VNIVERSITAT DE VALÈNCIA

Facultad de Química

Departamento de Química Analítica



DEVELOPMENT OF NOVEL SEPARATION SYSTEMS FOR DETERMINATION OF BIOMOLECULES IN VEGETAL SAMPLES

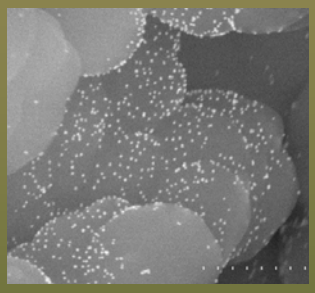
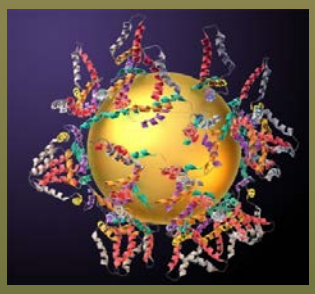

María Vergara Barberán
Mayo 2017

VNIVERSITAT DE VALÈNCIA

FACULTAD DE QUÍMICA

DEPARTAMENTO DE QUÍMICA ANALÍTICA

"DESARROLLO DE NUEVOS SISTEMAS SEPARATIVOS PARA LA DETERMINACIÓN DE BIOMOLÉCULAS EN MATRICES VEGETALES"

"DEVELOPMENT OF NOVEL SEPARATION SYSTEMS FOR DETERMINATION OF BIOMOLECULES IN VEGETAL SAMPLES"

Memoria para alcanzar el grado de Doctor en Química dentro del programa de doctorado en Química (RD 1393/2007) (Mención Internacional):

María Vergara Barberán

Directores:

Dr. Ernesto Francisco Simó Alfonso

Dr. José Manuel Herrero Martínez

Dra. María Jesús Lerma García

Valencia, Mayo 2017

VNIVERSITAT DE VALÈNCIA
Facultat de Química
Departament de Química Analítica

Dr. Ernesto Francisco Simó Alfonso, Dr. José Manuel Herrero Martínez, y Dra. María Jesús Lerma García, Catedrático, Profesor Titular del Departamento de Química Analítica de la Universidad de Valencia e Investigadora postdoctoral del Departamento de Tecnología de Alimentos de la Universidad Politécnica de Valencia.

Certifican

Que la presente memoria, que lleva por título "*Development of novel separation systems for determination of biomolecules in vegetal samples*" constituye la Tesis Doctoral de Dña. María Vergara Barberán.

Asimismo, certifican haber dirigido y supervisado tanto los distintos aspectos del trabajo como su redacción.

Y para que así conste a los efectos oportunos y a petición del interesado, firmamos la presente en Burjassot, a 25 de Mayo de 2017.

E. F.Simó Alfonso J. M. Herrero Martínez M. J. Lerma García

Preface

This Thesis is presented as "a compendium of publications", as it is regulated by the University of Valencia (Reglamento 29/11/2011, ACGUV 266/2011). Accordingly, the first part of the thesis contains a general introduction where all the articles are presented, with justification of the subject and also explaining the original contribution of the PhD candidate. The PhD student has contributed substantially in all stages of development of all the articles, from the development of the idea, literature search, experimental realization, analysis and interpretation of data, drafting and preparation of the manuscript, and monitoring and final correction thereof according to the recommendations of the referees. Then the published articles are included. These correspond entirely to indexed journals. The most recently submitted articles are also included. All articles have been written by María Vergara Barberán, with corrections and final review by the supervisors of this Thesis. According to the regulation quoted above, the last part of the thesis contains a summary of results, discussion and conclusions.

Esta Tesis se acoge a la modalidad “compendio de publicaciones”, contemplada en el Reglamento de la Universidad de Valencia de 29/11/2011 (ACGUV 266/2011). De acuerdo con dicha normativa, la primera parte de la Tesis contiene una introducción general, donde se presentan los trabajos compendiados, justificando su temática y explicando la aportación original del doctorando. El doctorando ha contribuido sustancialmente en todas las etapas de desarrollo, desde la elaboración de la idea, búsqueda bibliográfica, realización experimental, análisis e interpretación de datos, redacción y preparación del manuscrito, y seguimiento y corrección final del mismo de acuerdo con las recomendaciones de los evaluadores. A continuación se incluyen los artículos ya publicados, los cuales corresponden en su totalidad a revistas indexadas, más los artículos recientemente enviados. Todos los artículos han sido escritos por María Vergara Barberán, con correcciones y revisión final por parte de los supervisores de esta Tesis. De acuerdo con la normativa citada, la última parte de la Tesis contiene un resumen global de resultados, discusión y conclusiones.

Esta Tesis Doctoral ha sido realizada gracias a una
beca predoctoral (FPU) concedida por el Ministerio
de Educación, Ciencia y Deporte de España

A mi familia, y en especial a Él

AGRADECIMIENTOS

ACKNOWLEDGEMENTS

La realización de esta Tesis Doctoral no habría sido posible sin la ayuda y el apoyo de un gran número de personas:

En primer lugar, quisiera agradecer a mis Directores, Dr. Ernesto Francisco Simó Alfonso, Dr. José Manuel Herrero Martínez y Dra. María Jesús Lerma García por su ayuda, dedicación, por todos los conocimientos que me han transmitido y sobre todo por el tiempo que han invertido en mí. Su confianza, apoyo y paciencia han sido fundamentales para poder llevar a cabo este proyecto. Tampoco hay que olvidarse de los buenos momentos que hemos disfrutado juntos. Gracías María Jesús por ser primero mi compañera, y despúes mi codirectora, he aprendido mucho de ti, sobre todo a darle un valor importante al tiempo (a no estar parada…), y como no, nunca olvidaré nuestra estancia juntas en Milán, gracias a ti se hizo más llevadera.

Además, quisiera dar las gracias al Dr. Guillermo Ramis Ramos, por su contribución al desarrollo de mi trabajo y por haber estado dispuesto a ayudarme cuando lo he necesitado.

Ringraziare al Prof. P.G. Righetti e la Dott.ssa Elisa Fasoli per l'opurtunità che mi hanno datto di stare al suo laboratorio a Milano. Lì, ho potuto imparare una metodologia molto importante per lo svilupo della mia tesi. Grazie Elisa per il tuo tempo e il tuo aiuto.

Gracias también al Dr. Fernando Benavente, por brindarme la oportunidad de realizar una estancia en su laboratorio. Allí, pude ampliar mis conocimientos de CE acoplado a MS, los cuales espero den su fruto en un futuro no muy lejano.

Por otro lado, agradecer a mis compañeros del Laboratorio 10, con los que he compartido tantas horas… y tantas cosas buenas, otras no tan buenas, agobios, preocupaciones, trabajo, lloros… pero también muchos momentos buenos de diversión, risas, fiestas y bailes. A Aarón por estar siempre ahí, y hacer las veces de mi secretario, amigo, confidente, compañero de viajes y un largo etcétera. A Isabel, por sus conocimientos y su orden para hacer todo, gracias por prepararte tú las prácicas de cuali y dejarme todo el material, echaré de menos nuestras conversaciones de madres jóvenes e

incomprendidas. A Enrique por ser todo lo contrario a mi, sin ti mi paso por el lab habría sido más aburrido, pero en el fondo gracias por toda la ayuda que me has ofrecido en mis momentos de agobio. A Maria N, por los momentos locos y divertidos a las tantas de la tarde los viernes que acabábamos siempre en el bar con una buena cerveza. A la Miri, por su tranquilidad y sus momentos de escucharme, y por bajar a descansar cuando se lo pedía. No me olvido de todos mis pupilos (empezando por Ceci, Mireia, Pepe, Miriam, y como no de Óscar, sin duda el que más quebraderos de cabeza me ha dado y me sigue dando…), no sé si habréis aprendido algo de mí, pero yo de vosotros si. Tampoco me olvido de todos los que han pasado por el laboratorio: Agustín, José, Juan, Laura, Marta, Casandra y muchos otros.

No me puedo olvidar de Laura, Casandra y Juan por su apoyo y por todos los momentos juntos que hemos pasado. También agradecer a todos los profesores y personal del Departamento, con los que ha sido una verdadera satisfacción relacionarme y trabajar. No me voy a permitir olvidarme de mis amigas las “Barrieras”, porque los viernes de junta y las cenas al fresco no nos lo quita nadie. Y también a Sonia, Cris, Isa, y Anita las amigas que todo el mundo querría tener.

Gracias también al Ministerio de Educación, Cultura y Deporte por la beca predoctoral sin la cual no habría podido realizar esta tesis.

Y como no, agradecer enormemente a mi familia: mi madre, hermano, abuela y tios y primos, por demostrar siempre tanto interés en mi trabajo y por estar ahí. En especial a Carlos, por darme lo más bonito que puede existir, mi pequeña Valentina. Gracias por tu comprensión, tu ayuda y tu apoyo en los buenos y en los malos momentos.

Y por último, mi más profundo agradecimiento a mi Padre, que pese a que ya no está con nosotros, le daré gracias siempre porque he llegado hasta aquí gracias a su esfuerzo.

A todos vosotros, y a los que aunque no haya nombrado, pero que han sido partícipes de que todo haya llegado a buen fin, GRACIAS.

Abbreviations

ACN	Acetonitrile
AIBN	Azobisisobutyronitrile
ATR	Attenuated total reflectance
APS	Ammonium persulfate
BDDA	1,3-Butanediol diacrylate
BGE	Background electrolyte
BSA	Bovine serum albumin
BSE	Backscattered electrons
CEC	Capillary electrochromatography
CGE	Capillary gel electrophoresis
CHAPS	3-(3-Cholamidopropyl dimethyl ammonio)-1-propanesulfonate
CPLL	Combinatorial peptide ligand library
CZE	Capillary zone electrophoresis
DAD	Diode array detector
DIMS	Direct infusion mass spectrometry
DNA	Deoxyribonucleic acid
2-D	Two-dimensional
ECN	Equivalent carbon number
EDAX	Energy dispersive analysis of X-rays
EDMA	Ethylene dimethacrylate

ELSD	Evaporative light scattering detector
EIC	Extracted ion chromatogram
EOF	Electro-osmotic flow
ESI	Electrospray ionization
EVOO	Extra virgin olive oil
FAME	Fatty acid methyl ester
FID	Flame ionization detector
FTIR	Fourier transform infrared
GC	Gas chromatography
GLP	Germin-like protein
GMA	Glycidyl methacrylate
HAP	High-abundance protein
HPLC	High-performance liquid chromatography
LAP	Low-abundance protein
LDA	Linear discriminant analysis
LLE	Liquid-liquid extraction
LOD	Limit of detection
LPO	Lauroyl peroxide
MALDI	Matrix-assisted laser desorption/ionization
MeOH	Methanol
META	[2-(Methacryloyloxy)ethyl]trimethyl ammonium chloride
MS	Mass spectrometry
ML	Mistletoe lectin

MLR	Multiple linear regression
NARP	Non-aqueous reversed-phase
NP	Nanoparticles
NIR	Near infrared
NMR	Nuclear magnetic resonance
ODA	Octadecyl acrylate
PAGE	Polyacrylamide gel electrophoresis
PAH	Polycyclic aromatic hydrocarbons
PCA	Principal component analysis
PEG	Poly(ethylene glycol)
PS-DVB	Polystyrene-divinylbenzene
PVA	Poly(vinyl alcohol)
RI	Refractive index
RIP	Ribosome-inactivating protein
RP	Reversed phase
RSD	Relative standard deviation
Rubisco	Ribulose-1,5-bisphosphate carboxylase
SDS	Sodium dodecyl sulfate
SEM	Scanning electron microscope
SERS	Surface enhanced Raman spectroscopy
SOD	Superoxide dismutase
SPE	Solid-phase extraction
SSP	Seed storage proteins
TAG	Triacylglycerol

TCA	Trichloroacetic acid
TCEP	Tris(2-carboxyethyl)phosphine
TEMED	N,N,N',N'-tetramethylethylenediamine
TIC	Total ion chromatogram
TLC	Thin-layer chromatography
TLP	Thaumatin-like protein
TOF	Time of flight
Tris	Tris(hydroxymethyl)aminomethane
UHPLC	Ultra-high-pressure liquid chromatography

En esta sección de la Tesis Doctoral, tal y como lo exige la normativa de la Universidad de Valencia, se presenta un resumen indicando los objetivos, metodología y las conclusiones más relevantes.

La presente memoria se enmarca dentro de las líneas de investigación del grupo de investigación, entre las que se encuentran: i) el desarrollo de materiales poliméricos con fines separativos, y ii) la puesta a punto de metodologías analíticas rápidas y fiables para el control de calidad en la industria de aceites vegetales y otros productos de interés agroalimentario. Así pues, los objetivos planteados en la presente tesis pretenden dar continuidad a dichas líneas de investigación, conjugando además el interés, la calidad y la actualidad tanto en el aspecto científico como en el de transferencia tecnológica de los resultados obtenidos.

Objetivos

Los objetivos principales de esta Tesis Doctoral son: i) el diseño y optimización de soportes poliméricos modificados con nanopartículas metálicas (tales como el oro y la plata) para la extracción de proteínas en matrices vegetales, ii) la preparación y evaluación de sistemas de extracción de proteínas en dichas muestras asistida por enzimas y iii) el desarrollo de metodologías analíticas de separación rápidas y fiables con el fin de poder establecer el origen genético y botánico de diversos productos alimentarios.

El tratamiento de muestras de naturaleza vegetal constituye una tarea compleja, debido al amplio espectro de interferentes presentes en las mismas. Además, la separación, aislamiento y preconcentración de los analitos objetivo puede estar dificultada por posibles efectos sinérgicos negativos que pueden darse entre el analito y los interferentes presentes en la matriz. En este sentido, los métodos de extracción de proteínas desarrollados en los objetivos i y ii) suponen una interesante y prometedora alternativa al

empleo de las metodologías tradicionales de extracción de estas sustancias, las cuales son tediosas, poco selectivas, de cuestionada sostenibilidad medioambiental, y por lo general proporcionan rendimientos no especialmente altos. Por otro lado, los métodos desarrollados en el objetivo iii) presentan gran interés en las industrias alimentarias en lo referente al control de calidad de sus materias primas y/o productos, así como poder garantizar a los consumidores los cánones de calidad y seguridad de los mismos.

La presente memoria de Tesis Doctoral se divide en cuatro grandes bloques. El primer bloque consta de una introducción, donde se describen brevemente las muestras vegetales empleadas en esta Tesis Doctoral (fruto, hoja y aceite de olivo, frutos de la variedad *Citrus* (en concreto naranjas y mandarinas) y muérdago, correspondientes a los Capítulos 1-3, respectivamente). Además, se incluye una revisión actualizada de los métodos de extracción empleados durante la tesis: extracción en fase sólida (SPE), extracción asistida por enzimas y por último, el empleo de las bibliotecas combinatorias de ligandos peptídicos (CPLLs). El bloque de introducción concluye con una breve descripción de las técnicas analíticas empleadas en el desarrollo de la Tesis Doctoral (Capítulo 5).

El segundo bloque (que engloba los capítulos 6-11) está dedicado al desarrollo de nuevas técnicas de extracción de proteínas en matrices de origen vegetal. Para ello, se han puesto a punto nuevos sorbentes, basados en materiales poliméricos sintetizados a partir del metacrilato de glicidilo (GMA), que son posteriormente modificados con nanopartículas metálicas (de oro y plata) para su uso como sorbentes en SPE.

Por otro lado, la presencia de sistemas reticulares u organizados, presentes en los vegetales, requiere habitualmente de tratamientos relativamente “agresivos” con el fin de poder extraer los analitos diana. En este sentido, se han llevado a cabo estudios de extracción de proteínas

asistidos por enzimas, empleándose tanto enzimas individuales como mezclas de las mismas. Gracias a la acción de estas biomacromoléculas, se facilita la ruptura de las membranas celulares, y por ende la extracción de los analitos para su posterior análisis y cuantificación. Estos pretratamientos de la muestra, sin duda, permitirán obtener resultados de mayor calidad. En este caso, se ha empleado dicha tecnología para la extracción de proteínas de diversos productos del olivo (hojas, huesos y pulpa), así como para muestras de naranja y mandarina, incluyendo tanto la piel como la pulpa de las mismas. Por último, se ha llevado a cabo un estudio del proteoma del muérdago mediante la extracción del mismo empleando las CPLLs, que son capaces de extraer y preconcentrar las proteínas de baja abundancia. La identificación del mapa proteico de esta planta ha permitido profundizar en un mayor conocimiento de sus propiedades medicinales.

El tercer bloque (que engloba los capítulos 12-20) muestra el desarrollo de una amplia variedad de métodos de análisis para la determinación de diferentes compuestos en matrices de origen vegetal, tales como aceite de oliva, frutos y hojas de olivo, frutos de la variedad *Citrus* (naranjas y mandarinas), y muérdago). Dichas metodologías abarcan tanto técnicas de carácter cromatográfico (HPLC) y afines (CZE, CGE y CEC) así como de carácter espectrométrico (ATR-FTIR o DIMS). Se han desarrollado metodologías analíticas para la determinación de proteínas, TAGs, esteroles, ácidos grasos y péptidos. Además, en muchos de los capítulos, se han aplicado herramientas quimiométricas de análisis, en concreto, se han construido modelos de análisis discriminante lineal (LDA), para establecer la clasificación de muestras de aceites vegetales en función de su origen botánica, para la discriminación de productos del olivo, incluyendo aceites de oliva, en función de su variedad genética y en caso de los aceites de oliva, también para clasificarlos en función de su índice de madurez. En algunos de ellos, se ha aplicado la regresión lineal múltiple (MLR) para cuantificar mezclas binarias de diferentes variedades genéticas

Metodología y Conclusiones

En este apartado se describe la metodología y las conclusiones obtenidas para cada uno de los trabajos incluidos en la Tesis Doctoral. Los trabajos han sido divididos en dos grandes grupos (A y B), que corresponden a los bloques II y III de la memoria, respectivamente, donde se indicará de forma desglosada por capítulos (cada capítulo corresponde a una publicación) la metodología adoptada en cada uno de ellos para alcanzar los objetivos planteados así como los conclusiones más relevantes obtenidas de los mismos.

A. Desarrollo de técnicas de extracción novedosas para la extracción de proteínas en muestras vegetales

A.1. Diseño y aplicación de soportes poliméricos modificados con nanopartículas metálicas

En este trabajo (**Capítulo 6** de la memoria) se ha desarrollado un nuevo sorbente basado en un monolito polimérico de GMA en polvo para la extracción en fase sólida (SPE) de proteínas. Para ello, en primer lugar, se procedió a la síntesis del polímero de GMA, se trituró y se llevó a cabo la modificación de su superficie mediante reacción con amoníaco, seguida de la posterior inmovilización de nanopartículas de oro (AuNPs) en su superficie. De esta manera, se obtiene un material polimérico modificado con AuNPs. Este soporte presenta una elevada afinidad por los grupos tiol y amino, habitualmente presentes en las biomoléculas (como las proteínas). El material obtenido se caracterizó mediante la adquisición de imágenes en microscopía electrónica de barrido con detector de retrodispersados SEM/BSE, observándose un alto recubrimiento de la superficie del polímero con las AuNPs. También, se evaluó el contenido de Au presente en el material mediante dos métodos diferentes (UV-vis y microanálisis por dispersión de energías de Rayos-X (EDAX)), obteniéndose en ambos casos

valores cercanos al 0.5 % (en peso) de Au. Posteriormente, el material sintetizado se empaquetó en un cartucho de SPE para su posterior empleo en la extracción de proteínas, en particular, se utilizó como solutos test, albumina de suero bovino (BSA), citocromo c (cyt c). Tras optimizar diversos parámetros que afectan al rendimiento de extracción, se obtuvieron buenos rendimientos (95-98 %) y una excelente capacidad de carga (16.6 mg proteína/ g de sorbente). Además, se realizó un estudio de su reutilización, obteniéndose resultados satisfactorios hasta un uso continuado de unas 20 veces, sin una pérdida significativa de sus prestaciones analíticas. Los resultados de este estudio demostraron que es posible aislar las proteínas de interés simplemente ajustando el pH de la etapa de carga y de lavado cerca de su punto isoeléctrico.

La aplicabilidad de dicho material como sorbente queda demostrada mediante la separación de una mezcla de las proteínas test (BSA y cyt c), así como la extracción de las lectinas (glicoproteínas) presentes en el muérdago, las cuales son de gran interés debido a sus propiedades medicinales como coadyuvante en el tratamiento del cáncer. Así pues, la metodología desarrollada supone una alternativa sencilla y fiable respecto a la cromatografía de afinidad, que es la técnica generalmente empleada para la purificación de dichas lectinas.

En un trabajo posterior (correspondiente al **Capítulo 7** de la memoria), se desarrollaron sorbentes para SPE con prestaciones mejoradas, y se aplicaron a la extracción selectiva de proteínas en muestras vegetales. Para ello, al igual que el trabajo anterior, se utilizó como material de partida un monolito de GMA pulverizado. Este material fue tratado con dos ligandos diferentes (amoníaco y cisteamina), con el fin de introducir en la superficie del polímero terminaciones amino y tiol. La introducción de estos grupos funcionales permitirá la posterior inmovilización de las Au o AgNPs. La presencia de dichas NPs en los cuatro sorbentes sintetizados se confirmó

mediante la adquisición de imágenes SEM, y su contenido en Au o Ag se midió mediante espectrometría de masas con plasma de acoplamiento inductivo (ICP-MS). Tal y como se ha indicado en el trabajo anterior, los materiales desarrollados se empaquetaron en cartuchos de SPE, utilizando BSA como soluto test. Tras la optimización de las condiciones de elución, se llevó a cabo una comparación de los materiales diseñados en base a su nivel de recuperación y capacidad de carga, observándose que el material modificado con grupos tiol y Au proporcionó los mejores resultados (>90% y 29.3 mg /g sorbente). Además, los sorbentes desarrollados se aplicaron a la extracción selectiva de viscotoxinas (tioninas) presentes en el muérdago. Dichos tratamientos permitieron obtener extractos enriquecidos en viscotoxinas, las cuales fueron analizadas mediante MALDI-TOF.

A.2. Aplicación de metodologías de extracción asistida por enzimas a productos alimentarios

En este trabajo (**Capítulo 8** de la memoria) se ha desarrollado una metodología basada en la extracción de proteínas asistida por enzimas en muestras complejas (hojas de olivo). Para ello, se empleó la enzima celulasa, ya que ésta es capaz de hidrolizar los componentes de la pared celular de las hojas de olivo favoreciendo así la extracción de los componentes intracelulares. Se evaluó la influencia de diversos parámetros que afectan al rendimiento de la extracción (contenido de enzima, pH, temperatura y tiempo de extracción). Las condiciones óptimas se obtuvieron con 30% ACN, 5 % (v/v) Celluclast® 1.5L a pH 5.0 y 55 ºC durante 15 minutos. Bajo estas condiciones, se obtuvieron extractos proteicos procedentes de diferentes variedades genéticas de hojas de olivo, y se realizó su posterior análisis mediante SDS-PAGE. Se observaron diferencias en los perfiles electroforéticos obtenidos, lo cual puede ser de gran utilidad para distinguir hojas de oliva en función su origen genético.

La metodología propuesta en este capítulo presenta una serie de ventajas frente a las metodologías tradicionales de extracción de proteínas. Entre dichas ventajas destacan: las condiciones "suaves" de extracción empleadas, bajo impacto medioambiental, reducción en el uso de disolventes orgánicos y tiempos cortos de procesado de muestras.

En este estudio (**Capítulo 9** de la memoria), se adoptó la metodología propuesta en el capítulo anterior para llevar a cabo la extracción de proteínas de pulpa y hueso de aceituna. En primer lugar, se estudió el empleo de otras enzimas diferentes a la celulasa, ya que las matrices tienen naturaleza diversa. Se utilizaron enzimas individuales (lipasa, celulasa y fosfolipasa), así como un preparado multienzimático comercial (arabanasa, celulasa, beta-glucanasa, hemicelolosa y silanasa). Se optimizaron las variables fundamentales que afectan a la extracción (tipo enzima, concentración, pH, tiempo y la temperatura de extracción). Las mejores condiciones de extracción para pulpa fueron: 5% (v/v) Palatase® 20000 L a pH 7, 30 ºC durante 15 minutos, mientras que para hueso fueron: 50 % Lecitase® Ultra a pH 7, 40ºC durante 15 minutos. Bajo estas condiciones, se analizaron muestras de pulpa y hueso de aceituna de diferentes orígenes genéticos por SDS-PAGE. Los resultados mostraron diferentes perfiles electroforéticos para las diferentes variedades genéticas estudiadas, lo cual confirmó la enorme utilidad de las proteínas, tras una extracción eficiente de las mismas, como marcadores moleculares para distinguir las muestras analizadas en función de la variedad genética.

Este trabajo (**Capítulo 10** de la memoria) también se enmarca dentro de la extracción asistida por enzimas en matrices vegetales. En particular, en este estudio se plantearon tres objetivos, i) verificar la efectividad del uso de enzimas en la extracción de proteínas tanto en la piel como en la pulpa de naranjas y mandarinas, ii) comparar la metodología enzimática con otras

metodologías no enzimáticas y iii) obtener los perfiles proteicos mediante CGE para su posterior tratamiento quimiométrico.

En primer lugar, se llevó a cabo la extracción de proteínas de pulpa y piel de naranja y mandarina mediante el uso de diferentes tratamientos: extracción asistida por enzimas y extracción empleando el tampón tradicional Tris-HCl. Los mejores resultados se obtuvieron utilizando las enzimas celulasa y lipasa (en ambos casos con un 5% fue suficiente) en la extracción de proteínas de piel y pulpa, respectivamente. A continuación, se procesaron muestras de estos cítricos de origen español pero de diferente variedad genética. Las proteínas extraídas se caracterizaron mediante CGE, observándose un total de 14 y 8 proteínas comunes para piel y pulpa, respectivamente. Además, se evaluó la reproducibilidad del método, obteniéndose valores satisfactorios de RSDs (3.6 y 3.7% para piel y pulpa, respectivamente). Seguidamente, se procedió a la normalización de los picos electroforéticos (área de cada pico dividida por el área de cada uno de los picos restantes), se utilizaron como variables predictoras en la construcción de modelos LDA. Dichos modelos fueron capaces de discriminar las muestras según su variedad genética, observándose una clasificación correcta de todas las muestras analizadas.

Este trabajo pone de nuevo de manifiesto el potencial que ofrece la extracción asistida con enzimas en combinación con la separación de las proteínas extraídas mediante CGE y el uso de herramientas quimiométricas adecuadas.

A.3. Aplicación de CPLLs a la caracterización el muérdago

En este trabajo (**Capítulo 11** de la memoria) se propone el uso de la tecnología basada en librerías peptídicas (CPLLs) acoplada a MS para investigar el proteoma del muérdago. Dicha tecnología permite preconcentrar las proteínas de baja concentración, reduciendo al mismo

tiempo la concentración de las más abundantes. Para ello, en primer lugar se llevó a cabo la "captura" de proteínas con CPLLs a dos pHs diferentes (2.2 y 7.2). A continuación, se eluyeron las proteínas con SDS y se caracterizaron mediante SDS-PAGE. Las bandas del gel fueron cortadas y digeridas con tripsina para su posterior análisis en MS. Los datos espectrales fueron cruzados con dos bases de datos teniendo en cuenta la especie estudiada (*Viscum álbum L.),* encontrándose un total de 295 y 257 proteínas en la muestra sin tratar (control) y en la muestra tratada con las CPLLs, de las cuales sólo 96 proteínas eran comunes.

La metodología propuesta fue capaz de extraer no solamente las lectinas y viscotoxinas presentes en el muérdago, las cuales han sido ampliamente descritas en la bibliografía, sino también se identificaron otras proteínas de interés biológico con actividad farmacológica.

B. Desarrollo de métodos para la discriminación de productos derivados de la aceituna según su origen genético y botánico

En este trabajo (**Capítulo 12** de la memoria) se ha desarrollado un método de CZE para separar las proteínas presentes en hoja y pulpa de aceituna. Las proteínas se aislaron mediante los métodos enzimáticos mencionados anteriormente (empleándose celulasa y lipasa, **Capítulos 8** y **9** de la memoria). Se optimizó el tampón de separación y otros aspectos instrumentales (voltaje e inyección). Los mejores resultados se obtuvieron con un tampón de separación compuesto por 50 mM fosfato, 50 mM tetraborato conteniendo 0.1% PVA a pH 9, a un voltaje de separación de +10 kV e inyección hidrodinámica (50 mbar durante 3 s). La metodología propuesta en este capítulo proporciona menores tiempos de análisis comparados con otros procedimientos descritos en la literatura. Bajo las condiciones óptimas de separación, se analizaron muestras de hojas y pulpa de diferentes variedades genéticas, observándose un total de 9 y 14 picos de proteínas comunes para hoja y pulpa, respectivamente. Las áreas de las

proteínas identificadas se emplearon como predictores en la construcción de modelos LDA, los cuales fueron capaces de clasificar correctamente todas las muestras estudiadas en función de su variedad genética.

En este trabajo (**Capítulo 13** de la memoria), la clasificación de hojas y pulpa de aceituna de acuerdo a su origen genético utilizando los perfiles proteicos obtenidos mediante CGE. Las proteínas se extrajeron utilizando los métodos enzimáticos de extracción descritos anteriormente (**Capítulos 8** y **9).** Tras el análisis de las muestras, se observaron 10 y 9 proteínas comunes para hoja y pulpa, respectivamente. Posteriormente, se llevó a cabo un estudio quimiométrico, y para ello se construyeron modelos LDA empleando las áreas de los picos observados. En ambos casos (hoja y pulpa de aceituna), se consiguió una clasificación correcta de todas las muestras con una excelente resolución entre categorías, lo cual demostró de nuevo que los perfiles proteicos son característicos de cada variedad y pueden ser utilizados para su correcta clasificación.

En este artículo (**Capítulo 14** de la memoria), se obtuvieron los perfiles de los TAGs mediante HPLC acoplado a dos detectores diferentes (UV y ELSD) con la finalidad de clasificar según la variedad genética y el índice de madurez muestras de EVOO provenientes de Túnez. Así pues, se realizó una comparación entre los resultados proporcionados por ambos detectores para los analitos estudiados, seleccionándose las señales obtenidas en ELSD, ya que en términos generales, proporcionaron una mejor relación señal/ruido que el detector UV.

Tras una simple dilución de la muestra, se llevó a cabo la separación de los TAGs, seleccionándose un total de 19 picos característicos de las diferentes muestras investigadas. Después de realizar un tratamiento estadístico de los datos, los modelos LDA obtenidos proporcionaron una correcta clasificación de todas muestras analizadas de acuerdo tanto a su origen genético (7 variedades fueron incluidas en el estudio) como a su

índices de madurez. Así pues, se ha demostrado que los perfiles de TAGs pueden ser empleados como marcadores genéticos para la diferenciación de muestras de diferentes orígenes y con diferentes índices de madurez.

En este estudio (**Capítulo 15** de la memoria), se analizaron los esteroles presentes en muestras de diferentes variedades genéticas e índice de madurez de EVOO procedentes de Túnez. Para ello, los esteroles se aislaron siguiendo el procedimiento indicado por la normativa Europea, y seguidamente se inyectaron en el sistema cromatográfico (HPLC-MS). Se pudieron identificar 12 esteroles (en base a su *m/z* y tiempo de retención), usándose como variables útiles para realizar estudios de análisis clasificatorio. Así pues, se realizó un tratamiento estadístico de los datos obtenidos y se construyeron modelos LDA, los cuales fueron capaces de discriminar de forma satisfactoria entre variedades genéticas y, también entre diferentes índices de madurez con una excelente capacidad predictora.

En este trabajo (**Capítulo 16** de la memoria) se ha desarrollado un método de CE para la determinación de ácidos grasos en muestras de aceites vegetales. Para ello, se utilizó detección indirecta UV-vis, ya que los ácidos grasos no contienen en su estructura grupos cromóforos, para que puedan ser detectados de forma directa. Además, la metodología propuesta evita las típicas reacciones de derivatización de los ácidos grasos empleadas en CG, las cuales pueden ser una fuente de interferentes e incluso conducir a una conversión incompleta de los analitos de interés. Para ello, en primer lugar, se optimizó la composición del electrolito de fondo (BGE) (contenido y naturaleza del surfactante Brij, y concentración de modificador orgánico). Se obtuvo la siguiente composición óptima de BGE: 10 mM p-hidroxibenzoato, 5 mM Tris a pH 8.8, 80 mM Brij 98, 40% ACN y 10% 2-propanol. Se establecieron los parámetros de calidad del método, entre ellos la precisión y LODs, obteniéndose valores cercanos de RSD de 3% y 0.020 mM, respectivamente. El método propuesto se aplicó a la cuantificación de ácidos

grasos presentes en 5 aceites procedentes de diferente origen vegetal (aguacate, avellana, maíz, oliva extra virgen y soja). Finalmente, se construyeron modelos LDA utilizando las áreas de los picos de los analitos como variables predictoras, obteniéndose en todos los casos una buena resolución entre las categorías incluidas en los modelos.

La metodología propuesta en este trabajo constituye una herramienta eficaz tanto para el control rutinario de calidad de aceites como para la detección de adulteraciones de aceites de mayor calidad con otros aceites de menor precio.

En este trabajo (**Capítulo 17** de la memoria) se ha desarrollado un método de CEC usando columnas monolíticas de acrilato (de fabricación propia) para análisis de TAGs en diferentes aceites vegetales. Para ello, se utilizó como monómero funcional, ODA, optimizándose la composición de la mezcla de polimerización. Los mejores resultados en términos de resolución, eficacia y en tiempos de análisis de los TAGs se obtuvieron a las siguientes condiciones: 40:60% (p/p) monómeros/porógenos, 60:40% (p/p) ODA/1,3-butanodiol diacrilato y 23:77% (p/p) 1,4-butanodiol/1-propanol (14 % 1,4-butanodiol en la mezcla de polimerización). Bajo las condiciones óptimas, se analizaron muestras de aceites de distinto origen botánico fueron analizadas. Se pudieron reconocer hasta un total de 9 TAGs (en menos de 12 min), los cuales fueron usados como variables útiles para estudios clasificatorios. Tras el correcto tratamiento estadístico de las señales obtenidas, se diseñaron modelos LDA capaces de clasificar las muestras según su origen botánico. La capacidad de predicción del modelo fue excelente, ya que todas las muestras analizadas fueron correctamente asignadas a su categoría.

En comparación con otras metodologías analíticas de TAGs mediante HPLC, con el método propuesto se redujo considerablemente el tiempo de análisis.

Resumen

En este trabajo (**Capítulo 18** de la memoria) se ha llevado a cabo dos objetivos: i) desarrollar un método basado en el uso de la técnica de ATR-FTIR, rápido y fiable para la clasificación de aceitunas de diferente variedad genética y ii) comparar diferentes tratamientos estadísticos como son el PCA y el LDA usando los datos espectrales obtenidos. Para ello, en primer lugar se obtuvo el espectro IR de un total de 136 muestras de aceitunas de diferente origen genético (17 variedades procedentes de España). A continuación, se dividió el espectro en 24 regiones, integrándose el área de cada una de éstas, y tras su normalización, se emplearon como variables predictoras en la construcción de modelos LDA, con el fin de poder discernir las aceitunas en función del origen genético. El modelo obtenido se ensayó con muestras de un conjunto de evaluación, obteniéndose una capacidad de predicción de 100%. Sin embargo, cuando se llevó a cabo un segundo modelo quimiométrico basado en PCA-LDA, se observó la incorrecta clasificación de algunas de las muestras, mostrando tan sólo un 56% de capacidad predictora. A la vista de estos resultados, así como su mayor simplicidad y rapidez, se seleccionó el modelo LDA como herramienta clasificatoria.

En este estudio (**Capítulo 19** de la memoria) se demuestra la aplicabilidad con fines clasificatorios de la metodología ATR-FTIR propuesta en el trabajo anterior, seguida del correcto tratamiento estadístico de los datos espectrales obtenidos. Para ello, se emplearon muestras de EVOO de diferentes variedades genéticas y diferente índice de madurez procedentes de Túnez. Además, los datos espectrales fueron también empleados en el diseño de modelos MLR capaces de distinguir entre mezclas binarias de EVOOs de diferentes orígenes genéticos. Los modelos construidos presentaron errores de predicción inferiores al 6%.

Los resultados obtenidos en este estudio y en el anterior demostraron que la técnica ATR-FTIR junto con la aplicación de tratamientos

quimiométricos, como LDA o MLR, representando metodologías rápidas, fiables y de bajo coste.

El objetivo de este último estudio (**Capítulo 20** de la memoria) fue la utilización del perfil de ácidos grasos (obtenidos mediante infusión directa en MS) como herramienta para poder clasificar muestras de EVOOs (procedentes de Túnez) de acuerdo a su variedad genética. También, se llevó a cabo la discriminación de muestras en función de su índice de madurez. Para ello, tras una sencilla dilución de la muestra (con propanol/metanol), los aceites se inyectan de forma directa en el espectrómetro de masas midiéndose las abundancias de los picos de los ácidos grasos. Los perfiles de estos compuestos se utilizaron con el fin de construir modelos de LDA capaces de discriminar los aceites según su origen genético e índices de madurez.

INDEX

SECTION I. INTRODUCTION

Chapter 1. Olive fruit, leaf and oil

1.1. Introduction

Olive tree (*Olea europaea*) is one of the most important and the oldest cultivated tree around world, especially in the Mediterranean area, where almost 98% of olive trees are located. Currently, the major producers of olive oil are Spain, Turkey, Italy, Tunisia and Greece.

The olive tree and its products (olive fruit, olive leaves, and oil) have a rich history of nutritional, medicinal and commercial purposes (Soni, 2006). In the last decade, consumption of olives and olive oil has increased significantly, since they are important components in the daily diet of a large part of the world's population. Moreover, in high-income countries such as United States, Japan, Canada and Australia, where olive trees are not traditionally cultivated, the consumption has increased in the last years (Ghanbari, 2012).

1.2. Olive fruit

Olive fruits can be directly consumed as table olives or manufactured to produce olive oil. The major commercial table olives include Spanish style green fermented olives, American style canned ripe olives and Greek style black (naturally ripe) olives.

As indicated in **Figure 1.1**, olive fruits are constituted by three parts. The epicarp or skin (*ca.* 3% of the olive weight), the mesocarp or pulp (70-80% of the whole fruit, which comprises the major part of nutrients), and the endocarp (18–22% of the olive weight), containing the seed (Bianchi, 2003).

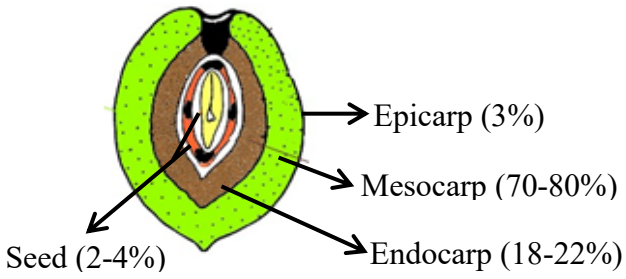

Figure 1.1. Cross schematic section of olive fruit.

Epicarp. The epicarp presents a bright green color at an earlier maturity stage due to its high content in pigments (chlorophylls, carotenoids and anthocyanins). However, during maturation, the olive color changes to purple pink and finally to black. In the case of table olives, this parameter is fairly important, since the skin minimizes mechanical damage to cells, inhibiting fungal and insect attack and it plays a determining role in the processing and the final product quality (Bianchi, 2003).

M*esocarp.* The major part of the olive is constituted by the mesocarp or flesh. It is mainly composed by water (50 % of the total weight) and oil (*ca.* 15% in green olives and 30% in black olives) (Zamora, 2001; Conor, 2005). In addition, it is composed by free organic acids (*ca.* 2% of the dry flesh), sugars (such as saccharose and mannitol, which accounted *ca.* 4% of the dry flesh) and proteins (*ca.* 2% of the fruit weight) (Zamora, 200l; Conor, 2005). Free phenols and their glycosides (1-3% of the olive weight) are also present. Finally, other minor compounds are polysaccharides and pectic substances, which play an important role in the textural quality of olives.

Endocarp. The endocarp or stone is characteristic of the olive variety. It represents 18-22% of the olive weight. The enclosed kernels (or seed) comprise 2-4% of the weight. The major components of the seeds are cellulose, hemicellulose and lignin (31, 21 and 26 % of dry weight, respectively) (Rodriguez, 2008). Then, the seed contains a relevant amount of oil (22-27% of the total seed weight) (Zamora, 200l; Conor, 2005; Rodriguez, 2008), whereas the woody shell contains at most 1%. Phenolic compounds comprise between 1–3% of the fresh pulp weight (Silva, 2006). The size, weight, shell conformation of the stone and its easy separation from the flesh are important parameters that determine the quality of the final product (Bianchi, 2003).

The study of the composition in the different parts of the olive fruit has been focused on the isolation and characterization of the major components, such as fatty acids (Leon, 2004; Aydin, 2009; De la Rosa, 2013) or bioactive compounds such as phenols (Silva, 2006; Malheiro, 2014). However, proteins present in olive fruit have been scarcely investigated (Montealegre, 2010; Esteve, 2011). Since one of the objectives of this thesis is the determination of proteins in both olive pulp and seed, a brief description is next included.

Recent studies have demonstrated that the most abundant proteins in the mature olive seeds belong to a certain type of proteins called seed storage proteins (SSPs). These SSPs are classified according to their solubility into albumins (water soluble), globulins (soluble in dilute saline buffer), prolamins (soluble in alcohol/water mixtures), and glutelins (soluble in dilute acid or alkali). Globulins are the most widely distributed group of SSPs (Alché, 2006), concretely the 11S protein family, which are approximately 70% of the total SSPs (Alché, 2006, Montealegre, 2012). These storage proteins are formed during seed development and deposited predominantly in specialized storage tissues, like the cotyledon or endosperm. Furthermore, oleosins have been found in the seed (Huang,

1992; Ross, 1993). Other identified proteins are thaumatin-like proteins (TLPs), which are related to host defense, or acyl carrier proteins, which are universal and highly conserved carrier of acyl intermediates during fatty acid biosynthesis.

Moreover, the role of some enzymes present in olive fruit and oils has attracted much attention. In this sense, some enzymes such as lipoxygenase, which is related to the responsible compounds of virgin olive oil aroma, and/or Cu/Zn and Mn superoxide dismutases (SODs), which belong to a part of the cellular defense system against oxidative stress, have been also studied (Salas, 1999; Esteve, 2011). These enzymes are responsible for several nutritional and organoleptic properties of olive fruits (Ortega-Garcia, 2008).

1.3. Olive leaf

Olive leaf, which is generated during pruning of trees, is a by-product of the olive tree cultivation. It can be found in huge amounts in olive oil industry (5% of the total weight of the olives). Olive leaves are used as a cheap raw source of anti-oxidants (polyphenols), since they constitute the main constituents. Moreover, olive leaves contain triterpenes, flavonoids and tannins (Briante, 2002). The chemical composition of olive leaves varies depending on several factors such as origin, proportion of branches on the tree, moisture content, storage and climatic conditions. In addition, the structural carbohydrates and nitrogen content in olive leaves depends on factors such as the variety of the olive tree, climatic conditions, year, proportion of wood, etc (Sedef, 2009).

Besides, it has been demonstrated the usefulness of olive leaves in the prevention of some diseases due to their anti-oxidative, anti-inflammatory, antiviral (De Leonardis, 2008) and antimicrobial properties (Pereira, 2007;

Leonardis, 2008; Sudjana, 2009), atherosclerosis inhibition and hypotensive action (Somova, 2003). Moreover, olive leaves show anti-carcinogenic properties that lead to the prevention of some cancers (Owen, 2000) and also to the stimulation of the thyroid gland (Al-Qarawi, 2002).

Since this thesis has been focused in the determination of proteins, as mentioned above, a brief introduction about olive leaf proteins is next found.

The protein content in olive leaves is *ca.* 2.46 mg g^{-1} of aged leaf (Wang, 2003). The most abundant protein is the ribulose-1,5-bisphosphate carboxylase (Rubisco). Moreover, another protein at 63 kDa, named β-glucosidase, whose function is related to chemical defense response and lignification or cell-wall catabolism, has been described (Dietz, 2000; Lee, 2006; Koudounas, 2015). Another group of proteins, SOD isozymes, is also found at a range comprised between 17 to 27 kDa (Corpas, 2006).

1.4. Olive oil

Olive oil is obtained by physical methods from the fruits *Olea europaea L.* (Manai, 2008; Ouni, 2011). It is well-known that the beneficial effect of olive oil is attributed to its favorable fatty acid profile and minor components such as carotenoids, phospholipids and phenolic compounds (Soler-Rivas, 2000). The constituents of the olive oil can be grouped in saponifiable and unsaponifiable fractions.

The saponifiable fraction, which accounts for 98.5 - 99.5% of oils, is mainly composed by triacylglycerols (TAGs) and free fatty acids, although other compounds as sterols are also found. TAGs are esters derived from the union of glycerol (1,2,3-propanetriol) and fatty acids. The fatty acids at the central or 2-position of the glycerol molecule are generally unsaturated. Saturated acids are found at this position only when the total concentration

of saturated fatty acids in the oil is very high. Major olive oil triacylglycerols are POO (18.4%), SOO (5.1%), POL (5.9%), OOO (43.5%), and OOL (6.8%) (P, palmitic acid; O, oleic acid; S, stearic acid; L: linoleic acid) (Fedeli, 1977). On the other hand, free fatty acids proportion in the oil depends on the hydrolysis degree of triacylglycerols, being their composition variable according to the genetical and botanical origin, climatic conditions, fruit maturity and geographical origin of olives (D' Imperio, 2007; Lerma-Garcia, 2011; Quintero, 2015). Major fatty acids in olive oils are palmitic (7.5 – 20%), stearic (0.5 – 5%), palmitoleic (0.3 – 3.5%), oleic (55 – 85%), linoleic (7.5 – 20%) and linolenic (7.5 – 20%) and linolenic (0.0 – 1.5%) acids, although traces of myristic, arachidic and margaric acids could be also found.

On the other hand, the unsaponifiable fraction of olive oils (0.5 - 1.5% of the total oil) contains different compounds which are not chemically related to fatty acids, such as free sterols. There are four classes of sterols in olive oils: 4-α-desmethylsterols, 4-α-methylsterols, 4,4-dimethyl sterols (commonly named as triterpene alcohols) and triterpene dialcohols. 4-α-Desmethylsterols are the most abundant sterols found in olive oil, being its content ranged between 100 and 200 mg/100 g. In this group, β-sitosterol (75 – 90%), Δ^5-avenasterol (5 – 36%) and campesterol (approximately 3% of the total sterol fraction) are the main compounds. Other 4-α-desmethylsterols, present at trace levels, are cholesterol, campestanol, stigmasterol, Δ^7-campesterol, chlerosterol, sitostanol, $\Delta^{5,24}$-stigmastadienol, Δ^7-stigmasterol and Δ^7-avenasterol (Boskou, 2002). Then, 4-α-methylsterols, whose concentration is approximately 20 – 70 mg/100 g, represent small quantities in the oils (Boskou, 1996). The most abundant 4-α-methylsterols are obtusifoliol, cycloeucalenol, gramisterol and citrostadienol. On the other hand, major triterpene alcohols present in olive oil, whose content ranged between 100 and 150 mg/100 g oil (Kiosseoglou, 1987), are α- and b-amiryn, cycloartenol, butyrospermol, 24-

methylenecycloartanol, taraxerol, dammaradienol and 24-methylene-24-dihydroparkeol (Paganuzzi, 1982; Boskou, 2002; Kiritsakis, 2003). Finally, erythrodiol and uvaol are the main triterpene dialcohols found in olive oils. Their total content in olive oil ranged from 1 to 20 mg/100 g, although it may be as high as 280 mg/100g (Mariani, 1987; Boskou, 2002). In this thesis, sterols have been studied, since their profiles can be used as a tool to discriminate between cultivars and maturity index (**Chapter 15**).

1.5. Methods of analysis of olive tree constituents

The discussion of this section will be focused only in the determination of the compounds that have been studied in this thesis. Thus, a brief description regarding the determination of tryacylglycerols, fatty acids, sterols and proteins, have been next included.

1.5.1. Determination of TAGs

TAGs have been traditionally analyzed using thin-layer chromatography (TLC) (Christie, 1992) and reversed-phase high-performance liquid chromatography (RP-HPLC) (Ranalli, 2002; Holčapek, 2005; Cunha, 2006). Regiospecific analysis of TAG composition in olive fruit have been also conducted by using ^{13}C Nuclear Magnetic Resonance (NMR) in order to investigate the distribution of fatty acids into TAGs (Vlahov, 1999; Ranalli, 2002). Regarding HPLC, columns packed with silver ions have been employed, since their presence in the stationary phase promote the selective retention of unsaturated compounds (Macher, 2001). In addition, a non-aqueous RP-HPLC with mobile phase systems of low polarity, where TAG are separated according to the equivalent carbon number (ECN), have been also used (Jakab, 2002; Fauconnot, 2004). On the other hand, a satisfactory selectivity and high peak capacities have been achieved by using comprehensive two-dimensional chromatography (2D-

HPLC), based on the combination of a C18 column and a second column load with silver ions (Dugo, 2006; van der Klift, 2008). Also, 2D-HPLC using a single column has been done by simply altering the mobile phase between acetonitrile (ACN) and methanol (MeOH), which exhibited a higher selectivity for the separation of TAGs in vegetable oils with high efficiency and rapid speed (Wei, 2015).

The official method of TAG analysis involves the use of an HPLC coupled with a refractive index (RI) (Parcerisa, 1995). However, RI detectors are not suitable for gradient elution due to insufficient dynamic range and extended waiting periods to allow for thermal equilibration of the flow cells (Wade, 2013). As alternative, other detectors as UV (Lerma-García, 2011) or mass spectrometry (MS) (Nagy, 2005; Ruiz-Samblás, 2011) have been employed. Nevertheless, UV detection offers a low sensitivity for saturated TAG (Gutiérrez, 1999; Dag, 2011). For this reason, some reports have described the use of evaporative light scattering detector (ELSD) to analyze TAGs (Baccouri, 2007; Rombaut, 2009). ELSD is a mass-sensitive detector that responds to any analyte less volatile than the mobile phase, compatible with a broad range of solvent, and its signal is independent of the chain length unsaturation degree. Thus, it has been successfully used for many researches in the separation of TAGs. In this thesis TAGs profiles have been employed for discrimination of different edible oils and EVOO cultivars (**Chapters 14 and 17**).

1.5.2. Determination of fatty acids

According to the official method, fatty acids are commonly determined by gas chromatography (GC) coupled to flame ionization detector (FID) after conversion of fatty methyl esters (FAMEs), calculating their composition as percentage of the total fatty acids for olive fruit and olive oil (Commission Regulation (EC) Nº 2568/91; León, 2004; Aydyn, 2009;

Lerma-García, 2009; de la Rosa, 2013). Moreover, GC coupled with MS has been used (Yang, 2013; Boggia, 2014). However, underivatized fatty acids have been determined by using capillary zone electrophoresis (CZE) (Sato, 2014) and direct infusion MS (Lerma-García, 2007). In the latter case, instantaneous information about the composition of a given sample, without any previous sample treatment or chromatographic separation is obtained.

1.5.3. Determination of sterols

As indicated in **Section 1.4**, sterols are present in the unsaponifiable fraction. These compounds are isolated from the oil matrix by TLC on silica gel plates (Commission Regulation (EC) Nº 2568/91). Then, sterol identification and quantification have been carried out using GC coupled with different detectors such as FID (Ranalli, 2002; Matos, 2007; Chehade 2016) and MS (Cunha, 2006; Cercaci 2007). However, GC requires thermally stable columns and chemical derivatization prior to analysis. For this reason, alternative methods have been described based on the use of HPLC-MS (Cañabate-Díaz, 2007; Segura-Carretero, 2008) and capillary electrochromatography (CEC) (Abidi, 2004; Lerma-García, 2008).

1.5.4. Determination of proteins

The determination of proteins from olive fruits and leaves implies a tedious extraction, which is a critical step in the extraction methodology. Several procedures involve the use of aqueous solutions containing detergents, such as sodium dodecyl sulfate (SDS), and reducing agents (mercaptoethanol), or trichloroacetic acid (TCA)/acetone combined to methanol washes to remove the interferences followed by protein extraction with a phenol solution equilibrated with 10 mM tris(hydroxymethyl)aminomethane (Tris) HCl (Wang, 2001; Alché, 2006;

Wang, 2007; Wang, 2008; Esteve, 2011). Regarding olive oil protein extraction, several procedures have been based on precipitation of proteins with acetone (Hidalgo, 2001) or acetone-hexane (Martin-Hernández, 2008). The quantification of the total amount of proteins has been conducted using different methods as Kjeldahl, Lowry or Bradford. In order to characterize the extracted protein fraction, 1D- and 2D-polyacrylamide gel electrophoresis (PAGE) have been widely used. Nevertheless, other techniques have been also employed for protein detection from olive fruit and oils, as CE (Montealegre, 2012) and ultra performance HPLC (Esteve, 2010; Esteve 2011).

1.6. Genetic varieties

Currently, there are more than 1500 olive varieties around the world (Bartolini, 1998). This enormous genetic diversity has attracted much attention in the last decade. The consumption of olive oils has increased due to their excellent organoleptic and nutritional properties. Besides, an increase in the extra virgin olive oil (EVOO) consumption has been observed in the last decades. For this reason, more EVOOs are being produced.

The composition of these EVOOs varies depending on the genetic variety of the olives employed for their production (Tura, 2007; Baccouri, 2008). As shown in **Figure 1.2**, the main Spanish genetic varieties of olives (*ca.* 95% of produced olives) are: Arbequina, Hojiblanca and Picual, although the number of other varieties grown in Spain is also high and very diverse, depending on the geographic region where the crop is located. Many of the olives employed in this thesis arise from Castellón (Canetera and Serrana), Alicante (Blanqueta and Gordal) and Córdoba (Arbequina, Frantoio, Hojiblanca and Picual).

Other genetic varieties of particular interest in the development of this thesis are those grown in Tunisia, which occupies the second position after European Union as olive oil manufacturer. There are some reports that have studied the composition of oils coming from the most important cultivars (Chétoui and Chemlali) (Baccouri, 2007; Baccouri, 2008; Jabeur, 2014) (**Figure 1.3**). However, there is a lack of information related to the minor cultivars, which can provide a better oil quality (higher phenolic content, better organoleptic properties, etc.). For this reason, in this thesis some Tunisian minor cultivars, such as Chemchali, Chemlali, Dhokar, Fouji, Jemri, Zalmati and Zarrazi, have been studied.

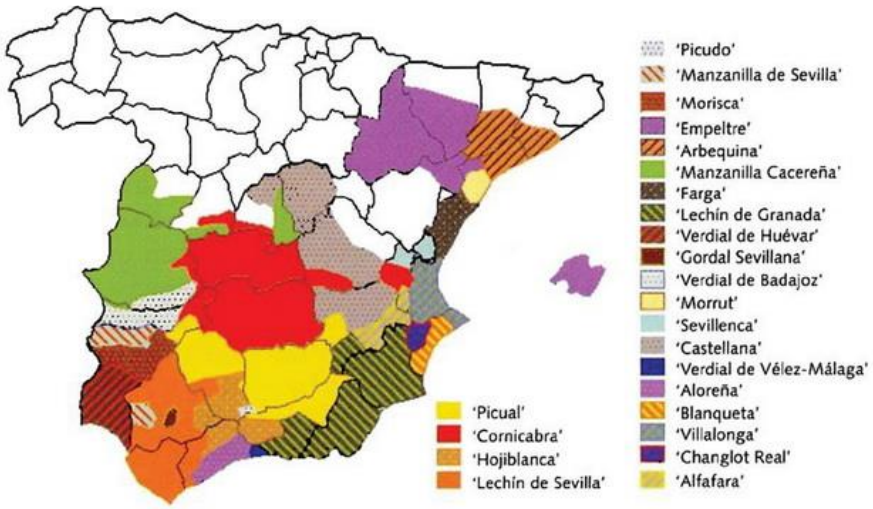

Figure 1.2. Geographical distribution of Spanish genetic varieties of EVOO.

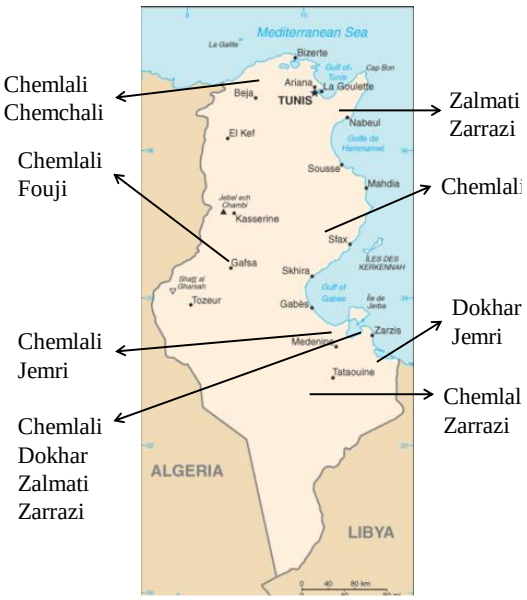

Figure 1.3. Geographical distribution of Tunisianan olive varieties (ONH, 2015).

1.7. Olive fruit and oil authenticity

Olive fruit and oil authenticity involves not only the detection of possible adulterations but also the determination of its genuineness mainly in terms of geographical origin and botanical or genetic variety (García-Gonzalez, 2010). In the last years, the authenticity and traceability of olive fruits and oils has been the object of numerous studies. For this purpose, HPLC and GC techniques have usually been employed since they offer the possibility for reliable and rapid separation and also quantitative determination of major and minor compounds (Nollet 2003; Cserháti, 2005). Also, spectroscopic approaches associated with multivariate analysis have been used to detect adulteration of virgin olive oil. Among these spectroscopic methods are vibrational techniques such as near-infrared spectroscopy (NIR) (Christy, 2004), Fourier transform infrared (FT-IR) (Lerma-García, 2010) and Fourier transform Raman (FT-Raman)

(Ozen, 2002), and nuclear magnetic resonance (NMR) spectroscopies (Alonso-Salces, 2010).

With regard to major components of olive oil, fatty acid profiles have been used as a fingerprint of genetic variety of olive oils (D'Imperio, 2007; Lerma-García, 2009). In another study, TAG profiles have been examined by HPLC-UV (Lerma-García, 2011) or HPLC-ELSD (Baccouri, 2007) in order to discriminate oils according to their botanical origin.

Amongst the minor compounds, volatile compounds have been determined by GC-FID (Koprivnjak, 2005) or GC-MS (Nagy, 2005) in order to distinguish between refined and crude olive oil. Phenolic fraction has been also subjected to MS analysis to predict the genetic variety of Spanish EVVOs (Lerma-García, 2008A). Furthermore, Farrés-Cebrián *et al* (Farrés-Cebrián, 2016) have obtained HPLC-UV polyphenolic profiles to classify olive oils according to their botanical and genetic origin. In addition, tocopherols have also been employed to detect olive oil adulteration with low-cost edible oils (Cerretani, 2010). Additionally, free sterol profiles have been used to discriminate oils according to their botanical origin (Vichi, 2001; Lerma-García, 2008B).

As regard other minor compounds, proteins from olive fruits have been employed to discriminate olive oil varieties (Esteve, 2010; Esteve 2011) and raw and table olives samples (Montealegre, 2010). Besides, Martins-Lopes' group has used DNA-based markers to establish a relationship between small-scale-produced monovarietal and commercial olive oil samples for certification purposes (Martins-Lopes, 2008).

1.8. References

Abidi, S.L. (**2004**). Capillary electrochromatography of sterols and related steryl esters derived from vegetable oils. *Journal of Chromatography A, 1059*, 199-208.

Alché, J.D.; Jiménez-López, J.C.; Wang, W.; Castro-López, A.J.; Rodríguez-García, M.I. (**2006**). Biochemical characterization and cellular localization of 11S type storage proteins in olive (*Olea europaea L.*) seeds. *Journal of Agriculture and Food Chemistry, 54*, 5562-5570.

Alonso-Salces, R.M.; Héberger, K.; Holland, M.V.; Moreno-Rojas, J.M.; Mariani, C.; Bellan, G.; Reniero, F.; Guillou, C. (**2010**). Multivariate analysis of NMR fingerprints of the unsaponifiable fraction of virgin olive oils for authentification purposes. *Food Chemistry, 118*, 956-965.

Al-Qarawi, A.A.; Al-Damegh, M.A.; ElMougy, S.A. (2002) Effect of freeze dried extract of *Olea europaea* on the pituitary-thyroid axis in rats. *Phytotherapy Research, 16*, 286-287.

Aydin, C.; Musa Özcan, M.; Gümüş, T. (**2009**). Nutritional and technological characteristics of olive (*Olea europea L.*) fruit and oil: two varieties growing in two different locations of Turkey. *International Journal of Food Sciences and Nutrition, 60*, 365-373.

Baccouri, O.; Cerretani, L.; Bendini, A.; Caboni, M.F.; Zarrouk, M.; Pirrone, L.; Daoud Ben Miled, D. (**2007**). Preliminary chemical characterization of Tunisian monovarietal virgin olive oils and comparison with Sicilian ones. European *Journal of Lipid Science and Technology, 109*, 1208-1217.

Baccouri, O.; Guerfel, M.; Baccouri, B.; Cerretani, L.; Bendini, A.; Lercker, G.; Zarrouk, M.; Daoud Ben Miled, D. (**2008**). Chemical

composition and oxidative stability of Tunisian monovarietal virgin olive oils with regard to fruit ripening. *Food Chemistry, 109*, 743-754.

Bartolini, G.; Prevost, G.; Messeri, C.; Carignani, C.; Menini, U.G.(**1998**). Olive germplasm: cultivars and world-wide collections. Rome, Italy: FAO.

Bianchi, G. (**2003**). Lipids and phenols in table olives. *European Journal of Lipid Science and Technology, 105,* 229-242.

Boggia, R.; Borgogni, C.; Hysenaj, V.; Leardi, R.; Zunin, P. (**2014**). Direct GC-(EI) MS determination of fatty acid alkyl esters in olive oils. *Talanta, 119*, 60-67.

Boskou, D. (**1996**). Olive oil, chemistry and technology. AOCS Press, Champaign, IL, USA.

Boskou, D. (**2002**). Olive Oil, in Gunstone, F.D. Vegetable oils in food technology. CRC Press, Blackwell Publishing Ltd., Oxford, UK pp. 244-277.

Briante, R.; Patumi, M.; Terenziani, S.; Bismuto, E.; Febbraio, F.; Nucci, R. (**2002**). *Olea europaea L*. leaf extract and derivatives: antioxidant properties. *Journal of Agriculture and Food Chemistry 50*, 4934-40.

Cabañate-Díaz, B.; Segura-Carretero, A.; Fernández-Gutiérrez, A.; Belmonte-Vega, A.; Garrido-Frenich, A.; Martínez-Vidal, J.L.; Duran-Martos, J. (**2007**). Separation and determination of sterols in olive oil by HPLC-MS. *Food Chemistry, 102*, 593-598.

Cercaci, L.; Passalacqua, G.; Poerio, A.; Rodriguez-Estrada, M.T.; Lercker, G. (**2007**). Composition of total sterols (4-desmethyl-sterols) in extravirgin olive oils obtained with different extraction technologies and their influence on the oil oxidative stability. *Food Chemistry, 102*, 66-76.

Cerretani, L.; Lerma-García, M.J.; Herrero-Martínez, J.M.; Gallina-Toschi, T.; Simó-Alfonso, E.F. (**2010**). Determination of tocopherols and tocotrienols in vegetable oils by nanoliquid chromatography with ultraviolet-visible detection using a silica monolithic column. *Journal of Agriculture and Food Chemistry, 58*, 757-761.

Chehade, A.; Bitar, A.E.; Kadri, A.; Choueiri, E.; Nabbout, R.; Youssef, H.; Smeha, M.; Awada, A.; Chami, Z.A.; Dubla, E.; Trani, A.; Mondelli, D.; Famiani, F. (**2016**). In situ evaluation of the fruit and oil characteristics of the main Lebanese olive germplasm. *Journal of the Science of Food and Agriculture, 96*, 2532-2538.

Christie, W.W. (**1992**). Advances in lipid methodology. The Oily Press, Ayr, UK, 239-271.

Christy, A.A.; Kasemsumran, S.; Du, Y.; Ozaki, Y. (2004). The detection and quantification of adulteration in olive oil by near-infrared spectroscopy and chemometrics. *Analytical Science, 20*, 935-940.

Commission Regulation (EEC). (**1991**). No 2568/91 of 11 July 1991 on the characteristics of olive oil and olive-residue oil and on the relevant methods of analysis, Off. J. Eur. Union L128.

Conor, D.J.; Fereres, E. (**2005**). The physiology of adaptation and yield expression in olive. *Horticultural reviews, 31*, 155-229.

Corpas, F.J.; Fernández-Ocaña, A.; Carreras, A.; Valderrama, R.; Luque, F.; Esteban, F.J; Rodríguez-Serrano, M.; Chaki, M.; Pedrajas, J.R.; Sandalio, L.M.; Del Río, L.A.; Barroso, J.B. (**2006**). The expression of different superoxide dismutase forms is Ccell-type dependent in olive (*Olea europaea L.)* leaves. *Plant and Cell Physiology, 47*, 984-994.

Cserháti, T.; Forgács, E.; Deyl, Z.; Miksik, I. (**2005**). Chromatography in authenticity and trace ability tests of vegetable oils and dairy products: a review. *Journal Biomedical Chromatography, 19*, 183-90.

Cunha, S.C.; Oliveira, M.B.P.P. (**2006**). Discrimination of vegetable oils by triacylglycerols evaluation of profile using HPLC/ELSD. *Food Chemistry, 95,* 518-524.

D 'Imperio, M.; Dugo, G.; Alfa, M.; Mannina, L.; Segre, A. L. (**2007**). Statistical analysis on Sicilian olive oils. *Food Chemistry*. 102, 956-965.

Dag, A.; Kerem, Z.; Yogev, N.; Zipori, I.; Lavee, S.; Ben-David, E. (**2011**). Influence of time of harvest and maturity index on olive oil yield and quality. *Scientia Horticulturae, 127,* 358-366.

De la Rosa, R.; Talhaoui, N.; Rouis, H.; Velasco, L.; León, L. (**2013**). Fruit characteristics and fatty acid composition in advanced olive breeding selections along the ripening period. *Food Research International, 54,* 1890-1896.

De Leonardis, A.; Aretini, A.; Alfano, G.; Macciola, V.; Ranalli, G. (**2008**). Isolation of a hydroxytyrosol-rich extract from olive leaves (*Olea Europaea L.)* and evaluation of its antioxidant properties and bioactivity. *European Food Research and Technology, 226,* 653-659.

Dietz, K.J.; Sauter, A.; Wichert, K.; Messdaghi, D.; Hartung, W. (**2000**). Extracellular β-glucosidase activity in barley involved in the hydrolysis of ABA glucose conjugate in leaves. *Journal of Experimental Botany 51,* 937-944.

Dugo, P.; Kumm, T., Crupi, M.L.; Cotroneo, A.; Mondello, L. (**2006**). Comprehensive two-dimensional liquid chromatography combined with mass spectrometric detection in the analyses of triacylglycerols in natural lipidic matrixes. *Journal of Chromatography A, 1112,* 269-275.

Esteve, C.; Cañas, B.; Moreno-Gordaliza, E.; Del Río, C.; García, M.C.; Marina, M.L. (**2011**). Identification of Olive (*Olea europaea*) pulp proteins by matrix-assisted laser desorption/ionization time-of-flight mass spectrometry and nano-liquid chromatography tandem mass

spectrometry. *Journal of Agriculture and Food Chemistry, 59*, 12093-12101.

Esteve, C.; Del Río, C.; Marina, M.L.; García, M.C. (**2010**). First ultraperformance liquid chromatography based strategy for profiling intact proteins in complex matrices: application to the evaluation of the performance of olive (*Olea europaea L.)* stone proteins for cultivar fingerprinting. *Journal of Agriculture and Food Chemistry, 58*, 8176-8182.

Farrés-Cebrián, M.; Seró, R.; Saurina, J.; Nuñéz. (**2016**). HPLC-UV polyphenolic profiles in the classification of olive oils and other vegetable oils via principal component analysis. *Separations, 3,* 33-46.

Fauconnot, L.; Hau, J.; Aeschlimann, J.M.; Fay, L.B.; Dionisi, F. (**2004**). Quantitative analysis of triacylglycerol regioisomers in fats and oils using reversed-phase high-performance liquid chromatography and atmospheric pressure chemical ionization mass spectrometry. *Rapid Communications in Mass Spectrometry, 18*, 218-222.

Fedeli, E. (**1977**). Lipids of olives, in Ralph, E; Holman, T. Progress on chemistry of fats and other lipids. Pergamon Press, Paris, France pp. 15-74.

García-González, D.; Aparicio, R. (**2010**). Coupling MOS sensors and gas chromatography to interpret the sensor responses to complex food aroma: application to virgin olive oil. *Food Chemistry, 120*, 572-579.

Ghanbari, R.; Anwar, F.; Alkharfy, K.M.; Gilani, A.H.; Saari, N. (**2012**). Valuable nutrients and functional bioactives in different parts of olive (*Olea europaea L.*). A Review. *International Journal of Molecular Sciences, 13*, 3291-3340.

Gutiérrez, F.; Jiménez, B.; Ruiz, A.; Albi, M.A. (**1999**). Effect of olive ripeness on the oxidative stability of virgin olive oil extracted from the

varieties Picual and Hojiblanca and on the different components involved. *Journal of Agricultural and Food Chemistry, 47*, 121-127.

Hidalgo, F.J.; Alaiz, M.; Zamora, R. (**2001**). Determination of peptides and proteins in fats and oils. *Analytical Chemistry, 73*, 698–702.

Holčapek, M.; Lísa, M.; Jandera, P.; Kabátová, N. (**2005**). Quantitation of triacylglycerols in plant oils using HPLC with APCI-MS, evaporative light-scattering, and UV detection. *Journal of Separation Science, 28*, 1315-1333.

Huang, A.H.C. (**1992**). Oil bodies and oleosins in seeds. *Annual Review of Plant Physiology and Plant Molecular Biology, 43*, 177-200.

Jabeur, H.; Zribi, A.; Makni, J.; Rebai, A.; Abdelhedi, R.; Bouaziz, M. (**2014**). Detection of Chemlali Extra-Virgin Olive Oil adulteration mixed with soybean oil, corn oil, and sunflower oil by using GC and HPLC. *Journal of Agricultural and Food Chemistry, 62*, 4893-4904.

Jakab, A.; Héberger, K.; Forgács, E. (**2002**). Comparative analysis of different plant oils by high-performance liquid chromatography-atmospheric pressure chemical ionization mass spectrometry. *Journal of Chromatography A, 976*, 255-63.

Kiosseoglou, B.; Vlachopoulou, I.; Boskou, D. (**1987**). Esterified 4-monomethyl- and 4,4-dimethyl-sterols in some vegetable oils. *Grasas y Aceites, 38*, 102-103.

Kiritsakis, A.; Christie, W.W. (**2003**). Análisis de aceites comestibles, in Aparicio, R.;Hardwood, J. Manual del aceite de oliva. Ed. Mundi-Prensa, Madrid, Spain, 135-162.

Koprivnjak, O.; Moret, S.; Populin, T.; Lagazio, C.; Conte, L.S. (**2005**). Variety differentiation of virgin olive oil based on n-alkane profile. *Food Chemistry, 90*, 603-608.

Koudounas, K.; Banilas, G.; Michaelidis, C.; Demoliou, C.; Rigas, S.; Hatzopoulos, P. (**2015**). A defence-related Olea europaea β-glucosidase hydrolyses and activates oleuropein into a potent protein cross-linking agent. *Journal of Experimental Botany*, *66*, 2093-2106.

Lee, K.H.; Piao, H.L.; Kim, H.Y.; Choi, S.M.; Jiang, F.; Hartung, W.; Hwang, I.; Kwak, J.M.; Lee, I.J.; Hwang, I. (**2006**). Activation of glucosidase via stress induced polymerization rapidly increases active pools of abscisic acid. *Cell*, *126*, 1109-1120.

León, L.; Uceda, M.; Jiménez, A.; Martín, L.; M.; Rallo, L. (**2004**). Variability of fatty acid composition in olive (*Olea europaea L.)* progenies. *Spanish Journal of Agricultural Research*, *2*, 353-359.

Lerma-García, M.J.; Simó-Alfonso, E.F.; Bendini, A.; Cerretani, L. (**2009**). Rapid evaluation of oxidized fatty acid concentration in virgin olive oils using metal oxide semiconductor sensors and multiple linear regression. *Journal of Agricultural and Food Chemistry*, *57*, 9365-9369.

Lerma-García, M.J.; Lusardi, R.; Chiavaro, E.; Cerretani, L.; Bendini, A.; Ramis-Ramos, G.; Simó-Alfonso, E.F. (**2011**). Use of triacylglycerol profiles established by high performance liquid chromatography with ultraviolet-visible detection to predict the botanical origin of vegetable oils. *Journal of Chromatography A*, *42*, 7521-7527.

Lerma-García, M.J.; Ramis-Ramos, G.; Herrero-Martínez, J.M.; Simó-Alfonso, E.F. (**2007**). Classification of vegetable oils according to their botanical origin using amino acid profiles established by direct infusion mass spectrometry. *Rapid Communications in Mass Spectrometry*, *21*, 3751-3755.

Lerma-García, M.J.; Ramis-Ramos, G.; Herrero-Martínez, J.M.; Simó-Alfonso, E.F. (**2008A**). Prediction of the genetic variety of Spanish extra virgin olive oils using fatty acid and phenolic compound profiles

established by direct infusion mass spectrometry. *Food Chemistry, 108*, 1142–1148.

Lerma-García, M.J.; Ramis-Ramos, G.; Herrero-Martínez, J.M.; Simó-Alfonso, E.F. (**2008B**). Classification of vegetable oils according to their botanical origin using sterol profiles established by direct infusion mass spectrometry. *Rapid Communications in Mass Spectrometry, 22*, 973-978

Lerma-García, M.J.; Ramis-Ramos, G.; Herrero-Martínez, J.M.; Simó-Alfonso, E.F. (**2010**). Authentication of extra virgin olive oils by Fourier-transform infrared spectroscopy. *Food chemistry, 118*, 78-83.

Macher, M.B.; Holmqvist, A. (**2001**). Triacylglycerol analysis of partially hydrogenated vegetable oils by silver ion HPLC. *Journal of Separation Science, 24*, 179-185.

Malheiro, R.; Mendes, P.; Fernandes, F.; Rodrigues, N.; Bento, A.; Pereira, J.A. (**2014**). Bioactivity and phenolic composition from natural fermented table olives. *Food Function, 5*, 3132-3142.

Manai, H.; Mahjoub-Haddada, F.; Oueslati, I.; Daoud, D.; Zarrouk, M. (**2008**). Characterization of monovarietal virgin olive oils from six crossing varieties. *Scientia Horticulturae, 115*, 252-260.

Mariani, C.; Fedeli, E.; Morchio, G.(**1987**). Absolute erythrodiol content as a possibility to detect olive husk oil in olive oil. *Rivista Italiana Delle Sostanze Grasse 64*, 359-363.

Martín-Hernández, C.; Bénet, S.; Obert, L. (**2008**). Determination of proteins in refined and nonrefined oils. *Journal of Agricultural and Food Chemistry. 56*, 4348-4351.

Martins-Lopes, P.; Gomes, S.; Santos, E.; Guedes-Pinto, H. (**2008**). DNA markers for Portuguese olive oil fingerprinting. *Journal of Agricultural and Food Chemistry, 56*, 11786–11791.

Matos, L.C.; Cunha, S.C.; Amaral, J.S.; Pereira, J.A.; Andrade, P.B.; Seabra, R.M.; Oliveira, B. (**2007**). Chemometric characterization of three varietal olive oils (cvs. Cobrancosa, Madural and Verdeal Transmontana) extracted from olives with different maturation indices. *Food Chemistry*, *102*, 406-414.

Montealegre, C.; García, M.C.; Del Río, C.; Marina M.L.; García-Ruiz, C. (**2012**). Separation of olive proteins by capillary gel electrophoresis. *Talanta*, *97*, 420-424.

Montealegre, C.; Marina, M.L.; García-Ruiz, C. (**2010**). Separation of olive proteins combining a simple extraction method and a selective CE approach. Application to raw and table olive samples. *Journal of Agricultural and Food Chemistry, 58*, 11808-11813.

Nagy, K.; Bongiorno, D.; Avellone, G.; Agozzino, P.; Ceraulo, L.; Vékey, K. (**2005**). High performance liquid chromatography-mass spectrometry based chemometric characterisation of olive oils. *Journal of Chromatography A, 1078*, 90-97.

Nollet, L.M.L. (**2003**). High-pressure liquid chromatography (HPLC) in food authentication. In: Lees M, editor. Food authenticity and traceability. Boca Raton, Florida: CRC Press. 218-238

Ofiice Nationale de l'Huile (ONH). Available on the website: www.internationaloliveoil.org/estaticos/view/136-contry-profiles. Accessed May 22,2015.

Ortega-García, F.; Blanco, S.; Peinado, M.A.; Peragón, J. (**2008**). Polyphenol oxidase and its relationship with oleuropein concentration in

fruits and leaves of olive (*Olea europaea*) cv. 'Picual' trees during fruit ripening. *Tree Physiology, 28*, 45-54.

Ouni, Y.; Guido, F.; Daoud, D.; Zarrouk, M. (**2011**). Effect of cultivar on minor components in Tunisia olive fruits cultivated in microclimate. *Journal of Horticulture and Forestry, 3*, 13-20.

Owen, R.W.; Giacosa, A.; Hull, W.E.; Haubner, R.; Spiegelhalder, B.; Bartsch, H. (**2000**). The antioxidant/anticancer potential of phenolic compounds isolated from olive oil. *European Journal of Cancer, 36*, 1235-1247.

Ozen, B.F.; Mauer, L.J. (**2002**). Detection of hazelnut oil adulteration using FT-IR spectroscopy. *Journal of Agricultural and Food Chemistry, 50*, 3898-3901.

Paganuzzi, V. (**1982**) Use of argentation-TLC [thin layer chromatography] in olive oil triterpene alcohol analysis. 2: Virgin oils and raw husk oils. *Rivista Italiana Delle Sostanze Grasse*, 59 415-421.

Parcerisa, J.; Boatella, J.; Codony, R.; Rafecas, M.; Castellote, A. I.; García, J.; López, A.; Romero, A. (**1995)**. Comparison of fatty acid and triacylglycerol compositions of different hazelnut varieties (*Corylus avellana L.)* cultivated in Catalonia (Spain). *Journal of Agriculture and Food Chemistry, 43*, 13-16.

Pereira, A.P.; Ferreira, I.C.F.R.; Marcelino, F.; Valentão, P.; Andrare, P.B.; Seabra, R.; Estevinho, L.; Bento, A.; Pereira, J.A. (**2007**). Phenolic compounds and antimicrobial activity of olive *(Olea europaea L. Cv. Cobrançosa)* leaves. *Molecules, 12*, 1153-1162.

Quintero-Flórez, A.; Sinausia Nieva, L.; Sánchez-Ortíz, A.; Beltrán, G.; Perona J.S. (**2015**). The fatty acid composition of virgin olive oil from different cultivars is determinant for foam cell formation by

macrophages. *Journal of Agriculture and Food Chemistry, 63*, 6731-6738.

Ranalli, A.; Pollastri, L.; Contento, S.; Di Loreto, G.; Lannucci, E.; Lucera, L.; Russi, F. (**2002**). Acylglycerol and fatty acid components of pulp, seed, and whole olive fruit oils. Their use to characterize fruit variety by chemometrics. *Journal of Agriculture and Food Chemistry, 50*, 3775-3779.

Rodríguez, G.; Lama, A.; Rodríguez, R.; Jiménez, A.; Guillén, R.; Fernández-Bolaños, J. (**2008**). Olive stone an attractive source of bioactive and valuable compounds. *Bioresource Technology, 99*, 5261-5269.

Rombaut, R.; De Clercq, N.; Foubert, I.; Dewettinck, K. (**2009**). Triacylglycerol analysis of fats and oils by evaporative light scattering detection. *Journal of the American Oil Chemists' Society, 86*, 19-25.

Ross, J.H.E.; Sanchez, J.; Millan, F.; Murphy, D.J. (**1993**). Differential presence of oleosins in oleogenic seed and mesocarp tissues in olive (*Olea europaea*) and avocado (*Persea americana*). *Plant Science, 93*, 203-210.

Ruiz-Samblás, C.; Cuadros-Rodríguez, L.; González-Casado, A.; Rodríguez García, F.P.; De la Mata-Espinosa, P.; Bosque-Sendra, J.M. (**2011**). Multivariate analysis of HT/GC-(IT) MS chromatographic profiles of triacylglycerol for classification of olive oil varieties. *Analytical and Bioanalytical Chemistry, 399*, 2093-2103.

Salas, J.J.; Williams, M.; Harwood, J.L.; Sánchez, J. (**1999**). Lipoxygenase activity in olive (*Olea europaea*) fruit. *Journal of the American Oil Chemists' Society, 76*, 1163-1168.

Sato, R.; Coelho, T.; Castro, R.J.; De Castro Barra, P.M.; De Oliveira, M.A.L. (**2014**). Rapid separation of free Fatty acids in vegetable oils by capillary zone electrophoresis. *Phytochemical Analysis, 25*, 241-246.

Sedef, N.E.; Karakaya, S. (**2009**). Olive tree (*Olea europaea*) leaves: potential beneficial effects on human health. *Nutrition Reviews, 67*, 632-638.

Segura-Carretero, A.; Carrasco-Pancorbo, A.; Cortacero, S.; Gori, A.; Cerretani, L.; Fernández-Gutíerrez, A. (**2008**). A simplified method for HPLC-MS analysis of sterols in vegetable oil. *European Journal of Lipid Science and Technology, 110*, 1142-1149.

Silva, S.; Gomes, L.; Leitão, F.; Coelho, A.V.; Vilas-Boas, L. (**2006**). Phenolic compounds and antioxidant activity of *Olea europaea L*. fruits and leaves. *Food Science and Technology International, 12*, 385-396.

Soler-Rivas, C.; Espin, I.C.; Wichers, I. (**2000**). An easy and fast to compare total free radical scavenger capacity of food studies. *Phytochemical Analysis, 11*, 330-338.

Somova, L.I.; Shode, F.O.; Ramnanan P.; Nadar, A. (**2003**). Antihypertensive, antiatherosclerotic and antioxidant activity of triterpenoids isolated from *Olea europaea*, subspecies *africana* leaves. *Journal of Ethnopharmacology, 84*, 299-305.

Soni, M.G.; Burdock G.A.; Christian, M.S.; Bitler, C.M.; Crea, R. (**2006**). Safety assessment of aqueous olive pulp extract as an antioxidant or antimicrobial agent in foods. *Food and Chemical Toxicology, 44,* 903–915.

Sudjana, A.N.; D'Orazio, C.; Ryan, V.; Rasool, N.; Ng, J.; Islam, N.; Riley, T.V.; Hammer, K.A. (**2009**). Antimicrobial activity of commercial Olea europaea (olive) leaf extract. *International Journal of Antimicrobial Agents, 33*, 461-463.

Tura, D.; Gigliotti, C.; Pedo, S.; Failla, O.; Bassi, D.; Serraiocco, A. (**2007**). Influence of cultivar and site of cultivation on levels of lipophilic and hydrophilic antioxidants in virgin olive oils (*Olea Europea L.)* and correlations with oxidative stability. *Scientia Horticulturae, 112*, 108-119.

Van der Klift, E.J.C.; Vivó-Truyols, G.; Claassen, F.W.; van Holthoon, F.L.; van Beek, T. A. (**2008**). Comprehensive two-dimensional liquid chromatography with ultraviolet, evaporative light scattering and mass spectrometric detection of triacylglycerols in corn oil. *Journal of Chromatography A, 1178*, 43-55.

Vichi, S.; Pizzale, L.; Toffano, E.; Bortolomeazzi, R.; Conte, L. (**2001**). Detection of hazelnut oil in virgin olive oil by assessment of free sterols and triacylglycerols. *Journal of AOAC International, 84*, 1534-1542.

Vlahov, G.; Schiavone, C.; Simone, N. (**1999**). Triacylglycerols of the olive fruit (*Olea europaea L.):* characterization of mesocarp and seed triacylglycerols in different cultivars by liquid chromatography and ^{13}C NMR spectroscopy. *European Journal of Lipid Science and Technology, 101*, 146-150.

Wade, J.H.; Bailey, R. (**2014**). Refractive index-based detection of gradient elution liquid chromatography using chip-integrated microring resonator arrays *Analytical Chemistry, 86*, 913-919.

Wang, W.; Alché, J.D.; Castro, A.J.; Rodríguez-García, M.I. (**2001**). Characterization of seed storage proteins and their synthesis during seed development in Olea europaea. *International Journal of Developmental Biology, 45*, 63-64.

Wang, W.; Alché, J.D.; Rodríguez-García, M.I. (**2007**). Characterization of olive seed storage proteins. *Acta Physiologiae Plantarum, 29*, 439-444.

Wang, W.; Scali, M.; Vignani, R.; Spadafora, A.; Sensi, E.; Mazzuca, S.; Cresti, M. (**2003**). Protein extraction for two-dimensional electrophoresis from olive leaf, a plant tissue containing high levels of interfering compounds. *Electrophoresis, 24*, 2369-2375.

Wang, W.; Tai, F.; Chen, S. (**2008**). Optimizing protein extraction from plant tissues for enhanced proteomics analysis. *Journal of Separation Science, 31*, 2032-2039.

Wei, F.; Hu, N.; Lv, X.; Dong, X.Y.; Chen, H. (**2015**). Quantitation of triacylglycerols in edible oils by off-linecomprehensive two-dimensional liquid chromatography–atmospheric pressure chemical ionization mass spectrometry using a single column. *Journal of Chromatography A, 1404*, 60-71.

Yang, Y.; Ferro, M.D.; Cavaco, I.; Liang, Y. (**2013**). Detection and identification of extra virgin olive oil adulteration by GC-MS combined with chemometrics. *Journal of Agriculture and Food Chemistry, 61*, 3693-3702.

Zamora, R.; Alaiz, M.; Hidalgo, F.J. (**2001**). Influence of cultivar and fruit ripening on olive (*Olea europaea*) fruit protein content, composition, and antioxidant activity. *Journal of Agriculture and Food Chemistry, 49*, 4267-4270.

Chapter 2. Orange and tangerine fruits (*Citrus sinensis and tangerine*)

2.1. Introduction

Citrus fruits belong to the *Rutaceae* family, in which several major cultivated species can be found, such as sweet orange (*Citrus sinensis*), tangerine (*Citrus tangerine*), lemon *(Citrus limon*) and grapefruit *(Citrus paradisi*), among others. In 2014, the global production of *Citrus* fruits was 121.3 million tons (FAO, 2015), being Spain one of world's leading *Citrus* fruit-producing countries. Concretely, Comunidad Valenciana is the main Spanish *Citrus* producer (60% of Spanish total production) with a great variety of *Citrus* cultivars, mainly oranges (*Citrus sinensis*) and tangerines (*Citrus tangerine*) (Xu, 2013). There are available a high number of genetical varieties of both oranges and tangerines. As regard oranges, the most cultivated species are Navelina, Salustiana, Sanguinelli and Navel. In the case of tangerines, Clemenrubí, Oronules or Nadorcott are the most expended.

Consumption of *Citrus* fruits has been found to be beneficial in preventing coronary diseases and chronic asthma, and its extracts show anti-inflammatory, antitumor and antifungal inhibition activities (Abeysinghe, 2007; Carballo, 2014). The *Citrus* benefits are due to the presence of some compounds such as certain types of phenols, vitamin C, vitamin A and other compounds such as vitamin E and selenium (Carballo, 2014; Jandríc, 2017; Rafiq, 2015).

Morphologically, the *Citrus* fruit is composed of three parts: epicarp (flavedo), mesocarp (albedo) and endocarp (pulp). Generally, *Citrus* peels, which are the primary waste, are subdivided into the epicarp (coloured peripheral surface) and mesocarp (white soft middle layer), while endocarp is commonly employed to obtain *Citrus* fruit extracts as shown in **Figure 2.1.**

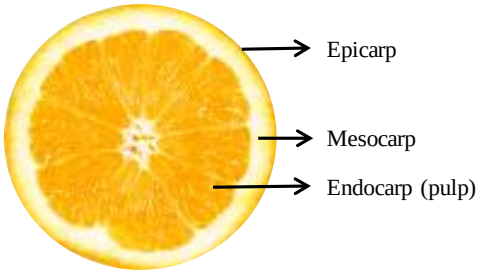

Figure 2.1. Scheme of *Citrus* fruit.

As regard the epicarp, it is the major source of various bioactive compounds such as phenolics, carotenoids, flavonoids and ascorbic acid, among others. These bioactive compounds can be used as natural antioxidants (Kato, 2004; Khan, 2010; Serra, 2013).

Then, the mesocarp or albedo is considered an important source of pectins (Lliso, 2007) and flavonoids (Sun, 2010). In fact, these compounds represent a total of 21% of the peel weight (Ververis, 2007). As regard pectins, it is well-known their important role as a dietary fibre product, whose consumption have proved to be useful in threatening chronic diseases such as gastrointestinal disorders, obesity and diabetes (Rafiq, 2015). The thickness of the albedo varies with the species. For example, mandarins generally have very thin albedo while the one in citrons is very thick. Both flavedo and albedo form the non-edible part of the fruit called the pericarp, and they are commonly known as the rind or peel.

Finally, the endocarp or pulp, which is formed by large juice sacs, accumulates high amounts of some organic acids such as tartaric, malic, ascorbic and citric acid (Pintagaro, 2010; Scherer, 2012). Moreover, it is a potential source of reducing sugars (Guimarães, 2010; Abad-García, 2014) and phenolic compounds, especially flavanones, flavones and flavonols (Sun, 2010; Abad-García, 2014). These latter families of compounds are the main antioxidant compounds, being present in high amounts in *Citrus* pulp.

In addition, carotenoids (Mouly, 1999), pectins (Lliso, 2007) are also found. Other compounds found in *Citrus* pulp comprise terpenoids, alcohols, aldehydes, and esters (Pichersky, 2006; Schwab, 2008).

Regarding protein composition (which are the compounds determined in this thesis), several proteins and peptides from *Citrus* peel (flavedo and albedo) and pulp have been studied and characterized due to their allergenic properties (Ahrazem, 2005; Ebo, 2007; Serra, 2013). They can be grouped into three different families: germin-like proteins (GLPs), such Cit s 1; profilins, as Cit s 2; and non-specific lipid transfer proteins (nsLTPs). GPLs and profilins are responsible for many cross-reactions between pollens and food (Serra, 2013). As regard nsLTPs, Cit s 3 and Cit r 3 have been recognized as allergens in sweet orange and tangerine, respectively. These proteins are involved in plant defense mechanisms against bacteria and fungi and, possibly, in the assembly of hydrophobic protective layers of surface polymers, such as cutin (Ahrazem, 2005; Ebo, 2007).

2.2. Methods of analysis of *Citrus* fruit constituents

Citrus fruit composition has been extensively studied using the extracted juice from the pulp/endocarp. HPLC has been employed to characterize carotenoid profiles from mandarin and orange juices (Goodner, 2001). Then, several publications have described *Citrus* phenolic compound determination, using HPLC coupled to diode array detector (DAD) (Mouly, 1998; Saraji, 2010) or to electrospray ionization (ESI) and MS/MS detection (Ignat, 2011). In addition, organic acids have been determined by UV-Vis (Nour, 2010; Scherer, 2012), HPLC-MS (Kelebek, 2009; Flores, 2012), capillary zone electrophoresos (CZE) (Navarro-Pascual, 2015B) or Fourier transform infrared (FTIR) (Regmi, 2012). In addition, compounds such as glucose, fructose and sucrose have been determined through HPLC coupled to a RI (Kelebek, 2011), ELSD (Cheong, 2012) or a pulsed amperometric

detector (White, 1990). Using these sugar profiles, CZE has been applied for rapid differentiation of commercial juices and blends (Navarro Pascual-Ahuir, 2015B). Furthermore, pyrolysis followed by MS has been applied to *Citrus* juices (Garcia-Wass, 2000). Lastly, proteomic analysis has been carried out to characterize allergens by 2D-PAGE in combination with MS detection (Zucas, 2005; Lliso, 2007). Also, IgE immunoblotting, N-terminal sequencing, IgE-inhibition assays have been conducted (Crespo, 2006) to identify allergenic orange proteins.

2.3. Detection of adulteration

As mentioned above, consumption of *Citrus* juices has increased in the last years. Their economic value makes *Citrus* fruits a target for misrepresentation and their juices a target for adulteration. Concretely, orange (*Citrus sinensis*) juices are adulterated with cheaper fruit juices like tangerine (*Citrus tangerine*). This has a negative impact on both industry and consumers, since high quality authentic products have to compete with less expensive adulterated ones (Jandríc, 2017). To guarantee the quality control demanded by food producers and consumers, the development of analytical methods able to detect the adulteration of *Citrus* juices is required. Also, there is a need of verifying the adulteration of specific varieties of *Citrus* fuits and the juices prepare from them. In this sense, the analysis of the citrus compositions followed by statistical analysis has been employed to classify juices into various categories. The usefulness of the ^{1}H nuclear magnetic resonance (^{1}H NMR), IR spectroscopy or HPLC-MS for authenticity assessment of fruit juices in combination with different chemometrics tools has been demonstrated (Cuny, 2008; Vaclavik, 2012; Jandric, 2017). Moreover, the presence of some specific flavonoids has been employed to detect the adulteration of sweet orange (*Citrus sinensis*) juice with grapefruit *(Citrus paradise)* and bitter orange (*Citrus aurantium)* juices (Ooghe, 1994;

Rouseff, 1988). On the other hand, DNA markers have also been used for the characterization of different sweet orange varieties grown in India (Malik, 2012; Sankar, 2014). Most of the studies reported in literature to discriminate orange varieties are based on the content of some micro constituents present in the juices of *Citrus sp*. However, few studies have been conducted using the whole fruit without processing or other parts (like leaves). Thus, some works have described using near infrared (NIR) spectroscopy (Cen, 2007; Suphamitmongkol, 2013) to differentiate varieties of Chinese and Thai oranges. Other studies (Zucas, 2005) have employed the profiles of *Citrus* leaf proteins using 2D-PAGE to distinguish different *Citrus* cultivars.

Additionally, six genetically different cultivars of *Citrus* were analyzed by Zucas *et al*. In this case, the authors found different protein profiles from *Citrus* leaves using 2D-PAGE (Zucas, 2005).

2.4. References

Abad-García, B.; Garmón-Lobato, G.; Sánchez-Ilárduya M.B.; Berrueta L.A.; Gallo, B.; Vicente, F.; Alonso-Salces, R.M. (**2014**). Polyphenolic contents in Citrus fruit juices: authenticity assessment. *European Food Research and Technology 238*, 803-818.

Abeysinghe, D.C.: Li, X.; Sun, C.D.; Zhang, W.S.; Zhou, C.H.; Chen, K.S. (**2007**). Bioactive compounds and antioxidant capacities in different edible tissues of citrus fruit of four species. *Food Chemistry, 104*, 1338-1344.

Ahrazem, O.; Ibáñez, M.D.; López-Torrejón, G.; Sanchez-Monge, R.; Sastre, J.; Lombardero, M.; Barber, D.; Salcedo, G. (**2005**). Lipid transfer proteins and allergy to oranges. *International Archives of Allergy and Immunology, 137*, 201-210.

Carballo, S.; Zingarello, F.A.; Maestre, S.E., Todolí, J.L.; Prats, M.S. (**2014**). Optimisation of analytical methods for the characterization of oranges, clementines and citrus hybrids cultivated in Spain on the basis of their composition in ascorbic acid, citric acid and major sugars. *International Journal of Food Science and Technology, 49*, 146-152.

Cen, H.; He, Y.; Huang, M. (**2007**). Combination and comparison of multivariate analysis for the differentiation of orange varieties using visible and near infrared reflectance spectroscopy. *European Food Research and Technology, 225*, 699-705.

Cheong, M.W.; Zhu, D.; Sng, J.; Liu, S.Q.; Curran, P.; Yu, B. (**2012**). Characterisation of calamansi (*Citrus microcarpa*). Part II: volatiles, physicochemical properties and non-volatiles in the juice. *Food Chemistry, 134*, 696-703.

Crespo, J.F.; Retzek, M.; Foetisch, K.; Sierra-Maestro, E. (**2006**). Germin-like protein Cit s 1 and profilin Cit s 2 are major allergens in orange (*Citrus sinensis*) fruits. *Molecular Nutrition & Food Research 50*, 282-290.

Cuny, M.; Vigneau, E.; Le Gall, G.; Colquhoun, I.; Lees, M.; Rutledge, D.N. (**2008**). Fruit juice authentication by 1H NMR spectroscopy in combination with different chemometrics tools. *Analytical and Bioanalytical Chemistry 390*, 419-427.

Ebo, D.G.; Ahrazem, O.; López-Torrejón, G.; Bridts, C.H.; Salcedo, G.; Stevens, W.J. (**2007**). Anaphylaxis from mandarin (*Citrus reticulata*): identification of potential responsible allergens. *International Archives of Allergy and Immunology, 144*, 39-43.

FAO. (**2015**). Food and Agriculture Organization of the United Nations. URL http://www.fao.org/3/a-i5558e.pdf

Flores, P.; Hellin, P.; Fenoll, J. (**2012**). Determination of organic acids in fruits and vegetables by liquid chromatography with tandem-mass spectrometry. *Food Chemistry, 132*, 1049-1054.

García-Wass, F.; Hammond, D.; Mottram, D.S.; Gutteridge, C.S. (**2000**). Detection of fruit juice authenticity using pyrolysis mass spectroscopy. *Food Chemistry, 69*, 215-220.

Goodner, K.L.; Rouseff, R.L.; Hofsommer, H.J. (**2001**). Orange, mandarin, and hybrid classification using multivariate statistics based on carotenoid profiles. *Journal of Agriculture and Food Chemistry, 49*, 1146-1150.

Guimarães, R.; Barros, L.; Barreira, J.C.M.; Sousa, M.J.; Carvalho, A.M.; Ferreira, I.C.F.R. (**2010**). Targeting excessive free radicals with peels and juices of citrus fruits: Grapefruit, lemon, lime and orange. *Food and Chemical Toxicology, 48*, 99-106.

Ignat, I.; Volf, I.; Popa, V.I. (**2011**). A critical review of methods for characterisation of polyphenolic compounds in fruits and vegetables. *Food Chemistry, 126*, 1821-1835.

Jandríc, Z.; Islam, M.; Singh, D.K.; Cannavan, A. (**2017**). Authentication of Indian citrus fruit/fruit juices by untargeted and targeted metabolomics. *Food Control, 72*, 181-188.

Kato, M.; Ikoma, Y.; Matsumoto, H.; Sugiura, M.; Hyodo, H.; Yano, M. (**2004**). Accumulation of carotenoids and expression of carotenoid biosynthetic genes during maturation in *Citrus* Fruit. *Plant Physiology, 134*, 824-837.

Kelebek, H.; Selli, S. (**2011**). Determination of volatile, phenolic, organic acid and sugar components in a Turkish cv. Dortyol (*Citrus sinensis L. Osbeck*) orange juice. *Journal of the Science of Food and Agriculture, 91*, 1855-1862.

Kelebek, H.; Selli, S.; Canbas, A.; Cabaroglu, T. (**2009**). HPLC determination of organic acids, sugars, phenolic compositions and antioxidant capacity of orange juice and orange wine made from a Turkish cv. Kozan. *Microchemical Journal, 91*, 187-192.

Khan, M. K., Abert-Vian, M., Fabiano-Tixier, A. S., Dangles, O., Chemat, F. (**2010**). Ultrasound-assisted extraction of polyphenols (flavanone glycosides) from orange (*Citrus sinensis L.*) peel. *Food Chemistry, 119*, 851-858.

Lliso, I.; Tadeo, F.R.; Phinney, B.S; Wilkerson, C.G.; Talón, M. (**2007**). Protein changes in the albedo of *Citrus* fruits on post harvesting storage. *Journal of Agriculture and Food Chemistry, 55*, 9047-9053.

Malik, S.K.; Rohini, M.R.; Kumar, S.; Choudhary, R.; Pal, D.; Chaudhury, R. (**2012**). Assessment of genetic diversity in sweet orange [*Citrus*

sinensis (L.) Osbeck] cultivars of India using morphological and RAPD markers. *Agricultural Research, 1*, 317-324.

Mouly, P.; Gaydou, E.M.: Auffray, A. (**1998**). Simultaneous separation of flavanone glycosides and polymethoxylated flavones in Citrus juices using liquid chromatography. *Journal of Chromatography A, 800*, 171-179.

Mouly, P.P.; Gaydoub, E.M.; Corsettia, J. (**1999**). Determination of the geographical origin of Valencia orange juice using carotenoid liquid chromatographic profiles. *Journal of Chromatography A, 844*, 149-159.

Navarro Pascual-Ahuir, M.; Lerma-García, M.J.; Simó Alfonso, E.F.; Herrero-Martínez, J.M. (**2015A**). Quality control of fruit juices by using organic acids determined by capillary zone electrophoresis with poly(vinyl alcohol)-coated bubble cell capillaries. *Food Chemistry, 188,* 596-603.

Navarro Pascual-Ahuir, M.; Lerma-García, M.J.; Simó Alfonso, e.f.; Herrero-Martínez, J.M. (**2015B**). Rapid differentiation of commercial juices and blends by using sugar profiles obtained by capillary zone electrophoresis with indirect UV detection. *Journal of Agriculture and Food Chemistry, 63,* 85-94.

Nour, V.; Trandafir, I.; Ionica, M.E. (**2010**). HPLC organic acid analysis in different citrus juices under reversed phase conditions. *Notulae Botanicae Horti Agrobotanici Cluj-Napoca, 38*, 44-48.

Ooghe, W.C.; Ooghe, S.J.; Detavernier, C.M.; Huyghebaert, A. (**1994**). Characterization of orange juice by flavanone glycosides. *Journal of Agriculture and Food Chemistry, 42*, 2183-2190.

Pichersky, E.; Noel, J.P.; Dudareva, N. (**2006**). Biosynthesis of plant volatiles: nature's diversity and ingenuity. *Science, 311,* 808-811.

Pintagaro, V.; Canton, C.; Spadafora, A.; Mazzuca, S. (**2010**). Proteome from lemon fruit flavedo reveals that this tissue produces high amounts of the Cit s1 germin-like isoforms. *Journal of Agriculture and Food Chemistry, 58,* 7239-7244.

Rafiq, S.; Kaul, R.; Sofi, S.A.; Bashir, N.; Nazir, F.; Nayik, G.A. (**2015**). Citrus peel as a source of functional ingredient: A review. *Journal of the Saudi Society of Agricultural Sciences*, https://doi.org/ 10.1016/ j.jssas.2016.07.006.

Regmi, U.; Palma, M.; Barroso, C.G. (**2012**). Direct determination of organic acids in wine and wine-derived products by Fourier transform infrared (FT-IR) spectroscopy and chemometric techniques. *Analytica Chimica Acta, 732,* 137-144.

Rouseff, R.L. (**1988**). Adulteration of fruit juices beverages. In S. Nagy, M.E. Rhodes, J.A. Attaway (Eds.), Differentiating citrus juices using flavanone glycoside concentration profiles. New York and Basel: Marcel Dekker Inc. 49-64.

Sankar, T.G.; Gopi, V.; Deepa, B.; Gopal, K. (**2014**). Genetic diversity analysis of sweet orange (*Citrus sinensis osbeck*) varieties/clones through RAPD markers. *International Journal of Current Microbiology and Applied Sciences, 3,* 75-84

Saraji, M.; Mousavi, F. (**2010**). Use of hollow fibre-based liquid-liquid-liquid microextraction and high-performance liquid chromatography-diode array detection for the determination of phenolic acids in fruit juices. *Food Chemistry, 123,* 1310-1317.

Scherer, R.; Poloni Rybka, A.C.; Ballus, C.A.; Dillenburg Meinhart, A.; Teixeira Filho, j.; Teixeira Godoy, H. (**2012**). Validation of a HPLC

method for simultaneous determination of main organic acids in fruits and juices. *Food Chemistry, 135*, 150-154.

Schwab, W.; Davidovich-Rikanati, R.; Efraim Lewinsohn, E. (**2008**). Biosynthesis of plant-derived flavor compounds. *The Plant Journal, 54*, 712-732.

Serra, I. A.; Bernardo, L.; Spadafora, A.; Faccioli, P.; Canton, C.; Mazzuca, S. (**2013**). The *Citrus* clementina putative allergens: from proteomic analysis to structural features. *Journal of Agriculture and Food Chemistry, 61*, 8949-8958.

Sun, Y.; Wang, J.; Gu, S.; Liu, Z.; Zhang, Y.; Zhang, X. (**2010**). Simultaneous determination of flavonoids in different parts of *Citrus reticulata* "Chachi" fruit by high performance liquid chromatography-photodiode array detection. *Molecules, 15*, 5378-5388.

Suphamitmongkol, W.; Nie, G.; Liu, R.; Kasemsumran, S.; Shi, Y. (**2013**). An alternative approach for the classification of orange varieties base don near infrared spectroscopy. *Conputers and Electronics in Agriculture, 91*, 87-936.

Vaclavik, L.; Schreiber, A.; Lacina, O.; Cajka, T.; Hajslova, J. (**2012**). Liquid chromatography–mass spectrometry-based metabolomics for authenticity assessment of fruit juices. *Metabolomics 8*, 793-803.

Ververis, C.; Georghiou, K.; Danielidis, D.; Hatzinikolaou, D.G. Santas, P.; Santas, R.; Corleti, V. (**2007**).Cellulose, hemicelluloses, lignin and ash content of some organic materials and their suitability for use as paper pulp supplements. *Bioresource Technology 98*, 296-301

White, D.R.; Widmer, W.W. (**1990**). Application of high-performance anion-exchange chromatography with pulsed amperometric detection to

sugar analysis in citrus juices. *Journal of Agricultural and Food Chemistry, 38,* 1918-1921.

Xu, Q.; Chen, L.; Ruan, X.; Chen, D. (**2013**). The draft genome of sweet orange (*Citrus sinensis*). *Nature genetics, 45,* 59-69.

Zukas, A.A.; Breksa, A.P. (**2005**). Extraction methods for analysis of *Citrus* leaf proteins by two-dimensional gel electrophoresis. *Journal of Chromatography A, 1078,* 201-205.

Chapter 3. Mistletoe (*Viscum album L.*)

3.1. Introduction

European mistletoe *(Viscum album L.*) is a hemi-parasitic plant, which grows on the branches of other trees, absorbing nutrients from the host plant (Olsner, 1982). Thus, *Viscum album L* is able to infect a large number of trees such as oaks, white poplars, apples, pines, sprunes, etc. Extracts from this plant material have been used since ancient time as therapeutic agent for oncological applications, being frequently prescribed for cancer therapy in central European countries (Lutter, 2001). Its composition is a complex mixture of several biological active substances such glycoproteins (in particular the mistletoe lectins I, II and III), polypeptides (e.g. viscotoxins), flavonoids, amino acids, and oligo- and polysaccharides. Among all the components, mistletoe lectins as well as viscotoxins, which are considered in this thesis, are described below.

3.2. Mistletoe lectins

The mistletoe lectins (MLs) belong to an A-B family of toxins, which is named as ribosome-inactivating proteins (RIPs) of type II (Krauspenhaar, 1999; Lutter, 2001). This type of heterodimeric proteins is composed of an enzyme (A-chain), which inactivates the ribosomes, and a lectin (B-chain) that recognizes receptors on the membrane and allows the holotoxin to bind to the glycan part of glycoproteins or glycolipids located on the surface of target cells. In any case, the cellular cytotoxicity of the lectins seems to require both A- and B-chains (Siegle, 2001; Mishra, 2003; Thiest, 2005) (**Figure 3.1**).

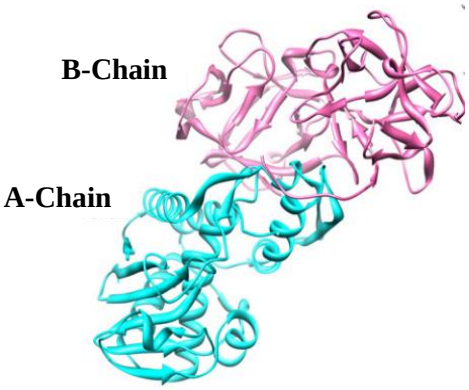

Figure 3.1. Molecular structure of mistletoe lectin. A-chain is the ribosome inactivator moiety, whereas the B-chain is responsible for its immuno-modulatory efficacy.

MLs have been used as recognizing tools to differentiate malignant tumors from benign and their degree of glycosylation is associated with metastasis (Liu, 2010; Podlech, 2012). Three MLs have widely been identified in crude mistletoe extracts studied: ML-I, ML-II and ML-III. Molecular weight of these glycosylated cytotoxic proteins ranges between 60 and 66 kDa. MLs can be classified according to their sugar specificities: ML-I (galactose-specific), ML-II (galactose- and N-acetylgalactosamine-specific) and ML-III (N-acetylgalactosamine-specific) (Lee, 1999).

The most important and most often studied lectin has been ML-I, called also viscumin, since it is the major component of therapeutically active substances present in commercially available mistletoe extracts applied for the treatment of human cancer (Huguet-Soler, 1996). It consists of a cytotoxic A-chain with a molecular weight of 29 kDa and a carbohydrate binding B-chain of 34 kDa that is responsible for its immune-modulatory efficacy. ML-II and ML-III could also be degradation products of ML-I in the plants themselves (Olsnes, 1982; Dietrich, 1992). At present, the consideration of the origin of ML-II and ML-III are not in agreement. Some research groups have only found two groups of isolectins: ML-I and N-

acetylgalactosamin-specific ML-II. The structural analysis of ML-I and its physical, chemical as well as biological characteritics reveal many similarities with the ricin molecule (Luther, 1986; Dietrich, 1992). Several authors have isolated MLs from mistletoe extracts and then its structure has been characterized by different techniques such as molecular replacement (Krauspenhaar, 1999) or solid-phase binding assays with matrix-assisted laser desorption/ionization coupled to time-of-flight (MALDI-TOF) (Müthing, 2004). Thus, these authors have suggested that ML-I has to be considered as a sialic acid- and not a galactose-specific lectin.

3.3. Mistletoe viscotoxins

In the last years, viscotoxins from *Viscum album L* have also attracted much attention. They are located in mistletoe seed, leaves and branches (Guidici, 2003). They come from a family named thionins, which are best known for their toxicity to bacteria and fungi, as well as to animal and plant cells (Romagnoli, 2000).

Viscotoxins are polypeptides, with a molecular mass of 5 kDa, composed by 45-50 aminoacids that contain 3–4 internal disulfide bonds. According to the amino acid sequence, disulphide bridge arrangement and distribution in plant tissues, seven isoforms of viscotoxins, namely A1, A2, A3, B, B2, 1-PS and C1 have been reported (Urech, 1995; Schaller, 1996). The cytotoxicity of these viscotoxins is quite different due to these structural changes. In fact, among them, viscotoxin A3 is the most cytotoxic whereas B is the least cytotoxic (Büssing, 1998). Moreover, the toxicity of viscotoxins has been found to be about 100 times less toxic than lectins on human tumor cells (Olson, 1972). However, in preparation of tea or medical decoction in anticancer therapy, lectins are denatured and lose their toxicity, whereas viscotoxins due to their heat resistance and stable structure remains as a

major cytotoxic component in these oncological treatments or tumors (Khwaja, 1986).

3.4. Methods of characterization of MLs and viscotoxins

The characterization of MLs has been traditionally conducted in two steps; the first step is the extraction of lectins in an aqueous solution, using commonly a phosphate or Tris buffer (pH 7-8), followed by their isolation using a carbohydrate affinity chromatography column (Sephadex G-50 and Sepharose 4B) (Franz, 1980; Park, 1998; Müthing, 2004; Jiménez, 2005). However, in some cases additional separation techniques have to be used subsequently to purify the lectins, such as immunoaffinity (Müthing 2004; Kang, 2007), ion-exchange chromatography and/or gel filtration. After its purification, classical methods such as SDS-PAGE, Western blot analysis (Olsner, 1982; Park, 1997; Kang, 2007) and more sophisticated techniques (e.g. MALDI-TOF) (Müthing, 2004) have been used for their characterization.

On the other hand, the selective extraction of viscotoxins also requires several purification steps. Thus, the use of a cation-exchange column (Sephadex C-25), followed by fractionation by preparative HPLC has been carried out to identify the different isoforms (Debreczeni, 2003). In addition, Hussain *et al*. have reported the use of novel materials based on poly(styrene-co-divinylbenzene) hollow-monoliths containing zirconium silicate nano-powder (Hussain, 2013) and aluminum silicate (mullite) powder (Hussain, 2014) as sorbents in solid-phase extraction (SPE) to selectively extract viscotoxins.

3.5. References

Brinkworth, C.S. (**2010**). Identification of ricin in crude and purified extracts from castor beans using on-target tryptic digestion and MALDI mass spectrometry. *Analytical Chemistry, 82*, 5246-5252.

Büssing, A.; Schaller, G.; Pfüller, U. (**1998**). Generation of reactive oxygen intermediates (ROI) by the thionins from *Viscum album L*. *Anticancer Research, 18*, 4291-4296.

Debreczeni, J.E.; Girmann, B.; Zeeck, A.; Krätzner, R.; Sheldrick, G.M. (**2003**). Structure of viscotoxin A3: disulfide location from weak SAD data. *Acta Crystallographica, 59*, 2125-2132.

Dietrich, J.B.; Ribereau-Gayon, G.; Jung, M.L.; Franz, H.; Beck, J.P.; Anton, R (**1992**). Identity of the N-terminal sequences of the three A chains of mistletoe (Viscum album L.) lectins: homology with ricin-like plant toxins and single-chain ribosome-inhibiting proteins. *Anticancer Drug, 3*, 507-511.

Franz, H.; Ziska, P.; Kindt, A. (**1981**). Isolation and properties of three lectins from mistletoe (*Viscum album L.*). *Biochemical Journal, 195*, 481-484.

Giudici, M.; Pascual, R.; Canal, L.; Pfüller, K.; Pfüller, U.; Villalaín, J.(**2003**). Interaction of Viscotoxins A3 and B with membrane model systems: Implications to their mechanism of action. *Biophysical Journal, 85*, 971-981.

Hussain, S.; Güzel, Y.; Pezzei, C.; Rainer, M.; Huck, C.W.; Bonn, G.K. (**2014**). Solid-phase extraction of plant thionins employing aluminum silicate based extraction columns. *Journal of Separation Science, 37*, 2200–2207.

Hussain, S.; Güzel, Y.; Schönbichler, S.A.; Rainer, M.; Huck, C.W.; Bonn, G.K. (**2013**). Solid-phase extraction method for the isolation of plant thionins from European mistletoe, wheat and barley using zirconium silicate embedded in poly(styrene-co-divinylbenzene) hollow-monoliths. *Anal Bioanalytical Chemistry, 405*, 7509-7521.

Huguet-Soler, M.; Stoeva, S.; Schwamborn, C.; Wilhelm, S.; Stiefel, T.; Voelter, W. (**1996**). Complete amino acid sequence of the A chain of mistletoe lectin I. *FEBS Letters, 399*, 153-157.

Jiménez, M.; Sáiz, J.L.; André, S.; Gabius, H.J.; Solís, D. (**2005**). Monomer/dimer equilibrium of the AB-type lectin from mistletoe enables combination of toxin/agglutinin activities in one protein: analysis of native and citraconylated proteins by ultracentrifugation/gel filtration and cell biological consequences of dimer destabilization. *Glycobiology, 12*, 1386-1395.

Kang, T.B.; Song, S.K.; Yoon, T.J.; Yoo, Y.C.; Lee, K.H.; Her, E.; Kim, J.B. (**2007**). Isolation and characterization of two Korean mistletoe lectins. *Journal of Biochemistry and Molecular Biology, 40*, 959-65.

Khwaja, T.A.; Dias, C.B.; Pentecost, S. (**1986**). Recent studies on the anticancer activities of misletoe (Viscumin álbum) and its alkaloids. *Oncology, 43*; 42-50.

Krauspenhaar, R.; Eschenburg, S.; Perbandt, M.; Kornilov, V. (**1999**). Crystal Structure of Mistletoe Lectin I from Viscum album. *Biochemical and Biophysical Research Communications 257*, 418-424.

Lee, H.S.; Kim, Y.S.; Kim, S.B.; Choi, B.E.; Woo, B.H.; Lee, K.C. (**1999**). Isolation and characterization of biologically active lectin from Korean mistletoe, Viscum album var. Coloratum. *Cellular and Molecular Life Science 55*, 679-682.

Liu, B.; Bian, H.; Bao, J. (**2010**). Plant lectins: Potential antineoplastic drugs from bench to clinic. *Cancer Letters 287*, 1-12.

Luther, P.; Uhlenbruck, G.; Reutgen, H.; Samtleben, R.; Sehrt, I.; Ribereau-Gayon, G. (**1986**). Are lectins of Viscum album interesting tools in lung diseases? A review of recent results. *Z Erkr Atmungsorgane, 166*, 247-256.

Luther, P.; Meyer, H.E.; Langer, M.; Witthohn, K.; Dormeyer, W.; Sickmann, A.; Bluggel, M. (**2001**). Investigation of charge variants of rViscumin by two-dimensional gel electrophoresis and mass spectrometry. *Electrophoresis 22*, 2888-2897.

Mishra, V.; Sharma, R.S.; Yadav, S.; Babu, C.R.; Singh T.P. (**2003**). Purification and characterization of four isoforms of Himalayan mistletoe ribosome-inactivating protein from *Viscum album* having unique sugar affinity. *Archives of Biochemistry and Biophysics 423*, 288-301.

Müthing, J.; Meisen, I.; Bulau, P.; Langer, M.; Witthohn, K.; Lentzen, H.; Neumann, U.; Peter-Katalinic, J. (**2004**). Mistletoe lectin I is a sialic acid-specific lectin with strict preference to gangliosides and glycoproteins with terminal Neu5AcR2-6Galâ1-4GlcNAc residues. *Biochemistry, 43*, 2996-3007.

Olson, T.; Samuelson, G. (**1972**). The amino acid sequence of Viscotoxin A2 from the European Mistletoe (*Viscumin album L., Loranthaceae*). *Acta Chemica Scandinavica, 26*, 585-595.

Park, W.B.; Han, S.K.; Lee, M.H.; Han, K.H. (**1997**). Isolation and characterization of lectins from stem and leaves of Korean mistletoe (Viscum album var.coloratum) by affinity chromatography. *Archives of Pharmacal Research, 20*, 306-312.

Patočka, J.; Středa, L. (**2006**). protein biotoxins of military significance. *Acta Medica, 49,* 3-11.

Podlech, O.; Harter, P.N.; Mittelbronn, M.; Pöschel, S.; Naumann, U. (**2012**). Fermented mistletoe extract as a multimodal antitumoral agent in gliomas. *Evidence-Based Complementary and Alternative Medicine, 2012,* 501796.

Schaller, G.; Urech, K.; Giannattasio, M. (**1996**). Cytotoxicity of different viscotoxins and extracts from the European subspecies of *Viscum album L*. *Phytotherapy Research, 10,* 473-477.

Siegle, I.; Fritz, P.; McClellan, M.; Gutzeit, S.; Murdter, T.E. (**2001**). Combined cytotoxic action of Viscum album agglutinin-1 and anticancer agents against human A549 lung cancer cells. *Anticancer Research, 21,* 2687-2691.

Thies, A.; Nugel, D.; Pfüller, U.; Moll, I.; Schumacher, U. (**2005**). Influence of mistletoe lectins and cytokines induced by them on cell proliferation of human melanoma cells in vitro. *Toxicology. 207,* 105-16.

Urech, K.; Schaller, G.; Ziska, P.; Giannattasio, M. (**1995**). Comparative study on the cytotoxic effect of viscotoxin and mistletoe lectin on tumour cells in culture. *Phytotherapy Research, 9,* 49-55.

.

Chapter 4. Sample preparation techniques

The choice of an appropriate sample preparation method is a critical factor in the success of an analysis, and the whole analytical process can be failed if an inadequate sample preparation is conducted (Vas, 2004; Hyötyläinen, 2009). The process of extraction and preconcentration of samples such food or biological matrices is usually complex, tedious and time consuming (Saunders, 2009). Thus, an ideal sample preparation method should be as simple as possible, fast, reproducible and with a high extraction recovery of the target analytes. In addition, it should require a minimum number of processing steps, minimize reagent consumption, be environmentally friendly, improve detection limits, and have potential for its use in on-line work stations (Abdel-Rehim, 2001; Nováková, 2009).

In the following sections, an overview of the different extraction techniques currently employed for the family of compounds studied in this thesis has been included.

The typical extraction techniques used for aqueous matrices can be classified in two groups according to the nature of the extracting reagent: liquid-liquid extraction (LLE) and solid-phase extraction (SPE).

4.1 Liquid-liquid extraction (LLE)

LLE is a separation process, which is produced due to the relative solubilities of the compounds of interest in two liquid phases. It is based on the use of a separator funnel to separate two liquid phases, one immiscible organic solvent and an aqueous solvent, followed by evaporation of the organic solvent to dryness and reconstitution prior to analysis. However, this technique is labor-intensive (it includes multiple stages), non-selective, susceptible to errors, time consuming, needs a large volume of high-purity solvents with expensive disposal requirements for environmental pollutants that add extra cost to the analytical procedure, creates health hazards to the

laboratory personnel, and is difficult to automate and connect with analytical instruments. In addition, LLE can lead to analyte losses due to an incomplete extraction, and commonly it has practical problems such as emulsion formation.

4.2. Solid-phase extraction (SPE)

4.2.1. General features

SPE can be described as a sample preparation method that provides analyte enrichment and a sample clean-up from solution by sorption onto a solid extracting phase. Thus, in this technique, the analytes are firstly transferred from a liquid sample to a solid sorbent (loading step). Then, matrix interferences can be removed from the sorbent using an appropriate solvent (washing step), and finally, the analytes of interest are totally released from solid sorbent using an organic solvent (elution step) followed by instrumental analysis.

SPE shows several advantages compared with LLE, such as higher recoveries, larger reproducibility and accuracy, less time-consuming and more environmentally friendly. Moreover, the eluent of the SPE can be injected directly into chromatographic systems, while the extracted analytes using LLE need to be dried and the residue redissolved in a suitable solvent before analysis (Simpson, 2000).

However, there are some disadvantages of SPE; for example, SPE supports can be quite expensive and are manufactured for single use only (Shen, 2001). In addition, if the sample solution contains any solid particles, they can block the sorbent (Lingeman, 1997).

The design of efficient supports for SPE has been developed over years. Thus, sorptive materials are commercially available in different formats,

such as cartridges, syringes and disks. Recent miniaturized SPE formats are pipette tips and 96-well plates, which allow processing of a large number of small samples with a semi-automated handle system, which is suitable for biological, pharmaceutical and proteomic analysis. Despite these advantages, cartridges still constitute the most preferred SPE format, due to the extensively availability of commercial sorbents with satisfactory extraction efficiencies for retaining a large number of analytes of interest.

The SPE technique can be carried out in two working modes: off-line or on-line. In the last mode, there is a direct and automated coupling between SPE (sample preparation) and the chromatographic system. However, some drawbacks are present when this approach is applied, such as the incompatibility of elution solvent with chromatographic techniques (e.g. mobile phase in HPLC) or the small amount of solvent in the precolumn, which may lead to low loading capacity (Ota, 2007; Lin, 2009).

Due to its versatility, SPE has become a very popular separation and preconcentration approach for extracting a broad range of compounds with different chemical properties from liquid samples (Du, 2007).

In the optimization of a SPE procedure, the experimental parameters that affect the retention efficiencies of the species of interest, the enrichment factors, and the gradient/sequential isolation of similar species must be carefully investigated. These factors include the nature of the target species, the surface properties of the packing sorbent, the acidity of the reaction system, the sampling flow rate, and the appropriate choice of eluents. Among all of them, sorbent selection is the most critical parameter to achieve efficient extraction of the analytes of interest from liquid samples.

4.2.2. Materials used as SPE sorbents

The choice of sorbent in SPE depends on factors such as the properties of target analytes, type of sample matrix, and the interfering components to be removed. The ideal sorbent material to be used for SPE should be chemically stable and not react with the solvents or reagents used in the process. In addition, a high surface area is highly desirable in a SPE sorbent in order to increase its loadability. Another important feature is the permeability in order to decrease the processing time by increasing the flow rate without detrimental increase in backpressure. Additionally, a suitable sorbent for SPE should be able to separate desired from undesired components, and give batch-to-batch reproducibility (Simpson, 2000). The common materials that have been used as SPE sorbents are packed beds and monoliths, which will be discussed in the following sections. **Figure 4.1** shows the classification of these main sorptive materials for SPE depending on their chemical structure.

4.2.2.1. Packed-bed materials

Micro- and nanoscale particles packed in SPE supports can be considered as the conventional solution commonly employed in chromatographic or SPE columns. In particular, silica-based particles are the most common material used as sorbents. Due to the well-established technology of chemically-bonded silica packings for HPLC columns, the development of SPE materials has constituted a simple task. Thus, the modification of silica particles has led to the design of many sorbents used in retention mechanisms like reversed-phase (RP), normal-phase and ion-exchange, such as octadecyl (C18), octyl (C8), phenyl, cyanopropyl, diol, aminopropyl, sulfonic acid bonded silica sorbents, among others.

Despite the advantages of these silica-packed particles (high surface area to volume ratio, wide range of functionalities, etc.), their main drawback is

their narrow pH stability range and the presence of residual silanol groups in its structure, which can have a negative effect on the retention of certain analytes (Lin, 2009).

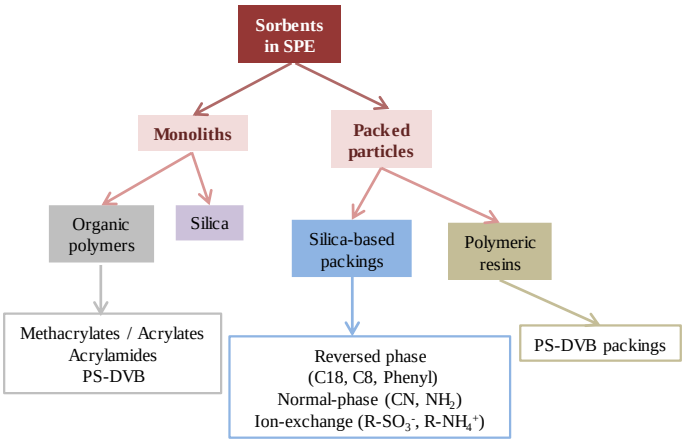

Figure 4.1. Classification of the main SPE sorbents on the basis of their chemical properties.

In order to overcome the disadvantages of these materials, porous polymeric resins based on polystyrene-divinylbenzene (PS-DVB) as sorbent material were introduced (Girault, 2004; Rhee, 2004). The behavior of these polymeric sorbents (commercially available) is mainly hydrophobic (through van der Waals forces and π-π interactions of aromatic rings), and they have displayed acceptable capability for extracting low and moderate polar compounds from complex matrices. However, they showed a poor retention of highly polar compounds.

In any case, the preparation of packed-silica or polymeric particles requires special instruments and skilled abilities to obtain a packing of enough quality that assures an efficient extraction of analytes of interest. Furthermore, both types of particles require the existence of frits to keep the integrity of packing. Other limitations of packed SPE columns include restricted flowrates, particle size and plugging of the frits.

4.2.2.2. Monolithic materials

The word “monolith” is derived from the Greek word “monolithos”, which means “single stone”. It defines a geological or technological feature such as a mountain or boulder, consisting of a large block of stone. In the context of functional materials for analytical sciences, the term monolith describes a continuous single rod with a porous structure made of macropores and mesopores (Viklund, 1996). The macropores or through-pores (>50 nm) act as flow-through channels for solvent transport (through the monolithic materials), whereas mesopores (2-50 nm) provide a high surface area for the efficient interaction with analytes, and increased loadability of the monolith. **Figure 4.2** shows the structural differences between a conventional chromatographic support packed with particles (**part A**) and a monolithic column (**part B**). As evidenced from these pictures, the monolithic bed contains a much greater number of channels penetrating the chromatographic bed compared with the column packed with particles.

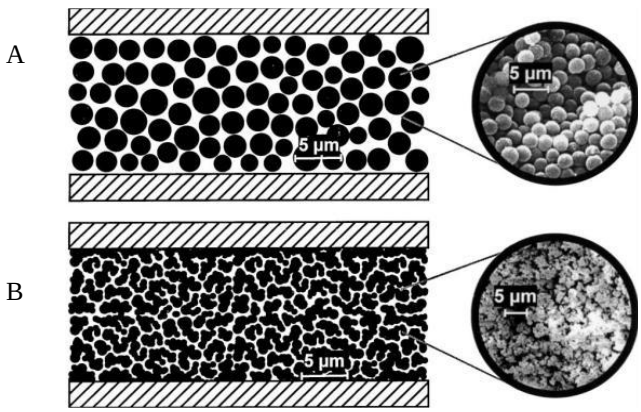

Figure 4.2. Structural characteristics of (A) packed, and (B) monolithic chromatographic beds.

Monolithic materials have several potential advantages compared with packed particles. For example, they usually offer low backpressure

depending on their structure and also the effective surface area of the monolithic column is larger than that of the packed column, even if the chemistry of both surfaces is very similar, providing the same elution order for many analytes.

The large permeability can increase the efficiency of extraction or separation and decrease the backpressure (Leinweber, 2003; Svec, 2004). However, since the density of monolithic columns is considerable lower, the load capacity of a conventional column of the same size is much higher. Also, the monolithic stationary phase does not require frits compared to the packed particles, which could be a source of secondary adsorption and clogging of the column during its use (Leinweber, 2002; Klampfl, 2004).

Pioneer studies, conducted independently by Hjertén *et al.* (Hjertén, 1989) and Svec and Frechet (Svec, 1992) on organic monoliths further supplemented by the contributions of Tanaka's group (Minakuchi, 1996) on silica-based monoliths; have revolutionized the field of column technology.

To date, the range of monolithic related applications is extensive in all fields of analytical chemistry. Thus, these supports have been used as stationary phases in various modes of chromatography, such as GC, HPLC, and CEC. These applications have been described in many reviews (Zou, 2002). However, less common applications of monoliths are as carriers for immobilization of enzymes, static mixers, thermally responsive gates and valves, as well as a solid-phase support for extraction and preconcentration (Svec, 2006; Aoki, 2009; Thabano, 2009). Monolithic materials can be broadly classified into inorganic silica-based monoliths and organic polymer-based monoliths, both of which will be described in the following sections.

***A) Silica-based monoliths*.** These monoliths with a well-defined homogenous structure are commonly prepared by a sol-gel process

(Nakanishi, 1997). This process implies the preparation of a siloxane network by the sequential hydrolysis and polycondensation of a silane compound (or a mixture of alkoxysilanes) under acidic (acetic acid) or basic (urea) conditions in the presence of a porogenic solvent (e.g. polyethylene glycol (PEG)). **Figure 4.3** shows the SEM micrograph of a silica-based monolith, where macropores and mesopores were evidenced.

Although silica-based monoliths can offer high permeability and excellent mechanical stability, their preparation is laborious, especially when is performed *in situ* (Lin, 2009; Svec, 2010). Moreover, the monolithic silica rods need to be wrapped in column materials, such as PEEK, when they are prepared in a mould (Guiochon, 2007). Besides, thermal treatment associated with its preparation make that the literature was mainly focused on fused-silica capillaries, being difficult to transfer to cartridge or microfluidic chip formats.

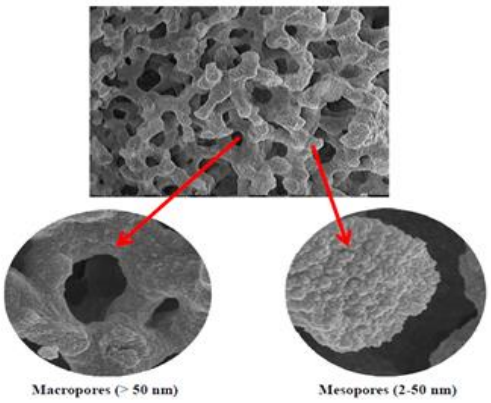

Macropores (>50 nm) Mesopores (2-50 nm)

Figure 4.3. SEM micrograph of the porous structure of a silica-based monolith.

Silica monoliths also suffer from some of the same limitations as silica-based particles, such as the limited pH range over which these monoliths are

stable (approximately pH 2-7). Despite of these limitations, silica-based monoliths have been successfully introduced as separation media for small molecules in GC, CEC and HPLC (Adam, 2000; Luo, 2005). However, there are few papers describing their use as materials for biomolecule extraction (DNA and proteins) (Miyazaki, 2004; Nema, 2014).

Thus, Miyazaki *et al*. (Miyazaki, 2004) have developed a monolithic silica extraction tip for the analysis of peptides and proteins. After fabrication, the monolithic silica rod was cut and fixed inside a 200 μL pipette tip using supersonic adhesion. Following this, the silica surface was chemically modified with either an octadecyl group in order to make it hydrophobic and enrich proteins, or the silica surface was coated with a titania phase and used for the concentration of phosphorylated peptides. The results showed that the C18-bonded monolithic silica extraction tip has the ability to purify different standard proteins varying in molecular weight up to 40000 Da; however, the extraction of proteins decreased with increasing molecular weight of the proteins. In addition, the fabricated monolith was not optimized nor its porous structure characterized.

Nema and co-workers (Nema, 2010) have fabricated silica-based monoliths into a 2 mL plastic syringe connected to a SPE vacuum manifold. The unmodified silica-based monolith with ionizable silanol groups was used in off-line cation-exchange for preconcentration of polar parapharmaceutical compounds (epinephrine, normetanephrine, and metanephrine) from biological samples.

B) Organic polymer-based monoliths. Polymeric monoliths are commonly synthesised via free-radical polymerization. Some of the benefits of these materials are its fast and easy separation, wide variety in monomers and readily available surface chemistries and higher chemical stability compared to silica counterparts. This thesis is exclusively focused on organic

polymer monoliths. In comparison to silica-based monoliths, polymeric monoliths have some advantages. Thus, organic based-monoliths are easily constructed *in-situ* almost independently from the shape and nature of the confining support (frequently a silica capillary tube, but also a variety of other materials and shapes). Polymeric monoliths have the necessary versatility to be easily adapted when small volumes of biological samples (containing valuable analytes of a wide range of molecular masses and polarities), should be handled. This is a great advantage to fill up micro-fluidic devices with a stationary phase, particularly when the mold has a complex geometry. In addition, the variety of synthesis procedures and the different materials that can be employed provides large flexibility of the surface chemistries, and allows the use in a wide range of separation methodologies.

The preparation of polymeric monoliths is carried out by filling the support with a polymerization mixture consisting of monomer/s, cross-linker, porogenic solvents and a radical initiator. The initiation of a polymerization reaction can be performed by thermal initiation (heat) (Svec, 2010), by chemical reactions (Joldsvendová, 2003; Cantó-Mirapeix, 2008), or UV radiation (Carrasco-Correa, 2013), which can only be carried out in a transparent mould such as a quartz tube, fused silica capillary, glass microchip (Svec, 2004) or polypropylene tip. The photochemical approach provides advantages such as short polymerization time and easy site-specific immobilization and surface functionalization of monolith using photomask technology (Stachowiac, 2003; Guerrouache, 2012). However, this initiation mode requires of UV transparent moulds (with a small size in one dimension) and UV transparent monomers.

Prior to polymerization reaction, the inner walls of confining support (e.g. capillary) are silanized in order to prevent the displacement of the monolith during its application. For this purpose, the wall is silanized using 3-

(trimethoxysilyl)propyl methacrylate. After polymerization reactions, the resulting monolith is chemically bound to the inner walls of support.

As mentioned above, the formation of polymeric monoliths is based on a radical reaction (**Figure 4.4**). First, the radical initiator is decomposed to afford free radicals and these active centers are transferred to the surrounding monomers. During propagation, the chain length of the polymers increases. Once a chain has been initiated, it propagates until there is no more available monomer or until termination by deactivation of the radical. Also, the reaction between the monomer and crosslinking agent takes place. As a result of this process, a system of two phases will be accomplished: one continuous monolithic solid and inert porogenic liquid filling the process of the monolithic structure.

The resulting morphology of the polymeric monoliths is a complex system with a structure consisting of a series of interconnected microglobules partially aggregated in larger clusters that form the body of the polymer (**Figure 4.5**). Irregular voids between clusters of microglobules are macropores. The optimization of the globules and their aggregates depends both on the composition of the polymerization mixtures and on the reaction conditions used in the preparation of the monolith.

Polymeric monoliths can be fabricated by using a wide range of monomers and crosslinking agents enabling the porous properties of the monolith to be controlled; for example, acrylate/methacrylate- (Cantó-Mirapeix, 2008; Cantó-Mirapeix, 2009A; Cantó-Mirapeix, 2009B; Bernabé-Zafón, 2009), styrene (Petro, 1996; Wang, 1995), and acrylamide-based stationary phases (Bedair, 2004).

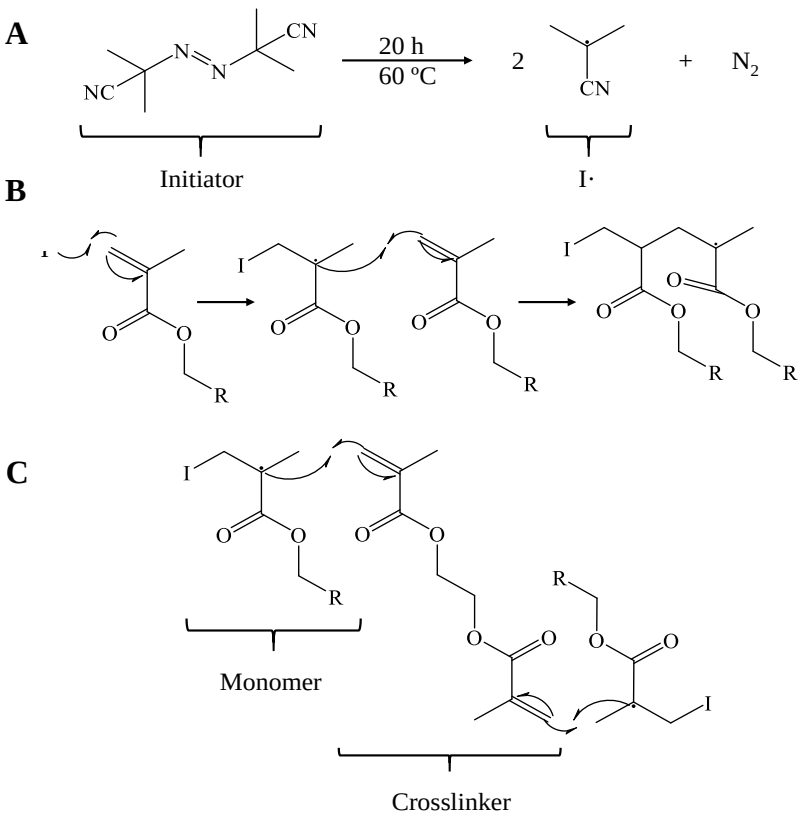

Figure 4.4. Polymerization mechanism. (A) Decomposition of the initiator; (B) radical monomer initiation and polymeric chain growth; (C) radical polymerization between monomer and crosslinker.

Svec and coworkers (Svec, 1992; Peters, 1998; Svec, 2005) have extensively reviewed the studies on polymeric support materials with special emphasis on methacrylate monoliths. These stationary phases were selected in the present thesis. **Figure 4.6** shows some common monomers and their crosslinking agents that have been used for fabrication of methacrylate-based monoliths.

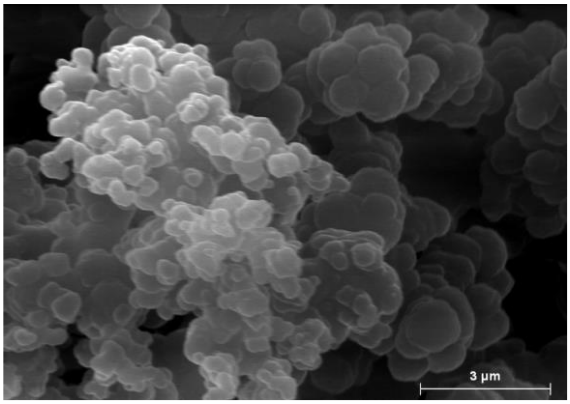

Figure 4.5. Cross-section SEM image of a metharcylate monolithic stationary phase.

Lauryl methacrylate (LMA)

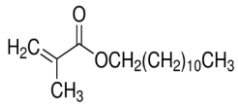

Octadecyl acrylate (ODA)

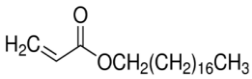

Glycidyl methacrylate (GMA)

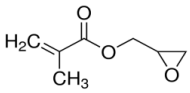

1,3-Butanediol diacrylate (BDDA)

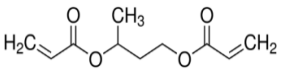

Ethylene dimethacrylate (EDMA)

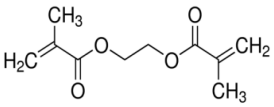

Figure 4.6. Example of monomers and crosslinkers used for the preparation of porous monoliths.

Most studies (Merhar, 2003; Eeltink, 2007) dealing with the development of methacrylate monoliths have demonstrated that the porous properties of stationary phases and their chromatographic performance depend on a number of factors such as the composition and concentration of porogens, degree of crosslinker, type of monomer, type of initiation, reaction time, etc. The monolith can be also functionalized by co-polymerization or post-polymerization in order to convert it into a sorbent with the desired chromatographic binding properties (Gusev, 1999).

In spite of the good features of these macroporous polymeric monoliths, they have relatively low surfaces areas (compared to its silica counterparts) due to the absence of an adequate micro- or mesoporous structure, which results in reduced sample load capacity and weak retention for chromatographic applications. Low surface area also limits other applications which also rely on interactions with surface active sites, such as catalysis and adsorption. In order to overcome this limitation, several strategies (new column chemistries and polymerization conditions, hypercrosslinking, incorporation of nanomaterials, etc) have been proposed and recently reviewed (Lv, 2015). In this sense, the approaches consisting of incorporation of nanoparticles (NPs) to the monoliths have emerged as an effective and promising way of increasing the surface-to-volume ratio, as well as to serve as new platforms to further or more efficiently modify the surface chemistry (Carrasco-Correa, 2015). NPs can offer numerous advantages; for example, their large surface-to-volume ratio can potentially facilitate mass transfer and enhance separation efficiency. Further, the larger surface should result in enhanced retention and increased sample loading capacity.

The NPs can be introduced into the monolith supports by simple entrapment during polymerization (Li, 2012) or attachment onto pore surface of monolithic matrix (Wen, 2012). The first method is performed by admixing the NPs into the reaction mixture before polymerization. This way is technically feasible and straightforward; however, most of them would be buried within the monolithic matrix and not be available at the pore surface for the desired interactions (Navarro-Pascual-Ahuir, 2013). Also, there might be some limitations regarding the amount of NPs that can be added to the incompatibility in the polarity of the NPs and the polymerization mixture.

Alternatively, attachment of NPs on pore surface of polymeric monolith using covalent bonds or electrostatic interactions can be performed after

synthesis of monolithic matrix. Several NPs such as latex (Valcárcel, 2005), AuNPs (Xu, 2010) and hydroxyapatite (Krenkova, 2010) have been introduced into monolith by attaching them onto pore surface of monolith. However, to perform a modification in the surface chemistry of polymeric monoliths, materials with reactive functionalities ("reactive monoliths") are required. In particular, glycidyl methacrylate (GMA)-based monoliths (with epoxy groups) constitute the typical platform to modify the surface chemistry once polymerization has been completed (Frankovic, 2008; Svec, 1992; Wang, 1995, Carrasco-Correa, 2013). For example, GMA-based monoliths can be reacted with ammonia (see **Figure 4.7A)** or with cystamine (**Figure 4.7B**) followed by reduction with tris(2-carboxyethyl)phosphine (TCEP) to provide stationary phases with different selectivity (Lv, 2012; Carrasco-Correa, 2013). Then, the immobilization of AuNPs on the pore surface of these modified monoliths can be easily accomplished based on the high affinity of these NPs toward the amino or thiol functionalities (Cao, 2010; Xu, 2010; Lv, 2012).

In an extension of this surface modification, Svec *et al*. (Lv, 2012) have exploited the dynamic nature of the bond between Au and thiol groups to tailor the surface chemistry through the binding of a variety of "exchangeable" thiol-containing moieties. The modified columns were examined in nano-LC for the rapid separation of a standard protein mixture. Despite the promising combination of NPs with polymeric monoliths, most examples of application of these novel hybrid supports are described in the chromatographic area (Hilder, 2004; Cao, 2010; Xu, 2010; Lv, 2012). However, studies of polymeric monoliths modified with NPs for peptide and protein enrichment purposes have been reported (Rainer, 2008; Alwael, 2011; Cao, 2010; Xu, 2010; Lv, 2012). Thus, Rainer *et al.* (Rainer, 2008) formed a polymer monolith within a pipette-tip with incorporated titanium dioxide nanoparticles for the selective enrichment of phosphopeptides.

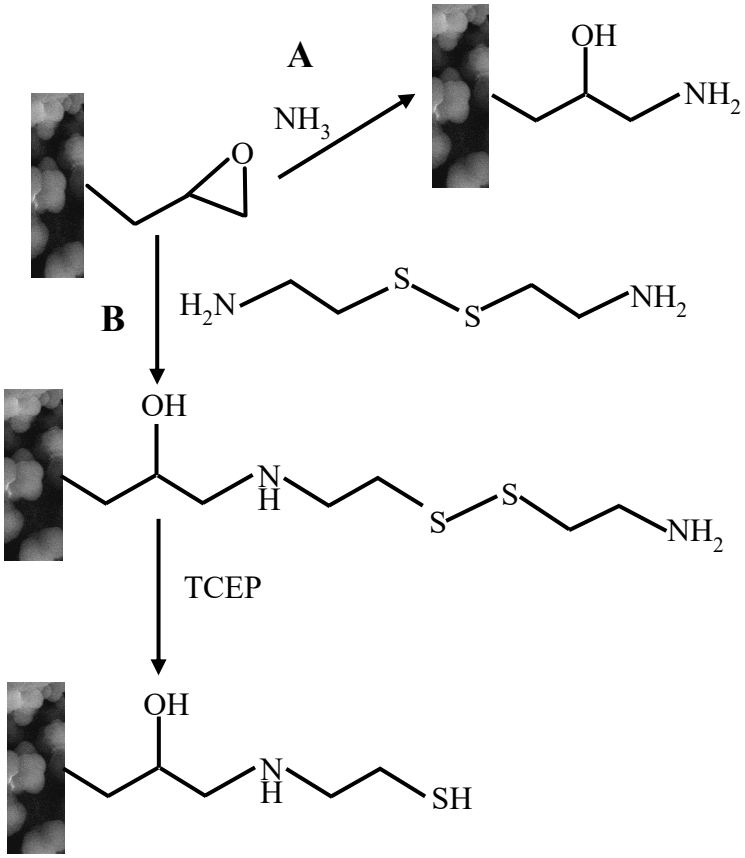

Figure 4.7. Reaction scheme of functionalization of poly(GMA-co-EDMA) material with A) ammonia and B) cystamine.

Moreover, Hussain *et al*. (Hussain 2013, Hussain 2014) have carried out the extraction of thionins (sulphur-rich proteins) using hollow-monolithic extraction tips based on poly(PS-DVB) with embedded zirconium silicate nano-powder and aluminum silicate powder as a sorbent in extraction columns. Xu *et al.* (Xu, 2010) has synthesized a gold modified polymeric monolith to selectively capture and separate cysteine-containing peptides in capillary format. Alwael *et al.* (Alwael, 2011) have also demonstrated the potential of a gold modified polymeric material to isolate glycoproteins. Although in most of these reports satisfactory enrichment of target analytes was achieved, in the fabrication process of nano-structured polymeric

monoliths, most part of NPs were buried within polymeric network or only partially exposed at the polymeric surface leading to limitations on loading capacity. Besides, the extraction systems developed were prepared in pipette-tips or capillary format, being desirable its extension to larger formats (such syringe, cartridges or disks) in order to exploit its full adsorption properties.

In this thesis, the development of polymeric materials modified with AuNPs (**Chapter 6 and 7**) or AgNPs (**Chapter 7**) for selective and effective extraction of several proteins and peptides using cartridges as SPE supports has been described.

4.3. Enzyme-assisted extraction

In recent years, enzyme-assisted extraction methods have gained attention as an effective tool to improve the extraction yield of bioactive compounds. The mechanism that makes the enzymes able to extract intracellular compounds is based on the hydrolysis and subsequently degradation of the cell wall constituents, rendering the intracellular materials more accessible for extraction (Li, 2006).

The main advantage of using enzyme-assisted extraction methods is that they are considered to be environmentally friendly processes. The analytes can be extracted from many complex matrices by using water as extraction medium instead of organic solvents. Moreover, the enzyme-assisted methods eliminate the use of solvent consumption reducing the investment cost and increase the yield of extractable compounds (Rosenthal, 1996; Sharma, 2002; Gibbins, 2012).

There are several parameters that can affect the enzyme-assisted recovery such as enzyme content, extraction temperature, extraction time and pH. For

this reason, these parameters need to be optimized. With regard to extraction temperature and pH, they are important parameters, since the enzyme can become inactivated at high temperatures or extreme pH conditions, thus giving low recoveries (Gupta, 1993). As previously mentioned, the enzyme content should be also evaluated in order to obtain good recoveries. Many authors have observed that high amounts of enzyme did not produce an improvement of the extraction yield (Fu, 2008; Shen, 2008). This fact is explained taking into account the so-called competitive inhibition, in which the extracted molecules are supposed to act as inhibitors combining with the enzyme to form a complex and thereby preventing its activity (Laidler, 1973).

Since the field of enzyme-assisted extraction has increased in the last decade, several types of enzymes are commercially available to perform this process. The types and combination of enzymes depend on the nature of raw materials (Puri, 2012). A brief description of the enzymes used in this thesis is next included.

4.3.1. Type of enzymes

Hydrolitic enzymes. This group is constituted by cellulases, beta-glucosidases and pectinases. They play an important role in hydrolyzing cellulose, hemi-cellulose and pectins from the cell walls (Fu, 2008). Thus, cellulase and hemicellulase enhanced the oil yield extracted from oilseeds with high cellulose and hemicellulose content (Sharma, 2012; Gibbins, 2012).

Lipolytic enzymes. Lipases and phospholipases are included in this group. These enzymes hydrolyze hydrophobic ester linkages of triacylglycerols and phospholipids. Lipases have been commonly used for the preparation of enantiomeric compounds ranging from pharmaceutical intermediates to neutraceuticals (Gotor-Fernández, 2006). On the other hand, phospholipases

produce 2-acyl lysophospholipids and hydrolyzed lecithin products for food compositions (Mishra, 2009).

Proteolytic enzymes. Proteases are able to partially hydrolyze proteins and convert them to peptides or even aminoacids. Thus, their action can cause a breakdown in the protein network feature of the cotyledon cells cytoplasm, and in the protein (oleosin)-based membranes that surround the lipid bodies thereby liberating more quantity of the oil (Roshental, 2001).

4.3.2. Application of enzyme-assisted methods

The use of enzyme-assisted extraction has been mostly described in literature to extract several bioactive compounds such as polyphenols, carotenoids, carbohydrates, oils and proteins from a variety of sources (plants, bacteria, fungi, algae and animals) (Fu, 2008; Moura, 2008; Latif, 2011; Camargo, 2016). The specific details of enzyme-assisted extractions vary with the biomolecules of interest and its source material.

Among all the bioactive compounds, proteins are the most important as a nutritional and dietary supplement. Proteins and peptides together contribute as major constituents of regular food and can be obtained from plants as well as from animal sources. The presence of indigenous proteases in plant tissue makes the extraction of proteins complicated (Puri, 2012). Proteins are usually found in protein bodies (also called as aleurone grains) inside the cells. Hence, the complete solubilization and extraction of proteins depends on cell disruption. The method used for cell disruption depends on the types of plant material used (leaf, fruit, root, seed, etc.) or even on the stage of development of plant.

A number of chemical methods (using alkaline treatments or solvents such as hexane, acidified alcohol, and chloroform) have been used for the disruption of cells and protein extraction. However, these classical methods

have several trackbacks, including safety and environmental aspects, high energy input and low product recovery. In this sense, as previously mentioned, aqueous extraction process using enzyme represents a promising alternative.

The extraction yield of proteins can further be increased by using enzyme-assisted aqueous extraction. Different cellulases can be used to release proteins from raw materials. Guan *et al.* (Guan, 2008) used viscozyme L to hydrolyze the cell wall by cleaving the linkages within polysaccharides that effectively release intracellular protein from oat bran. Jung *et al.* (Jung, 2006) showed successful use of pectinase to improve extractability of soy protein without protein degradation. The protein recovery was increased by 50% as compared to control with improved foam stability. Recently, the focus has been shifted to use proteases to hydrolyze the proteins partially and convert them to peptides. This increases the solubility of peptides making their extraction effective. Oil seed meal that is obtained as by-product after meal production is a potential source of protein. Proteases have been used to extract proteins from oilseed meals such as rapeseed, soybeans, and microalgae meals. The addition of proteases enhances the yield of protein extraction to 90% from soybean meals (Siow, 2013; Ngoh, 2016), rapeseeds and microalgae meals (Sari, 2013) and sesame seeds (Latif, 2011). The use of proteases has also been explored for the extraction of peptides of interest for various pharmacological actions (Sari, 2013).

In this thesis, we have investigated the enzyme-assisted extraction of proteins from *Citrus* fruits and olive materials (pulp, peel, leaf, and stone (**Chapters 8, 9 and 10**). In particular, commercial enzymes such as cellulase, lipase, phospholipase and a mixture of very different enzymes (arabanase, cellulase, beta-glucanase and hemicellulose) have been applied to these vegetal matrices.

4.4. Combinatorial peptide ligand libraries (CPLLs)

Evidencing low-abundance proteins (LAPs) from any kind of sample always remains a challenging task. Thus, minimizing the presence of high-abundance proteins (HAPs) has attracted the attention of scientists and contributed to important findings about interesting biomarkers. Methodologies based on sample pretreatment or prefractionation have been developed over the years in an attempt to minimize protein overload. In addition, immunosorbents have been also employed to minimize the presence of HAPs with a potential risk of protein depletion and a subsequently loss of hundreds of proteins (Boschetti, 2012; Righetti, 2015). As an alternative to these methods, CPLLs have been proposed by Righetti and coworkers (D'Amato, 2010, D'Amato, 2011; Fasoli, 2010A; Fasoli, 2011; Esteve, 2012; Lerma-García, 2015), as a well-established technique to enrich LAPs in complex samples. This approach consists in the use of peptide ligand libraries in peptides made of different mixtures of amino acids with different lengths (comprised between 4 to 6, being this last one size the best) (Santucci, 2012). These set of hexapeptides are covalently bound to chromatographic supports (porous silica beads). Each bead carries a large number (billions) of copies of the same peptide bait; the beads are thus different from each other, and all combinations of hexapeptides are present. Depending on the number of amino acids used, a library contains a population of millions of different ligands. When a complex protein extract is exposed to such a ligand library under large overloading conditions, each bead with affinity to an abundant protein will rapidly become saturated, and the vast majority of the same protein will remain unbound. In contrast, trace proteins will not saturate the corresponding partner beads, but are captured in progressively increasing amounts as the beads are loaded with additional protein extract. (**Figure 4.8**) As a result, LAPs are enriched on basis of the normalization effect on the protein abundance in an entire proteome,

concretely, reducing the concentration of the most abundant components, while enhancing the concentration of the most diluted species. The type and the topology of interaction points are at the origin of the specificity of interaction for the targeted proteins.

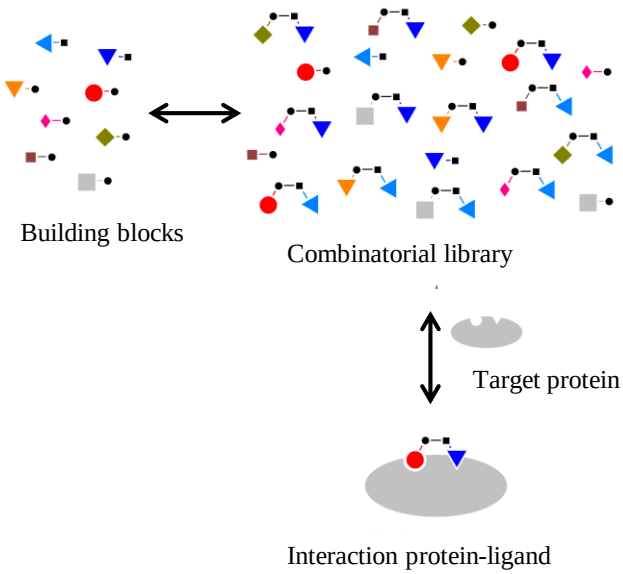

Figure 4.8. Principle of protein-ligand library interaction.

CPLLs methodology requires a strict control of several parameters as pH, ionic strength and temperature since they play an important role that can influence the thermodynamic equilibria (Fasoli, 2010A). However, its use allows the access to very LAPs to a level at which they would be detectable and identifiable via standard analytical tools, such as an ELISA test or MS.

The applicability and feasibility of CPPLs have been demonstrated since they have been widely applied to many types of matrices as orine (Castagna, 2005), serum (Sennels, 2007), human eritrocites (Roux-Dalvai, 2008), vegetable tissues (Boschetti, 2009), and also to detect rare protein impurities in rADN used for human consumption products (Antonioli, 2007). In

addition to those reported by the scientific community (especially in the bio-medical field), Righetti's group has focused their on the analysis of a variety of foodstuff such as wine (Cereda, 2010; D'Amato, 2010), beer (Fasoli, 2010B), almond milk (Fasoli, 2011), vinagre de vino blanco (Di Girolamo, 2011), cola drink (D'Amato, 2011), cocnut milk (D'Amato, 2012), Ginger drink (Fasoli, 2012A), Braulio aperitif (Fasoli, 2012B), orange juice (Lerma-García, 2015) and olive oil (Esteve, 2012). In this thesis, CPLLs were employed frowe applied for proteomic characterization of mistletoe samples (**Chapter 11**).

4.5. References

Abdel-Rehim, M.; Andersson, M.; Portelius, E.; Norsten, C.; Blomberg, L.G. (**2001**). Determination of ropivacaine and its metabolites in human plasma using solid phase microextraction and GC-NPD/GC-MS. *Journal of Microcolumn Separations, 13,* 313-321.

Adams, T.; Unger, K.K.; Dittmann, M.M.; Rozing, G.P. (**2000**). Towards the column bed stabilization of columns in capillary electroendosmotic chromatography: Immobilization of microparticulate silica columns to a continuous bed. *Journal of Chromatography A, 887,* 327-337.

Alwael, H.; Connolly, D.; Clarke, P.; Thompson, C.; Twamley, B.; O'Connor, B.; Paull, B. (**2011**). Pipette-tip selective extraction of glycoproteins with lectin modified gold nano-particles on a polymer monolithic phase. *Analyst, 136,* 2619-2629.

Antonioli, P.; Fortis, F.; Guerrier, L.; Rinalducci, S.; Zolla, L.; Righetti, P.G.; Boschetti E. (**2007**). Capturing and amplifying impurities from purified recombinant monoclonal antibodies via peptide library beads: a proteomic study. *Proteomics, 7,* 1624-33.

Aoki, H.; Kubo, T.; Ikegami, T.; Tanaka, N.; Hosoya, K.; Tokuda, D.; Ishizuka, N. (**2006**). Preparation of glycerol dimethacrylate-based polymer monolith with unusual porous properties achieved via viscoelastic phase separation induced by monodisperse ultra high molecular weight poly(styrene) as a porogen. *Journal of Chromatography A, 1119,* 66-79.

Bedair M.; El Rassi, Z. (**2004**). Recent advances in polymeric monolithic stationary phases for electrochromatography in capillaries and chips. *Electrophoresis, 25*, 4110-4119.

Bernabé-Zafón, V.; Cantó-Mirapeix, A.; Simó-Alfonso, E.F.; Ramis-Ramos G.; Herrero-Martínez, J.M. (**2009**). Photo-polymerized lauryl methacrylate monolithic columns for CEC using lauroyl peroxide as initiator. *Electrophoresis, 1929*, 3748-5376.

Boschetti, E.; Righetti P.G. (**2012**). Breakfast at Tiffany's? Only with a low-abundance proteomic signature! *Electrophoresis, 33*, 2228-2239.

Camargoa, A.; Aparecida M.; Regitano-d'Arceb,M.; Camarão Telles Biasotoc A.; Shahidia, F. (**2016**). Enzyme-assisted extraction of phenolics from winemaking by-products: Antioxidant potential and inhibition of alpha-glucosidase and lipase activities. *Food Chemistry, 212*, 395-402.

Cantó-Mirapeix, A. Herrero-Martínez, J.M. Mongay-Fernández, C. Simó-Alfonso, E.F. (**2009B**). CEC column behaviour of butyl and lauryl methacrylate monoliths prepared in non-aqueous media. *Electrophoresis, 30*, 607-615.

Cantó-Mirapeix, A.; Herrero-Martínez, J.M.; Mongay-Fernández, C.; Simó-Alfonso, E.F. (**2008**). preparation and evaluation of butyl acrylate-based monolithic columns for cec using ammonium peroxodisulfate as a chemical initiator. *Electrophoresis, 29*, 3858-3865.

Cantó-Mirapeix, A.; Herrero-Martínez, J.M.; Mongay-Fernández, C.; Simó-Alfonso, E.F. **(2009A)**. Chemical initiation for butyl and lauryl acrylate monolithic columns for CEC. *Electrophoresis, 30*, 599-606

Cao, Q.; Xu, Y.; Liu, F.; Svec, F.; Frechet, J.M.J. (**2010**). Polymer monoliths with exchangeable chemistries: use of gold nanoparticles as intermediate ligands for capillary columns with varying surface functionalities, *Analytical Chemistry, 82*, 7416-7421.

Carrasco-Correa, E.J.; Ramis-Ramos, G.; Herrero-Martínez, J.M. (**2013**). Methacrylate monolithic columns functionalized with epinephrine for capillary electrochromatography applications. *Journal of Chromatography A, 129*, 61-67.

Carrasco-Correa, E.J.; Ramis-Ramos, G.; Herrero-Martínez, J.M. (**2015**). Hybrid methacrylate monolithic columns containing magnetic nanoparticles for capillary electrochromatography. *Journal of Chromatography A, 1385*, 77-84.

Castagna, A.; Cecconi, D.; Sennels, L. (**2005**). Exploring the hidden human urinary proteome via ligand library beads. *Journal of Proteome Research, 4*, 1917-1930.

Cereda, A.; Kravchuk, A.V.; D'Amato, A.; Bachi, A.; Righetti, P.G. (**2010**). Proteomics of wine additives: mining for the invisible via combinatorial peptide ligand libraries. *Journal of Proteomics, 73,* 1732-1739.

D'Amato, A.; Fasoli, E.; Kravchuk, A.V.; Righetti, P.G. (**2011**). Going Nuts for Nuts? The Trace Proteome of a Cola Drink, as Detected via Combinatorial Peptide Ligand Libraries. *Journal of Proteome Research, 10,* 2684-26896.

D'Amato, A.; Fasoli, E.; Righetti, P.G. (**2012**). Harry Belafonte and the secret proteome of coconut milk. *Journal of Proteomics, 75*, 914-920.

D'Amato, A.; Kravchuk, A.V.; Bachi, A.; Righetti, P.G. (**2010**). Noah's nectar: The proteome content of a glass of red wine. *Journal of Proteomics, 73*, 2370-2378.

Di Girolamo, F.; D'Amato, A.; Righetti, P.G. (**2011**). Horam nonam exclamavit: sitio. The trace proteome of your daily vinegar. *Journal of Proteomics, 75*, 718-724.

Du, Z.; Yu Y.L.; Chen, X.W.; Wang, J.H. (**2007**) The isolation of basic proteins by solid-phase extraction with multiwalled carbon nanotubes. *Chemical European Jouranl, 13*, 9679-9685.

Eeltink, S.; Hilder, E.F.; Geiser, L.; Svec, F.; Fréchet, J.M.J.; Rozing, G.P.; Schoenmakers, P.J.; Kok, W.T. (**2007**). Controlling the surface chemistry and chromatographic properties of methacrylate-ester based monolithic capillary columns via photografting. *Journal of Separation Science, 30,* 407-413.

Esteve, C.; D'Amato, A.; Marina, M.L.; García, M.C.; Citterio, A.; Righetti, P.G. (**2012**). Identification of olive (*Olea europaea*) seed and pulp proteins by nLC-MS/MS via combinatorial peptide ligand libraries. *Journal of Proteomics, 75,* 2396-2403.

Fasoli, E.; Aldini, G.; Regazzoni, L.; Kravchuk, A.V.; Citterio, A.; Righetti, P.G. (**2010B**). Les Maîtres de l'Orge: the proteome content of your beer mug. *Journal of Proteome Research, 9,* 5262-5269.

Fasoli, E.; D'Amato, A.; Citterio, A.; Righetti, P.G. (**2012**). Anyone for an aperitif? Yes, but only a Braulio DOC with its certified proteome. *Journal of Proteomics, 75,* 3374-3379.

Fasoli, E.; D'Amato, A.; Citterio, A.; Righetti, P.G. (**2012**). Ginger Rogers? No, Ginger Ale and its invisible proteome. *Journal of Proteomics, 75,* 1960-1965.

Fasoli, E.; D'Amato, A.; Kravchuk, A.V.; Citterio, A.; Righetti, P.G. (**2011**). In-depth proteomic analysis of non-alcoholic beverages with peptide ligand libraries. I: Almond milk and orgeat syrup. *Journal of Proteomics, 74,* 1080-1090.

Fasoli, E.; Farinazzo, A.; Sun, C.J.; Kravchuk, A.V.; Guerrierc, L.; Fortis, F.; Boschetti, E.; Righetti. P.G. (**2010A**). Interaction among proteins and

peptide libraries in proteome analysis: pH involvement for a larger capture of species. *Journal of Proteomics, 73*, 733-742.

Frankovic, V.; Podgornik, A.; Kranjc, N.L.; Smrekar, F.; Krajnc, P.; Strancar, A. (**2008**). Characterisation of grafted weak anion-exchange methacrylate monoliths. *Journal of Chromatography A, 1207*, 84-93..

Fu, Y.J.; Liu W.; Zu, Y.G. (**2008**). Enzyme assisted extraction of luteolin and apigenin from pigeonpea (*Cajanus cajan (L.) Millsp.)* leaves. *Food Chemistry*, *111*, 508–512.

Gibbins, R.D. Aksoy, H. Ustun. GA.. (**2012**). Enzyme-assisted aqueous extraction of safflower oil: optimisation by response surface methodology. *International Journal of Food Science and Technology, 47,* 1055–1062

Gotor-Fernández, V.; Brieva, R.; Gotor. V. (**2006**). Lipases: Useful biocatalysis for the preparation of pharmaceuticals. Journal of Molecular *Catalysis B: Enzymatic, 40*, 111-120

Guan, X.; Yao, H. (**2008**). Optimization of Viscozyme L-assisted extraction of oat bran protein using response surface methodology. *Food Chemistry, 106*, 345-351.

Guerrouache, M.; Mahouche-Chergui S.; Chehimi, M.M.; Carbonnier, B. (**2012**). Site-specific immobilisation of gold nanoparticles on a porous monolith surface by using a thiol–one click photopatterning approach. *Chemical Communications, 48*, 7486-7488.

Guiochon, G. (**2007**). Monolithic columns in high-performance liquid chromatography. *Journal of Chromatography A, 1168*, 101-168.

Gupta, S.; Gupta, M.N. (**1993**). Mechanisms of Irreversible Thermoinactivation and Medium Engineering, in Thermostability of

Enzymes. Edited by M.N. Gupta, Narosa, India/Springer Verlag, Germany,114-142.

Gusev, I. Huang X. Horváth, C. (**1999**). Capillary columns with in situ formed porous monolithic packing for micro high-performance liquid chromatography and capillary electrochromatography. *Journal of Chromatography A, 855,* 273-290.

Hilder, E.F.; Svec, F.; Fréchet, J.M.J. (**2004**) Latex-functionalized monolithic columns for the separation of carbohydrates by micro anion-exchange chromatography. *Journal of Chromatography A, 1053,* 101-106.

Hjerten, S. Liao, J.L. Zhang R. (**1989**). High-performance liquid chromatography on continuous polymer beds. *Journal of Chromatography A, 473,* 273-289.

Hussain, S.; Güzel, Y.; Pezzei, C.; Rainer, M.; Huck, C.W.; Bonn, G.K. (**2014**). Solid-phase extraction of plant thionins employing aluminum silicate based extraction columns. *Journal of Separation Science, 37,* 2200-2207

Hussain, S.; Güzel, Y.; Schönbichler, S.A.; Rainer, M.; Huck, C.W.; Bonn, G.K. (**2013**). Solid-phase extraction method for the isolation of plant thionins from European mistletoe, wheat and barley using zirconium silicate embedded in poly(styrene-co-divinylbenzene) hollow-monoliths. *Analytical Bioanalytical Chemistry, 405,* 7509-7521.

Hyötyläinen, T. (**2009**). Critical evaluation of sample pretreatment techniques. *Analytical and Bioanalytical Chemistry, 394,* 743-758.

Joldsvendová, P.; Coulfal, P.; Suchánková, J.; Tesaøová, E.; Bosáková, Z. (**2003**). Methacrylate monolithic columns for capillary liquid

chromatography polymerized using ammonium peroxodisulfate as initiator. *Journal of Separation Science, 26,* 1623-1628.

Jung, S.; Lamsal, B.P.; Stepien, V.; Johnson, L.A.; Murphy, P.A. (**2006**). Functionality of soy protein produced by enzyme-assisted extraction. *Journal of the American Oil Chemists' Society, 83*, 71–78.

Klampfl, C.W. (**2007**). Review coupling of capillary electrochromatography to mass spectrometry. *Journal of Chromatography A, 1044*, 131-144.

Krenkova, J.; Lacher, N.A.; Svec, F. (**2010**). Control of selectivity via nanochemistry: monolithic capillary column containing hydroxyapatite nanopaticles for separation of proteins and enrichment of phosphopeptides, *Analytical Chemistry, 82*, 8335-8341.

Laidler, K.J., Bunting, P.S. (**1973**). The chemical kinetics of enzyme action (2nd ed.). Clarendon Press.

Latif, S.; Diosady, L.L.; Anwar, F. (**2008**). Enzyme-assisted aqueous extraction of oil and protein from canola (*Brassica napus L.*) seeds. *European Journal of Lipid Science and Technology. 110,* 887–892

Leinweber, F.C.; Lubda, D.; Cabrera, K.; Ulrich, T. (**2002**). Characterization of Silica-Based Monoliths with Bimodal Pore Size Distribution. *Analytical Chemistry, 74*, 2470-2477.

Leinweber, F.C.; Tallarek, U. (**2003**). Chromatographic performance of monolithic and particulate stationary phases: Hydrodynamics and adsorption capacity. *Journal of Chromatography A, 1006,* 207-228.

Lerma-García, M.J.; D'Amato, A.; Simó-Alfonso, E.F.; Righetti, P.G.; Fasoli, E. (**2016**). Orange proteomic fingerprinting: From fruit to commercial juices. *Food Chemistry, 196,* 739–749

Li, B.B.; Smith, B.; Hossain, M.M. (**2006**). Extraction of phenolics from citrus peels II. Enzyme-assisted extraction method. *Separation and Purification Technology, 48,* 189-196.

Li, W. (**2012**). Novel hybrid organic-inorganic monolithic column containing mesoporous nanoparticles for capillary electrochromatography. *Talanta 98,* 277-281.

Lin, Z.; Yang, F.; He, X.; Zhao, X.; Zhang, Y. (**2009**). Preparation and evaluation of a macroporous molecularly imprinted hybrid silica monolithic column for recognition of proteins by high performance liquid chromatography. *Journal of Chromatography A, 1216,* 8612-8622.

Lingeman H.; Hoekstra-Oussoren, S.J.F. (**1997**). Particle-loaded membranes for sample concentration and/or clean-up in bioanalysis. *Journal of Chromatography B, 689,* 221-237.

Luo Q.; Shen, Y.; Hixson, K.K.; Zhao, r.; Yang, F.; Moore, R.J.; Mottaz, H.M.; Smith, R.D. (**2005**). Preparation of 20-μm-i.d. silica-based monolithic columns and their performance for proteomics analyses. *Analytical Chemistry, 77*, 5028-5035.

Lv, Y.; Maya, A.; Frechet, J.M.J.; Svec, F. (**2012**). Preparation of porous polymer monoliths featuring enhanced surface coverage with gold nanoparticles, *Journal of Chromatography A, 1261*, 121-128.

Merhar, M.; Podgornik, A.; Barut, M.; Žigon, M.; Štrancar, A. (**2003**). Methacrylate monoliths prepared from various hydrophobic and hydrophilic monomers – Structural and chromatographic characteristics. *Journal of Separation Science, 26,* 322-330.

Minakuchi, H.; Nakanishi, K.; Soga, N.; Ishizuka, N.; Tanaka, N. (**1996**). Octadecylsilylated Porous silica rods as separation media for reversed-phase liquid chromatography, *Analytical Chemistry, 68,* 3498-3501.

Mishra, M.K.; Kumaraguru, T.; Sheelu, G.; Fadnavis N.W. (**2009**). Lipase activity of Lecitase Ultra: characterization and applications in enantioselective reactions. *Tetrahedron: Asymmetry, 20,* 2854-2860.

Miyazakia, S.; Morisatob, k.; Ishizuka, N.; Minakuchi, H.; Shintani, Y.; Furuno, M.; Nakanishi, K. (**2004**). Development of a monolithic silica extraction tip for the analysis of proteins. *Journal of Chromatography A, 1043,* 19-25.

Nakanishi, K.; Minakuchi, H.; Soga, N.; Tanaka, N. (**1997**). Double pore silica gel monolith applied to liquid chromatography. *Journal of Sol-Gel Science and Technology, 8,* 547-581.

Navarro-Pascual-Ahuir, M.; Lerma-García, M.J.; Ramis-Ramos, G.; Simó-Alfonso, E.F.; Herrero-Martínez, J.M. (**2013**). Preparation and evaluation of lauryl methacrylate monoliths with embedded silver nanoparticles for capillary electrochromatography. *Electrophoresis, 34,* 925-934,

Nema, T.; Chan E.; Ho, P. (**2010**). Application of silica-based monolith as solid phase extraction cartridge for extracting polar compounds from urine. Talanta, 82, 488-494.

Nema, T.; Chan, E.C.Y.; Ho, P.C. (**2014**). Applications of monolithic materials for sample preparation. *Journal of Pharmaceutical and Biomedical Analysis, 87,* 130-141.

Ngoh, Y.Y.; Gan, C.Y. (**2016**). Enzyme-assisted extraction and identification of antioxidative and a-amylase inhibitory peptides from pinto beans (Phaseolus vulgaris cv. Pinto). *Food Chemistry, 190,* 331–337.

Nováková, L.; Vlcková, H. (**2009**). A review of current trends and advances in modern bio-analytical methods: chromatography and sample preparation. *Analytica Chimica Acta, 656,* 8-35.

Peters, E.C. Petro, M. Svec, F. Frechet, J.M.J. (**1998**). Molded rigid polymer monoliths as separation media for capillary electrochromatography. 1. Fine Control of porous properties and surface chemistry. *Analytical Chemistry, 70,* 2288-2295.

Petro, M. Svec, F. Fréchet, J.M.J. (**1996**). Molded continuous poly(styrene-co-divinylbenzene) rod as a separation medium for the very fast separation of polymers Comparison of the chromatographic properties of the monolithic rod with columns packed with porous and non-porous beads in high-performance liquid chromatography of polystyrenes. *Journal of Chromatography A, 752,* 59-66.

Puri, M.; Sharma, D.; Barrow, C.J. (**2012**). Enzyme-assisted extraction of bioactives from plants. *Trends in Biotechnology, 30,* 37-44.

Rainer, M.; Sonderegger, H.; Bakry, R.; Huck, C.K.; Morandell, S.; Huber, L.A.; Gjerde, DT.; Bonn, G.K. (**2008**). Analysis of protein phosphorylation by monolithic extraction columns based on poly(divinylbenzene) containing embedded titanium dioxide and zirconium dioxide nano-powders. *Proteomics, 8,* 4593-4602.

Righetti, P.G.; Candiano, G.; Citterio, A.; Boschetti, E. (**2015**). Combinatorial peptide ligand libraries as a "Trojan Horse" in deep discovery proteomics. *Analytical Chemistry, 87*, 293-305.

Rosenthal, A.; Pyle, D.L.; Niranjan, K.; Gilmour, S.; Trinca. L. (**2001**). Combined effect of operational variables and enzyme activity on aqueous enzymatic extraction of oil and protein from soybean. *Enzyme and Microbial Technology, 28,* 499–509

Roux-Dalvai, F.; González de Peredo, A.; Simó, C. (**2008**). Extensive analysis of the cytoplasmic proteome of human erythrocytes using the

peptide ligand library technology and advanced mass spectrometry. *Molecular & Cellular Proteomics, 7,* 2254-2270.

Santucci, L.; Candiano, G.; Bruschi, M.; D'Ambrosio, C.; Petretto, A.; Scaloni, A.; Urbani, A.; Righetti, P.G.; Ghiggeri, G.M. (**2012**). Combinatorial peptide ligand libraries for the analysis of low-expression proteins: Validation for normal urine and definition of a first protein MAP. *Proteomics, 12,* 509-515.

Sari, Y.W. Bruins, M.E.; Sanders, J.P.M. (**2013**). Enzyme assisted protein extraction from rapeseed, soybean, and microalgae meals. *Industrial Crops and Products, 43*, 78–83.

Saunders, K.C.; Ghanem, A.; Hon, B.; Hilder, F.E.; Haddad, P.R. (**2009**). Separation and sample pre-treatment in bioanalysis using monolithic phases: A review. *Analytica Chimica Acta, 652*, 22-31.

Sennels, L.; Salek, M.; Lomas, L. (**2007**) Proteomic analysis of human blood serum using peptide library beads. *Journal of Proteome Research, 6*, 4055-4062.

Sharma, A.; Khare, S.K. Gupta, M.N. (**2002**). Enzyme-Assisted Aqueous Extraction of Peanut Oil. *Journal of the American Oil Chemists' Society, 79*, 215-218.

Shen G.; Lee, H.K. (**2001**). Hollow fiber-protected liquid-phase microextraction of triazine herbicides. *Analytical Chemistry, 74*, 648-654.

Shen, L.; Wang, X.; Wang, Z.; Wua, Y.; Chen, J. (**2008**). Studies on tea protein extraction using alkaline and enzyme methods. *Food Chemistry, 107*, 929-938.

Simpson, N. (**2000**). Solid-Phase Extraction: Principles, Techniques, and Applications, Marcel Dekker, New York.

Siow, H.L.; Gan, C.Y. (**2013**). Extraction of antioxidative and antihypertensive bioactive peptides from Parkia speciosa seeds. *Food Chemistry, 141,* 3435–3442.

Stachowiak, T.B.; Rohr, T.; Hilder, E.F.; Peterson, D.S.; Yi, M.; Svec, F.; Fréchet, J.M. (**2003**). Fabrication of porous polymer monoliths covalently attached to the walls of channels in plastic microdevices. *Electrophoresis. 24*, 3689-93.

Svec, F. (**2004**). Preparation and HPLC applications of rigid macroporous organic polymer monoliths. *Journal of Separation Science, 27,* 747-766.

Svec, F. (**2006**). Less common applications of monoliths: Preconcentration and solid-phase extraction. *Journal of Chromatography B, 841,* 52-64.

Svec, F. (**2010**). Porous polymer monoliths: Amazingly wide variety of techniques enabling their preparation. *Journal of Chromatography A, 1217,* 902-924.

Svec, F.; Frechet, J.M.J. (**1992**). Continuous rods of macroporous polymer as high-performance liquid chromatography separation media. *Analytical Chemistry, 64,* 820-829.

Thabano, J.R. (**2009**). Silica nanoparticle-templated methacrylic acid monoliths for in-line solid-phase extraction-capillary electrophoresis of basic analytes. *Journal of Chromatography A, 1216,* 4933-4940.

Valcárcel, M.; Simonet, B.M.; Cárdenas, S.; Suárez, B. (**2005**). Present and future applications of carbon nanotubes to analytical science. *Analytical and Bioanalytical Chemistry, 382,* 1783-1790.

Vas, G.; Vékey, K. (**2004**). Solid-phase microextraction: a powerful sample preparation tool prior to mass spectrometric analysis. *Journal of Mass Spectrometry, 39,* 2333-2354.

Viklund, C.; Svec, F.; Fréchet, J.M.J.; Irgum, K. (**1996**). Monolithic, "molded", porous materials with high flow characteristics for separations, catalysis, or solid-phase chemistry: control of porous properties during polymerization. *Chemistry of Materials, 8* 744-750.

Wang, Q.C.; Svec, F.; Fréchet, J.M.J. (**1995**). Hydrophilization of porous polystyrene-based continuous rod column. *Analytical Chemistry, 67,* 670-674.

Wen, L. (**2012**). Hybrid monolithic columns with nanoparticles incorporated for capillary electrochromatography. *Journal of Chromatography A, 1239,* 67-71.

Xu, Y.; Cao, Q.; Svec, F.; Fréchet, J.M.J. (**2010**). Porous polymer monolithic column with surface-bound gold nanoparticles for the capture and separation of cysteine-containing peptides. *Analytical Chemistry, 82,* 3352-3358.

Zou, H.; Huang, X.; Ye M.; Luo, Q. (**2002**). Monolithic stationary phases for liquid chromatography and capillary electrochromatography. *Journal of Chromatography A, 954,* 5-32.

Chapter 5. Analytical techniques

5.1. HPLC

HPLC is a well-known separation technique, in which analytes are separated on the basis of different solubilities between a liquid mobile phase and a solid stationary phase. Thus, the mobile phase is forced through a column by a pumping system, and the stationary phase is constituted by porous particles densely packed inside the column (**Figure 5.1**).

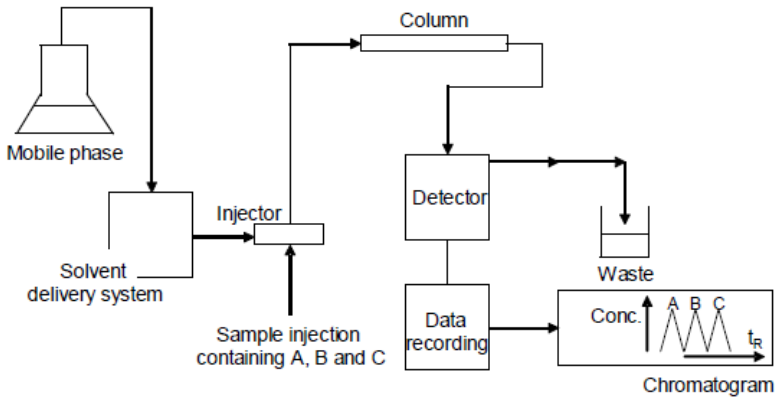

Figure 5.1. Block diagram of the components of a liquid chromatograph.

Within the HPLC modes, RP is the most widely used due to its large flexibility. Since it has a hydrophobic stationary phase, this modality has been used to separate both non-polar and polar compounds.

With regard to detection, HPLC coupled to a UV or DAD is the simplest and the most popular technique employed to detect and identify a wide range of solutes. Thus, UV or DAD detectors are commonly used to identify compounds containing chromophore groups such as phenolic compounds, flavonoids, carotenoids, proteins or peptides.

The employment of ELSD has experimented an increase in the last years, since it is an alternative of detection of non-chromophore groups. The main

advantages of using ELSD are related to its ability to be a mass sensitive detector that responds to any analyte less volatile than the mobile phase. In addition, it is compatible with a broad range of solvents and it is independent of the chain length unsaturation degree. In this thesis, a HPLC method with hyphenated UV and ELSD detection is described for simultaneous determination of tryacylglycerols (**Chapter 14**).

5.2. Electromigration techniques

Electromigration techniques are characterized by the separation of components of a sample (on the basis of differential ion migration) through a support (gel, capillary, etc.) under the influence of an electric field.

Classical electromigration methods (i.e. conventional electrophoresis and isoelectric focusing) have been in use for years to separate biomolecules and their fragments. Also, the separations achieved in narrow fused silica capillaries (25 to 100 μm i.d.) (namely capillary electromigration techniques) have proved to be highly effective and very attractive. These techniques present several advantages such as short analysis times and extremely high separation efficiencies (from 100.000 up to few millions theoretical plates). Other important features are the capability to handle micro samples (1 to 50 nL are injected), low reagent consumption and high flexibility. In addition, automated commercial instrumentation is available, which allows repeatable and reliable operation in routine analysis.

Due to the numerous techniques available, in this thesis, only those techniques employed in this thesis will next briefly described. These techniques are: sodium dodecyl sulfate polyacrylamide gel electrophoresis (SDS-PAGE), capillary zone electrophoresis (CZE), capillary gel electrophoresis (CGE) and capillary electrochromatography (CEC).

5.2.1. SDS-PAGE

This technique has been employed in protein and peptide separation. The separation of analytes (by electrophoresis) uses discontinuous polyacrylamide gels as a support medium and SDS to denature the proteins. In SDS-PAGE, molecules are separated according to their molecular sizes.

Polyacrylamide gels are composed of acrylamide (monomer) chains with interconnections formed from the methylenebisacrylamide (crosslinker). The polymerization, which proceeds via a free-radical mechanism, requires also ammonium persulfate (APS) in the presence of the tertiary aliphatic amine N,N,N',N'-tetramethylethylenediamine (TEMED) to produce free oxygen radicals (**Figure 5.2).** To describe the polyacrylamide gel composition, a standard nomenclature has been widely adopted. Concretely, T constutites the total percentage concentration (w/v) of monomer (acrylamide plus crosslinker) in the gel, and the term C refers to the percentage of the total monomer represented by the crosslinker. Moreover, it is possible controlling the pore size of gel by changing the T and C values. For example, an increase in the T value leads to a decrease in pore size, allowing the separation of small molecules.

In SDS-PAGE, proteins are denatured by treating the sample with the surfactant SDS. Proteins bind the detergent uniformly along their length to a level of 1.4 g SDS/g protein, thus losing their secondary, tertiary or quaternary structure. Moreover, by the addition of SDS, all the proteins have approximately the same mass-to-charge ratio and separation occurs in basis of the molecular mass. This means that small proteins travel faster during separation than the larger proteins.

Then, when the protein-SDS complexes are loaded onto a gel, and placed in an electric field, a migration towards the anode (positively charged electrode) is produced (**Figure 5.3**).

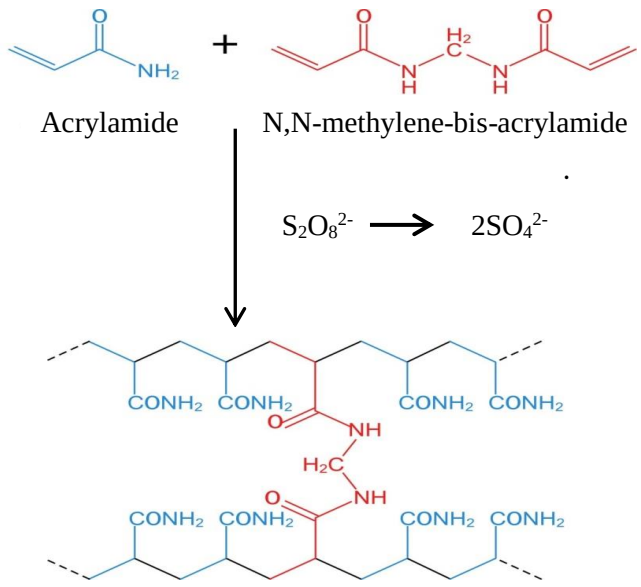

Figure 5.2. Polymerization of acrylamide monomers and cross-linking N,N'-methylenebisacrylamide components.

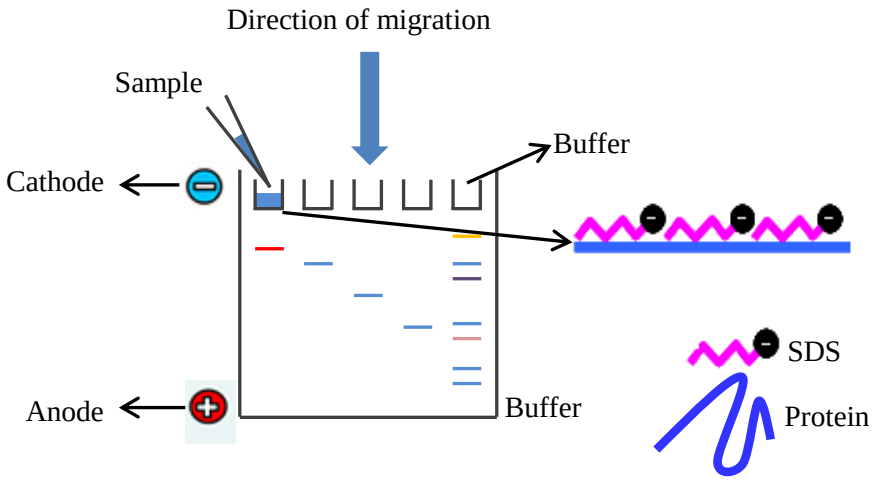

Figure 5.3. Scheme of SDS-PAGE separation.

With regard to the detection of proteins in SDS-PAGE, the most popular gel staining method is based on the use of Coomassie reagent. There are two Coomassie dyes (R-250 and G-250), which bind to proteins through ionic interactions between dye sulfonic acid groups and positive protein amine groups as well as through van der Waals attractions.

The size of a protein can be calculated by comparing its migration distance with that of a known molecular weight ladder (marker), which has been run in the same gel. For this purpose, the relative migration distance of each band of the protein standards and the unknown protein is calculated using this equation:

$$R_f = \frac{Migration\ distance\ of\ the\ protein\ problem}{Migration\ distance\ of\ the\ dye\ front} \qquad (1)$$

Then, the logarithm of the molecular weight of each standard and its relative migration distance (R_f) is plotted into a graph. The obtained regression equation is used to interpolate the R_f value of the unknown protein and thus establishing its molecular weight (**Figure 5.4**).

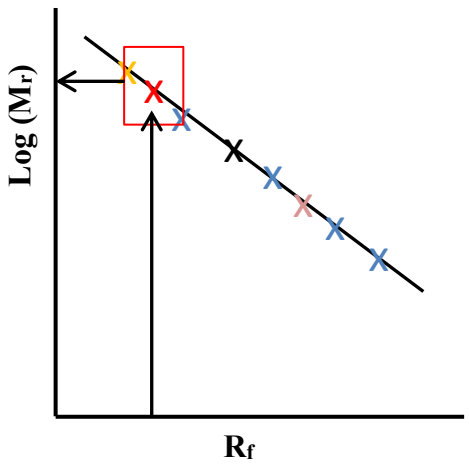

Figure 5.4. Calculated standard curve of standard proteins.

This technique offers the possibility of digest the separated proteins via in gel tryptic digestion for MS identification. There are available thousands of articles describing this procedure (Jafari, 2012). In this sense, gels are sliced and each fraction is digested with trypsin and subsequently analyzed by nanoLC-ESI-MS/MS.

5.2.2. CZE

According to IUPAC definition (Riekkola, 2004), this technique is based solely on the differences in the electrophoretic mobilities (charge-to-size-ratios) of charged species either in aqueous or non-aqueous background electrolyte (BGE) solution in the presence of an electric field. Therefore, ions with large electrophoretic mobilities will move faster than those with low mobilities, thus migrating in discrete zones at different velocities.

The electric field can be also used for a second purpose: to transport the bulk flow of liquid in the capillary in two ways, i.e. forward with respect to either the inlet or the outlet ends, and also with respect to the detector location. This is achieved due to the interfacial phenomenon known as electro-osmotic flow (EOF). The EOF results from the influence of the applied electric field on the charge of the double layer at the inner surface of capillary. Depending on the pH of the BGE, silanol groups of the internal wall are deprotonated. The negative charge attracts cations from BGE, giving as a result a diffuse layer, next to the wall, in which the population of these buffer cations predominates. The application of an electric field along the capillary produces that these cations (forming the diffuse layer) move towards the cathode, dragging the bulk buffer solution withthem (**Figure 5.5**).

An important feature of EOF is that the thickness of the diffuse layer is very much smaller than the radios of the capillary, giving a flat profile. As a consequence, EOF allows high separation efficiencies compared to parabolic profile characteristic of pressure-driven flow. The rate of EOF can be controlled by change of the capillary surface charge or BGE viscosity. The EOF direction can be modified on basis of a specific analyte separation. The rate of EOF can be controlled by changing the capillary surface charge or BGE viscosity.

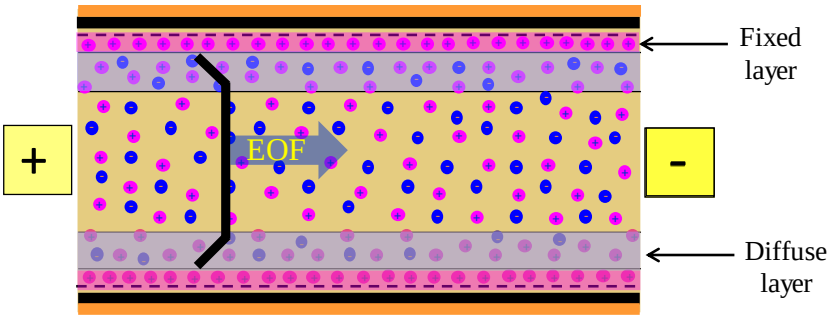

Figure 5.5. Scheme of EOF generation due to an electric field.

The EOF direction can be modified on basis of a specific analyte separation. For instance, if there is a need to analyze anions (whose migration times are very long), a reversed EOF could be applied to shorten the analysis time. Thus, it is possible to invert the EOF direction by coating the capillary wall with dynamic coatings (e.g. addition of cationic surfactant). In this case, the capillary walls will be negatively charged and the EOF will be reversed, that is, towards the anode.

The applicability of CZE has been widely demonstrated by separating a wide range of organic and inorganic analytes, from small to very large molecular masses (proteins, deoxyribonucleic acid (DNA) fragments and synthetic polymers) (Righetti, 1996). Although solutes without net electric charge (uncharged and double ions) cannot be separated by CZE; it is

possible to achieve the separation by adding charged reagents which associates to the target analyte in the solution (e.g. an ionic surfactant, even below its critical micellar concentration).

5.2.3. CGE

CGE is an electrophoretic technique commonly used to separate proteins and ADN, in which the interior wall of capillaries is filled with a cross-linked gel or viscous solution. In CGE, it is necessary to coat the capillary walls with a gel because the uncoated wall can interact with proteins electrostatically and/or hydrophobically (if part of the protein is positively charged or contain hydrophobic groups, respectively), thus avoiding a worsening in separation efficiencies. In addition, CGE is performed at low or zero EOF conditions, since the existence of a strong EOF would produce the movement of sieving matrix (from anode to cathode), thus losing its discrimination effect on molecular size. The viscous medium acts as "molecular sieve", and retards more the larger molecules than the smaller ones, giving a separation based on the molecular size of the charged analytes. In the area of protein separations, much research described is related to SDS-gels for size-based separation (Zhu, 2012). Thus, proteins are treated with SDS (like in classical SDS-PAGE; **Section 5.2.1**) to form SDS-protein complexes. These negatively charged complexes migrate to anode according its molecular size.

Thus, CGE has been recognized and established as an important tool in biopharmaceutical industry to support analytical characterization, process development, and quality control of therapeutic recombinants antibodies (Tous, 2005). Also, current CGE methods have been routinely used for the analysis of protein-based pharmaceuticals (Feng, 2008), biological fluids (Gomis, 2003) and quality controls in food area (Debaugnies, 2011).

5.2.4. CEC

In CEC, the movement of the mobile phase through a capillary filled with a particle-packed or monolithic stationary phase is achieved by EOF. Since the driving force is this phenomenon, the surface of the stationary phase should have a net electrical charge. The separation mechanism in CEC is double. On the one hand, solutes are separated by true chromatographic distribution between the mobile and stationary phases. On the other hand, charged analytes are also simultaneously separated by an electrophoretic mechanism, which is based on the differences in electrophoretic mobility. In CEC, it is of great importance the nature of stationary phase of the column, since it determines the EOF and influences on the separation performance.

The instrumentation used in CEC is quite similar to the CE system commonly employed in electromigration capillary techniques (**Figure 5.6).** In particular, the CEC system is provided by external pressure supply (2-15 bars) to avoid the formation of bubbles, which can disturb the detector baseline and current.

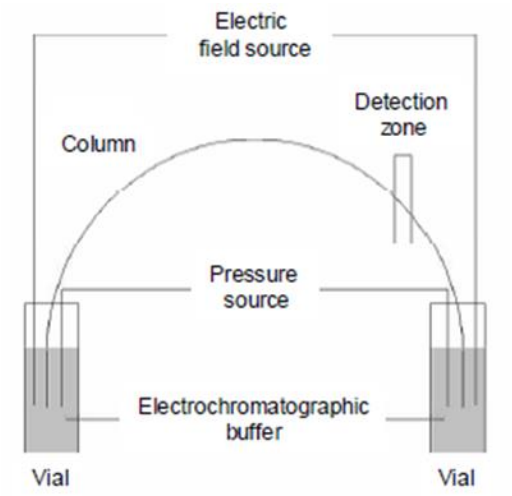

Figure 5.6. Scheme of a CEC instrument.

5.2.4.1. Columns used in CEC

CEC columns are usually prepared from fused-silica capillaries with internal diameters comprised between 50 and 100 μm. Different types of chromatographic supports can be distinguished: packed, open-tubular and monolithic columns.

The potential of packed capillary columns in CEC was demonstrated in the 1980s (Dittman, 1997). However, several technical problems slowed the development of this separation technique (Fujimoto, 1995). These problems include the difficult fabrication of frits within a capillary, the packing of beads into a tube with a very small diameter, the limited stability of packed columns, and the formation of bubbles capable of disrupting the current during the analysis.

Compared to packed columns, open-tubular columns have no bubble formation because end-frits are not needed; however, their small sample loading capability (low phase ratio) and difficult detection (Tang, 2000) have led to search for other options.

The development of monolithic columns has provided a very good solution to overcome all these problems. As mentioned above in **Section 4.2**, these stationary phases can be molded within the capillary and can be chemically linked to its walls, without the need of retaining frits. Besides, its preparation process is simple, in a single step, which enables the incorporation of different monomers, charged positively or negatively needed to generate the desirable EOF, plus other monomers with the ability to control functionality and the porous properties (Eeltink, 2007; Svec, 2009). Within the two types of monoliths, as commented in **Section 4.2**, the preparation of organic polymeric based beds is easier, their chemical stability is higher than silica-based ones, and there is a wide variety of monomers available to synthesize polymers with different functionalities

(Rozenbrand, 2011; Huber, 2004). As mentioned in Section 4.2, acrylate- or methacrylate-based monoliths are among the most popular polymer chemistries used as separation media.

Up to now, most of the publications dealing with the set-up of monolithic columns in CEC have been focused on the monolithic structure for enhancing column performance and on new column chemistries for tailoring selectivity (Svec, 2015) using sets of standard mixtures. However, to our knowledge, few CEC methods with polymeric monoliths have been reported for the integration of these systems in the analysis of complex samples such as biological (Aturki, 2009) and food matrices (e.g. olive oil) (Lerma-García, 2007; Lerma-García, 2008). In this thesis, a CEC method using acrylate-based monoliths for the analysis of triacylglycerols in vegetable oils has been described (**Chapter 17**).

5.3. Mass spectrometry

In MS, the detector is an instrument that provides high-level information about analyte molecular structures, distinguishing between functional groups, chemical elements and isotopes, separating the fragments according to their *m/z* ratio. As illustrated in **Figure 5.7,** a mass spectrometer is composed by an entry system that allows the introduction of a small amount of sample into the mass spectrometer. There are different entry systems depending on the type of sample to be analyzed (solid, liquid or gaseous). Sample can be introduced in a discrete manner using a syringe or continuously by coupling mass spectrometer with flow in injection system or with chromatographic or electrophoretic system.

Mass spectra are obtained by conversion of sample components in their gas-phase ions, which are separated according to their *m/z* ratio, being the analytical signal the abundance or intensity for each *m/z* value. **Figure 5.7** shows a diagram with the main components of a mass spectrometer.

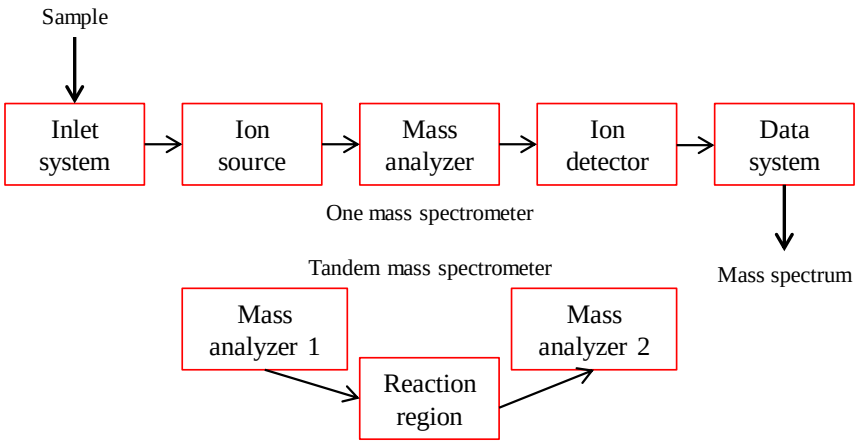

Figure 5.7. Principal components of a mass spectrometer.

There are different ionization techniques in MS, such as atmospheric pressure photoionization and atmospheric pressure chemical ionization, but electrospray ionization (ESI) and matrix-assisted laser desorption/ionization (MALDI) are the most commonly used in proteomic analysis. In the following sections, a brief description of both techniques is included.

5.3.1. ESI

The most popular ion source, especially in the LC-MS coupling, is the ESI one. Sample in solution is passed through a capillary nebulizer jointly with a coaxial N_2 flow. Then, a high electric potential is applied at the exit of the nebulizer that, in combination with nebulizer gas, creates a fine spray of charged particles (**Figure 5.8**). The gas present at atmospheric pressure in the spray chamber carries the ions into the capillary entrance of mass analyzer, where the pressure is reduced to about 3 mbar by a vacuum pump.

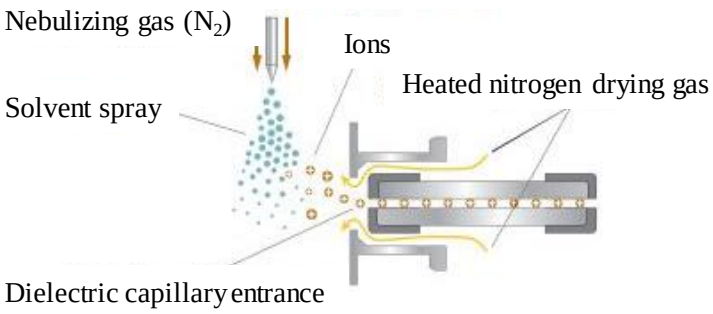

Figure 5.8. Scheme of an ESI source.

5.3.2. MALDI

MALDI is commonly applied to the analysis of peptides, proteins and polymers. It is characterized by its sensibility, versatility and feasibility. The target molecules crystalize with an aromatic matrix, which consists in an organic molecule that absorbs at the laser wavelength. The crystals are irradiated with laser pulses under vacuum conditions. The matrix absorbs the most of the energy of the laser and transfers this energy to the peptide/protein, which then ionizes into the gas phase (as a result of the relatively large amount of energy absorbed). MALDI ion source is often coupled to time-of-flight (TOF) analyzer. The resulting ions are subjected to a high electrical field and accelerated into a flight-tube in the mass spectrometer with a detector at its end. Then, the ions take different time to reach the detector, being separated according to their *m/z* ratio (**Figure 5.9**). The relationship that allows determining the *m/z* of ions ratio is next indicated:

$$E = \frac{1}{2}(m/z)\, v^2 \qquad (2)$$

where E is the energy imparted on the charged ions (as a result of the voltage applied by the instrument) and v is the velocity of the ions down the flight

path. Thus, according to the above equation, ions that have larger mass will have lower velocities and will require longer times to reach the detector, thus forming the basis for *m/z* determination by a mass spectrometer equipped with TOF detector.

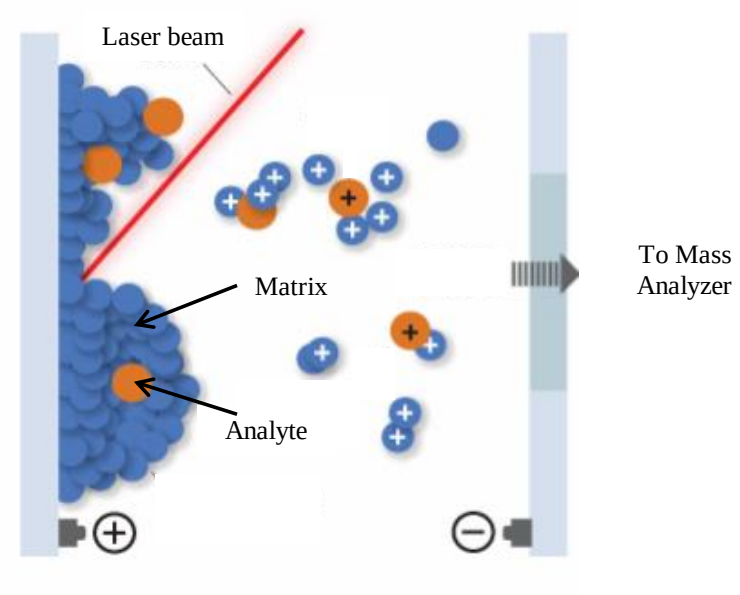

Figure 5.9. Scheme of MALDI ionization.

5.4. ATR-FTIR

Attenuated total reflectance (ATR)–FTIR spectroscopy is a versatile tool for measuring infrared spectra of a broad range of samples and systems. This technique is characterized by the use of an ATR accessory, which operates by measuring the changes that occur in a totally internally reflected infrared beam when the beam comes into contact with a sample (**Figure 5.10**). The infrared beam is directed onto an optically dense crystal with a high refractive index at a certain angle. This internal reflectance produces an evanescent wave that extends beyond the surface of the crystal into the sample held in contact with the crystal. This evanescent wave protrudes only

a few microns (0.5 - 5 μm) beyond the crystal surface and into the sample. Therefore, a good contact between the sample and the crystal surface is required. In the IR regions where the sample absorbs energy, the evanescent wave will be attenuated or altered. The attenuated energy from each evanescent wave is passed back to the IR beam, which then exits the opposite end of the crystal and is passed to the detector. The system then generates an IR spectrum. The number of reflections at each surface of the crystal is usually between five and ten, depending on the length and thickness of the crystal and the angle of incidence (**Figure 5.10**).

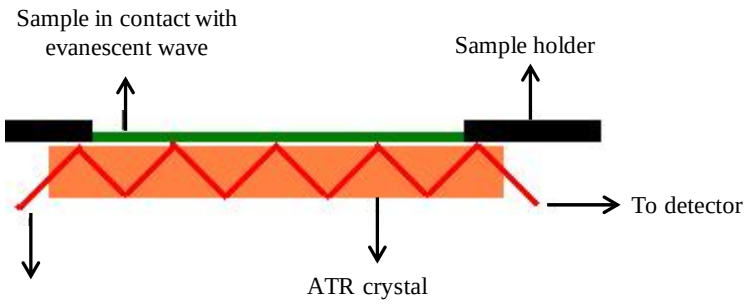

Figure 5.10. Scheme of a multiple reflection ATR system.

The most frequently crystal is diamond because it has the best durability and chemical inertness. Nevertheless, there are other materials accessible for ATR, such as zinc selenide (ZnSe) and germanium. A crystal of ZnSe, is the one employed in this thesis.

Two requirements are needed in this technique to be successful:

i) Sample has to be in direct contact with the ATR crystal.

ii) The refractive index of the crystal must be considerable higher than that of the sample or internal reflectance will not occur.

The use of ATR-FTIR technique to analyze biomedical samples (Baker, 2016), to follow crystallization processes (Zhang, 2014), or to evaluate the adulteration and authentication of food (Lerma-García, 2011), has been reported by many authors in literature.

5.5. Data statistical treatment

Currently, analytical instruments play an important role in quality control, process analysis, material identification, etc; however, the volume of collected data is increasingly larger. Thus, the reduction of dimensionality of data is essential for pattern recognition purposes to obtain a significant information. According to whether supervised information (*a priori* knowledge of categories of samples) is available or not, reduction methodologies can be classified into supervised and unsupervised ones. Principal component analysis (PCA) and linear discriminant analysis (LDA) are the most well-known unsupervised and supervised dimensionality deduction methods, respectively.

In the first part of this section a brief description of both techniques will be done, whereas the second one will include a description of multiple linear regression (MLR), since these techniques have been omployed in this thesis (**Chapters 10, 12-20**).

Unsupervised analysis. In PCA, a set of orthogonal vectors, which are linear combinations of the original variables, is created. These vectors are constructed in order to decrease the explained variance, thus; the first vector covers as much of the variation in data as possible. The second vector, which is orthogonal to the first one, covers as much of the remaining variance as possible, and so on. By plotting the projection of the samples on the planes of the first-second, first-third and second-third vectors, one can have the best possible views of the internal structure of the data matrix, thus interpreting sample relationships such as correlation and groups. Before using PCA,

standardization of the data matrix is usually performed in order to give the same weight to all the original variables.

Supervised analysis. It consists in constructing models able to predict if an object belongs to a certain class. The data matrix comprises at least one categorical variable that indicates the category to which each object belongs, which constitutes the variable to be predicted. Data matrix also contains one or more scale variables that describe object characteristics. These variables are used as predictors. To construct a model, it is necessary to have a data set with known information of both, category and predictors (although data belonging to a category could be assumed). The object assignment to the categories should be exhaustive (all objects belong to a category) and mutually exclusive (any object belongs to more than one category). These objects form the training set, which is used to construct the classification model. Once constructed, the model is used to predict the category of new objects from the measurement of predictors. The prediction of an evaluation set allows the validation of the model, which will be applied to predict the category of unknown samples.

In LDA, an algorithm that searches functions or discriminant vectors, i. e, linear combinations of the variables that maximize the variance between categories, while minimizing the intra-category variance, is used. To construct the model, it is required to assign the objects of the training set to a given category. To do this, a categorical variable is added to the data matrix containing as many categories as needed.

The LDA estimates the coefficients a_1, a_2, ..., a_m of the linear discriminant function, *f*, which is able to predict the object belonging to one or another category:

$$f = a_1 x_1 + a_2 x_2 + \cdots + a_m x_{1m} \qquad (3)$$

The discriminant functions are constructed one at a time, looking for directions in space that maximize the expression:

$$\lambda' = \frac{SC_D}{SC_I} \qquad (4)$$

where SC_D is the sum of squares of the Euclidean distances between objects belonging to different categories in the direction of the discriminant function, and SC_I is the sum of squares of the Euclidean distances between objects belonging to the category, also in the direction of the discriminant function. From the *q* categories, *q-1* discriminant functions are obtained (although if the number of predictor variables, *N*, is lower than *q*, *N-1* discriminant functions will be obtained). The discriminant functions are obtained in decreasing order of their value λ', and maintaining orthogonality between them.

The λ' function varies widely with the number of objects and the separation between them. Therefore, instead of maximizing λ', is often minimized Wilks' lambda, which is defined as:

$$\lambda_W = \frac{1}{1+\lambda'} = \frac{SC_I}{SC_I + SC_D} \qquad (5)$$

This function takes values between 0 and 1. Categories with a clear separation gave λ_w values close to 0, while largely overlapping categories gave λ_w values close to unity.

Multiple Linear Regression (MLR). It is defined as a multivariate technique for determining the correlation between an independent variable *y* (response variable) and some combination of *x* independent variables (predictors). Thus, the MLR model can be written as:

$$y = b_0 + b_1x_1 + b_2x_2 + \cdots + b_Qx_Q + e = b_0 + \sum_{q=1}^{Q} b_qx_q + e \quad (6)$$

where y is the response variable, x_q is the ith observation of the independent variable, b_0, b_1, …, b_Q are regression coefficients, and e_i is the error associated with the ith observation when the model is accepted. Once the model is obtained, the final objective is to predict future values of the dependent variables from the predictor variables.

One of the critical operations in MLR is the selection of predictor variables to be included in the model. The model should include a single predictor variable that represents each of the sources of variance of data, that being relevant, are also correlated with the response. If all significant sources of variance are not considered, “underfitted" models will be obtained, which would translate in error. In the opposite case, when the model included more sources of variance than those strictly necessary, "overfitted” models are obtained. In this case, model predictions will be affected by an excessive error. A simple procedure for variables selection is to initially include in the model all variables that have some probability of influencing the response. Thus, regression coefficients are obtained, and then the variable associated to the lowest regression coefficient is eliminated. The process is repeated until all variables have non-negligible values of the regression coefficient. However, this technique should be applied with caution, since the presence in the model of correlated variables reduces its regression coefficient. Therefore, when there is a group of strongly correlated variables, only one variable should be selected to represent the group. On the other hand, there are more rigorous selection procedures known as "forward", "backward" and "stepwise". These procedures are usually found in statistical packages, and are very helpful when a large number of variables are handled, and when it is not easy to assign the variables to specific sources of variance. In the three methods, the variables are entered or removed from the model following a criterion of "in-out". Thus, in the "forward" algorithm, linear correlations of

all variables with the response are calculated, and it is chosen as candidate the variable with the highest r^2 value. The variable is only introduced if it exceeds the entrance threshold of the following $F_{\text{-test}}$:

$$F = \frac{SC'_{\text{exp}} - SC_{\text{exp}}}{\frac{SC'_{res}}{n-p}} \qquad (7)$$

where SC'_{exp} and SC_{exp} are the sums of squares of the variance explained by the models constructed including and excluding the variable candidate, respectively, and SC_{res} is the sum of squares of the residual variance of the model constructed including the candidate variable. If the first variable entered the model, it is considered as the next candidate the variable that has a higher correlation with the model residuals, that is, the variable which is more correlated with response after removing the variance due to the first variable. The second variable entered the model if it also exceeds the entrance threshold. The process continues with a third candidate, and ends when there are no variables with a partial correlation with the response significantly different from zero, and that also exceeds the entrance threshold. In the "backwards" algorithm, all variables are initially introduced in the model, and then are sequentially eliminated according to the F_{test}. The first variable to be eliminated is the variable that has the lowest correlation with the response. The process ends when there are no variables in the model that satisfy the rejection threshold. Finally, in "stepwise" algorithm, variables are sequentially introduced, as in the "forward" algorithm. However, the entrance of a new variable modifies the significance of those variables which are already present in the model. For this reason, after the inclusion of a new variable, a rejection threshold is used to decide if one of the other variables should be removed from the model. The process terminates when there are no variables entering or being eliminated from the model. Once the model is

obtained, it is necessary to evaluate the goodness of fit. This can be estimated based on the coefficient of multiple determinations, R^2, and also by the sum of squared residuals. However, if the sum of squares is calculated considering only the objects of the calibration set, the ability of the model to accurately predict new objects, not included in this set, could be excessively optimistic. To solve this problem, cross-validation techniques are used, such as leave-one-out, which is the most common used. Leave-one-out validation involves the use of a single object from the original sample matrix as the validation set, and the remaining objects as the training set. This is repeated until each object in the sample matrix is used once as the validation set. In addition to this, the prediction capability of a model could be also evaluated using an independent evaluation set, which will determine the percentage of correctly predicted objects.

5.6. References

Aturki, Z.; D'Orazio, G.; Fanali, S.; Rocco, A.; Bortolotti, F.; Gottardo, R.; Tagliaro, F. (**2009**). Capillary electrochromatographic separation of illicit drugs employing a cyano stationary phase. *Journal of Chromatography A, 1216,* 3652-3659.

Debaugnies, F.; Cotton, F.; Boutique, C.; Gulbis, B (**2011**). Acta Clinica Belgica, 66, 165-165

Dittmann, K.; Wlenand, F.; Bek, G.; Rozing, P. (**1995**). Theory and practice of capillary electrochromatography. *Journal of Chromatography A, 13,* 800-821.

Eeltink, S.; Svec, F. (**2007**). Recent advances in the control of morphology and surface chemistry of porous polymer-based monolithic stationary phases and their application in CEC. *Electrophoresis, 28,* 137-147.

Feng, J.; Arriaga, E.A. (**2008**). Quantification of carbonylated proteinsin rat skeletal muscle mitochondria usingcapillary sieving electrophoresis withlaser-induced fluorescence detection. *Electrophoresis, 29,* 475-482.

Fujimoto, C. (**1995**). Charged polyacrylamide gels for capillary electrochromatographic separations of uncharged, low molecular weight compounds. *Analytical Chemistry, 67,* 2050-2053.

Gomis, D.B.; Junco, S.; Expósito, Y.; Gutiérrez, M.D. (**2003**). Size-based separations of proteins by capillary electrophoresis using linear polyacrylamide as a sieving medium: model studies and analysis of cider proteins. *Electrophoresis, 24,* 1391-1396.

Huber, C.G.; Walcher, W.; Timperio, A.M.; Troiani, S.; Porceddu, A.; Zolla, L. (**2004**). Multidimensional proteomic analysis of photosynthetic

membrane proteins by liquid extraction-ultracentrifugation-liquid chromatography-mass spectrometry. *Proteomics, 4,* 3909-3920

Lerma-García, M.J.; Simó-Alfonso, E.F.; Ramis-Ramos, G.; Herrero-Martínez, J.M. (**2008**). Rapid determination of sterols in vegetable oils by CEC using methacrylate ester-based monolithic columns. *Electrophoresis, 29,* 4603-4611.

Lerma-García, M.J.; Simó-Alfonso, E.F.; Ramis-Ramos, G.; Herrero-Martínez, J.M. (**2007**). Determination of tocopherols in vegetable oils by CEC using methacrylate ester-based monolithic columns. *Electrophoresis, 28,* 4128-4135.

Riekkola, M.L.; Jönsson, J.A.; Smith, R.A. (**2004**). Terminology for analytical capillary electromigration techniques (IUPAC Recommendations 2003).*Pure and Applied Chemistry, 76,* 443-451.

Righetti, P.G. (**1996**). Capillary electrophoresis in analytical biotechnology. CRC Series in Analytical Biotechnology. Boca raton, Florida

Rozenbrand, J.; van Bennekom W.P. (**2011**). Silica-based and organic monolithic capillary columns for LC: recent trends in proteomics. *Journal of Separation Science, 34,* 1934-1944.

Svec, F. (**2009**). CEC: selected developments that caught my eye since the year 2000. *Electrophoresis, 30,* 568-582.

Tang, Q.; Lee, M. **(2000**). Column technology for capillary electrochromatography. *TrAC Trends in Analytical Chemistry, 11,* 648-666.

Tous G.I.; Wei, Z.; Feng, J.; Bilbulian, S.; Bowen, S.; Smith, J.; Strouse, R.; McGeehan, P.; Casas-Finet, J.; Schenerman, M. (**2005**). Characterization

of a novel modification to monoclonal antibodies: Thioether cross-link of heavy and light chains. *Analytical Chemistry, 77,* 2675-2682.

Zhu, Z.; Lu, J.; Liu, S. (**2012**). Protein separation by capillary gel electrophoresis: A review. *Analytical Chimica Acta, 709;* 21-31.

SECTION II. DEVELOPMENT OF NOVEL EXTRACTION TECHNIQUES FOR PROTEIN EXTRACTION IN VEGETABLE SAMPLES

II.A Design and application of polymeric supports modified with metallic nanoparticles

Chapter 6. Solid-phase extraction based on ground methacrylate monolith modified with gold nanoparticles for isolation of proteins

Analytica Chimica Acta 917 (2016) 37–43

Contents lists available at ScienceDirect

Analytica Chimica Acta

journal homepage: www.elsevier.com/locate/aca

Solid-phase extraction based on ground methacrylate monolith modified with gold nanoparticles for isolation of proteins

María Vergara-Barberán**, María Jesús Lerma-García, Ernesto Francisco Simó-Alfonso, José Manuel Herrero-Martínez*

Department of Analytical Chemistry, University of Valencia, C. Doctor Moliner 50, E-46100 Burjassot, Valencia, Spain

In this study, a novel polymeric material functionalized with AuNPs was prepared as SPE sorbent for isolation of proteins. The sorbent was synthesized from a powdered poly(glycidyl-co-ethylene dimethacrylate) monolith, and modified with ammonia, followed by immobilization of AuNPs on the pore surface of the material. To evaluate the performance of this SPE support, proteins were selected as test solutes, being the extraction conditions and other parameters (loading capacity and regenerative ability of sorbent) established. The results indicated that this sorbent could be employed to selectively capture proteins according to their pI, on the basis of the strong affinity of these biomacromolecules towards to AuNPs surface. The applicability of this sorbent was demonstrated by isolating protein species of interest (BSA, cytochrome c and lectins in European mistletoe leaves), followed by SDS-PAGE analysis.

Keywords: gold nanoparticles; glycidyl methacrylate monolith; proteins; solid-phase extraction

6.1. Introduction

Porous polymer monoliths are a category of materials developed during the last two decades, which have attracted much interest (Svec, 2015). Their simple in situ preparation, high permeability, stability along wide pH-ranges, and versatile surface chemistries have made these materials to be a competitive alternative to the conventional packed chromatographic columns (Smith, 2008). Due to their singular porous structure, polymer monoliths provide rapid conventional mass transport with very low resistance to flow. As a result, these stationary phases have been used in HPLC (Liu, 2013) and capillary electroseparation techniques (Ou, 2015). Recently, the application of polymeric monoliths has undergone a rapid growing in the field of sample pretreatment (Bunch, 2013; Namera, 2013). Thus, the performance of extraction efficiency of organic monoliths could be modified by tailoring its pore structure and surface chemistry.

GMA material has been used as "reactive support" to provide monoliths with different chromatographic properties (ion exchange, hydrophobic/hydrophilic, chiral, etc.) (Sykora, 1999; Prenerstorfer, 2005; Dong, 2007; Carrasco-Correa, 2013). GMA-based monoliths have been also used for holding silver and gold nanostructures to generate a good surface enhanced Raman spectroscopy (SERS) performance (Liu, 2011; Li, 2012; Wang, 2014). In addition, GMA-based materials in powder have been demonstrated to be helpful in ultrasensitive SERS detection (Li, 201; Wang, 2014) as an "entrapment support" to immobilize biomacromolecules (Benčina, 2007). The powder material could be easily processed into a thin packed column and contains active epoxy groups that can susceptible of undergoing functionalization.

AuNPs have unique properties such as special stability, quantum and surface effect, and great biocompatibility (Yeh, 2012). Since AuNPs have

high surface-area-to-volume ratios, easy chemical modification and strong affinity for thiol-containing ligands, they have already been used for extracting and enriching analytes from complex matrices (Shen, 2009; Li, 2009; Sykora, 2010; Chang, 2010). Thus, Tseng *et al.* (Shen, 209) used AuNPs to selectively extract thiol-containing compounds as a result of the specific formation of Au–S bonds. In a similar way, they have also developed methods for determining aminothiols in human urine and protein-bound aminothiols in human plasma (Li, 2009; Chang, 2010). Also, the AuNPs have been suspended in the BGE (Lin, 2003) or attached (Yang, 2005) on the inner wall of capillary in electrodriven separation techniques. In spite of its excellent properties, the combination of AuNPs with organic monoliths has been slightly explored. Thus, Svec's research group (Cao, 2010; Xu, 2010; Lv, 2012) has studied the attachment of AuNPs on the pore surface of reactive polymer-based monolithic supports. In particular, a GMA-based monolithic capillary column was functionalized with cysteamine to afford a pore surface with thiol groups, to which the AuNPs were attached. These capillary monolithic columns have proved to be useful for the capture and separation of cysteine-containing peptides (Xu, 2010) and as platforms to facilitate further variations in surface functionalities (Cao, 2010; Lv, 2012). However, the extension of this novel hybrid material as extraction phase has been scarcely reported (Wang, 2014).

SPE is a powerful tool to preconcentrate and purify analytes of interest from a great variety of sample matrices. In particular, this technique is among the widely employed alternatives for protein separation and preconcentration in protein analysis schemes and proteomics techniques (Chen, 2007). However, a limited choice of sorbents for protein species is available at present, consequently, the development of novel sorbent materials with satisfactory extraction efficiency and selectivity for protein species is highly desirable.

The aim of this study was the development of a novel SPE sorbent based on the modification of a polymer monolith with AuNPs. For this purpose, a GMA-based monolith was first synthesized; ground and subsequently amino groups were introduced onto the surface of the material by reacting epoxy groups with ammonia. Then, the AuNPs were immobilized onto the amino-functionalized GMA powder material surface on the basis of the strong interaction between the amino group and AuNPs (Joshi, 2004; Aureau, 2010). The prepared materials were filled into an empty plastic SPE column tube and its extraction efficiency was evaluated by using proteins as test solutes. The conditions for the extraction of proteins (bovine serum albumin and cytochrome c) were optimized. Loading capacity and regenerative ability of the SPE monolithic material was also evaluated. The ability of the developed sorbent to isolate proteins in several samples was also evaluated.

6.2. Experimental

6.2.1. Chemicals and reagents

GMA, ethylene dimethacrylate (EDMA), 3-(trimethoxysilyl) propyl methacrylate, ACN and MeOH were purchased from Scharlab (Barcelona, Spain). Azobisisobutyronitrile (AIBN) was from Fluka (Buchs, Switzerland). AuNP suspension (particle size, 20 nm, stabilized with sodium citrate) and Coomassie Blue were from Alfa Aesar (Landcashire, United Kingdom). Monosodium and disodium phosphate (NaH_2PO_4 and Na_2HPO_4, respectively) and orthophosphoric (H_3PO_4) acid were from Merck (Darmstadt, Germany). APS, acrylamide, bisacrylamide, BSA, cytochrome c (cyt c), gold (III) chloride trihydrate, HCl, 2-mercaptoethanol, HNO_3, lactose, sodium bromide, SDS, TEMED, Tris and trisodium citrate were obtained from Sigma-Aldrich (St. Louis, MO, USA). A molecular-weight-size protein standard (6.5 to 200 kDa) was also provided by Sigma-Aldrich.

Deionized water (Barnstead deionizer, Sybron, Boston, Mass., U.S.A.) was used in all procedures.

Stock solutions of BSA and cyt c (1 mg mL^{-1}) were prepared by dissolving appropriate amounts of each protein in deionized water, and working standard solutions were obtained by dilution of the stock solutions. Phosphate buffer solutions (PBS) of 20 mM at several pH values were prepared by mixing appropriate amounts of Na_2HPO_4, NaH_2PO_4 and H_3PO_4 according to the required pH.

6.2.2. Instrumentation

SEM/backscattered electron (BSE) images and energy dispersive X-ray (EDAX) analysis were obtained with a Philips XL 330 ESEM integrated with backscattered electron detector and a QUANTAX 400 energy dispersive spectrometer (Bruker, Germany). For these measurements, the monoliths were coated with a very thin-layer of conductive carbon instead of the more usual Au/Pd coating.

Elemental analysis of synthesized material was performed using an EA 1110 CHNS elemental analyzer (CE Instruments, Milan, Italy). The determination of Au in synthesized materials and Bradford protein assay were carried out by measuring in UV-vis with an 8453 diode-array UV-vis spectrophotometer (Agilent Technologies, Waldbronn, Germany). For Bradford's assay (Bradford, 1976)], a calibration curve up to 1 mg mL^{-1} of BSA and cyt c was prepared in the elution solvent (see **section 6.3.2**). SDS-PAGE experiments were performed using a vertical minigel Hoefer SE260 Mighty Small system (Hoefer, MA, USA).

6.2.3. Preparation and functionalization of GMA-based monolith

The GMA-co-EDMA monolithic material was based on a previous work (Carrasco-Correa, 2013). Briefly, a polymerization mixture was prepared in a 10 mL glass vial by weighing GMA (20 wt%), EDMA (5 wt%), and a binary porogenic solvent mixture containing cyclohexanol (70 wt%) and 1-dodecanol (5 wt%). AIBN (1 wt% with respect to the monomers) was added as initiator. This mixture was sonicated for 5 min and then purged with nitrogen to remove oxygen for 10 more min. The polymerization was carried out in an oven at 60ºC for 24 h. Next, the polymeric material was washed with methanol to remove the porogenic solvents and possible unreacted monomers. Then, the monolithic bulk material was ground with a mortar and sieved with a steel sieve with sizes ≤ 100 µm. The synthesized powder porous material was treated with aqueous 4.5 M ammonia in a round bottomed-flask at 60ºC (water bath) for 2 h under continuous stirring. Upon completion of the reaction, the material was washed with ultra-pure water to remove the excess of ammonia until the eluent was neutral. The poly(GMA-co-EDMA) powdered material functionalized with amino group was obtained for further use.

6.2.4. Functionalization of amino modified GMA-co-EDMA powder material with AuNPs

The amino modified powder material (400 mg) was placed in a Falcon tube, and then 20 mL AuNPs solution were added, and the mixture was allowed to react under stirring for 10 h. A GMA-co-EDMA powder attached with AuNPs (pink colour) was obtained. Then, the material was washed with deionized water (containing 38.8 mM sodium citrate at pH 6.6) in order to remove the AuNPs, which had not been attached on the amino-modified material. The AuNP-modified material was characterized by SEM and the Au content was evaluated using both UV-vis and EDAX. For UV-vis

detection, the dried methacrylate material with AuNPs was first calcinated at 550 °C for 1 h. Then, the remaining product (which contained the gold material), was treated with freshly prepared *aqua regia*, which was subsequently left to evaporate nitric acid vapor and cool down to room temperature. The solution was properly diluted with HCl 1 M and was subjected to UV-vis analysis. The colorimetric determination of Au was based on the formation of the bromoaurate $[Au(Br)_4]^-$ ion (McBryde, 1948; Gitis, 2006), which is obtained through the reaction of chloroauric acid with potassium bromide and measured at 380 nm. A stock solution of 200 µg mL^{-1} of Au(III) was prepared from its chloride salt. A calibration curve (1-20 µg mL^{-1}) was obtained by appropriate dilution of the stock solution in presence of an excess of NaBr (4 %).

6.2.5. SPE protocol

Fifty milligrams of AuNP-modified polymer was packed between two frits (1/16', 20 µm, Análisis Vínicos, Tomelloso, Spain) into 1 mL empty propylene disposable SPE cartridge (Análisis Vínicos). Activation of the sorbent was done with ACN (200 µL) and then equilibrated with water (500 µL). 200 µL of protein standard was loaded on the SPE material at a flow rate of 0.1 mL min^{-1}. After loading the protein standard, the material was washed with water (500 µL) at 0.7 mL min^{-1}, collecting the washing step solution. Retained analytes were eluted with 30 mM PBS (500 µL) and the eluted proteins were also collected. Next, the sorbent surface was regenerated with water at 80 ºC during 2h. During the SPE process, the proteins left in the effluent (loading solution) passing through the microcolumn were quantified by Bradford assay (measurement of absorbance at 595 nm), in order to evaluate the retention efficiency of proteins on the AuNP-modified material. Afterwards, the proteins were eluted from the microcolumn and quantified in the same way. The same

procedure was applied to prepare a blank sorbent constituted by the GMA-co-EDMA polymer (50 mg).

6.2.6. Extraction of mistletoe proteins

European mistletoe (*Viscum Album L.*) grown on *Pinus halepensis* was collected and the green parts were wased with water to eliminate bacterial and surface contamination from human hands. Then, the green parts were sliced and transferred to a mortar and frozen in liquid nitrogen. The frozen material was ground to a fine powder in a pre-cooled mortar and pestle. Then, the protein extraction protocol was carried out according to Olsner *et al.* (Olsner, 1982). Briefly, 10 g of this powder was mixed with 100 mL of 10 mM Tris-HCl at pH 8.3, which contained 100 mM lactose to avoid the bind of lectins to carbohydrate components in the homogenate. Then, the suspension was mildly shaken at 4ºC overnight and centrifuged at 10000 x g for 10 min. Then, 500 µL of supernatant adjusted at pH 6 was passed through the SPE sorbent. As described above, the retained proteins were eluted with 30 mM PBS at pH 12 and an aliquot of 20 µL was loaded into the gel.

6.2.7. SDS-PAGE analysis

SDS-PAGE of proteins was carried out with 40% acrylamide/bis solution, and standard discontinuous buffer systems as described by Laemmli (Laemmli, 1970). The protein bands were visualized with staining by using Coomassie Blue. Molecular sizes of the model proteins were analyzed by comparison with an SDS-PAGE standard marker.

6.3. Results and discussion

6.3.1. Preparation and characterization of the AuNP-modified monolith

A generic poly(GMA-*co*-EDMA) monolith was first synthesized (Carrasco-Correa, 2013), ground into fine powder and then functionalized with ammonia to prepare the amino modified column (**Figure 6.1**). Elemental analysis of this bulk material indicated the presence of 1.54 wt% nitrogen (1.10 mmol /g monolith), which is in agreement with previous studies related to the preparation of other amino-based monoliths (Sykora, 1999; Carrasco-Correa, 2015). Then, a citrate-stabilized AuNP colloidal dispersion of 20 nm was used to functionalize the resulting amino until the polymer surface was fully covered with Au (**Figure 6.2**).

It was visually confirmed by a change of color in the powdered monolith from white to pink. In addition, SEM micrographs of this material were taken with a BSE detector, giving a satisfactory surface coverage with AuNPs (white spots randomly distributed) (**Figure 6.2B**). The coverage of AuNPs was estimated by both UV-vis spectroscopy (see **Section 2.4**) and EDAX. Thus, UV-vis spectroscopy analysis showed the presence of 0.5 wt% Au, being EDAX analysis consistent with this value (0.42 wt% Au). Next, this material was used as SPE sorbent for enrichment of proteins.

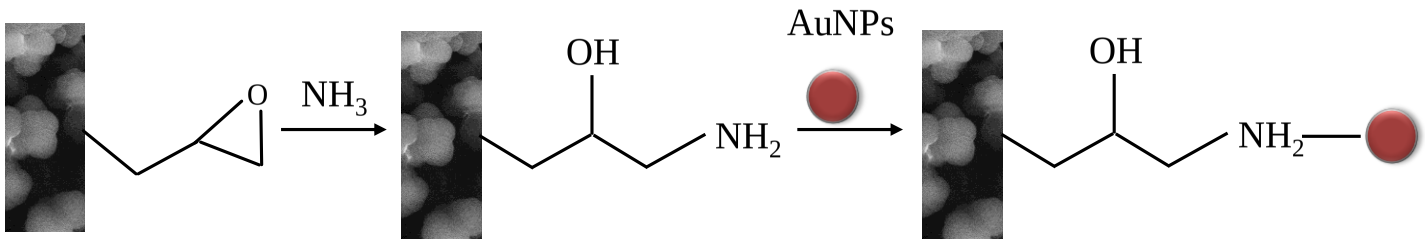

Figure 6.1. Preparation of poly(GMA-co-EDMA) monolith and its modifications with ammonia and immobilization of AuNPs.

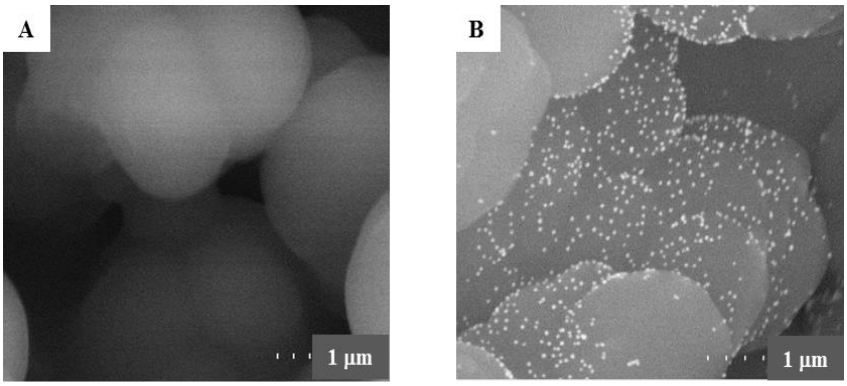

Figure 6.2. SEM/BSE micrograph of GMA-co-EDMA powder material without AuNPs (A) and modified with AuNPs (B).

6.3.2. Retention of proteins using AuNP-modified GMA material as SPE sorbent

The sample loading flow rate (0.1-0.5 mL min^{-1}) was first studied. This variable has not only a significant effect on the recovery of proteins, but also determines the time of the whole analytical process. The experimental results indicated that low loading flow rates (0.1 mL min^{-1}) allowed higher retention efficiencies of proteins on the AuNP-modified polymeric material. Lower flow-rates than 0.1 mL min^{-1} were not tested since they require longer processing times. Next, the effect of the elution flow rate on the recovery was also investigated, being the best elution flow rate 0.1 mL min^{-1} for protein species, which was employed for further studies. The adsorption of proteins onto solid surfaces is a complex process in which several driving forces could be involved, such as hydrophobic, electrostatic, and hydrogen bonding interactions.

In general, hydrophobic and electrostatic interactions tend to rule the entire process (Gray, 2004; Lacerda, 2010; Gagner, 2011). A preliminary study have showed that within an appropriate pH range, the surfaces of AuNPs could effectively retain proteins, thus providing a potential medium for isolation of these species of interest from several sample matrices (Du, 2007). For this reason, the effect of sample pH (2.5-11) on the loading SPE step was first studied (**Figure 6.3**). Solutions (200 µL) containing 200 µg mL^{-1} of BSA (pI 4.7) or cyt c (pI 10.5) were selected as test solutes to perform the sorption studies.

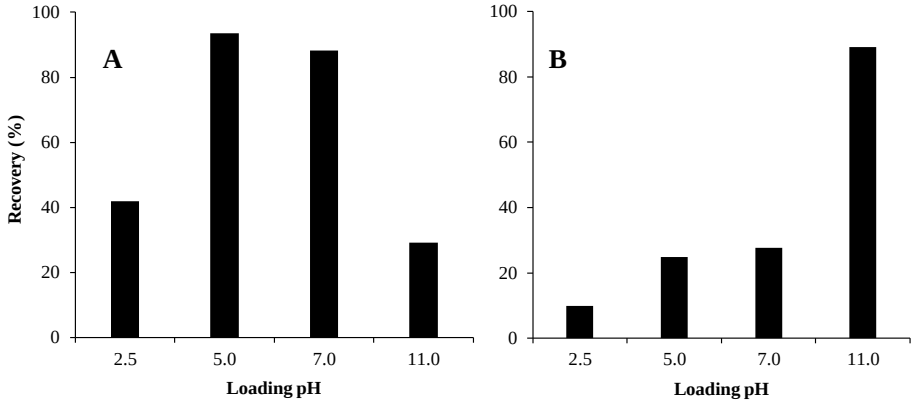

Figure 6.3. Effect of loading pH solution on elution step of BSA (part A) and cyt c (part B).

As shown in **Figure 6.3A**, for BSA, the highest retention in the loading step was achieved at pH 5.0. This result is in agreement with the findings reported in literature, where the maximum adsorption from aqueous protein solutions onto the metal surface was usually observed at the pI (Yoon, 1998; Yoon, 1999; Thobhani, 2010). The adsorption of proteins to AuNPs could be explained taking into account both electrostatic interactions and ligand displacement reactions (Brewer, 2005; Glomm, 2007). The electrostatic interactions are related to the attraction between the positive surface residues of the protein and the negative charge from the citrate-coated Au surfaces.

The displacement phenomena implies that citrate is displaced by the protein upon adsorption with amino acids (functional groups) such as lysine (amine), histidine (imidazole), or cysteine (thiol) interacting directly with the gold surface (Brust, 1994). At pH close to the pI, the electrostatic interactions between the protein molecule and the sorbent are minimized, being the hydrophobic interactions (displacement mechanism) predominant. When the pH was modified to other values different from the optimal one, a less favorable adsorption or retention was obtained owing to electrostatic interactions (repulsion) between protein molecules-support and/or between adjacent adsorbed protein molecules onto Au surface. On the other hand, several authors (Dobson, 1997; Guo, 2008; Tsai, 2011) have reported that structural changes (displacement by the protein in its native structure or denaturation of the protein on the surface) can occur as the result of adsorption on the surface while the protein displaces the citrate stabilizer. In this way, the protein unfolds near the surface, exposing hydrophobic residues and presenting specific functional groups which interact by dispersive and van der Waals forces with the Au surface. Taking into account all above considerations, the washing step was done at pH close to pI (buffer at pH 5.0), giving small losses of BSA (< 5%).

Concerning to the elution step, at higher pH values (pH ≥ 11.0) recoveries higher than 94.8% were yielded. As mentioned above, at this pH, the desorption of this protein was facilitated owing to electrostatic interactions. Additionally, a generic GMA-based polymer (parent-material) was used as sorbent in the optimal conditions found for the material modified with AuNPs. Low retention (15 %) was obtained in the parent polymer after loading step, which confirmed the selectivity of the AuNP-modified GMA material.

A similar study was done with cyt c. As shown in **Figure 6.3B**, the maximum adsorption of this protein was achieved at a loading pH solution

close to its pI (10.7). A similar explanation than that previously described for BSA can be extended for cyt c (Rezwan, 2005). This may be the result of electrostatic repulsions between the negatively charged protein molecules (pH > pI) and negatively charged AuNPs or even between adjacent proteins retained onto the AuNP surface, giving a decrease in the interaction between protein and the sorbent. Accordingly, the washing and elution steps were adequately adjusted to pH conditions to achieve the highest extraction efficiency. In particular, washing step was performed at pH 11, whereas the elution step was done at pH 12. Also, a comparison in terms of retention was also performed with the parent material. Again a high selectivity of the developed procedure was proven since a retention *ca*. 27 % of cyt c was observed in the parent polymer.

In SPE, the breakthrough volume is another important parameter, which could affect the extraction efficiency. For this purpose, different sample volumes (100-2000 µL) of the standard protein solutions were passed through to the SPE material by keeping constant the amount of protein (1000 µg). **Figure 6.4** shows the breakthrough curves obtained for BSA and cyt c using the developed sorbent. As shown in this figure, high recoveries (89.5-97.8%) up to 1000 µL were achieved for BSA; however, a considerable decrease in the recovery values of cyt c was observed at volumes >200 µL. For this reason, a volume of 200 µL was chosen for further SPE studies.

The loading capacity of SPE sorbent (50 mg) was also evaluated by passing different amounts of BSA. The maximum loading capacity of the polymer monolith modified with AuNPs was 16.6 mg per g sorbent. Typical capacity values for porous media are 1–10% of the bed weight (Sigma-Aldrich and Waters websites), meaning that 10 mg of analyte could be potentially retained (under the proper condition) per g of sorbent material.

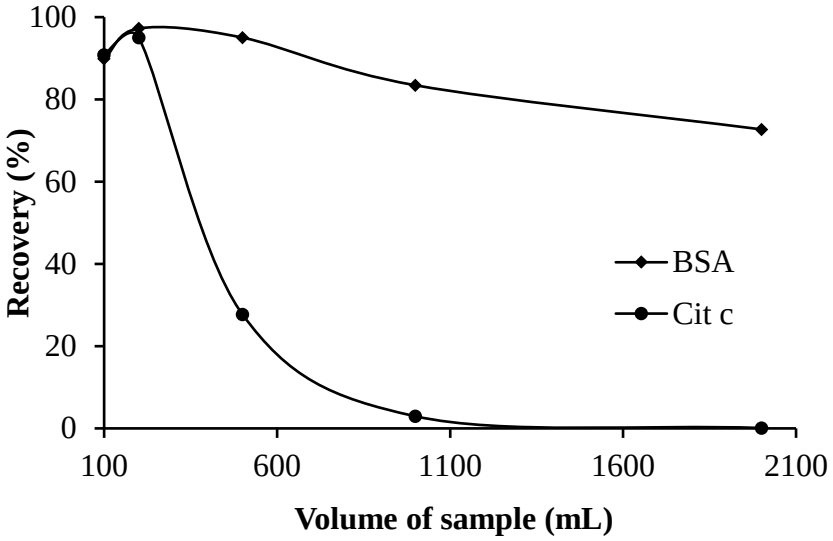

Figure 6.4. Effect of sample volume on the recoveries of BSA and cyt c in the GMA-co-EDMA material modified with AuNPs.

In order to ensure a satisfactory loading capacity of the SPE sorbent, its reusability was also evaluated. Svec *et al.* (Xu, 2010) have described that rinsing with water at elevated temperatures (80ºC) allowed a satisfactory regeneration of AuNP-modified columns after treatment with different ligands. On the basis on this study, the regeneration of the AuNP-modified material was carried out by washing it with water at 80ºC for 2 h. After this treatment, the loading capacity was again checked, giving *ca*. 87% of the original capacity. Further, SEM/BSE micrograph of the regenerated AuNP-modified sorbent was performed, where AuNPs were attached onto the polymer surface (data not shown) Also, UV-vis and EDAX measurements of Au content were conducted, with values *ca*. 0.42 wt%, which confirmed the feasibility of the rinsing protocol. Following this procedure, the sorbent can be reused for 20 times without significant efficiency losses (or with satisfactory recoveries comprised between 81.3-97.6%).

The proposed SPE sorbent described here could be favorably compared with recent reports related to the use of functionalized polymeric films for protein purification (Jain, 200; Dong, 2015). Thus, the loading capacity was higher than that reported using membranes-based devices modified with poly(acrylic acid) (PAA) brushes (Dai, 2006). However, the derivatization of PAA films with metal-ion complexes developed by these authors in several works (Jain, 2009; Dong, 2015; Ning, 2015) allowed an increase in the binding capacity of the platform (5.8 μg/cm^2 for BSA (Dai, 2006) and *ca*. 90 mg/mL for His-tagged ubiquitin (Jain, 2010; Ning, 2015) and its specificity to protein with accessible histidine groups. From these results, a 12 cm × 12 cm membrane area would be needed to retain the same amount of protein (830 μg BSA) previously found for 50 mg sorbent per cartridge, being this SPE device adequate to process small amounts of sample. In spite of the satisfactory binding capacities of these films, the membrane-modification process to achieve these platforms is laborious (several reaction steps). Moreover, brush synthesis is complicated and controlling the polymer-chain density, which undoubtedly affects the amount of protein binding, is challenging (Yang, 2011). In our case, the preparation of sorbent (synthesis and modification protocol) involved few simple steps.

Another aspect to be considered in these films is that they should be thin enough to prevent clogging and maintain flow. In our case, the resulting polymeric sorbent showed some residual permeable porous monolithic structure, which minimizes the probability of sorbent clogging.

Other strength of the proposed sorbent is its large reusability (see data above). In this regard, in some of the related works of polymeric films, these devices were reused at least 4 (Dai, 2006) or 6 times (Bhattacharjee, 2012).

6.3.3. Application to protein isolation

The feasibility of the present extraction method for the isolation of proteins according to their pI was demonstrated by isolating cyt c from BSA. A 200 μg mL^{-1} of BSA sample solution prepared at pH 5 and spiked with 100 μg mL^{-1} of cyt c was employed. The extraction process was conducted as detailed above and the different fractions were subjected to SDS-PAGE as illustrated in **Figure 6.5**.

As observed, BSA was effectively isolated from cyt c, which is not retained onto the sorbent at pH 5. The SDS-PAGE showed the cyt c band around 12 kDa in the loading fraction (lane 3); whereas the presence of proteins was not observed in the washing step solution (lane 4). On the other hand, BSA band at 66 kDa was observed in the elution fraction after pass through the column buffer solution at pH 11 (lane 5).

To demonstrate the application of this sorbent in complex real samples, the isolation of lectins from a European mistletoe sample was done. The extracts from this plant material have been used for a long time as therapeutic agents, mainly for oncological applications. In particular, the cytotoxic and immune stimulant properties of this plant material have been attributed to lectins (Baxevanis, 1998; Bantel, 1999). These glycoproteins are constituted by two polypeptide chains, the cytotoxic A-chain (Mr ≈ 29 kDa) and the carbohydrate-binding B-chain (Mr ≈ 32 kDa), linked by a disulfide bond, and they can be classified as mistletoe lectins (ML): ML-1, ML-2, and ML-3, depending on sugar-binding specificities (Franz, 1981; Samtleben, 1985; Eifler, 1993). In particular, most of the European MLs belong to ML-1 group, being it well characterized. Thus, the chains of ML-1 were distributed over a pI range comprised between 6.6 and 7.0 (Lutherm 1980; Yoon, 19999; Lutter, 2001).

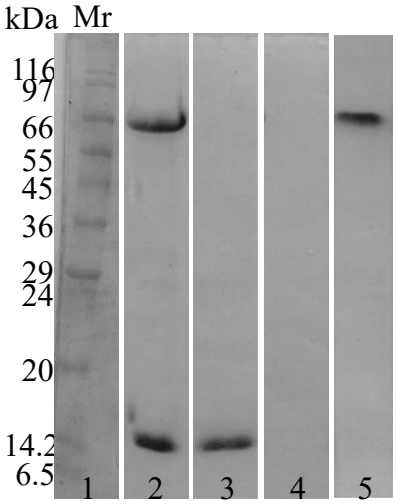

Figure 6.5. SDS-PAGE of the isolated cyt c from BSA. Identification: lane 1, molecular weight standards (Mr in kDa); lane 2, a 200 μg mL^{-1} of BSA sample solution spiked with 100 μg mL^{-1} of cyt c without pre-treatment; lane 3, the loading step solution passing through the GMA-co-EDMA material modified with AuNPs; lane 4, the washing step solution; lane 4: the elution step solution with the recovered BSA from the sample solution.

The isolation of lectins from complex samples is often complicated and requires many purification steps (ammonium precipitation, ionic and affinity chromatography, etc.) (Nascimento, 2012). These chromatographic methods can be time-consuming and expensive, leading to a low yield of the entire process. In addition, the affinity chromatography maintenance is a hardy task when plant crude extracts are loaded into columns since such samples contain pigments, oily components, and other complex substances that could damage the column and worsen the purification (de Santana, 2008). These awkward purification protocols can be considerably simplified by using the sorbent developed here. For this purpose, the extraction process detailed in **Section 6.3** was followed and then SDS-PAGE analysis of the collected fractions was carried out. **Figure 6.6** shows the SDS-PAGE analysis of the

mistletoe extract without (lane 2) and with pretreatment (lane 3) using this sorbent under non-reducing conditions.

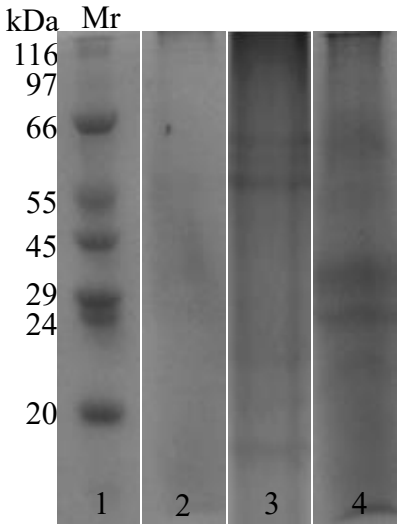

Figure 6.6. SDS-PAGE analysis demonstrating isolation of ML lectins from a European mistletoe extract. Lane 1: molecular weight marker, lane 2: mistletoe extract without pretreatment with this sorbent using non-reducing conditions; lane 3: mistletoe extract after pretreatment with this sorbent using non-reducing conditions; lane 4: mistletoe extract after pretreatment with this sorbent using reducing conditions.

Lane 2 did not yield a clearly visible band at the position of the ML proteins, whereas the lane 3 gave two major bands corresponding to Mr = 60,000 and 58,000 Da. These two prominent bands were identified as ML-1 and ML-3, respectively, which was in agreement with previous studies (Wacker, 2005). Also, SDS-PAGE analysis was performed under reducing conditions (presence of 2-mercaptoethanol) (**Figure 6.6,** lane 4), where two major bands originated from the heterodimeric lectins were evidenced, which corresponded to Mr = 28,000 and 34,000 Da, being ascribed to the corresponding A- and B-chains of ML-1 and ML-3, respectively (Wacker,

2005). In addition, a misty band at Mr = 60,000 Da was found, which was caused by uncompleted reaction of 2-mercaptoethanol.

6.4. Conclusions

A novel material based on a powdered GMA-based polymeric monolith modified with AuNPs has been developed and used as a sorbent in SPE for proteins separation. Several parameters of the SPE procedure have been optimized and protein recoveries have been evaluated by using Bradford assay. By simply adjusting the pH of the loading and washing solution close to pI values of proteins of interest, the biomacromolecules were readily adsorbed onto the AuNPs surface, and could afterwards be eluted by a proper variation of the pH of the eluent. Satisfactory results in terms of recovery efficiencies (95-98%), loading capacity (16.6 mg/g sorbent) and reusability (at least 20 times) of this sorbent have been also obtained. The feasibility of this methodology was also successfully demonstrated by the isolation of cyt c from BSA followed by SDSPAGE analysis. Moreover, the practical applicability of the sorbent was demonstrated by an efficient isolation of lectins from mistletoe samples. The results obtained here showed that the developed sorbent could be useful for the selective separation and/or preconcentration of protein species of interest (according to pI) in complex real samples.

Acknowledgements

This work was supported by project CTQ2014-52765-R (MINECO of Spain and FEDER). M. V-B thanks the MEC for an FPU grant for PhD studies. The authors also thank Dr. Salomé Laredo-Ortíz and Dr. Enrique Navarro-Raga from the Atomic spectroscopy and Microscopy sections of the SCSIE (University of Valencia), respectively, for their help in elemental analysis and SEM/EDAX measurements.

6.5. References

Aureau, D.; Varin, Y.; Roodenko, K.; Seitz, O.; Pluchery, O.; Chabal, Y.J. (**2010**). Controlled deposition of gold nanoparticles on well-defined organic monolayer grafted on silicon surfaces, *Journal of Physical Chemistry C, 114*, 14180-14186.

Bantel, H.; Engels, I.H.; Voelter, W.; Schulze-Osthoff, K.; Wesselborg, S. (**1999**). Mistletoe lectin activates caspase-8/FLICE independently of death receptor signaling and enhances anticancer drug-induced apoptosis. *Cancer Research, 59*, 2083-2090.

Baxevanis, C.N.; Voutsas, I.F.; Soler, M.H.; Gritzapis, A.D.; Tsitsilonis, O.E.; Stoeva, S.; Voelter, W.; Arsenis, P.; Papamichail, M. (**1998**). Mistletoe lectin I-induced effects on human cytotoxic lymphocytes. I. Synergism with Il-2 in the induction of enhanced lak cytotoxicity. *Immunopharmacology and Immunotoxicology, 20*, 355-372.

Benčina, K. Benčina, M. Podgornika, A. Štrancara, A. (**2007**). Influence of the methacrylate monolith structure on genomic DNA mechanical degradation, enzymes activity and clogging, *Journal of Chromatography A*, 1160, 176-183.

Bhattacharjee, S.; Dong, J.; Ma, Y.; Hovde, S.; Geiger, J.H.; Baker, G.L.; Bruening, M.L. (**2012**). Formation of high-capacity protein-adsorbing membranes through simple adsorption of poly(acrylic acid)-containing films at low pH. *Langmuir, 28*, 6885-6892.

Bradford, M.M. (**1976**). A rapid and sensitive method for the quantitation of microgram quantities of protein utilizing the principle of protein-dye binding. *Analytical Biochemistry, 72*, 248-54.

Brewer, S.H.; Glomm, W.R.; Johnson, M.C.; Knag, M.K.; Franzen, S. (**2005**). Probing BSA binding to citrate-coated gold nanoparticles and surfaces. *Langmuir, 21,* 9303-9307.

Brust, M.; Walker, M.; Bethell, D.; Schiffrin, D.J.; Whyman, R. (**1994**). Synthesis of thiol-derivatised gold nanoparticles in a two-phase liquid-liquid system. *Journal of the Chemical Society, Chemical Communications, 70*, 801-802.

Bunch, D.R.; Wang, S. (**2013**). Applications of monolithic solid-phase extraction in chromatography-based clinical chemistry assays, *Analytical and Bioanalytical Chemistry, 405,* 3021-3033.

Cao, Q.; Xu, Y.; Liu, F.; Svec, F.; Fréchet, J.M.J. (**2010**). Polymer monoliths with exchangeable chemistries: use of gold nanoparticles as intermediate ligands for capillary columns with varying surface functionalities. *Analytical Chemistry, 82*, 7416-7421.

Carrasco-Correa, E.J.; Ramis-Ramos, G.; Herrero-Martínez, J.M. (**2013**). Methacrylate monolithic columns functionalized with epinephrine for capillary electrochromatography applications, *Journal of Chromatography A, 1298,* 61- 67.

Carrasco-Correa, E.J.; Ramis-Ramos, G.; Herrero-Martínez, J.M. (**2015**). Evaluation of 2,3-epoxypropyl groups and functionalization yield in glycidyl methacrylate monoliths using gas chromatography. *Journal of Chromatography A, 1379*, 100-105.

Chang, C.W.; Tseng, W.L. (**2010**) Gold nanoparticle extraction followed by capillary electrophoresis to determine the total, free, and protein-bound aminothiols in plasma. *Analytical Chemistry, 82*, 2696-2702.

Chen, W.Z.; Shen, J.; Yin, X.F.; Yu, Y.N. (**2007**). Optimization of microfabricated nanoliter-scale solid-phase extraction device for

detection of gel-separated proteins in low abundance by matrix-assisted laser desorption/ionization mass spectrometry. *Rapid Communications in Mass Spectrometry, 21,* 35-43.

Dai, J.; Bao, Z.; Sun, L.; Hong, S.U.; Baker, G.L.; Bruening, M.L. (**2006**). High-capacity binding of proteins by poly(acrylic acid) brushes and their derivative. *Langmuir, 22,* 4274-4281.

De Santana, M.A.; Santos, A.M.; Oliveira, M.E.; de Oliveira, J.S.; Baba, E.H.; Santoro, M.M.; de Andrade, M.H. (**2008**). A novel and efficient and low-cost methodology for purification of Macrotyloma axillare (Leguminosae) seed lectin. *International Journal of Biological Macromolecules*, *43*, 352-358.

Dobson, K.D. Connor, P.A. McQuillan, A.J. **(1997**). Monitoring hydrous metal oxide surface charge and adsorption by STIRS. *Langmuir*, *13*, 2614-2616.

Dong, J. Ou, R. Dong, X. Wu, R. Ye, M. Zou, H. (**2007**). Preparation and evaluation of rigid porous polyacrylamide-based strong cation-exchange monolithic columns for capillary electrochromatography, *Journal of Separation Science, 30,* 2986-2992.

Dong, J.; Bruening, M.L. (**2015**) Functionalizing microporous membranes for protein purification and protein digestion. *Annual Review of Analytical Chemistry, 8,* 81-100.

Du, Z.; Yu, Y.L.; Chen, X.W.; Wang, J.H. (**2007**). The isolation of basic proteins by solid-phase extraction with multiwalled carbon nanotubes. *Chemistry - A European Journal, 13,* 9679-9685.

Eifler, R.; Pfüller, K.; Göckeritz, W.; Pfüller, U. (**1993**). Improved procedures for isolation of mistletoe lectins and their subunits: lectin

pattern of the European mistletoe. *Lectins: Biology, Biochemistry, Clinical Biochemistry, 9,* 144-151.

Franz, H.; Ziska, P.; Kindt, A. (**1981**). Isolation and properties of three lectins from mistletoe (*Viscum album L.*). *Biochemical Journal, 195,* 481-484.

Gagner, J.E.; Lopez, M.D.; Dordick, J.S.; Siegel, R.W. (**2011**). Effect of gold nanoparticle morphology on adsorbed protein structure and function. *Biomaterials, 32,* 7241-7252.

Gitis, V.; Haught, R.C.; Clark, R.M.; Gun, J.; Lev, O. (**2006**). Nanoscale probes for the evaluation of the integrity of ultrafiltration membranes, *Journal of Membrane Science, 276,* 199-207.

Glomm, W.R.; Halskau, Ø.; Hanneseth, A.M.D.; Volden, S. (**2007**). Adsorption behavior of acidic and basic proteins onto citrate-coated Au surfaces, correlated to their native fold, stability, and pI. *Journal of Physical Chemistry B, 111,* 14329-14345.

Gray, J.J. (**2004**). The interaction of proteins with solid surfaces. *Current Opinion in Structural Biology, 14,* 110-115.

Guo, S.H.; Tsai, S.J.; Kan, H.C.; Tsai, D.H.; Zachariah, M.R.; Phaneuf, R.J. (**2008**). The effect of an active substrate on nanoparticle-enhanced fluorescence. *Advanced Materials, 20,* 1424-1428.

http: // www.sigmaaldrich.com/ analytical-chromatography/ sample-preparation/ spe/ tube- configuration-guide .html

http:/ /www.waters.com/ waters/ en_US/ SPE-Method-Development /nav.htm?cid=10083845&locale=en_US.

Jain, P. Baker, G.L. Bruening, M.L. (**2009**). Applications of polymer brushes in protein analysis and purification. *Annual Review of Analytical Chemistry, 2,* 387-408.

Jain, P.; Vyas, M.K.; Geiger, J.H.; Baker, G.L.; Bruening, M.L. (**2010**). Protein purification with polymeric affinity membranes containing functionalized poly(acid) brushes. *Biomacromolecules, 11*, 1019-1026.

Joshi, H.; Shirude, P.S.; Bansal, V.; Ganesh, K.N.; Sastry, M. (**2004**). Isothermal titration calorimetry studies on the binding of amino acids to gold nanoparticles. *Journal of Physical Chemistry B, 108*, 11535-11540.

Lacerda, S.H.; Park, J.J.; Meuse, C.; Pristinski, D.; Becker, M.L.; Karim A.; Douglas, J.F. (**2010**). Interaction of gold nanoparticles with common human blood proteins. *ACS Nano, 26*, 365-379.

Laemmli. U.K. (**1970**) Cleavage of structural proteins during the assembly of the head of bacteriophage T4. *Nature, 227*, 680-685.

Li, M.D.; Cheng, T.L.; Tseng, W.L. (**2009**). Nonionic surfactant-capped gold nanoparticles for selective enrichment of aminothiols prior to CE with UV absorption detection. *Electrophoresis, 30*, 388-395.

Li, Q.; Du, Y.; Tang, H.; Wang, X.; Chen, G.; Iqbal, J.; Wang, W.; Zhang, W. (**2012**). Ultra sensitive surface-enhanced Raman scattering detection based on monolithic column as a new type substrate, *Journal of Raman Spectroscopy, 43*, 1392-1396.

Lin, Y.W.; Huang, M.J.; Chang, H.T. (**2003**). Analysis of double-stranded DNA by microchip capillary electrophoresis using polymer solutions containing gold nanoparticles. *Journal of Chromatography A, 1014*, 47-55.

Liu, J.; White, I.; DeVoe, D.L. (**2011**) Nanoparticle-functionalized porous polymer monolith detection elements for surface-enhanced Raman scattering. *Analytical Chemistry, 83,* 2119-2124.

Liu, K.; Aggarwal, P.; Lawson, J.S.; Tolley, H.D.; Lee, M.L. (**2013**). Organic monoliths for high-performance reversed-phase liquid chromatography. *Journal of Separation Science, 36,* 2767-2781.

Luther, P.; Theise, H.; Chatterjee, B.; Karduck, D.; Uhlenbruck, G. (**1980**). The lectin from Viscum *Album L*. isolation, characterization, properties and structure. International *Journal of Biochemistry, 11,* 429-435.

Lutter, P.; Meyer, H.E.; Langer, M.; Witthohn, K.; Dormeyer, W.; Sickmann, A.; Blüggel, M. (**2001**). Investigation of charge variants of rViscumin by two-dimensional gel electrophoresis and mass spectrometry. *Electrophoresis, 22,* 2888-2897.

Lv, Y.; Maya A.; Fréchet, J.M.J.; Svec, F. (**2012**). Preparation of porous polymer monoliths featuring enhanced surface coverage with gold nanoparticles. *Journal of Chromatography A,* 1261, 121-128.

McBryde, W.A.E.; Yoe, J.H. (1948). Colorimetric determination of gold as bromoaurate. Analytical Chemistry, 20, 1094-1099.Namera, A.; Saito, T. (**2013**). Advances in monolithic materials for sample preparation in drug and pharmaceutical analysis. *Trends in Analytical Chemistry, 45,* 182-196.

Nascimento, K.S.; Cunha, A.I.; Nascimento, K.S.; Cavada, B.S.; Azevedo, A.M.; Aires-Barros, M.R. (**2012**). An overview of lectins purification strategies. *Journal of Biological Chemistry, 25*, 527-541.

Ning, W.; Bruening, M.L. (**2015**). Rapid protein digestion and purification with membranes attached to pipet tips, *Analytical. Chemistry, 87*, 11984-11989.

Olsnes, S.; Stirpe, F.; Sandvig, K.; Pihl, A. (**1982**). Isolation and characterization of Viscumin, a toxic lectin from Viscum *album L.* (Mistletoe). *Journal of Biological Chemistry, 257,* 13263-13270.

Ou, J. Liu, Z. Wang, H. Lin, H. Dong, J. Zou, H. (**2015**). Recent development of hybrid organic-silica monolithic columns in CEC and capillary LC. *Electrophoresis, 36,* 62-75.

Preinerstorfer, B.; Lindner, W.; Laemmerhofer, M. (**2005**) Polymethacrylate-type monoliths functionalized with chiral amino phosphonic acid-derived strong cation exchange moieties for enantioselective nonaqueous capillary electrochromatography and investigation of the chemical composition of the monolithic polymer. *Electrophoresis, 26,* 2005-2018.

Rezwan, K.; Studart, A.R.; Voros, J.; Gauckler, L.J.J. (**2005**). Change of ζ potential of biocompatible colloidal oxide particles upon adsorption of bovine serum albumin and lysozyme. *Physical Chemistry, 109,* 14469-14474.

Samtleben, R.; Kiefer, M.; Luther, P. (**1985**). Characterization of the different lectins from *Viscum album* (Mistletoe) and their structural relationships with the agglutinins from *Abrus precatorius* and *Ricinus communis*. *Lectins: Biology, Biochemistry, Clinical Biochemistry, 4*, 617-626.Shen, C.C.;

Smith, N.; Jiang, Z. (**2008**). Developments in the use and fabrication of organic monolithic phases for use with high-performance liquid chromatography and capillary electrochromatography. *Journal of. Chromatography A, 1184,* 416-440.

Svec, F.; Lv, Y. (**2015**). Advances and recent trends in the field of monolithic columns for chromatography. *Analytical Chemistry, 87*, 250-273.

Sykora, D. Svec, F. Frechet, J.M.J. (**1999**). Separation of oligonucleotides on novel monolithic columns with ion-exchange functional surfaces. *Journal of Chromatography A, 852,* 297-304.

Sykora, D.; Kasicka, V.; Miksik, I.; Rezanka, P.; Zaruba, K.; Matejka, P.; Kral, V. (**2010**). Application of gold nanoparticles in separation sciences. *Journal of Separation Science, 33*, 372-387.

Thobhani, S.; Attree, S.; Boyd, R.; Kumarswami, N.; Noble, J.; Szymanski, M.; Porter, R.A. (**2010**). Bioconjugation and characterisation of gold colloid-labelled proteins. *Journal of Immunological Methods, 356*, 60-69.

Tsai, H.; Davila-Morris, M.; Del Rio, F.W.; Guha, S.; Zachariah, M.R.; Hackley, V.A. (**2011**). Quantitative determination of competitive molecular adsorption on gold nanoparticles using Attenuated Total Reflectance-Fourier Transform Infrared Spectroscopy. *Langmuir, 27,* 9302-9313.

Tseng, W.L.; Hsieh, M.M. (**2009**). Selective enrichment of aminothiols using polysorbate 20-capped gold nanoparticles followed by capillary electrophoresis with laser-induced fluorescence. *Journal of Chromatography A, 1216,* 288-293.

Wacker, R.; Stoeva, S.; Betzel C.; Voelter, W. (**2005**). Complete structure determination of N-acetyl-Dgalactosamine-binding mistletoe lectin-3 from *Viscum album L. album. Journal of Peptide Science, 11,* 289-302.

Wang, X.; Du, Y.; Zhang, H.; Xu, Y.; Pan, Y.; Wu, T.; Hu, H. (**2014**). Fast enrichment and ultrasensitive in-situ detection of pesticide residues on oranges with surface-enhanced Raman spectroscopy based on Au nanoparticles decorated glycidyl methacrylate ethylene dimethacrylate material. *Food Control, 46,* 108-114.

Xu, Y.; Cao, Q.; Svec, F.; Fréchet, J.M.J. (**2010**). Porous polymer monolithic column with surface-bound gold nanoparticles for the capture and separation of cysteine-containing peptides. *Analytical Chemistry, 82,* 3352-3358.

Yang, L.; Guihen, E.; Holmes, J.D.; Loughran, M.; O'Sullivan, G.P.; Glennon, J.D. (**2005**). Gold nanoparticle-modified etched capillaries for open-tubular capillary electrochromatography. *Analytical Chemistry, 77,* 1840-1846.

Yang, Q.; Adrus, N.; Tomicki, F.; Ulbricht M. (**2011**). Composites of functional polymeric hydrogels and porous membranes. *Journal of Materials Chemistry, 21*, 2783-2811.

Yeh, Y-C.; Creran, B.; Rotello, V.M. (**2012**). Gold nanoparticles: preparation, properties, and applications in bionanotechnology. *Nanoscale, 4*, 1871-1880.

Yoon, J.Y.; Kim, J.H.; Kim, W.S. (**1998**). Interpretation of protein adsorption phenomena onto functional microspheres. *Colloids and Surfaces B, 12*, 15-22.

Yoon, J.Y.; Kim, J.H.; Kim, W.S. (**1999**). The relationship of interaction forces in the protein adsorption onto polymeric microspheres. *Colloids and Surfaces A, 153*, 413-419.

Chapter 7. Polymeric sorbents modified with gold and silver nanoparticles for solid-phase extraction of proteins followed by MALDI-TOF analysis

Microchim Acta
DOI 10.1007/s00604-017-2168-5

ORIGINAL PAPER

Polymeric sorbents modified with gold and silver nanoparticles for solid-phase extraction of proteins followed by MALDI-TOF analysis

María Vergara-Barberán[1] · María Jesús Lerma-García[1] · Ernesto Francisco Simó-Alfonso[1] · José Manuel Herrero-Martínez[1]

The authors describe four different kinds of sorbents for SPE and preconcentration of proteins from complex samples. All are based on the use of a poly(glycidyl-co-ethylene dimethacrylate) host monolith that was chemical ly functionalized by using two different ligands (ammonia and cysteamine). AuNPs or AgNPs were then assembled to the amino or thiol groups. The resulting materials are shown to be viable stationary phases for use in SPE cartridges. The sorbents can selectively retain bovine serum albumin, and the thiol modified sorbents containing AuNPs and AgNPs provide the highest recoveries (>90%) and satisfactory loading capacities (29.3 and 17.6 μg·mg^{-1} of sorbent, respectively). The applicability of these nanosorbents was demonstrated by preconcentrating viscotoxins from mistletoe extracts. The enriched fractions were subjected to MALDI-TOF analysis to underpin their selectivity.

Keywords: metal nanoparticles; sorption; preconcentration; poly(glycidyl-co-ethylene dimethacrylate); BSA; SPE; stationary phase; MALDI-TOF; mistletoe viscotoxins

7.1. Introduction

Protein/peptide purification and isolation constitute important steps in almost all branches of biosciences and biotechnologies. For this reason, a considerable interest in developing selective and efficient methods to isolate target proteins from complex matrices has attracted much attention (Zhou, 2007). Besides, it is very important that these methodologies present high loading capacities, which will lead to lower detection limits in protein analysis (Du, 2007). In this sense, SPE is the most popular sample treatment procedure employed in protein separation and preconcentration techniques (Du, 2007). Thus, SPE is characterized by its high efficiency, low running cost, simplicity, easy automation, and avoidance of the use of toxic organic solvents (Du, 2007). However, the selection of an appropriate sorbent is a critical factor to achieve high extraction efficiency, since there is a limited number of sorbents for protein species available at present. Thus, interest has been focused in the development of SPE sorbents for protein isolation using novel materials such as metal-organic frameworks (Yang, 2016) and polymer monoliths (Namera, 2013). Particularly, these latter sorbents represent an alternative class of stationary phases to traditional packed columns. In this sense, organic polymeric monoliths have many advantages when they are used in sample treatment. For instance, its porous structure can aid to increase the loading capacity of the extraction and offer a good permeability, which allows the use of larger flow rate, thus reducing analysis time (Namera, 2013). Another important point of monolithic materials is that their extraction efficiency can be changed by tailoring its pore structure and by introducing chemical modifications in the pore surface, which may produce monoliths with enhanced selectivity properties. In this regard, the modification of monoliths via attachment of metallic nanoparticles (NPs) onto the monolithic surface has focused much attention (Cao, 2010; Xu, 2010; Alwael, 2011). Thus, the most common way to immobilize metallic

NPs to polymeric structures is by incorporating amine or thiol functionalities onto their pore surface (Cao, 2010; Alwael, 2011; Vergara-Barberán, 2016). However, up to date, most of these publications have been applied in chromatographic area, being few reports focused on sample treatment (Alwael, 2011; Vergara-Barberán, 2016). Thus, Alwael *et al.* (Alwael, 2011) have described the immobilization of AuNPs onto the amine modified monoliths in pipette tips using ethylenediamine to extract glycoproteins. Vergara *et al.* (Vergara-Barberán, 2016) have immobilized AuNPs onto ground monolithic powder (previously modified with ammonia) to isolate proteins from complex samples. This ground monolithic powder has been also used in ultrasensitive SERS detection (Li, 2012) as an "entrapment support" to immobilize biomacromolecules (Benčina, 2007).

On the other hand, AgNPs have demonstrated to possess distinctive properties compared to other metallic NPs such as their antimicrobial (Sharm, 2009) and optical properties (González, 2007). For instance, Banerjee et *al*. (Banerjee, 2013) investigated changes in their surface plasmon resonance band in presence of different protein concentrations to study the type of interaction (hydrophobic and/or electrostatic) in the binding of proteins to AgNP surface. However, few applications (Shrivas, 2008) describing its use as preconcentrating supports to retain proteins have been reported. Thus, Shrivas *et al.* (Shrivas, 2008) have used modified AgNPs to preconcentrate hydrophobic peptides and proteins from biological samples previous MALDI analysis.

This work focuses on the study of different SPE sorbents especially designed for protein isolation from complex samples. For this purpose, polymeric sorbents were prepared from a ground poly(glycidyl-co-ethylene dimethacrylate) based polymer and then treated with different ligands (ammonia or cysteamine). The resulting materials (containing amine or thiol groups, respectively) were functionalized with AuNPs or AgNPs. These SPE

sorbents were evaluated in terms of extraction parameters to retain proteins (using BSA as probe) and other performance features (loading capacity, reusability and limit of detection) were established. In addition, the ability of these materials to specifically retain small basic and cysteine-rich proteins (thionins) in European mistletoe extract was demonstrated.

7.2. Experimental

7.2.1. Chemicals and reagents

GMA, EDMA, ACN and MeOH were purchased from Scharlab (Barcelona, Spain, http://www.scharlab.com). AIBN was purchased from Fluka (Buchs, Switzerland, http://www.sigmaaldrich.com). AuNP and AgNP suspensions (both with a particle size of 20 nm and stabilized with sodium citrate) and Coomassie Blue were from Alfa Aesar (Landcashire, United Kingdom, http://www.alfa.com). Monosodium and disodium phosphate (NaH_2PO_4 and Na_2HPO_4, respectively) and orthophosphoric (H_3PO_4) acid were from Merck (Darmstadt, Germany, http://www.merckgroup.com/en/index.html). BSA, α-cyano-4-hydroxycinnamic acid (HCCA), gold (III) chloride trihydrate, HCl, 2-mercaptoethanol, nitric acid (HNO_3), potassium bromide, Tris and trisodium citrate were obtained from Sigma-Aldrich (St. Louis, MO, USA, http://www.sigmaaldrich.com). A molecular-weight-size protein standard (6.5 to 200 kDa) was also provided by Sigma-Aldrich. Deionized water (Barnstead deionizer, Sybron, Boston, Mass., USA, http://www.barnstead-water.com) was used in all procedures.

A stock solution of BSA (1 mg mL^{-1}) was prepared with deionized water, and working standard solutions were obtained by dilution of the stock solution. Phosphate buffer solutions of 20 mM at several pH values were prepared by dissolving appropriate amounts of Na_2HPO_4, NaH_2PO_4 and H_3PO_4 according to the required pH.

7.2.2. Instrumentation

Scanning electron microscopy /backscattered electron (SEM/BSE) micrographs were obtained with a Hitachi S4800 (Ibaraki, Japan, www.hitachi.com) provided with a field emission gun, and an EMIP 3.0 image acquisition system. Previous to the SEM measurements, the polymeric sorbents were coated with a very thin-layer of conductive carbon.

An EA 1110 CHNS elemental analyzer (CE Instruments, Milan, Italy, http://www.ceinstruments.co.uk) was used for elemental analysis of synthesized materials. An 8453 diode-array UV-vis spectrophotometer (Agilent Technologies, Waldbronn, Germany, http://www.agilent.com/) was used for Bradford assay and for gold determination. An ICP-MS (Agilent model 7900) was employed to determine silver content in the sorbents. Raman spectra of materials were recorded with an XploRA One Raman microscope (Horiba Scientific, Villeneuve d'Ascq, France, http://www.horiba.com/) from 150 to 3500 cm^{-1} using 532 nm as excitation wavelength with a laser power of 90 μW. A 5800 MALDI-TOF/TOF-MS (AB SCIEX, Foster City, CA, https://sciex.com/) was used to determine viscotoxin masses.

7.2.3. Preparation and modification of GMA-based polymer

The GMA-co-EDMA monolithic material was obtained as described in previous works (Carrasco-Correa, 2013; Vergara-Barberán, 2016). Briefly, the polymerization mixture composed by GMA (20 wt%), EDMA (5 wt%), cyclohexanol (70 wt%), 1-dodecanol (5 wt%) and AIBN (1 wt% with respect to the monomers) was sonicated for 10 min to obtain a clear solution and, and then, purged with nitrogen for 10 min. The polymerization was carried out in an oven at 60ºC for 24 h. A rinse with methanol was employed to remove the unreacted monomers and the pore-forming solvents a wash with methanol was carried out. The bulk material was ground with a mortar

and sieved with a steel sieve (with sizes ≤ 100 µm). The resultant GMA powder was chemically modified with ammonia (procedure A) and with cysteamine (procedure B). The procedure A was carried out according to Vergara-Barberán *et al*. (Vergara-Barberán, 2016). Briefly, the material was treated with aqueous 4.5 M ammonia at 60ºC for 2 h. The functionalized GMA-based material with amino groups ("GMA-NH_2") was washed with water until neutral pH and kept at room temperature for further use. Regarding to procedure B, the parent polymer was allowed to react with 2.5 M cysteamine aqueous solution during 2 h at room temperature and finally a washing step was conducted with water until neutral pH (Cao, 2010; Xu, 2010). The resulting modified thiol-GMA material was referred to as "GMA-SH". **Figure 7.1** shows the reaction of GMA-based material with both ligands.

7.2.4. Functionalization of amino- or thiol-modified GMA material with AuNPs or AgNPs

To obtain the four types of sorbents used in this work, 400 mg of GMA-NH_2 or GMA-SH were treated with AuNP or AgNP dispersion. In order to detect the saturation of the monolithic material with metallic NPs, the UV-vis spectra of the supernatants were recorded before and after the addition of AuNPs or AgNPs at several times until the NP surface plasmon resonance band appeared in the UV-vis spectrum. In the case of GMA-NH_2 material, a total volume of 20 mL of metallic NPs was enough to saturate the material, while GMA-SH was saturated after adding a total of 100 mL of metallic NP suspension. In both cases, the color of the GMA-co-EDMA powders indicated that metallic NPs are attached (pink for AuNPs and yellowish for AgNPs). After attachment of NPs, the materials were washed with 38.8 mM sodium citrate at pH 6.6 in order to remove the non-immobilized AuNPs and AgNPs.

These four materials (designated as GMA-NH_2-Au, GMA-SH-Au, GMA-NH_2-Ag and GMA-SH-Ag) were characterized by SEM. Moreover, the Au and Ag contents were evaluated using UV-vis and ICP-MS, respectively. For these measurements, all materials were previously calcined at 550 °C for 1 h. In the case of sorbents containing AuNPs, the remaining product (which contained Au) was dissolved in *aqua regia*, properly diluted with HCl 1 M and then subjected to UV-vis analysis (Gitis, 2006). On the other hand, the materials with AgNPs were dissolved in concentrated HNO_3, adequately diluted with water and analyzed by ICP-MS.

7.2.5. SPE protocols

SPE cartridges were prepared according to the literature (Vergara-Barberán, 2016). For this purpose, 50 mg of AuNP- or AgNP-modified polymer sorbents was placed into 1 mL empty propylene disposable SPE cartridge (Análisis Vínicos, Tomelloso, Spain) using two frits (1/16', 20 µm, Análisis Vínicos). In all cases, the SPE sorbents were activated with 200 µL ACN and equilibrated with 500 µL H_2O. Then, 200 µL BSA (200 mg L^{-1} in phosphate buffer, adjusted to a proper pH) was loaded on the SPE material at a flow of 0.1 mL min^{-1}. The washing step was carried out with phosphate buffer (under the same pH conditions as the loading step) at 0.7 mL min^{-1}. The elution step was done with 200 µL of 30 mM phosphate buffer (pH 12.0) at 0.1 mL min^{-1}. In all steps, the fractions were collected and subjected to Bradford assay (Bradford, 1976) in order to evaluate the retention efficiency of proteins on these AuNP- and AgNP-modified materials. The regeneration of sorbents was accomplished with water at 80 ºC during 2h (Xu, 2010). The same procedure was applied to prepare a blank sorbent (GMA-based polymer) (50 mg).

To establish the capability of our SPE protocol to preconcentrate proteins, the limit of detection (LOD) of BSA was evaluated. For this purpose, BSA solutions of several concentrations (0.1-100 nM) were prepared in deionized water and subjected to the extraction process. The resulting eluates were then mixed with the matrix solution (0.5 g/L HCCA in 70% aqueous acetonitrile and 0.1% TFA), and were deposited onto an ABSCiex MALDI plate and analyzed in a 5800 MALDI TOF/TOF instrument (ABSciex) in the positive ion mode (3000 shots every position). The MS and MS/MS information was sent to be identified by the MASCOT software (v 2.3.02; Matrix Science) via the Protein Pilot (ABSciex).

7.2.6. Extraction of mistletoe viscotoxins and MALDI-TOF analysis

European mistletoe (*Viscum Album L.*) grown on *Pinus halepensis* was collected and the green parts were separated. To eliminate bacterial and surface contamination these parts were rinsed with water, and subsequently sliced, transferred to a mortar and ground into powder using liquid nitrogen. Then, the viscotoxin extraction protocol was adapted from Hussain *et al.* (Hussain, 2013). Briefly, 5 g of this powder was treated with 20 mL of 10 mM phosphate buffer at pH 7.4, mildly shaken at 4ºC overnight and centrifuged at 10000 × g for 10 min. For viscotoxin isolation, 500 µL of the supernatant were directly subjected to the SPE procedure.

As mentioned before, the protein elution was made with 30 mM phosphate buffer at pH 12. In this case of mistletoe extract these fractions were subjected to both, Bradford assay and MALDI-TOF measurements.

MALDI samples were prepared by mixing equal volumes of the extract and the matrix solution before spotting on the MALDI plate followed by MALDI-TOF analysis.

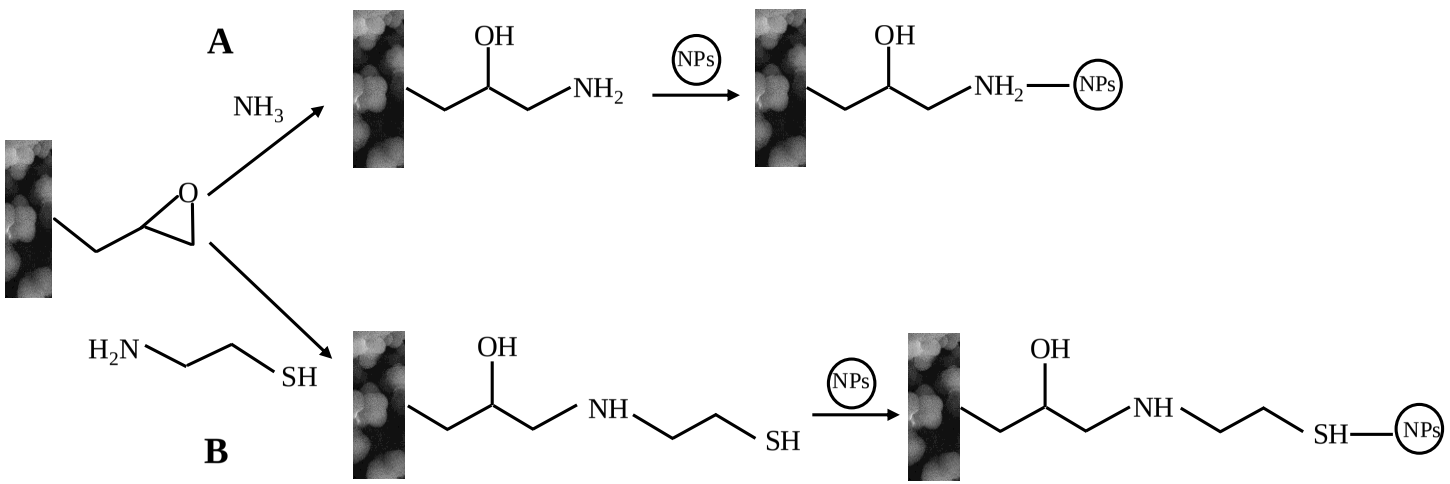

Figure 7.1. Scheme of functionalization of poly(GMA-co-EDMA) material with ammonia (A) and cysteamine (B), and subsequently immobilization with metallic nanoparticles (AuNPs or AgNPs).

7.3. Results and discussion

7.3.1. Choice of materials

As already mentioned in Introduction, organic polymer monoliths exhibit several benefits such as their simple in situ preparation and large permeability due to their large through pores. In particular, GMA-based polymers are chemically and mechanically stable materials containing reactive functionalities (epoxy groups) susceptible of undergoing functionalization, thus allowing the attachment of organic material or even metallic NPs such as gold (Cao, 2010; Xu, 2010; Vergara-Barberán, 2016). Taking into account these good features, and the strong affinity of both gold and silver surfaces for thiol-containing compounds, the development of novel SPE sorbents in sample treatment for selective extraction and preconcentration of proteins is highly desirable to translate the benefits of this fruitful combination.

7.3.2. Studies with GMA-based materials modified with AuNPs

The use of SPE sorbents based on AuNPs immobilized onto amino-modified GMA materials has been previously implemented in our research group (Vergara-Barberán, 2016). In fact, this sorbent provided advantageous features in terms of extraction efficiency (easy preparation, satisfactory loading capacity (16.6 mg/g sorbent) and reusability); however, its gold content was low (0.5 wt%). In order to increase this content, and consequently the loading capacity of material, another ligand (cysteamine) was considered. This ligand has been previously used by Svec and co-workers (Xu, 2010) to enrich the surface of GMA-based monoliths with thiol groups for posterior attachment of AuNPs. Thus, the ground GMA modified with cysteamine (GMA-SH) was obtained and then subjected to elemental analysis, giving 1.31 wt% sulfur (0.4 mmol thiol groups /g monolith). This

value was lower than those found by Svec's group (1.05 mmol/g) (Cao, 2010; Xu, 2010). These differences can be attributed to the format employed in the synthesis of monoliths. In our case, bulk monoliths (prepared in glass vials) were carried out, while the reported data of the functionalized monoliths were made in capillaries. Evidence on the different properties (e.g. number of accessible reactive and unfunctionalized groups) of monoliths prepared in rather different formats has been previously reported (Carrasco-Correa, 2015); where the accessible number of epoxy groups was lower for the bulk polymers than for the corresponding capillary monolith.

After functionalization with AuNPs, the GMA-SH-Au material led to a 2.90 wt% Au, which is higher than that previously obtained for GMA-NH_2-Au sorbent. It can be explained by the high amount of thiol groups present in the sorbent surface, which bind strongly to AuNPs. Moreover, SEM micrographs of the GMA-SH-Au materials, taken with a BSE detector, show the presence of large number of AuNPs compared with the GMA-NH_2-Au (**Figure 7.S1**). Raman spectroscopy was also employed to verify the binding of AuNPs onto the surface of the modified GMA-based polymers (**Figure 7.S2**). Thus, the characteristic stretching modes of primary amine groups (appeared at 3100-3300 and ~1560 cm^{-1}) and thiol groups (appeared at 2510 cm^{-1}) were evidenced for GMA-NH_2 and GMA-SH, respectively. After attachment of AuNPs onto the surface of these polymers, the characteristic stretching modes of amine and thiol groups diminished or even disappeared. It indicates that the AuNPs were assembled to GMA-based materials.

Then, the loading capacity of the GMA-SH-Au sorbent was evaluated. For this purpose, different amounts of BSA (200-5000 μg mL^{-1}) were passed through this SPE device by keeping constant the working conditions of SPE procedure detailed in our previous work (Vergara-Barberán, 2016). The maximum loading capacity obtained for GMA-SH-Au material was 29.3 mg/g sorbent, which was higher than that found previously for GMA-NH_2-

Au material. The reusability of this sorbent was also evaluated. For this purpose, the regeneration protocol described in SPE protocol Section was applied. Thus, the BSA adsorption capacity decreased only 5.3% after 20 cycles.

7.3.3. Studies with GMA-based materials modified with AgNPs

In order to extend the application of SPE supports for protein analysis, sorbents based on the immobilization of AgNPs were also prepared using the parent materials described in the previous section (GMA-NH_2 and GMA-SH). After attachment of AgNPs, the silver content in both materials (GMA-NH_2-Ag and GMA-SH-Ag) was measured by ICP-MS giving 0.29 and 2.7 wt% Ag, respectively. These results were in agreement with SEM micrographs of both sorbents (**Figure 7.S1**). Also, Raman spectra of parent and AgNP-modified polymers were done (data not shown), giving similar results to those found for AuNP-based materials (**Figure 7.S2**), thus confirming the binding of AgNPs onto the surface of amino- or thiol-modified polymers. As mentioned above, these differences in silver content can be explained by the higher affinity of these NPs or other metallic nanostructures (such as AuNPs) towards to thiol groups than the amino functionalities. In fact, several authors have suggested that the amino-Ag bond (resulting from a mixed mechanism of electrostatic and donor-acceptor interactions) is weaker than the thiol-Ag bond, which has a strongly covalent behavior (Joshi, 2004; Jiang, 2013; Park, 2016).

In any case, the retention of proteins onto these Ag modified sorbents was next considered. Both, loading sample and elution pHs were next optimized (see supplementary material text and **Figure 7.S3** and **S4**). The best results were obtained at pH values of 7 and 12 for loading sample and elution steps, respectively. Once the working SPE conditions were optimized, the breakthrough volume was evaluated for both Ag modified sorbents using

BSA as probe. For this purpose, different sample volumes (25-2000 μL) of the standard protein solutions were passed through to the SPE material by keeping constant the amount of protein (0.1 mg). Experimental results showed that for both AgNP-based sorbents excellent recovery values (> 95%) were achieved up to 200 μL of sample volume. Then, the loading capacities of GMA-NH_2-Ag and GMA-SH-Ag were established, giving values of 9.7 and 17.6 mg of BSA per g sorbent, respectively. These values were in strong correlation with the content of Ag found for each sorbent (see values above). The reusability of both sorbents was also tested using the protocol previously described (Vergara-Barberán, 2016). Thus, the GMA-NH_2-Ag and GMA-SH-Ag materials can be reused until 9 and 12 times, respectively, without significant efficiency losses (satisfactory recovery comprised between 80.2-92.4%). During these cycle experiments, the Ag content (measured by ICP-MS) was evaluated, and no significant changes in Ag concentration were found (data not shown), which demonstrated the viability of the regeneration protocol.

A comparison in terms of extraction performance using the sorbents was next considered. Under their respective SPE optimum conditions, the recoveries values of BSA were higher than 98.2% for all sorbents investigated, whereas for the loading capacity, the GMA-SH-Au sorbent shows the highest value (29.3 mg/g). This fact can be explained taking into account the large Au content present in this material and the large affinity of this metallic NP towards to thiol functionalities present in GMA support, as we discussed above.

Prior to evaluate the applicability of the current approach to real samples, experiments were conducted to establish the LOD of standard BSA spiked in water using the GMA-SH-Au sorbent, achieving a LOD value for BSA in water of 0.1 nM.

Then, the SPE sorbent described here was compared with reports related to the use of other nanomaterials for protein/peptide preconcentration prior MALDI-MS analysis. Thus, the LOD assayed in this study was similar (Chang, 2007; Chen, 2007; González, 2007) or even better (Shrivas, 2008; Bhat, 2010; Kailasa, 2008; Shrivas, 2010; Shastri, 2015; Yan, 2014) than those described in studies given in **Table 7.1**.

Besides, our SPE support method offers an increased surface area-to-volume ratio, without losses of material and analyte compared to some of these microextraction techniques (such as NP-LLME or dSPE) (Shrivas, 2008; Kong, 2005; Bjat, 2010; Kailisa, 2008; Shrivas, 2010), where analyte loss or desorption from the surface of NPs occurred during washing or centrifugation steps. Moreover, our SPE protocol simplifies the handling of more samples simultaneously and speeds the preconcentration process of proteins. In particular, this method allowed a sample throughput of 10 samples h^{-1}, whereas a rate of 1-2 samples h^{-1} could be achieved with other NP-based protocols. Other strength of the proposed sorbents is its satisfactory reusability (see data above). In this regard, in the related studies of NP-based materials (see **Table 7.1**), this important parameter was not evaluated or this information was missing. This suitable reusability combined with the possibility of manufacturing several SPE cartridges (*ca*. 7) from the bulk NPs-modified material (see Experimental section) undoubtedly makes this protocol economically attractive.

Table 7.1

An overview on reported nanomaterial-based methods for preconcentration of proteins and peptides using MALDI-TOF analysis.

Material	Analyte	Matrix	Extraction technique	LOD (nM)	Ref.
ZipTip C_{18}	Cytochrome c, myoglobin and BSA	Blood serum	SPE	0.5-1	(Kong, 2005)
AgNPs	Myoglobin, ubiquitin BSA and gramicidin D	Urine and plasma	NP-LLME	130-160	(Shrivas, 2008)
PdNPs	Insulin, ubiquitin Lysozyme and gramidicin D	Water and urine	NP-LLME	17-37	(Bhat, 2010)
Diamond NPs	Cytochrome c, myoglobin and BSA	Blood serum	dSPE	0.1	(Kong, 2005)
ZnSNPs	Ubiquitin and insulin	Aqueous solution, Oyster mushroom and biological samples	dSPE	85-91	(Kailasa, 2008)
MWCNT/CdSNPs	Cytochrome c and lysozyme	Milk and urine	dSPE	1-7	(Shrivas, 2010)
Bidentate AgNPs	Cytochrome c and insulin	Milk and human urine	SDME	1-80	(Shastri, 2015)

Cont. Table 7.1

Fe_3O_4 NPs-TiO_2	Angiotensin I, insulin, cytochrome c and trypsinogen	Aqueous solution	MSPE	50	(Chen, 2005)
Fe_3O_4 NPs (coated with carboxylate groups)	Angiotensin I, insulin, myoglobin and cytochrome C digest	Aqueous solution	MSPE	0.1-10	(Chang, 2007)
Alumina-coated Fe_3O_4 NPs	Digests of α-and β-caseins, human protein phosphatase inhibitor 1, egg white and a cell lysate	Tryptic digest products	MSPE	0.05	(Chen, 2007)
TiO_2 coated Fe_3O_4-MWCNTs	Phosphopeptides	BSA digest	MSPE	20	(Yan, 2014)
GMA-SH-Au	BSA, viscotoxins	Aqueous solution	SPE	0.1	This work

Abbreviations: SPE, solid-phase extraction; NP-LLME, nanoparticle liquid-liquid microextraction; SDME, single drop microextraction; dSPE; dispersive solid-phase extraction; MWCNTs, multiwalled carbon nanotubes; MSPE, magnetic solid-phase extraction.

7.3.4. Application to the isolation of viscotoxins from European mistletoe

The designed sorbent materials were employed to selective isolate and preconcentrate viscotoxins from European mistletoe samples. These small basic and cysteine-rich polypeptides (with molecular weights *ca*. 5 kDa), belonging to the thionin family, consist of a 45-50 amino acids residues with 3-4 internal disulfide bonds. They display cytotoxic activity against different types of tumor cells (Büssing, 1999). Their biological activity can be related to plant defense since its high expression gives enhanced resistance to pathogens (Holtorf, 1998). According to the amino acid sequence, disulphide bridge arrangement and distribution in plant tissues, seven isoforms of viscotoxins, namely A1, A2, A3, B, B2, 1-PS and C1 have been reported (Pal, 2008; Hussain, 2013). From these thionins, viscotoxin A3 is the most cytotoxic whereas viscotoxin B is the less potent (Schaller, 1996). The pI of the viscotoxins is comprised in a range from 8.9 to 9.3.

The extraction and isolation of the viscotoxins is generally a tedious task that implies several purification steps (cation-exchange columns, fractionation by preparative HPLC, etc) (Guidici, 2003). To avoid these time-consuming processes, the sorbents previously developed to isolate mistletoe viscotoxins were used. The experimental procedure is detailed in Extraction of mistletoe viscotoxins Section, and subsequently the collected fractions were subjected to MALDI-TOF analysis. **Figure 7.2** shows the MALDI-TOF MS spectra of mistletoe extract before SPE (A), the wash fraction (B) and the eluted viscotoxins using the GMA-SH-Au sorbent (C).

The trace A represents the entire range of peptides (up to *m/z* 6000) found in Mistletoe extract, whereas in the washing fraction (trace B), any signal around 4800 (molecular masses of viscotoxins) is observed. Trace C shows the eluted fraction (including an expanded mass region around 4800 *m/z*), being the identified viscotoxins listed in **Table 7.2**. Protein information resource software (MASCOT) was used for the determination of the exact

mass of peptides. These peptides were also detected in the eluates obtained from the other sorbents of this study (data not shown).

Table 7.2

Identified viscotoxins from the SPE elution fractions of mistletoe extracts and their theoretical mass reported in literature.

Viscotoxin	Observed mass (Da)	Theretical mass (Da)*
A2	4835.8	4834.42
A3	4835.8	4835.53
B	4857.7	4857.45
A1	4889.9	4889.53
1-PS	4904.3	4904.02

* (Hussain, 2013; Hussain, 2014).

As shown in **Figure 7.2C**, the most abundant viscotoxin found was B in contrast to that reported by Hussain *et al.* (Hussain, 2013; Hussain, 2014), where the isoforms predominant were A2 and A3. These differences in isoform contents can be explained by taking into account several factors such as the *V. album* subspecies considered and seasonal changes. In our case, the Mistletoe leaves were from the subspecie *Viscum album austriacum*, which were found over *Pinus nigra*, where the viscotoxin B showed a large content (Urech, 2011). Besides, the content of this viscotoxin remained unchanged during the seasonal course of leaves of *V. album*, whereas viscotoxins A1, A2, and A3 showed degradation (Urech, 2011).

7.4. Conclusions

In this work, several SPE sorbents based on a methacrylate polymer modified with both AuNPs and AgNPs have been used for protein isolation. The ability of two ligands (ammonia and cysteamine) to prepare parent supports to be subsequently functionalized with these NPs was evaluated. The results show that the materials containing thiol functionalities afford a large coverage of AuNPs or AgNPs onto the polymer surface due to the large affinity of thiol moieties and these NPs. After SPE protocol optimization, the sorbents show large recovery efficiencies, loading capacities (up to 29.3 mg/g sorbent) and satisfactory reusabilities. Compared to the existing NP-based methods for sample preparation in MALDI-TOF analysis, our SPE protocol is simpler, more cost-effective, and shorter in terms of processing time; however, it requires more sorbent amount (50 mg) than these (micro)extraction techniques. To demonstrate the practical applicability of these materials, the GMA-SH-Au sorbent, which provided the highest loading capacity and excellent LOD, was chosen and successfully applied to selectively isolate viscotoxins from European mistletoe extracts. The sorbents used in this work open an alternative avenue to facilitate satisfactory separation of peptides/proteins from complex samples using very simple extraction methodologies.

Acknowledgements

This work was supported by project CTQ2014-52765-R (MINECO of Spain and FEDER) and PROMETEO/2016/145 (Generalitat Valenciana). M. V-B thanks the MEC for an FPU grant for PhD studies. The authors also thank Dr. Luz Valero Rustarazo from the Proteomic section of the SCSIE (University of Valencia), for her help in MALDI-TOF-MS measurements.

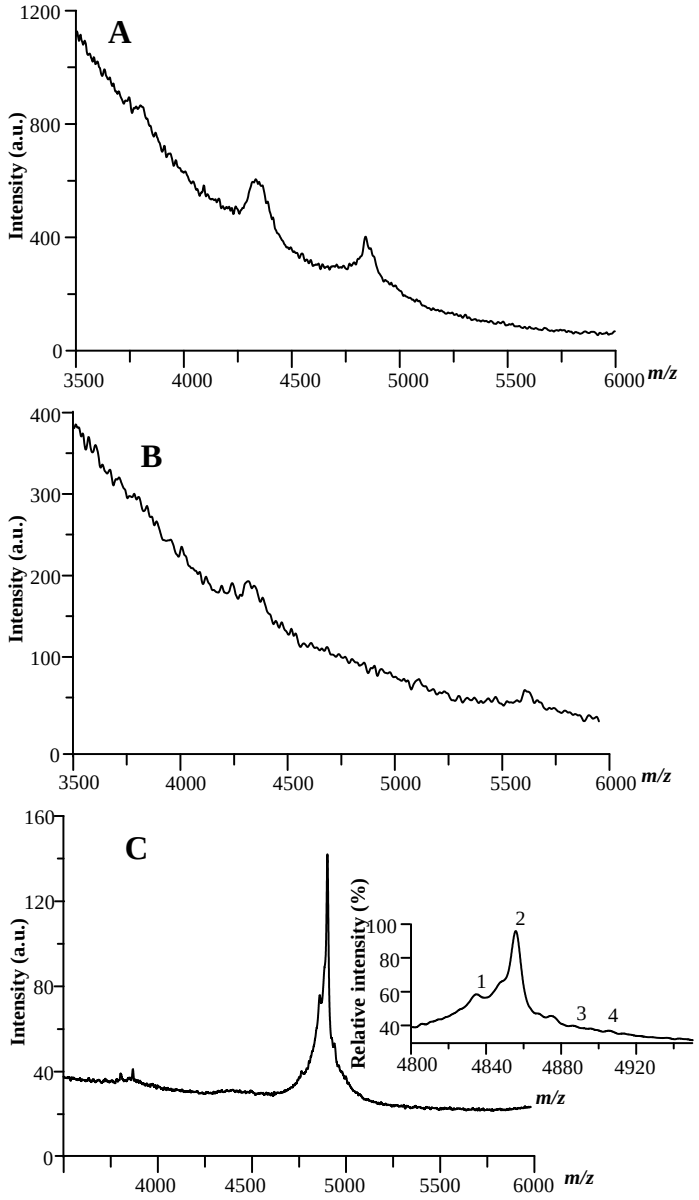

Figure 7.2. MALDI-TOF MS spectra of mistletoe extract. Mass spectra of extract before SPE procedure (A), wash fraction after SPE procedure (B) and the elution of the retained viscotoxins (C) using the GMA-SH-Au sorbent.

7.5. References

Alwael, H.; Connolly, D.; Clarke, P.; Thompson, R.; Twamley, B.; O'Connor, B.; Paull, B. (**2011**). Pipette-tip selective extraction of glycoproteins with lectin modified gold nano-particles on a polymer monolithic phase. *Analyst, 136*, 2619-2628.

Banerjee, V.; Das, K.P. (**2013**). Interaction of silver nanoparticles with proteins: A characteristic protein concentration dependent profile of SPR signal. *Colloids and Surfaces B, 111*, 71-79.

Benčina, K.; Benčina, M.; Podgornik, A.; Štrancar, A. (**2007**). Influence of the methacrylate monolith structure on genomic DNA mechanical degradation, enzymes activity and clogging. *Journal of Chromatography A, 1160*, 176-183.

Bhat, A.R.; Wu, H.F. (**2010**). Synthesis, characterization and application of modified Pd nanoparticles as preconcentration probes for selective enrichment/analysis of proteins via hydrophobic interactions from real-world samples using nanoparticle liquid-liquid microextraction coupled to matrix-assisted laser desorption/ionization time-of-flight mass spectrometry. *Rapid Communications in Mass Spectrometry, 24*, 3547-3552.

Bradford, M.M. (**1976**). A rapid and sensitive method for the quantitation of microgram quantities of protein utilizing the principle of protein-dye binding. *Analytical Biochemistry, 72*, 248-254.

Büssing, A.; Schietzel, M. (**1999**). Apoptosis-Inducing properties of *Viscum album L*. extracts from different host trees, correlate with their content of toxic mistletoe lectins. *Anticancer Research, 19*, 23-28.

Cao, Q.; Xu, Y.; Liu, F.; Svec, F.; Fréchet, J.M.J. (**2010**). Polymer monoliths with exchangeable chemistries: use of gold nanoparticles as intermediate ligands for capillary columns with varying surface functionalities. *Analytical Chemistry, 82*, 7416-7421.

Carrasco-Correa, E.J.; Ramis-Ramos, G.; Herrero-Martínez, J.M. (**2013**). Methacrylate monolithic columns functionalized with epinephrine for capillary electrochromatography applications. *Journal of Chromatography A, 1298*, 61-67.

Carrasco-Correa, E.J.; Ramis-Ramos, G.; Herrero-Martínez, J.M. (**2015**). Evaluation of 2,3-epoxypropyl groups and functionalization yield inglycidyl methacrylate monoliths using gas chromatography. *Journal of Chromatography A, 1379*, 100-105.

Chang, S.Y.; Zheng, N.Y.; Chen, C.S.; Chen, C.D.; Chen, Y.Y.; Wang, C.R.C. (**2007**). Analysis of peptides and proteins affinity-bound to iron oxide nanoparticles by MALDI-MS. *Journal of the American Society for Mass Spectrometry, 18*, 910-918.

Chen, C.T.; Chen, W.Y.; Tsai, P.J.; Chien, K.Y.; Yu, J.S.; Chen, Y.C. (**2007**). Rapid enrichment of phosphopeptides and phosphoproteins from complex samples using magnetic particles coated with alumina as the concentrating probes for MALDI MS analysis. *Journal of Proteome Research, 6*, 316-325.

Chen, C.T.; Chen, Y.C. (**2005**). Fe_3O_4/TiO_2 Core/Shell nanoparticles as affinity probes for the analysis of phosphopeptides using tio_2 surface-assisted laser desorption/ionization mass spectrometry. *Analytical Chemistry, 77*, 5912-5919.

Du, Z.; Yu, Y.L.; Chen, X.W.; Wang, J.H. (**2007**). The isolation of basic proteins by solid-phase extraction with multiwalled carbon nanotubes. *Chemistry European Journal, 13,* 9679-9685.

Gitis, V.; Haught, R.C.; Clark, R.M.; Gun, J; Lev, O. (**2006**). Nanoscale probes for the evaluation of the integrity of ultrafiltration membranes. *Journal of Membrane Science, 276,* 199-207.

Giudici, M.; Pascual, R.; Canal, L.; Pfüller, K.; Pfüller, U.; Villalaín, J. (**2003**). Interaction of Viscotoxins A3 and B with membrane model systems: Implications to their mechanism of action. *Biophysical Journal, 85,* 971-981.

González, L.; Noguez, C. (**2007**). Optical properties of silver nanoparticles. *Physica Status Solidi, 11,* 4118-4126.

Holtorf, S.; Ludwig-Müller, J.; Apel, K.; Bohlmann, H. (**1998**). High level expression of a viscotoxin in Arabidopsis thaliana gives enhanced resistance against *Plasmodiophora brassicae*. *Plant Molecular Biology, 36,* 673-680.

Hussain, S.; Güzel, Y.; Pezzei, C.; Rainer, M.; Huck, C.W.; Bonn, G.K. (**2014**). Solid-phase extraction of plant thionins employing aluminum silicate based extraction columns. *Journal of Separation Science, 37,* 2200-2207.

Hussain, S.; Güzel, Y.; Schönbichler, S.A.; Rainer, M.; Huck, C.W.; Bonn, G.K. (**2013**). Solid-phase extraction method for the isolation of plant thionins from European mistletoe, wheat and barley using zirconium silicate embedded in poly(styrene-co-divinylbenzene) hollow-monoliths. *Analytical and Bioanalytical Chemistry, 405,* 7509-7521.

Jiang, X.; Yang, M.; Meng, Y.; Jiang, D.W.; Zhan, J. (**2013**). Cysteamine-modified silver nanoparticle aggregates for quantitative SERS sensing of

pentachlorophenol with a portable Raman spectrometer. *Applied Materials & Interfaces, 5,* 6902-6908.

Joshi, M.; Shirude, P.S.; Bansal, V.; Gaxesh, K.; Sostry, M. (**2004**). Isothermal titration calorimetry studies on the binding of amino acids to gold nanoparticles. *Journal of Physical Chemistry B, 108,* 11535-11540.

Kailasa, S.K.; Kiran, K.; Wu, H.F. (**2008**). Comparison of ZnS semiconductor nanoparticles capped with various functional groups as the matrix and affinity probes for rapid analysis of cyclodextrins and proteins in surface-assisted laser desorption/ionization time-of-flight mass spectrometry. *Analytical Chemistry, 80*, 9681-9688.

Kong, X.L.; Huang, L.C.L.; Hsu, C.M.; Chen, W.H.; Han, C.C.; Chang, H.C. (**2005**). High-affinity capture of proteins by diamond nanoparticles for mass spectrometric analysis. *Analytical Chemistry, 77*, 259-265.

Li, Q.; Du, Y.; Tang, H.; Wang, X.; Chen, G.; Iqbal, J.; Wang, W.; Zhang, W. (**2012**). Ultra sensitive surface-enhanced Raman scattering detection based on monolithic column as a new type substrate. *Journal of Raman Spectroscopy, 43*, 1392-1396.

Namera, A.; Saito, T. (**2013**). Advances in monolithic materials for sample preparation in drug and pharmaceutical analysis. *Trends in Analytical Chemistry, 45,* 182-196.

Pal, A.; Debreczeni, J.E.; Sevvana, M.; Gruene, T.; Kahle, B.; Zeeck, A.; Sheldrick, G.M. (**2008**). Structures of viscotoxins A1 and B2 from European mistletoe solved using native data alone. *Acta Crystallographica Section D, 64*, 985-992.

Park, S.H.; Ko, Y.S.; Park, S.; Lee, J.S.; Cho, J.; Baek, K.Y.; Kim, I.T.; Woo, K.; Lee, J.H. (**2016**). Immobilization of silver nanoparticle-

decorated silica particles on polyamide thin film composite membranes for antibacterial properties. *Journal of Membrane Science, 499*, 80-91.

Schaller, G.; Urech, K. (**1996**). Cytotoxicity of different viscotoxins and extracts from the European subspecies of *Viscum album L*. *Phytotherapy Research, 10*, 473-477.

Sharm, V.K.; Yngard, R.A.; Lin, Y. (**2009**). Silver nanoparticles: Green synthesis and their antimicrobial activities. *Advances in Colloid and Interface Science, 145*, 83-96.

Shastri, L.; Abdelhamid, H.N.; Nawaza, M.; Wu, H.F. (**2015**). Synthesis, characterization and bifunctional applications of bidentate silver nanoparticle assisted single drop microextraction as a highly sensitive preconcentrating probe for protein analysis. *RSC Advances, 5*, 41595-41603.

Shrivas, K.; Wu, H.F. (**2008**). Modified silver nanoparticle as a hydrophobic affinity probe for analysis of peptides and proteins in biological samples by using liquid-liquid microextraction coupled to AP-MALDI-Ion trap and MALDI-TOF mass spectrometry. *Analytical Chemistry, 80*, 2583-2589.

Shrivas, K.; Wu, H.F. (**2010**). Multifunctional nanoparticles composite for MALDI-MS: Cd^{2+}-doped carbon nanotubes with CdS nanoparticles as the matrix, preconcentrating and accelerating probes of microwave enzymatic digestion of peptides and proteins for direct MALDI-MS analysis. *Journal of Mass Spectrometry, 45*, 1452-1460.

Urech, K.; Schaller, G.; Ramm, H.; Baumgartner, S. (**2011**). Organ specific and seasonal accumulation of viscotoxin-isoforms in *Viscum album ssp. album*. *Phytomedicine, 18S*, S7-S9.

Vergara-Barberán, M.; Lerma-García, M.J.; Simó-Alfonso, E.F.; Herrero-Martínez, J.M. (**2016**). Solid-phase extraction based on ground methacrylate monolith modified with gold nanoparticles for isolation of proteins. *Analytica Chimica Acta, 917*, 37-43.

Xu, Y.; Cao, Q.; Svec, F.; Fréchet, J.M.J. (**2010**). Porous polymer monolithic column with surface-bound gold nanoparticles for the capture and separation of cysteine-containing peptides. *Analytical Chemistry, 82*, 3352-3358.

Yan, Y.; Zheng, Z.; Deng, C.; Zhang, X.; Yang, P. (**2014**). Selective enrichment of phosphopeptides by titania nanoparticles coated magnetic carbon nanotubes. *Talanta, 118*, 14-20.

Yang, X.; Xia, Y. (**2016**). Urea-modified metal-organic framework of type MIL-101(Cr) for the preconcentration of phosphorylated peptides. *Microchimica Acta, 183*, 2235-2240.

Zhou, M.; Veenstra, T.D. (**2007**). Proteomic analysis of protein complexes. *Proteomics, 7*, 2688-2697.

Electronic Supplementary Material (ESM)

SEM micrographs of NP-modified materials

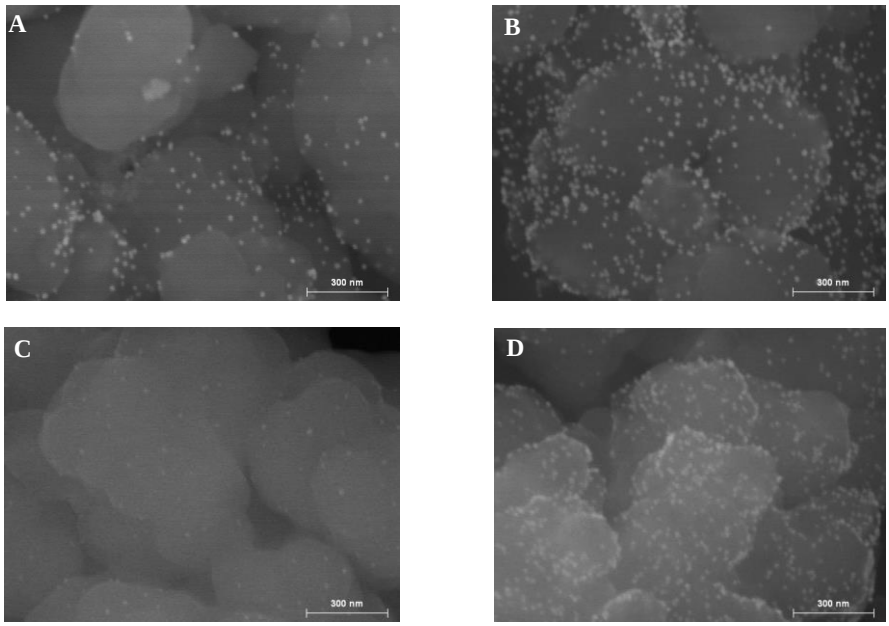

Figure 7.S1. SEM micrographs of NP-modified materials: (A) GMA-NH_2-Au, (B) GMA-SH-Au, (C) GMA-NH_2-Ag and (D) GMA-SH-Ag.

Raman Spectra

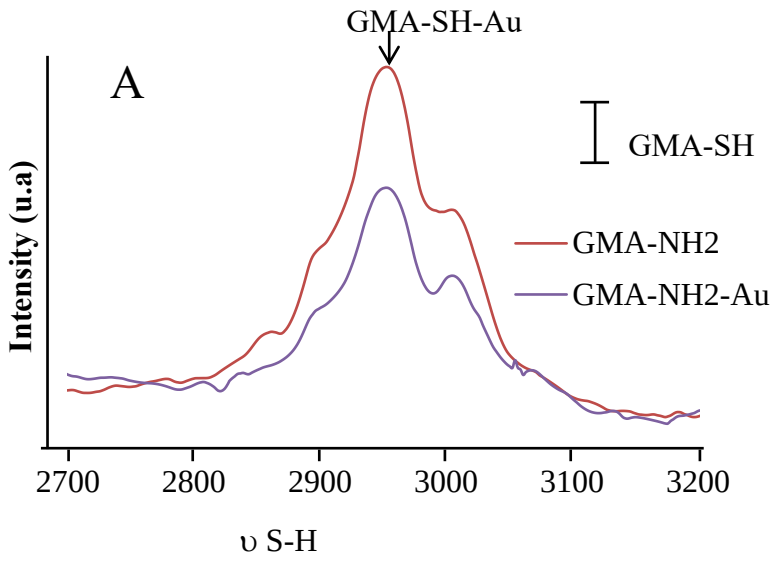

Figure 7.S2. Raman spectra of amino- or thiol-modified GMA-based materials functionalized with AuNPs.

Optimization of loading sample and elution pHs

Several studies have demonstrated that pH plays an important role to efficiently retain proteins onto the surface of NPs (Vergara-Barberán, 2016; Du, 2007). For this reason, the effect of loading sample pH (2-11) was evaluated using BSA 200 μg mL^{-1} (200 μL) as test protein (**Figure 7.S3**). As it can be seen for both sorbents, the retention of BSA was excellent at a pH range comprised between 5 and 7. This observation is consistent with the results reported in literature for AuNPs (Yoon, 1998;Yoon, 1999; Thobani, 2010), where the protein retention onto these metal surfaces reaches its maximum close to its protein pI value (Brewer, 2005; Glomm, 2007). In our case, when the pH was modified beyond this range, a less favorable

adsorption took place owing to electrostatic interactions (repulsions between proteins and sorbent). Taking into consideration this, a pH of 7 was selected in the loading step (giving slightly higher recoveries than those found at pH 5) for both sorbents. The washing step was performed at pH 7, leading to minor losses of BSA (*ca*. 5%). According to our previous study (Vergara-Barberán, 2016), several pH values (9-13) were then tried in the elution step (see **Figure 7.S4**). As observed, at pH higher than 11, higher recoveries (> 70%) were found for both Ag modified sorbents.

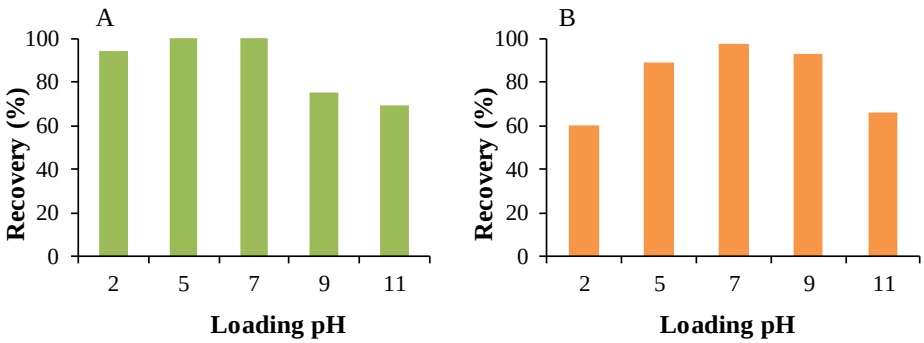

Figure 7.S3. Influence of loading sample pH of BSA on the SPE procedure for: (A) GMA-NH_2-Ag and (B) GMA-SH-Ag.

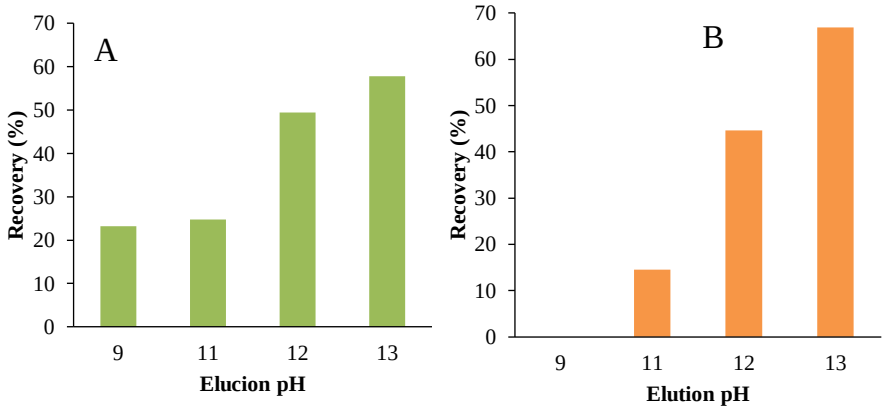

Figure 7.S4. Influence of elution pH of BSA on the SPE procedure for: (A) GMA-NH_2-Ag and (B) GMA-SH-Ag.

References of Electronic Supplementary Material.

Vergara-Barberán, M.; Lerma-García, M.J.; Simó-Alfonso, E.F.; Herrero-Martínez, J.M. (**2016**). Solid-phase extraction based on ground methacrylate monolith modified with gold nanoparticles for isolation of proteins. *Analytica Chimica Acta, 917*, 37-43.

Du, Z.; Yu, Y.L.; Chen, X.W.; Wang, J.H. (**2007**). The isolation of basic proteins by solid-phase extraction with multiwalled carbon nanotubes. *Chemistry - A European Journal, 13*, 9679-9685.

Yoon, J.Y.; Kim, J.H.; Kim, W.S. (**1998**). Interpretation of protein adsorption phenomena onto functional microspheres. *Colloids Surfaces B, 12*, 15-22.

Yoon, J.Y.; Kim, J.H.; Kim, W.S. (**1999**). The relationship of interaction forces in the protein adsorption onto polymeric microspheres. *Colloids Surfaces A, 153*, 413-419.

Thobhani, S.; Attree, S.; Boyd, R.; Kumarswami, N.; Noble, J.; Szymanski, M.; Porter, R.A. (**2010**). Bioconjugation and characterisation of gold colloid-labelled proteins. *Journal of Immunological Methods, 356,* 60-69.

Brewer, S.H.; Glomm, W.R.; Johnson, M.C.; Knag, M.K.; Franzen, S. (**2005**). Probing BSA binding to citrate-coated gold nanoparticles and surfaces. *Langmuir, 21*, 9303-9307.

Glomm, W.R.; Halskau, Ø.; Hanneseth, A.M.D.; Volden, S. (2007). Adsorption behavior of acidic and basic proteins onto citrate-coated Au surfaces, correlated to their native fold, stability, and Pi. *The Journal of Physical Chemistry B, 111*, 14329-14345.

II.B. Application of enzyme-assisted methodologies in food materials

Chapter 8. Use of an enzyme-assisted method to improve protein extraction from olive leaves

Food Chemistry 169 (2015) 28–33

Contents lists available at ScienceDirect

Food Chemistry

journal homepage: www.elsevier.com/locate/foodchem

Analytical Methods

Use of an enzyme-assisted method to improve protein extraction from olive leaves

M. Vergara-Barberán, M.J. Lerma-García, J.M. Herrero-Martínez, E.F. Simó-Alfonso *

Department of Analytical Chemistry, University of Valencia, C. Doctor Moliner 50, E-46100 Burjassot, Valencia, Spain

The improvement of protein extraction from olive leaves using an enzyme-assisted protocol has been investigated. Using a cellulase enzyme (Celluclast® 1.5L), different parameters that affect the extraction process, such as the influence and amount of organic solvent, enzyme amount, pH and extraction temperature and time, were optimized. The influence of these factors was examined using the standard Bradford assay and the extracted proteins were characterized by SDS-PAGE. The optimum extraction parameters were: 30% acetonitrile, 5% (v/v) Celluclast® 1.5L at pH 5.0 and 55 °C for 15 min. Under these conditions, several protein extracts from olive leaves of different genetic variety (with a total protein amount comprised between 1.87 and 6.64 mg g^{-1}) were analyzed and compared by SDS-PAGE, showing differences in their electrophoretic protein profiles. The developed enzyme-assisted extraction method has shown a faster extraction, higher recovery and reduced solvent usage with respect to the use of the non-enzymatic methods described in literature.

Keywords: enzyme-assisted extraction; genetic variety; olive leaf protein profiles; SDS-PAGE

8.1. Introduction

Olive tree (*Olea europeaea*, Oleaceae) is an important crop in the Mediterranean area, which produces 98% of the world total amount of olive oil. The olive tree and its products (leaves, olive fruit and its beneficial oil) have a rich history of nutritional, medicinal and commercial purposes (Soni, 2006). In particular, olive leaves are one of the harvest by-products which can be found in high amounts in olive oil industries (5% of the total weight of the olives) since they accumulate during the pruning of the olive trees (Molina-Alcaide, 2008). Olive leaves are considered as a cheap raw material which can be used as a useful source of high-value added products, such as phenolic compounds (Briante, 2002). Recently, the interest in the chemical composition of olive leaves has been increased since they are capable to prevent certain diseases and present a large number of health benefits such as anti-oxidative, anti-inflammatory and antimicrobial properties (Pereira, 2007; Sudjana, 2009). The olive leaf composition varies depending on its origin, proportion of branches, storage and climatic conditions, moisture content, and degree of contamination with soil and oils (Molina-Alcaide, 2008). The analysis of proteins in leaves has received less attention (García, 2000; Wang, 2003; Malik, 2005) than those of olive pulp (Esteve, 2011; Hidalgo, 2001; Montealegre, 2012; Salas, 1999; Zamora, 2001), seed (Alché, 2006; Montealegre, 2012; Ross, 1993; Wang, 2001; Wang, 2007) and oil (Georgalaki, 1998; Martín-Hernández, 2008; Montealegre, 2010; Zamora, 2001). Some of these works have employed the protein profiles to understand its accumulation during the fruit maturation (Wang, 2007), its role in oil stability (Georgalaki, 1998) and to differentiate between different genetic varieties (Montealegre, 2010; Montealegre, 2012; Wang, 2007).

The analysis of olive leaf proteins is fairly difficult due to the low crude protein content present (70-129 g/kg dry matter) (Molina-Alcaide, 2008) and the high levels of interfering components (such as pigments, polyphenols,

etc. (Granier, 1988)) during its extraction procedure and subsequent electrophoretic separation. Several extraction protocols have been proposed (García, 2000; Malik, 2005; Wang, 2003) to overcome this troublesome. Thus, García *et al*. (García, 2000) employed an aqueous sodium borate buffer, followed by cold methanolic ammonium acetate isolation of juvenile-related proteins in olive leaves; however, the protein profiles in SDS-PAGE showed a background due to the presence of interfering compounds. To improve protein extraction, Wang *et al*. (Wang, 2003) developed a procedure based on phenol extraction of proteins from olive leaves in presence of SDS for their determination by two-dimensional electrophoresis. Slight modifications of this protocol were introduced by Malik *et al*. (Malik, 2005) to achieve a higher protein yield. However, these latter extraction methods employed several cleanup steps using acetone and/or trichloroacetic acid, being laborious, time-consuming and non-environmentally friendly protocols. Enzyme-assisted protein extraction can be an alternative method due to its mild extraction condition and lower environmental impact (Sari, 2013; Shen, 2008). Thus, several specific enzymes have been employed in protein extraction in tea leaves (Shen, 2008), in *Leguminosae* gums (Sebastián-Francisco, 2004) and in different oilseed meals (Sari, 2013), providing improved protein extraction yields compared to alkaline or acidic extractions. However, to our knowledge, this methodology has been not applied to the olive leaves protein extraction.

The aim of this work was to investigate the possible use of cellulase enzyme (Celluclast® 1.5L) in assisting the extraction of proteins from olive leaves. The protein extraction was optimized in terms of several experimental conditions such as organic solvent and enzyme amounts, pH and extraction temperature and time. To monitor the extraction, the total protein amount was measured using the standard Bradford assay, and protein profiles were characterized by SDS-PAGE. Additionally, a comparison of

the resulting protein profiles from olive leaves belonging to different genetic varieties was performed.

8.2. Materials and methods

8.2.1. Chemicals

ACN, acetone, MeOH, 2-propanol and glycerine were purchased from Scharlau (Barcelona, Spain). PSA, TEMED, Tris, acrylamide, bisacrylamide, SDS, Coomassie Brilliant Blue R and bovine serum albumin (BSA) were obtained from Sigma-Aldrich (St. Louis, MO, USA). 2-Mercaptoethanol and HCl were purchased from Merck (Darmstadt, Germany) and bromophenol blue from Riedel-de-Haën (Hannover, Germany). Two molecular weight size protein standards (6.5-66 kDa and 36-200 kDa) were also provided by Sigma-Aldrich. A Protein Quantification Kit-Rapid from Fluka (Steinheim, Germany) was used for Bradford protein assay. A cellulase enzyme (Celluclast® 1.5L) was donated by Novozymes (Bagsvaerd, Denmark). This enzyme is produced by submerged fermentation of a selected strain of the fungus *Trichoderma reesei* (ATCC26921) and catalyzes the breakdown of cellulose into glucose, cellobiose and higher glucose polymers. Celluclast® 1.5L activity is 1500 NCU/g (NCU = Novo Cellulase Unit). For practical applications, the optimal working conditions are about pH 4.5 - 6.0 and 50 – 60 ºC. Deionized water (Barnstead deionizer, Sybron, Boston, MA) was also employed.

8.2.2. Samples

The olive leaves employed in this study (**Table 8.1**) were kindly donated by different olive oil manufacturers. To assure a correct sampling, olive leaves were collected at the same period (end of November 2011) directly from trees located in different Spanish regions. The genetic variety of

samples was guaranteed by the suppliers. The leaves were previously selected to assume the absence of mold or other microorganisms, washed with water to remove dust or airborne particles settled on the leaf surface and then stored at -20 ºC prior their use.

8.2.3. Instrumentation

SDS-PAGE experiments were performed using a vertical minigel Hoefer SE260 Mighty Small system (Hoefer, MA, USA). Protein extraction was carried out with a Sigma 2-15 centrifuge (Sigma Laborzentrifugen, Osterode am Harz, Germany) and a D-78224 ultrasonic bath (Elma, Germany). To measure the absorbance at 595 nm for the Bradford protein assay, a Model 8453 diode-array UV-vis spectrophotometer (Agilent Technologies, Waldbronn, Germany), provided with a 1-cm optical path quartz cell (Hellma, Müllheim, Germany), was used.

Table 8.1

Genetic variety, geographical origin and total protein content (mg g^{-1} fresh leaf), established using the enzyme-assisted method developed in this work, of the olive leaves used in this study.

Genetic variety	**Geographical origin**	**Protein content (mg g^{-1} fresh leaf) (n = 3)**
Solà	Castellón	3.67 ± 0.18
Cornicabra	Castellón	1.87 ± 0.10
Hojiblanca	Córdoba	4.84 ± 0.22
Picual	Murcia	6.64 ± 0.24
Arbequina	Murcia	5.68 ± 0.23
Manzanilla	Valencia	5.06 ± 0.26
Blanqueta	Valencia	6.09 ± 0.23
Grosol	Valencia	5.87 ± 0.29

8.2.4. Protein extraction

Protein extraction was performed as follows. 10 g of fresh leaves were frozen in liquid nitrogen and ground to a fine powder in a pre-cooled mortar and pestle, and next lyophilized. The lyophilized powder was then homogenized, and 0.3 g were treated with 3 mL of a water:ACN mixture (7:3, v/v) containing a 5% (v/v) Celluclast® 1.5L enzyme at pH 5.0, sonicated at 55 ºC for 15 min using an ultrasound power of 0.5 W/mL, and centrifuged at 10000 × *g* for 10 min. An aliquot of the supernatant was taken and used for Bradford's assay, and the rest of solution was stored at -20 ºC until their use.

For SDS-PAGE analysis, 200 µL of protein extract were precipitated by adding 800 µL of ice-cold acetone for 20 min. The proteins were collected by centrifugation at 10000 ×*g* for 10 min at 4 ºC, and the resulting pellet was dissolved in 100 µL of SDS sample buffer (0.0625 M Tris-HCl pH 6.8, 10% (v/v) glycerol, 5% (w/v) SDS, 0.004% (w/v) bromophenol blue and 5% (v/v) 2-mercaptoethanol) (Laemmli, 1970). Then, the sample was heated for 5 min at 95 ºC and an aliquot was loaded on the gel.

For Bradford's assay (Bradford, 1976), a calibration curve up to 1 mg mL^{-1} of BSA was prepared in the extraction solvent (water:ACN mixture (7:3, v/v)). Sample protein amount was measured according to the protocol described in the Bradford assay Protein Quantitation Kit-Rapid (Fluka). A sample blank containing 5% (v/v) Celluclast® 1.5L enzyme was also made in order to remove its contribution to the final sample absorbance.

8.2.5. SDS-PAGE separation

In order to determine the molecular weight of the extracted proteins, their separation was carried out on 10 cm long gels under reducing conditions. The running gels were composed by 30% (w/w) total acrylamide and 8%

(w/w) bisacrylamide. Electrophoresis was performed for 1.5 h at constant voltage (180 V) using a running buffer containing 3.03 g L^{-1} Tris, 14.4 g L^{-1} glycine and 1 g L^{-1} SDS. Then, gels were stained overnight in a solution of 0.2% (w/v) Coomassie Brilliant Blue R. Gels were washed with a solution composed of 40% (v/v) MeOH and 10% (v/v) acetic acid. Then, the gels were stored using an aqueous solution containing 5% (v/v) glycerol.

8.3. Results and discussion

8.3.1. Influence of organic solvent amount on protein extraction

First, the optimization of a method for the extraction of proteins was performed to minimize interfering compounds previous to its posterior analysis. Based on the results previously published by Sebastián-Francisco *et al*. (Sebastián-Francisco, 2004), the use of an organic solvent extractant (such as ACN) in combination with an enzyme was investigated. In this work, a cellulase enzyme (Celluclast® 1.5L) was selected for the protein extraction, since its function is to hydrolyze the mesocarp tissue structure, which is a lipid deposition in fruits and leaves, and thereby helps to liberate the leaf components.

Thus, the influence of ACN amount on the protein extraction was firstly studied, keeping constant the Celluclast® 1.5L concentration at 3.5% (v/v) at pH 5.0, sonicated at 25 ºC for 20 min. Villalonga variety leaves were selected to carry out the optimization studies. For this purpose, the standard Bradford assay was first used. As shown in **Figure 8.1A**, an increase in the absorbance was obtained when ACN percentage was increased up to 30 %. However, when the ACN percentage was further increased, a signal decrease was observed. This behavior could be explained taking into account that protein solubility decreased when high ACN percentages were used, which provided a high hydrophobicity in the medium.

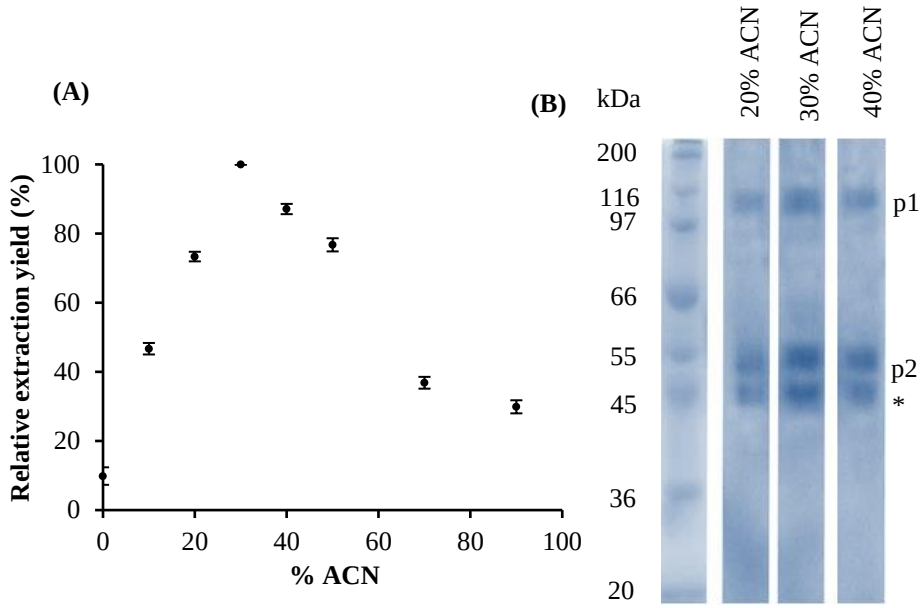

Figure 8.1. Influence of ACN percentage on the olive leaf protein extraction monitored by (A) Bradford assay and (B) SDS-PAGE. Band identification: asterisk, 44 kDa (Celluclast® 1.5L); p1, 110 kDa; p2, 55 kDa. The proteins were extracted at 25 ºC for 20 min using a Celluclast® 1.5L percentage of 3.5% (v/v) at pH 5.0.

The influence of the ACN percentage in the separation of olive leaf protein extracts was also tested by SDS-PAGE. For this purpose, eight molecule markers were used to establish the molecular weight band (**Figure 8.1B**). As observed in this figure, when a 30% ACN percentage was used, clear bands were identifiable with higher intensity than those obtained at 20% and 40 % ACN. Three prominent protein bands, located at 44, 55 and 110 kDa were distinguished. The band located at 44 kDa was identified as Celluclast® 1.5L enzyme, whereas the 55 kDa protein was assigned as ribulose-1,5-bisphosphate carboxylase (Rubisco), which was characteristic of leaf protein fractions of many plant species (García, 2000; Wang, 2003). However, the protein located at 110 kDa has not been previously reported in

literature. As a result of both Bradford assay and SDS-PAGE results, a 30% ACN was selected for further studies.

8.3.2. Influence of enzyme amount on protein extraction

Next, the effect of enzyme amount on the protein extraction was examined by keeping constant the optimum percentage of organic modifier (30% ACN) at pH 5.0, sonicated at 25 ºC for 20 min. For this purpose, enzyme concentrations were varied from 0 to 8% (v/v). In all cases, and as mentioned above, a reagent blank was also employed. As observed in **Figure 8.2A** (standard Bradford assay), an increase in the total protein amount was obtained when the Celluclast® 1.5L percentage was increased up to a 5% (v/v). However, when the enzyme amount was further increased, a decrease in the signal was observed. This behavior could be explained taking into account two effects: i) the appearance of turbidity in the protein extracts by using enzyme percentages higher than 5% (v/v) and ii) the so-called competitive inhibition, in which the extracted protein molecules are supposed to act as inhibitors combining with the enzyme to form a complex and thereby preventing its activity, although there is no evidence of this mechanism (Laidler, 1973). This fact was in agreement with other studies reported (Shen, 2008). In addition to this, an increase in enzyme concentration would normally enhance the solubility of protein into the solvent and, therefore, increase the extraction yield. However, the existence of free enzyme in the solvent could interact with the protein and cause degradation of protein molecules, which could also explain signal decrease. This fact was in agreement with previously published studies (Shen, 2008).

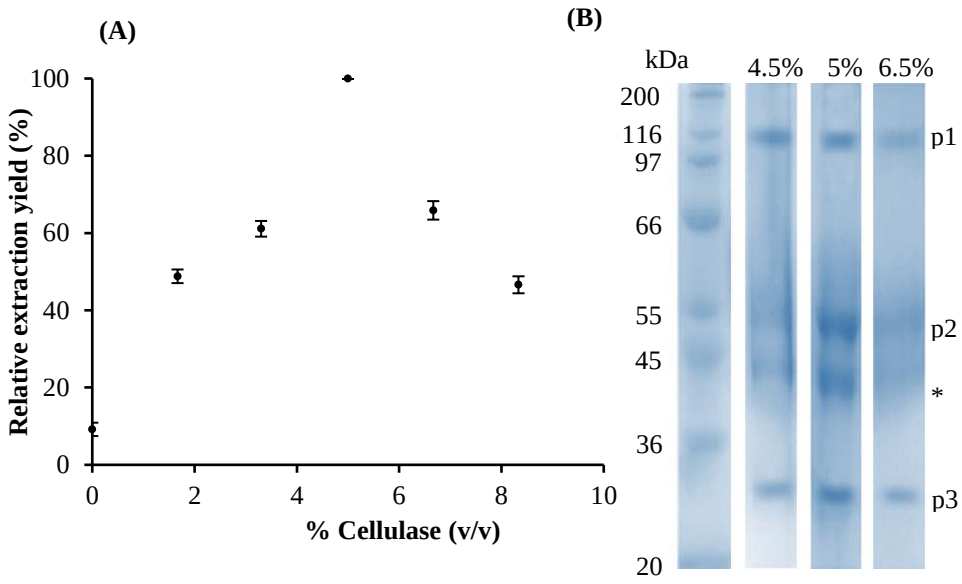

Figure 8.2. Influence of Celluclast® 1.5L percentage on the olive leaf protein extraction monitored by (A) Bradford assay and (B) SDS-PAGE. Band identification: p3, 29 kDa; other bands as in **Figure 8.1**. The proteins were extracted at 25 ºC for 20 min using 30 % ACN at pH 5.0.

Also in this case, the influence of the enzyme percentage was tested by SDS-PAGE. As shown in **Figure 8.2B**, similar molecular weight distributions as those reported in **Figure 8.1B** were observed. Nevertheless, the bands provided higher intensity and the presence of a protein at 29 kDa was clearly evidenced, especially at 5% (v/v). Consequently, the optimum enzyme concentration was set at 5% (v/v) for further studies.

8.3.3. Influence of pH, temperature and extraction time on protein extraction

The effect of pH, temperature and extraction time on protein extraction in the selected medium was also investigated. Thus, pH was varied from 4.5 – 6.0, as recommended by the enzyme supplier. Since small differences in the total protein amount were observed along the pH range studied, a pH 5.0 was selected for the following studies (data not shown).

Next, the influence of temperature was tested by varying it from 25 to 65 ºC under the previously optimized conditions (30% ACN, 5% (v/v) Celluclast® 1.5L at pH 5.0). As shown in **Figure 8.3A**, temperature had a significant effect on the enzyme's capability in extracting proteins up to 55 ºC, however, higher temperatures led to a decrease in protein extraction, which could be explained by a possible degradation of proteins. These results were consistent with those observed by SDS-PAGE (see **Figure 8.3B**). Thus, 55 ºC was selected as the optimum extraction temperature.

Finally, the extraction time was also tested by varying it from 5 to 25 min. As observed in **Figure 8.4**, an increase in the total protein amount was obtained when extraction time was increased up to 15 min, while at higher times (20 and 25 min), the total protein amount obtained remained practically the same. Thus, an extraction time of 15 min was selected as the optimal one for further studies.

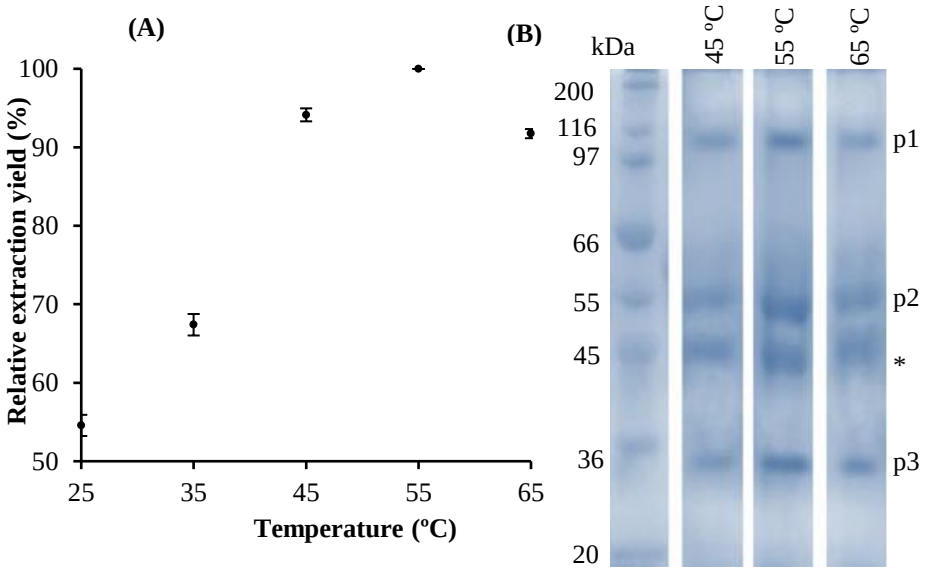

Figure 8.3. Influence of temperature on the olive leaf protein extraction monitored by (A) Bradford assay and (B) SDS-PAGE. Band identification as in **Figure 8.2**. The proteins were extracted for 20 min using 30 % ACN and 5% (v/v) Celluclast® 1.5L at pH 5.0.

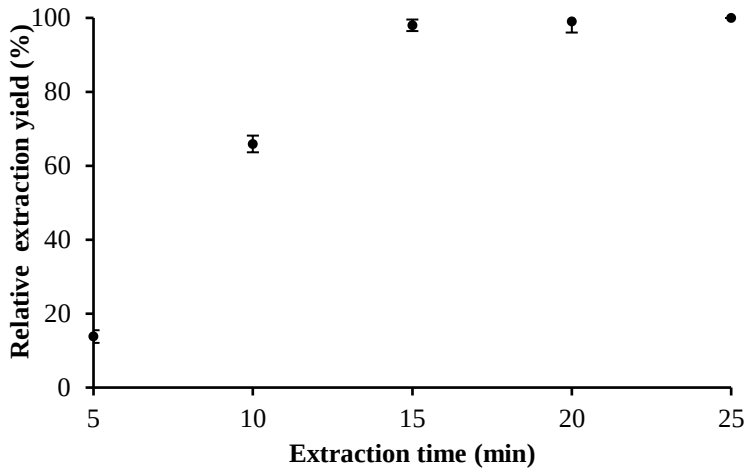

Figure 8.4. Influence of extraction time on the olive leaf protein extraction monitored by Bradford assay. The proteins were extracted at 55 ºC using 30 % ACN and 5% (v/v) Celluclast® 1.5L at pH 5.0.

8.3.4. Analysis of olive leaves from different genetic variety

Under the optimal extraction conditions (55 ºC for 15 min using 30 % ACN and 5% (v/v) Celluclast® 1.5L at pH 5.0), the protein amount of the olive leaf tissues from the different genetic varieties was determined using the standard Bradford assay (see **Table 8.1**). The total amount of protein mass on fresh weight basis was comprised between 1.87 mg g^{-1} (Cornicabra variety) and 6.63 mg g^{-1} (Picual variety). A study of repeatability of the recommended extraction protocol from the same tissue was also performed. In all cases, satisfactory relative standard deviation (RSD) values (below 5.2 %) were obtained. In addition, these contents were higher (*ca*. 2-3 folds) than those found by other extraction protocols reported for the same genetic varieties (Wang, 2003).

Thus, the protein distribution of the different genetic varieties was studied by SDS-PAGE. From the examination of the electrophoretic patterns (**Figure 8.5**), a new protein band at 63 kDa, present in Solà, Hojiblanca and Picual varieties, was identified. This protein was assigned to oleuropein β-glucosidase (Hatzopoulos, 2002). The band observed at 110 kDa was observed in Solà, Cornicabra, Hojiblanca and Grosol, being less intense in Grosol variety. On the other hand, the band observed at 29 kDa was only observed in Picual, Arbequina, Manzanilla, Blanqueta and Grosol varieties, being in this case the intensity observed very similar. Finally, the band at 55 kDa was the only one present in all the genetic varieties considered in this study. Thus, the differences observed could be helpful to distinguish the olive leaf tissues according to their genetic variety.

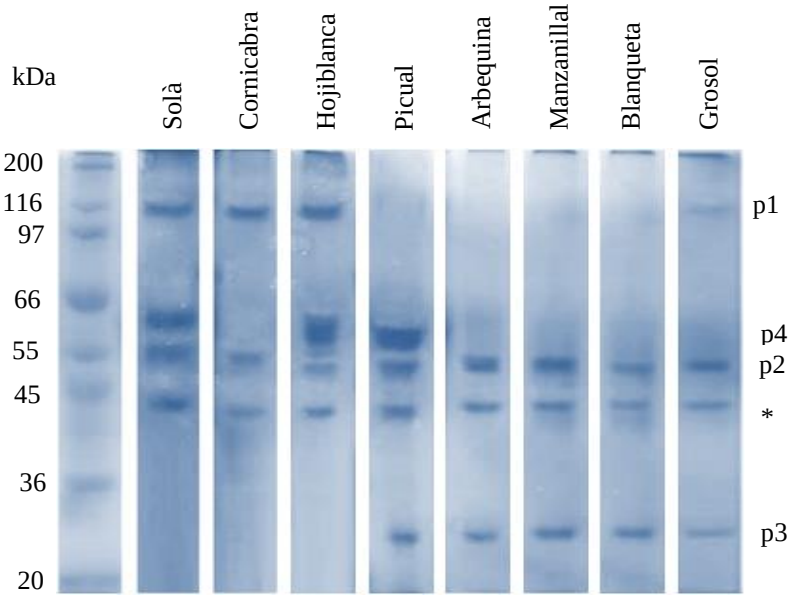

Figure 8.5. SDS-PAGE electrophoretic protein profiles obtained from the different olive leaf genetic varieties considered in this study. Band identification: p4, 63 kDa; other bands as in **Figure 8.2**. The proteins were extracted at 55 ºC for 15 min using 30 % ACN and 5% (v/v) Celluclast® 1.5L at pH 5.0.

8.4. Conclusions

In conclusion, this work demonstrated that the employment of a Celluclast® 1.5L enzyme is a fast, feasible and effective method to extract proteins from olive leaves. Several parameters affecting Celluclast® 1.5L assisted extraction of proteins were optimized, e.g., organic solvent percentage, Celluclast® 1.5L concentration, pH, and extraction temperature and time. It was found that the use of Celluclast® 1.5L improve the protein extraction, which is due to the breakdown of the cell wall rendering the intracellular materials more accessible for extraction. The mild extraction

conditions were environmentally sustainable and faster than other protocols described in the literature. In addition, electrophoretic protein profiles from diverse genetic varieties were evaluated finding differences, which could be useful to classify the olive leaves according to their genetic variety.

Acknowledgements

Work supported by project CTQ2010- 15335 (MINECO of Spain and FEDER) ACOMP/2013/196 (Generalitat Valenciana). M. V-B thanks the MINECO for an FPU grant for PhD studies. M.J. L-G thanks the Generalitat Valenciana for a VALi+d postdoctoral contract.

8.5. References

Alché, J.D.; Jiménez-López, J.C.; Wang, W.; Castro-López, A.J.; Rodríguez-García, M.I. (**2006**). Biochemical characterization and cellular localization of 11s type storage proteins in olive (*Olea europaea L.*) seeds. *Journal of Agricultural and Food Chemistry*, *54*, 5562-5570.

Bradford, M.M. (**1976**). A rapid and sensitive method for the quantitation of microgram quantities of protein utilizing the principle of protein-dye binding. *Analytical Biochemistry, 72*, 248-254.

Briante, R.; Patumi, M.; Terenziani, S.; Bismuto, E.; Febbraio, F. (**2002**). *Olea europaea L*. leaf extract and derivatives: antioxidant properties. *Journal of Agricultural and Food Chemistry, 50*, 4934-4940.

Esteve, C.; Del Río, C.; Marina, M.L.; García, M.C. (**2011**). Development of an ultra-high performance liquid chromatography analytical methodology for the profiling of olive (*Olea europaea L*.) pulp proteins. *Analytica Chimica Acta*, *690*, 129-134.

García, J.L.; Avidan, N.; Troncoso, A.; Sarmiento, R.; Lavee, S. (**2000**). Possible juvenile-related proteins in olive tree tissues. *Scientia Horticulturae, 85*, 271-284.

Georgalaki, M.D.; Sotiroudis, T.G.; Xenakis, A. (**1998**). The presence of oxidizing enzyme activities in virgin olive oil. *Journal of the American Oil Chemists Society*, 75, 155–159.

Granier, F. (**1988**). Extraction of plant proteins for two-dimensional electrophoresis. *Electrophoresis*, *9*, 712-718.

Hatzopoulos, P.; Banilas, G.; Giannoulia, K.; Gazis, F.; Nikoloudakis, N.; Milioni, D.; Haralampidis, K. (**2002**). Breeding, molecular markers and molecular biology of the olive tree. *European Journal of Lipid Science and Technology*, *104*, 574-586.

Hidalgo, F.J.; Alaiz, M.; Zamora, R. (**2001**). Determination of peptides and proteins in fats and oils. *Analytical Chemistry*, *73*, 698-702.

Laemmli, U.K. (**1970**). Cleavage of structural proteins during the assembly of the head of bacteriophage T4. *Nature*, *227*, 680-685.

Laidler, K.J.; Bunting, P.S. (**1973**). The chemical kinetics of enzyme action (2nd ed.) Oxford, (Chapter 3).

Malik, N.S.A.; Bradford, J.M. (**2005**). A simple protein extraction method for proteomic studies on olive leaves. *Journal of Food Agriculture and Environment*, *3*, 246-248.

Martín-Hernández, C.; Bénet, S.; Obert, L. (**2008**). Determination of proteins in refined and nonrefined oils. *Journal of Agricultural and Food Chemistry*. *56*, 4348-4351.

Molina-Alcaide, E.; Yáñez-Ruiz, D.R. (**2008**). Potential use of olive by-products in ruminant feeding: A review. *Animal Feed Science and Technology*, *147*, 247–264.

Montealegre, C.; García, M.C.; Del Río, C.; Marina, M.L.; García-Ruiz, C. (**2012**). Separation of olive proteins by capillary gel electrophoresis. *Talanta, 97,* 420-424.

Montealegre, C.; Marina, M.L.; García-Ruiz, C. (**2010**). Separation of proteins from olive oil by CE: An approximation to the differentiation of monovarietal olive oils. *Electrophoresis*, *31*, 2218-2225.

Mylonaki, S.; Kiassos, E.; Makris, D.P.; Kefalas, P. (**2008**). Optimisation of the extraction of olive (*Olea europaea*) leaf phenolics using water/ethanol-based solvent systems and response surface methodology. *Analytical and Bioanalytical Chemistry, 392*, 977-985.

Pereira, A.P.; Ferreira, I.C.F.R.; Marcelino, F.; Valentão, P.; Andrade, P.B.; Seabra, R.; Estevinho, L.; Bento, A.; Pereira, J.A. (**2007**). Phenolic compounds and antimicrobial activity of olive (*Olea europaea L. Cv. Cobrançosa*). leaves. *Molecules, 12*, 1153–1162.

Ross, J.H.E.; Sanchez, J.; Millan, F.; Murphy, D.J. (**1993**). Differential presence of oleosins in oleogenic seed and mesocarp tissue in olive (*Olea europaea*) and avocado (*Persea Americana*). *Plant Science,* 93, 203–210.

Salas, J.J.; Sánchez, J. (**1998**). Alcohol dehydrogenases from olive (*Olea europaea*). *Phytochemistry*, *48*, 35–40.

Salas, J.J., Williams, M., Harwood, J.L., Sanchez, J. (**1999**). Lipoxygenase activity in olive (*Olea europaea*) fruit. *Journal of the American Oil Chemists Society, 76*, 1163–1168.

Sari, Y. W.; Bruins, M.E.; Sanders, J.P.M. (**2013**). Enzyme assisted protein extraction from rapeseed, soybean, and microalgae meals. *Industrial Crops and Products, 43*, 78-93.

Sebastián-Francisco, I.; Simó-Alfonso, E.F.; Mongay-Fernández, C.; Ramis-Ramos, G. (**2004**). Improvement of the electrophoretic protein profiles of Leguminosae gums extracts using gamanase and application to the evaluation of carob–guar mixtures. *Analytica Chimica Acta, 508*, 135-140.

Shen, L.; Wang, X.; Wang, Z.; Wu, Y.; Chen, J. (**2008**). Studies on tea protein extraction using alkaline and enzyme methods. *Food Chemistry, 107*, 929-938.

Soni M. G.; Burdock, G.A.; Christian, M.S.; Bitler, C.M.; Crea, R. (**2006**). Safety assessment of aqueous olive pulp extract as an antioxidant or antimicrobial agent in foods. *Food and Chemical Toxicology*, *44,* 903–915.

Sudjana, A.N.; D' Orazio, C.; Ryan, V.; Rasool, N.; Ng, J.; Islam, N., Riley, T.V.; Hammer, K.A. (**2009**). Antimicrobial activity of commercial *Olea europaea* (olive) leaf extract. *International Journal of Antimicrobial Agents*, *33*, 461-463.

Wang, W.; Alché, J.D.; Castro, A.J.; Rodríguez-García, M.I. (**2001**). Characterization of seed storage proteins and their synthesis during seed development in *Olea europaea*. *International Journal of Developmental Biology*, *45(s1*), 63-64.

Wang, W.; Alché, J.D.; Rodríguez-García, M.I. (**2007**). Characterization of olive seed storage proteins. *Acta Physiologiae Plantarum*, *29,* 439-444.

Wang, W.; Scali, M.; Vignani, R.; Spadafora, A.; Sensi, E.; Mazzuca, S.; Cresti, M. (**2003**). Protein extraction for two-dimensional electrophoresis from olive leaf, a plant tissue containing high levels of interfering compounds. *Electrophoresis*, *24*, 2369-2375.

Zamora, R.; Alaiz, M.; Hidalgo, F.J. (**2001**). Influence of cultivar and fruit ripening on olive (*olea europaea*) fruit protein content, composition, and antioxidant activity. *Journal of Agricultural and Food Chemistry*, *49,* 4267-4270.

Chapter 9. Efficient extraction of olive pulp and stone proteins by using an enzyme-assisted method

Efficient Extraction of Olive Pulp and Stone Proteins by using an Enzyme-Assisted Method

María Vergara-Barberán, María Jesús Lerma-García, José Manuel Herrero-Martínez, and Ernesto Francisco Simó-Alfonso

An efficient protein extraction protocol for proteins from olive pulp and stone by using enzymes was developed. For this purpose, different parameters that affect the extraction process, such as enzyme type and content, pH, and extraction temperature and time, were tested. The influence of these factors on protein recovery was examined using the standard Bradford assay, while the extracted proteins were characterized by SDS-PAGE. The best extraction conditions for pulp and stone proteins were achieved at pH 7.0 and 5% (v/v) Palatase® 20000 L (lipase) or Lecitase® Ultra (phospholipase) content, respectively. The optimal extraction temperature and time were 30 and 40 ºC for 15 min for pulp and stone tissues, respectively. Under these conditions, several protein extracts coming from olive fruits of different genetic variety were analyzed, their profiles being compared by SDS-PAGE. The developed enzyme-assisted extraction method showed faster extraction, higher recovery and reduced solvent usage than the non-enzymatic methods previously described in the literature. In the case of stone proteins, different electrophoretic profiles and band intensities were obtained which could be helpful to distinguish samples according to their genetic variety.

Keywords*:* olive pulp; olive stone; enzyme-assisted extraction; SDS-PAGE; protein profiles

C1298 Journal of Food Science • Vol. 79, Nr. 7, 2014

doi: 10.1111/1750-3841.12499

9.1. Introduction

The fruit of the olive tree (*Olea europeaea, Oleaceae*) is an important crop in the Mediterranean area, which produces 98% of the worlds' total amount of olive oil. Olive fruits and its appreciated oil have been investigated for many years due to their economic importance and potential health benefits (Zamora, 2001). Olive fruit is composed by mesocarp (70% to 90%), endocarp (9% to 27%), and seed (2% to 3%). When fruits are collected at the usual harvest time, mesocarp composition is 30% oil, 60% water, 4% sugars, 3% proteins, being the other components mainly fiber and ash. On the other hand, endocarp composition is 1% oil, 10% water, 30% cellulose, and 40% other carbohydrates (Conde, 2008).

Olive fruit proteins (pulp and stone) have been scarcely studied, although several reports have demonstrated their importance in the manufacturing and quality of olives and its oil (Georgalaki, 1998a, 1998b; Koidis, 2006). Moreover, there are data showing that proteins present in oils could cause allergic reactions (Martín-Hernández, 2008; Esteve, 2011). Olive fruit proteins, which are mainly contained in the olive seed, belong to 2 main families: SSPs and oleosins. Storage proteins are formed during seed development (Alché, 2006). According to Alché and others (Alché, 2006), the most abundant SSPs in the olive seed belong to the 11S protein family, which accounts for approximately 70% of the total seed proteins. SSPs in olive seed consist of 2 hydrogen-bonded subunits of 41 and 47.5 kDa (Wang, 2001; Wang, 2007; Alché, 2006). Under reducing conditions, these subunits generate different polypeptides of 20.5, 21.5, 25.5, 27.5, and 30 kDa (11S protein family) (Alché, 2006). In addition to the SSPs, proteins associated with fatty bodies called oleosins, of 22 and 50 kDa, have also been found in olives (Ross, 1993).

Since the content of crude proteins in olive fruit is very low (about 2%) (Zamora, 2001), and there are several interfering components, such as lipids and phenolic compounds, that can interfere with protein determination, the analysis of these proteins is rather difficult. Thus, to overcome this problem, several extraction protocols have been proposed in the literature. One of the protocols consists of a classical TCA/acetone precipitation to eliminate undesired compounds and the extraction of proteins with an aqueous buffer, while another procedure is based on a phenol extraction of proteins (Wang, 2008). Moreover, the combination of both protocols has also been reported (Wang, 2003; Esteve, 2011). Nevertheless, these strategies are not always efficient enough, being laborious, time-consuming, and non-environmentally friendly protocols. Enzyme-assisted protein extraction can be an alternative method since it presents a low environmental impact and due to its mild extraction conditions (Shen, 2008; Sari, 2013). Thus, several specific enzymes have been employed in protein extraction from tea leaves (Shen, 2008), from Leguminosae gums (Sebastián-Francisco, 2003), and from different oilseed meals (Sari, 2013) providing improved protein extraction yields compared to alkaline or acidic extractions. However, to our knowledge, the enzyme-assisted methodology has not been applied to olive fruit protein extraction.

The aim of this work was to investigate the use of different enzymes, such as lipase, cellulase, phospholipase, and an enzymatic mixture made up of arabanase, cellulase, beta-glucanase, hemicellulose, and xylanase in assisting the extraction of proteins from olive pulp and stone. Several experimental parameters that could affect protein extraction, such as enzyme type and content, pH, and extraction temperature and time, were tested. To monitor the extraction, the total protein content was measured using the standard Bradford assay, and protein profiles were characterized by sodium dodecyl sulfate–polyacrylamide gel electrophoresis (SDS-PAGE). Additionally, a comparison of the resulting protein profiles from olive pulps and stones belonging to different genetic varieties was performed.

9.2. Materials and methods

9.2.1. Chemicals

ACN, acetone, MeOH, 2-propanol, and glycerine were purchased from Scharlau (Barcelona, Spain). APS, TEMED, Tris, acrylamide, bisacrylamide, SDS, Coomassie Brilliant Blue R, and BSA were obtained from Sigma-Aldrich (St. Louis, Mo., U.S.A.). 2-Mercaptoethanol and HCl were purchased from Merck (Darmstadt, Germany) and bromophenol blue from Riedel-de-Häen (Hannover, Germany). Two molecular-weight-size protein standards (6.5 to 66 kDa and 36 to 200 kDa) were also provided by Sigma-Aldrich. A Protein Quantification Kit-Rapid from Fluka (Steinheim, Germany) was used for the Bradford protein assay. The following enzymes, kindly donated by Novozymes (Bagsvaerd, Denmark) were used: lipase (Palatase® 20000 L; activity 20000 LU-MM/g (LU = lipase unit); optimal working conditions, pH 7 and 25 - 45 ºC), cellulase (Celluclast® 1.5L, activity 1500 NCU/g (NCU = novo cellulase unit), working conditions, pH 4.5 - 6.0 and 50 - 60 ºC), phospholipase (Lecitase® Ultra; activity 10 KLU/g; optimal working conditions, pH 6 - 7 and 40 ºC), and an enzymatic mixture containing arabanase, cellulase, beta-glucanase, hemicellulose, and xylanase (Viscozyme® L; activity 100 FBG/g (FBG = beta-glucanase unit); optimal working conditions, pH 4 and 45 - 65 ºC). Deionized water (Barnstead deionizer, Sybron, Boston, MA) was used in all procedures.

9.2.2. Samples

The olive fruits used in this study (**Table 9.1**) were kindly donated by various olive oil manufacturers. To assure a correct sampling, olives were collected at the same period (end of November 2011) directly from trees located in different Spanish regions. The genetic variety of samples was guaranteed by the suppliers. The olives were selected to assure the absence of mold or other

microorganisms, washed with water to remove dust or airborne particles settled on the olive, and then stored at -20 ºC prior their use.

9.2.3. Instrumentation

SDS-PAGE experiments were performed using a vertical minigel Hoefer SE260 Mighty Small system (Hoefer, MA, USA). Protein extraction was carried out with a Sigma 2-15 centrifuge (Sigma Laborzentrifugen, Osterode am Harz, Germany) and a D-78224 ultrasonic bath (Elma, Germany). To measure the absorbance at 595 nm for the Bradford protein assay, a Model 8453 diode-array UV-vis spectrophotometer (Agilent Technologies, Waldbronn, Germany) with a 1-cm optical path quartz cell (Hellma, Müllheim, Germany) was used.

9.2.4. Protein extraction

In order to proceed to protein extraction, olive pulp and stone were first separated and then treated as follows: about 20 g of fresh pulp or stone was frozen in liquid nitrogen and ground to a fine powder with a pre-cooled mortar and pestle, lyophilized, and the resulting powder was homogenized. For the extraction of olive pulp proteins, 0.3 g of the powder was treated with 3 mL water at pH 7.0 containing 5% (v/v) Palatase® 20000 L and sonicated at 30 ºC for 15 min. On the other hand, for the extraction of olive stone proteins, the same conditions described for pulp proteins were used, although in this case the enzyme employed was phospholipase (Lecitase® Ultra), and the extraction temperature was 40 ºC. Next, both pulp and stone protein extracts were centrifuged at 10000 × *g* for 10 min. An aliquot of the supernatant was taken and used for Bradford's assay, and the rest of the solution was stored at -20 ºC until-use.

Table 9.1

Genetic variety, geographical origin, and total protein content (mg g^{-1}) of the olive pulps and stones used in this study.

Genetic variety	Geographical origin	Pulp protein content (mg g^{-1}) (n = 6)	Stone protein content (mg g^{-1}) (n = 6)
Solà	Castellón Valencia	0.38 ± 0.01	0.35 ± 0.03
Cornicabra	Castellón Murcia	0.90 ± 0.01	0.52 ± 0.01
Hojiblanca	Córdoba Murcia	0.64 ± 0.02	0.96 ± 0.05
Picual	Córdoba Murcia	0.98 ± 0.01	1.26 ± 0.07
Arbequina	Castellón Murcia	0.88 ± 0.01	2.71 ± 020
Manzanilla	Cáceres Valencia	0.88 ± 0.02	1.20 ± 0,12
Blanqueta	Alicante Valencia	0.37 ± 0.02	1.51 ± 0.14
Grosol	Alicante Valencia	0.27 ± 0.01	0.42 ± 0.04

For SDS-PAGE analysis, 200 µL of the protein extract was mixed with 800 µL of ice-cold acetone, and the resulting mixture was kept at -20 ºC for 20 min. The precipitated proteins were collected by centrifugation at 10000 × *g* for 10 min at 4 ºC, and the resulting pellet was dissolved in 100 µL of SDS sample buffer (0.0625 M Tris-HCl pH 6.8, 10% (v/v) glycerol, 5% (w/v) SDS, 0.004% (w/v) bromophenol blue, and 5% (v/v) 2-mercaptoethanol) (Laemmli, 1970). Then, the sample was heated for 5 min at 95 ºC and an aliquot was loaded onto the gel.

For Bradford's assay (Bradford, 1976), a calibration curve up to 1 mg mL^{-1} of BSA was prepared. The sample protein content was measured according to the protocol described in the Bradford assay Protein Quantitation Kit-Rapid (Fluka). A sample blank containing 5% (v/v) of the corresponding enzyme was also made to remove its contribution to the final sample absorbance.

9.2.5. SDS-PAGE separation

In order to determine the molecular weight of the extracted proteins, their separation was carried out on 10-cm-long gels under reducing conditions. The running gels were composed of 30% (w/w) total acrylamide and 8% (w/w) bisacrylamide. Electrophoresis separation was performed for 1.5 h at constant voltage (180 V) using a running buffer containing 3.03 g L^{-1} Tris, 14.4 g L^{-1} glycine, and 1 g L^{-1} SDS. Then, gels were stained overnight in a solution of 0.2% (w/v) Coomassie Brilliant Blue R and washed with a solution composed of 40% (v/v) MeOH and 10% (v/v) acetic acid. Finally, gels were stored using an aqueous solution containing 5% (v/v) glycerol.

9.3. Results and discussion

9.3.1. Influence of enzyme type on protein extraction

Enzyme-assisted extraction of proteins from both olive pulp and stone were conducted with the 4 different enzyme types (lipase, cellulase, phospholipase and the enzymatic mixture) previously described in "Chemicals" section. For this purpose, enzyme type was changed by keeping the enzyme concentration constant at 5% (v/v), at pH 6.0, and sonicated at 25 ºC for 20 min. Blanqueta variety olives from Valencia (**Table 9.1**) were selected for the selection of the best conditions. For this purpose, the standard Bradford assay was first used. In all cases, measurements were performed considering a blank which contained the same type and concentration of enzyme. The obtained results are shown in

Figure 9.1. As deduced from this figure for pulp proteins, the highest extraction was achieved using a lipase enzyme (Palatase® 20000 L), which has a hydrolytic activity on triacylglycerol bonds. On the other hand, the best results for stone proteins were obtained using a phospholipase (Lecitase® Ultra) enzyme, which produces the breakdown of phospholipid bonds. Thus, these enzymes, lipase and phospholipase, for pulp and stone, respectively, were next selected for further studies.

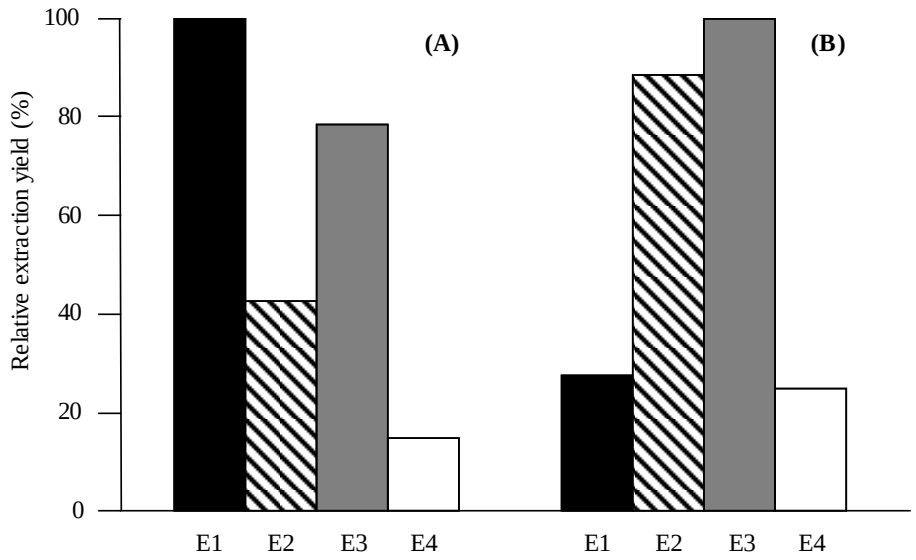

Figure 9.1. Influence of enzyme type on pulp (A) and (B) stone protein extraction monitored by Bradford assay. Enzyme identification: E1, lipase; E2, cellulase; E3, phospholipase, and E4, enzymatic mixture containing arabanase, cellulase, beta-glucanase, hemicellulose, and xylanase. Experimental conditions: 5% (v/v) enzyme, at pH 6.0, sonicated at 25 °C for 20 min.

9.3.2. Influence of enzyme content on protein extraction

Next, the effect of enzyme content on the protein extraction was examined at pH 6.0 and by sonication at 25 ºC for 20 min. In both cases, Palatase® 20000 L and Lecitase® Ultra content, for pulp and stone, respectively, was varied from 0

to 8% (v/v). In all cases, and as mentioned above, a reagent blank was also employed. As observed in **Figure 9.2A** (standard Bradford assay) for both the pulp and stone protein extracts, an increase in the total protein content was obtained when the enzyme content was increased up to 5% (v/v). However, when the enzyme content was increased from 5 to 8% (v/v), the extraction yield decreased. This behavior could be explained by taking into account 2 effects: i) the appearance of turbidity in the protein extracts, when using enzyme contents higher than 5% (v/v) and ii), the so-called competitive inhibition, in which the extracted protein molecules are supposed to act as inhibitors in combination with the enzyme to form a complex, thus preventing its activity, although there is no evidence of this mechanism (Laidler, 1973). This fact was in agreement with previously reported results (Shen, 2008). In addition, an increase in enzyme concentration would normally enhance the solubility of protein into the solvent and, therefore, increase the extraction yield. However, the existence of free enzyme in the solvent could interact with the protein and cause degradation of protein molecules, which could also explain signal decrease. This fact was in agreement with previously published studies (Shen, 2008).

Next, the influence of the enzyme content was also tested by SDS-PAGE. For this purpose, 9 molecule markers were used to establish the molecular-weight band (**Figure 9.2B** and **C**). In both cases, when a 5% (v/v) enzyme content was used, clear bands were identifiable with higher intensity than those obtained at 3.5% and 6.5% (v/v) enzyme content. In pulp protein extracts, 4 prominent protein bands, located at 22, 30, 41, and 48 kDa were distinguished. The bands located at 30 and 48 kDa were identified as lipase enzyme, whereas the 22 and 41 kDa proteins could be related to an oleosin (Ross, 1993) and to a precursor of storage proteins, respectively. On the other hand, in stone protein extracts, 6 protein bands, located at 20.5, 25.5, 30, 47.5, 50, and 110 kDa, were distinguished.

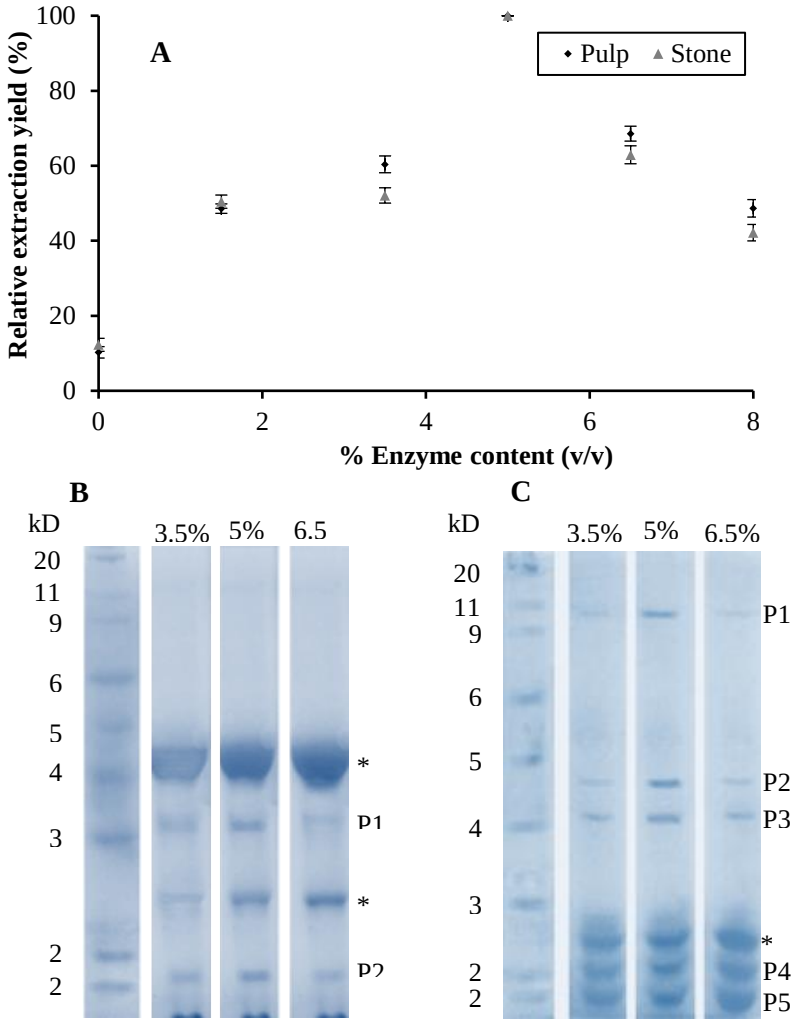

Figure 9.2. Influence of enzyme content on the olive pulp and stone protein extraction monitored by Bradford assay (A) and SDS-PAGE (part B for pulp and part C for stone proteins). Band identification (pulp, part B): asterisk, 30 and 48 kDa (lipase); P1, 41 kDa; P2, 22 kDa. Band identification (stone, part C): asterisk, 30 kDa (phospholipase); P1', 110 kDa; P2', 50 kDa; P3', 47.5 kDa; P4', 25.5 kDa; P5', 21.5 kDa. Experimental conditions: pH 6.0, sonicated at 25 ºC for 20 min.

The band located at 30 kDa was identified as phospholipase enzyme, whereas the band at 50 kDa was attributed to a polypeptide which had previously been proposed as a member of the oleosin family (Ross, 1993).

On the other hand, both 20.5 and 25.5 bands were assigned as SSPs of the 11S protein family, the band located at 47.5 kDa being its precursor (Alché, 2006). However, the protein located at 110 kDa has not been previously reported in the literature. Thus, as a result of both Bradford assay and SDS-PAGE results, the optimum enzyme concentration for both pulp and stone was set at 5% (v/v) for further studies.

9.3.3. Influence of pH on protein extraction

The effect of pH on protein extraction was next investigated, by keeping constant the optimum percentage of enzyme (5% (v/v)) and by sonication at 25 ºC for 20 min. For this purpose, pH was varied between 6.0 and 9.0. As observed in **Figure 9.3A** (standard Bradford assay), for both pulp and stone, an increase in the total protein content was obtained when the pH was increased up to 7.0. However, when the pH was further increased a decrease in the signal was observed. This behavior was in agreement with the optimal pH values provided by the enzyme supplier.

Next, the influence of pH was tested by SDS-PAGE. As shown in **Figure 9.3B** and **C**, similar molecular weight distributions than those reported in **Figure 9.2B** and **C** for pulp and stone proteins, respectively, were observed. However, a new band, at 27.5 kDa was evidenced in stone protein extracts. This band was also assigned as a SSP of the 11S protein family (**Figure 9.2C**). As observed, the bands at pH 7.0 provided the highest intensity. Consequently, the optimum pH was set at 7.0 for further studies.

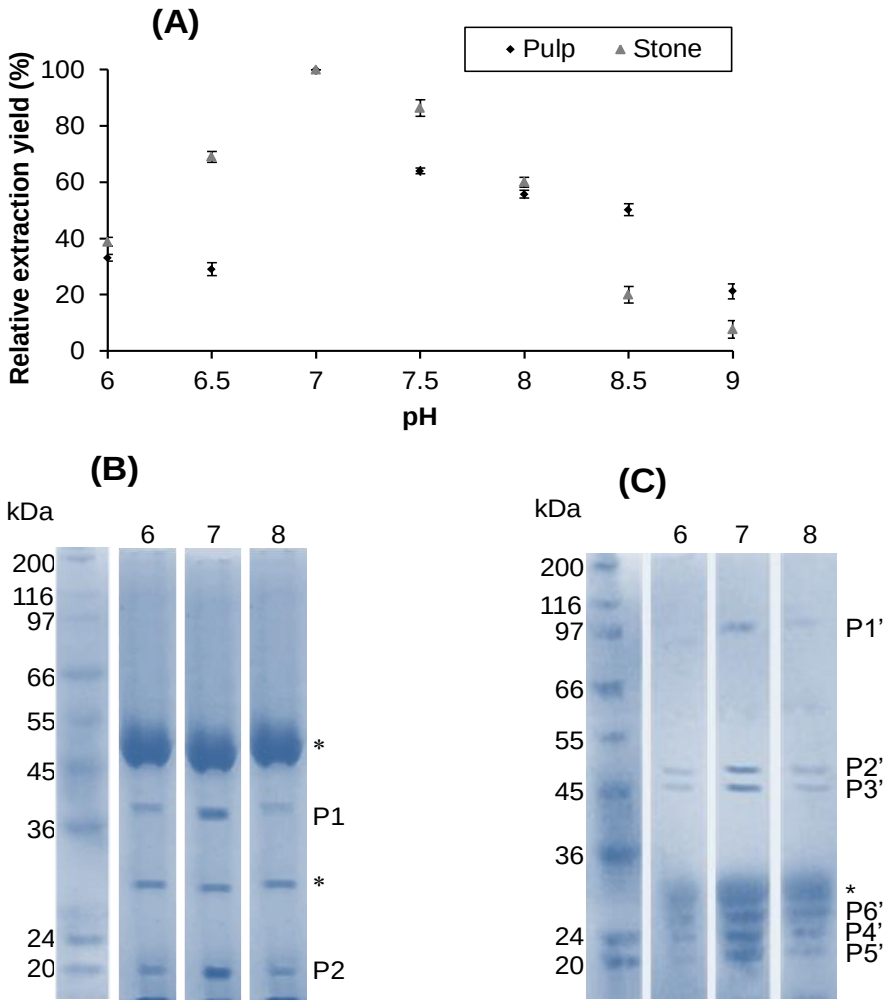

Figure 9.3. Influence of pH on the olive pulp and stone protein extraction monitored by Bradford assay (A) and SDS-PAGE (part B for pulp and part C for stone proteins). New band in part C (stone) is P6', 27.5 kDa. Other band identification as in **Figure 9.2**. Experimental conditions: 5% (v/v) enzyme sonicated at 25 ºC for 20 min.

9.3.4. Influence of extraction temperature and time on protein recovery

The influence of temperature and extraction time on protein extraction under the selected conditions (5% (v/v) enzyme at pH 7.0) was also investigated. First, the influence of temperature was tested by varying it from 25 to 50 ºC. As shown in **Figure 9.4A** for pulp proteins, temperature had a significant effect on the enzyme's capability in extracting proteins up to 30 ºC; however, higher temperatures led to a decrease in protein extraction. This behavior was in agreement with the data reported by Novozymes, which stated that enzyme stability decreases at temperatures higher than 30 ºC. On the other hand, for stone proteins, the higher signal was obtained when temperature was set at 40 ºC, being also observed a decrease in protein extraction when temperature was further increased. This behavior could be explained taking into account that a high reaction temperature could cause irreversible enzyme denaturation, which decreased enzyme activity, as previously stated in the literature for phospholipase (Primozic, 2003; Wang, 2010). This fact was also in agreement with the supplier who has declared that the maximum phospholipase activity is obtained at 40 ºC.

The results obtained by the standard Bradford assay were consistent with those observed by SDS-PAGE (**Figure 9.4B** and **C**). Thus, 30 ºC and 40 ºC, for pulp and stone proteins, respectively, were selected as the optimum extraction temperatures.

Finally, the extraction time was also studied from 5 to 25 min using the previously selected conditions. As observed in **Figure 9.5**, an increase in the total protein content was obtained when extraction time was increased up to 15 min, while at higher times (20 and 25 min) the total protein content obtained remained practically constant. Thus, an extraction time of 15 min was selected as the optimal one for further studies.

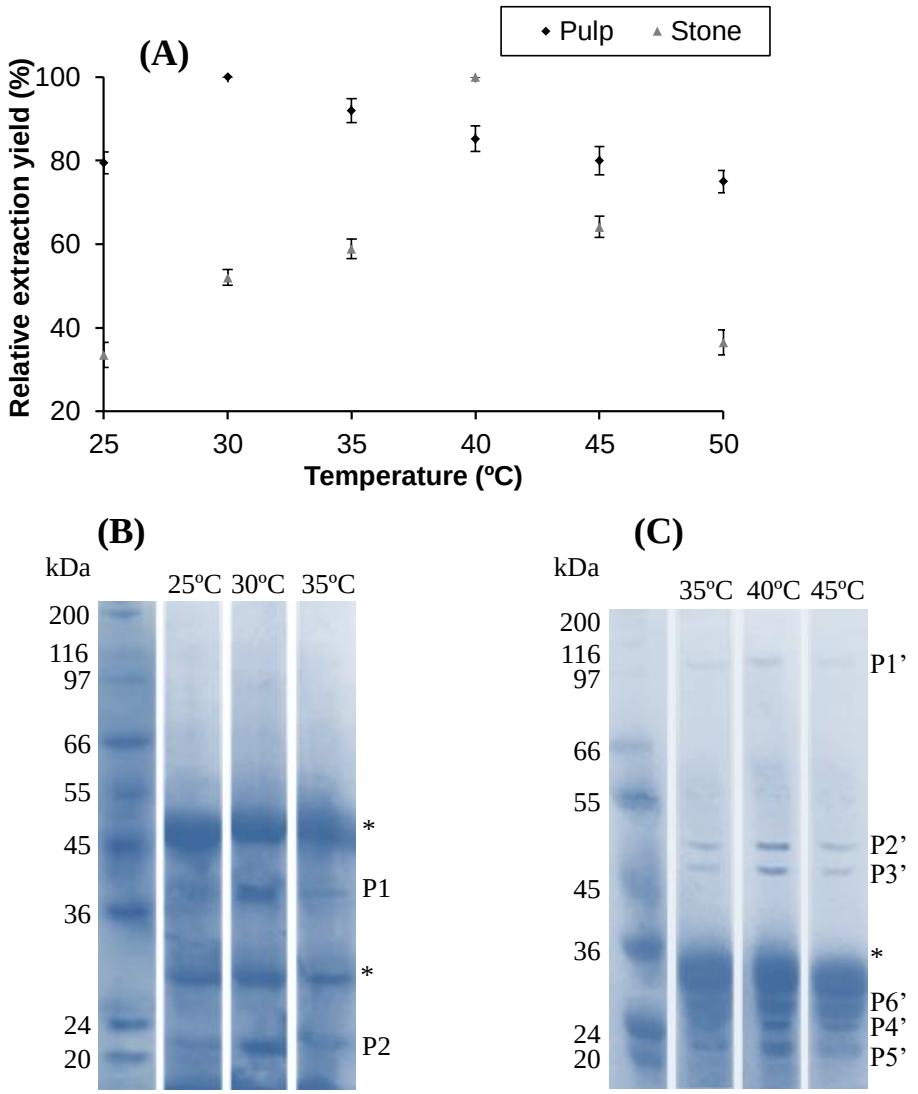

Figure 9.4. Influence of temperature on the olive pulp and stone protein extraction monitored by Bradford assay (A) and SDS-PAGE (part B for pulp and part C for stone proteins). Band identification as in **Figure 9.3.** Experimental conditions: 5% (v/v) enzyme, at pH 7.0, sonicated for 20 min.

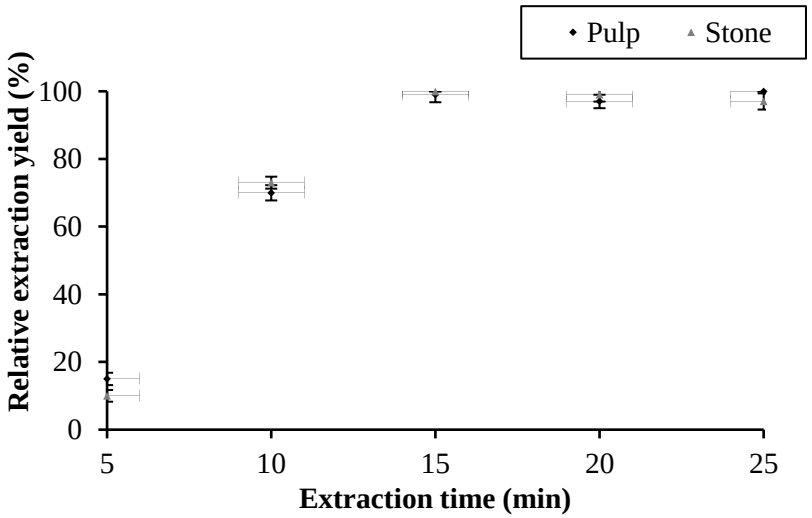

Figure 9.5. Influence of extraction time on the olive pulp and stone protein extraction monitored by Bradford assay. Experimental conditions: 5% (v/v) enzyme, at pH 7.0, sonicated at 30 ºC for pulp and 40 ºC for stone proteins.

9.3.5. Analysis of olive pulp and stone proteins from different genetic varieties

The developed extraction method was applied to the evaluation of the protein content of olive pulps and stones from different genetic varieties obtained from different geographical Spanish regions (**Table 9.1**). The total amount of protein mass, on a fresh weight basis, which was calculated using the standard Bradford assay, was between 0.27 mg g^{-1} (Grosol variety) and 0.98 mg g^{-1} (Picual variety) for pulp, while for stone it was between 0.35 mg g^{-1} (Solà variety) and 1.51 mg g^{-1} (Blanqueta variety). A study of repeatability of the recommended extraction protocol from the same tissues was performed. In all cases, satisfactory RSD values (4.8 and 5.1 %) were obtained for pulp and stone proteins, respectively.

Thus, the protein distribution of the different genetic varieties was studied by SDS-PAGE. The results obtained are shown in **Figure 9.6**. For pulp proteins (**Figure 9.6A**), all genetic varieties provided the same protein distribution. However, when stone protein profiles were compared (see **Figure 9.6B**), several differences were observed, which suggested that some of these proteins seem to be cultivar-dependent. A new protein band at 66 kDa, present in Solà, Cornicabra, Picual, Blanqueta, and Grosol varieties, was evidenced. A protein with the same molecular mass has been previously described by Tazzari (1995) in olive leaves. The band observed at 110 kDa was observed in Cornicabra, Picual, Arbequina and Grosol, being more intense in Arbequina variety. On the other hand, the band at 50 kDa was observed in all the studied genetic varieties except in Manzanilla and Grosol.

Finally, regarding the SSPs, all the investigated varieties showed three 11S proteins (21.5, 25.5, and 27.5 kDa) except Solà and Arbequina, which did not show the band at 25.5 kDa. Moreover, the same SDS-PAGE protein profiles were observed for the olive fruits from different Spanish regions for a same genetic variety. Thus, the differences observed in stone protein profiles could be helpful to distinguish them according to their genetic variety.

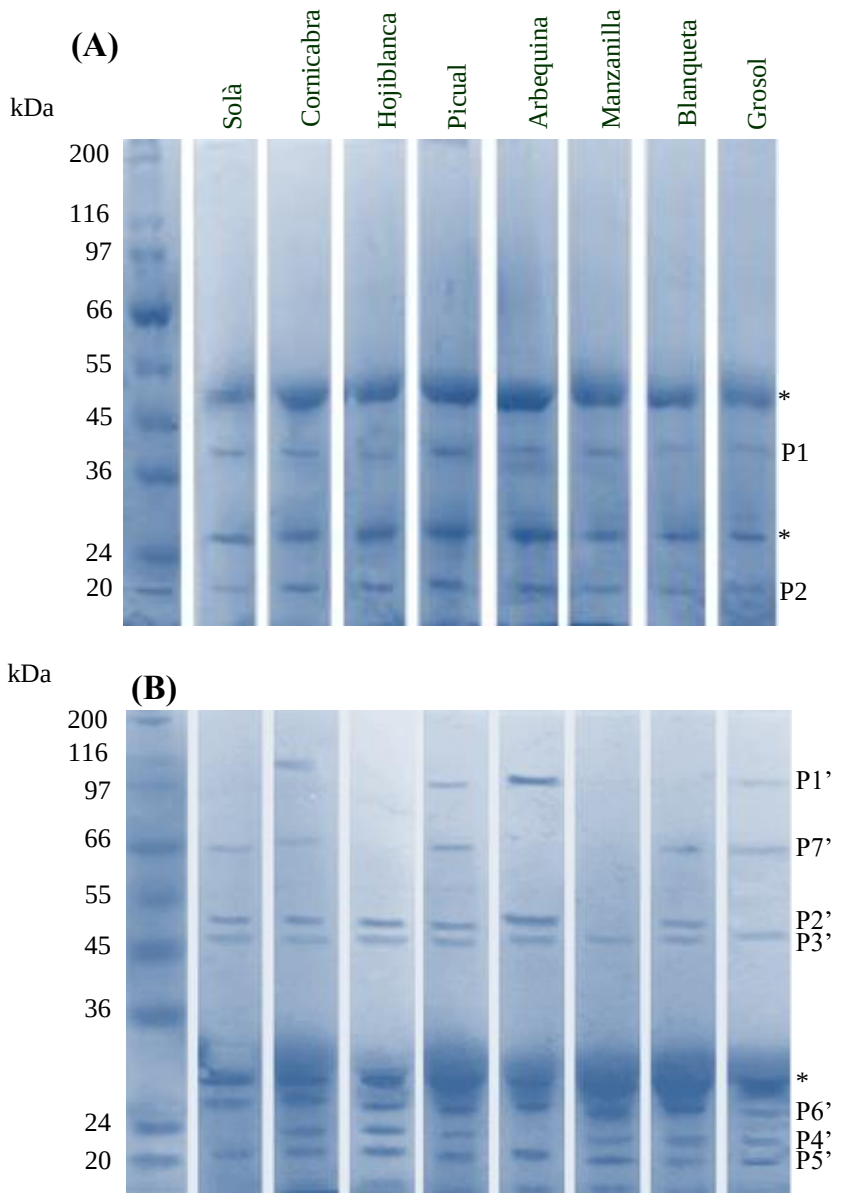

Figure 9.6. SDS-PAGE electrophoretic protein profiles obtained for the different olive pulp (A) and stone (B) genetic varieties considered in this study. Band identification (stone, part B): P7', 66 kDa. Other bands as in **Figure 9.3**. Experimental conditions: 5% (v/v) enzyme, at pH 7.0, sonicated for 15 min at 30 ºC for pulp and 40 ºC for stone proteins.

9.4. Conclusions

The use of enzymes to effectively extract the proteins from olive pulp and stone is described in this paper. Several parameters that affect the extraction process, such as enzyme type and content, pH, and extraction temperature and time, were tested. For pulp proteins, the best extraction yields were obtained at pH 7.0 and 5% (v/v) Palatase® 20000 L (lipase) content, being extraction temperature and time 30 ºC and 15 min, respectively. Regarding stone proteins, the selected enzyme was Lecitase® Ultra (phospholipase) content, being the other conditions the same as for pulp proteins except extraction temperature that was 40ºC in this case. These enzymes were selected for pulp and stone, since they were capable of breaking down triacylglycerol and phospholipid bonds, respectively. The mild extraction conditions are environmentally sustainable and faster than other protocols described in the literature. Moreover, in the case of stone proteins, different electrophoretic profiles and band intensities were obtained which could be helpful to distinguish stone samples according to their genetic variety or origin.

Acknowledgements

M. V-B thanks the MINECO for an FPU grant for PhD studies. M.J. L-G thanks the Generalitat Valenciana for a VALi+d postdoctoral contract. The authors also thank Ramiro Martínez from Novozymes (Spain) for his support.

9.5. References

Alché, J.D.; Jiménez-López, J.C.; Wang, W.; Castro-López, A.J.; Rodríguez-García, M.I. (**2006**). Biochemical characterization and cellular localization of 11s type storage proteins in olive (*Olea europaea L.*) seeds. *Journal of Agriculture of Food Chemistry, 54*, 5562-5570.

Bradford, M.M. (**1976**). A rapid and sensitive method for the quantitation of microgram quantities of protein utilizing the principle of protein-dye binding. *Analytical Biochemistry*, *72*, 248-254.

Conde, C.; Delrot, S.; Gerós, H. (**2008**). Physiological, biochemical and molecular changes occurring during olive development and ripening. *Journal of Plant Physiology, 165*, 1545-1562.

Esteve, C.; Del Río, C.; Marina, M.L.; García, M.C. (**2011**). Development of an ultra-high- performance liquid chromatography analytical methodology for the profiling of olive (*Olea europaea L.*) pulp proteins. *Analytica Chimica Acta, 690*, 129-134.

Georgalaki, M.D.; Sotiroudis, T.G.; Xenakis, A. (**1998A**). The presence of oxidizing enzyme activities in virgin olive oil. *Journal of the American Oil Chemists' Society*, *75*, 155-159.

Georgalaki, M.D.; Bachmann, A.; Sotiroudis, T.G.; Xenakis, A.; Porzel, A.; Feussner, I. (**1998B**). Characterization of a 13-lipoxygenase from virgin olive oil and oil bodies of olive endosperms. *European Journal of Lipid Science and Technology*, *100*, 554-560.

Koidis, A.; Boskou, D. (**2006**). The content of proteins and phospholipids in cloudy (veiled) virgin olive oils. *European Journal of Lipid Science and Technology*, *108*, 323-328.

Laemmli, U.K. (**1970**). Cleavage of structural proteins during the assembly of the head of bacteriophage T4. *Nature 227*, 680-685.

Laidler, K.J.; Bunting, P.S. (**1973**). The chemical kinetics of enzyme action, second ed., Oxford, UK.

Martín-Hernández, C.; Bénet, S.; Obert, L. (**2008**). Determination of proteins in refined and nonrefined oils. *Journal of Agriculture of Food Chemistry, 56,* 4348-4351.

Primozic, M.; Habulin, M.; Knez, Z. (**2003**). Parameter optimization for the enzymatic hydrolysis of sunflower oil in high-pressure reactors. *Journal of the American Oil Chemists' Society, 80,* 643-646.

Ross, J.H.E.; Sanchez, J.; Millan, F.; Murphy, D.J. (**1993**). Differential presence of oleosins in oleogenic seed and mesocarp tissue in olive (*Olea europaea*) and avocado (Persea americana). *Plant Science, 93,* 203-210.

Sari, Y.W.; Bruins, M.E.; Sanders, J.P.M. (**2013**). Enzyme-assisted protein extraction from rapeseed, soybean, and microalgae meals. *Industrial Crops and Products 43*, 78-93.

Sebastián-Francisco, I.; Simó-Alfonso, E.F.; Mongay-Fernández, C.; Ramis-Ramos, G. (**2003**). Improvement of the electrophoretic protein profiles of Leguminosae gum extracts using gamanase and application to the evaluation of carob–guar mixtures. *Analytica Chimica Acta*, 508, 135-140.

Shen, L.; Wang, X.; Wang, Z.; Wu, Y.; Chen, J. (**2008**). Studies on tea protein extraction using alkaline and enzyme methods. *Food Chemistry, 107,* 929-938.

Tazzari, L.; Bartolini, G.; Mslallem, M.; Pestelli, P. (**1995**). Phase change in *Olea europaea L.*: leaf proteins in juvenile and adult shoots. In: Ninth

Consultation of the Inter-regional Cooperative Research Network on Olives, Hammamet, Tunisia. Coordination Centre, CIDA, Cordoba, Spain, p. 65.

Wang, W.; Alché, J.D.; Castro, A.J.; Rodríguez-García, M.I. (**2001**). Characterization of seed storage proteins and their synthesis during seed development in Olea europaea. *International Journal of Developmental Biology*, *45*, 63-64.

Wang, W.; Alché, J.D.; Rodríguez-García, M.I. (**2007**). Characterization of olive seed storage proteins. *Acta Physiologiae Plantarum, 29,* 439-444.

Wang, W.; Scali, M.; Vignani, R.; Spadafora, A.; Sensi, E.; Mazzuca, S.; Cresti, M. (**2003**). Protein extraction for two-dimensional electrophoresis from olive leaf, a plant tissue containing high levels of interfering compounds. *Electrophoresis, 24*, 2369-2375.

Wang, W.; Tai, F.; Chen, S. (**2008**). Optimizing protein extraction from plant tissues for enhanced proteomics analysis. *Journal of Separation Science, 31,* 2032-2039.

Wang, Y.; Zhao, M.; Song, K.; Wang, L.; Tang, S.; Riley, W.W. (**2010**). Partial hydrolysis of soybean oil by phospholipase A_1 (Lecitase Ultra). *Food Chemistry*, *121*, 1066-1072.

Zamora, R.; Alaiz, M.; Hidalgo, F.J. (**2001**). Influence of cultivar and fruit ripening on olive (*Olea europaea*) fruit protein content, composition, and antioxidant activity. *Journal of Agricultural and Food Chemistry*, *49*, 4267-4270.

Chapter 10. Enzyme-assisted extraction of proteins from *Citrus* fruits and prediction of their cultivar using protein profiles obtained by capillary gel electrophoresis

Food Control 72 (2017) 14–19

Contents lists available at ScienceDirect

Food Control

journal homepage: www.elsevier.com/locate/foodcont

Enzyme-assisted extraction of proteins from *Citrus* fruits and prediction of their cultivar using protein profiles obtained by capillary gel electrophoresis

María Vergara-Barberán, Óscar Mompó-Roselló, María Jesús Lerma-García, José Manuel Herrero-Martínez, Ernesto Francisco Simó-Alfonso*

Department of Analytical Chemistry, University of Valencia, C. Doctor Moliner 50, E-46100 Burjassot, Valencia, Spain

The suitability of protein profiles established by CGE as a tool to discriminate between 11 cultivars of *Citrus* (orange and tangerine) peel and pulp was evaluated in this work. Before CGE analysis, different extraction buffers (which included enzyme-assisted treatments) were compared. The best results were achieved using 5% (*v/v*) Celluclast® 1.5L and 5% (*v/v*) Palatase® 20000 L buffers for *Citrus* peel and pulp protein extracts, respectively. The resulting protein profiles obtained were used to construct LDA models able to distinguish *Citrus* peel and pulp samples according to their cultivar. In both cases, all samples were correctly classified with an excellent resolution among all categories, which demonstrated that protein patterns are a powerful tool to discriminate *Citrus* samples coming from different cultivars.

Keywords: *Citrus*; cultivar; protein profile; capillary gel electrophoresis; enzyme-assisted extraction

10.1. Introduction

Orange (*Citrus sinensis*) and tangerine (*Citrus tangerine*) fruits and juices are frequently consumed in Europe and North America. The total annual *Citrus* production was estimated at over 145 million tons in 2013 (FAO, 2010). Within *Citrus* fruit production, orange juice processing constitutes the largest volume percentage (75%) of the world marker (FAO, 2010). In this sense, it is of prime importance to the *Citrus* industry to maintain and improve product quality, to remain competitive and to fulfill consumer demands (Klavons, 1991).

Among the different compounds present in *Citrus* fruits, flavonoids (Kawaii, 1999), carotenoids (Goodner, 2001; Moulya, 1999) and phenolic compounds (Cieslik, 2006; Khan, 2010) have been largely described in comparison to other components, such as proteins, that have been scarcely studied. This could be due to the fact that the extraction of fruit proteins is difficult due to the low solubility of these biomacromolecules. This fact is due to the complex formed between protein and pectin compounds (Klavons, 1991). In this regard, different extraction protocols have been described for the extraction of proteins from *Citrus* tissues (Saravanan, 2004; Zukas, 2004). Saravanan *et al.* (Saravanan, 2004) compared two protein extraction methods (TCA and phenol extraction protocols) to obtain a high number of protein spots from 2D electrophoresis gel of several tissues (tomato, avocado, banana and orange peel). The best results were obtained using the phenol extraction protocol, which provided the greatest protein yield (2.08 mg/g fresh weight). On the other hand, Zukas *et al*. (Zukas, 2005) compared three extraction protocols (Tris–HCl, KCl and phenol) followed by precipitation to purify and concentrate proteins from *Citrus* leaves coming from 6 different varieties (Sour and Navel orange, mandarin, citron and lemon). In this case, the best results were obtained using the Tris-HCl extraction protocol. However, these

latter extraction protocols employed several cleanup steps, which are laborious, time-consuming and in some cases non-environmentally friendly protocols.

Enzyme-assisted protein extraction constitutes an alternative method due to its mild extraction conditions and lower environmental impact (Sari, 2013; Shen, 2008; Vergara-Barberán, 2014A; Vergara-Barberán, 2015). Thus, several specific enzymes have been employed in protein extraction in tea leaves (Shen, 2008) in Leguminosae gums (Sebastián-Francisco, 2004), in different oilseed meals (Sari, 2013) and in olive fruit and leaves, (Vergara-Barberán, 2014A; Vergara-Barberán, 2015) providing improved protein extraction yields compared to alkaline or acidic treatments. However, to our knowledge, this methodology has not been applied to *Citrus* fruit protein extraction.

In previous works, it has been demonstrated that protein profile is a good marker of sample origin (Lliso, 2007; Montealegre, 2010; Vergara-Barberán, 2014B; Vergara-Barberán, 2014C; Wang, 2014).

As an example, the protein profiles established by both GCE (Vergara-Barberán, 2014B) and CZE (Vergara-Barberán, 2014C), followed by LDA, have been used to classify olive leaves and pulps according to their cultivar. On the other hand, Montealegre *et al*. (Montealegre, 2010) have used SDS-CGE to differentiate proteins from raw and table olive samples from some cultivars. Moreover, Wang et al. (Wang, 2014) studied different protein profiles of peanut cultivars using SDS-PAGE followed by LDA, finding that the different varieties could be grouped according to their storage proteins.

In this work, different enzyme-assisted extraction protocols have been studied in order to obtain a satisfactory protein yield. To monitor the extraction, the total protein content was measured using the standard Bradford assay. Next, protein extracts were analyzed by CGE, and the resulting protein

profiles were used to develop LDA models able to distinguish *Citrus* peel and pulp samples according to their cultivar.

10.2. Materials and methods

10.2.1. Chemicals

Tris, SDS, sodium chloride (NaCl), 3-[3-cholamidopropyl dimethylammonio]-1-propanesulfonate (CHAPS) and BSA were from Sigma-Aldrich (St. Louis, MO, USA). 2-Mercaptoethanol, sodium hydroxide (NaOH) pellets and hydrochloric acid (HCl) were purchased from Merck (Darmstadt, Germany). Molecular mass standard mixture solution (eight proteins comprised between 6.5 to 66 kDa) provided by Sigma-Aldrich was used. In order to perform Bradford protein assay, a Protein Quantification Kit-Rapid from Fluka (Steinheim, Germany) was employed. Different enzymes, which were kindly provided by Novozymes (Bagsvaerd, Denmark) were used: lipase (Palatase® 20000 L; activity 2,000 LU-MM/g (LU = lipase unit); working conditions, pH 7 and 25-45 ºC) and cellulase (Celluclast® 1.5L; activity 1,500 NCU/g (NCU = novo cellulose unit); working conditions, pH 4.5-6.0 and 50-60 ºC). SDS-MW gel buffer (pH 8, 0.2% SDS) (Beckman Coulter, Inc., Fullerton, CA) was utilized for CGE analysis. Deionized water (Barnstead deionizer, Sybron, Boston, MA) was also used.

10.2.2. Instrumentation

In order to quantify proteins using Bradford assay, UV–vis data were recorded at 595 nm using a diode array UV–visible spectrophotometer from Agilent Technologies (Waldbronn, Germany) equipped with a 1-cm optical path quartz cell from Hellma (Müllheim, Germany).

Protein separations by CGE were performed using an HP^{3D} CE system from Agilent, which is equipped with a diode-array spectrophotometric detector. Bare fused-silica capillaries of 33.5 cm (25 cm effective length) and 375 µm od x 50 µm id (Polymicro Technologies, Phoenix, AZ, USA) were used. These capillaries were initially activated with 1 and 0.1 M NaOH and water at 60º C for 10 min each before its first use.

Every day, the capillary was sequentially conditioned with 0.1 M NaOH for 5 min, 0.1 M HCl and water for 2 min each, and SDS-MW gel buffer for 10 min before use. The protein samples were injected at -30 kV x 7 s. Separations were performed at -15 kV at 25 ºC. UV detection was done at 214 nm.

10.2.3. Citrus fruits and protein extraction

Citrus fruit samples (both oranges and tangerines) coming from 11 different cultivars were employed in this study (see **Table 10.1**). In all cases, the cultivar origin of samples was guaranteed by the supplier (Fontestad S.A., Museros, Valencia, Spain).

Both, *Citrus* peel and pulp were subjected to protein extraction. For this purpose, the surface of *Citrus* fruits was washed with lukewarm 1% SDS solution, in order to eliminate bacterial and surface contamination from human hands. Next, the thin flavedo peel was carefully excised and reduced to very small fragments via a treatment in a fruit blender for 10 min at maximum power. Regarding pulp, 200 g were first lyophilized and the resulting powder next homogenized before their use.

Table 10.1

Description of the *Citrus* fruits considered in this work.

Oranges			
Cultivar	**Geographical origin**	**Nº samples**	**Crop season**
Salustiana	Montserrat (Valencia)	1	2013/2014
		1	2014/2015
	Campredó (Tarragona)	1	2013/2014
		1	2014/2015
	Palma del río (Córdoba)	1	2013/2014
		1	2014/2015
Navel	Gandía (Valencia)	1	2014/2015
	Alzira (Valencia)	1	2013/2014
		1	2014/2015
	Agost (Alicante)	1	2013/2014
		2	2014/2015
	Écija (Sevilla)	1	2014/2015
Navelate	Alzira (Valencia)	2	2013/2014
		1	2014/2015
	Palma del Río (Córdoba)	1	2013/2014
		1	2014/2015
Navelina	Alcàsser (Valencia)	1	2013/2014
		1	2014/2015
	Peñíscola (Castellón)	1	2013/2014
		1	2014/2015
	Barxeta (Valencia)	1	2013/2014
		1	2014/2015
Nulera	Tavernes de la Valldigna (Valencia)	1	2013/2014
		2	2014/2015
	Pulpí (Almería)	1	2014/2015
Fukumoto	Cabanes (Castellón)	1	2013/2014
		1	2014/2015
	Xiva (Valencia)	1	2013/2014
		2	2014/2015
	Alcanar (Tarragona)	1	2013/2014
	Domeño (Valencia)	1	2013/2014
		1	2014/2015

Cont. Table 10.1

Tangerines			
Cultivar	**Geographical origin**	**Nº samples**	**Crop season**
Ortanique	Burriana (Castellón)	1	2013/2014
		1	2014/2015
	Petrés (Valencia)	1	2013/2014
		1	2014/2015
	Castelló (Castellón)	1	2013/2014
		1	2014/2015
	Sagunt (Valencia)	1	2013/2014
Nadorcott	Alcalá del Río (Sevilla)	1	2013/2014
		1	2014/2015
	Vinaròs (Castellón)	1	2013/2014
		2	2014/2015
	Carcaixent (Valencia)	1	2013/2014
		1	2014/2015
Clemenrubi	Lorca (Murcia)	1	2013/2014
		1	2014/2015
	Isla del Marquesado (Huelva)	1	2013/2014
		1	2014/2015
	Jimena de la Frontera (Cadíz)	1	2013/2014
Clemenpons	Agost (Alicante)	2	2013/2014
		1	2014/2015
	Massamagrell (Valencia)	1	2013/2014
		1	2014/2015
	Alcalá del Río (Sevilla)	1	2013/2014
		1	2014/2015
Orogrande	Burriana (Castellón)	1	2013/2014
		1	2014/2015
	Sagunto (Valencia)	1	2013/2014
		1	2014/2015

Three different extraction buffers were tested with both, *Citrus* peel and pulp. The native buffer contained 50 mM Tris–HCl (pH 7.2), 50 mM NaCl and 2% (*w/v*) CHAPS (buffer I) (Lerma-García, 2016), and buffer II and III containing 5 % (*v/v*) Celluclast® 1.5L and 5 % (*v/v*) Palatase® 20000 L, respectively. The extraction procedure was carried out as follows. 15 g of minced peel or 5 g of lyophilized pulp were mixed with 40 and 30 mL,

respectively, of each extraction buffer, and mildly shaken for 8 h at different temperatures depending on the optimal working conditions of each buffer (Vergara-Barberán, 2014B) (buffer I, 25 ºC; buffer II, 55 ºC and buffer III, 30 ºC). Next, the homogenates were centrifuged at 10,000 rpm for 10 min and the supernatants of protein extracts from *Citrus* peel and pulp were used for further analysis.

A calibration curve up to 1 mg mL^{-1} of BSA was prepared for Bradford assay (Bradford, 1976). The procedure indicated in the Bradford assay Protein Quantitation Kit-Rapid (Fluka) was followed in order to measure sample protein content. A sample blank containing the corresponding buffer was also made in order to remove its contribution to the final sample absorbance.

For CGE, a proper volume of protein extract was taken to provide a final concentration comprised between 0.2 and 2 mg mL^{-1}. Then, this aliquot was mixed with 100 μL of sample buffer (0.1 M Tris–HCl pH 9.0, 1 % (w/v) SDS, and 1% (v/v) 2-mercaptoethanol). Next, this mixture was heated at 95 °C for 5 min and allowed to cool in a water bath for 5 min. Next, samples were analyzed per triplicate into the CE system. Method reproducibility was also evaluated by measuring the migration times of the three replicates of each sample.

10.2.4. Molecular masses determination and construction of LDA models

The molecular mass standard mixture solution was injected under the selected CGE conditions, and employed to determine the molecular masses of sample protein peaks. For this purpose, a calibration curve was obtained by plotting the logarithm of the standard protein molecular masses versus the t_{ref}/t_i ratio, where t_{ref} is the migration time of electroosmotic flow (EOF) peak (or reference peak) and t_i is the migration time of sample proteins. The

obtained calibration curve was described by the following regression equation: log MW = -2.980 (t_{ref}/t_i) + 2.609 (r = 0.9904).

After integrating protein peaks of all samples, LDA models were constructed. For this purpose, a data matrix using the areas of all protein peaks as original variables was constructed. To reduce the variability associated with sources of variance, as injected sample volume or sample preparation, the area of each peak was divided by each one of the areas of the other peaks, taking into account that each pair of peaks should be considered only once. These ratios were used as predictor variables. Next, using these variables, LDA models able to distinguish *Citrus* fruits according to their cultivar were constructed using SPSS (v. 15.0, Statistical Package for the Social Sciences, Chicago, IL). LDA, a supervised technique for data classification, could be used to distinguish samples of unknown origin, having a set of cases whose sample origin is known *a priori.* In order to select the variables to be included in the model, the Wilks' lambda (λ_w) criterion was used (Vandeginste, 1998). This criterion maximizes the distance between classes and minimizes the distance between the objects for each class. In this work, the stepwise algorithm was used to select the predictors that will be included in the LDA models (Vergara-Barberán, 2014B), being the probability values adopted for variable inclusion (F_{in}) or removal (F_{out}) of 0.05 and 0.10, respectively.

10.3. Results and discussion

10.3.1. Comparison of the different protein extraction buffers

In order to maximize the amount of extracted proteins from *Citrus* peel and pulp, different protein extraction buffers were compared (native, cellulose- and lipase -assisted buffers), using a tangerine sample from Clemenpons cultivar. These enzyme-assisted buffers have been previously employed by our research group (Vergara-Barberán, 2014A; Vergara-Barberán, 2015) and it

was demonstrated that they improved protein extraction from olive leaf, pulp and stone. The enzymes employed in this study (cellulase and lipase) were selected taking into account the sample tissues, since the function of these enzymes is to hydrolyze the mesocarp tissue structure. Thus, and taking into account the satisfactory results previously obtained (Vergara-Barberán, 2014A; Vergara-Barberán, 2015), after optimization of buffer compositions, the extraction efficiencies of these buffers (II and III) were compared to the efficiency provided by the native buffer (I), which was largely employed in literature (Fasoli, 2013; Esteve, 2011; Lerma-García, 2014; Lerma-García, 2016). In order to verify the extraction efficiency of the three buffers, the Bradford protein assay was used. The results obtained for both, peel and pulp samples, are shown in **Table 10.2**.

Table 10.2

Total protein content (mg/g) of the peel and pulp of Clemenpons tangerine obtained using different extraction buffers.

	Extraction buffer	**Protein content (mg/g) (n=6)**
Peel	I (native)	0.34
	II (5% (v/v) Celluclast® 1.5L)	5.45
	III (5% (v/v) Palatase® 20000 L)	0.50
Pulp	I (native)	1.09
	II (5% (v/v) Celluclast® 1.5L)	0.06
	III (5% (v/v) Palatase® 20000 L)	1.67

For peel protein extracts, the buffer II (containing 5% (*v/v*) Celluclast® 1.5L) provided the highest protein content (5.45 mg/g) compared with the other two buffers (0.34 and 0.50 for buffer I and III, respectively). Taking into account that one of the major components in cell walls is fibre (Figuerola, 2005), the use of cellulase enzyme allows the extraction of a high amount of components from peel; consequently, buffer II was selected for further studies.

On the other hand, for pulp protein extracts, the highest protein content (1.67 mg/g) was obtained with buffer III (5% (*v/v*) Palatase® 20000 L). This could be explained since in general, the pulp fruit contains a considerable content of lipids (Marx, 1997; Marx, 1998); thus, this buffer was chosen for pulp protein extraction of all samples.

10.3.2. Characterization of protein profiles of Citrus peel and pulp

After protein extraction of *Citrus* fruit samples (see **Table 10.1**) with their corresponding buffers, all protein extracts were subjected to SDS-CGE analysis. Illustrative electropherograms of peel and pulp extracts of a Navel orange and a Clemenpons tangerine are depicted in **Figure 10.1.**

A total of 14 common peaks were obtained in the peel extracts of all the cultivars studied (see **Figure 10.1A** and **10.1B**). The molecular masses of these peaks were determined using a molecular marker as above indicated (see **Section 10.2.4**). The molecular masses of the peel proteins were comprised between 20 (peak 1) to 56 kDa (peak 14), while the enzyme peak was found at 44 kDa. The molecular masses of the most abundant proteins for all orange peel samples analyzed were 24 (peak 5), 27 (peak 7) and 36 kDa (peak 10), while for tangerine peel samples were 24 (peak 5), 24.5 (peak 6), 27 (peak 7), 37 (peak 11) and 37.6 kDa (peak 12). The peak located at 24 kDa could be attributed to a germin-like protein (GLP), which is a major allergen in orange fruit (Crespo, 2006; Serra, 2013). In addition, the protein peaks found at 27 and 35 kDa have been previously identified as a manganese superoxide dismutase (Mn SOD) and as Cit S1, which is also a GLP (Crespo, 2006; Lliso, 2007).

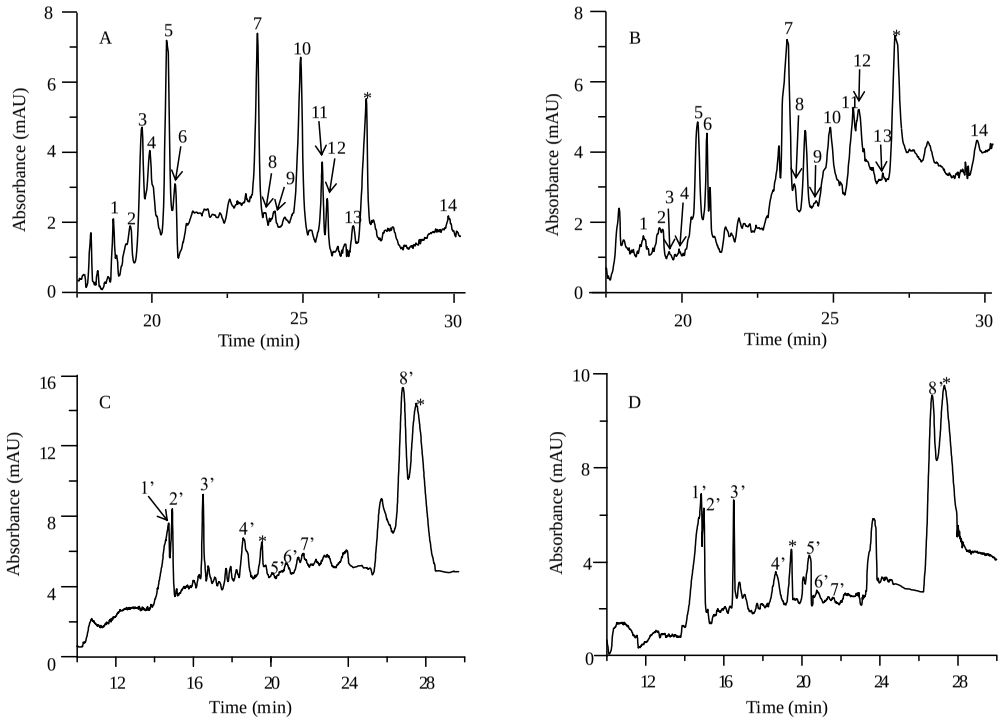

Figure 10.1. Electropherograms of Navel (A) and Clemenpons (B) peels, and Navel (C) and Clemenpons (D) pulps. Experimental conditions: electrokinetic injection at -30 kV for 7 s; separation voltage, −15 kV; temperature, 25 °C; detection wavelength, 214 nm. Enzyme peaks were labelled with an asterisk

For pulp extracts (**Figure 10.1C and 10.1D**), a total of 8 peaks were detected for all the cultivars studied. The range of molecular masses of these peaks was from 16 to 59 kDa, being the lipase enzyme identified at 31.6 and 59 kDa. The molecular masses of the most abundant proteins for all orange and tangerine pulp samples analyzed were 16 (peak 1), 16.8 (peak 2), 21.9 (peak 3) and 58.6 KDa (peak 8). According to Crespo *et al.* (Crespo, 2006), the peak at 16 kDa could be attributed to a profilin Cit s2, which has been described as a predominant IgE-binding protein in orange allergic children and adolescents. Moreover, the peak found at 21.9 could be a translationally controlled tumor protein, which appears to be a cytoplasmic calcium-binding protein, with a role in maintenance of Ca^{2+} homeostasis (Figuerola, 2005). Finally, the 58.6 kDa peak has been identified as an ATP synthase subunit (ATPase) (Lliso, 2007).

Next, precision of the method was evaluated by studying the intra- and interday reproducibilities of migration times of some proteins obtained by injecting the peel and pulp protein extracts of the Clemenpons sample three times per day during three days. The RSD values (see **Table 10.3**) were lower than 3.6% for peel, whereas for pulp samples the values were below 3.7%.

10.3.3. Variable normalization and construction of LDA models

Before proceeding with the construction of the LDA models, all the previously selected peaks, except the peaks that corresponded to the enzymes used to extract proteins, were considered as original variables. These variables were then normalized as previously indicated in section 2.4; thus, taking into consideration the 14 and 8 protein peaks identified for peel and pulp samples, respectively, a total of 91 ((14x13)/2) and 28 ((8x7)/2) non redundant peak ratios were obtained; then, these peak ratios will be used as predictor variables.

Next, using these predictor variables, two LDA models, one for peel and another for pulp samples, were constructed in order to distinguish the samples according to their cultivar. Then, two matrices were built using the 66 samples of **Table 10.1** and the corresponding number of predictor variables (91 for peel and 28 for pulp samples, respectively). A response variable, containing the 11 classes corresponding to the 11 cultivars of *Citrus* peel and pulps, was added to these matrices. Both matrices were next divided to obtain the training and evaluation sets, which were constituted by 55 objects (5 objects for each cultivar) and by 11 objects, respectively.

The constructed LDA model able to distinguish *Citrus* peel samples according to their cultivar is shown in **Figure 10.2.** For this model, the λ_w value obtained was 0.128, which agrees with the excellent resolution observed between all class pairs. The standardized coefficients of the discriminant functions found to construct the LDA model are given in **Table S.10.1** of supplementary material. As deduced from this table, the protein peak ratios that provided the highest discriminant capabilities corresponded to 1/5, 1/14 and 4/5 ratios. Using this model and leave-one-out validation, all the objects of the training set were correctly classified. Furthermore, all the objects of the evaluation set (labelled with crosses in **Figure 10.2**) were correctly assigned within a 95% probability level, which confirmed the satisfactory prediction capability of the model.

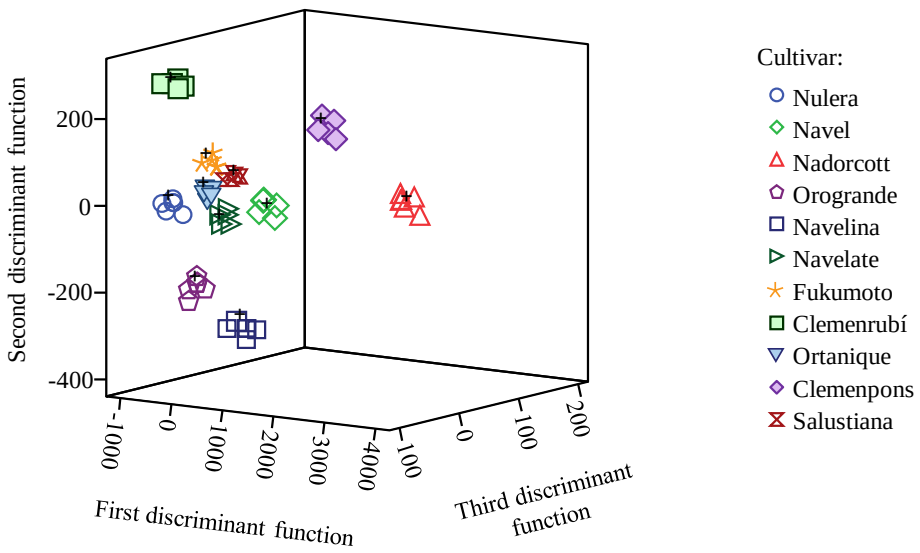

Figure 10.2. LDA score plot obtained by representing the three first discriminant functions on an oblique plane of the 3D space to differentiate *Citrus* peel samples in accordance to their cultivar. Evaluation set samples are labelled with a cross symbol.

Next, another LDA model was constructed to differentiate the *Citrus* pulp samples according to their cultivar. A 3D plot obtained by representing the three first discriminant functions obtained for this model is given in **Figure 10.3**. As it can be observed, a good resolution between all class pairs was also found (λ_w = 0.104). The standardized coefficients of the discriminant vectors of the LDA model are given in **Table S.10.2** of supplementary material. In this case, the protein peak ratios that provided the largest discriminant capabilities corresponded to 2'/6', 6'/8', 1'/6' and 5'/8' ratios. For this model, and using leave-one-out validation, all the objects of the training set were correctly classified. Finally, the evaluation set was used to check model prediction ability, providing an excellent classification of all the objects, with a prediction capability of 100%.

Table 10.3

Reproducibility of migration times obtained for *Citrus* peel and pulp proteins from Clemenpons cultivar.

Peel			Pulp		
Parameter[a]	**RSD[b] ,% (n=3)**	**RSD[c] ,% (n=9)**	**Parameter[a]**	**RSD[b] ,% (n=3)**	**RSD[c] ,% (n=9)**
t_{eof} (min)	1.8	2.9	t_{eof} (min)	1.8	2.3
t_5 (min)	2.0	3.4	$t_{2'}$ (min)	2.1	3.7
t_7 (min)	2.2	2.9	$t_{3'}$ (min)	1.9	2.4
t_{10} (min)	2.5	3.3	$t_{4'}$ (min)	2.6	3.1
t_{11} (min)	2.6	3.6	$t_{8'}$ (min)	2.7	2.2

[a] Migration times of protein number identified in **Figure 10.1** (traces A-B) and (traces C-D) for peel and pulp, respectively.

[b] Intra-day relative standard deviation (3 injections per day).

[c] Inter-day relative standard deviation, (3 injections per day during 3 days).

10.4. Conclusions

This work demonstrated that the use of an enzyme-assisted procedure is a feasible, fast and effective method to extract proteins from *Citrus* peel and pulp tissues. The resulting protein patterns gave a total of 14 and 8 common peaks for peel and pulp, respectively. After normalization of these peak areas, two LDA models have been constructed. All the samples studied in this work, arising from different Spanish regions, were correctly assigned with very good resolution. This study demonstrated that protein profiles represent an excellent tool to discriminate among different classes of *Citrus* fruits (peel and pulp from orange and tangerine samples), being these profiles distinctive of each cultivar.

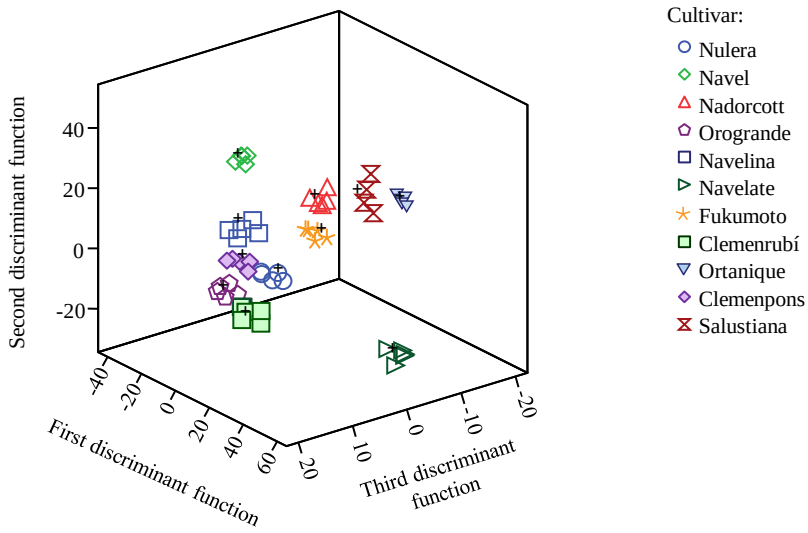

Figure 10.3. LDA score plot obtained by representing the three first discriminant functions on an oblique plane of the 3D space to distinguish *Citrus* pulp samples in accordance to their cultivar. Evaluation set samples are labelled with a cross symbol.

Acknowledgements

Work financed by MINECO of Spain and FEDER (ref. CTQ2014-52765-R). M. Vergara-Barberán acknowledge her PhD FPU grant granted by the MEC of Spain, while M.J. Lerma-García thanks her VALi+d postdoctoral contract granted by the Generalitat Valenciana. The support of Novozymes (Spain) and Fontestad S.A (Museros, Valencia, Spain) is also acknowledged.

10.5. References

Bradford, M.M. (**1976**). A rapid and sensitive method for the quantitation of microgram quantities of protein utilizing the principle of protein–dye binding. *Analytical Biochemistry*, *72*, 248-254.

Cieslik, E.; Greda, A.; Adamus, W. (**2006**). Contents of polyphenols in fruit and vegetables. *Food Chemistry*, *94*, 135-142.

Crespo, J.F.; Retzek, M.; Foetisch, K.; Sierra-Maestro, E.; Cid-Sanchez, A.B.; Pascual, C.Y.; Conti, A.; Feliu, A. (**2006**). Germin-like protein Cit s 1 and profilin Cit s 2 are major allergens in orange (*Citrus sinensis*) fruits. *Molecular Nutrition & Food Research*, *50*, 282-290.

Esteve, C.; Del Río, C.; Marina, M.L.; García, M.C. (**2011**). Development of an ultra-high performance liquid chromatography analytical methodology for the profiling of olive (*Olea europaea L.)* pulp proteins. *Analytica Chimica Acta*, *690*, 129-134.

Fasoli, E.; Righetti, P.G. (**2013**). The peel and pulp of mango fruit: A proteomic samba. *Biochimica et Biophysica Acta*, *1834*, 2539-2545.

FAO. (**2010**). Food and Agriculture Organization of the United Nations. URL http://www.fao.org/docrep/006/y5143e/y5143e12.htm

Figuerola, F.; Hurtado, M.L.; Estevez, A.M.; Chiffelle, I.; Asenjo, F. (**2005**). Fibre concentrates from apple pomace and citrus peel as potential fibre sources for food enrichment. *Food Chemistry*, *91*, 395-401.

Goodner, K.L.; Rouseff, R.L.; Hofsommer, H.J. (**2001**). Orange, mandarin, and hybrid classification using multivariate statistics based on carotenoid profiles. *Journal of Agriculture and Food Chemistry*, *49*, 1146-1150.

Kawaii, S.; Tomono, Y.; Katase, E.; Ogawua, K.; Yano M. (**1999**). Quantitation of flavonoid constituents in *Citrus* fruits. *Journal of Agriculture and Food Chemistry, 47*, 3565-3571.

Khan, M.K.; Abert-Vian, M.; Fabiano-Tixier, A.S.; Dangles, O.; Chemat, F. (**2010**). Ultrasound-assisted extraction of polyphenols (flavanone glycosides) from orange (*Citrus sinensis L.*) peel. *Food Chemistry, 119*, 851-858.

Klavons, J.A.; Bennett, R.D.; Vannier S.H. (**1991**). Nature of the protein constituent of commercial orange juice cloud. *Journal of Agriculture and Food Chemistry*, *9*, 1545-1548.

Lerma-García, M.J.; D'Amato, A.; Simó-Alfonso, E.F.; Righetti, P.G.; Fasoli, E. (**2016**). Orange proteomic fingerprinting: From fruit to commercial juices. *Food Chemistry*, *196*, 739-749.

Lerma-García, M.J.; D'Amato, A.; Fasoli, E.; Simó-Alfonso, E.F.; Righetti P.G. (**2014**). According to the CPLL proteome sheriffs, not all aperitifs are created equal! *Biochimica et Biophysica Acta*, *1844*, 1493-1499.

Lliso, I.; Tadeo, F.R.; Phinney, B.S; Wilkerson, C.G; Talón, M. (**2007**). Protein changes in the albedo of *Citrus* fruits on postharvesting storage. *Journal of Agriculture and Food Chemistry, 55*, 9047-9053.

Marx, F.; Andrade, E.H.A.; Maia, J.G. (**1997**). Chemical composition of the fruit pulp of *Caryocar villosum*. *Z Lebensm Unters Forsch A, 204*, 442-444.

Marx, F.; Andrade, E.H.A.; Maia, J.G. (**1998**). Chemical composition of the fruit of *Solanum sessiliflorum*. *Z Lebensm Unters Forsch A, 206*, 364-366.

Montealegre, C.; Marina, M.L.; Ruiz, C.G. (**2010**). Separation of proteins from olive oil by CE: An approximation to the differentiation of monovarietal olive oils. *Electrophoresis, 31,* 2218-2225.

Moulya, P.P.; Gaydoub, E.M.; Corsettia, J. (**1999**). Determination of the geographical origin of Valencia orange juice using carotenoid liquid chromatographic profiles. *Journal of Chromatography A, 844,* 149-159.

Saravanan, R.S.; Rose, J.K.C. (**2004**). A critical evaluation of sample extraction techniques for enhanced proteomic analysis of recalcitrant plant tissues. *Proteomics*, *4*, 2522-2532.

Sari, Y.W.; Bruins, M.E.; Sanders, J.P.M. (**2013**). Enzyme assisted protein extraction from rapeseed, soybean, and microalgae meals. *Industrial Crops and Products*, *43*, 78- 83.

Sebastián-Francisco, I.; Simó-Alfonso, E.F.; Mongay-Fernández, C.; Ramis-Ramos, G. (**2004**). Improvement of the electrophoretic protein profiles of *Leguminosae* gum extracts using gamanase and application to the evaluation of carob–guar mixtures. *Analytica Chimica Acta, 508,* 135-140.

Serra, I.A.; Bernardo, L.; Spadafora, A.; Faccioli, P.; Canton, C.; Mazzuca, S. (**2013**). The *Citrus* clementina putative allergens: from proteomic analysis to structural features. *Journal of Agriculture and Food Chemistry*, *61*, 8949-8958.

Shen, L.; Wang, X.; Wang, Z.; Wua, Y.; Chen, J. (**2008**). Studies on tea protein extraction using alkaline and enzyme methods. *Food Chemistry*, *107*, 929-938.

Vandeginste, B.G.M.; Massart, D.L.; Buydens, L.M.C.; De Jong, S.; Lewi, P.J.; Smeyers-Verbeke, J. (**1998**). Data handling in science and technology Part B, Elsevier, Amsterdam.

Vergara-Barberán, M.; Lerma-García, M.J.; Herrero-Martínez, J.M.; Simó-Alfonso E.F. (**2014A**). Efficient extraction of olive pulp and stone proteins by using an enzyme-assisted method. *Journal of Food Science, 79,* 1298-1304.

Vergara-Barberán, M.; Lerma-García, M.J.; Herrero-Martínez, J.M.; Simó-Alfonso, E.F. (**2014B**). Classification of olive leaves and pulps according to their cultivar by using protein profiles established by capillary gel electrophoresis. *Analytical and Bioanalytical Chemistry, 406,* 1731-1738.

Vergara-Barberán, M.; Lerma-García, M.J.; Herrero-Martínez, J.M.; Simó-Alfonso, E.F. (**2014C**). Use of protein profiles established by CZE to predict the cultivar of olive leaves and pulps. *Electrophoresis, 35,* 1652-1659.

Vergara-Barberán, M.; Lerma-García, M.J.; Herrero-Martínez, J.M.; Simó-Alfonso E.F. (**2015**). Use of an enzyme-assisted method to improve protein extraction from olive leaves. *Food Chemistry, 169,* 28-33.

Wang, L.; Liu, H.; Liu, L.; Wang, Q.; Li, Q.; Du, Y.; Zhang, J. (**2014**). Protein contents in different peanut varieties and their relationship to gel property. *International Journal of Food Properties, 17,* 1560-1576.

Zukas, A.A.; Breksa, A.P. (**2005**). Extraction methods for analysis of *Citrus* leaf proteins by two-dimensional gel electrophoresis. *Journal of Chromatography A, 1078,* 201-205.

Table S.10.1

Standardized coefficients of the predictors selected by the LDA model constructed to discriminate *Citrus* peel samples in accordance to their cultivar.

Predictors[a]	f_1	f_2	f_3	f_4	f_5	f_6	f_7	f_8	f_9	f_{10}
1/5	30.51	-3.43	-2.13	-0.35	-0.39	-0.15	-0.71	-0.16	-0.24	-0.06
1/14	-14.19	25.62	8.19	-2.20	2.19	-1.82	0.14	0.79	1.41	0.50
2/6	9.31	-13.25	4.64	-2.59	-0.51	0.74	0.51	1.19	-0.01	0.04
2/12	-9.84	13.18	-3.40	2.92	0.51	-0.99	-1.28	-0.79	0.30	-0.29
3/7	0.03	0.15	4.52	3.41	1.14	1.98	3.76	0.91	0.66	0.21
3/12	-0.71	0.72	2.09	0.66	-0.14	0.69	0.25	2.48	-1.25	-0.16
4/5	11.69	28.19	-6.59	-0.03	1.87	0.49	1.21	1.93	1.45	0.17
4/12	-3.24	2.85	-1.05	0.72	-0.47	-0.61	-1.43	-0.54	-0.01	-0.47
4/14	2.79	-5.08	-2.36	2.12	-0.70	1.15	-0.32	0.40	0.12	0.10
5/7	-1.61	3.06	-7.52	-0.79	0.30	0.35	0.71	0.91	0.17	-0.05
6/7	0.81	5.15	20.43	-0.47	-0.21	0.04	1.87	-0.71	-0.24	0.58
6/12	9.04	-17.85	-0.90	-0.20	0.72	-0.83	-0.26	-0.45	0.52	0.05
6/14	2.83	-10.63	-6.39	3.03	0.12	0.91	-0.37	1.08	-0.70	-1.16
7/9	-0.61	-0.06	0.91	-0.65	1.10	0.65	0.12	0.18	0.06	0.09
7/12	-2.87	5.72	2.87	1.33	0.22	1.06	2.12	2.42	-0.74	0.61

[a] Ratios of protein peak areas.

Table S.10.2

Standardized coefficients of the predictors selected by the LDA model constructed to discriminate *Citrus* pulp samples in accordance to their cultivar.

Predictors[a]	f_1	f_2	f_3	f_4	f_5	f_6	f_7	f_8	f_9	f_{10}
1’/2’	6.70	10.54	3.68	0.21	0.23	0.32	0.48	0.45	-0.32	-0.49
1’/5’	-10.91	-4.31	-1.59	4.01	-0.43	0.60	0.66	0.51	0.08	-0.46
1’/6’	-14.30	-12.98	10.32	5.21	-1.84	6.05	1.67	0.47	-0.79	0.65
1’/8’	7.21	0.85	-8.94	1.41	1.67	-2.33	-1.68	-0.88	1.27	-0.03
2’/6’	21.77	15.98	-10.33	-8.26	1.40	-5.51	-1.22	-0.80	0.53	-0.36
2’/8’	-5.62	-0.58	10.12	-1.27	-1.95	3.80	1.56	0.86	-1.22	0.32
3’/6’	-4.05	-3.84	8.24	-0.73	3.10	0.65	0.42	1.09	0.72	0.26
3’/7’	1.48	0.20	2.62	-0.95	-0.80	0.91	-0.93	0.30	0.13	0.03
3’/8’	6.61	6.16	-3.25	0.37	-2.82	-3.35	0.12	-2.01	0.70	-0.15
4’/8’	1.25	-10.12	4.39	-1.21	1.01	2.37	0.86	1.30	-1.13	-0.04
5’/8’	-12.81	8.11	-14.67	6.68	-2.84	-0.19	-0.53	0.64	0.35	-0.18
6’/8’	19.31	5.12	15.96	-5.63	4.14	-0.48	0.08	-1.28	0.60	0.61
7’/8’	-6.27	2.32	-2.37	1.38	-0.31	0.87	-1.07	1.62	-0.64	0.04

[a] Ratios of protein peak areas.

II.C. Application of CPLLs to mistletoe characterization

Chapter 11. Proteomic fingerprinting of Mistletoe (*Viscum Album L*) via combinatorial peptide ligand libraries and mass spectrometry analysis

JOURNAL OF PROTEOMICS
An official journal of the European Proteomics Association (EuPA)

Proteomic fingerprinting of Mistletoe (*Viscum Album L)* via combinatorial peptide ligand libraries and mass spectrometry analysis[1]

María Vergara-Barberán[a], María Jesús Lerma-García[a], Maria Nicoletti[b], Ernesto Francisco Simó-Alfonso[a], José Manuel Herrero-Martínez[a], Elisa Fasoli*[b], Pier Giorgio Righetti[b]

a Department of Analytical Chemistry, University of Valencia, C. Doctor Moliner 50, E-46100 Burjassot, Valencia, Spain
b Department of Chemistry, Materials and Chemical Engineering "Giulio Natta", Politecnico di Milano, 20131 Milan, Italy

[1] State: Accepted

CPLLs, coupled to MS analysis, have been used to investigate in depth the proteome of *Viscum album L*. (VA), commonly named European mistletoe, in order to provide a first proteomic fingerprinting. For this purpose, the proteins were captured via CPLLs at two different pH values (acidic and neutral). A total of 648 non-redundant proteins were identified by using two different databases. The two pH values, chosen for bead incubations, have contributed to increment the capture ability: 56% and 31% of CPLLs species were respectively recognized at pH 7.2 and at pH 2.2. Finally the biological function of identified proteins was evaluated in order to understand their role on human health and the potential benefits of mistletoe extracts in medicine.

Keywords: European mistletoe; proteomic fingerprinting; combinatorial peptide ligand library; mass spectrometry

11.1. Introduction

Mistletoe is defined as a "hemiparasite" because as a parasitic plant, it grows on the branches or trunk of a tree but it is also capable of growing on its own. The name mistletoe originally referred to the species *Viscum album L.* (VA), a European mistletoe belonging to *Santalaceae* family in the order *Santalales* native to Great Britain and much of Europe. However, a different species, *Viscum cruciatum*, occurs in Southwest Spain and Southern Portugal, as well as North Africa, Australia and Asia. Extracts of VA have been used in traditional medicine for treatment of jaundice, indigestion, common fever and asthma (Arndt, 2000). Recently, some biological activities of mistletoe preparations were investigated, such as anticancer function (Bock, 2014), probably due to induction of tumor cell death (Kienle, 2003) and to exertion of direct necrotic effects or apoptosis (Podlech, 2012). For this reason, VA extracts have been tested in clinical trials (Kienle, 2003) as supporting medicine for cancer therapy, improving patients' survival (Osterman, 2009; Singh, 2016) and increasing their quality of life (Melzer, 2009; Troger, 2014). Despite the development of individualized medicine, chemotherapy and surgery remain the preferred choice especially for advanced malignancies (Jackson, 2015) For this reason, the possible additive antitumor activity of VA extracts with a chemotherapy drug, doxorubicin, was recently investigated, demonstrating an increase of drug antileukemic effectiveness (Srdic, 2016). Furthermore, recent literature has showed that VA modulates immune system and exerts immune-adjuvant activities, influencing tumor regression (Sha, 2016).

Although the knowledge of VA medical effects is increasing, the role of its components is still unclear. The mistletoe plant contains many kinds of metabolites like several pentacyclic triterpenes, among them oleanolic acid, betulinic acid, ursolic acid and lupeol (Krzaczek, 1997; Urek, 2005), flavonoids, long-chain fatty acids and hydrocarbons as well as trace amounts

of volatile components including loliolide and vomifoliol (Cebovic, 2008). Due to their insolubility in water, these compounds are not present in significant amounts in aqueous mistletoe extracts (Jager, 2007); however, they have exhibited anti-angiogenic activities (Delebinski, 2012A; Delebinski, 2012B; Struh, 2012; Struh, 2013) and pro-inflammatory and anti-apoptotic effects (Weissentein, 2012). Moreover VA extracts, often used as adjuvant in cancer therapy, contain several hydrophilic bioactive compounds like lectins (Wacker, 2004; Khil, 2007), viscotoxins, oligosaccharides and polysaccharides (Bussing, 2000; Arda, 2003).

Although mistletoes have been shown to have other pharmacological activities, including nervine, hypertensive (Poruthukaren, 2014), cardiac depressant, hypolipidemic action (Kim, 2014), vasodilator and relaxant effects, as yet no studies have explored the entire proteome of *VA*. In the present research, a deep investigation on proteins, extracted from *Viscum album L.* leaves, has been performed by the application of CPLLs technology, coupled to MS analysis, in order to enlarge the identification of the VA proteome. The related biological functions, in order to understand the biomedical role of proteomic profiling on human health, have been also evaluated.

11.2. Materials and methods

11.2.1. Chemicals and biologicals

ProteoMiner™ (combinatorial hexapeptide ligand library beads, PM), Laemmli buffer, 40% acrylamide/bis solution, TEMED, molecular mass standards (Precision Plus Protein Standard) and electrophoresis apparatus for one-dimensional electrophoresis were from Bio-Rad Laboratories (Hercules CA). β-mercaptoethanol, ammonium persulphate, ACN, trifluoroacetic acid (TFA), SDS, dithiothreitol (DTT), APS, MeOH, ammonium bicarbonate

(AmBic), formic acid (FA) and all other chemicals used all along the experimental work were pure analytical grade products and purchased from Sigma-Aldrich (St Louis, MO). Complete protease inhibitor cocktail tablets and sequencing grade trypsin were from Roche Diagnostics, (Basel, CH).

11.2.2. Extraction of mistletoe proteins

Mistletoe (*Viscum album L.)* growing on host tree, called *Pinus nigra*, located in El Toro (Castellón de la Plana, Spain, UTM coordinates: X= 692600 and Y= 4422700) was collected in January 2015. The green parts (leaves) were selected and washed with water to eliminate bacterial and surface contamination from human hands. The age of mistletoe was estimated by counting the total number of nodes (or branch nodes) on the longest stem of mistletoe. In our case, a large number of node branches was found, being 10-year-old mistletoe. Then, the green parts were sliced and transferred to a mortar and frozen in liquid nitrogen. The frozen material was ground to a fine powder in a pre-cooled mortar and pestle and then this powder was homogenized. The protein extraction protocol was adapted from Olsner *et al*. (Olsnes, 1982). Briefly, 10 g of powdered mistletoe were solubilized in 10 volumes of 10 mM Tris-HCl at pH 8.3, containing 100 mM lactose in order to avoid the interaction among carbohydrate components in the homogenate. The addition of lactose was considered as the best compromise considering the diversity of sugar specificity of lectins (galactose and N-acetyl-D-galactosamine) (Olsnes, 1982). Next, the suspension was mildly shaken at 4ºC overnight. To study the whole proteome of mistletoe, 5 mL of this protein extract were diluted with 45 mL of a buffer containing 50 mM Tris-HCl at pH 7.2 and 50 mM NaCl.

Prior to capture with CPLLs, the extract was centrifuged at 18,000 rpm for 10 min to isolate the clarified protein solution from the insoluble residue, *ca.* 40 mL of mistletoe solution being thus recovered. Two biological replicas

were performed. To determine the protein concentration, a Bio-Rad DC Protein Assay was performed in mistletoe extract. It was a colorimetric assay based on Lowry assay where proteins create complexes with copper in alkaline medium able to reduce the Folin reagent, producing a blue color, proportional to protein concentration, with maximum absorbance at 750 nm. This extract was divided into two fractions (20 mL each containing 28.8 mg of proteins), one of which was maintained at pH 7.2, whereas the other was adjusted at pH 2.2 by adding FA and 0.1 % TFA. To all mentioned aliquots, 30 µL of ProteoMiner (CPLL) bead volume were added and protein capture was carried out via gentle shaking overnight at room temperature; then the beads were collected by filtration and washed with the appropriate extraction buffer.

The captured proteins from the peptide library were desorbed twice (each time with 30 µL) by washing with a boiling solution composed of 4% SDS and 20mM DTT for 15 min (Candiano, 2009). The entire eluates (60 µL each) and 50 µL of mistletoe extract (untreated by CPLLs), were precipitated with MeOH/chloroform as follows: to one volume of protein solution, 4 volumes of cold MeOH were added, mixed and kept at 4 °C for 5 min. One volume of chloroform and 3 volumes of water were added, mixed and centrifuged at 14,000 rpm for 15 min. The supernatant was rejected and the pellet was washed twice with cold MeOH and finally centrifuged at 14,000 rpm for 5 min. The obtained pellet was dissolved in 20 µL of Laemmli buffer for SDS-PAGE (which was performed according to Candiano *et al*.(Candiano, 2009).

12.2.3. SDS-PAGE analysis

The three pellets obtained in the previous step (one for control and the others for eluates at pH 2.2 and 7.2), which were disoolved in 20 uL of Laemmli buffer, were loaded onto an SDS-PAGE gel. The gel was composed by a 4% polyacrylamide stacking gel (125 mM Tris–HCl, pH 6.8, 0.1%, m/v,

SDS) and a 12% resolving polyacrylamide gel (in 375 mM Tris–HCl, pH 8.8, 0.1%, m/v, SDS buffer). A Tris-glycine buffer at pH 8.3 (with 0.1% SDS, m/v) was employed to fill the cathode, whereas a Tris buffer at pH 8.8 was used in the anode. Electrophoresis was set at 100 V until the dye front reached the bottom of the gel. Staining and destaining were performed with Colloidal Coomassie Blue and 7% (v/v) acetic acid in water, respectively (Candiano, 2009). Finally, the SDS-PAGE gels were scanned with a VersaDoc imaging system (Bio-Rad).

12.2.4. Mass spectrometry and data analysis

All sample bands obtained by SDS-PAGE were cut out and destained by washing with ACN and 50 mM ammonium bicarbonate (AmBic) at 56 ºC (Shevchenko, 2007). Afterwards, the gel pieces were reduced and alkylated with 1.5 mg/mL DTT (in 50 mM AmBic) at 56 ºC and 10 mg/mL iodoacetamide (in 50 mM AmBic) at room temperature, respectively. Finally, proteins were digested with 0.02 µg/µL trypsin (in 25 mM AmBic) at 37 ºC overnight. The tryptic mixtures were acidified with FA up to a final concentration of 10%. Eight microliters of trypsin digested sample was injected on a reversed phase trap column (Acclaim PepMap100, C18, 100 Å, 5 µm, 100 µm ID × 2 cm length, Thermo Scientific) for peptide clean-up and preconcentration. After clean-up, the trap column was placed in series with a fused silica reverse-phase column (pico Frit column, C18 HALO, 90 Å, 75 µm ID, 2.7 µm, 10.5 cm length, New Objective). Separations were performed using a nano chromatographic system (UltiMate 3000 RSLCnano System, Thermo Scientific) at a constant flow rate of 300 nL/min with a gradient from 4% buffer A (2% ACN and 0.1% FA in water) to 96% buffer B (2% water and 0.1% FA in ACN) in 60 min.

The eluting peptides were on-line sprayed in a LTQ XL mass spectrometer (Thermo Scientific). Full scan mass spectra were collected in the linear ion

trap in the mass range *m/z* 350 to *m/z* 1800 Da and the 5 most intense ions were selected and fragmented in the ion trap. Target ions already selected for fragmentation were dynamically excluded for 30 s.

The MS data were analyzed by the Mascot search engine (Version 2.3.01); using the Proteome Discoverer software (v. 1.2.0 Thermo) and consulting Uniprot_*Viridiplantae* (30264 sequences, 184678199 residues) and *Santatales* databases (1261 sequences, 411601 residues), all databases were downloaded by UniProtKB/Swiss-Prot web site (www.uniprot.org). Oxidation of methionine residues was set as variable modifications; one missed cleavages were allowed to trypsin; peptide mass tolerance was set to 1 Da, fragment mass tolerance to 0.8 Da, and an ion source cut-off of 20 was chosen. The false discovery rate obtained by Proteome Discoverer, consulting the Mascot decoy database, was less than 1%. MS analysis was performed in biological duplicates, obtained by two different extraction performed in the same experimental conditions. For each biological sample, three technical MS runs were carried out. All recorded raw.file of technical replicates were used to generate one single mgf.file useful for a final search by Mascot.

11.3. Results

The SDS-PAGE profiles of Mistletoe extracts, characterized by control (untreated sample) and two eluates from CPLLs beads after capture at pH 2.2 and 7.2 are depicted in **Figure 11.1**. The protein profiles in the original extract (Ctrl) and in the eluate at pH 2.2 were considerably similar, showing intense protein bands distributed along the 10 and 50 kDa regions, whereas in eluate at pH 7.2 only few bands were resolved after electrophoresis run. As typical of in vegetal samples, a streaking in the lower Mr region was observed, due to the presence of tannins and polyphenols and other plant polymers not completely eliminated during the protein extraction. All lanes were excised in segments as shown by numbers on red lines across the gel, digested by trypsin

and subjected to MS analysis in order to evaluate the different protein composition before and after CPLLs treatment.

For this reason, in **Figure 11.2A**, a Venn diagram was constructed to investigate the role of CPLLs in the discovery of mistletoe's proteome. A total of 648 non-redundant proteins were identified in the Mistletoe extracts using Uniprot *Viridiplantae*: 295 were found only in untreated sample and 257 were present in both CPLLs eluates, while 96 were commonly recognized in both samples. These identification number derives considering both biological replicate, 238 and 234 unique gene products respectively were identified in control and both eluates of first replica, 186 and 224 in control and both eluates of the second one. In order to evaluate the biological role of total identified proteins (648), a Gene Ontology (GO) analysis was performed using the web available software QuickGO (www.ebi.ac.uk/QuickGO) (**Figure 11.2B**). The proteins, found in both untreated sample and CPLLs eluates, belonged to similar cellular components like chloroplast, nucleus and plastid.

Furthermore, a second Venn diagram has compared the MS identifications obtained from CPLLs incubations at different pH values (**Figure 11.3A**): the CPLLs treatment at pH 7.2 captured 196 specific proteins, while 109 species were found only after CPLL's incubation at pH 2.2. The predicted molecular functions of eluted proteins are shown in the histogram reported in **Figure 11.3B**.

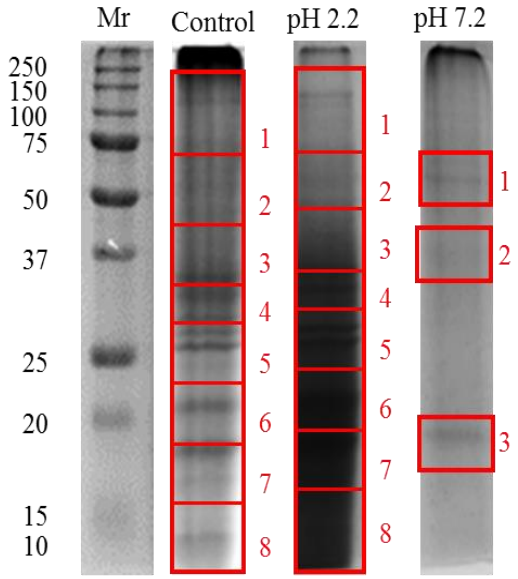

Figure 11.1. SDS-PAGE profiling of an untreated sample of Mistletoe (Ctrl) and of two eluates from CPLLs capture, labelled pH 2.2 and pH 7.2. Mr: molecular mass ladder. Staining with micellar Coomassie blue. The numbered bands were excised, digested by trypsin, and analyzed by nano-LC–MS/MS.

Finally, the MS spectra were matched with Uniprot_*Santalales* database with a more restricted taxonomy referred to mistletoe. In this case, 16 and 23 species were identified in eluates of CPLLs incubated at pH 2.2 and pH 7.2 respectively (**Tables 11.1** and **11.2**).

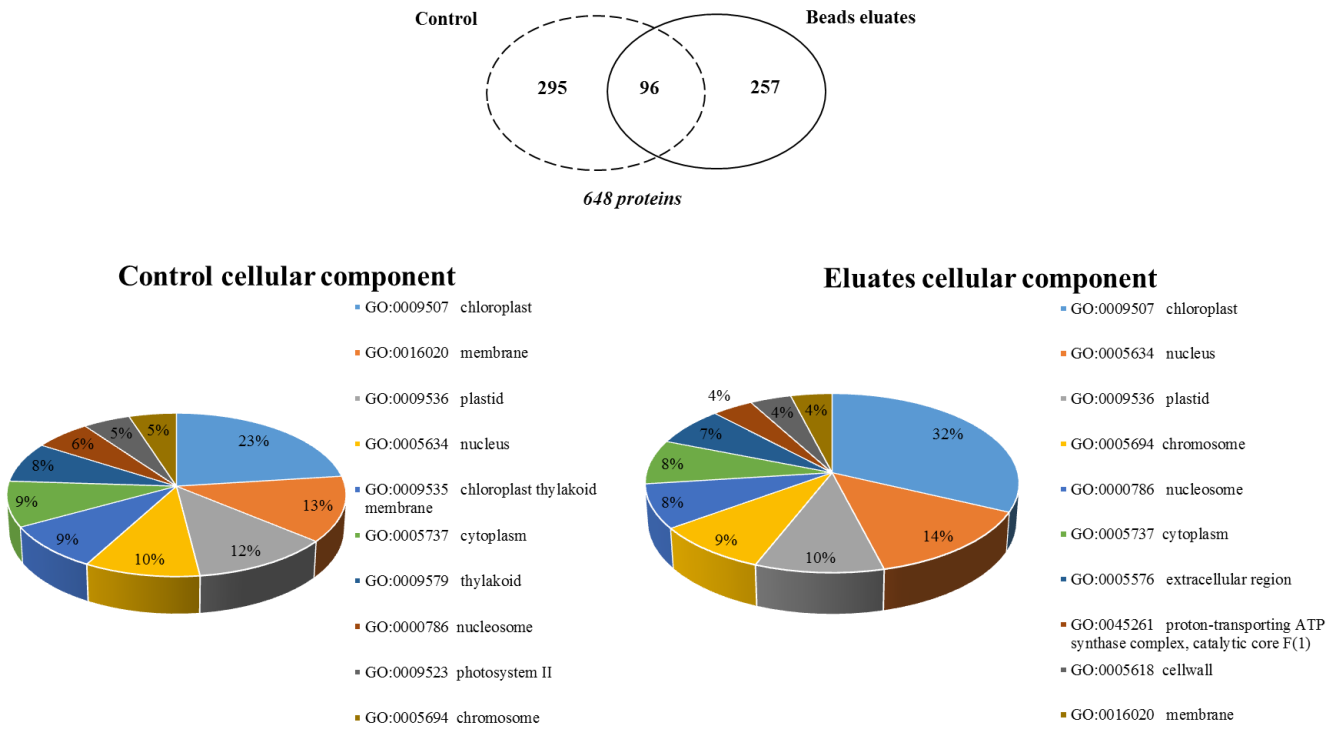

Figure 11. 2. A) Venn diagram of the total proteins identified in mistletoe: untreated sample (Crtl) and in the two combined eluates from the pH 2.2 and 7.2 captures. B) Pie chart of cellular component classification of the 648 unique gene products described in mistletoe.

11.4. Discussion

The principal aim of this research was to increase the knowledge on VA proteome in order to understand the benefits of mistletoe extracts in medicine and to evaluate the potential role in human health (Konopa, 1980; Woynarowski, 1980; Kuttan, 1988; Jung, 1990). Therefore the CPLLs methodology was adopted to identify low and very-low abundance proteins (LAPs): CPLLs are commonly used to reduce the dynamic protein range concentration by concomitantly decreasing the concentration of high-abundance proteins while increasing the trace ones (Righetti, 2015). In order to figure out the best conditions for proteins capture, two pH values were tested considering that pH can affect the interactions between hexapeptides bound to beads and their respective protein partner (Fasoli, 2010; Saez, 2013). The chosen pH values, acidic pH (2.2) and neutral pH (7.2), have increased the ability of the CPLLs to capture proteins, which were finally identified using two different databases. The most general Uniprot_*Viridiplantae*, referred to all green plants, has generated the global list of identifications referred to both biological replicates, respectively named Supplementary Table 11.1 and Supplementary Table 11.2. Among the 648 total recognized proteins, 96 were present in both control and CPLL eluates, while 257 were specifically captured by CPLLs, thus demonstrating the capacity to enrich by more than 39% the number of total identifications (**Figure 11.2A**).

Although the identified species mostly populated the same cellular components in both control and CPLLs eluates, the CPLLs treatment has increased the percentage of species present in the extracellular region and in plant cell wall, important not only to provide cellular support but also to regulate intracellular communication and cellular growth (**Figure 11.2B**). The protein composition of extracellular matrix is important in the comprehension of potential cytotoxic effects of mistletoe extracts and for this reason the CPLLs technology could be useful to investigate the VA synergistic antitumor

action (Marvibaigi, 2014). The highest percentage of identified proteins belongs to the chloroplast. Most of them, like D2XUU_CAPAN, F2VPP4_SOLNI and A3QSS2_MARPO, are involved in different steps of photosynthetic process with specific functions. A considerable percentage of proteins, belonging to nucleosome, was due to the identification of high number of histones in eluates, such as P25469/H2A1_SOLLC, B3SGL7/B3SGL7_MEDTR, Q6V9/H4_SOLCH and Q43566_NARPS. Although their role in regulating gene expression is well-known in all eukaryotes, their presence in plants may have important DNA-independent function like the determination of cell shape and growth (Over, 2014).

In order to understand the contribution of CPLLs in the discovery of VA proteome, the Venn diagram of **Figure 11.3A** shows total CPLLs captures of both biological replicates at the two pH values: 196 species were specific for pH 7.2 (56% of total identifications), 109 proteins were found at pH 2.2 (31% of total identifications) and the remaining 48 identifications were present in both eluates (13% of total identifications). The diversity on numbers of identified species reflected peculiar molecular functions as described in the graph of **Figure 11.3B**, demonstrating that both CPLL incubations have permitted a deeper proteome investigation than the traditional protocol. While incubation at pH 2.2 has enriched proteins able to bind DNA or metal ions, and characterized by peroxidase activity, the capture at pH 7.2 was specific for species with oxidoreductase, catalytic and nucleotide-binding activities.

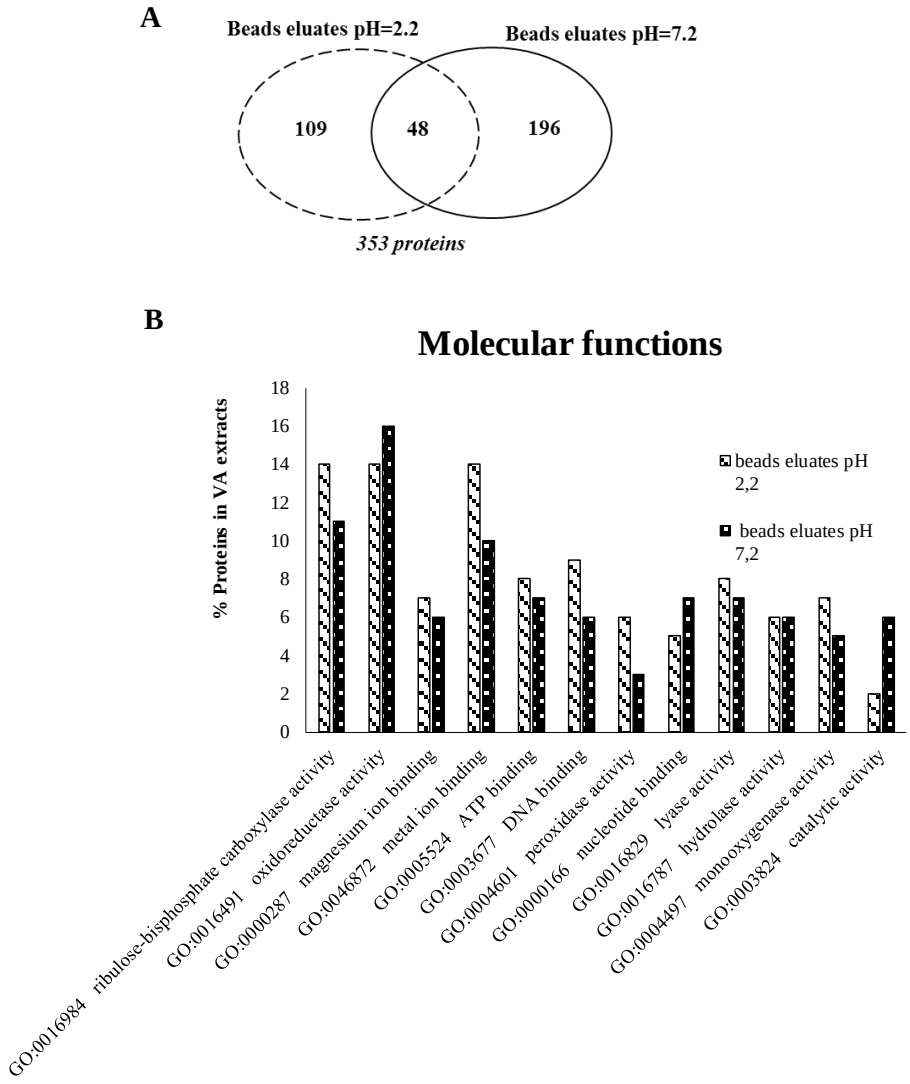

Figure 11.3. Venn diagram of CPLL captured proteins at pH 2.2 vs. and CPLL captured proteins at pH 7.2. B) Histogram of predicted molecular functions of the eluted proteins, drawn after Gene ontology analysis.

Table 11.1

Proteins identified in Mistletoe after CPLLs treatment at pH 2.2

Prot. Number	Accession Number	Protein Name	Mascot Score	Mr	N° peptides
1	ML1_VISAL	Beta-galactoside-specific lectin 1 OS=Viscum album PE=1 SV=3	10241	63159	22
2	ML3_VISAL	Beta-galactoside-specific lectin 3 OS=Viscum album PE=1 SV=2	4149	63330	17
3	ML4_VISAL	Beta-galactoside-specific lectin 4 OS=Viscum album PE=1 SV=1	2850	57378	11
4	THNB_VISAL	Viscotoxin-B (Fragment) OS=Viscum album GN=THI2.2 PE=1 SV=2	1470	11685	2
5	ML2_VISAL	Beta-galactoside-specific lectin 2 OS=Viscum album PE=2 SV=1	918	64054	10
6	B3F5I6_9MAGN	rRNA N-glycosidase OS=Viscum articulatum PE=3 SV=1	759	62551	6
7	THN1_VISAL	Viscotoxin-1-PS OS=Viscum album GN=THI2.4 PE=1 SV=1	742	5243	4
8	S4S3F2_9MAGN	Ribosome-inactivating protein (Fragment) OS=Viscum ovalifolium PE=2 SV=1	723	59791	4
9	Q8LKQ3_9MAGN	Lectin chain B isoform 1 (Fragment) OS=Viscum coloratum PE=2 SV=1	475	30032	4

Table 11.1

Cont.

Prot. Number	Accession Number	Protein Name	Mascot Score	Mr	N° peptides
10	RBL_VISAL	Ribulose bisphosphate carboxylase large chain OS=Viscum album GN=rbcL PE=3 SV=1	464	52813	10
11	Q32726_9MAGN	Ribulose-1,5-bisphosphate carboxylase/oxygenase large subunit (Fragment) OS=Opilia amentacea GN=rbcL PE=3 SV=1	456	52830	9
12	A0A0D3MEH8_9MAGN	Ribulose bisphosphate carboxylase large chain (Fragment) OS=Scorodocarpus borneensis GN=rbcL PE=3 SV=1	453	19069	4
13	A2VAT9_9MAGN	Ribulose bisphosphate carboxylase large subunit (Fragment) OS=Septulina glauca GN=rbcL PE=3 SV=1	423	52073	13
14	Q32249_9MAGN	Ribulose 1,5-bisphosphate carboxylase (Fragment) OS=Ginalloa arnottiana GN=rbcL PE=3 SV=1	313	52770	9
15	SMST_SANMU	Probable sesquiterpene synthase OS=Santalum murrayanum GN=STPS PE=3 SV=1	54	66195	4
16	Q1HG95_VISAL	Sucrose synthase (Fragment) OS=Viscum album subsp. album PE=2 SV=1	54	92607	2

Table 11.2

Proteins identified in Mistletoe after CPLLs treatment at pH 7.2

Protein Num.	Accession Number	Protein Name	Mascot Score	Mr	N° peptides
1	ML1_VISAL	Beta-galactoside-specific lectin 1 OS=Viscum album PE=1 SV=3	2245	63159	15
2	A6XHX2_9MAGN	Ribulose-1,5-bisphosphate carboxylase/oxygenase large subunit (Fragment) OS=Cansjera leptostachya GN=rbcL PE=3 SV=1	2129	51974	15
3	RBL_VISAL	Ribulose bisphosphate carboxylase large chain OS=Viscum album GN=rbcL PE=3 SV=1	2108	52813	17
4	THNC_VISAL	Viscotoxin-C1 OS=Viscum album PE=1 SV=1	1928	5285	4
5	THNB_VISAL	Viscotoxin-B (Fragment) OS=Viscum album GN=THI2.2 PE=1 SV=2	1907	11685	2
6	Q32726_9MAGN	Ribulose-1,5-bisphosphate carboxylase/oxygenase large subunit (Fragment) OS=Opilia amentacea GN=rbcL PE=3 SV=1	1856	52830	15
7	ML2_VISAL	Beta-galactoside-specific lectin 2 OS=Viscum album PE=2 SV=1	1725	64054	20
8	Q9MW36_9MAGN	ATP synthase subunit beta (Fragment) OS=Opilia sp. Chase 1902 GN=atpB PE=3 SV=1	1489	51985	12
9	A0A0K1Z6G6_COMUM	ATP synthase CF1 beta subunit OS=Comandra umbellata GN=atpB PE=4 SV=1	1480	53858	11
10	D3WCJ3_PHOSE	ATP synthase subunit beta, chloroplastic OS=Phoradendron serotinum GN=atpB PE=3 SV=1	1451	53881	11
11	D3WCJ2_PHOSE	ATP synthase subunit alpha, chloroplastic OS=Phoradendron serotinum GN=atpA PE=3 SV=1	1410	56168	6

Table 11.2

Cont.

Protein Num.	Accession Number	Protein Name	Mascot Score	Mr	N° peptides
11	D3WCJ2_PHOSE	ATP synthase subunit alpha, chloroplastic OS=Phoradendron serotinum GN=atpA PE=3 SV=1	1410	56168	6
12	Q95FT6_DENCL	ATP synthase beta subunit (Fragment) OS=Dendrophthora clavata GN=atpB PE=4 SV=1	1354	30166	11
13	Q32249_9MAGN	Ribulose 1,5-bisphosphate carboxylase (Fragment) OS=Ginalloa arnottiana GN=rbcL PE=3 SV=1	1070	52770	12
14	THN1_VISAL	Viscotoxin-1-PS OS=Viscum album GN=THI2.4 PE=1 SV=1	994	5243	5
15	ML3_VISAL	Beta-galactoside-specific lectin 3 OS=Viscum album PE=1 SV=2	895	63330	9
16	Q9MRF4_HEIPA	ATP synthase subunit beta (Fragment) OS=Heisteria parvifolia GN=atpB PE=3 SV=1	822	52336	9
17	Q7ITP8_VISAL	ATP synthase subunit beta (Fragment) OS=Viscum album GN=atpB PE=3 SV=1	541	49432	7
18	Q8LKQ3_9MAGN	Lectin chain B isoform 1 (Fragment) OS=Viscum coloratum PE=2 SV=1	359	30032	6
19	Q4U4N0_9MAGN	Lectin (Fragment) OS=Viscum coloratum PE=2 SV=1	329	63419	7
20	B3F5I6_9MAGN	rRNA N-glycosidase OS=Viscum articulatum PE=3 SV=1	307	62551	5
21	D0VWT3_VISAL	Viscotoxin A1 OS=Viscum album PE=1 SV=1	130	5228	2
22	Q1HG95_VISAL	Sucrose synthase (Fragment) OS=Viscum album subsp. album PE=2 SV=1	62	92607	2
23	A6XI45_9MAGN	Maturase K (Fragment) OS=Maburea trinervis GN=matK PE=4 SV=1	61	45672	2

Additionally, considering the extension of *Viridiplantae* database, the MS analysis has been focused on identification of proteins belonging to *Santalales*, the order of mistletoe plants, using the Uniprot_*Santalales* database more suitable to this specific context. In this case, 16 identifications were found in CPLLs eluates at pH 2.2 (**Table 11.1**) vs. 23 in CPLLs eluates at pH 7.2 (**Table 11.2**). In both CPLLs eluates, beta-galactoside-specific lectins 1, 2, and 3 (ML1_VISAL, ML2_VISAL, ML3_VISAL) were identified, while beta-galactoside-specific lectins 4 (ML4_VISAL) was found in CPLLs sample at pH 2.2. The CPLL treatment has detected the three major types of lectins described in literature: ML-1, ML-2 and ML-3, which are associated to antitumor activity, due to suppression of cancer growth and to inhibition of metastasis (Yoon, 2003; Kang, 2008), to immunological action (Kang, 2007) and to antidiabetic effects (Kin, 2014). Generally, lectins are composed by two disulphide–bond-linked subunits A and B: the toxic chain A is responsible for ribosome inactivation and chain B interacts with cell surface glycans to favor the internalization of toxic subunit (Jiménez, 2005). For its unique anti-tumor mechanisms, ML-1 has been often used as therapeutic agent in cancer therapy (Hajto, 1990; Beuth, 1997; Stauder, 2002; Mengs, 2002; Jiménez, 2005). ML-2 is a galactose- and N-acetylgalactosamine-specific protein, characterized by a similar biological activity to ML-1: the differences, due to specific glycosylation patterns and to diverse carbohydrate binding sites, provide peculiar physiological activities (Wacker, 2005).

Moreover, the CPLL treatment was able to capture several viscotoxin isoforms: viscotoxin 1-PS (THN-1_VISAL) and viscotoxin B (THNB_VISAL) were identified in both eluates, while viscotoxin C (THNC_VISAL) and viscotoxin A1 (DOVWT3_VISAL) only after CPLLs application at pH 7.2. Viscotoxins, isolated from mistletoe, have been classified as belonging to thionin family on the basis of sequence homology (Florack, 1994); they are basic low molecular mass proteins, containing cysteine residues involved in disulfide bridges, fundamental to stabilize three-

dimensional (3D) structure (Romagnoli, 2000; Romagnoli, 2003). Their specific 3D structure has an important role in the interaction with cell membranes, showing a cytotoxic effect against tumour cells (Romagnoli, 2000; Coulon, 2003). These anti-tumoral properties are of particular interest since viscotoxins occur in some mistletoe-derived medicines used in anti-cancer therapy (Guidici, 2003; Hussain, 2013). Moreover they are also endowed with antimicrobial activity, for this reason they are physiologically involved in plant defense (Hughes, 2000). Again both CPLLs eluates have detected ribulose-1,5-biphosphate carboxylase/oxygenase (RuBisCO) and related enzymes, such as ATP synthase and sucrose synthase, involved in carbon fixation pathway. Other two ribosomal enzymes, present in low concentration and detected only after CPLLs treatment, were rRNA glycosidase and ribosome-activating protein: they are involved in hydrolysis of specific N-glycosidic bond on rRNA during plant defensive processes. Furthermore, our idea to perform CPLLs incubation at different pH values to favor specific interactions with different proteins was successful because two distinct species were captured at different conditions: ATP-dependent Clp protease at pH 7.2 and sesquiterpene synthase at pH 2.2. The first is normally present in chloroplasts for degradation of misfolded proteins, hydrolyzing them into small peptides in presence of ATP. The second is involved in the synthesis of terpenes, which are organic compounds and the presence of functional groups transforms terpenes into terpenoids, isolated also in VA extract (Renata, 2002; Stein, 2002).

11.5. Conclusions

The present study was focused on investigation of the VA proteome, contributing to improve the knowledge of proteins' role in the medical effects attributed to this plant. The combinatorial peptide ligand libraries (CPLLs) have been chosen, in order to reduce the dynamic concentration range present in VA samples, as an alternative procedure to traditional protocols previously described in literature, which apply affinity chromatography for isolation of lectins from mistletoe extracts (Stoeva, 2001; Wacker, 2005). The MS analysis performed on CPLL eluates, has identified a fair number of unique gene products belonging to *Santalales*, the plant order of VA. Considering their molecular functions, the recognized proteins are involved in defense processes and in metabolic pathways like photosynthesis. CPLLs have efficiently captured not only abundant proteins like RuBisCO, lectins and viscotoxins, whose therapeutic effects are deeply described in literature, but also other enzymes involved in metabolic reactions probably related to well-known pharmacological activities. Therefore, the results obtained in this work could be considered as a useful starting point for a future deeper investigation on the mistletoe proteome aware that many efforts should be done in order to obtain its complete identification and comprehension.

Acknowledgements

This work was supported by projects CTQ2014-52765-R (MINECO of Spain and FEDER) and GV-PROMETEO2016-145 (Conselleria de Educación, Investigación, Cultura y Deporte, Generalitat Valenciana, Spain). M. V-B thanks the MEC for an FPU grant for PhD studies.

Conflict of interest

The authors declare that they have no conflict of interest.

11.6. References

Arda, N.; Onay, E.; Koz, O.; Kirmizigul, S. (**2003**). Monosaccharides and polyols from mistletoes (*Viscum álbum L.*) growing on two different host species. *Biologia (Bratislava), 58*, 1037-1041.

Arndt, B. (**2000**). The Genus Viscum Medicinal and aromatic plant, industrial profiles. Harwood Academic, Amsterdam, 45.

Beuth, J. (**1997**). Clinical relevance of immunoactive mistletoe lectin-I. *Anti-Cancer Drugs.8*, S53-S55.

Bock, P.R.; Hanisch, J.; Matthes, H.; Zanker, K.S. (**2014**). Targeting inflammation in cancer-related-fatigue: A rationale for mistletoe therapy as supportive care in colorectal cancer patients. *Inflammation & Allergy - Drug Targets, 13*, 105-111.

Bussing, A. (**2000**). Mistletoe, the genus *Viscum*. Harwood Academic Publishers Amsterdam.

Candiano, G.; Dimuccio, V.; Bruschi, M.; Santucci, L.; Gusmano, R.; Boschetti, E.; Ghiggeri, G.M. (**2009**). Combinatorial peptide ligand libraries for urine proteome analysis: investigation of different elution systems. *Electrophoresis, 30,* 405-2411.

Cebovic, T.; Spasic, S.; Popovic, M. (**2008**). Citotoxic effects of the *Viscum album L*. extract on Ehrlich tumour cells in vivo. *Phytotherapy Research, 22*, 1097-1103.

Coulon, A.; Mosbah, A.; Lopez, A.; Sautereau, A.M.; Schaller, G.; Urech, K.; Rouge, P.; Darbon, H. (**2003**). Comparative membrane interaction study of viscotoxins A3, A2 and B from mistletoe (*Viscum album*) and connections with their structures. *Biochemical Journal, 374*, 71-78.

Delebinski, C.; Jäger, S.; Kauczor, G.; Hassanin, K.; Seeger, K.; Henze, G.; Lode, H.; Seifert, G. (**2012**). A new development of triterpene acids-containing extracts from *Viscum album L*. displays synergistic induction of apoptosis in childhood leukaemia. *BMC Journal of Alternative and Complementary Medicine, 12*, 1-33.

Delebinski, C.I.; Hassanin, K.; Henze, G.; Lode, H.N.; Seifert, G.J. (**2012**). A new development of triterpene acid-containing extracts from *Viscum album L*. displays synergistic induction of apoptosis in acute lymphoblastic leukaemia. *Cell Proliferation, 45*, 176-187.

Fasoli, E.; Farinazzo, A.; Sun, C.J.; Kravchuk, A.V.; Guerrier, L.; Fortis, F.; Boschetti, E.; Righetti, P.G. (**2010**). Interaction among proteins and peptide libraries in proteome analysis: pH involvement for a larger capture of species. *Journal of Proteomics, 73*, 733-742.

Florack, D.E.; Stiekema, W.J. (**1994**). Thionins: properties, possible biological roles and mechanisms of action. *Plant Molecular Biology, 26*, 25-37.

Giudici, M.; Pascual, R.; Canal, L.; Pfüller, K.; Pfüller, U.; Villalaín, J. (**2003**). Interaction of Viscotoxins A3 and B with membrane model systems: Implications to their mechanism of action. *Biophysical Journal, 85*, 971-981.

Hajto, T.; Hostanska, K.; Frei, K.; Rordorf, C.; Gabius, H.J. (**1990**). Increased secretion of tumor necrosis factor α, interleukin 1, and interleukin 6 by human mononuclear cells exposed to β-galactoside-specific lectin from clinically applied mistletoe extract. *Cancer Research, 50*, 3322-3326.

Hughes, P.; Dennis, E.; Whitecross, M.; Llewellyn, D.; Gage, P. (**2000**). The cytotoxic plantprotein, β-purothionin, forms ion channels in lipid membranes. *Journal of Biological Chemistry, 275*, 823-827.

Hussain, S.; Güzel, Y.; Schönbichler S.A.; Rainer M.; Huck C.W.; Bonn GK. (**2013**). Solid-phase extraction method for the isolation of plant thionins from European mistletoe, wheat and barley using zirconium silicate embedded in poly(styrene-co-divinylbenzene) hollow-monoliths. *Analytical and Bioanalytical Chemistry, 405*, 7509-7521.

Jackson, S.E.; Chester, J.D. (**2015**). Personalised cancer medicine. *International Journal of Cancer, 137*, 262-266.

Jager, S.; Winkler, K.; Pfuller, U.; Scheffler, A. (**2007**). Solubility studies of oleanolic acid and betulinic acid in aqueous solutions and plant extracts of *Viscum album L. Planta Medica, 73*, 157-162.

Jiménez, M.; Sáiz, J.L.; André, S.; Gabius, H.J.; Solís, D. (**2005**). Monomer/dimer equilibrium of the AB-type lectin from mistletoe enables combination of toxin/agglutinin activities in one protein: analysis of native and citraconylated proteins by ultracentrifugation/gel filtration and cell biological consequences of dimer destabilization. *Glycobiology, 15*, 1386-1395.

Jung, M.L.; Baudino, S.; Ribereau-Gayon, G.; Beck, J.P. (**1990**). Characterization of cytotoxic proteins from mistletoe (*Viscum album L.*). *Cancer Letters, 51*, 103-108.

Kang, T.B.; Song, S.K.; Yoon, T.J. (**2007**). Isolation and characterization of two Korean mistletoe lectins. *Journal of Biochemistry and Molecular Biology, 40*, 959-965.

Kang T.B.; Yoo Y.C.; Lee K.H. (**2008**). Korean mistletoe lectin (KML-IIU) and its subchains induce nitric oxide (NO) production in murine macrophage cells. *Journal of Biomedical Science, 15*, 197-204.

Khil, L.Y.; Kim, W.; Lyu, S.; Park, W.B.; Yoon, J.W.; Jun H.S. (**2007**). Mechanisms involved in Korean mistletoe lectin-induced apoptosis of cancer cells. *World Journal of Gastroenterology*, *13*, 2811-2818.

Kienle, G.S.; Berrino, F.; Bussing, A.; Portalupi, E.; Rosenzweig, S.; Kiene, H. (**2003**). Mistletoe in cancer-A systematic review on controlled clinical trials. *European Journal of Medical*, *8*, 109-119.

Kim, S.; Lee, D.; Kim, J.K.; Kim, J.H.; Park, J.H.; Lee, J.W.; Kwon, J. (**2014**). Viscothionin isolated from Korean mistletoe improves nonalcoholic fatty liver disease via the activation of adenosine monophosphate-activated protein kinase. *Journal of Agricultural and Food Chemistry*, *62*, 11876-11883.

Kin, K.W.; Yang, S.H.; Kim, J.B. (**2014**). Protein fractions from Korean mistletoe (*Viscum album coloratum*) extracts induce insulin secretion from pancreatic beta cells. *Evidence-Based Complementary and Alternative Medicine*, *2014*, 703624.

Konopa, J.; Woynarowski, J.M.; Lewandowska-Gumieniak, M. (**1980**). Isolation of viscotoxins. Cytotoxic basic polypeptides from *Viscum album L*. *Hoppe-Seyler's Zeitschrift Fur Physiologische Chemie*, *361*, 1525-1533.

Krzaczek, T. (**1997**). Pharmocobotanical research on the sub-species *Viscum album L*. terpenes and sterols (author's transl). *Annales Univ Mariae Curie-Skodowska Medical*, *32*, 125-134.

Kuttan, G.; Vasudevan D.M.; Kuttan, R. (**1988**). Isolation and identification of a tumor reducing component from mistletoe extract (Iscador). *Cancer Letters*, *41*, 307-314.

Marvibaigi, M.; Supryanto, E.; Amini, N.; Majid, F.A.; Janathan, S.K. (**2014**). Preclinical and clinical effects of mistletoe against breast cancer. *BioMed Research International*, *2014*, 785479.

Melzer, J.; Iten, F.; Hostanska, K.; Saller, R. (**2009**). Efficacy and safety of mistletoe preparations (*Viscum album*) for patients with cancer diseases. A systematic review. *Forsch Komplementmed, 6,* 217-226.

Mengs, U.; Gothel, D.; Leng-Peschlow, E. (**2002**). Mistletoe extracts standardized to mistletoe lectins in oncology: review on current status of preclinical research. *Anticancer Research, 22,* 1399-1407.

Olsnes, S.; Stirpe, F.; Sandvig, K.; Pihl, A. (**1982**). Isolation and characterization of Viscumin, a toxic lectin from *Viscum album L.* (Mistletoe). *Journal of Biological Chemistry, 257,* 13263-13270.

Osterman, T.;, Raak, C.A. Bussing, T.(**2009**). Survival of cancer patients treated with mistletoe extract (Iscador): a systemic literature review. *BMC Cancer, 9,* 451.

Over, R.S.; Michaelis, S.C. (**2014**). Open and closed: the roles of linker histones in plants and animals. *Molecular Plant, 7,* 481-491.

Podlech, O.; Harter, P.N.; Mittelbronn, M.; Poschel, S.; Naumann, U. (**2012**). Fermented mistletoe extract as a multimodal antitumoral agent in gliomas. *Evidence-Based Complementary and Alternative Medicine, 50,* 1796.

Poruthukaren, K.J.; Palatty, P.L.; Baliga, M.S.; Suresh, S. (**2014**). Clinical evaluation of *Viscum album* mother tincture as an antihypertensive: a pilot study. *Evidence-Based Complementary and Alternative Medicine, 19,* 31-35.

Renata, J.; Piotrowski, A. (**2002**). Characterization and antiglycation activity of phenolic constituents from *Viscum album* (European Mistletoe). *Canadian Journal of Plant Pathology, 24,* 21-28.

Righetti, P.G.; Candiano, G.; Citterio, A.; Boschetti, E. (**2015**). Combinatorial peptide ligand libraries as a "Trojan Horse" in deep discovery proteomics. *Analytical Chemistry, 87*, 293-305.

Romagnoli, S.; Fogolari, F.; Catalano, M.; Zetta, L.; Schaller, G.; Urech, K.; Giannattasio, M.; Ragona, L.; Molinari, H. (**2003**). NMR solution structure of viscotoxin C1 from *Viscum album* species *Coloratum ohwi*: toward a structure-function analysis of viscotoxins. *Biochemical Journal, 42,* 12503-12510.

Romagnoli, S.; Ugolini, R.; Fogolari, F.; Schaller, G.; Urech, K.; Giannattasio, M.; Ragona, L.; Molinari, H. (**2000**). NMR structural determination of viscotoxin A3 from *Viscum album.L*. *Biochemical Journal, 350,* 569-577.

Saez, V.; Fasoli, E.; D'Amato, A.; Simó-Alfonso, E.F.; Righetti, P.G. (**2013**). Artichoke and Cynar liqueur: Two (not quite) entangled proteomes. *Biochimica et Biophysica Acta, 1834*, 119-126.

Sha, C.; Das, M.; Stephen-Victor, E.; Friboulet, A.; Bayry, J.; Kaver, S.V. (**2016**). Differential effects of *Viscum album* preparations on the maturation and activation of human dendritic cells and $CD4^+$ T cell responses. *Molecules, 21*, 912-925.

Shevchenko, A.; Tomas, H.; Havli, J.; Olsen, J.V.M. (**2007**). In-gel digestion for mass spectrometric characterization of proteins and proteomes. *Nature Protocols, 1*, 2856-2860.

Singh, B.N.; Saha, C.; Galun, D.; Upreti, D.K.; Bayry, J.; Kaveri, S.V. (**2016**). European *Viscum album*: A potent phytotherapeutic agent with multifarious phytochemicals, pharmacological properties and clinical evidence. *RSC Advances, 6*, 23837-23857.

Srdic-Rajic, T.; Tisma-Miletic, N.; Cavic, M.; Kanjier, K.; Savikin, K.; Galun, D.; Konic-Ristic, A.; Zoranovic, T. (**2016**). Sensitization of K562 leukimia

cells to doxorubicin by the *Viscum album* extract. *Phytotherapy Research, 30,* 485-495.

Stauder, H.; Kreuser, E.D. (**2002**). Mistletoe extracts standardized in terms of mistletoe lectins (ML I) in oncology: current state of clinical research. *Onkologie, 25,* 374-380.

Stein, G.M.; Pfuller, U.; Schietzel, M.A. Bussing, M. (**2002).** Intracellular expression of IL-4 and inhibition of IFN-gamma by extracts from European mistletoe is related to induction of apoptosis. *Anticancer Research, 20,* 2987-2994.

Stoeva, S.; Franz, M.; Wacker, R.; Krauspenhaar, R.; Guthöhrlein, E.; Mikhailov, A.; Betzel, C.; Voelter, W. (**2001**). Primary structure, isoforms, and molecular modeling of a chitin-binding mistletoe lectin 1. *Archives of Biochemistry and Biophysics, 1,* 23-31.

Struh, C.M.; Jager , S.; Schempp, C.M.; Scheffler, A.; Martin, S.F. (**2012**). A novel triterpene extract from mistletoe induces rapid apoptosis in murine B16.F10 melanoma cells. *Phytotherapy Research, 26,* 1507-1512.

Struth C.M.; Jager, S.; Kersten, A.; Schempp, C.M.; Scheffler, A.; Martin, S.F. (**2013**). Triterpenoids amplify anti-tumoral effects of mistletoe extracts on murine B16.f10 melanoma in vivo. *PloS One, 8,* 62168.

Troger, W.; Galun, D.; Reif, M.; Schumann, A.; Stankovic, N.; Milicevic, M. (**2014**). Quality of life of patients with advanced pancreatic cancer during treatment with mistletoe: a randomized controlled trial. *Deutsches Ärzteblatt International, 111,* 493-502.

Urek, K.; Scher, J.M.; Hostanska, K.; Becker, H. (**2005**). Aptosisi inducing activity of viscin, a lipophilic extract from *Viscum album L. Journal of Pharmacy and Pharmacology, 57,* 101-109.

Wacker, R.; Stoeva, S.; Betzel, C.; Voelter, W. (**2005**). Complete structure determination of N-acetyl-Dgalactosamine-binding mistletoe lectin-3 from *Viscum album L. album*. *Journal of Peptide Science, 11,* 289-302.

Wacker, R.; Stoeva, S.; Pfuller, K.; Voelter, W. (**2004**). Complete structure determination of the A chain of mistletoe lectin III from *Viscum album L*. *Journal of Peptide Science, 10,* 138-148.

Weissenstein, U.; Toffol, U.; Baumgartner, S.; Urech, K. (**2012**). Immunmodulatory and anti-apoptotic effects of *Viscum album* lopophilic extract and oleanolic acid on human peripheral blood lymphocytes and monocytes in vitro. *European Journal of Integrative Medicin, 4,* 124.

Woynarowski, J.M.; Konopa, J. (**1980**). Interaction between DNA and viscotoxins. Cytotoxic basic polypeptides from *Viscum album L*. *Hoppe-Seyler's Zeitschrift fur physiologische Chemie, 361*, 1535-1545.

Yoon, T.S.; Yoo, Y.C.; Choi, B. (**2003**). Antitumor activity of Korean mistletoe lectin is attributed to activation of macrophages and NK cells. *Archives of Pharmacal Research, 26,* 861-867.

SECTION III. DEVELOPMENT OF METHODS FOR THE DISCRIMINATION OF OLIVE PRODUCTS ACCORDING TO THEIR GENETIC AND BOTANICAL ORIGIN

III.A. Application of chromatographic and related techniques

Chapter 12. Use of protein profiles established by CZE to predict the cultivar of olive leaves and pulps

1652 *Electrophoresis* 2014, *35*, 1652–1659

María Vergara-Barberán
María Jesús Lerma-García
José Manuel Herrero-Martínez
Ernesto Francisco Simó-Alfonso

Research Article

Use of protein profiles established by CZE to predict the cultivar of olive leaves and pulps

Intact protein profiles established by CZE have been used to predict the cultivar of olive leaves and pulps. For this purpose, proteins were extracted using a mild enzyme-assisted extraction method, which provided higher protein recoveries and a lower environmental impact than other previously described methods. These extracts were subjected to CZE determination under basic conditions using a BGE composed by 50 mM phosphate, 50 mM tetraborate and 0.1% PVA at pH 9. Nine and fourteen common peaks, for leaf and pulp samples, respectively, were identified in the nine cultivars studied in this work. In addition, and using linear discriminant analysis of the CZE data, olive leaf and pulp samples belonging to nine cultivars from different Spanish regions were correctly classified with an excellent resolution among all categories, which demonstrated that intact protein profiles are characteristic of each cultivar.

Keywords: cultivar; CZE; linear discriminant analysis; intact protein profiles; olive leaf and pulp

12.1. Introduction

Olive tree (Olea europeaea, Oleaceae), an important crop in the Mediterranean area, produces 98% of the world total amount of olive oil. Olive tree and its products (leaves, olive fruit and oil) have a rich history of nutritional, medicinal and commercial purposes (Soni, 2006). For these reasons, several molecular markers have been established in order to distinguish, characterize or identify cultivars, to estimate germplasm variability and to trace olive origin (Hatzopoulos, 2002).

Olive leaf and pulp proteins have been scarcely studied when compared to other olive leaf and pulp compounds, although several reports have demonstrated their important role in the processing and quality of olive fruits and olive oil (Georgalaki, 1998A; Giogalaki, 1998; Boidis, 2006). Additionally, it has been also demonstrated that olive oil proteins can elicit allergic reactions in sensitive individuals (Martín-Hernández, 2008; Esteve, 2011).

Different protocols to determine olive leaf and pulp proteins have been published in literature. SDS-PAGE (García, 2000; Wang, 2003; Esteve, 2011; Esteve, 2012; Esteve 2013), UHPLC (Esteve, 2011), nLC-MS/MS (Esteve, 2011; Esteve 2013), MALDI-TOF (Esteve, 2011; Esteve, 2013), CZE (Montealegre, 2010) and CGE (Montealegre, 2012) techniques have been proposed to carry out leaf and pulp protein separation. García *et al.* compared by SDS-PAGE the protein composition of juvenile and adult olive leaf, bark and bud tissues (García, 2000), founding that the proteins observed in each sample were highly dependent of the maturation stage of the tissue. Also leaf proteins have been characterized by 1- and 2-D gel electrophoresis (Wang, 2003); being the protein observed in this work the same that has been previously described as a characteristic protein of other plant species (Meyer, 1988; Hubbs, 1992; Saha, 1997). In other work, proteins from olive pulp were extracted using TCA and precipitated with acetone. The resulting proteins

were subjected to SDS-PAGE, being only one band observed and excised for MALDI-TOF and nLC-MS/MS determination. Different proteins were observed, although only differences for the same peptides coming from the thaumatin-like protein were evidenced when four different olive varieties were analyzed (Esteve, 2011). Esteve *et al*. (Esteve, 2011) have separated pulp peptides and proteins from different cultivars by both SDS-PAGE and UHPLC after testing several olive pulp protein extraction methods. When UHPLC protein profiles were compared, several differences were evidenced. The same research group, in collaboration with the group of Prof. Righetti, has exploited the potential of combinatorial peptide ligand libraries (CPLLs) to amplify the signal of the low-abundant proteins present in olive pulp and seeds. After SDS-PAGE protein separation and nLC-MS/MS determination, a quite large number of compounds have been identified (Esteve, 2012). On the other hand, olive pulp and seed proteins have been also examined by IEF-SDS-PAGE (Esteve, 2013). The same CPLLs were also applied to the determination of olive oil proteins (Esteve, 2012); however, when the electrophoretic profiles obtained with the olive oil and those corresponding to the olive seed and pulp were compared, only the smaller proteins in the seed and the pulp seem to pass to the oil while the bigger proteins probably remain in the pellet resulting from the oil extraction. On the other hand, Montealegre *et al*. (Montealegre, 2012) separated proteins from olive fruits of different cultivar and geographical origin using CGE. In all cases, seven common peaks were identified. Furthermore, proteins from raw and table olives were also determined by CZE using acid media (Montealegre, 2010), and the resulting profiles were compared, showing differences according to their botanical variety and geographical region.

The potential of chemometric tools to discriminate among different types and classes of foodstuffs by using proteins and peptides as predictors has been previously demonstrated in literature (Herrero-Martínez, 2000; García-Ruiz, 2007; Lerma-García, 2009; Herrero, 2010; Castro-Puyana, 2012). Herrero-

Martínez *et al.* (Herrero-Martínez, 2000) have constructed a LDA model able to classify cheeses according to both genetic origin and ripening time by using protein profiles obtained by CZE. In another work, García-Ruiz *et al*. (García-Ruiz, 2007) successfully differentiated among soybeans with different pigmentation, and between transgenic and non-transgenic soybeans by using as predictors for the construction of a discriminant analysis model several protein peak areas also established by CZE. On the other hand, CZE analysis of the peptide fraction of Spanish dry-cured hams allowed their classification according to their curing time by using LDA (Lerma-García, 2009). Only one work has been published regarding the employment of discriminant analysis to distinguish olive fruits according to their geographical origin by using proteins obtained by CGE as predictors (Montealegre, 2012), being the prediction capability of this model 80%. However, and as far as we are concerned, any work has been published using protein profiles obtained by CZE as predictors to discriminate among different olive leaf and pulp cultivars.

The aim of this work was the development of a CZE method for the determination of intact proteins from olive leaves and pulps from nine cultivars collected from different Spanish regions. Two discriminant analysis (LDA) models were constructed using the normalized protein peak areas obtained from the electropherograms as predictors in order to check if these models are able to classify the olive leaves and pulps according to their cultivar. For this purpose, an enzyme-assisted protocol previously optimized by our research group in terms of different experimental parameters that could affect protein extraction was used.

12.2. Material and methods

12.2.1. Reagents and samples

The following analytical grade reagents were used: ACN, HCl, monosodium hydrogen phosphate (Panreac, Barcelona, Spain), sodium tetraborate decahydrate (Probus, Barcelona), NaOH and polyvinyl alcohol (PVA, average molecular mass 133 000; Sigma, St. Louis, MO, USA). The following enzymes, kindly donated by Novozymes (Bagsvaerd, Denmark) were used: lipase (Palatase® 20000 L; activity 20000 LU-MM/g (LU = lipase unit); optimal working conditions, pH 7 and 25 - 45 ºC) and cellulase (Celluclast® 1.5L; activity 1500 NCU/g (NCU = novo cellulase unit); working conditions, pH 4.5 - 6.0 and 50 - 60 ºC). Deionized water (Barnstead deionizer, Sybron, Boston, MA) was also employed.

The olive leaves and fruits employed in this study (**Table 12.1**) were kindly donated by different olive oil manufacturers. To assure a correct sampling, both olive leaves and fruits were collected at the same period (end of November 2011) directly from trees located in different Spanish regions. The cultivar of samples was guaranteed by the suppliers. Both olive leaves and fruits were previously selected to assume the absence of mold or other microorganisms, washed with water to remove dust or airborne particles settled on the olive and then stored at -20ºC prior their use.

12.2.2. Intact protein extraction

Protein extraction was performed following the procedure previously optimized by our research group (unpublished data). In this procedure, 10 g of fresh leaves / pulps were frozen in liquid nitrogen and ground to a fine powder in a pre-cooled mortar and pestle, lyophilized, and the resulting powder was next homogenized. For the extraction of olive leaf proteins, 0.3 g lyophilized powder were treated with 3 mL of a water:ACN mixture (7:3, v/v) containing

a 5% (v/v) cellulase enzyme at pH 5.0, and sonicated at 55 ºC for 15 min. On the other hand, for the extraction of pulp proteins, 0.3 g of powder were treated with 3 mL of water at pH 7.0 containing a 5% (v/v) lipase, and sonicated at 30 ºC for 15 min. Next, both leaf and pulp protein extracts were centrifuged at 10000 x g for 10 min, and stored at -20 ºC until their use. For CZE determination, samples were 1:1 (v/v) diluted with BGE and injected by triplicate into the CE system.

12.2.3. Instrumentation and working conditions

An HP3D CE system (Agilent, Waldbronn, Germany) provided with a diode-array spectrophotometric detector and uncoated fused-silica capillaries (Polymicro Technologies, Phoenix, AZ) of 33.5 cm length (25 cm effective length) x 50 µm id (375 µm od) were used. New capillaries were successively flushed with 1 M NaOH, 0.1 M HCl, 0.1 M NaOH and water at 60º C for 10 min each. At the beginning of each working session and between runs, the capillary was successively rinsed with 0.1 M NaOH for 5 min, water for 5 min, and BGE for 10 min. Hydrodynamic injections at 50 mbar × 3 s were performed. Separations were conducted at +10 kV at 25 ºC. The detector was set at 214 nm with 450 nm as reference. The optimal BGE consisted of 50 mM phosphate, 50 mM tetraborate and 0.1% PVA, adjusted at pH 9 with 0.1M NaOH.

Table 12.1

Cultivar, geographical origin and number of samples of the olive leaves and pulps used in this study

Cultivar	No. of samples	Geographical origin
Arbequina	2	Jumilla (Murcia)
	2	Les Garrigues (Lleida)
	1	Puente Genil (Córdoba)
	1	Vila Franca del Penedés (Barcelona)
Canetera	2	Altura (Castellón)
	1	Adzaneta (Castellón)
	2	La Plana comarca (Castellón)
	1	Maestrat *comarca* (Castellón)
Cornicabra	2	Daimiel (Ciudad Real)
	1	Jumilla (Murcia)
	2	Requena (Valencia)
	1	Villapalacios (Albacete)
Frantoio	1	Altura (Castellón)
	2	Cabra (Córdoba)
	1	Jumilla (Murcia)
	1	Mengíbar (Jaén)
	1	Puente Genil (Córdoba)
Grosal de	1	Pobla del Duc (Valencia)
Albocácer	2	Requena (Valencia)
	3	La Noguera (Lleida)
Hojiblanca	1	Aguilar de la Frontera (Córdoba)
	1	Estepa (Sevilla)
	2	Fuente de Piedra (Málaga)
	1	Jumilla (Murcia)
	1	Villapalacios (Albacete)
Manzanilla	1	Ahigal (Cáceres)
	2	Altura (Castellón)
	1	Puente Genil (Córdoba)
	2	Requena (Valencia)

Cont. Table 12.1

Cultivar	No. of samples	Geographical origin
Picual	1	Jumilla (Murcia)
	2	Puente Genil (Córdoba)
	1	Requena (Valencia)
	2	Villapalacios (Albacete)
Serrana	1	Altura (Castellón)
	2	Artana (Castellón)
	1	Jérica (Castellón)
	2	Viver (Castellón)

12.2.4. Data treatment and statistical analysis

The peak area of each protein was measured from the electropherograms, and a data matrix was constructed using the areas of all the peaks as original variables. After normalization of the variables, LDA analysis was performed using SPSS (v. 15.0, Statistical Package for the Social Sciences, Chicago, IL, USA). LDA, a supervised classificatory technique, is widely recognized as an excellent tool to obtain vectors showing the maximal resolution between a set of previously defined categories. In LDA, vectors minimizing the Wilks' lambda, λ_w, are obtained (Vandeginste, 1998). This parameter is calculated as the sum of squares of the distances between points belonging to the same category divided by the total sum of squares. Values of λw approaching zero are obtained with well resolved categories, whereas overlapped categories made λw to approach one. Up to $N-1$ discriminant vectors are constructed by LDA, being N the lowest value for either the number of predictors or the number of categories. The selection of the predictors to be included in the LDA models was performed using the SPSS stepwise algorithm. According to this algorithm, a predictor is selected when the reduction of λ_w produced after its inclusion in the model exceeds F_{in}, the entrance threshold of a test of

comparison of variances or F_{test}. However, the entrance of a new predictor modifies the significance of those predictors which are already present in the model. For this reason, after the inclusion of a new predictor, a rejection threshold, F_{out}, is used to decide if one of the other predictors should be removed from the model. The process terminates when there are no predictors entering or being eliminated from the model. The probability values of F_{in} and F_{out}, 0.05 and 0.10, respectively, were adopted.

12.3. Results and discussion

12.3.1. Optimization of enzyme-assisted protocol

In a previous work (unpublished data), different parameters that affect the extraction process, such as the enzyme type and content, organic solvent percentage, pH and extraction temperature and time, were optimized. The influence of these factors was examined using the standard Bradford assay and the extracted proteins were characterized by SDS-PAGE. The best results for the extraction of olive leaf proteins were achieved using 3 mL of a water:ACN mixture (7:3, v/v) containing a 5% (v/v) cellulase enzyme at pH 5.0, and sonicated at 55 ºC for 15 min. On the other hand, for the extraction of pulp proteins, the best results were obtained with 3 mL of water at pH 7.0 containing a 5% (v/v) lipase, and sonicated at 30 ºC for 15 min. The SDS-PAGE obtained under these conditions for two representative olive leaf and pulp samples (Picual variety) are shown in **Figure 12.1.**

As observed in this figure for the leaf protein extract, four prominent protein bands, located at 29, 44, 55 and 63 kDa were distinguished. The band located at 44 kDa was identified as cellulase enzyme, whereas the 55 kDa protein was assigned as ribulose-1,5-bisphosphate carboxylase (Rubisco), which was characteristic of leaf protein fractions of many plant species

(García, 2000; Wang, 2003). In addition, the band located at 63 kDa, was assigned to oleuropein β-glucosidase (Hatzopoulos, 2002).

On the other hand, for the olive pulp protein extract, 4 prominent protein bands, located at 22, 30, 41 and 48 kDa were distinguished. The bands located at 30 and 48 kDa were identified as lipase enzyme, whereas the 22 kDa protein could be related to an oleosin (Ross, 1993). Using this protocol, the total amount of protein mass on fresh weight basis was comprised between 1.87 mg g^{-1} (Cornicabra variety) and 6.63 mg g-1 (Picual variety) for leaf extract, and between 0.27 mg g^{-1} (Grosol variety) and 0.98 mg g^{-1} (Picual variety) for pulp extract. These contents were higher (*ca.* 2-3 folds) than those found by other extraction protocols reported for the same genetic varieties (Wang, 2003), being also a more environmentally sustainable and faster than other protocols described.

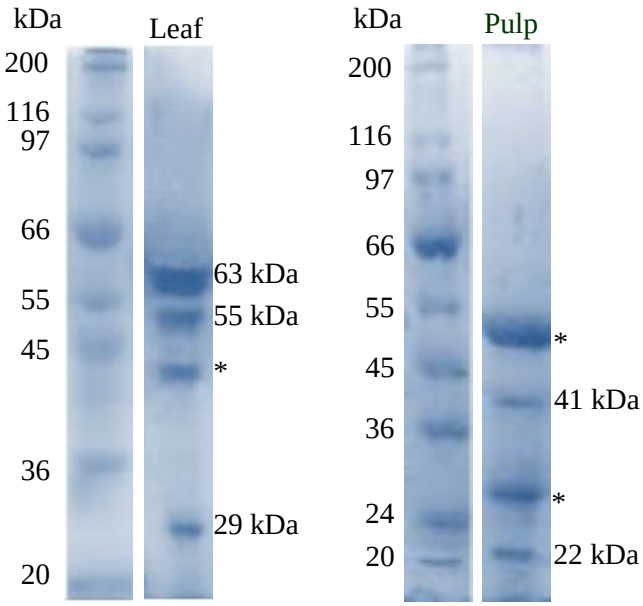

Figure 12.1. SDS-PAGE electrophoretic protein profiles obtained from olive leaf and pulp samples from Picual variety. The bands corresponding to the enzyme used are labeled with an asterisk.

12.3.2. Optimization of CZE conditions

In order to optimize the separation of both olive leaf and pulp proteins, a protein extract from Picual cultivar was used. Montealegre *et al*. (Montealegre, 2010) have described that the use of a basic BGE (with commercial additives, to minimize the adsorption of proteins) gave poor reproducible results in the separation of olive pulp proteins. However, some previously reports (Ruíz-ángel, 2002; Sebastián-Francisco, 2003) have stated that the use of BGE containing PVA is able to alleviate protein adsorption on the capillary walls, thus reducing background noise and improving migration time reproducibility. Therefore, a BGE composed by 50 mM phosphate, 25 mM tetraborate and 0.1% PVA at pH 9 (Sebastián-Francisco, 2003) was initially tested in this study. Under these conditions and for the Picual leaf extract, a total of 9 peaks (7 protein + 2 cellulase enzyme peaks) were observed (see **Figure 12.2A**). When the tetraborate content was increased up to 50 mM (see **Figure12.2B**), two more peaks were observed, which were overlapped when a 25 mM tetraborate content was used (**Figure 12.2A**). A further increase in tetraborate content up to 100 mM only led to higher analysis times; thus, 50 mM tetraborate content was selected as the best comprise between both peak resolution and analysis time.

A similar optimization was also performed to the Picual pulp extract (see **Figure 12.3**). As observed for a 25 mM tetraborate content, several peak pairs overlapped, being resolved when a 50 mM tetraborate content was used (**Figure 12.3B**). When a 100 mM tetraborate content was tried, peak resolution remained practically the same, except for lipase and no. 9 peak pair, which was improved, but at expenses of higher analysis times (35 min vs 15 min). Therefore, a tetraborate content of 50 mM was selected for further studies.

Next, the applied voltage for protein separation was optimized. For this purpose, different applied voltages, ranging from 5 to 20 kV, were tried. In all cases, migration time decreased when voltage was increased. Thus, a voltage of 10 kV was selected as the best compromise between migration time and separation efficiency. Moreover, capillary temperature was also set at 25 ºC and a good separation of proteins was obtained.

On the other hand, hydrodynamic injection was selected since more reproducible results were obtained when compared to electrokinetic injection. Injection time and pressure were also optimized. Injection time was varied between 2 and 10 s, being 3 s selected as the optimum value taking into account that longer times provided an intense enzyme peak, which disguised some protein peaks. Regarding injection pressure, values ranging from 30 to 60 mbar were tried. A pressure of 50 mbar was selected since it provides the best protein sensitivities.

Next, precision was evaluated by studying the intra- and interday reproducibilities of migration times of some proteins obtained by injecting the olive leaf and pulp protein extract of the Picual cultivar 3 times per day during 3 days. In all cases, the RSD values were lower than 2.8% and 2.4% for leaf and pulp protein peaks, respectively (see **Table 12.2**). The developed method provided a lower analysis time (15 min vs. 40 min) and a satisfactory and better reproducibility in migration times (below 3%) than other previously reported protocols for the same matrix in literature (Montealegre, 2010).

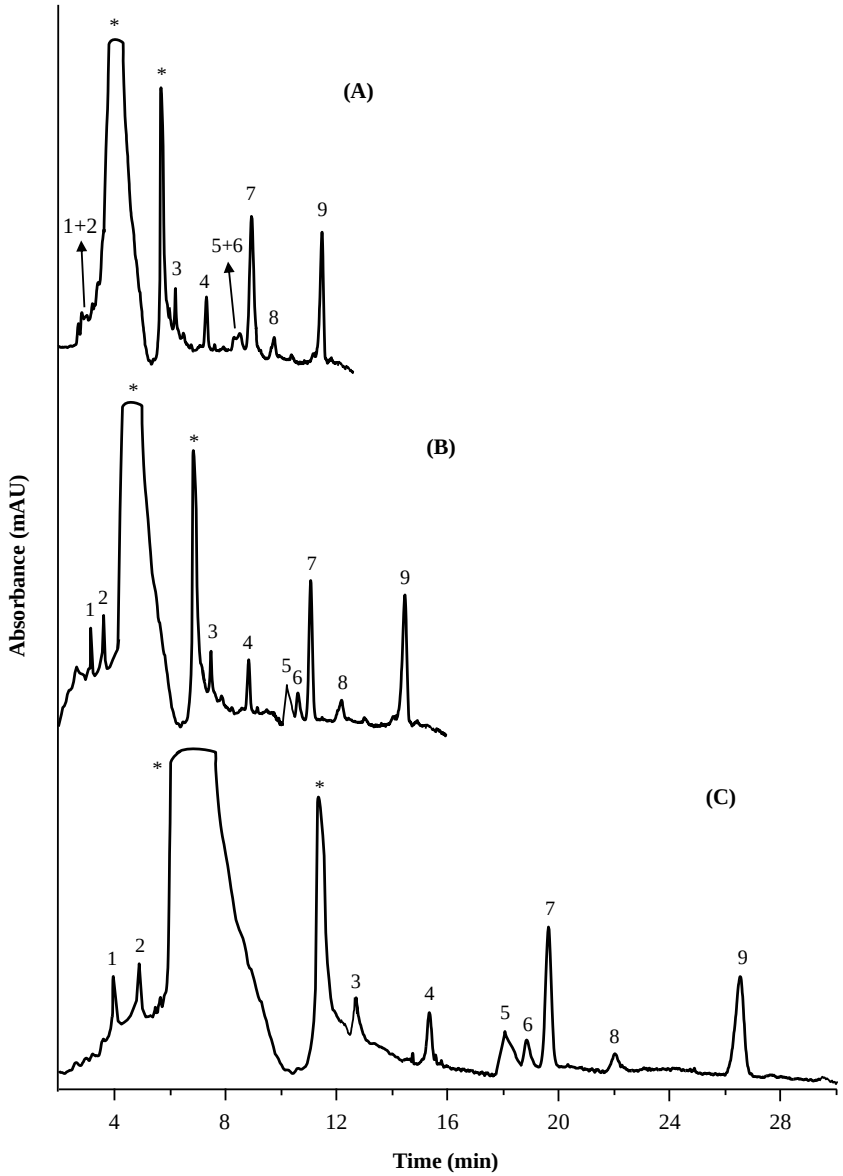

Figure 12.2. Influence of tetraborate content on the separation of intact proteins extracted from a Picual cultivar leaf using a 25 mM (A), 50 mM (B) and 100 mM borate content on a BGE composed by 50 mM phosphate and 0.1% PVA at pH 9. CZE conditions: Hydrodynamic injection, 50 mbar for 3 s; separation voltage, +10 kV at 25 ºC; detection, 214 nm. Peaks marked with an asterisk corresponded to cellulase enzyme peaks.

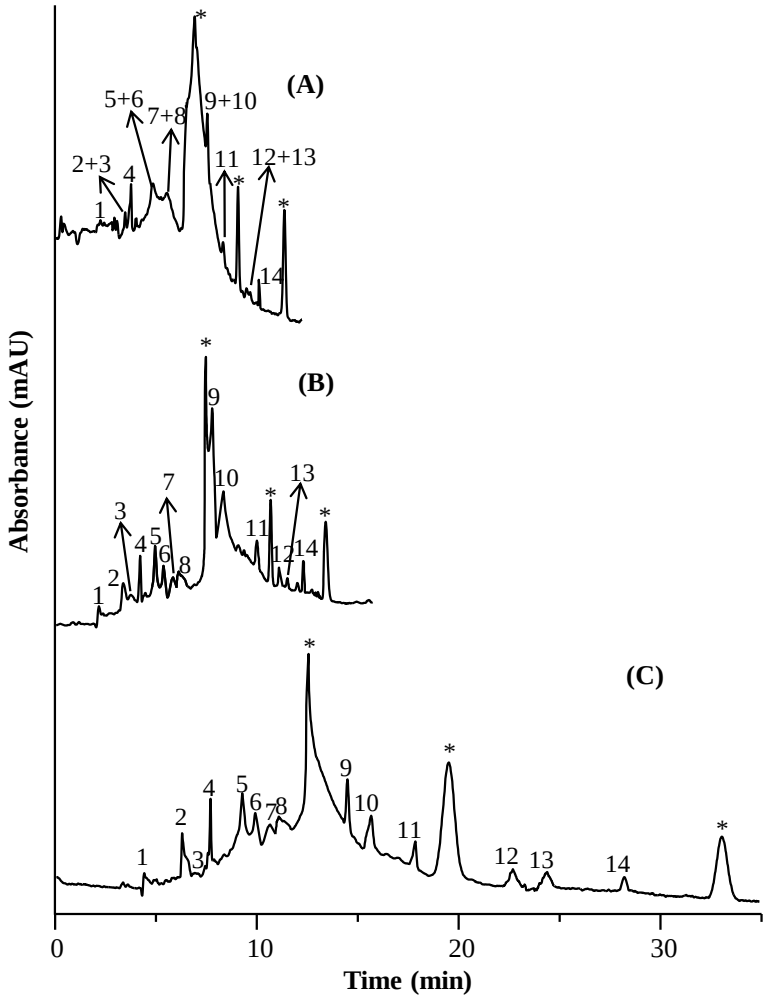

Figure 12.3. Influence of tetraborate content on the separation of intact proteins extracted from a Picual cultivar pulp using a 25 mM (A), 50 mM (B) and 100 mM borate content on a BGE composed by 50 mM phosphate and 0.1% PVA at pH 9. CZE conditions as in **Figure 12.2.** Peaks marked with an asterisk corresponded to lipase enzyme peaks.

Table 12.2

Migration times reproducibility for olive leaf and pulp proteins from Picual cultivar.

Leaf			Pulp		
Parameter	RSD[a] ,% (n=3)	RSD[b] ,% (n=9)	Parameter	RSD[a] ,% (n=3)	RSD[b] ,% (n=9)
t_{eof} (min)	0.5	0.9	t_{eof} (min)	0.3	0.9
t_1 (min)	0.8	2.8	t_1 (min)	0.2	0.7
t_2 (min)	0.4	1.2	t_5 (min)	0.3	2.4
t_7 (min)	1.0	2.1	t_{10} (min)	0.8	2.0
t_9 (min)	0.3	0.8	t_{14} (min)	0.7	1.1

[a] Intraday RSD, obtained injecting 3 times per day
[b] Interday RSD, obtained injecting 3 times per day during 3 days

12.3.3. Characterization of intact protein profiles of olive leaves and pulps

Under the optimized conditions, the protein extracts of all olive leaf and pulp samples included in **Table 12.1** were subjected to CZE analysis. Representative CZE electropherograms of an Arbequina (A), Canetera (B), Manzanilla (C) and Picual (D) olive leaf proteins are shown in **Figure 12.4**. As observed, the most abundant protein of Arbequina and Canetera varieties is protein no. 9, while for Manzanilla the most abundant proteins were those labelled as no. 4 and 7, and for Picual proteins no. 7 and 9. Thus, the profiles observed were different, which should be related with their different cultivar.

On the other hand, representative CZE electropherograms of an Arbequina (A), Canetera (B), Manzanilla (C) and Picual (D) olive pulp proteins are shown in **Figure 12.5.** As observed in this figure, protein no. 5 is more abundant in Canetera than in the other varieties, while protein no. 10 is the most abundant in Arbequina variety. Thus, the differences observed in both olive leaf and pulp profiles were enhanced when chemometric analysis of the data was performed.

14.3.4. Normalization of the variables and construction of LDA models

In order to reduce the variability associated to the random error when the total amount of intact proteins was recovered from the olive leaves and pulps, and to minimize other sources of variance also affecting the sum of the areas of all the peaks, normalized rather than absolute peak areas were used. In order to normalize the variables, the area of each peak taken from the CZE electropherogram was divided by each one of the areas of the other peaks; in this way, and taking into account that each pair of peaks should be considered only once, (9x8)/2 = 36 and (14x13)/2 = 91 nonredundant peak ratios, for leaf and pulp samples, respectively, were obtained to be used as predictors.

Using the normalized variables, LDA models capable of classifying the olive leaf and pulp samples according to their respective cultivar were constructed. From the 54 samples of **Table 12.1,** two matrices, one for leaf and another for pulp samples, were constructed. These matrices contained 162 objects (which correspond to the three replicates of each sample) and the corresponding number of predictors (36 for leaf and 91 for pulp samples). A response column, containing the 9 categories corresponding to the 9 cultivars of olive leaves and pulps, was added to these matrices, which were used as an evaluation sets.

To construct the LDA training matrices, only the means of the three replicates of each sample were included (54 objects); in this way, the internal dispersion of the categories was reduced, which was important to reduce the number of variables selected by the SPSS stepwise algorithm during model construction.

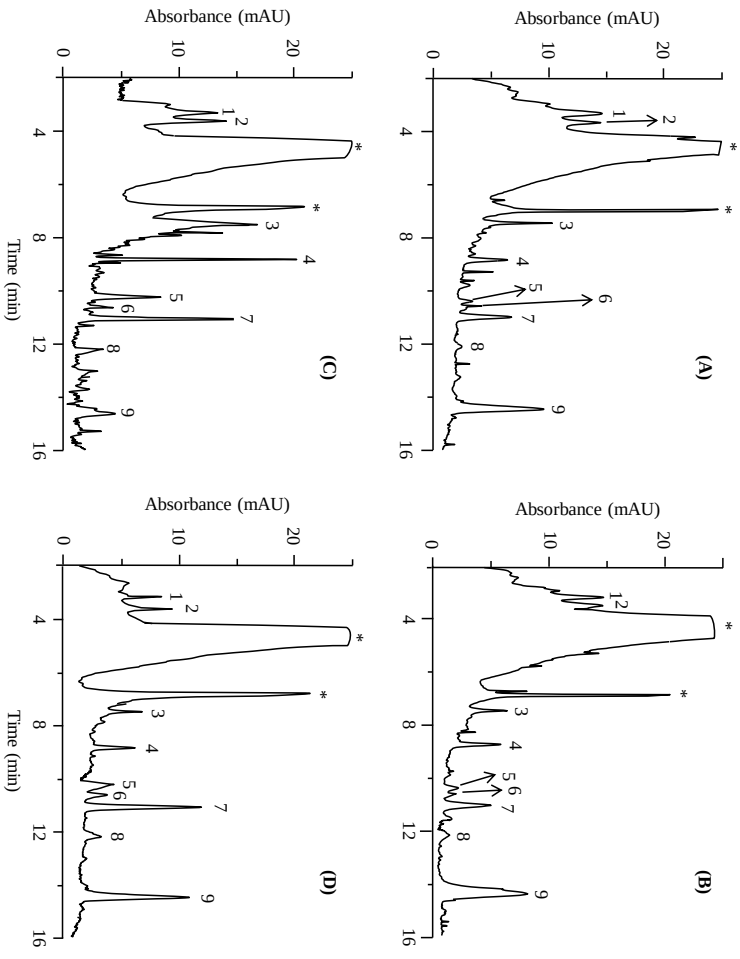

Figure 12.4. Representative CZE-electropherograms of Arbequina (A), Canetera (B), Manzanilla (C) and Picual (D) cultivar leaf samples. CZE conditions as in **Figure 12.1**.

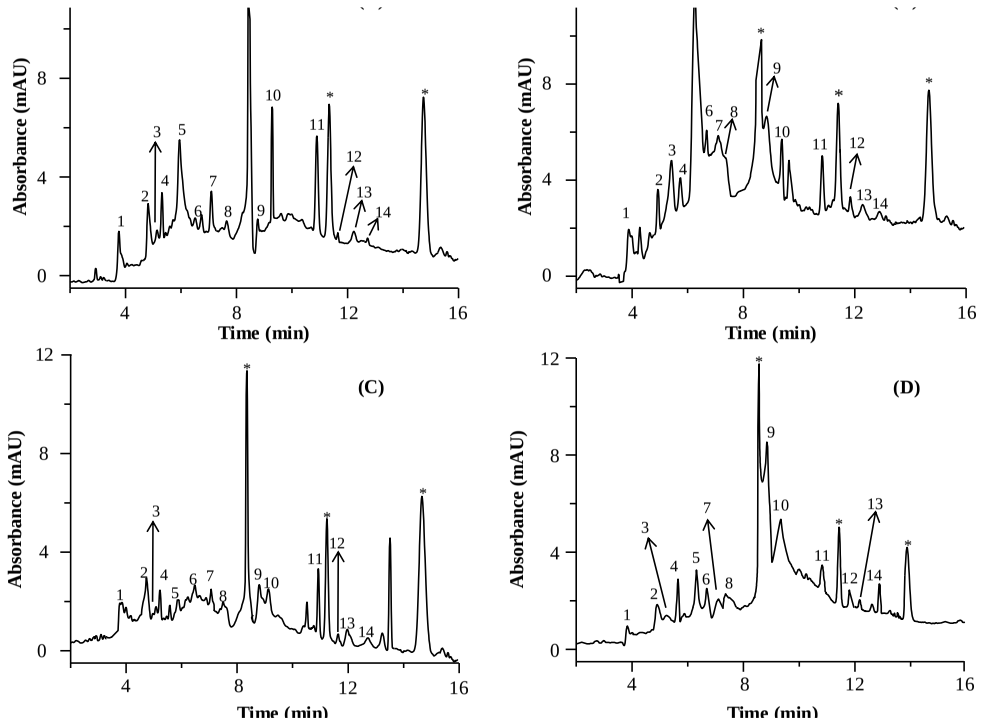

Figure 12.5. Representative CZE-electropherograms of Arbequina (A), Canetera (B), Manzanilla (C) and Picual (D) cultivar pulp samples. CZE conditions as in **Figure 12.1.**

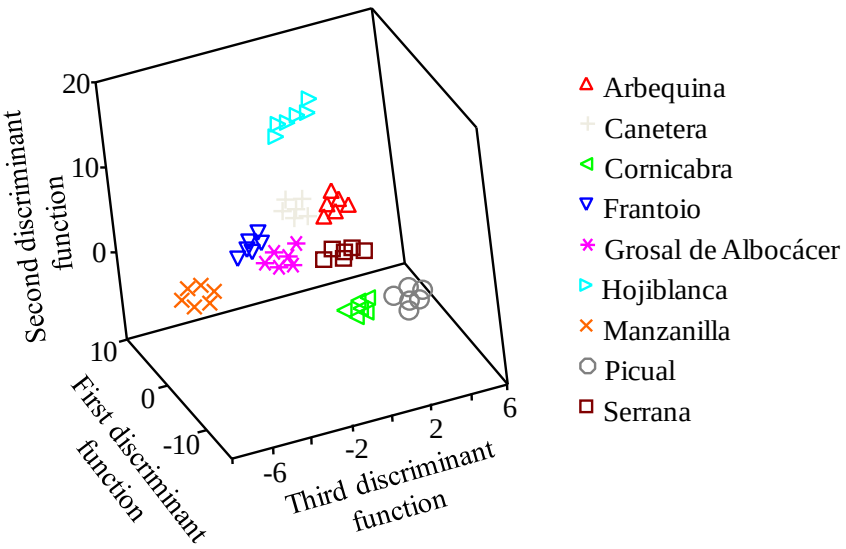

Figure 12.6A. Score plot on an oblique plane of the three-dimensional space defined by the three first discriminant functions of the LDA model constructed to classify olive leaves according to their cultivar.

First, and LDA model to classify the olive leaf samples was constructed. As it was shown in **Figure 12.6A,** an excellent resolution between all category pairs was achieved (λ_w = 0.18). The variables selected by the SPSS stepwise algorithm, and the corresponding standardised coefficients of the model, showing the predictors with large discriminant capabilities, are given in **Table 12.3A**. According to this table, the main protein peak ratios selected by the algorithm to construct the LDA model corresponded to 6/4 and 3/4 ratios. All the points of the training set were correctly classified by leave-one-out validation. To estimate the prediction capability of the model, the evaluation set, constituted by 54 original data points, was used. Using a 95% probability, all the objects were correctly classified; thus, the prediction capability was 100%.

Table 12.3A

Predictors selected and corresponding standardized coefficients of the LDA model constructed to classify olive leaf samples according to their cultivar.

Predictors[a]	f_1	f_2	f_3	f_4	f_5	f_6
9/7	0.66	0.69	0.47	-0.05	-0.09	-0.34
8/2	0.23	0.85	-0.80	0.48	0.50	0.51
6/5	0.13	-0.42	0.35	0.78	-0.66	0.31
6/4	-3.38	0.88	0.29	-0.58	0.05	-0.23
3/4	3.01	-0.87	0.39	0.52	0.88	-0.21
3/2	0.39	-0.50	0.69	-0.74	-0.49	0.58

[a] Ratios of intact protein peak areas.

Finally, another LDA model to classify the olive pulp samples was constructed. Also in this case, an excellent resolution between the all category pairs was obtained, being $\lambda_w = 0.11$ (see **Figure 12.6B**).

The variables selected and the corresponding model standardized coefficients are given in **Table 12.3B.** According to this table, the main protein peak ratios selected by the algorithm to construct the LDA model corresponded to 3/6, 6/10, 2/10 and 11/5 ratios. When leave-one-out cross-validation was applied to the training set, all the points were correctly classified. Finally, when the prediction capability of the model was tested by using the evaluation set, all the objects were correctly classified; thus, the prediction capability was 100%.

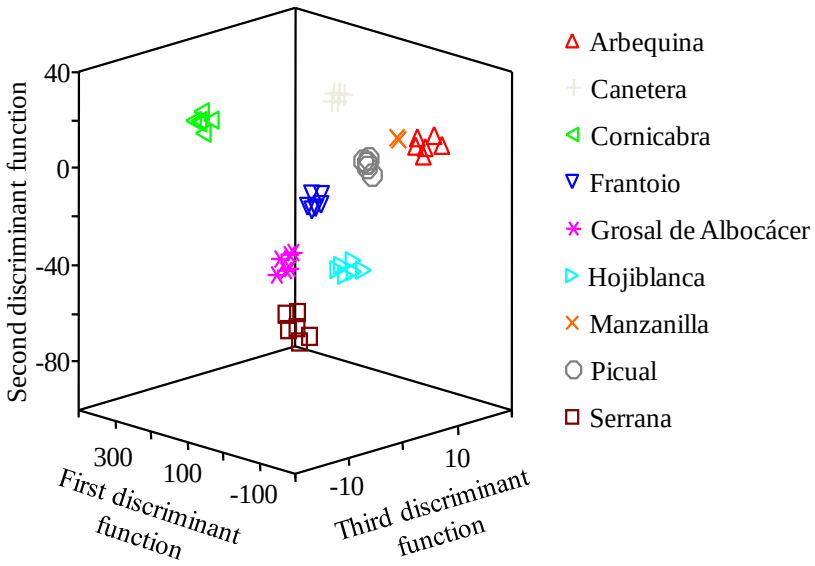

Figure 12.6B. Score plot on an oblique plane of the three-dimensional space defined by the three first discriminant functions of the LDA model constructed to classify olive pulps according to their cultivar.

Table 12.3B

Predictors selected and corresponding standardized coefficients of the LDA model constructed to classify olive pulp samples according to their cultivar.

Predictors[a]	f_1	f_2	f_3	f_4	f_5	f_6	f_7	f_8
11/5	17.41	3.07	4.85	-3.85	-0.90	0.60	0.10	-1.07
11/4	-8.52	1.60	0.75	2.39	-0.01	-0.15	-0.58	0.82
13/10	-0.18	-3.44	-3.35	-0.50	0.09	-0.54	0.05	-1.02
9/5	-7.53	-2.13	-4.80	2.38	0.89	-0.98	0.001	1.34
9/3	4.21	7.78	3.21	1.28	0.15	0.98	1.21	0.40
5/4	5.22	3.09	1.88	-0.70	0.72	0.004	0.09	-0.41
4/8	14.24	1.85	-2.16	-0.40	0.003	0.25	-0.25	0.04
2/10	-17.66	-3.94	2.24	-0.61	0.001	0.91	-0.73	0.12
3/6	28.05	7.60	-0.77	1.57	0.09	0.34	1.51	1.03
6/10	19.76	5.01	-1.79	-0.94	0.69	-0.28	0.37	0.70
6/8	3.70	-3.02	0.89	0.33	-0.14	0.04	0.05	-0.08

[a] Ratios of intact protein peak areas.

12.4. Conclusions

A quick and simple CZE method to separate proteins from olive leaves and pulps has been developed. In the proposed procedure, separation is performed within 15 min, which is significantly lower than the 40 min required in other CE procedure described in the literature for the same matrix. In addition, another non-negligible advantage is the use of an environmental friendly extraction protocol compared with traditional organic solvent extraction. Moreover, the possibility of distinguishing olive leaves and pulps according to their cultivar by using intact protein profiles obtained by CZE has been demonstrated in this work. Different protein profiles, with 9 and 14 common peaks, for leaf and pulp samples, respectively, were observed in all the cultivars considered in this study. Thus, the normalized protein peak areas were employed as predictors to construct LDA models. Both, olive leaf and pulp samples belonging to nine cultivars from different Spanish regions were correctly classified with an excellent resolution among all the categories, which demonstrated that intact protein profiles are characteristic of each cultivar.

Acknowledgements

This work was supported by project CTQ2010- 15335 (MINECO of Spain and FEDER) ACOMP/2013/196 (Generalitat Valenciana). M. V-B thanks the MEC for an FPU grant for PhD studies. M.J. L-G thanks the Generalitat Valenciana for a VALi+d postdoctoral contract. Authors also thank Ramiro Martínez from Novozymes (Spain) for his support.

12.5. References

Castro-Puyana, M.; García-Cañas, V.; Simó, C.; Cifuentes, A. (**2012**). Recent advances in the application of capillary electromigration methods for food analysis and Foodomics. *Electrophoresis, 33,* 147-167.

Esteve, C.; Cañas, B.; Moreno-Gordaliza, E.; Del Río, C.; García, M.C.; Marina, M.L. (**2011**). Identification of Olive (*Olea europaea*) pulp proteins by matrix-assisted laser desorption/ionization time-of-flight mass spectrometry and nano-liquid chromatography tandem mass spectrometry. *Journal of Agriculture and Food Chemistry, 59,* 12093-12101.

Esteve, C.; D' Amato, A.; Marina, M. L.; García, M. C.; Citterio, A.; Righetti, P.G. (**2012**). Identification of olive (Olea europaea) seed and pulp proteins by nLC-MS/MS via combinatorial peptide ligand libraries. *Journal of Proteomics, 75,* 2396-2403.

Esteve, C.; D' Amato, A.; Marina, M.L.; García, M.C.; Righetti, P.G. (**2013**). Analytical approaches for the characterization and identification of olive (*Olea europaea*) oil proteins. *Journal of Agriculture and Food Chemistry,* 61, 10384-10391.

Esteve, C.; Del Río, C.; Marina, M.L.; García, M.C. (**2011**). development of an ultra-high performance liquid chromatography analytical methodology for the profiling of olive (*Olea Europaea L.)* pulp proteins. *Analytica Chimica Acta, 690***,** 129-134.

García, J.L.; Avidan, N.; Troncoso, A.; Sarmiento, R.; Lavee, S. (**2000**). Possible juvenile-related proteins in olive tree tissues. *Scientia Horticulturae, 85,* 271-284.

García-Ruiz, C.; García, M.C.; Cifuentes, A.; Marina, M.L. (**2007**). Characterization and differentiation of diverse transgenic and

nontransgenic soybean varieties from CE protein profiles. *Electrophoresis, 28*, 2314–2323.

Georgalaki, M.D.; Bachmann, A.; Sotiroudis, T.G.; Xenakis, A.; Porzel, A.; Feussner, I. (**1998A**). Characterization of a 13-lipoxygenase from virgin olive oil and oil bodies of olive endosperms. *Fett-Lipid, 100*, 554-560.

Georgalaki, M.D.; Sotiroudis, TG.; Xenakis, A. (**1998B**). The presence of oxidizing enzyme activities in virgin olive oil. *Journal of the American Oil Chemists' Society, 75*, 155-159.

Hatzopoulos, P.; Banilas, G.; Giannoulia, K.; Gazis, F.; Nikoloudakis, N.; Milioni, D.; Haralampidis, K. (**2002**). Breeding, molecular markers and molecular biology of the olive tree. *European Journal of Lipid Science and Technology*, *104*, 574-586.

Herrero, M.; García-Cañas, V.; Simó, C.; Cifuentes, A. (**2010**). Recent advances in the application of capillary electromigration methods for food analysis and Foodomics. *Electrophoresis, 31*, 205-228.

Herrero-Martínez, J.M.; Simó-Alfonso, E.F.; Ramis-Ramos, G.; Gelgi, C.; Righetti, P.G. (**2000**). Determination of cow's milk and ripening time in nonbovine cheese by capillary electrophoresis of the ethanol-water protein fraction. *Electrophoresis, 21*, 633-640.

Hubbs, A.; Roy, H. (**1992**). Synthesis and assembly of large subunits into ribulose bisphosphate carboxylase/oxygenase in chloroplast extracts. *Plant Physiology, 100*, 272-281.

Koidis, A.; Boskou, D. (**2006**). The contents of proteins and phospholipids in cloudy (veiled) virgin olive oils. *European Journal of Lipid Science and Technology, 108*, 323-328

Lerma-García, M.J.; Herrero-Martínez, J.M.; Ramis-Ramos, G.; Mongay-Fernández, C.; Simó-Alfonso, E.F. (**2009**). Prediction of the curing time of

Spanish hams using peptide profiles established by capillary zone electrophoresis. *Food Chemistry, 113,* 635–639.

Martín-Hernández, C.; Bénet, S; Obert, L. (**2008**). Determination of proteins in refined and nonrefined oils. *Journal of Agricultural and Food Chemistry, 56,* 4348-4351.

Meyer, Y.; Grosser, J.; Chartier, Y.; Cleyet-Marel, J.C.C. (**1988**). Preparation by two-dimensional electrophoresis of proteins for antibody production: antibody against proteins whose synthesis is reduced by auxin in tobacco mesophyll protoplasts. *Electrophoresis, 9,* 704-712.

Montealegre, C.; García, M.C.; Del Río, C.; Marina, M.L.; García-Ruiz, C. (**2012**). Separation of olive proteins by capillary gel electrophoresis. *Talanta, 97,* 420-424.

Montealegre, C.; Marina, M.L.; García-Ruiz, C. (**2010**). separation of olive proteins combining a simple extraction method and a selective capillary electrophoresis (CE) approach: application to raw and table olive samples. *Journal of Agriculture and Food Chemistry. 58,* 11808-11813.

Ross, J.H.E.; Sanchez, J.; Millan, F.; Murphy, D.J. (**1993**). Differential presence of oleosins in oleogenic seed and mesocarp tissue in olive (*Olea europaea*) and avocado (*Persea Americana*). *Plant Science, 93,* 203-210.

Ruiz-Ángel, M.J.; Simó-Alfonso, E.F.; Mongay-Fernández, C.; Ramis-Ramos, G. (**2002**). Identification of Leguminosae gums and evaluation of carob-guar mixtures by capillary zone electrophoresis of protein extracts. *Electrophoresis, 23,* 1709-1715.

Saha, S.; Callahan, F.E.; Dollar, D.A.; Creech, J.B. (**1997**). Effect of lyophilization of cotton tissue on the quality of extractible DNA, RNA and protein. *Journal of Cotton Science, 1,* 10-14.

Sebastián-Francisco, I.; Simó-Alfonso, E.F.; Mongay-Fernández, C.; Ramis-Ramos, G. (**2004**). Improvement of the electrophoretic protein profiles of *Leguminosae* gum extracts using gamanase and application to the evaluation of carob–guar mixtures. *Analytica Chimica Acta, 508*, 135-140.

Soni M. G.; Burdock, G.A.; Christian, M.S.; Bitler, C.M.; Crea, R. (**2006**). Safety assessment of aqueous olive pulp extract as an antioxidant or antimicrobial agent in foods. *Food and Chemical Toxicology, 44,* 903–915.

Vandeginste, B.G.M.; Massart, D.L.; Buydens, L.M.C.; De Jong, S.; Lewi, P.J.; Smeyers-Verbeke, J. (**1998**). Data Handling in Science and Technology, Part B, Elsevier, Amsterdam

Wang, W.; Scali, M.; Vignani, R.; Spadafora, A.; Sensi, E.; Mazzuca, S.; Cresti, M. (**2003**). Protein extraction for two-dimensional electrophoresis from olive leaf, a plant tissue containing high levels of interfering compounds. *Electrophoresis 24*, 2369-2375.

Chapter 13. Classification of olive leaves and pulps according to their cultivar by using protein profiles established by capillary gel electrophoresis

Anal Bioanal Chem (2014) 406:1731–1738
DOI 10.1007/s00216-013-7585-7

RESEARCH PAPER

Classification of olive leaves and pulps according to their cultivar by using protein profiles established by capillary gel electrophoresis

María Vergara-Barberán · María Jesús Lerma-García · José Manuel Herrero-Martínez · Ernesto Francisco Simó-Alfonso

A method to classify olive leaves and pulps according to their cultivar using protein profiles obtained by CGE has been developed. For this purpose, proteins were extracted using an enzyme-assisted method, which provided higher protein recoveries than other previously described methods. Ten and nine common peaks, for leaf and pulp samples, respectively, were identified in the twelve cultivars studied in this work. In addition, and using linear discriminant analysis of the CGE data, olive leaf and pulp samples belonging to twelve cultivars from different Spanish regions were correctly classified with an excellent resolution among all the categories, which demonstrated that protein profiles are characteristic of each cultivar.

Keywords: Olive leaf; olive pulp; protein profiles; CGE; cultivar; linear discriminant analysis

13.1. Introduction

Olive (*Olea europeaea* L.) is a typical tree species present throughout the Mediterranean countries. It is among the oldest known cultivated trees in the world and it is an economically important crop due to the high quality of its oil. Thus, the olive tree and its products (leaves, olive fruit and oil) have a rich history of nutritional, medicinal and commercial purposes (Soni, 2006). For these reasons, several molecular markers have been established in order to distinguish, characterize or identify cultivars, to estimate germplasm variability and to trace olive origin (Hatzopoulos, 2002).

Among the different compounds that contain olive tree products (leaves and fruits), proteins have been less studied than other components, such as phenolic compounds (El-Khawaga, 2010; Salah, 2012), although several reports have demonstrated their important role in the processing and quality of olives and olive oil (Georgalaki, 1998A; Georgalaki, 1998; B Koidis, 2006). Moreover, there are works showing that proteins present in oils may elicit allergic reactions in sensitive individuals (Martín-Hernández, 2008; Esteve, 2011).

The determination of olive leaf proteins has been conducted by SDS-PAGE (García, 2000; Wang, 2003). García *et al*. (García, 2000) have compared the protein composition of juvenile and adult leaves, bark and bud tissues. Protein groups at 14, 29, 55 and 63 kDa were found in juvenile leaves, while the most expressed protein group found in adult tissues was located at 35 kDa. Wang et al. (Wang, 2003) have also separated leaf proteins using 1- and 2-dimensional gel electrophoresis. In this case, only a protein at 55 kDa was observed, which was assigned as Rubisco. This protein is characteristic of leaf protein fractions of many plant species (Meyer, 1988; Hubbs, 1992; Saha, 1997). On the other hand, different techniques, such as SDS-PAGE, UHPLC (Esteve, 2011), CZE (Montealegre, 2010) and CGE (Montealegre, 2012), have been proposed to

carry out pulp protein separation. After testing several olive pulp protein extraction methods, Esteve *et al* (Esteve, 2011) have separated pulp peptides and proteins from different cultivars by both SDS-PAGE and UHPLC. In most cultivars, a protein group at 20-25 kDa was observed. In addition to this, when UHPLC protein profiles were compared, several differences were evidenced. On the other hand, Montealegre *et al*. (Montealegre, 2010) employed CZE to separate proteins from raw and table olive samples. The resulting profiles were compared, showing differences according to their botanical variety and geographical region. Furthermore, CGE was also used to separate proteins from olive fruits of different cultivar and geographical origin. In all cases, seven common peaks were identified, being their molecular masses comprised between 10 to 50 kDa. Using these peaks, a discriminant analysis model was constructed to classify samples according to their geographical origin. The prediction capability of this model was 80%. However, to our knowledge, any work has been reported using CGE protein profiles as predictor variables to discriminate among diverse olive leaf and pulp cultivars.

The aim of this work was to study the possibility of distinguishing olive leaves and pulps according to their cultivar by using protein profiles established by CGE. For this purpose, olive leaf and pulp samples from 12 cultivars collected from different Spanish regions were employed. The normalized protein peak areas obtained from the CGE electropherograms were employed as predictors to construct two LDA models.

13.2. Materials and methods

13.2.1. Chemicals

ACN and acetone were purchased from Scharlau (Barcelona, Spain). Tris and SDS, were obtained from Sigma-Aldrich (St. Louis, MO, USA). 2-Mercaptoethanol, sodium hydroxide pellets and hydrochloric acid (HCl) were

purchased from Merck (Darmstadt, Germany). Two molecular weight size protein standards (6.5-66 kDa and 36-200 kDa) were also provided by Sigma-Aldrich. A Protein Quantification Kit-Rapid from Fluka (Steinheim, Germany) was used for Bradford protein assay. The following enzymes, kindly donated by Novozymes (Bagsvaerd, Denmark) were used: lipase (Palatase® 20000 L; activity 20000 LU-MM/g (LU = lipase unit); optimal working conditions, pH 7 and 25 - 45 ºC) and cellulase (Celluclast® 1.5L; activity 1500 NCU/g (NCU = novo cellulase unit); working conditions, pH 4.5 - 6.0 and 50 - 60 ºC). For CGE analysis, a SDS-MW analysis gel buffer (pH 8, 0.2% SDS) from Beckman (Coulter, Inc., Fullerton, CA) was employed. Deionized water (Barnstead deionizer, Sybron, Boston, MA) was also used.

13.2.2. Samples

The olive leaves and fruits employed in this study (**Table 13.1**) were kindly donated by different olive oil manufacturers. To assure a correct sampling, both olive leaves and fruits were collected at the same period (end of November 2011) directly from trees located in different Spanish regions. The cultivar of samples was guaranteed by the suppliers. Both olive leaves and fruits were previously selected to assume the absence of mold or other microorganisms, washed with water to remove dust or airborne particles settled on the olive and then stored at -20ºC prior their use.

13.2.3. Instrumentation

An HP^{3D} CE system (Agilent, Waldbronn, Germany) provided with a diode-array spectrophotometric detector and uncoated fused-silica capillaries (Polymicro Technologies, Phoenix, AZ) of 33.5 cm length (25 cm effective length) x 50 µm id (375 µm od) were used. New capillaries were successively flushed with 1 and 0.1 M NaOH and water at 60º C for 10 min each. Daily, before use, the capillary was successively rinsed with 0.1 M NaOH for 5 min,

0.1 M HCl and water for 2 min each, and SDS-MW analysis gel buffer for 10 min. This conditioning was also applied after 6 successive injections. Electrokinetic injections at -30 kV x 7 s were performed. Separations were carried out at -15 kV at 25 ºC. Detection was done at 214 nm.

13.2.4. Sample preparation

In order to proceed to protein extraction, olive leaves and pulps were treated as follows: *ca.* 20 g of fresh leaves / pulps were frozen in liquid nitrogen and ground to a fine powder in a pre-cooled mortar and pestle, lyophilized, and the resulting powder was next homogenized. For the extraction of olive leaf proteins, 0.3 g lyophilized powder were treated with 3 mL of a water:ACN mixture (7:3, v/v) containing a 5% (v/v) cellulase enzyme at pH 5.0, and sonicated at 55 ºC for 15 min. On the other hand, for the extraction of pulp proteins, 0.3 g of powder were treated with 3 mL of water at pH 7.0 containing a 5% (v/v) lipase, and sonicated at 30 ºC for 15 min. Next, both leaf and pulp protein extracts were centrifuged at 10000 × *g* for 10 min, and stored at -20 ºC until their use.

For CGE analysis, samples were prepared by taking the proper volume of protein extract (to give a final protein concentration range of 0.2 – 2 mg mL^{-1}), 10 µL of 2-mercaptoethanol and 85 µL of sample buffer (0.1 M Tris-HCl pH 9.0, 1% (w/v) SDS). 2-Mercaptoethanol was used since it reduces protein disulfide bonds, providing a more accurate assessment of the molecular weight of the olive leaf and pulp proteins. To complete protein reduction, the resulting mixtures were heated at 95 ºC for 5 min, cooled in a room-temperature water bath for 5 min, and injected by triplicate into the CE system. The migration times of the three replicates were used to evaluate the method reproducibility. Also, the mean of the area of the replicates was used for the construction of LDA training matrices, while the area of the individual replicates was employed for the construction of LDA evaluation set.

Table 13.1

Cultivar, geographical origin, number of samples and total protein content (mg g^{-1}) of the olive leaves and pulps used in this study

Cultivar	Geographical origin	Nº samples	Leaf protein content (mg g^{-1}) (n = 6)	Pulp protein content (mg g^{-1}) (n = 6)
Arbequina	Altura (Castellón)	2	0.88 ± 0.01	2.71 ± 0.13
	Puente Genil (Córdoba)	2		
	Jumilla (Murcia)	1		
	Alicante	1		
Blanqueta	Alicante	1	0.37 ± 0.02	1.51 ± 0.07
	Alcalatén *comarca* (Castellón)	2		
	Pobla del Duc (Valencia)	3		
Canetera	Altura (Castellón)	2	0.78± 0.02	0.99 ± 0.05
	Adzaneta (Castellón)	2		
	La Plana *comarca* (Castellón)	2		
Cornicabra	Requena (Valencia)	2	0.90 ± 0.01	0.52 ± 0.01
	Daimiel (Ciudad Real)	2		
	Jumilla (Murcia)	1		
	Villapalacios (Albacete)	1		
Frantoio	Puente Genil (Córdoba)	2	0.82 ± 0.01	0.92 ± 0.04
	Jumilla (Murcia)	1		
	Altura (Castellón)	3		
Gordal	Altura (Castellón)	2	0.52 ± 0.01	1.51 ± 0.07
	Pobla del Duc (Valencia)	2		
	Jérica (Castellón)	2		

Table 13.1

Cont.

Cultivar	Geographical origin	Nº samples	Leaf protein content (mg g^{-1}) (n = 6)	Pulp protein content (mg g^{-1}) (n = 6)
Grosal de Albocácer	Pobla del Duc (Valencia)	2	0.27 ± 0.01	0.62 ± 0.04
	Requena (Valencia)	1		
	La Noguera (Lleida)	3		
Hojiblanca	Puente Genil (Córdoba)	1	0.64 ± 0.02	0.96 ± 0.03
	Estepa (Sevilla)	2		
	Jumilla (Murcia)	2		
	Fuente de Piedra (Málaga)	1		
Lechín de Granada	Jumilla (Murcia)	3	0.67 ± 0.01	1.92 ± 0.09
	Tabernas (Almeria)	3		
Manzanilla	Ahigal (Cáceres)	2	0.88 ± 0.02	1.20 ± 0.06
	Altura (Castellón)	2		
	Requena (Valencia)	2		
Picual	Santaella (Córdoba)	2	0.98 ± 0.01	1.06 ± 0.05
	Villapalacios (Albacete)	1		
	Jumilla (Murcia)	3		
Serrana	Altura (Castellón)	1	0.45 ± 0.01	1.88 ± 0.09
	Viver (Castellón)	2		
	Artana (Castellón)	1		
	Jérica (Castellón)	2		

13.2.5. Molecular masses calculation and statistical analysis

In order to determine the molecular masses corresponding to the electrophoretic peaks, two calibration curves, for leaf and pulp proteins, were obtained by using 8 (comprised from 29 to 200) and 6 (from 20 to 66) molecular weight size protein standards, respectively, which were injected under the same CGE conditions as samples. To construct these curves, the logarithm of the standard protein molecular masses was plotted against the ratio of the migration time of reference (t_{ref}) peak (EOF peak) and the migration time of sample proteins (t_i). The calibration curves obtained for leaf and pulp proteins were: log MW = -3.094 (t_{ref}/t_i) + 3.4811 (r = 0.9959) and log MW = -2.634(t_{ref}/t_i) + 3.239 (r = 0.9946).

Once the peak are of each protein was measured, a data matrix was constructed using the areas of all protein peaks as original variables. After normalization of the variables, statistical data treatment was performed using SPSS (v. 15.0, Statistical Package for the Social Sciences, Chicago, IL). LDA, a supervised classificatory technique, is widely recognized as an excellent tool to obtain vectors showing the maximal resolution between a set of previously defined categories. In LDA, vectors minimizing the Wilks' lambda, λ_w, are obtained (Vandeginste, 1998). This parameter is calculated as the sum of squares of the distances between points belonging to the same category divided by the total sum of squares. Values of λ_w approaching zero are obtained with well-resolved categories, whereas overlapped categories made λ_w approach one. Up to N-1 discriminant vectors are constructed by LDA, with N being the lowest value for either the number of predictors or the number of categories. The selection of the predictors to be included in the LDA models was performed using the SPSS stepwise algorithm. According to this algorithm, a predictor is selected when the reduction of λ_w produced after its inclusion in the model exceeds F_{in}, the entrance threshold of a test of comparison of variances or F test. However, the entrance of a new predictor

modifies the significance of those predictors that are already present in the model. For this reason, after the inclusion of a new predictor, a rejection threshold, F_{out}, is used to decide if one of the other predictors should be removed from the model. The process terminates when there are no predictors entering or being eliminated from the model. The default probability values of F_{in} and F_{out}, 0.05 and 0.10, respectively, were adopted.

13.3. Results and discussion

13.3.1. Characterization of protein profiles of olive leaves and pulps

All the olive leaf and pulp protein extracts of the samples included in **Table 13.1** were subjected to SDS-CGE analysis. Representative electropherograms of Canetera (A), Frantoio (B), Manzanilla (C) and Picual (D) olive leaf samples are shown in **Figure 13.1.**

A total of 11 common peaks were obtained for all the cultivars studied. The molecular masses of these peaks were determined by using the calibration curve previously described. Two different protein groups, at 20 - 25 kDa (peaks 1 and 2) and at 29 kDa (peak 3) were identified. These results were in agreement with those described by García *et al*. (García, 2000) in juvenile olive leaves.

Next, peak 4 was the peak provided by the enzyme used to extract leaf proteins (cellulase, 44 kDa), peak 5 was assigned as an oleosin protein of 50 kDa (Ross, 1993; Montealegre, 2012), and peak 6 was attributed as ribulose-1,5-bisphosphate carboxylase (Rubisco, 55 kDa) (Meyer, 1988; Hubbs, 1992; Saha, 1997; García, 2000). The molecular masses of the other peaks (7 – 11), which were comprised between *ca.* 80 and 300 kDa, could be assigned as protein dimers.

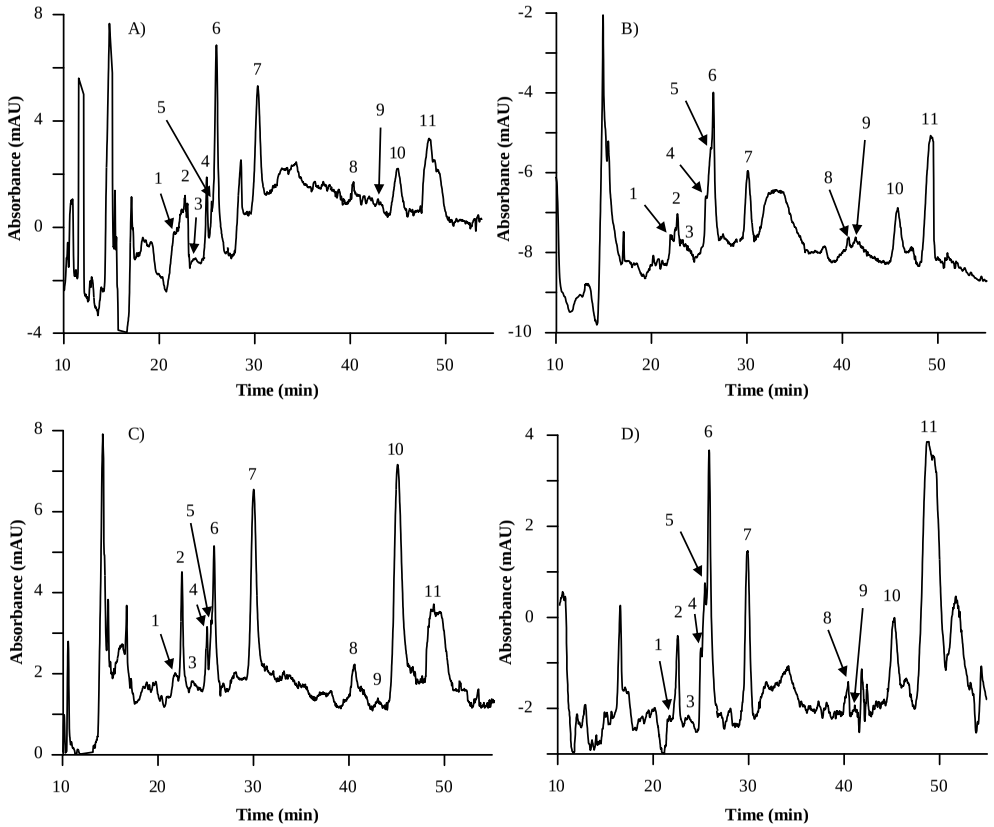

Figure 13.1. Representative CGE-electropherograms of Canetera (A), Frantoio (B), Manzanilla (C) and Picual (D) cultivar leaf samples. CGE conditions: Electrokinetic injection, -30 kV for 7 s; separation

On the other hand, representative SDS-CGE electropherograms of Blanqueta (A), Cornicabra (B), Frantoio (C) and Gordal (D) olive pulp proteins are shown in **Figure 13.2**. Also in this case, 11 common peaks were observed in all cultivars, being their molecular masses determined with the corresponding calibration curve. Peaks 1 to 4 were attributed to polypeptides, whose masses were lower than 20 kDa. Other polypeptides derived from the precursor of 41 kDa and 47.5 kDa were observed at 22-30 kDa (peaks 5-7), which could be attributed to storage proteins. Peak 9 was identified as a precursor at 47.5 kDa, while peak 10 was attributed to an oleosin at 50 kDa. Finally, peaks 8 and 11 were the peaks provided by the enzyme used to extract pulp proteins (lipase, 30 and 60 kDa).

Next, precision of the method was evaluated by studying the intra- and interday reproducibilities of migration times of some proteins obtained by injecting the olive leaf and pulp protein extract of the Frantoio sample from Jumilla 3 times per day during 3 days. In all cases, the RSD values were lower than 2.1 % and 2.6 % for leaf and pulp protein peaks, respectively (see **Table 13.2**).

Table 13.2

Migration times reproducibility for olive leaf and pulp proteins from Frantoio cultivar (Jumilla).

Parameter	Leaf RSD[a] ,% (n=3)	RSD[b] ,% (n=9)	Parameter	Pulp RSD[a] ,% (n=3)	RSD[b] ,% (n=9)
t_{eof} (min)	**0.5**	**0.9**	**t_{eof} (min)**	**1.3**	**1.9**
t_2 (min)	0.8	1.4	t_2 (min)	1.6	2.2
t_6 (min)	1.1	1.8	t_4 (min)	1.2	2.4
t_7 (min)	0.7	1.6	t_8 (min)	1.2	2.6
t_{10} (min)	1.2	2.1	t_{10} (min)	0.8	1.6

[a] Intraday RSD, obtained injecting 3 times per day

[b] Interday RSD, obtained injecting 3 times per day during 3 days

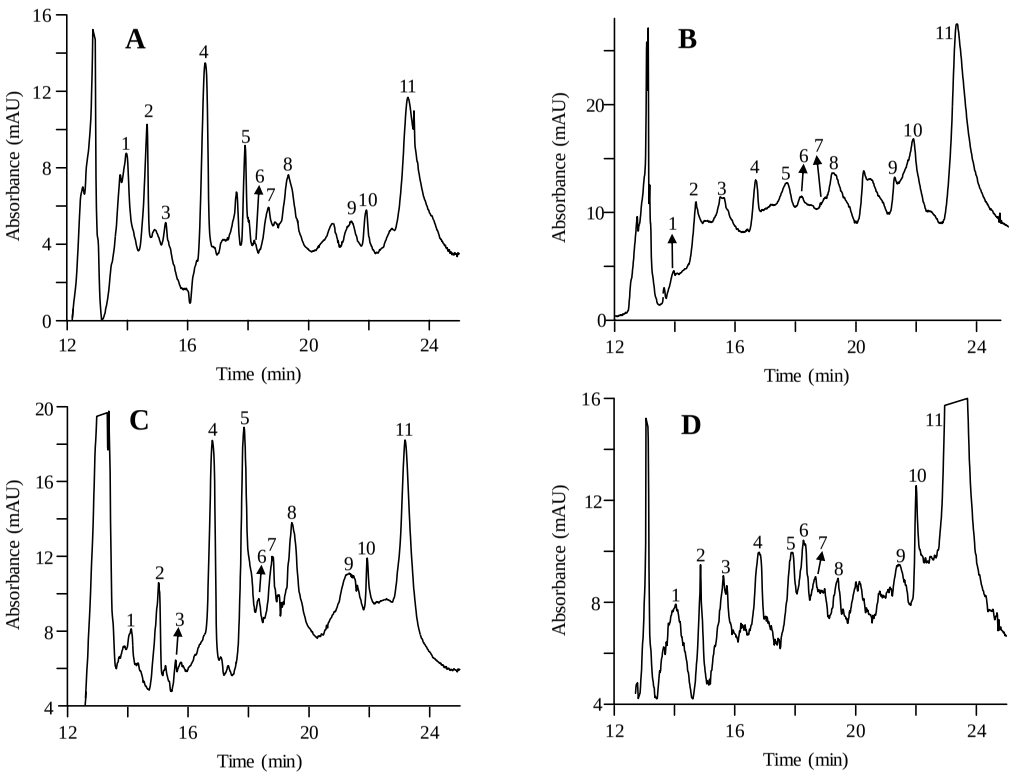

Figure 13.2 Representative CGE-electropherograms of Blanqueta (A), Cornicabra (B), Frantoio (C) and Gordal (D) cultivar pulp samples. CGE experimental conditions as in **Figure 13.1.**

13.3.2. Normalization of the variables and construction of LDA models

For the construction of LDA models, all the previously identified peaks were selected as variables, except the peaks provided by the enzyme used to extract proteins (peak 4 in leaf and peaks 8 and 11 in pulp samples). Before the construction of the models, these peaks were normalized to reduce the variability associated with sources of variance that can affect the sum of the areas of all peaks. To normalize the variables, the area of each peak was divided by each one of the areas of the other peaks; in this way, and taking into account that each pair of peaks should be considered only once, (10x9)/2 = 45 and (9x8)/2 = 36 nonredundant peak ratios, for leaf and pulp samples, respectively, were obtained to be used as predictors.

Using the normalized variables, LDA models capable of classifying the olive leaf and pulp samples according to their respective cultivar were constructed. From the 72 samples of **Table 13.1**, two matrices, one for leaf and another for pulp samples, were constructed. These matrices contained 216 objects (which correspond to the three replicates of each sample) and the corresponding number of predictors (45 for leaf and 36 for pulp samples). A response column, containing the 12 categories corresponding to the 12 cultivars of olive leaves and pulps, was added to these matrices, which were used as an evaluation sets. To construct the LDA training matrices, only the means of the three replicates of each sample were included (72 objects); in this way, the internal dispersion of the categories was reduced, which was important to reduce the number of variables selected by the SPSS stepwise algorithm during model construction.

First, and LDA model to classify the olive leaf samples was constructed. As it was shown in **Figure 13.3**, an excellent resolution between all category pairs was achieved (λ_w = 0.14). As shown in the score plot of the plane of the first and second discriminant functions (**Figure 13.3A**), Arbequina, Frantoio, Grosal de Albocácer, Lechín de Granada, Picual and Serrana categories were

clearly resolved from the other six categories. All these categories appeared separated when the plane of the second and third discriminant functions was represented. Finally, as illustrated in **Figure 13.3C**, by using a plane oblique to the three first discriminant functions, all the possible pair of categories were very well resolved from each other. The variables selected by the SPSS stepwise algorithm, and the corresponding standardised coefficients of the model, showing the predictors with large discriminant capabilities, are given in **Table 13.3**. According to this table, the main protein peak ratios selected by the algorithm to construct the LDA model corresponded to 7/10, 3/10, and 9/11 ratios. All the points of the training set were correctly classified by leave-one-out validation. To estimate the prediction capability of the model, the evaluation set, constituted by 72 original data points, was used. Using a 95% probability, all the objects were correctly classified; thus, the prediction capability was 100 %. Finally, another LDA model to classify the olive pulp samples was constructed. Also in this case, an excellent resolution between the all category pairs was obtained, being λ_w = 0.12. According to **Figure 13.4A** (score plot of the plane of the two first discriminant functions), all categories appeared clearly resolved from each other except Arbequina–Hojiblanca and Canetera–Cornicabra pairs, which partially overlapped. Arbequina–Hojiblanca pair was resolved in the plane formed by the first and the third discriminant functions (**Figure 13.4B),** while the Canetera–Cornicabra pair was resolved in the plane formed by the first and the fourth discriminant functions (data not shown). Finally, all the possible category pairs were very well resolved from each other when a plane oblique of the three first discriminant functions was represented (**Figure 13.4C**). The variables selected and the corresponding model standardized coefficients are given in **Table 13.4**. According to this table, the main protein peak ratios selected by the algorithm to construct the LDA model corresponded to 4/6, 4/5, and 1/6 ratios.When leave-one-out cross-validation was applied to the training set, all the points were correctly classified. Finally, when the

prediction capability of the model was tested by using the evaluation set, all the objects were correctly classified; thus, the prediction capability was 100 %.

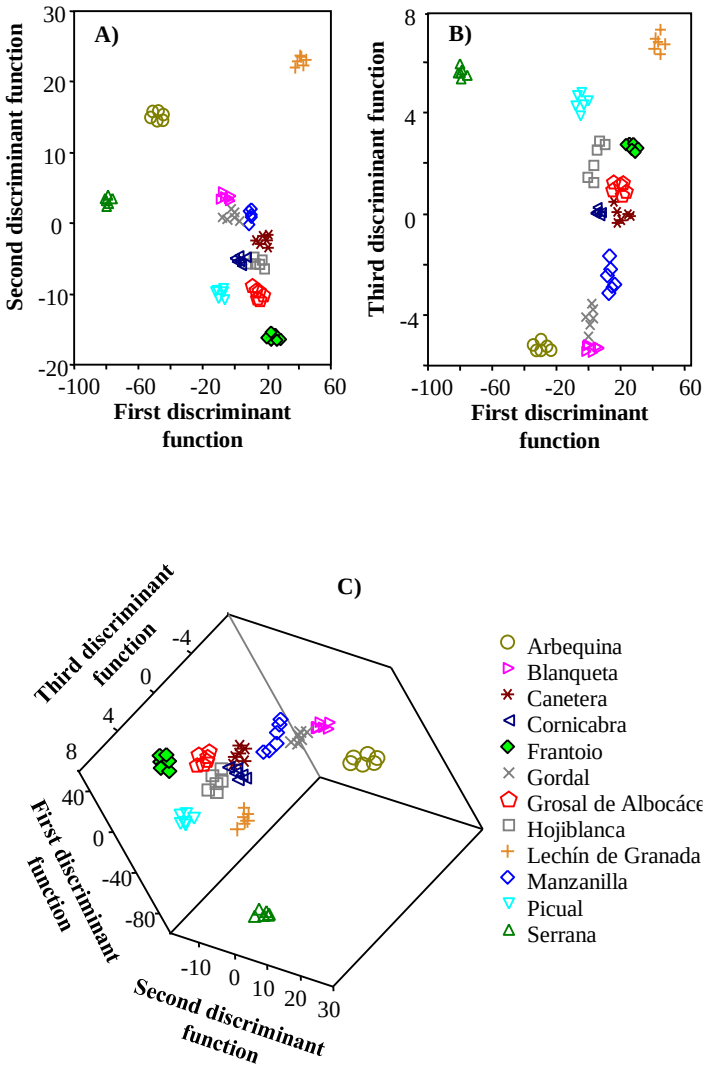

Figure 13.3. Score plot on the plane of the first and second (A), and first and third discriminant functions (B), and on an oblique plane of the three-dimensional space defined by the three first discriminant functions (C) of the LDA model constructed to classify olive leaves according to their cultivar.

Table 13.3

Predictors selected and corresponding standardized coefficients of the LDA model constructed to classify olive leaf samples according to their cultivar.

Predictors[a]	f_1	f_2	f_3	f_4	f_5	f_6	f_7	f_8	f_9	f_{10}
1/2	-2.72	-1.24	1.04	2.47	-0.84	-0.27	-0.37	0.06	-0.17	-0.13
3/7	-4.83	-0.66	0.52	1.84	-0.10	0.44	-1.12	0.45	0.13	0.04
3/10	13.08	-2.96	-0.26	-0.88	0.84	-0.34	1.05	-0.14	-0.64	-0.45
5/11	1.84	1.87	2.01	-2.40	-0.23	0.30	0.35	0.33	0.17	-0.24
6/10	8.36	-0.70	0.57	2.01	0.95	0.46	0.70	-0.19	0.82	0.47
7/9	1.43	1.54	-0.90	0.66	-0.14	0.84	0.37	0.40	0.09	0.14
7/10	-30.90	5.22	1.14	-0.09	0.02	0.20	-1.27	0.16	-0.07	0.06
7/11	0.50	0.40	-1.60	2.64	0.30	-0.35	-0.43	-0.23	0.05	-0.26
8/10	7.71	-11.23	-2.12	1.91	-2.58	-1.61	-0.28	1.02	0.14	-1.36
9/11	10.62	9.21	0.15	-4.78	1.89	1.22	1.10	-0.05	-0.33	1.76

[a] Ratios of protein peak areas.

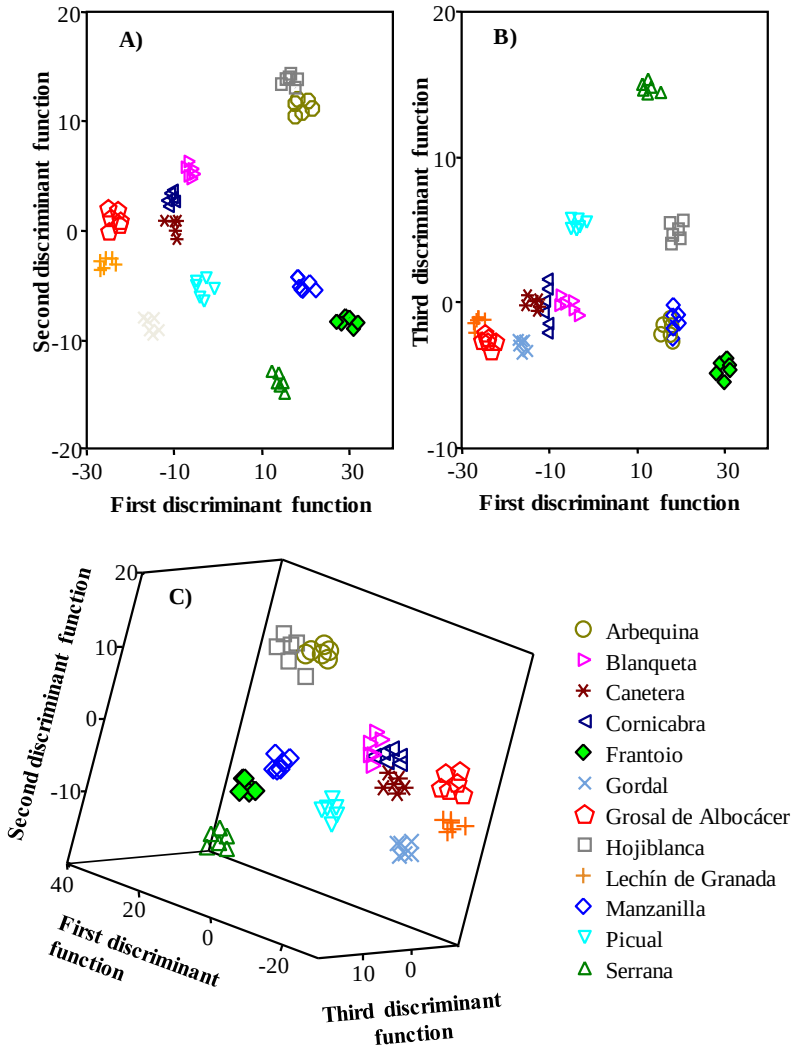

Figure 13.4. Score plot on the plane of the first and second (A), and first and third discriminant functions (B), and on an oblique plane of the three-dimensional space defined by the three first discriminant functions (C) of the LDA model constructed to classify olive pulps according to their cultivar.

Table 13.4

Predictors selected and corresponding standardized coefficients of the LDA model constructed to classify olive pulp samples according to their cultivar

Predictors[a]	f_1	f_2	f_3	f_4	f_5	f_6	f_7	f_8	f_9
1/4	-1.15	-0.15	0.49	0.26	1.28	0.24	0.15	0.04	-0.04
1/6	7.21	-2.50	-0.15	-1.71	-0.23	-0.66	0.19	0.18	-0.14
3/9	-3.50	0.75	-0.39	1.04	-0.52	0.21	0.62	0.49	0.08
4/5	8.42	-3.23	3.59	-0.08	0.09	0.17	1.00	-0.10	-0.06
4/6	-12.21	5.34	-3.69	0.80	-0.16	0.89	-1.83	0.67	-0.06
4/10	1.68	2.39	0.69	1.25	0.58	-0.43	-0.14	0.13	0.08
5/6	4.98	-0.65	2.11	0.89	0.70	-0.54	0.57	-0.08	1.13
5/10	2.30	-1.84	-0.19	-0.12	-0.33	0.62	0.44	-0.25	-0.45
7/9	4.18	1.56	0.01	-0.59	-0.26	0.06	0.05	0.06	0.07

[a] Ratios of protein peak areas.

13.4. Conclusions

The possibility of distinguishing olive leaves and pulps according to their cultivar by using protein profiles obtained by CGE has been demonstrated in this work. Different proteins profiles, with 11 common peaks, were observed in all the cultivars considered in this study. Thus, the normalized protein peak areas were employed as predictors to construct LDA models. Both, olive leaf and pulp samples belonging to 12 cultivars from different Spanish regions were correctly classified with an excellent resolution among all the categories, which demonstrated that protein profiles are characteristic of each cultivar.

Acknowledgements

This work was supported by project CTQ2010- 15335 (MINECO of Spain and FEDER) ACOMP/2013/196 (Generalitat Valenciana). M. V-B thanks the MEC for an FPU grant for PhD studies. M.J. L-G thanks the Generalitat Valenciana for a VALi+d postdoctoral contract. Authors also thank Ramiro Martínez from Novozymes (Spain) for his support.

13.5. References

El-Khawaga, O.Y.; Abou-Seif, M.A.M. (**2010**). Biochemical studies on antioxidant and oxidant activities of some plant extracts. *European Review for Medical and Pharmacological Sciences, 14*, 731-738.

Esteve, C.; Del Río, C.; Marina, M.L.; García, M.C. (**2011**). Development of an ultra-high performance liquid chromatography analytical methodology for the profiling of olive (*Olea europaea L.)* pulp proteins. *Analytica Chimica Acta, 690,* 129-134.

Garcia, J.L.; Avidan, N; Troncoso, A.; Sarmiento, R.; Lavee, S. (**2000**). Possible juvenile-related proteins in olive tree tissues. *Scientia Horticulturae, 85*, 271-284.

Georgalaki, M.D.; Bachmann, A.; Sotiroudis, T.G.; Xenakis, A.; Porzel, A.; Feussner, I. (**1998A**). Characterization of a 13-lipoxygenase from virgin olive oil and oil bodies of olive endosperms. *Fett-Lipid, 100,* 554-560.

Georgalaki, M.D.; Sotiroudis, TG.; Xenakis, A. (**1998B**). The presence of oxidizing enzyme activities in virgin olive oil. *Journal of the American Oil Chemists' Society, 75*, 155-159.

Hatzopoulos, P.; Banilas, G; Giannoulia, K.; Gazis, F.; Nikoloudakis, N.; Milioni, D.; Haralampidis, K. (**2002**). Breeding, molecular markers and molecular biology of the olive tree. *European Journal of Lipid Science and Technology, 104,* 574-586.

Hubbs, A.; Roy, H. (**1992**). Synthesis and assembly of large subunits into ribulose bisphosphate carboxylase/oxygenase in chloroplast extracts. Plant Physiology, 100, 272-281.

Koidis, A.; Boskou, D. (**2006**). The contents of proteins and phospholipids in cloudy (veiled) virgin olive oils. *European Journal of Lipid Science and Technology, 108,* 323-328

Martín-Hernández, C.; Bénet, S; Obert, L. (**2008**). Determination of proteins in refined and nonrefined oils. *Journal of Agricultural and Food Chemistry, 56,* 4348-4351.

Meyer, Y.; Grosser, J.; Chartier, Y.; Cleyet-Marel, J.C.C. (**1988**). Preparation by two-dimensional electrophoresis of proteins for antibody production: antibody against proteins whose synthesis is reduced by auxin in tobacco mesophyll protoplasts. *Electrophoresis, 9,* 704-712.

Montealegre, C.; Marina, M.L.; García-Ruiz, C. (**2010**). Separation of proteins from olive oil by CE: An approximation to the differentiation of monovarietal olive oils. *Electrophoresis, 31,* 2218-2225.

Montealegre, C.; García, M.C.; Del Río, C.; Marina, M.L.; García-Ruiz, C. (**2012**). Separation of olive proteins by capillary gel electrophoresis. *Talanta, 97,* 420-424.

Ross, J.H.E.; Sanchez, J.; Millan, F.; Murphy, D.J. (**1993**). Differential presence of oleosins in oleogenic seed and mesocarp tissue in olive (*Olea europaea*) and avocado (*Persea Americana*). *Plant Science, 93,* 203-210.

Saha, S.; Callahan, F.E.; Dollar, D.A.; Creech, J.B. (**1997**). Effect of lyophilization of cotton tissue on the quality of extractible DNA, RNA and protein. *Journal of Cotton Science, 1,* 10-14.

Salah, M.B.; Abdelmelek, H.; Abderraba, M. (**2012**). Study of phenolic composition and biological activities assessment of olive leaves from different varieties grown in Tunisia. *Journal of Medicinal Chemistry, 2,* 107-111.

Soni, M.G.; Burdock, G.A., Christian, M.S., Bitler, C.M.; Crea R. (**2006**). Safety assessment of aqueous olive pulp extract as an antioxidant or antimicrobial agent in foods. *Food and Chemical Toxicology, 44,* 903-915.

Vandeginste, B.G.M.; Massart, D.L.; Buydens, L.M.C.; De Jong, S.; Lewi, P.J.; Smeyers-Verbeke, J. (**1998**). Data Handling in Science and Technology, Part B, Elsevier, Amsterdam.

Wang, W.; Scali, M.; Vignani, R.; Spadafora, A.; Sensi, E.; Mazzuca, S.; Cresti, M. (**2003**). Protein extraction for two-dimensional electrophoresis from olive leaf, a plant tissue containing high levels of interfering compounds. *Electrophoresis 24,* 2369-2375.

Chapter 14. Use of triacylglycerol profiles established by HPLC-UV and ELSD to predict cultivar and maturity of Tunisian olive oils

Eur Food Res Technol
DOI 10.1007/s00217-016-2660-x

ORIGINAL PAPER

Use of triacylglycerol profiles established by HPLC–UV and ELSD to predict cultivar and maturity of Tunisian olive oils

Marwa Abdallah[1] · María Vergara-Barberán[2] · María Jesús Lerma-García[2] · José Manuel Herrero-Martínez[2] · Mokhtar Zarrouk[1] · Mokhtar Guerfel[1] · Ernesto Francisco Simó-Alfonso[2]

The usefulness of TAG profiles established by HPLC using both UV and ELSD detectors as a tool to discriminate between seven cultivars of Tunisian EVOOs was evaluated in this work. Moreover, the discrimination of EVOOs from the cultivars Chemchali, Fouji and Zarrazi, characterized with different maturity indexes, was also studied. With both detectors, a total of 19 peaks, which were common to all the EVOOs studied, were observed. However, ELSD peaks, which provided a higher signal-to-noise ratio than the UV peaks, were selected to construct LDA models for cultivar and maturity index prediction. In all cases, an excellent resolution between all category pairs was achieved, which demonstrated that TAG profiles are a good marker of both, cultivar and maturity index of EVOOs.

Keywords: Olive cultivar; HPLC; linear discriminant analysis; maturity index; triacylglycerols; Tunisian extra virgin olive oils

14.1. Introduction

EVOO is the principal source of fat in the Mediterranean diet with high nutritional value and significant health benefits. It is the only vegetable oil that can be consumed directly in its raw state, by cold-pressing of olive fruit, using exclusively mechanical procedures without any further treatments or chemical additions (Baccouri, 2008).

Olive oil plays an important role in the Tunisian agronomy and economy. Olive trees, which cover an area of 1.611.200 ha spread from north to south, accounting for more than 4% of the olive oil world production (Issaouri, 2010). The most cultivated Tunisian varieties are Chétoui and Chemlali (Baccouri, 2007; Baccouri, 2008; Ben Youssef, 2010; Vichi, 2012), although Tunisia has a great genetic diversity among its olive trees.

The quality of olive oil is influenced by a great number of factors such as geographic location (Ollivier, 2006; Mailer, 2011), agronomic practices (Krichene, 2010), extraction process (Gimeno, 2002), irrigation (Baccorui, 2007; Baccouri, 2008), harvest time (Dag, 2011), crop season (Salvador, 2001; Skevin, 2003) and climatic conditions (Morelló, 2006). It has been suggested that cultivar (Gutiérrez, 1999; Skevin, 2003; Kalua, 2005; Vichi, 2005; Cerretani, 2006; Baccouri, 2007; Haddada, 2007; Matos, 2007; Baccouri, 2008; Gómez-Rico, 2008; Oueslati, 2009; Mailer, 2011; Yorulmaz, 2013) and the olive maturity stage (degree of ripening) (Gutiérrez, 1999; Salvador, 2001; Skevin, 2003; Kalua, 2005; Baccouri, 2007; Matos, 2007; Baccouri, 2008; Gómez-Rico, 2008; Ben Youssef, 2010; Dag, 2011; Sakouri, 2011; Bengana, 2013; Fuentes de Mendoza, 2013; Yorulmaz, 2013), are two of the most important ones. When olive maturation proceeds, a number of changes occur in the fruit (weight, pulp-stone ratio, colour of skin, oil content) and several metabolic processes take place which involve subsequent variations in the profile of many compounds in olive oil. These changes are

reflected on the sensorial characteristics, especially in the aroma, the oxidative stability and/or nutritional value of obtained product, and in the quality parameters (Fuentes de Mendoza, 2013). However, the determination of the optimum maturity index is rather difficult as only few clear guidelines may be used by the producers to identify the optimum harvest period. Several authors have already studied the influence of maturity index on certain compounds of olive oil such as fatty acids (Baccouri, 2007; Baccouri, 2008; Ben Youssef, 2010; Mailer, 2011; Gimeno, 2002; Dag, 2011; Salvador, 2001; Skevin, 2003; Gutiérrez, 1999; Matos, 2007; Yoroulmaz, 2013; Sakouhi, 2011; Bengana, 2013; Fuentes de Mendoza, 2013), polyphenols (Skevin, 2003; Kalua, 2005; Baccouri, 2007; Gómez-Rico, 2008; Ben Youssef, 2010;Vichi, 2012; Bengana, 2013; Yoroulmas, 2013), volatile compounds (Kalua, 2005; Gómez-Rico, 2008), tocopherols (Gutiérrez, 1999; Gimeno, 2002; Baccouri, 2007; Matos, 2007; Mailer, 2011; Bengana, 2013; Yoroulmaz, 2013), sterols (Gutiérrez, 1999; Salvador, 2001; Matos, 2007; Mailer, 2011; Fuentes de Mendoza, 2013; Yoroulmaz, 2013), and pigments (Gutiérrez, 1999; Salvador, 2001; Skevin, 2003; Baccouri, 2007; Ben Youssef, 2010; Bengana, 2013; Yoroulmaz, 2013), with the aim to determine the optimum maturity index to produce an EVOO with a superior organoleptic profile and the highest possible chemical and nutritional properties. Among the different compounds affected by fruit maturity, triacylglycerols (TAGs), which represent up to 95-98% (w/w) of olive oil composition (Nagy, 2005; Vichi, 2012), are also affected by this parameter (Boskou, 1996; Vichi, 2005; Baccouri, 2007; Baccouri, 2008; Sakouhi, 2011; Fuentes de Mendoza, 2013; Yoroulmaz, 2013). With the determination of the optimum maturity index, the characterization of olive oil according to its cultivar and/or geographical origin is of a great importance to obtain a high quality product, which is demanded by producers and consumers. Several analytical techniques have been used to determine TAGs in olive oil. Chromatographic methods are commonly used, but HPLC has been particularly employed in the last years,

mainly coupled with UV (Lerma-García, 2011) MS detectors (Nagy, 2005; Ruíz-Samblás, 2011). However, TAGs determined with UV detector provide a linear response but a low sensitivity for saturated TAG. For this purpose, the use of ELSD has been increased in the last years. Several advantages are related to this detector: it is a mass-sensitive detector that responds to any analyte less volatile than the mobile phase, compatible with a broad range of solvent, and its signal is independent of the chain length unsaturation degree. Thus, it has been successfully used for many researches in the separation of TAGs (Rombaut, 2009; Baccouri, 2008).

TAG profiles have been proposed as a useful tool for olive oil characterization. The advantage of using these patterns when compared to fatty acid profiles is that the stereospecific distribution of fatty acids on the glycerol molecule is genetically controlled and thus, the information of intact TAGs is usually high (Aparicio, 2000). These profiles associated with different chemometric techniques has been successfully reported in several works to characterize olive oil (Cerretani, 2006; Ollivier, 2006), or to predict the botanical origin of some vegetable oils (Cunha, 2006).

Most research studies related to the Tunisian EVOOs have been focused on the improvement and characterization of the two main varieties (Chétoui and Chemlali) (Vichi, 2005; Baccouri, 2007; Baccouri, 2008). Thus, to diversify Tunisian olive oil resources and improve the quality of olive oil produced in Tunisia, more information is still needed especially for minor cultivars. As far as we are concerned, only few works (Haddada, 2007; Oueslati, 2009; Sakouhi, 2011) have been published regarding TAG composition of minor Tunisian cultivars. However, any work that describes the changes produced in TAG profiles of the Tunisian cultivars Chemchali, Fouji and Zarrazi with different maturity indexes has been previously published.

The aim of this work was to investigate the possibility of using TAG profiles established by HPLC coupled to both UV and ELSD detectors, followed by LDA of the data, to classify Tunisian EVOOs according to their cultivar (Chemchali, Fouji, Zarrazi, Dhokar, Chemlali, Jemri and Zalmati), and to classify Chemchali, Fouji and Zarrazi EVOOs by their maturity index.

14.2. Materials and methods

14.2.1. EVOO samples

A total of 55 EVOOs, coming from seven Tunisian cultivars, were employed in this study (see **Table 14.1**). All these samples were used to develop a classificatory method based on their cultivar. On the other hand, a study to classify the samples according to their maturity index was also carried out using only the samples of known maturity index. All EVOOs were obtained from *ca.* 1 kg of healthy and non-damaged olives, which have been hand picked during the 2012/2013 and 2013/2014 harvesting seasons (see **Table 14.1**) from olive orchards located in the Tunisian geographical areas indicated in **Table 14.1**. After harvesting, olives were immediately transported to the laboratory in ventilated storage trays to avoid oil compositional changes, being oil extracted within 24h. An abencor system (MC2 Ingeniería y Sistemas, Seville, Spain) was used to extract EVOOs at a laboratory scale, which simulates the industrial process of olive oil production. After harvesting, olives were deleafed, crushed with a hummer crusher (equipped with a 4-mm sieve) at a velocity of 3850 rpm, and the olive paste mixed in a thermobeater at 25ºC for 30 min and then centrifuged at 3500 rpm for 5 min; then, the obtained EVOOs were left for decantation, filtered and transferred into dark glass bottles and stored at 4 °C until analysis.

In order to obtain the EVOOs of different maturity indexes, *ca*. 10 kg olives were collected from a same olive tree at different periods: olive fruits from the Chemlali, Dhokar, Jemri and Zalmati varieties were picked at the end of November, while for the Chemchali, Fouji and Zarrazi varieties the harvesting started at the end of September and continue up to January in order to obtain olives with different maturity indexes. Then, for Chemchali and Fouji cultivars, five maturity levels were identified, while for Zarrazi cultivar only three were observed (see **Table 14.1**). For each one of these maturity levels, *ca.* 1 kg of healthy and non-damage olives were used to obtain the corresponding EVOO.

These maturity levels were established according to the National Institute of Agronomical Research of Spain and it is based on a subjective evaluation of olive skin and pulp colours (1, yellowish green; 2, green with reddish spots; 3, reddish brown; 4, black with white flesh and 5, black with < 50% purple flesh).

14.2.2. TAG analysis

EVOO samples were injected in a 1100 series liquid chromatograph (Agilent Technologies, Waldbronn, Germany) after a simple dilution to 0.5% (w/v) in a 2:2:1 ACN/2-propanol/*n*-hexane (v/v/v) ternary mixture (Lerma-García, 2011). Three dilutions were performed for each sample, and then injected. The chromatograph was equipped with a quaternary pump, an online vacuum degasser, an autosampler, a thermostated column compartment and a UV-Vis diode array detector online coupled to an Agilent 385-ELSD. TAG separation was performed using a Kinetex™ C18 100 Å column (150 mm × 4.6 mm, 2.6 µm; Phenomenex, Torrance, CA, USA) at a flow rate of 1 mL min^{-1}. Elution was performed by varying the proportion of ACN and *n*-pentanol as follows: 75:25 (v/v) ACN/*n*-pentanol for 20 min, followed by an increase of *n*-pentanol up to a ratio of 40% in 10 min. Column temperature

was set at 10 ºC, and injection volume was 10 µL. UV detection was performed at 205 ± 10 nm (360 ± 60 nm as reference) (Lerma-García, 2011). The ELSD parameters were: evaporation temperature, 40 ºC; nebulization temperature, 55 ºC; gas flow rate, 1.2 Standard Litres per Minute (SLM); gain factor, 1.0.

For TAG identification, an UPLC™ binary pump system (Acquity, Waters, Milford, USA) was interfaced to a triple quadrupole mass spectrometer (TQD, Waters, Manchester, UK). Separation was carried out with the above mentioned column, using the same mobile phase and stepwise elution. Other parameters were: column temperature, 25 ºC; flow rate, 1 mL min^{-1} and injection volume, 20 µL. MS experiments were performed using an atmospheric pressure chemical ionization (APCI) source. The MS working conditions were as follows: probe temperature, 600 ºC; corone discharge current, 20 µA; source temperature: 120 ºC; desolvation gas flow, 800 L/h; cone gas flow, 60 L/h. Drying and nebulizer gas was nitrogen (Praxair, Valencia, Spain). The mass spectrometer scanned within the *m/z* 150-1000 range in the positive ionization mode at one scan per second.

Table 14.1

Genetic variety, number of samples, crop season, maturity index and geographical origin of the EVOO samples employed in this study.

Genetic variety	No. of samples	Crop season	Maturity index	Geographical origin
Chemchali	1	2012/2013	1	Gafsa
	2	2013/2014		
	2	2012/2013	2	
	1	2013/2014		
	2	2012/2013	3	
	1	2013/2014		
	1	2012/2013	4	
	2	2013/2014		
	2	2012/2013	5	
	1	2013/2014		
Chemlali	1	2012/2013	3.1	Sousse
	1	2013/2014	3.7	Sfax
	2	2012/2013	3.5	Sidi Bouzid
		2013/2014	4.0	
Dhokar	2	2012/2013	3.9	Ben Gardène
		2013/2014	3.2	
	2	2012/2013	3.7	Tataouine
		2013/2014	3.5	
Fouji	2	2012/2013	1	Gafsa
	1	2013/2014		
	2	2012/2013	2	
	1	2013/2014		
	1	2012/2013	3	
	2	2013/2014		
	1	2012/2013	4	
	2	2013/2014		
	1	2012/2013	5	
	2	2013/2014		

Table 14.1

Cont.

Genetic variety	No. of samples	Crop season	Maturity index	Geographical origin
Jemri	2	2012/2013	4.2	Ben Gardène
		2013/2014	3.8	
	2	2012/2013	3.1	Medenine
		2013/2014	3.7	
Zalmati	2	2012/2013	3.3	Medenine
		2013/2014	3.6	
	2	2012/2013	3.1	Zarzis
		2013/2014	3.9	
Zarrazi	2	2012/2013	1	Gafsa
	1	2013/2014		
	2	2012/2013	3	
	1	2013/2014		
	2	2012/2013	4	
	1	2013/2014		

14.2.3. Data treatment and statistical analysis by LDA

The peak areas of the 19 TAGs identified by MS (see **Table 14.2**) were measured from the HPLC-ELSD chromatograms, and a data matrix was constructed using the areas of all the peaks as original variables. These variables were normalized as next indicated and used to construct LDA models using SPSS (v. 15.0, Statistical Package for the Social Sciences, Chicago, IL, USA). LDA is a statistical supervised classificatory technique that uses a linear combination of predictor variables to obtain new axes, called discriminant functions, which show the maximal resolution between a set of categorical variables (Vandeginste, 1998). LDA constructs as many discriminant functions as the number of predictors or categories minus one. In LDA, vectors minimizing Wilks' lambda (λ_w) are calculated as the sum of squares of the distances between points belonging to the same category, divided by the total sum of squares. Well-resolved categories give λ_w values

approaching zero, while overlapped categories give values approaching one. There are different methods to include predictors during LDA model construction. In this work, the SPSS stepwise method was used. In this method, the predictors to be included in the model are selected using a test of comparison of variances.

If a predictor exceeds the entrance threshold (F_{in}), it is included in the model, although its inclusion could modify the significance of those predictors which are already present. Then, after the inclusion of a new predictor, a rejection threshold (F_{out}), is used to decide if one of the other predictors should be removed from the model. The model is completed when there are no predictors entering or being eliminated from the model. In this work, the F_{in} and F_{out} probability values selected were 0.05 and 0.10, respectively.

In order to minimize the different sensitivity observed in ELSD for the TAGs identified, normalized rather than absolute peak areas were used. For this purpose, the area of each peak was divided by each one of the areas of the other 18 peaks; in this way, and taking into account that each pair of peaks should be considered only once, (19 x 18)/2 = 171 non-redundant peak area ratios were obtained to be used as predictors for LDA model construction.

Thus, taking into account the total number of samples (55 objects) and the 171 predictors obtained after application of the normalization procedure indicated above, a data matrix was constructed. A response column, containing the categories corresponding to the 7 cultivars, was added. This matrix was divided in two groups of objects to constitute the training and evaluation sets. The training set was composed by 38 objects (10 objects for Chemchali and Fouji, 6 for Zarrazi, 2 samples for each maturity index; and 3 objects from the other cultivars), while the evaluation set was constituted by the remaining samples (17 objects).

Table 14.2

TAGs identified by UPLC-MS analysis of EVOOs

Peak no.[a]	TAG[b]	PN	$[M+H]^+$	$[M+H-R_1COOH]^+$	$[M+H-R_2COOH]^+$	$[M+H-R_3COOH]^+$
1	LLLn	40	877.7	LL 599.5	LLn 597.5	-
2	LLL	42	879.7	LL 599.5	-	-
3	OLLn	42	879.7	LLn 597.5	OLn 599.5	OL 601.5
4	OLL	44	881.8	OL 601.5	LL 599.5	-
5	PaOL	44	855.74	PaO 575.50	PaL 573.48	OL 601.52
6	PLL	44	855.74	PL 575.50	-	LL 599.50
7	OLnO	44	881.8	OLn 599.5	OO 603.5	-
8	OOL	46	883.76	OO 603.53	OL 601.52	-
9	SLL	46	883.8	SL 603.5	LL 599.5	-
10	OLP	46	857.8	OL 601.5	LP 575.5	OP 577.5
11	MOO	46	831.74	MO 549.48	-	OO 603.53
12	PPL	46	831.74	PP 551.50	PL 575.50	-
13	OOO	48	885.8	OO 603.5	-	-
14	SLO	48	885.8	OL 601.5	SL 603.5	SO 605.5
15	OOP	48	859.8	OO 603.5	OP 577.5	-
16	PPO	48	833.8	OP 577.5	PP 551.5	-
17	SOO	50	887.8	OO 603.5	SO 605.5	-
18	SOP	50	861.8	OP 577.5	PS 579.5	SO 605.5
19	SSO	52	889.8	SO 605.5	SS 606.6	-

[a] Peak identification number according to **Figure 14.1**; TAGs identified according to the protonated molecule ($[M+H]^+$) and diacylglycerol ions ($[M+H-R_{1,2,3}COOH]^+$) observed in the mass spectra, and to the relative order of partition numbers (PN)

[b] Structure indicated by fatty acid composition (e.g. OOO for triolein) using the following abbreviations: L, linoleic acid; Ln, linolenic acid; M, myristic acid; O, oleic acid; Pa, palmitoleic acid; P, palmitic acid; S, stearic acid

14.3. Results and discussion

14.3.1. TAG Identification and comparison of TAG profiles of EVOOs from different cultivar and maturity index

Generally, the elution of TAGs in RP-HPLC occurs according to partition number (PN) (Ruíz-Gutiérrez, 1995; Sandra, 2002). The procedure for identifying the TAGs based on the PN is complicated due to the large number of fatty acid constituents and rather limited due to the coincidence of this parameter for several TAGs. For this reason, to achieve a reliable TAG identification, a fragmentation study resulting from the APCI-MS analysis of TAGs in the positive ionization mode was performed. As a result, a total of 19 TAG peaks were identified in the EVOO samples of all categories (peak assignments are given in **Table 14.2**).

Next, EVOOs were injected into the HPLC system with both UV and ELSD detectors coupled in series. Both detectors were employed in order to see if the obtained response is the same with both of them, and to check if there is an exaltation of the signal with one of the detectors with the aim of maximizing the possible differences between the different studied EVOOs. The chromatogram obtained with both detectors for an EVOO sample from Chemchali cultivar at maturity index 3 is shown in **Figure 14.1.** As it can be observed, different sensitivities were obtained when the profiles provided by both detectors were compared (see also **Table 14.4** and **Table 14.S1**).

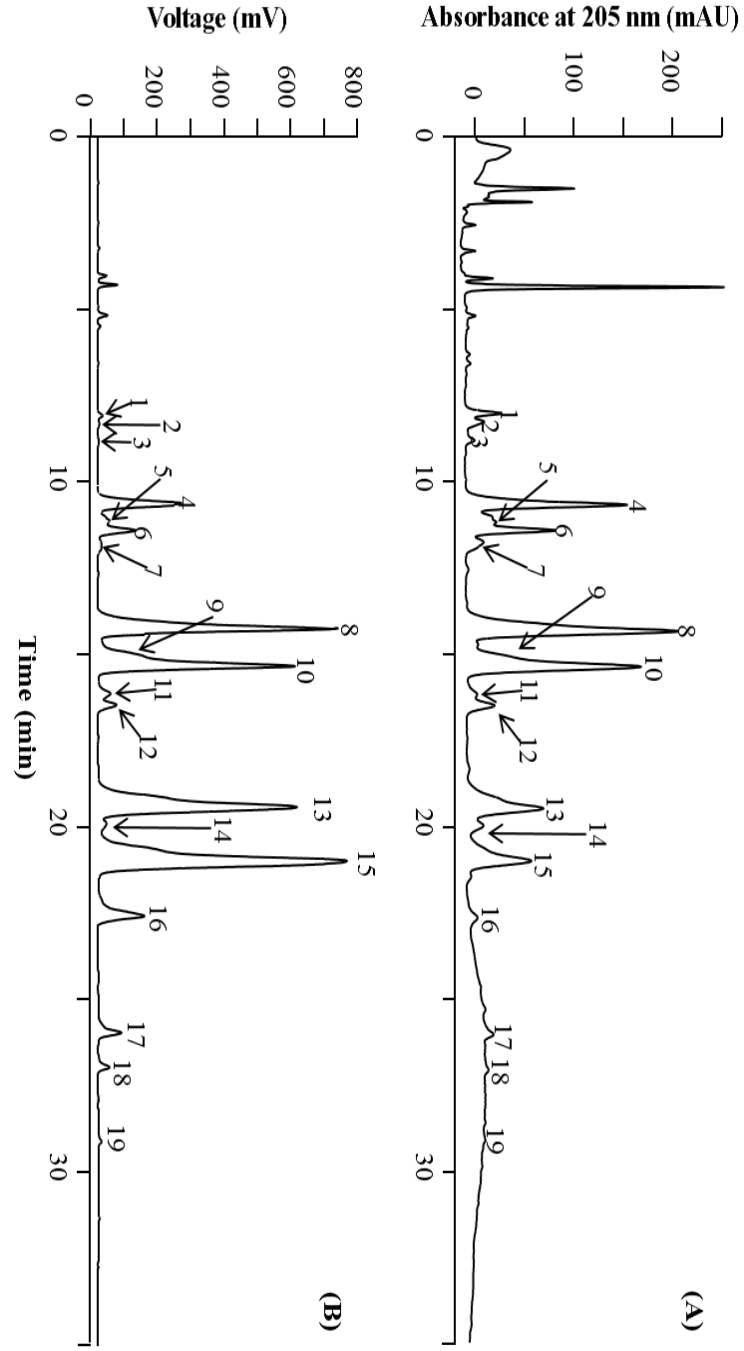

Figure 14.1. Chromatograms showing the TAGs profiles of an EVOO of the Chemchali cultivar of maturity index 3 with (A) UV and (B) ELSD detectors. Peak identification as in Table 2

Regarding ELSD, it has been described (Morera, 1998) that this detector provides a linear response with analyte concentration. Its response is function of the analyte refractive index, and then should be approximately constant for analytes with similar structure. However, previous studies (Cunha, 2006) have demonstrated that the HPLC–ELSD response follows a non-linear empirical model: $A=amb$, where A is the area of chromatographic peak, m the mass of analyte, being a and b two experimental parameters related to the ELSD configuration.

Thus, each change in the instrumental working conditions would require a new estimation of these parameters. In addition, it has been reported that the ELSD signal is influenced by peak shape (width and asymmetry), where a significant increase of the ELSD response factor was observed with a decrease of peak width and the closeness of symmetry factor to one (Mengerink, 2001). This increase could explain the differences observed for the TAG profiles obtained with UV and ELSD detectors. In order to check this behaviour, the areas of the TAG peaks obtained by both detectors were divided (ELSD/UV area ratios), and the efficiency and symmetry of all peaks was measured.

As an example, the results obtained for an EVOO sample (Chemchali at maturity index 3) are shown in **Table 14.3**. As it can be observed, in all cases the peak symmetry was close to 1. Moreover, an increase in the peak efficiency was observed for the peaks that eluted at high retention times, jointly with an increase in the ELSD/UV area ratio, which is in agreement with literature (Mengerink, 2001). The increase in the ELSD/UV area ratio was obtained for all peaks except for peaks 12 and 14, which presented higher UV absortivity than peaks 11 to 19, due to the presence of the linoleic fatty acid (L) which has two conjugated insaturations. A similar behaviour was obtained when the same measurements were performed to all the EVOOs analyzed. Therefore, and even if the sensitivity of some peaks, mainly peaks 1 to 3, was lower for ELSD than for the UV detector, the signal-to-noise ratio

was always higher for ELSD; thus, the ELSD peak areas were selected for the chemometric data treatment. The TAG profiles obtained with the ELSD detector for the Chemchali, Fouji and Zarrazi cultivars (at maturity index 3) are shown in **Figure 14.1B** and **Figure 14.2.**

Table 14.3

ELSD/UV area ratio, peak symmetry and peak efficiency of the 19 TAGs measured for a Chemchali EVOO at maturity index 3.

Peak no.[a]	ELSD/UV area ratio	Peak symmetry	Peak efficiency
1	0.40	1.142	3033
2	0.36	0.671	2394
3	1.25	0.834	3268
4	0.60	0.916	2558
5	1.26	1.091	3215
6	0.41	1.302	3095
7	1.43	0.986	4234
8	1.05	2.362	3060
9	1.31	1.135	3795
10	3.24	1.359	3794
11	3.55	1.048	4345
12	1.84	0.891	5384
13	8.02	1.245	4527
14	1.40	0.866	4892
15	11.57	1.044	5628
16	19.95	1.486	7533
17	18.12	1.495	9313
18	17.56	1.208	8719
19	15.51	1.222	9432

[a] Peak identification number according to **Figure 14.1.**

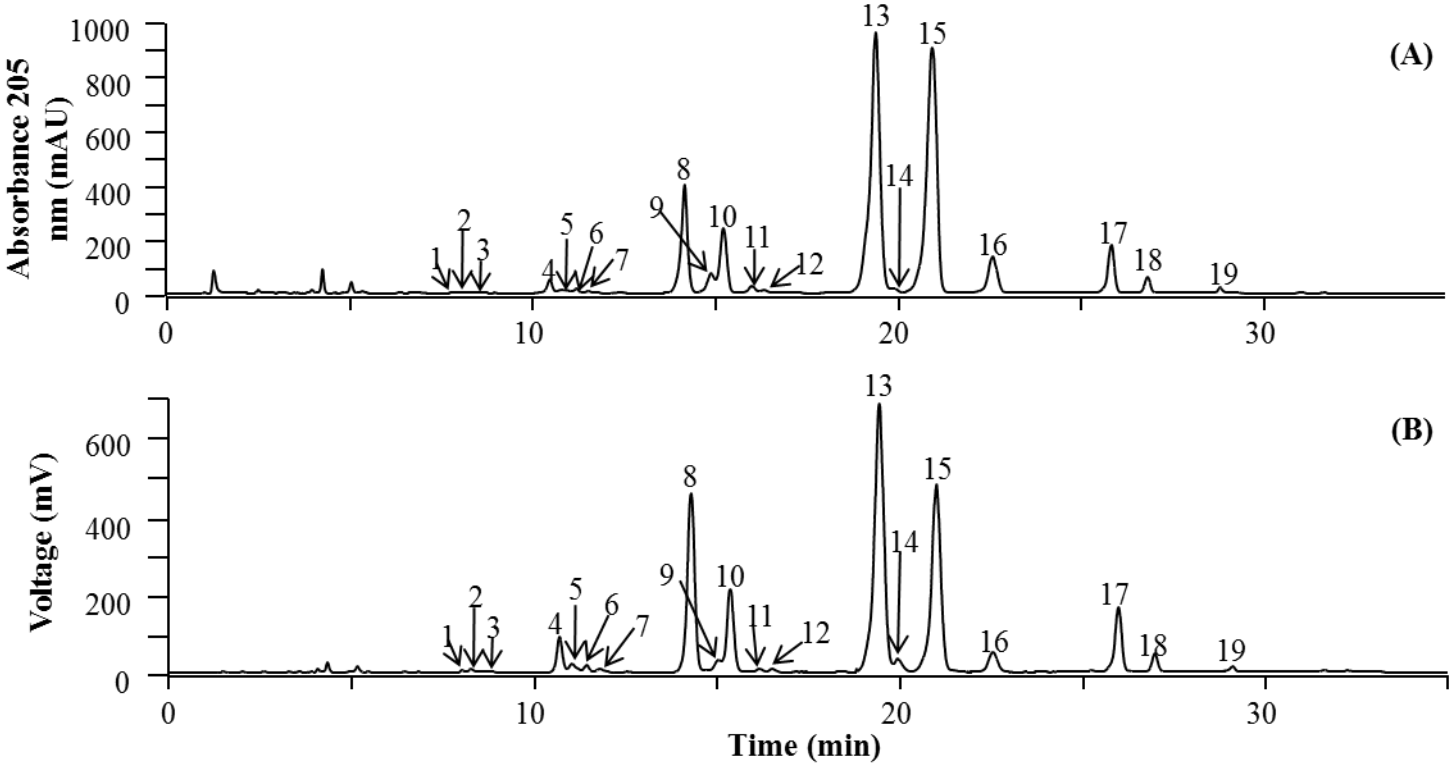

Figure 14.2. ELSD chromatograms showing the TAGs profiles of a (A) Fouji and (B) Zarrazi EVOOs of maturity index 3

A study of the TAG content was next performed. However, the establishment of reliable quantitation studies using ELSD peak areas, taking into account the previous exponential equation, implies the availability of each TAG identified in the samples, which are not commercially feasible. Thus, to overcome this problem, several quantitation approaches have been proposed in literature. Heron *et al*. (Heron, 2007) have developed an empirical methodology to evaluate the TAG content in vegetable oils based on the previous equation using a reduced number of standards.

However, the method provided a high variability (between 1 and 40%) with respect to the real mass percentage. Other authors (Cunha, 2006; Morera, 1998) have calculated the relative response factors (RRFs) of 5 pure TAG standards in relation to triolein (OOO) standard. In these studies, the RRFs found were comprised between 0.82 and 1.21. Thus, and since RRF values were close to one, it is possible to estimate the TAG content on the basis of percentage peak area. Therefore, and taking into account these results, the quantitative estimation of TAGs was established by dividing each TAG area by the sum of the areas of all TAGs identified (see **Table 14.4**).

As it can be observed, the most abundant TAGs identified were OOL, OOO, OLP and OOP, which were comprised between 77 and 94% of the total peak area in the chromatographic profiles. As shown in **Table 14.4**, the content of the main TAGs were comprised between 8.54-24.47% (OOL), 4.09-18.41% (OLP), 18.01-53.74% (OOO) and 20.00-37.71% (OOP). Thus, the Chemchali cultivar showed the highest contents of OOL and OLP, while the Fouji cultivar presented the highest OOO and OOP percentages. Chemchali and Dokhar also had high contents of OLP, while Zarrazi cultivar was also characterized by high OOO percentages. The contents found were similar with the ones published in literature for other Tunisian cultivars (Baccouri, 2007; Baccouri, 2008; Vichi, 2012).

On the other hand, TAG percentages varied widely according to the different maturity index. As ripening proceed, the content of OOO decreased while the content of OLP increased in the three cultivars studied, which is in agreement with previously studies of EVOOs (Baccouri, 2007; Mailer, 2011; Dag, 2011; Salvador, 2001; Sakouhi, 2011). The decrease in the OOO content could be explained by the decrease in the activities of lysophosphatidate acyltranspherase (LPAAT) and glycerol-3-phosphate acyltransferase (G3PAT) in the Kennedy pathway, since both LPAAT and G3PAT have a strong selectivity for oleoyl-CoA (Harword, 1994). Otherwise, OOL has an increasing tendency for Chemchali and Zarrazi cultivars during growth of olives (Sakouhi, 2011) while this trend was not very clear for the Fouji cultivar.

The increase in the accumulation of OOL during the ripening of olive could be explained by the increase in the activity of diacylglycerol acyltransferase (DAGAT), which has a broad specificity (Harword, 1994). Finally, OOP percentage decreased with maturation for Chemchali cultivar, and increased for Fouji variety.

Table 14.4

Percentages of TAGs found in the total TAG fraction using ELSD peaks of all the EVOO samples considered in this study.

Cultivar	Maturity index	LLLn	LLL	OLLn	OLL	PaOL	PLL	OLnO	OOL	SLL
Chemchali	1	0.050 ± 0.005(a)	0.030 ± 0.002(a)	0.009 ± 0.001(a)	2.11 ± 0.20(a)	0.32 ± 0.03(a)	0.73 ± 0.07(a)	0.16 ± 0.01(a)	16.8 ± 1.0(a)	0.83 ± 0.07(a)
	2	0.080 ±0.003(b)	0.054± 0.005(b)	0.022 ± 0.001(b)	2.92 ± 0.20(b)	0.39 ± 0.04(a)	1.04 ± 0.08(b)	0.18 ± 0.02(a)	18.9 ± 0.8(b)	0.88 ± 0.06(a)
	3	0.129 ± 0.009(c,1)	0.073 ± 0.006(c,1)	0.020 ± 0.001(b,1)	4.23 ± 0.30(c,1)	0.48 ± 0.02(b,1)	1.46 ± 0.07(c,1)	0.20 ± 0.01(a,1)	21.9 ± 2.0(c,1)	1.02 ±0.07(b,1)
	4	0.180 ± 0.009(d)	0.080 ± 0.004 (d)	0.021 ±0.001(b)	5.18 ± 0.40(d)	0.53 ± 0.03(c)	1.77 ± 0.11(d)	0.24 ± 0.02(b)	24.5 ± 2.0(c)	1.06 ± 0.06(b)
	5	0.311 ± 0.019(e)	0.101 ± 0.005(e)	0.021 ± 0.001(b)	6.64 ± 0.50(e)	0.67 ± 0.03(d)	2.32 ± 0.20(e)	0.28 ± 0.03(b)	22.4 ± 1.1(c)	0.56 ± 0.06(c)
Fouji	1	0.232 ± 0.018(a)	0.022 ± 0.001(a)	0.012 ± 0.001(a)	0.98 ± 0.04(a)	0.07 ± 0.03(a)	0.26 ± 0.02(a)	0.08 ± 0.01(a)	10.4 ± 1.0(a)	1.04 ± 0.10(a)
	2	0.011± 0.001(b)	0.023 ± 0.002(a)	0.020 ± 0.001(b)	0.76 ± 0.08(b)	0.13 ± 0.01(a)	0.17 ± 0.01(b)	0.10 ± 0.01(a)	12.6 ± 0.6(b)	1.36 ± 0.12(b)
	3	0.010 ± 0.001(b,2)	0.012 ± 0.001(b,2)	0.012 ± 0.001 (a,2)	0.45 ± 0.04(c,2)	0.08 ± 0.01(b,2)	0.14 ± 0.01(c,2)	0.10 ± 0.01(a,2)	8.5 ± 0.4(c,2)	0.94 ± 0.04(a,1)
	4	0.023 ± 0.080(c)	0.029 ± 0.003(a)	0.020 ± 0.001(b)	0.66 ± 0.06(d)	0.12 ± 0.01(a)	0.20 ± 0.02(d)	0.15 ± 0.01(b)	9.9 ± 1.0(a)	0.96 ± 0.08(a)
	5	0.050 ± 0.005(d)	0.105 ± 0.004(c)	0.062 ±0.005(c)	1.43 ± 0.06 (e)	0.53 ± 0.03(c)	0.24 ± 0.02(d)	0.11 ± 0.01(a)	16.9 ± 1.4(d)	0.49 ± 0.04(c)
Zarrazi	1	0.040 ± 0.002(a)	0.091 ± 0.005(a)	0.022 ± 0.002(a)	1.52 ± 0.11(a)	0.62 ± 0.04(a)	0.30 ± 0.02(a)	0.15 ± 0.01(a)	18.3 ± 0.7(a)	0.68 ± 0.03(a)
	3	0.052 ± 0.004(b,3)	0.092 ± 0.008(a,3)	0.023 ±0.002(a,1)	1.87 ± 0.13(b,3)	0.60 ± 0.06(a,3)	0.37 ± 0.02(b,3)	0.17 ± 0.01(a,3)	19.1 ± 1.5(a,1)	0.62 ± 0.06(a,2)
	4	0.124 ± 0.012(c)	0.133 ± 0.007(b)	0.019 ± 0.001(a)	2.90 ± 0.20(c)	0.75 ± 0.05(b)	0.58 ± 0.02(c)	0.24 ± 0.02(b)	21.8 ± 2.0(a)	0.74 ± 0.06(a)
Chemchali	-	0.140 ±0.010(1)	0.144 ± 0.010(4)	0.040 ± 0.002(3)	4.47 ± 0.40(1)	1.69 ± 0.12(4)	2.51 ± 0.10(4)	0.68 ± 0.04(4)	18.1 ± 0.9(1)	5.41 ± 0.50(3)
Dokhar	-	0.080 ± 0.006(2)	0.091 ± 0.007(3)	0.072 ± 0.006(4)	3.05 ± 0.15(4)	1.14 ± 0.05(5)	1.18 ± 0.06(5)	0.42 ± 0.03(5)	16.2 ± 1.5(3)	3.62 ± 0.36(4)
Jemri	-	0.140 ± 0.011(1)	0.140 ± 0.008(4)	0.042 ± 0.002(3)	3.38 ± 0.20 (4)	1.21 ± 0.07(5)	1.57 ± 0.14(6)	0.50 ± 0.04(6)	16.2 ± 1.3(3)	3.52 ± 0.24(4)
Zalmati	-	0.181 ± 0.009(4)	0.130 ± 0.008(4)	0.054 ± 0.004(5)	3.59 ± 0.20(5)	1.01 ±0.08(5)	2.21 ± 0.16(7)	0.52 ± 0.05(6)	15.2 ± 1.5(3)	2.06 ± 0.08(5)

Table 14.4

Cont

Cultivar	Maturity index	OLP	MOO	PPL	OOO	SLO	OOP	PPO	SOO	SOP	SSO
Chemchali	1	12.9 ± 1.3(a)	0.37 ± 0.04(a)	0.58 ± 0.04(a)	27.2 ± 3.0(a)	0.32 ± 0.02(a)	32.5 ± 3.0(a)	3.68 ± 0.30(a)	1.07 ± 0.06(a)	0.36 ± 0.02(a)	0.071 ± 0.007(a)
	2	14.8 ± 1.5(a)	0.39 ± 0.02(a)	0.63 ± 0.04(a)	24.9 ± 1.8(a)	0.33 ± 0.2(a)	30.4 ± 2.0(a)	2.89 ± 0.20(b)	0.88 ± 0.04(b)	0.24 ± 0.02(b)	0.059 ± 0.006(a)
	3	16.2 ± 0.7(b,1)	0.42 ± 0.04(a,1)	0.66 ± 0.03(a,1)	24.8 ± 2.0(a,1)	0.41 ± 0.04(b,1)	25.2 ± 1.2(b,1)	1.80 ± 0.09(c,1)	0.79 ± 0.07(b,1)	0.15 ± 0.01(c,1)	0.042 ± 0.004(b,1)
	4	16.6 ± 1.7(b)	0.34 ± 0.03(a)	0.56 ± 0.06(a)	24.8 ± 1.5(a)	0.48 ± 0.03(c)	21.6 ± 1.5(c)	1.26 ± 0.11(d)	0.74 ± 0.06(b)	0.09 ± 0.01(d)	0.042 ± 0.003(b)
	5	18.4 ± 1.7(b)	0.44 ± 0.02(a)	0.90 ± 0.05(b)	18.5 ± 1.7(b)	0.40 ± 0.03(b)	24.1 ± 1.7(b)	2.97 ± 0.18(e)	0.66 ± 0.04(b)	0.24 ± 0.02(b)	0.040 ± 0.003(b)
Fouji	1	4.1 ± 0.2(a)	0.25 ± 0.02(a)	0.11 ± 0.01(a)	53.7 ± 3.0(a)	0.29 ± 0.02(a)	25.2 ± 2.0(a)	0.92 ± 0.05(a)	1.99 ± 0.12(a)	0.18 ± 0.01(a)	0.121 ± 0.007(a)
	2	4.5 ± 0.2(a)	0.59 ± 0.02(b)	0.52 ± 0.05(b)	46.4 ± 1.9(b)	0.54 ± 0.04(b)	29.2 ± 3.0(a)	1.16 ± 0.07(b)	1.67 ± 0.08(b)	0.20 ± 0.01(a)	0.083 ± 0.006(b)
	3	5.0 ± 0.2(b,2)	0.35 ± 0.02(c,2)	0.17 ± 0.01(c,2)	39.8 ± 4.0(c,2)	0.27 ± 0.02(a,2)	37.7 ± 1.8(b,2)	3.26 ± 0.30(c,2)	2.46 ± 0.20(c,2)	0.60 ± 0.02(b,2)	0.119 ± 0.005(a,2)
	4	5.7 ± 0.3(c)	0.40 ± 0.2(d)	0.19 ± 0.02(c)	39.3 ± 2.0(c)	0.23 ± 0.02(c)	37.0 ± 1.5(b)	2.64 ± 0.19(d)	1.95 ± 0.08(a)	0.38 ± 0.04(c)	0.102 ± 0.006(a)
	5	6.9 ± 0.3(d)	0.14 ± 0.01(e)	0.18 ±0.01(c)	41.1 ± 2.0(c)	1.03 ± 0.09(d)	24.2 ± 1.0(a)	1.48 ± 0.06(e)	4.28 ± 0.40(d)	0.73 ± 0.06(d)	0.152 ± 0.009(c)
Zarrazi	1	6.4 ± 0.3(a)	0.13 ± 0.01(a)	0.17 ± 0.01(a)	46.2 ± 5.0(a)	0.92 ± 0.09(a)	20.0 ± 2(a)	0.93 ± 0.09(a)	3.03 ± 0.20(a)	0.39 ± 0.02(a)	0.151 ± 0.008(a)
	3	7.3 ± 0.7(b,3)	0.13 ± 0.01(a,3)	0.18 ± 0.01(a,2)	41.2 ± 3.0(a,3)	0.69 ± 0.06(b,3)	22.9 ± 1.1(a,3)	1.11 ± 0.06(b,3)	3.08 ± 0.15(a,3)	0.44 ± 0.03(a,3)	0.133 ± 0.012(b,2)
	4	8.4 ± 0.4(b)	0.14 ± 0.01(a)	0.20 ± 0.02(a)	39.1 ± 2.0(a)	0.75 ± 0.06(c)	20.6 ± 2.0(a)	0.82 ± 0.05(a)	2.33 ± 0.20(b)	0.25 ± 0.02(b)	0.109 ± 0.006(c)
Chemchali	-	16.3 ± 1.1(1)	1.48 ± 0.06(4)	1.36 ± 0.11(3)	18.1 ± 0.7(4)	0.44 ± 0.04(1)	24.6 ± 1.0(1)	3.43 ± 0.30(2)	0.79 ± 0.07(1)	0.37 ± 0.03(3)	0.073 ± 0.003(3)
Dokhar	-	12.7 ± 1.3(4)	1.24 ± 0.07(5)	0.91 ± 0.06(4)	24.7 ± 1.0(1)	0.46 ±0.03(2)	29.2 ± 2.0(4)	3.60 ± 0.30(2)	0.86 ± 0.06(1)	0.40 ± 0.02(3)	0.072 ± 0.004(3)
Jemri	-	13.4 ± 1.3(4)	1.20 ± 0.07(5)	0.97 ± 0.08(4)	24.2 ± 2.0(1)	0.34 ± 0.02(4)	28.0 ± 2.0(4)	3.72 ± 0.19(2)	0.95 ± 0.08(1)	0.44 ± 0.04(3)	0.102± 0.007(4)
Zalmati	-	15.7 ± 0.6(1)	1.03 ± 0.07(6)	1.26 ± 0.11(3)	23.5 ± 1.4(1)	0.36 ± 0.04(4)	28.0 ± 1.1(4)	3.68 ± 0.30(2)	1.09 ± 0.07(1)	0.40 ± 0.04(3)	0.091 ± 0.008(4)

14.3.2. Classification of EVOOs according to their cultivar

A first LDA model was constructed to classify the EVOO samples according to their cultivar (see **Table 14.1**) using the data matrix previously described. Only this objective was addressed in this first model since the construction of a single model able to predict both cultivar and maturity index is not possible, since the LDA model will try to group in a same category all the samples with the same maturity index not taking into consideration their corresponding cultivar. Then, when this first LDA model was constructed, an excellent resolution between all the category pairs was achieved (**Figure 14.3**, $\lambda_w < 0.01$). The variables selected by the SPSS stepwise algorithm, and the corresponding standardized coefficients of the model, showing the predictors with large discriminant capabilities, are given in **Table 14.5**. As it can be observed, the main peak area ratios selected by the algorithm to construct the

LDA model corresponded to the following TAG peak ratios: 6/8 (PLL/OOL) and 6/10 (PLL/OLP). Although for the construction of this model the number of samples for some cultivars is just four, an adequate fitting of the model is assured since the number of selected predictors is 13, and the total number of samples is 55.

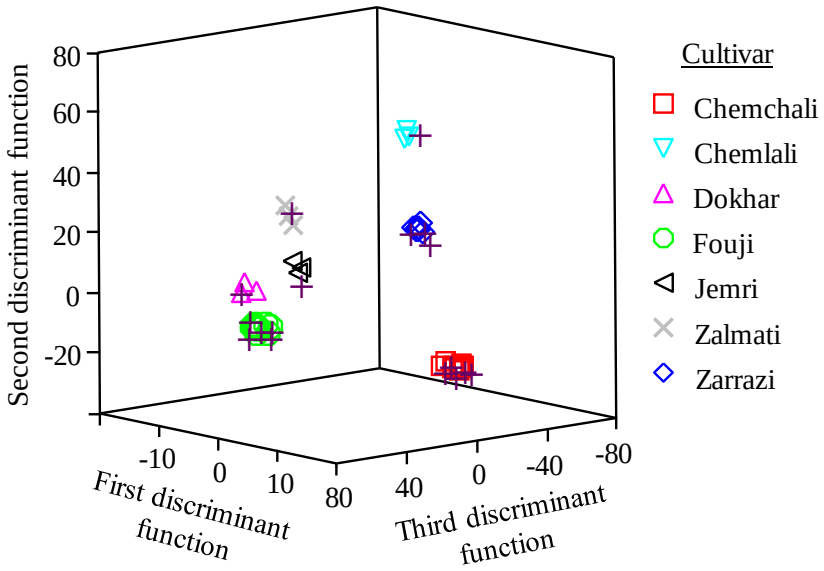

Figure 14.3. Score plot on an oblique plane of the 3D space defined by the three first discriminant functions of the LDA model constructed to classify EVOOs according to their cultivar. Evaluation set samples are labelled with a cross symbol.

Using this model and leave-one-out validation, all the objects of the training set were correctly classified. Concerning to the prediction capability of the model, all the objects of the evaluation set (represented with crosses in **Figure 14.3**) were correctly assigned within a 95% probability level.

Table 14.5

Predictors selected and corresponding standardized coefficients of the LDA model constructed to predict the cultivar of EVOOs.

Predictors[a]	f_1	f_2	f_3	f_4	f_5	f_6
4/5	2.18	-1.35	1.45	0.25	1.41	-0.10
4/10	-8.53	-3.97	-9.59	-6.10	-8.71	-4.69
4/12	8.86	-1.65	2.22	2.95	5.30	1.45
6/8	24.736	13.35	2.15	-13.29	3.37	-0.77
6/10	-13.87	-6.87	0.38	9.83	-0.39	1.77
8/11	-2.81	2.3	-0.17	-0.55	0.22	-0.43
9/10	7.18	-4.05	-0.34	0.58	3.30	-0.37
9/17	-7.22	-3.63	6.06	-0.65	1.68	-0.56
9/19	3.39	-0.08	-3.80	2.43	2.95	3.10
10/15	-8.98	-1.26	4.93	5.48	-0.98	2.91
11/12	-1.25	2.73	-2.40	-0.09	-2.27	0.03
15/16	-6.41	9.47	4.07	1.08	1.18	4.23
15/18	5.12	-4.26	-0.09	-2.66	-3.98	-3.50

[a] Pairs of peak areas identified according to figure labels

14.3.3. Classification of EVOO from the Chemchali, Fouji and Zarrazi cultivars according to their maturity index

Next, the EVOOs from the Chemchali, Fouji and Zarrazi cultivars were also classified according to their maturity index. For this purpose, three matrices were constructed: two matrices (for Chemchali and Fouji) containing 15 objects each, and one more matrix (for Zarrazi cultivar) with 9 objects. These matrices also contained the 171 predictors obtained after normalization and a response column in which the different maturity levels were included. All matrices were also divided in the training and evaluation sets. Thus the training sets were composed by 10 objects for Chemchali and Fouji cultivars and by 6 objects for Zarrazi cultivar, while the evaluation sets were composed by 5 objects (Chemchali and Fouji) and 3 objects (Zarrazi). Three LDA models, one for each cultivar, were next constructed. The corresponding score plots are shown in **Figure 14.4A, 4B and 4C**, for Chemchali, Fouji and

Zarrazi cultivars, respectively. In all cases, the λ_w was lower than 0.01. As it can be observed in **Figure 14.4** (A.2) for the Chemchali cultivar, the objects appeared in order along the first discriminant function according to their maturity index, except to the index 5. This is in agreement with the predictors selected to construct the LDA model (see **Table 14.6**), and the TAG percentages of **Table 14.4**. As it is observed in **Table 14.6** for the Chemchali cultivar, the first discriminant function was mainly constructed by predictors 8/18, 11/18 and 13/15. The percentages of peak 8 (OOL) increased according to maturity, except to the maturity index 5, that showed an intermediate value.

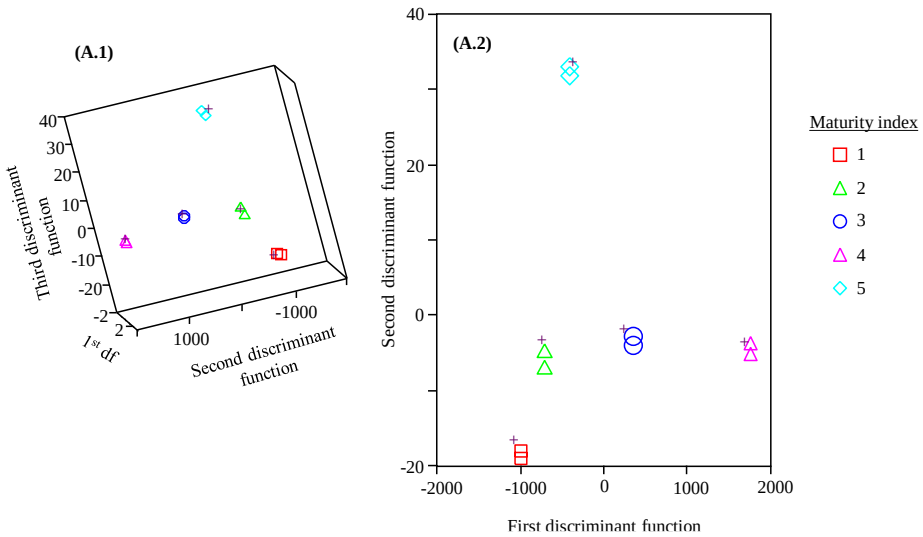

Figure 14.4A. Score plot on an oblique plane of the 3D space defined by the three first discriminant functions and on the plane of the first and second discriminant functions of the LDA model constructed to classify Chemlali.

The opposite tendency was observed for peak 18 (SOP), which percentage decreased when maturity index increased, except for index 5, which showed again an intermediate value. The 11/18 and 13/15 ratios showed a similar trend, although these predictors had lower discriminant capability. For this reason, when the samples were projected on the axis of the first discriminant function, the objects appeared at increasing maturity indexes, except for the index 5 that showed an intermediate value.

Similar results were obtained for the Fouji cultivar (**Figure 14.4(B.2**)), where the main peak area ratios selected by the algorithm to construct the LDA models corresponded to 4/12 (OLL/PPL) and 4/17 (OLL/SOO) ratios (see **Table 14.6**). Finally, the main predictors selected for the Zarrazi model corresponded to 5/18 (PaOL/SOP) and 5/10 (PaOL/OLP). When leave-one-out validation was applied to the three models, all the objects of the training set were correctly classified. The prediction capability of the models was also evaluated using the evaluation sets. Using a 95% probability, all the objects were correctly classified; thus, the prediction capability of the three models was 100%.

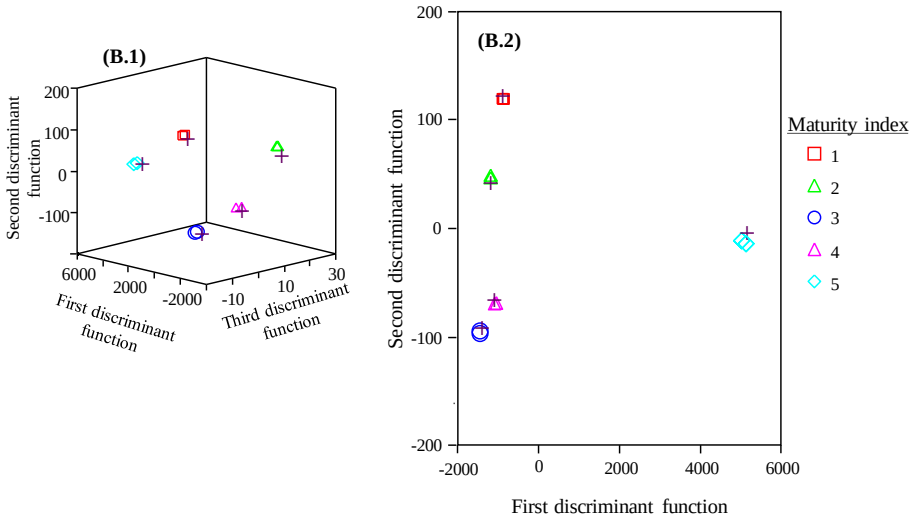

Figure 14.4B. Score plot on an oblique plane of the 3D space defined by the three first discriminant functions and on the plane of the first and second discriminant functions of the LDA model constructed to classify Fouji.

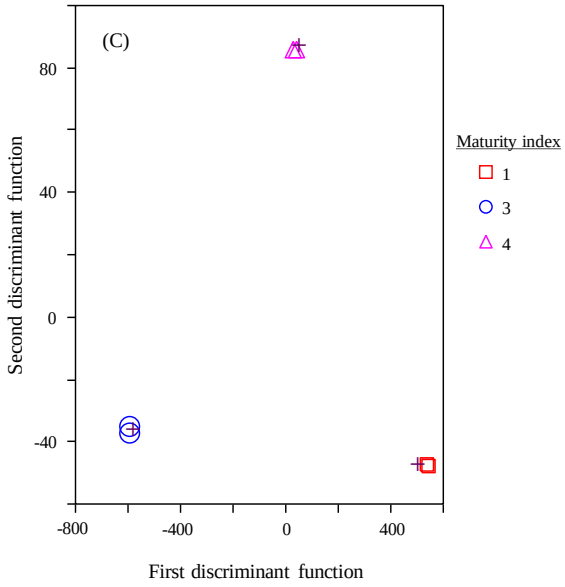

Figure 14.4C. Score plot on an oblique plane of the 3D space defined by the three first discriminant functions and on the plane of the first and second discriminant functions of the LDA model constructed to classify Zarrazi.

Table 14.6

Predictors selected and corresponding standardized coefficients of the LDA model constructed to predict the maturity index of EVOOs.

Cultivar	Predictors[a]	f_1	f_2	f_3	f_4
Chemchali	6/18	4.73	0.35	1.16	0.07
	8/18	31.32	-0.28	-0.79	-0.61
	10/18	7.99	1.10	0.27	0.19
	11/18	-25.35	-0.61	-0.22	0.64
	13/15	24.33	-0.30	0.12	0.54
Fouji	4/8	2.77	0.28	-0.37	0.84
	4/12	14.28	1.93	2.07	1.14
	4/17	18.26	0.04	0.02	-0.35
	13/15	-4.74	0.80	-0.50	-0.36
	15/18	-5.29	2.09	2.20	1.07
Zarrazi	4/13	-0.59	2.08	-	-
	5/10	18.77	0.92	-	-
	5/18	23.93	0.80	-	-

[a] Pairs of peak areas identified according to figure labels

14.4. Conclusions

The feasibility of distinguishing Tunisian EVOOs according to the selected cultivars and maturity index by using TAG profiles obtained by HPLC-ELSD followed by LDA has been demonstrated. Since different TAG patterns were observed for the EVOOs obtained from different cultivar and maturity index, TAGs were used as predictors for the construction of LDA models. EVOOs belonging to 7 Tunisian cultivars, and EVOOs from the Chemchali, Fouji and Zarrazi cultivars obtained at different maturity indexes, were correctly classified with an excellent resolution among all the categories, being in all cases the assignment probability of the models higher than 95%. Thus, it was demonstrated that TAG profiles present a high potential to discriminate EVOOs obtained from different cultivar and maturity index.

Acknowledgements

Project CTQ2014-52765-R (MINECO of Spain and FEDER funds). M. Vergara-Barberán thanks the MINECO for an FPU grant for PhD studies.

Conflict of Interest The authors declare no conflict of interest.

Compliance with ethics requirements This article does not contain any studies with human or animal subjects.

14.5. References

Aparicio, R.; Aparicio-Ruíz, R. (**2000**). Authentication of vegetable oils by chromatographic techniques. *Journal of Chromatography A, 881*, 93-104.

Baccouri, O.; Cerretani, L.; Bendini, A.; Caboni, M.F.; Zarrouk, M.; Pirrone, L.; Daoud Ben Miled, D. (**2007**). Preliminary chemical characterization of Tunisian monovarietal virgin olive oils and comparison with Sicilian ones. *European Journal of Lipid Science and Technology, 109*, 1208-1217.

Baccouri, O.; Guerfel, M.; Baccouri, B.; Cerretani, L.; Bendini, A.; Lercker, G.; Zarrouk, M.; Daoud, D. (**2008**). Chemical composition and oxidative stability of Tunisian monovarietal virgin olive oils with regard to fruit ripening. *Food Chemistry, 109*, 743-754.

Ben Youssef, N.; Zarrouk, W.; Carrasco-Pancorbo, A.; Ouni, Y.; Segura-Carretero, A.; Fernández-Gutiérrez, A.; Daoud, D.; Zarrouk, M. (**2010**). Effect of olive ripeness on chemical properties and phenolic composition of Chétoui virgin olive oil. *Journal of the Science of Food and Agriculture, 90*, 199-204.

Bengana, M.; Bakhouche, A.; Lozano-Sánchez, J.; Amir, Y.; Youyou A.; Segura-Carretero, A.; Fernandez-Gutiérrez, A. (**2013**). Influence of olive ripeness on chemical properties and phenolic composition of Chemlal extra-virgin olive oil. *Food Research International, 5*4, 1868–1875

Boskou, D (1996) Olive oil chemistry and technology, AOCS Press, Champaign, III, USA Boskou, D. (**2011**). Vegetable oils in food technology composition, properties and uses. Gunstone, F. D., Ed.; Blackwell Publishing., p. 252.

Cerretani, L.; Bendini, A.; Del Caro, A.; Piga, A.; Vacca, V.; Caboni, M.F.;

Gallina Toschi, T. (**2006**). Preliminary characterization of virgin olive oils obtained from different cultivars in Sardinia. Eur *Food Research Technology, 222,* 354–361

Cunha, S.C.; Oliveira, M.B.P.P. (**2006**). Discrimination of vegetable oils by triacylglycerols evaluation of profile using HPLC/ELSD. *Food Chemistry, 95,* 518-524.

Dag, A.; Kerem, Z.; Yogev, N.; Zipori, I.; Lavee, S.; Ben-David, E. (**2011**). Influence of time of harvest and maturity index on olive oil yield and quality. *Scientia Horticulturae, 127,* 358-366.

Fuentes de Mendoza, M.; Concepción, D.M.G.; Marín Expóxito, J.; Sánchez Casas, J. (**2013**). Chemical composition of virgin olive oils according to the ripening in olives. *Food Chemistry, 141*, 2575–2581.

Gimeno, E.; Castellote, A.I.; Lamuela-Raventos, R.M.; De la Torre, M.C.; Lopez-Sabater, M.C. (**2002**). The effects of harvest and extraction methods on the antioxidant content (phenolics, α-tocopherol, and β-carotene) in virgin olive oil. *Food Chemistry, 78,* 207-211.

Gómez-Rico, A.; Fregapane, G.; Salvador, M.D. (**2008**). Effect of cultivar and ripening on minor components in Spanish olive fruits and their corresponding virgin olive oils. *Food Research International, 41,* 433–440

Gutíerrez, F.; Jimenez, B.; Ruíz, A.; Albi, M. A. (**1999**). Effect of olive ripeness on the oxidative stability of virgin olive oil extracted from the varieties Picual and Hojiblanca and on the different components involved. *Journal of Agricultural and Food Chemistry, 47,* 121–127.

Haddada, F.M.; Manai, H.; Oueslati, I.; Daoud, D.; Sánchez, J.; Osorio, E.; Zarrouk, M. (**2007**). Fatty acid, triacylglycerol, and phytosterol composition in six Tunisian olive varieties. *Journal of Agricultural and Food Chemistry,* 55, 10941-10946.

Harwood JL, Page RA **(1994**). Biochemistry of oil synthesis. In: Murphy, D.J. (Ed.), Designer Oil Crops. VCH, Weinheim, pp. 165–194.

Heron, S.; Maloumbi, M.G.; Dreux, M.; Verette, E.; Tchapla, A. (**2007**). Method development for a quantitative analysis performed without any standard using an evaporative light-scattering detector. *Journal of Chromatography A, 1161*, 152–156.

Issaoui, M.; Flamini, G.; Brahmi, F.; Dabbou, S.; Ben Hassine, K.; Taamali, A., Chehab, H.; Ellouz, M.; Zarrouk, M;. Hammami, M.; (**2010**). Effect of the growing area conditions on differentiation between Chemlali and Chétoui olive oils. *Food Chemistry, 119*, 220–225.

Kalua, C.M.; Allen, M.S.; Bedgood, D.R.; Bishop, A.G.; Prenzler, P.D. (**2005**). Discrimination of olive oils and fruits into cultivars and maturity stages based on phenolic and volatile compounds. *Journal of Agricultural and Food Chemistry*, *53*, 8054–8062.

Krichene, D.; Allalout,A.; Mancebo-Campos, V.; Salvador, M.D.; Zarrouk, M.; Fregapane, G. (**2010**). Stability of virgin olive oil and behaviour of its natural antioxydants under medium temperature accelerated storage conditions. *Food Chemistry, 121,* 171–177.

Lerma-García, M.J.; Lusardi, R.; Chiavaro, E.; Cerretani, L.; Bendini, A.; Ramis-Ramos, G.; Simó-Alfonso, E.F. (**2011**). Use of triacylglycerol profiles established by high performance liquid chromatography with ultraviolet-visible detection to predict the botanical origin of vegetable oils. *Journal of Chromatography A, 1218*, 7521–7527.

Mailer R.J., Ayton J.; Graham K. (**2010**). The Influence of growing region, cultivar and harvest timing on the diversity of Australian olive oil. *Journal of the American Oil Chemists' Society*, 87, 877–884.

Matos, L.C.; Cunha, S.C.; Amaral, J.S.; Pereira, J.A.; Andrade, P.B.; Seabra, R.M.; Oliveira, B.P.P. (**2007**). Chemometric characterization of three varietal olive oils (Cvs. Cobrançosa, Madural and Verdeal Transmontana) extracted from olives with different maturation indices. *Food Chemistry, 102*, 406-414.

Mengerink, Y.; Peters, R.; de Koster, C.G.; Van der Wal, S.J.; Claessens, H.A.; Cramers, C.A. (**2001**). Separation and quantification of the linear and cyclic structures of polyamide-6 at the critical point of adsorption. *Journal of Chromatography A, 914*, 131–145.

Morelló, J.R.; Romero, M.P.; Motilva, M.J. (**2006**). Influence of seasonal conditions on the composition and quality parameters of monovarietal virgin olive oils. *Journal of the American Oil Chemists' Society, 83*, 683–690.

Morera Pons, S.; Castellote Bargallo, A.I.; Lopez Sabater, M.C. (**1998**). Analysis of human milk triacylglycerols by high-performance liquid chromatography with light-scattering detection. *Journal of Chromatography A, 823*, 475–482.

Nagy, K.; Bongiorno, D.; Avellone, G.; Agozzino, P.; Ceraulo, L.; Vékey, K. (**2005**). High performance liquid chromatography-mass spectrometry based chemometric characterisation of olive oils. *Journal of Chromatography A, 1078*, 90-97.

Ollivier, D.; Artaud, J.; Pinatel, C.; Durbec, J.P.; Guérère, M. (**2006**) Differentiation of French virgin olive oil RDOs by sensory characteristics, fatty acid and triacylglycerol compositions and chemometrics. *Food Chemistry, 97*, 382–393.

Oueslati, I.; Manai, H.; Haddada, F.M.; Daoud, D.; Sánchez, J.; Osorio, E.; Zarrouk, M. (**2009**). Sterol, triterpenic dialcohol, and triacylglycerol

compounds of extra virgin olive oils from some Tunisian varieties grown in the region of Tataouine. *Journal of Food Science and Technology, 15*, 5–13.

Rombaut, R.; De Clercq, N.; Foubert, I.; Dewettinck, K. (**2009**). Triacylglycerol analysis of fats and oils by evaporative light scattering detection. *Journal of the American Oil Chemists' Society, 86*, 19–25

Ruíz-Gutiérrez, V.; Barron, L.J. (**1995**). Methods for the analysis of triacylglycerols. *Journal of Chromatography B, 671*, 133–168.

Ruiz-Samblás, C.; Cuadros-Rodríguez, L.; González-Casado, A.; Rodríguez García, F.P.; De la Mata-Espinosa, P.; Bosque-Sendra, J.M. (**2011**). Multivariate analysis of HT/GC-(IT) MS chromatographic profiles of triacylglycerol for classification of olive oil varieties. *Analytical and Bioanalytical Chemistry, 399*, 2093–2103.

Sakouhi, F.; Herchi, W.; Sebei, K.; Absalon, C.; Kallel, H.; Boukhchina, S.(**2011**). Accumulation of total lipids, fatty acids and triacylglycerols in developing fruits of *Olea europaea* L. *Scientia Horticulturae, 132*, 7–11.

Salvador, M.D.; Aranda, F.; Fregapane, G. (**2001**). Influence of fruit ripening on "Cornicabra" virgin olive oil quality. A study of four successive crop seasons. *Food Chemistry, 73*, 45–53.

Sandra, P.; Medvedovici, A.; Zhao, Y.; David, F. (**2002**). Characterization of triglycerides in vegetable oils by silver-ion packed-column supercritical fluid chromatography coupled to mass spectroscopy with atmospheric pressure chemical ionization and coordination ion spray. *Journal of Chromatography A, 974*, 231–241.

Siouffi, A.M. (**2000**). Chapter 1: HPLC. In: Nollet, ML (Ed.), Food Analysis by HPLC. Marcel Dekker, Inc., New York, NY, 1-54.

Skevin, D.; Rade, D.; Strucelj, D.; Mokrovcak, Z.; Nederal, S.; Bencic, D. (**2003**). The influence of variety and harvest time on the bitterness and phenolic compounds of olive oil. *European Journal of Lipid Science and Technology*, *105*, 536-541.

Vandeginste, B.G.M.; Massart, D.L.; Buydens, L.M.C.; De Jong, S. (**1998**). Data handling in science and technology, Part B, 18th Edn., Elsevier, Ed., Amsterdam, p. 237.

Vichi, S.; Lazzez, A.; Grati-Kamoun, N.; Caixach, J. (**2012**). Modifications in virgin olive oil glycerolipid fingerprint during olive ripening by MALDI-TOF MS analysis. *LWT - Food Science and Technology*, *48*, 24-29.

Yorulmaz, A.; Erinc, H.; Tekin, A. (**2013**). Changes in olive and olive oil characteristics during maturation. *Journal of the American Oil Chemists' Society*, *90*, 647-658.

Chapter 15. Sterol profiles of Tunisian extra virgin olive oils: Classification among different cultivars and maturity indexes

European Journal of
Lipid Science and Technology

Sterol profiles of Tunisian extra virgin olive oils: Classification among different cultivars and maturity indexes

Marwa Abdallah[1,2a], María Vergara-Barberán[3a], María Jesús Lerma-García[3*], José Manuel Herrero-Martínez[3], Mokhtar Zarrouk[2], Mokhtar Guerfel[2] and Ernesto F. Simó-Alfonso[3]

[1] University of Tunis El Manar, Faculty of Sciences of Tunis, Campus University, Tunis 1060, Tunisia
[2] Center of biotechnology of Borj Cedria, Laboratory of biotechnology of olive, BP 901, 2050, Hammam-Lif, Tunisia
[3] Department of Analytical Chemistry, Faculty of Chemistry, University of Valencia, Burjassot, Valencia, Spain
[a] These authors equally contributed to this work and they should be considered co-first authors

The suitability of sterol profiles established by HPLC-MS as a tool to discriminate between seven cultivars of Tunisian extra virgin olive oils (EVOOs) was evaluated in this study. Moreover, some cultivars (Chemchali, Fouji and Zarrazi) have been also classified according to their maturity index. A total of nine sterol peaks, which appeared in all samples, were used to develop linear discriminant analysis (LDA) models able to distinguish Tunisian EVOOs according to their cultivar or maturity index. An excellent predictive classification was obtained since all samples were correctly categorized. Therefore, it has been demonstrated that sterol profiles are a powerful tool to discriminate EVOOs coming from different cultivars and maturity indexes.

Keywords: Cultivar; HPLC-MS; maturity index; sterols; Tunisian extra virgin olive oils

15.1. Introduction

Olive oil extracted from the fruit of Olea Europaea L. is the most characteristic source of fat in the Mediterranean diet. Its consumption is currently increasing due to the significant nutritional and healthy benefits. Olive oil plays an important role in the Tunisian agronomy and economy, being Tunisia the second most producer of EVOO in the world after the European Community (IOOC, 2004). There are two major varieties, Chemlali and Chétoui, however, a large genetic diversity among its olive trees can be found all over the country (Taamalli, 2012).

This appreciated edible oil is made up of triglycerides (more than 98%) and other minor compounds (about 1-2%) (Alonso-Salces, 2011) such as phenols, tocopherols or sterols. Among this chemical composition, sterols, also called phytosterols, present the greatest proportion of the non-saponifiable fraction of olive oil (Lagarda, 2006).

Several health benefits have been attributed to sterols. According to many researches, sterols are membrane constituents which regulate membrane fluidity and permeability (Giacometti, 2001), decreasing the plasma cholesterol levels by inhibiting its absorption from small intestine (Richelle, 2004), which may protect against cardiovascular diseases (Gylling, 2014). Sterols have been also considered as cancer preventive, abolishing the carcinogenesis process, mitigating cell division, modifying some hormones essential for tumor growth and stimulating the death of tumor cells (Sotiroudis, 2008). These compounds may have also anti-inflammatory activities (Cárdeno, 2014).

The most abundant sterol in olive oil is β-sitosterol, which represents a 75–90% of the total sterol fraction. Other sterols are found in considerable amounts, such as Δ^5-avenasterol (5–36%) and campesterol (approximately 3% of the total sterol fraction). However, other sterols, such as cholesterol,

campestanol, stigmasterol, $\Delta^{5,24}$-stigmastadienol, Δ^{7}-stigmastenol and Δ^{7}-avenasterol, among others, are present in olive oil in small amounts (Boskou, 2011). The content of these sterols in different olive oils is regulated by the European Union (EU), the International Olive Oil Council (IOOC) and Food and Agriculture Organization of the United Nations (FAO) to control against fraud (Sánchez, 2004).

The control of sterol fraction is an important issue for vegetable oil genuineness. Since several studies have demonstrated that each oily fruit has its characteristic sterol profile, its determination could provide abundant information about oil quality (Lerma-García, 2008) and therefore it could be used for authentication purposes. Regarding olive oil, sterol composition has been used for the detection of fraudulent admixtures of olive oil with other cheaper vegetable oils such as hazelnut (Azadmard-Damirchi, 2010), corn, soybean, sunflower and cotton seed oils (AL-Ismail, 2010). In addition, this profile has permitted the characterization of olive oils according to their genetic variety and quality grade (extra virgin, virgin, refined, solvent extracted, olive pomace oil, crude olive pomace oil, refined olive–pomace oil, and refined seed oil) (Cabañate, 2007; Martínez-Vidal, 2007). However, composition and total sterol contents are strongly influenced by many factors such as geographical area Ben Temime, 2008), crop season (Ilyasoglu, 2010) agronomic practices such as irrigation (Berenguer, 2006), soil conditions (Reboredo, 2014), storage time and temperature (Bouaziz, 2008). However, many researchers suggested that cultivar (Krichène, 2010) and fruit maturity (Fuentes de Mendoza, 2013) are the two most important factors.

Several techniques have been used to determine sterols from olive oils. The official methods for the determination of sterols involve the extraction of the unsaponifiable fraction and isolation of sterols by TLC. Quantification of the silanized sterol fraction is commonly performed by GC with FID (Manai, 2012), but GC with MS detection has been also used (Cunha, 2006). However,

the employment of GC has several disadvantages such as the requirement of both thermally stable columns and chemical derivatization before analysis. For this reason, other methods such as capillary electrochromatography with diode array UV-vis detection (Lerma-García, 2008A), direct infusion mass spectrometry (Lerma-García, 2008B) and HPLC-MS (Cabañate, 2007; Martínez-Vidal, 2008; Segura-Carretero, 2008) have been also developed to determine sterols in vegetable oils. However, and as far as we are concerned, only few works have been published regarding sterol composition of minor Tunisian cultivars because most research studies related to the Tunisian olive oil have been focused on the characterization of the two main varieties (Chétoui and Chemlali). This fact causes a lack of information of the chemical composition of several minor cultivars that could provide a better oil quality.

The aim of this work was to evaluate the possibility of using sterols profiles established by HPLC-MS, followed by LDA of the spectral data, to classify seven Tunisian EVOOs according to their cultivar, and to discriminate Chemchali, Fouji and Zarrazi EVOOs according to their maturity index.

15.2. Materials and methods

15.2.1. Chemicals

Ethanol, 2-propanol, acetic acid, ACN and anhydrous sodium sulphate were purchased from Scharlau (Barcelona, Spain); diethyl ether and chloroform from J. T. Baker (Deventer, The Netherlands). KOH from Probus (Barcelona); n-hexane from Riedel-de Haën (Seelze, Germany) and 2,7-dichlorofluorescein from Sigma-Aldrich (St. Louis, MO, USA). All these reagents were of suitable analytical grade. For TLC, glass plates coated with silica gel without fluorescent indicator (0.25 mm plate thickness, Merck, Darmstadt, Germany) were used. Deionized water obtained with a Barnstead deionizer (Sybron, Boston, MA) was also employed. The sterols used as

standards were erythrodiol (Fluka, Buchs, Switzerland), β-sitosterol (mixture containing 75% β-sitosterol and 10% campesterol), stigmasterol (Acros Organics, Morris Plains, NJ) and cholesterol (Aldrich, Milwaukee, WI).

15.2.2. EVOO samples

A total of fifty five EVOOs samples (see **Table 15.1**) were obtained in order to develop a classificatory method based on their different cultivar. Moreover, Chemchali, Fouji and Zarrazi samples were also used to obtain another classificatory method based on their different maturity index.

All EVOOs were obtained from *ca*. 1 kg of healthy and non- damage olives, which have been hand-picked during the 2012/2013 and 2013/2014 harvesting seasons from olive orchards located in the Tunisian geographical areas indicated in **Table 15.1**. After harvesting, olives were immediately transported to the laboratory, and the oil was extracted using an Abencor system (MC2 Ingeniería y Sistemas, Seville, Spain) within 24 h. After harvesting, olives were deleafed, crushed with a hammer crusher, mixed at ambient temperature for 30 min and centrifuged without addition of water or chemicals; then, EVOOs were transferred into dark glass bottles and stored at 4 °C until analysis.

In order to obtain the EVOOs of different maturity indexes, *ca.* 10 kg olives were collected from a same olive tree at different periods: olive fruits from the Chemlali, Dhokar, Jemri and Zalmati varieties were picked at the end of November, while for the Chemchali, Fouji and Zarrazi varieties the harvesting started at the end of September and continued up to January in order to obtain olives with different maturity indexes.

Table 15.1

Cultivar, number of samples, crop season, maturity index and geographical origin of the Tunisian EVOO samples employed in this study.

Genetic variety	No. of samples	Crop season	Maturity index	Geographical origin
Chemchali	1	2012/2013	1	Gafsa
	2	2012/2013	2	
	2	2012/2013	3	
	1	2012/2013	4	
	2	2012/2013	5	
Chemlali	1	2012/2013	3.1	Sousse
	1	2013/2014	3.7	Sfax
	2	2012/2013	3.5	Sidi Bouzid
		2013/2014	4.0	
Dhokar	2	2012/2013	3.9	Ben Gardène
		2013/2014	3.2	
	2	2012/2013	3.7	Tataouine
		2013/2014	3.5	
Fouji	2	2012/2013	1	Gafsa
	2	2012/2013	2	
	1	2012/2013	3	
	1	2012/2013	4	
	1	2012/2013	5	
Jemri	2	2012/2013	4.2	Ben Gardène
		2013/2014	3.8	
	2	2012/2013	3.1	Medenine
		2013/2014	3.7	
Zalmati	2	2012/2013	3.3	Medenine
		2013/2014	3.6	
	2	2012/2013	3.1	Zarzis
		2013/2014	3.9	
Zarrazi	2	2012/2013	1	Gafsa
	2	2012/2013	3	
	2	2012/2013	4	

Then, for Chemchali and Fouji cultivars, five maturity levels were identified, while for Zarrazi cultivar only three were observed (see **Table 15.1**). For each one of these maturity levels, *ca.* 1 kg of healthy and non-damage olives were used to obtain the corresponding EVOO. These maturity levels were established according to the National Institute of Agronomical Research of Spain, described by the IOOC (IOOC, 2004), which is based on a subjective evaluation of olive skin and pulp colours (1, yellowish green; 2, green with reddish spots; 3, reddish brown; 4, black with white flesh and 5, black with < 50% purple flesh).

15.2.3. Preparation of sterol extracts

EVOO sterol fractions were obtained following the procedure established by the European Union (CE Nº796/2002). Therefore, 5 g of oil was saponified by refluxing for 20 min with 2 M ethanolic KOH; then, 50 mL of distilled water was added, and the non-saponifiable fraction was extracted three times with diethyl ether. The ether extracts were combined and washed 3 times with 50 mL distilled water until neutral reaction. The organic extracts were dried with anhydrous sodium sulphate, filtered and then evaporated to dryness using a rotatory evaporator. The remaining unsaponifiables were dissolved in 2 mL of chloroform, and then the sterol fraction was separated by TLC using hexane/diethyl ether 60:40 (v/v). After TLC separation, the silica plate was sprayed lightly with 2,7-dichlorofluorescein. The sterol band was removed from the silica plate, dissolving the residue in 10 mL of diethyl ether. The solvent was evaporated, and the residue was dissolved in 500 μL of 2-propanol and stored at -20 ºC in amber vials. These solutions were properly diluted with the mobile phase and injected. For each sample of **Table 15.1**, three extracts were obtained, which were injected three times.

15.2.4. HPLC-MS conditions

Chromatographic separation was accomplished in an 1100 series HPLC (Agilent Technologies, Waldbronn, Germany) consisting of an automatic sampler, a solvent mixing module, an automatic degasser, a quaternary pump and a column oven compartment. Sterol separation was performed at 50 ºC using ACN containing 0.01% acetic acid as mobile phase at a constant flow of 1 mL min^{-1} under isocratic elution. A KinetexTM C18 100 Å column (150 mm × 4.6 mm, 2.6 μm; Phenomenex, Torrance, CA) was employed. 20 μL of samples was injected. As a detector, an HP 1100 series ion trap mass spectrometer (Agilent Technologies, Waldbronn, Germany) equipped with an electrospray ionization (ESI) source was used. The MS working conditions were: nebulizer gas pressure, 15 psi; drying gas flow rate, 12 L min^{-1} at 350 ºC; capillary voltage, -1.9kV; voltages of skimmers 1 and 2, 25.9, and 6.0 V, respectively. Nitrogen was used as nebulizer and drying gas (Gaslab NG LCMS 20 generator, Equcien, Madrid, Spain). The mass spectrometer was scanned within the m/z 200-500 range in the positive ion mode. The ion trap target mass was stablished at *m/z* 397 ($[M^{+} H^{-} H_2O]^{+}$ peak of β-sitosterol). Maximum loading of the ion trap and collection time were 3 x 10^4 counts and 200 ms, respectively. Total ion chromatograms (TIC) and extracted ion chromatograms (EIC) were smoothed using a Gaussian filter set at 5 points.

15.2.5. Statistical analysis by LDA

The peak area of each sterol was measured from the smoothed EIC, and a data matrix was constructed using the areas of all peaks as original variables. After normalization of the variables, statistical data treatment was performed using SPSS (v. 15.0, Statistical Package for the Social Sciences, Chicago, IL). This supervised technique allows the classification of a sample of unknown category between a set of classes whose category is known a priori. In order to select the variables to be included in the model, the Wilks' lambda (λ_w)

criterion was used (Vandeginste, 1998). This criterion maximizes the distance between classes and minimizes the distance between the objects for each class. In this work, the stepwise algorithm was used to select the predictors that will be included in the LDA models, being the probability values adopted for variable inclusion of F_{-test} (F_{in}) or removal (F_{out}) of 0.05 and 0.10, respectively.

15.3. Results and discussion

15.3.1. Comparison of sterol profiles of EVOOs from different cultivar and maturity index

All EVOO extracts were injected using the conditions described above. After acquiring the TICs of samples, EICs at different *m/z* values were performed, which led to the identification of 9 peaks, which corresponded to 12 possible sterols. A list of the identified sterols, and their corresponding retention times and *m/z* value is shown in **Table 15.2**.

Table 15.2

Peak labelling, retention time (t_R) and *m/z* value of the sterols considered in this work.

Peak no	Analytes	t_R (min)	*m/z*
1	Erythrodiol	2.3	425
2	Uvaol	2.3	425
3	Brassicasterol	6.0	381
4	Cholesterol	6.8	369
5	Δ^7-Avenasterol	7.0	395
6	Δ^5-Avenasterol	7.0	395
7	Campesterol	7.9	383
8	Campestanol	7.9	385
9	Stigmasterol	8.1	395
10	$\Delta^{5,24}$-Stigmastadienol	9.0	395
11	Δ^7-stigmastenol	9.1	397
12	β-Sitosterol	9.1	397

The TIC and EICs of EVOO samples from Chemchali, Fouji and Zarrazi cultivars at maturity index 3 are shown in **Figure 15.1**. As it can be observed, several differences between the peak profiles of the different cultivars were evidenced. The proportion of sterols found, established by dividing each sterol area (taken from its corresponding EIC) by the sum of the areas of all sterols identified are summarized in **Table 15.3**.

As it can be observed in both, **Figure 15.1** and **Table 15.3**, the most intense peaks found in all samples corresponded to β-sitosterol+ Δ^7-stigmastenol, Δ^7+ Δ^5-avenasterol and campesterol. Besides, brassicasterol, cholesterol, campestanol, stigmasterol, $\Delta^{5,24}$-stigmastadienol, Δ^7-stigmastenol and two triterpene dialcohols (erythrodiol and uvaol) were also found in a smaller proportion (see **Table 15.3**).

As previously reported by other authors (Ouni, 2011; Manai, 2012; Noorali, 2014), the composition of sterols in olive oil varied according to the cultivar and maturity index. In general, the most abundant sterol was β-sitosterol, its relative content was comprised between 71-89%, followed by Δ^7+Δ^5-avenasterol, which range was between 4-23%. The content of β-sitosterol generally decreases during ripening, while Δ^7+Δ^5-avenasterol content increases, which could be explained by de presence of desnaturase activity (Gutiérrez, 1999; Ouni, 2011).

The highest β-sitosterol content (88.72%) and the lowest one for Δ^7+Δ^5-avenasterol (4.59%) were found for Zarrazi cultivar, whereas Fouji and Dokhar are characterized by the lowest content of β-sitosterol (71.02 and 73.44%) and the highest of Δ^7+Δ^5-avenasterol (21.18 and 22.83%). These values are similar to those reported for other olive oil cultivars (Gutiérrez, 1999; Ouni, 2011; Manai, 2012; Fuentes de Mendoza, 2013).

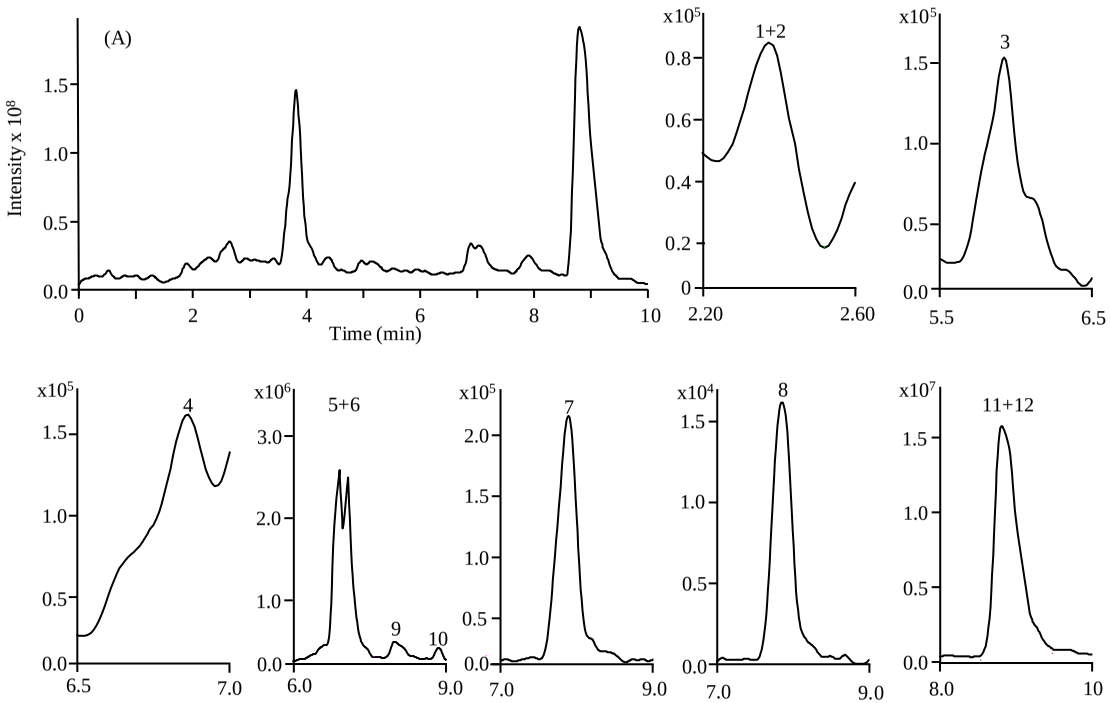

Figure 15.1A. TIC and EICs of Chemchali EVOO extracts of maturity index 3. EICs were obtained at the *m/z* values indicated in **Table 15.2**. Peak labelling is an indicated **Table 15.2**.

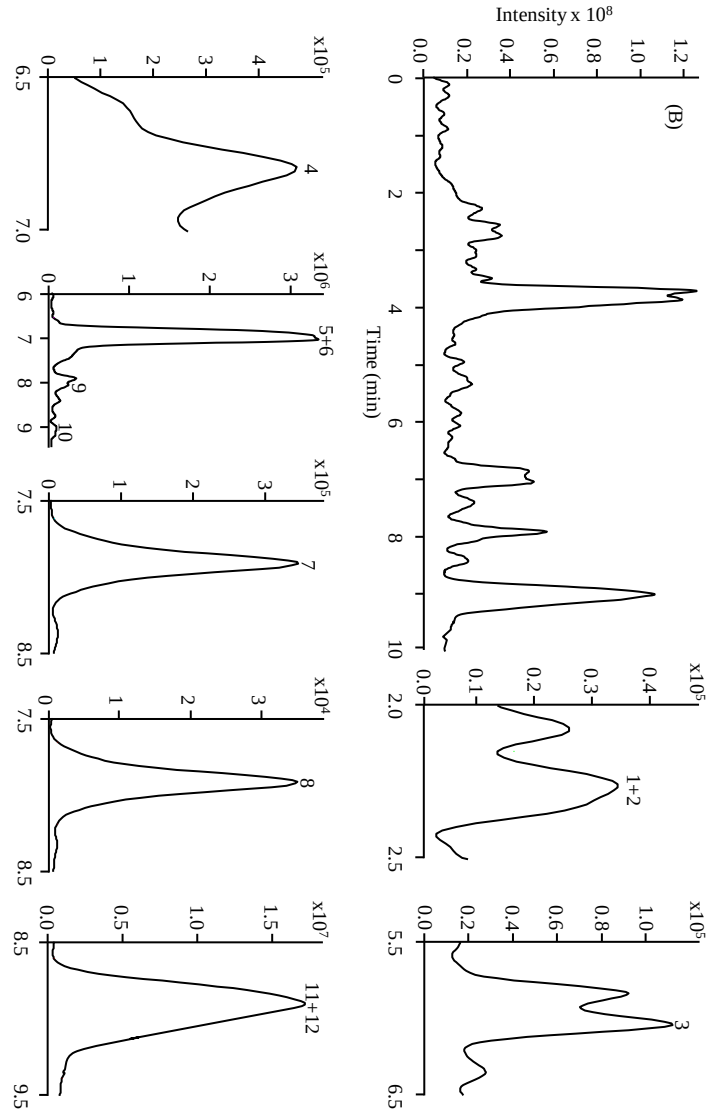

Figure 15.1B. TIC and EICs of Fouji EVOO extracts of maturity index 3. EICs were obtained at the *m/z* values indicated in **Table 15.2**. Peak labelling is an indicated **Table 15.2**.

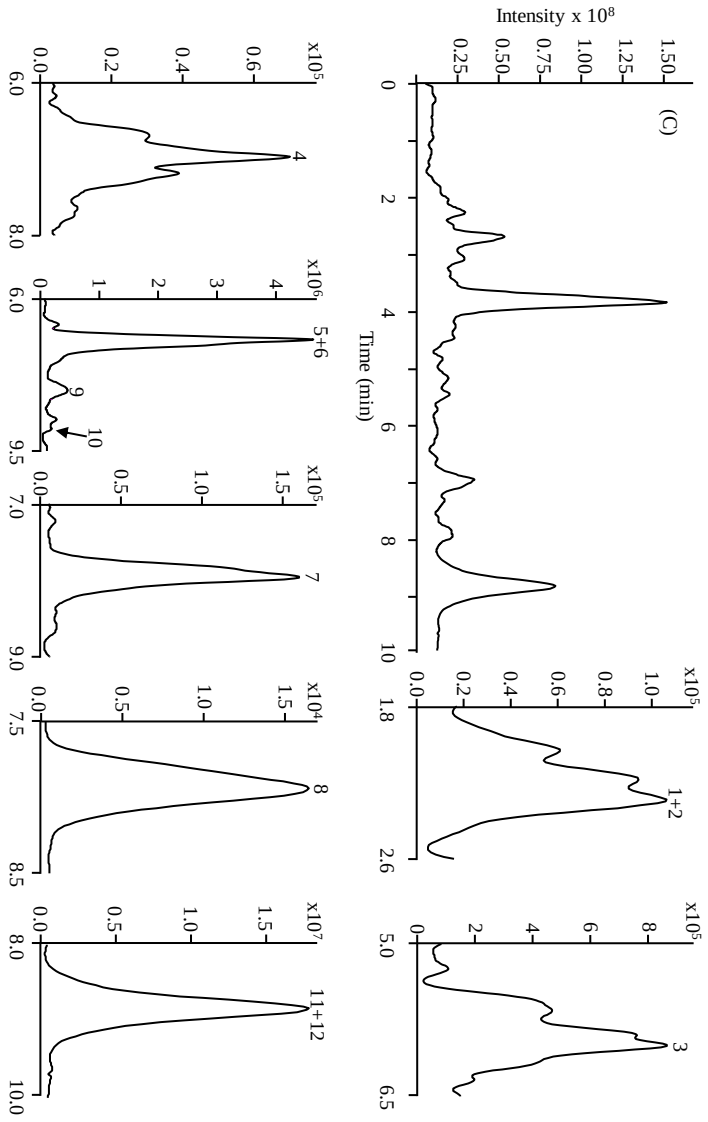

Figure 15.1C. TIC and EICs of Zarrazi EVOO extracts of maturity index 3. EICs were obtained at the *m/z* values indicated in **Table 15.2**. Peak labelling is an indicated **Table 15.2**.

The other most abundant sterol is campesterol. As it can be observed, its content varied with the cultivar (from 2.07 to 4.27%), although any tendency was observed between the different maturity indexes; however, in all cases the highest value was obtained for maturity index 3. For all samples, campesterol content was lower than the limit established by EU regulation (< 4%), except for Fouji cultivar at maturity index 3, which exceeds this value. It is possible to find other genetic varieties whit this peculiarity, for example Cornicabra (Spain) and Barnea (Australia), which showed contents about 4.5% (Rivera del Álamo, 2004; Mailer, 2010).

In the case of stigmasterol, its content in all samples (comprised between 0.16 and 0.81%) was lower than that of campesterol, which shows that all oil samples came from healthy fruits that were not obtained by forcing systems (Koutsaftakis, 1999).

It should be noted that the content of $\Delta^{5,24}$-stigmastadienol (0.07-0.68%) was lower in all the analysed EVOOs than other Tunisian EVOOs studied previously (0.67-0.90%) (Manai, 2012). On the other hand, the cholesterol content is lower than the maximum established (<0.5%). Finally, the erythrodiol and uvaol contents showed levels within the established limit (4.5%). In general, these results are in good agreement with those published for other cultivars from Spanish and Portugal. (Sanchez-Casas, 2004; Ouni, 2011; Manai, 2012).

Table 15.3

Proportions[a] of sterols found in the total sterol fraction of the Tunisian EVOOs considered in this study.

Cultivar	Maturity index	Erythrodiol + uvaol	Brassicasterol	Cholesterol	Δ^7+ Δ^5-Avenasterol	Campesterol	Campestanol	Stigmasterol	$\Delta^{5,24}$-Stigmastadienol	β-Sitosterol + Δ^7-stigmastenol
Chemchali	1	0.07±0.01	0.27±0.03	0.24±0.02	6.5±0.5	3.7±0.3	1.41±0.1	0.16±0.02	0.34±0.04	87±3
	2	0.07±0.01	0.20±0.03	0.37±0.04	7.6±0.5	3.6±0.3	1.23±0.09	0.24±0.02	0.28±0.03	86±2
	3	0.061±0.008	0.30±0.05	0.27±0.04	8.6±0.6	4.0±0.2	1.25±0.08	0.24±0.03	0.21±0.02	83±3
	4	0.062±0.007	0.36±0.06	0.38±0.05	9.1±0.6	3.4±0.2	0.81±0.06	0.30±0.02	0.24±0.03	83±3
	5	0.020±0.006	0.15±0.02	0.24±0.03	10.1±0.9	3.9±0.2	0.89±0.07	0.17±0.02	0.48±0.03	81±2
Fouji	1	0.070±0.009	0.39±0.07	0.39±0.08	8.1±0.7	2.7±0.2	0.79±0.07	0.18±0.03	0.071±0.008	84±3
	2	0.12±0.02	1.00±0.09	0.27±0.03	10.8±0.8	3.5±0.3	1.51±0.09	0.18±0.02	0.44±0.03	84±2
	3	0.031±0.009	0.21±0.05	0.42±0.06	10.9±0.9	4.3±0.4	2.0±0.1	0.46±0.03	0.24±0.03	82±4
	4	0.030±0.008	0.12±0.01	0.51±0.06	21±1	2.4±0.1	1.2±0.1	0.17±0.02	0.40±0.04	74±2
	5	0.072±0.009	0.51±0.06	0.21±0.04	21±1	2.9±0.2	1.3±0.1	0.56±0.04	0.68±0.05	71±2
Zarrazi	1	0.90±0.07	0.43±0.04	0.44±0.07	4.6±0.3	3.4±0.2	1.06±0.08	0.80±0.06	0.44±0.05	89±4
	3	0.17±0.03	0.77±0.08	0.13±0.03	12.2±0.9	3.6±0.2	1.16±0.07	0.62±0.05	0.28±0.02	83±3
	4	0.06±0.01	0.24±0.04	0.31±0.05	15 ±1	2.1±0.1	1.58±0.09	0.81±0.06	0.62±0.05	76±2

[a]Value corresponding to the mean of the three replicates, 3 extracts and the 3 samples

Table 15.3

Cont.

Cultivar	Erythrodiol + uvaol	Brassicasterol	Cholesterol	Δ^7+ Δ^5-Avenasterol	Campesterol	Campestanol	Stigmasterol	$\Delta^{5,24}$-Stigmastadienol	β-Sitosterol + Δ^7-
Chemlali	0.05±0.01	0.13±0.02	0.13±0.02	20±1	3.0±0.3	1.16±0.08	0.17±0.02	0.67±0.07	75±3
Dokhar	0.041±0.007	0.56±0.08	0.19±0.03	23±2	2.9±0.3	1.68±0.09	0.20±0.02	0.12±0.02	73±2
Jemri	0.022±0.003	0.30±0.05	0.24±0.04	17±1	3.9±0.6	1.22±0.06	0.19±0.02	0.30±0.04	79±3
Zalmati	0.05±0.02	0.4±0.2	0.07±0.03	20±1	3.4±0.2	0.95±0.07	0.25±0.03	0.26±0.03	79±3

15.3.2. Normalization of the variables for statistical analysis

To reduce the variability associated with the total amount of sterols recovered from the EVOO samples and to minimize other sources of variance also affecting the sum of the areas of all peaks, normalized rather than absolute peak areas were used. For this purpose, the area of each peak was divided by each one of the areas of the other 8 peaks; in this way, and taking into account that each pair of peaks should be considered only once, (9 x 8)/2=36 non-redundant peak area ratios were obtained to be used as predictors for LDA model construction.

15.3.3. Classification of EVOOs according to their cultivar

To classify the EVOO samples according to their cultivar (see **Table 15.1**) an LDA model was constructed. After variable normalization, a matrix containing the 36 predictors obtained and 55 objects (which corresponded to the mean of the replicates of the three extracts performed for each sample) was constructed. A response column, containing the 7 categories corresponding to the 7 cultivars of samples, was added. This matrix was divided in two groups, the training and the evaluation sets. The training set was composed by 38 objects, which corresponded to 10 objects for Chemchali and Fouji cultivars (2 samples x 5 maturity indexes), 6 objects for Zarrazi (2 samples x 3 maturity indexes) and 3 objects from the other cultivars. The evaluation set was constituted by the remaining samples (17 objects). A projection of the different cultivars in the plane defined by the three first discriminant functions is shown in **Figure 15.2**.

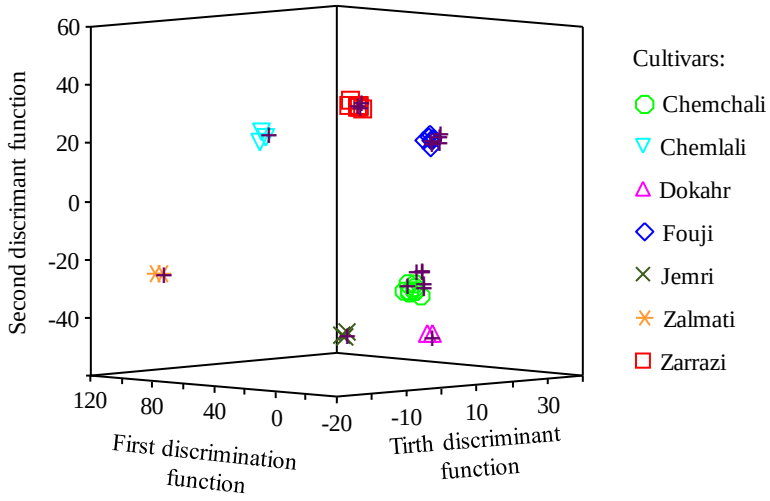

Figure 15.2. Score plot on an oblique plane of the three-dimensional space defined by the three first discriminant functions of the LDA model constructed to classify Tunisian EVOOs according to their cultivar. Evaluation set samples are labelled with a cross symbol.

An excellent resolution between all the category pairs was reached (**Figure 15. 2**, $\lambda w < 0.01$). The variables selected by the algorithm, and the standardized coefficients of the model, showing the predictors with large discriminant capabilities, are given in **Table 15.4**. According to this table, the main peak area ratios selected by the algorithm to construct the LDA model corresponded to the following sterol peak ratios: 3/4 (brassicasterol/ cholesterol), 3/8 (brassicasterol/ campestanol) and 5+6/10 ($\Delta^7+\Delta^5$-avenasterol/$\Delta^{5,24}$-stigmastadienol). Using this model and leave-one-out validation, all the objects of the training set were correctly classified. Concerning to the prediction capability of the model, all the objects of the evaluation set (represented with crosses in **Figure 15.2)** were correctly assigned within a 95% probability level.

15.3.4. Classification of EVOO from the Chemchali, Fouji and Zarrazi cultivars according to their maturity index

The EVOOs from the Chemchali, Fouji and Zarrazi cultivars were also classified according to their maturity index. For this purpose, three matrices were constructed: two matrices (for Chemchali and Fouji) containing 15 objects each, and one more matrix (for Zarrazi cultivar) with 9 objects. These matrices also contained the 36 predictors obtained after normalization and a response column in which the different maturity levels were included. All matrices were also divided in the training and evaluation sets.

Table 15.4

Predictors selected and corresponding standardized coefficients of the LDA model constructed to classify EVOOs according to their cultivar.

Predictors[a]	f_1	f_2	f_3	f_4	f_5	f_6
3/4	20.96	-1.45	-2.79	-1.23	0.42	1.61
3/8	-25.20	12.95	13.37	-1.65	-0.14	-0.92
4/5+6	11.19	1.59	-2.78	2.36	-1.50	-0.16
4/8	9.67	8.62	-10.58	-0.64	-0.44	0.16
4/9	-10.91	5.91	16.51	-1.68	2.64	1.98
5+6/8	-0.93	-8.60	-2.81	4.26	0.86	3.69
5+6/9	10.90	9.69	-6.96	0.59	-0.36	-2.18
5+6/10	16.85	-3.16	11.57	-0.79	-1.61	-3.37
8/10	-11.29	16.33	-12.64	2.61	2.46	4.75
7/10	1.82	2.04	4.61	-0.54	0.27	-0.06
9/11+12	4.49	13.21	2.42	0.19	-0.09	0.52
10/11+12	6.61	19.16	3.12	1.99	1.18	0.35

[a] *m/z* values of the ratios of sterol peaks according to peak labelling of **Table 15.2.**

Thus the training sets were composed by 10 objects for Chemchali and Fouji cultivars and by 6 objects for the Zarrazi one, while the evaluation sets were composed by 5 objects (Chemchali and Fouji) and 3 objects (Zarrazi).

Three LDA models, one for each genetic variety, were next constructed. The corresponding score plots are shown in **Figure 15.3**. For all models, an excellent resolution between all the category pairs was observed, being λw below 0.01 in all cases. The variables selected by the SPSS stepwise algorithm, and the corresponding standardized coefficients of the models are shown in **Table 15.5**.

Table 5.5

Predictors selected and corresponding standardized coefficients of the LDA model constructed to classify EVOOs according to their maturity index

Cultivar	Predictors[a]	f_1	f_2	f_3	f_4
Chemchali	1+2/11+12	-0.16	4.18	6.36	-0.49
	3/11+12	-1.77	-3.46	-7.71	0.59
	5+6/7	0.72	0.09	-0.12	3.24
	5+6/9	2.35	-0.48	-0.78	-0.94
	8/7	-0.80	-0.07	2.84	-0.80
	10/11+12	0.74	-0.004	-0.08	2.62
Fouji	1+2/11+12	-1.06	1.55	5.84	1.88
	4/10	1.97	-1.72	4.31	1.71
	5+6/9	0.60	-2.76	-5.76	-0.99
	8/7	-1.33	3.08	-3.89	-1.29
Zarrazi	1+2/11+12	1.04	0.41		
	4/10	-0.82	0.75		

[a] *m/z* values of the ratios of sterol peaks according to peak labelling of Table 15.2.

As it is observed, the sterol peak ratios with higher discriminant capabilities for the Chemchali samples are 5+6/9 (Δ^7+Δ^5-avenasterol/stigmasterol) and 3/11+12 (brassicasterol/Δ^7-stigmastenol+β-sitosterol), while those selected to discriminate among the maturiry indexes of Fouji EVOOs were peak ratios 4/10 and 8/7, which corresponded to cholesterol/$\Delta^{5,24}$-stigmastadienol and campestanol/campesterol ratios. Finally, the 1+2/11+12 peak ratio (erythrodiol+uvaol/Δ7-stigmastenol+β-sitosterol)

was the one with high discriminant capability for the Zarraki EVOOs. When leave-one-out validation was applied to all the models, all the objects of the training set were correctly classified. Finally, the evaluation sets were used to check model prediction abilities, providing an excellent classification of all the objects in the three models; thus, the prediction capability was 100%.

15.4. Conclusions

The results from this work showed that sterol profiles obtained by HPLC-MS followed by a chemometric treatment of the chromatographic data could be useful for distinguishing Tunisian EVOOs according to their cultivar and maturity index. These results are possible due to the differences observed between the sterol profiles of the different samples, which are enhanced by chemometric analysis. Thus, EVOOs coming from 7 cultivars, and EVOOs from the Chemchali, Fouji, and Zarrazi cultivars from different maturity indexes, were correctly classified with an excellent resolution among all the categories using sterol peak ratios as predictors. In all models, the assignment probabilities were higher than 95%, which proved the proposed method is of interest to control the genetic origin and the maturity index of the olives used to obtain the EVOOs.

Acknowledgements

This work was supported by project CTQ2014-52765-R (MINECO of Spain and FEDER). M. Vergara-Barberán thanks the MINECO for an FPU grant for PhD studies.

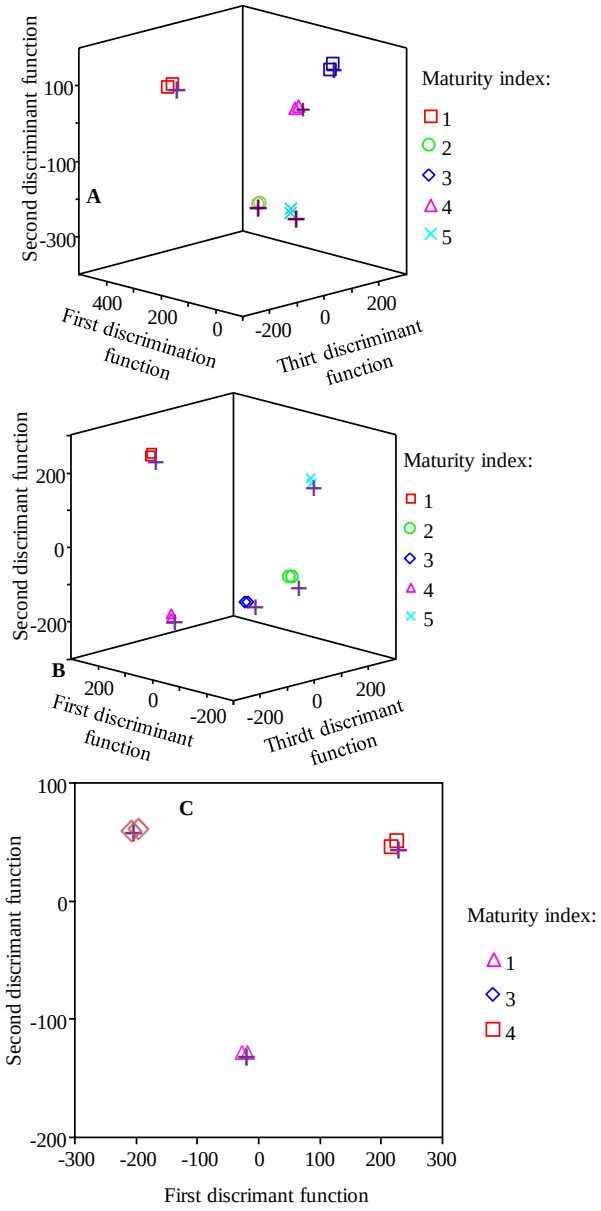

Figure 15.3. Score plots of the discriminant functions of the LDA models constructed to classify Chemchali (A), Fouji (B), and Zarrazi (C) EVOOs according to their maturity index. Evaluation set samples are labelled with a cross symbol.

15.5. References

Al-Ismail, K.M.; Alsaed, A.K.; Ahmad, R.; Al-Dabbas, M. (**2010**). Detection of olive oil adulteration with some plant oils by GLC analysis of sterols using polar column. *Food Chemistry, 121*, 1255–1259.

Alonso-Salces, R.M.; Holland, M.V.; Guillou, C. (**2011**). ^{1}H-NMR fingerprinting to evaluate the stability of olive oil. *Food Control, 22*, 2041-2046.

Azadmard-Damirchi, S. (**2010**). Phytosterol classes in olive oils and their analysis by common chromatographic methods. *Food Additives & Contaminants, 27,* 1–10.

Ben Temime, S.; Manai, H.; Methenni, K.; Baccouri, B. (**2008**). Sterolic composition of Chétoui virgin olive oil: Influence of geographical origin. *Food Chemistry, 110*, 368-374.

Berenguer, M. J.; Vossen, P. M.; Grattan, S. R.; Connell, J. H. (**2006**). Tree irrigation levels for optimum chemical and sensory properties of olive oil. *HortScience, 41*, 427–432.

Boskou, D. (**2011**). Vegetable oils in food technology composition, properties and uses. Gunstone, F. D., Ed.; Blackwell Publishing., p. 252.

Bouaziz, M.; Fki, I.; Jemai, H.; Ayadi, M. (**2008**). Effect of storage on refined and husk olive oils composition: Stabilization by addition of natural antioxidants from Chemlali olive leaves. *Food Chemistry, 108*, 253–262.

Cañabate Díaz, B.; Segura Carretero, A.; Fernández Gutiérrez, A.; Belmonte Vega, A. (**2007**). Separation and determination of sterols in olive oil by HPLC-MS. *Food Chemistry, 102,* 593–598.

Cárdeno, A.; Magnusson, M.K.; Strid, H.; Alarcón de La Lastra, G. (**2014**). The unsaponifiable fraction of extra virgin olive oil promotes apoptosis and attenuates activation and homing properties of T cells from patients with inflammatory bowel disease. *Food Chemistry, 161,* 353–360.

Commission Regulation (EC) No. 796/2002 of 6 May 2002, Off. J. Eur. Union (**2002),** L128, annex XIX, 23.

Cunha, S.S.; Fernandes, J.O.; Oliveira, M.B.P.P. (**2006**). Quantification of free and esterified sterols in Portuguese olive oils by solid-phase extraction and gas chromatography-mass spectrometry. *Journal of Chromatography A, 1128*, 220–227.

Fuentes de Mendoza, M.; Concepción, D.M.G.; Marín Expóxito, J.; Sánchez Casas, J. (**2013**). Chemical composition of virgin olive oils according to the ripening in olives. *Food Chemistry, 141,* 2575–2581.

Giacometti, J. (**2001**). Determination of aliphatic alcohols, squalene, α-tocopherol and sterols in olive oils: Direct method involving gas chromatography of the unsaponifiable fraction following silylation. *Analyst, 126*, 472–475.

Gutíerrez, F.; Jimenez, B.; Ruíz, A.; Albi, M. A. (**1999**). Effect of olive ripeness on the oxidative stability of virgin olive oil extracted from the varieties Picual and Hojiblanca and on the different components involved. *Journal of Agricultural and Food Chemistry, 47,* 121–127.

Gylling, H.; Plat, J.; Turley, S.; Ginsberg, H.N. (**2014**). Plant sterols and plant stanols in the management of dyslipidaemia and prevention of cardiovascular disease. *Atherosclerosis, 232,* 346–360.

Ilyasoglu, H.; Ozcelik, B.; Van Hoed, V.; Verhe, R, (**2010**). Characterization of Aegean olive oils by their minor compounds. *Journal of the American Oil Chemists' Society, 87,* 627–636.

IOOC. (**2004**). Olive Oil Exportations, International Olive Oil Council, http:// www.internationalolive oil.org 2011.

Koutsaftakis, A.; Kotsifaki, F.; Stefanoudaki, E., (**1999**). Effect of extraction system, stage of ripeness, and kneading temperature on the sterol composition of virgin olive oils. *Journal of the American Oil Chemists' Society, 76*, 1477–1481.

Krichène, D.; Allalout, A.; Salvador, M.D.; Fregapane, G.; Zarrouk, M. (**2010**). Fatty acids, volatiles, sterols and triterpenic alcohols of six monovarietal Tunisian virgin olive oils. *European Journal of Lipid Science and Technology, 112*, 400–409.

Lagarda, M.J.; García-Llatas, G.; Farré, R. (**2006**). Analysis of phytosterols in foods. *Journal of Pharmaceutical and Biomedical Analysis, 41*, 1486–1496.

Lerma-García, M.J.; Ramis-Ramos, G.; Herrero-Martínez, J.M.; Simó-Alfonso, E.F. (**2008**). Classification of vegetable oils according to their botanical origin using sterol profiles established by direct infusion mass spectrometry. *Rapid Communications in Mass Spectrometry*, *22*, 973–9.

Lerma-García, M.J.; Simó-Alfonso, E.F.; Ramis-Ramos, G.; Herrero-Martínez, J.M. (**2008**). Rapid determination of sterols in vegetable oils by CEC using methacrylate ester-based monolithic columns. *Electrophoresis, 29*, 4603–4611.

Lerma-García, M.J.; Simó-Alfonso, E.F.; Ramis-Ramos, G.; Herrero-Martínez, J.M. (**2008**). Rapid determination of sterols in vegetable oils by CEC using methacrylate ester-based monolithic columns. *Electrophoresis, 29*, 4603-4611.

Mailer R.J., Ayton J.; Graham K. (**2010**). The Influence of growing region, cultivar and harvest timing on the diversity of Australian olive oil. *Journal of the American Oil Chemists' Society*, 87, 877–884

Manai-Djebali, H.; Krichène, D.; Ouni, Y.; Gallardo, L. (**2012**). Chemical profiles of five minor olive oil varieties grown in central Tunisia. *Journal of Food Composition and Analysis, 27,* 109–119.

Martínez-Vidal, J.L.; Garrido-Frenich, A.; Escobar-García, M.A.; Romero-González, R. (**2007**). LC–MS determination of sterols in olive oil. *Chromatographia, 65*, 695–699.

Martínez-Vidal, J.L.; Garrido-Frenich, A.; Escobar-García, M.A.; Romero-González, R. (**2007**). LC-MS determination of sterols in olive oil. *Chromatographia, 65,* 695–699.

Noorali, M.; Barzegar, M.; Sahari, M. A. (**2014**). Sterol and fatty acid compositions of olive oil as an indicator of cultivar and growing area. *Journal of the American Oil Chemists' Society, 91,* 1571–1581.

Ouni, Y.; Flamini, G.; Ben Youssef, N.; Guerfel, M.; (**2011**). Sterolic composition and triacylglycerols of Oueslati virgin olive oil: comparison among different geographic areas. *Journal of Food Science and Technology, 46,* 1747–1754.

Reboredo-Rodríguez, P.; González-Barreiro, C.; Cancho-Grande, B.; Simal-Gándara, J. (**2014**). Quality of extra virgin olive oils produced in an emerging olive growing area in north-western Spain. *Food Chemistry, 164,* 418–426.

Richelle, M.; Enslen, M.; Hager, C.; Groux, M. (**2004**). Both free and esterified plant sterols reduce cholesterol absorption and the bioavailability of β-carotene and α-tocopherol in normocholesterolemic humans. *The American Journal of Clinical Nutrition, 80,* 171–177.

Rivera del Álamo, R.M.; Fregapane, G.; Aranda, F.; Gómez-Alonso, S. (**2004**). Sterol and alcohol composition of Cornicabra virgin olive oil: the campesterol content exceeds the upper limit of 4u` established by EU regulations. *Food Chemistry, 84*, 533–537.

Sánchez-Casas, J.; Osorio-Bueno, E.; Montana-Garcia, A.M.; Martínez-Cano, M. (**2004**). Sterol and erythrodiol+uvaol content of virgin olive oils from cultivars of Extremadura (Spain). *Food Chemistry, 87, 2*25–230.

Segura Carretero, A.; Carrasco Pancorbo, A.; Cortacero, S.; Gori, A., (**2008**). A simplified method for HPLC-MS analysis of sterols in vegetable oil. *European Journal of Lipid Science and Technology, 1110*, 1142–1149.

Sotiroudis, T.G.; Kyrtopoulos, S.A. (**2008**). Anticarcinogenic compounds of olive oil and related biomarkers. *European Journal of Nutrition, 47*, 69–72.

Taamalli, A.; Arráez-Román, D.; Zarrouk, M.; Valverde, J. (**2012**). The occurrence and bioactivity of polyphenols in Tunisian olive products and by-products: A review. *Journal of Food Science, 77*, 83-92.

Vandeginste, B.G.M.; Massart, D.L.; Buydens, L.M.C.; De Jong, S. (**1998**). Data handling in science and technology, Part B, 18th Edn., Elsevier, Ed., Amsterdam, p. 237.

Chapter 16. Capillary electrophoresis of free fatty acids by indirect ultraviolet detection: application to the classification of vegetable oils according to their botanical origin

JOURNAL OF AGRICULTURAL AND FOOD CHEMISTRY

ARTICLE

pubs.acs.org/JAFC

Capillary Electrophoresis of Free Fatty Acids by Indirect Ultraviolet Detection: Application to the Classification of Vegetable Oils According to Their Botanical Origin

María Vergara-Barberán,[†] Aarón Escrig-Doménech,[†] María Jesús Lerma-García,[‡] Ernesto Francisco Simó-Alfonso,[†] and José Manuel Herrero-Martínez*[,†]

A method for the determination of fatty acids in vegetable oils by capillary electrophoresis with indirect UV-vis detection has been developed. The separation of fatty acids was optimized in terms of Brij surfactant nature and concentration and organic modifier (2-propanol) percentage. The optimal background electrolyte consisted of 10 mM p-hydroxybenzoate, 5 mM Tris at pH 8.8, 80 mM Brij 98, 40% acetonitrile, and 10% 2-propanol. Under these conditions, vegetable oils from five botanical origins (avocado, corn, extra virgin olive, hazelnut, and soybean) were analyzed and the fatty acid contents established. LDA models were constructed using fatty acid peak areas as predictors. An excellent resolution among all category pairs was obtained, and all samples were correctly classified with assignment probabilities of >95%.

Keywords: botanical origin; CE; fatty acid; linear discriminant analysis; vegetable oils

16.1. Introduction

Authentication of edible quality oils is of great importance from the viewpoints of commercial value and health impact. The organoleptic properties, high nutritional value, and health benefits of quality oils are related to the presence of many components, such as fatty acids, the concentration profiles of which differ according to fruit variety. A relevant aspect of oil authenticity is the adulteration of quality oils by mixing them with oils of lower quality. Then, the evaluation of fatty acid profiles could be an excellent tool to assess oil authenticity.

Traditionally, analysis of fatty acids has been performed spectroscopically (De Greyt, 1998; Mossoba, 1999; Mossoba, 2000) and chromatographically (Gutnikov, 1995; Adlof, 1998; Nikolova, 2001; Williams, 2001; Brondz, 2002). The chromatographic technique most widely applied to determine fatty acid profiles of lipids has been gas chromatography (Gutnikov, 1995; Brondz, 2002), in which long chain fatty acids are analyzed as methyl or trimethylsilyl esters in polar columns. On the other hand, HPLC has been also used to determine fatty acids in lipid matrices, where several UV-absorbing derivatives have been usually employed, such as phenacyl (Durst, 1975) or naphthacyl (Jordi, 1978) esters and 2-nitrophenylhydrazides (Miwa, 1987). However, derivatization reactions often produce incomplete conversion of the analyte and undesirable interfering side products.

In the past decade, CE has been proposed as an interesting alternative for the analysis of underivatized long-chain fatty acids (Roldan-Assad, 1995; Collet, 1996; Vallejo-Córdoba, 1998; Chen, 1999; Haddadian, 1999; Mofaddel, 1999; Gallaher, 2000; de Oliveira, 2001; Öhman, 2002; Bohlin, 2003; de Oliveira, 2003; Otieno, 2008; Li, 2011). However, one of the major concerns in analyzing fatty acids by CE has been their limited solubility in aqueous electrolyte systems. To solve this problem, CE separation has been

described by using BGEs containing organic solvents, such as methanol (Roldan-Assad, 1995; Collet, 1996) ethanol (Liu, 2005), ACN (de Oliveira, 2001; de Oliveira, 2003; Surowiec, 2004), 1-octanol (de Oliveira, 2003; Surowiec, 2004) and methylformamidedioxane (Haddadian, 1999). In addition, the use of additives to the BGE, such as cyclodextrins (Collet, 1996; de Oliveira, 2001; Bohlin, 2003; Liu, 2005) or surfactants (SDS (Bohlin, 2003; Liu, 2005) and polyoxyethylene 23 lauryl ether (Brij 35) (Erim, 1995; Haddadian, 1999; Gallaher, 2000; de Oliveira, 2003; Surowiec, 2004) among others), has been described to modify selectivity on analyte separation. On the other hand, fatty acids do not possess strong chromophores in their structures, which makes difficult their sensitive detection in direct photometric mode. Then, direct UV or fluorescence detection was only employed when a previous derivatization step was performed, although the use of indirect UV and indirect fluorescence detection (Yeung, 1995) was preferred. The chromophoric agents used include p-anisate (Collet, 1996; Vallejo-Córdoba, 1998), diethylbarbiturate (Buchberger, 1996), adenosine monophosphate (Haddadian, 1999), dodecylbenzenesulfonate (Erim, 1995; Haddadian, 1999; Gallaher, 2000; de Oliveira, 2003; Surowiec, 2004) and p-hydroxybenzoate (Heinig, 1998), among others.

In this work, a CE method with an alkaline buffer in the presence of an anionic chromophore (p-hydroxybenzoate) for the indirect UV detection of fatty acids was developed. The separation of fatty acids was optimized in terms of Brij surfactant nature and concentration and organic modifier (2-propanol) percentage. The fatty acid content present in different vegetable oil samples was obtained. Moreover, the fatty acid profiles observed were used to construct LDA models to classify oil samples according to their botanical origin.

16.2. Materials and methods

16.2.1. Reagents and samples

The following analytical grade reagents were used: ACN, methanol, ethanol, 1-propanol, 2-propanol (Scharlau, Barcelona, Spain); Tris, Fluka, Buchs, Switzerland); polyethylene glycol dodecyl ether (Brij 30, $C_{12}EO_4$; EO = number of ethoxylate groups), polyoxyethylene 23 lauryl ether (Brij 35, $C_{12}EO_{23}$), polyoxyethylene (20) oleyl ether (Brij 98, $C_{18}EO_{20}$), sodium p-hydroxybenzoate (Sigma-Aldrich, St. Louis, MO); NaOH and ammonia (NH_3; Panreac, Barcelona, Spain). Deionized water (Barnstead deionizer, Sybron, Boston, MA) was also used. The fatty acids used as standards were myristic (C14:0), palmitoleic (C16:1), palmitic (C16:0), linolenic (C18:3), linoleic (C18:2), oleic (C18:1), and stearic (C18:0) (Sigma-Aldrich). Individual stock solutions of the fatty acid standards (7 mM) were prepared in a MeOH/1-propanol 85:15 (v/v) mixture containing 40 mM NH_4OH.

The vegetable oils employed in this study and their commercial brands are shown in **Table 16.1**. Monovarietal extra virgin olive oil (EVOO) samples (Hojiblanca, Arbequina, and Picual, the three most important varieties in Spanish production) were from four different geographical areas of Spain. Other vegetable oil samples from different areas of Europe and South America were also used. Most samples were bought in the Spanish market, except for hazelnut oil (Percheron, France), corn oils from Crystal, Gloria, and Mazola (Mexico), and peanut oil (Coppini, Italy). The genetic variety of the olive oils and the botanical and geographical origin of all samples were guaranteed by the suppliers.

16.2.2. Instrumentation and procedures

An HP^{3D}CE system (Agilent, Waldbronn, Germany) provided with a diode array spectrophotometric detector and uncoated fused-silica capillaries (Polymicro Technologies, Phoenix, AZ) of 80.5 cm length (72 cm effective length) x 50 μm id (375 μm o.d.) were used. New capillaries were successively flushed with 1 and 0.1M NaOH and water at 60 ºC for 10 min each. Daily, before use, the capillary was successively rinsed with 2-propanol, water, and 0.1 M NaOH for 5 min each, followed by the BGE for 10 min more. Between runs, the capillary was flushed with the BGE for 5 min. Hydrodynamic injections at 50 mbar x 3 s were performed. Separations were performed at 25 kV at 45 ºC. Indirect detection was done at 254 nm. The BGEs were prepared weekly and stored at 4 ºC. Before injection, all solutions were filtered through 0.45 μm pore size nylon filters (Albet, Barcelona, Spain). The optimal BGE consisted of 10 mM p-hydroxybenzoate, 5 mM Tris at pH 8.8, 80 mM Brij 98, 40% ACN, and 10% 2-propanol.

16.2.3. Sample preparation, data treatment, and statistical analysis

Oil samples (400 mg) were saponified by refluxing at 75-80 ºC for 25 min with 0.5 M ethanolic NaOH. After saponification, samples were 1:20 diluted with MeOH and directly injected or stored at 4 ºC until their use. All samples were injected three times. The peak area of each compound was measured, and a data matrix was constructed using the areas of all the peaks as original variables. After normalization of the variables, statistical data treatment was performed using SPSS (v. 15.0, Statistical Package for the Social Sciences, Chicago, IL). LDA, a supervised classificatory technique, is widely recognized as an excellent tool to obtain vectors showing the maximal resolution between a set of previously defined categories. In LDA, vectors minimizing the Wilks' lambda, λ_w, are obtained (Vandeginste, 1998).

Table 16.1

Botanical origin, number of samples, and brands of vegetable oil samples used in this work.

Origin	No. of samples	Brand
Avocado	2	Guinama
	2	Marnys
	2	Serra Vita
Corn	2	Guinama
	1	Asua
	1	Cristal
	1	Gloria
	1	Mazola
Extra virgin olive	1	Borges
	1	Carbonell
	1	Coosur
	1	Grupo Hojiblanca
	1	Vea
	1	Torrereal
Hazelnut	3	Guinama
	3	Percheron
Peanut	2	Coppini
	2	Guinama
	2	Maurel
Soybean	2	Coosur
	2	Guinama
	1	Biolasi
	1	Coppini

This parameter is calculated as the sum of squares of the distances between points belonging to the same category divided by the total sum of squares. Values of λ_w approaching zero are obtained with well-resolved categories, whereas overlapped categories made λ_w approach one. Up to N = 1 discriminant vectors are constructed by LDA, with N being the lowest value for either the number of predictors or the number of categories. The selection

of the predictors to be included in the LDA models was performed using the SPSS stepwise algorithm. According to this algorithm, a predictor is selected when the reduction of λ_w produced after its inclusion in the model exceeds F_{in}, the entrance threshold of a test of comparison of variances or F_{test}. However, the entrance of a new predictor modifies the significance of those predictors that are already present in the model. For this reason, after the inclusion of a new predictor, a rejection threshold, F_{out}, is used to decide if one of the other predictors should be removed from the model. The process terminates when there are no predictors entering or being eliminated from the model. The default probability values of F_{in} and F_{out}, 0.05 and 0.10, respectively, were adopted.

16.3. Results and discussion

16.3.1. Optimization of BGE

To optimize fatty acid separation in terms of BGE, a test mixture containing the seven fatty acid standards described in the Reagents and Samples section was used. The initial BGE composition was adapted from the literature (Heinigh, 1998), which contained 10 mM p-hydroxybenzoate, 5 mMTris, 40 mM Brij 35, and 50% ACN. However, under these conditions, the injection of most oil samples led to a disruption in current, probably due to the poor solubility of fatty acids in the BGE. Then, and in order to enhance the solubility of these compounds, 10% 2-propanol was initially added to the BGE, but keeping the organic percentage constant (40% ACN). The fatty acid separation obtained with this BGE is shown in **Figure 16.1A**. As observed, all peaks were separated except the C16:1/C18:3 peak pair. Several studies (Erim, 1995; Haddadian, 1999; de Oliveira, 2001; de Oliveira, 2003; Surowiec, 2004) have demonstrated that the use of Brij 35 as nonionic surfactant helps to

solubilize fatty acids, leading also to an increase in solvophobic interactions with analytes, which can improve peak resolution.

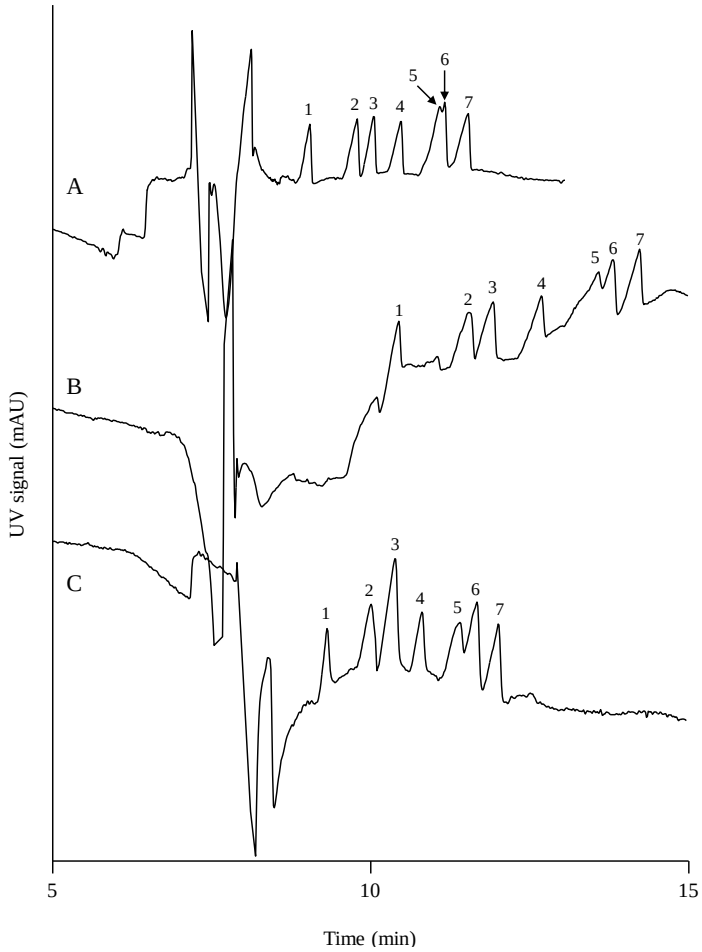

Figure 16.1. Influence of Brij surfactant nature on the separation of fatty acid standards: Brij 35 (A), Brij 30 (B), and Brij 98 (C) in a BGE composed of 10 mM p-hydroxybenzoate, 5 mM Tris at pH 8.8, 40 mM Brij, 40% ACN, and 10% 2-propanol. Working conditions: injection at 50 mbar x 3 s; separation at 25 kV at 45 C; indirect detection at 254 nm. Peaks: 1, C18:0; 2, C18:1; 3, C16:0; 4, C18:2; 5, C16:1; 6, C18:3; 7, C14:0.

However, to our knowledge, there are no reports about the influence of Brij series surfactants on the separation of fatty acids. For this purpose, fatty acid separation using Brij 30 and Brij 98 was evaluated. These surfactants were selected due to differences in both alkyl chain length and number of EO groups. Thus, for Brij 30 ($C_{12}EO_4$) the hydrophilic group is quite smaller than that of Brij 35 ($C_{12}EO_{23}$), whereas the alkyl chain length was the same. For Brij 98 ($C_{18}EO_{20}$), the hydrophilic group is slightly smaller than that of Brij 35 but the alkyl chain length increased from 12 to 18 carbon atoms. **Figure 16.1** shows the influence of the nature of Brij surfactant on the separation of fatty acids under the same concentration of Brij (40 mM). As observed, a reduction in the EO units of Brij surfactant from 23 (Brij 35, **Figure 16.1A**) to 4 (Brij 30, **Figure 16.1B**) led to an increase in analysis time jointly with an incipient separation of C16:1/C18:3 peaks. On the other hand, when the alkyl chain length increased from 12 (Brij 35, **Figure 16.1A**) to 18 (Brij 98, **Figure 16.1C**), an increase in resolution of C16:1/C18:3 peaks was observed with a concomitant increase in analysis time. This migration behavior can be explained by taking into account the solvophobic interactions between the alkyl chain of the surfactant and the polyoxyethylene moieties with the analytes. As evidenced in **Figure 16.1**, the hydrophobicity of polyoxyethylene moiety has a stronger effect than the hydrophobicity of the alkyl chain length. At the sight of these results, Brij 98 was selected for the following studies as the best compromise between resolution and analysis time.

Next, Brij 98 concentration was varied between 40 and 100mM. The results obtained are shown in **Figure 16.2**. As observed, an increase in the Brij 98 content led to longer migration times. This behavior could be explained by taking into account both EOF changes (due to an increase in the BGE viscosity) and the solvophobic interactions between the analytes and the surfactant.

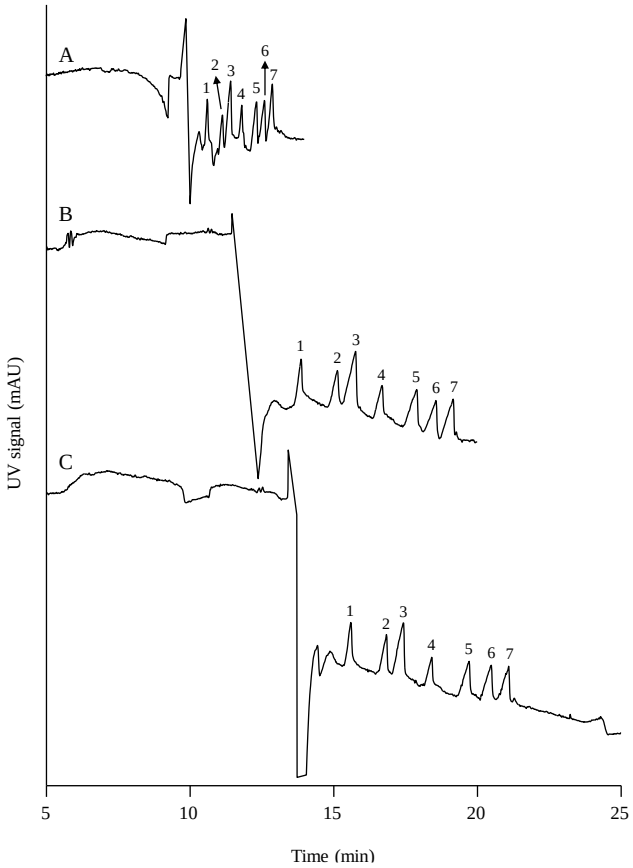

Figure 16.2. Influence of Brij 98 concentration in the BGE on the separation of fatty acid standards: 60 mM (A); 80 mM (B); 100 mM (C). Other working conditions were as in **Figure 16.1**.

On the other hand, an increase in peak resolution was observed up to 80 mM Brij 98, whereas a slight improvement in peak resolution was achieved at expenses of longer analysis time at 100 mM; then, a concentration of 80 mM was selected for further studies.

Finally, the percentage of 2-propanol was also optimized. Its percentage was varied between 5 and 15%. As evidenced in **Figure 16.3**, the addition of 2-propanol led to a progressive increase in migration times of fatty acids, which was due to the EOF reduction caused by 2-propanol (solvent with

higher viscosity and lower dielectric constant than ACN).On the other hand, when the content of 2-propanol was increased, an improvement in peak resolution was obtained. Then, a percentage of 10% was selected as the best compromise between resolution and analysis time.

16.3.2. Characterization of the fatty acid profiles of vegetable oils

The optimal method was applied to the analysis of vegetable oil samples. Representative electropherograms of avocado (A), corn (B), and hazelnut (C) oil samples are shown in **Figure 16.4**. As observed, the myristic acid (C14:0) peak was not observed in any sample; thus, this peak was not used in the following statistical treatments. On the other hand, different fatty acid fingerprints were obtained for the oils; then, fatty acid should be related with the different botanical origins of the oil samples. The differences observed in oil fingerprints were enhanced when chemometric analysis of the data was performed.

16.3.3. Quantitation studies

External calibration curves were constructed by injecting six standard solutions of each fatty acid between 0.1 and 5mM. Straight lines with $r^2 >$ 0.998 were obtained. Other analytical parameters of interest are given in **Table 16.2**. Precision was determined by studying the intra- and interday repeatabilities of migration times and peak areas obtained by injecting the same 0.5 mM solution for all analytes 10 times per day during 3 days. In all cases, the relative standard deviation values were lower than 2.9 and 3.7% for migration times and peak areas, respectively. The LOD were obtained for signal-to-noise ratio of 3, giving values of *ca.* 0.020 mM. These values were similar to those reported in the literature. (Heinig, 1998; Drange, 1997).

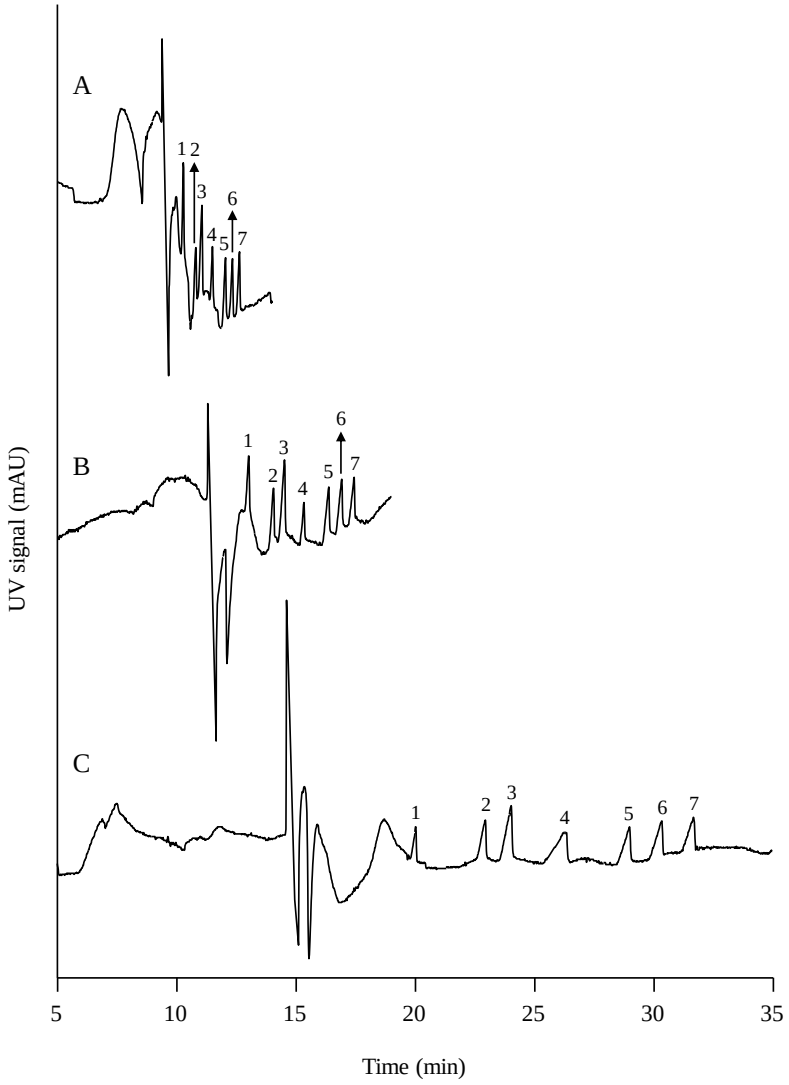

Figure 16.3. Effect of 2-propanol percentage in the BGE on the separation of fatty acid standards: 5% (A); 7% (B); 15%. BGE composed of 10 mM p-hydroxybenzoate, 5 mM Tris at pH 8.8, 80 mM Brij 98, and 45, 43, and 35% ACN, respectively. Other working conditions were as in **Figure 16.1.**

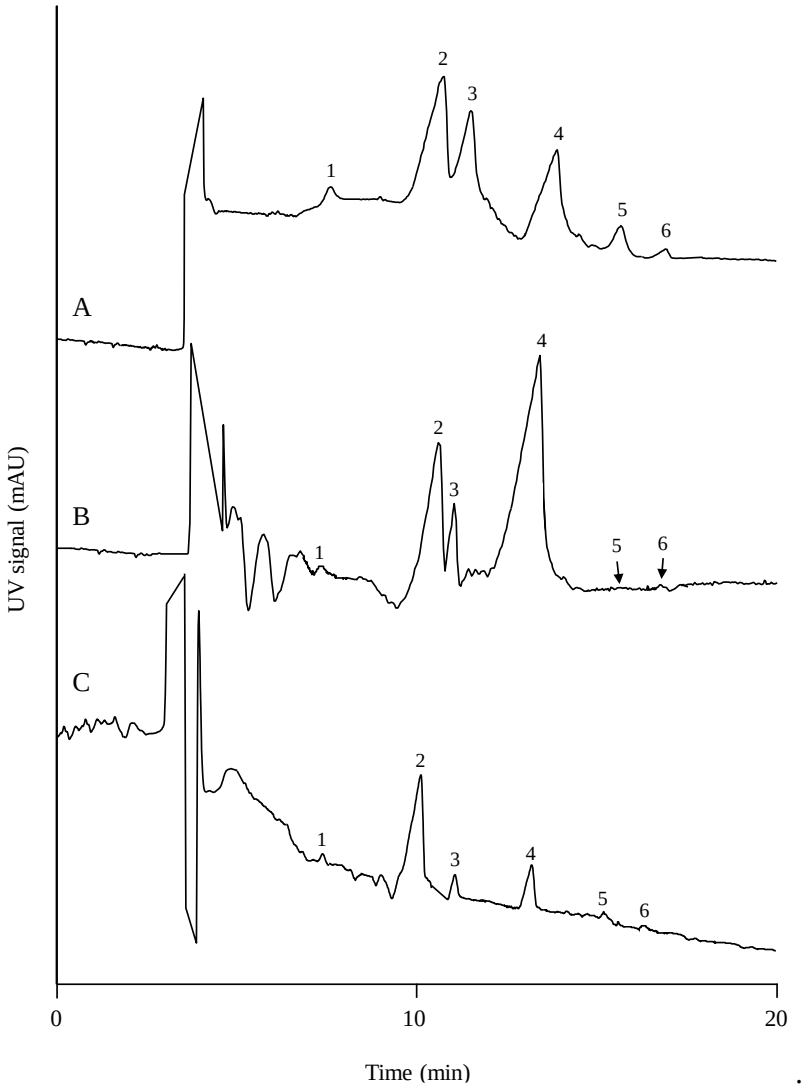

Figure 16.4. Representative electropherograms of avocado (A), corn (B), and hazelnut (C) oil samples. BGE composed of 10 mM p-hydroxybenzoate, 5 mM Tris at pH 8.8, 80 mM Brij 98, 40% ACN, and 10% 2-propanol. Other working conditions were as in **Figure 16.1.**

Table 16.2

Migration time (t_m) and peak area (A) repeatabilities[a] of the CE method.

Compound	tm (%)	A (%)
C14:0	1.5; 1.8	2.0;2.5
C16:0	1.7;2.2	2.4;2.7
C16:1	1.6;2.3	2.4;2.8
C18:0	1.8;2.5	2.8;3.2
C18:1	1.89;2.6	1.8;2.6
C18:2	1.8;2.8	1.8;2.8
C18:3	1.9;2.9	1.9;2.9

[a] As intra- and interday relative standard deviations.

The quantitative results of fatty acids found in the vegetable oils analyzed are shown in **Table 16.3**. In general, the levels of these compounds found in the samples are in good agreement with data reported in the literature (Gunstone, 2002; Jee, 2002; De Koning, 2001; Alves, 2004). Corn and soybean oils showed large quantities of linoleic acid (>50%) compared to those found in EVOOs. For this reason, the C18:2 peak has been used as an adulteration marker for detecting these seed oils in EVOOs at contents >21%. Consequently, two binary mixtures containing 25% corn or soybean oil with EVOO were prepared and injected. An electropherogram showing the EVOO spiked with 25% soybean oil is shown in **Figure 16.5B**.

Thus, the presence of this seed oil could be easily evidenced by an increase in the C18:2 peak area when compared with that obtained for the pure EVOO (**Figure 16.5A**). A similar increase was evidenced when the EVOO sample was spiked with 25% corn oil (data not shown).

Table 16.3

Percentages of fatty acids found in vegetable oils.

Fatty acid	Avocado	Corn	Extra virgin olive	Hazelnut	Soybean
C14:0	<LOD	<LOD	<LOD	<LOD	<LOD
C16:0	19.8	10.8	11.9	7.1	6.8
C16:1	6.1	<LOD	<LOD	0.6	<LOD
C18:0	1.2	2.3	2.2	1.8	4.8
C18:1	55.7	25.1	71.7	75.0	19.2
C18:2	16.3	61.0	14.3	15.0	68.1
C18:3	0.9	0.8	0.8	0.5	1.1

16.3.4. Normalization of the variables and construction of LDA models

To reduce the variability associated with sources of variance that can affect the sum of the areas of all peaks, normalized rather than absolute peak areas were used. To normalize the variables, the area of each peak was divided by each one of the areas of the other five peaks; in this way, and taking into account that each pair of peaks should be considered only once, (6 x 5)/2 =15 nonredundant peak ratios were obtained to be used as predictors. Using the normalized variables, LDA models capable of classifying the vegetable oil samples according to their respective botanical origin were constructed. From the 30 samples of **Table 16.1**, a matrix containing 90 objects (which correspond to the three replicates of each sample) and 15 predictors was constructed. A response column, containing the five categories corresponding to the five botanical origins of the oils, was added to this matrix. This matrix was used as an evaluation set. To construct the LDA training matrix, only the means of the three replicates of each sample were included (30 objects); in this way, the internal dispersion of the categories was reduced, which was important to reduce the number of variables selected by the SPSS stepwise algorithm during model construction.

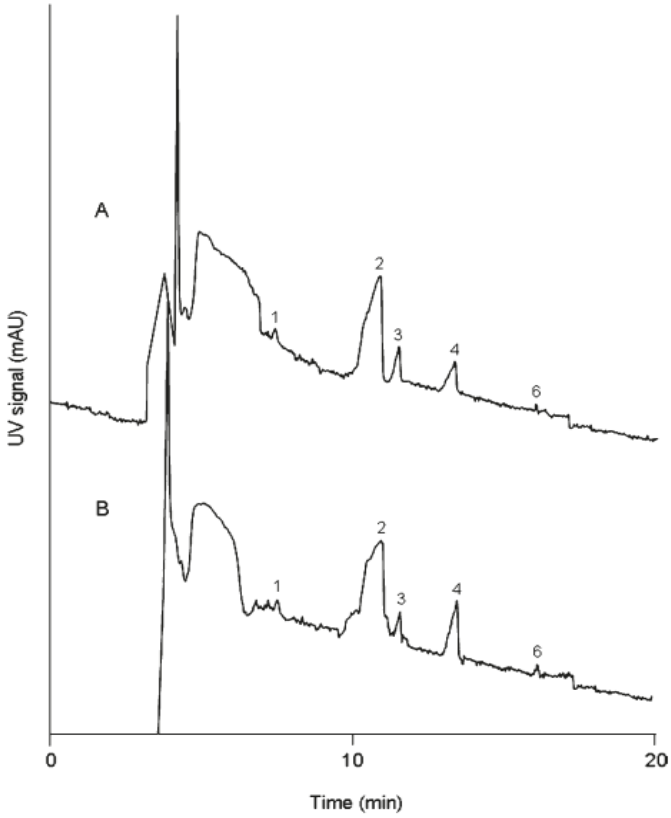

Figure 16.5. Electropherograms of (A) an EVOO sample and (B) an EVOO sample spiked with 25% soybean oil. Peak identification and working conditions were as in **Figure 16.4**.

To classify the vegetable oils according to the five botanical origins of **Table 16.1**, an LDA model was constructed. An excellent resolution between all category pairs was obtained (**Figure 16.6**, $\lambda w = 0.074$). The variables selected by the SPSS stepwise algorithm, and the corresponding model standardized coefficients, showing the predictors with large discriminant capabilities, are given in **Table 16.4**. According to this table, the main fatty acid ratios selected by the algorithm to construct the LDA model corresponded to C18:2/C18:1, C18:3/C18:1, and C16:0/C18:1. All the points of the training set were correctly classified by leave-one-out validation. The

evaluation set, containing the 30 original data points, was used to check the prediction capability of the model. Using a 95% probability, all the objects were correctly classified; thus, the prediction capability was 100%.

Table 16.4

Predictors selected and corresponding standardized coefficients of the discriminant functions *f1-f4* of the LDA model constructed to predict the botanical origin of vegetable oils.

Predictor[a]	***f1***	***f2***	***f3***	***f4***
C16:0/C18:2	-2.24	-3.94	0.76	0.04
C16:0/C18:3	1.24	2.98	0.07	0.34
C16:0/C18:1	14.41	-7.01	-0.44	-0.14
C18:3/C18:2	-1.39	7.55	-0.12	1.07
C18:3/C18:1	16.89	-5.55	0.02	-0.83
C18:2/C18:1	-24.77	9.06	1.04	0.31

[a] Ratios of fatty acid peak areas.

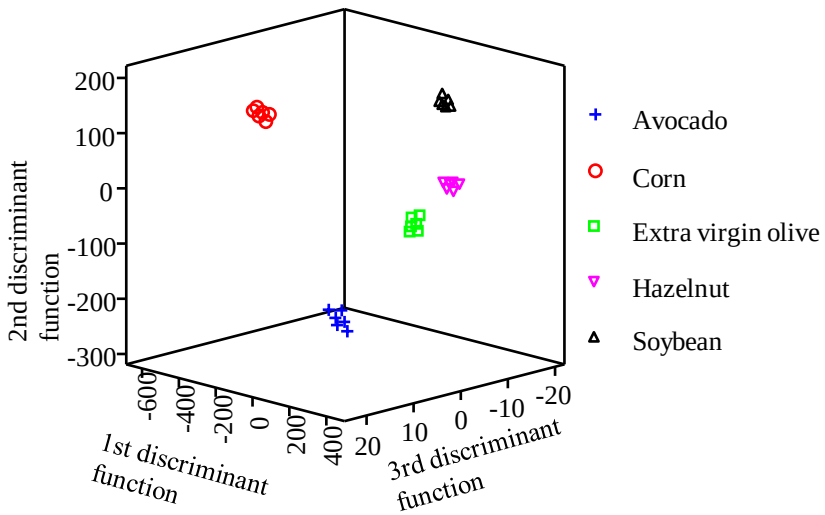

Figure 16.6. Score plot on an oblique plane of the 3-D space defined by the three first discriminant functions of the LDA model constructed to classify vegetable oils according to their botanical origin.

This classification model is compared with another classification approach previously published in the literature for the classification of vegetable oils according to their botanical origin using amino acid profiles established by HPLC-UVvis (Concha-Herrera, 2010). A lower λ_w value was obtained with the proposed model (0.074 vs 0.393 for the model constructed with amino acid profiles), being the categories resolved in the latter higher than those discriminated in the present work (7 vs 5 categories). On the other hand, a total of 6 predictors were selected by the LDA model constructed in the current work, which was lower than those selected by the model constructed with amino acid profiles (13 predictors). Taking into account all these aspects, a better model has been obtained in the present work.

In conclusion, the developed method provides a reliable protocol for the separation and determination of fatty acids in vegetable oils by CE with indirect photometric detection. The feasibility of classifying vegetable oils according to their botanical origin by using fatty acid profiles established by CE has been also demonstrated. Additionally, the method allows the detection of adulterations of contents >25% low-cost edible oils, such as soybean or corn in EVOO. To improve the sensitivity, further work is now in progress by the use of extended-path length capillaries.

The developed methodology is a promising alternative to the traditional GC method with the advantages of simplicity and lower consumption of reagents. Thus, the present procedure is of great interest for routine quality control or adulteration purposes in vegetable oil samples.

Funding Sources

Work supported by Project CTQ2010-15335/BQU (MEC and Feder funds). M.J.L.-G. thanks the Junta de Comunidades de Castilla La Mancha and the Fondo Social Europeo for a research postdoctoral fellowship.

16.4. References

Adlof, R.; Lamm, T. (**1998**). Fractionation of cis- and trans-oleic, linoleic, and conjugated linoleic fatty acid methyl esters by silver ion high-performance liquid chromatography. *Journal of Chromatography A, 799,* 329-332.

Alves, M.R.; Oliveira, M.B. (**2004**). Predictive and interpolative biplots applied to canonical variate analysis in the discrimination of vegetable oils by their fatty acid composition. *Journal of Chemometrics, 18*, 393-401.

Bohlin, M.E.; Ohman, M.; Hamberg, M.; Blomberg, L.G. (**2003**). Separation of conjugated trienoic fatty acid isomers by capillary electrophoresis. *Journal of Chromatography, A, 985*, 471-478.

Buchberger, W.; Winna, K. (**1996**). Determination of free fatty acids by capillary zone electrophoresis. *Microchimica Acta, 122*, 45-52.

Brondz, I. (**2002**). Development of fatty acid analysis by high-performance liquid chromatography, gas chromatography, and related techniques. *Analytica Chimica Acta, 465*, 1-37.

Chen, M.J.; Chen, H. S.; Lin, C.Y.; Chang, H.T. (**1999**). Indirect detection of organic acids in non-aqueous capillary electrophoresis. *Journal of Chromatography A, 853*, 171-180.

Collet, J.; Gareil, P. **(1996**). Selectivity in capillary electrophoresis: Application to chiral separations with cyclodextrins. *Journal of Capillary Electrophoresis, 3*, 77-82.

Concha-Herrera, V.; Lerma-García, M.J.; Herrero-Martínez, J.M.; Simo-Alfonso, E.F. (**2010).** Classification of vegetable oils according to their botanical origin using amino acid profiles established by high performance liquid chromatography with UVvis detection: a first approach. *Food Chemistry, 120,* 1149-1154.

De Greyt, W.; Kint, A.; Kellens, M.; Huyghebaert, A. (**1998**). Determination of low trans levels in refined oils by Fourier transform infrared spectroscopy. *Journal of the American Oil Chemists' Society, 75,* 115-118.

De Koning, S.; van der Meer, B.; Alkema, G.; Janssen, H.G.; Brinkman, U.A.T. (**2001**). Automated Determination of fatty acid methyl ester and cis/trans methyl ester composition of fats and oils. *Journal of Chromatography, A, 922,* 391-397.

De Oliveira, M.A.L.; Micke, G.A.; Bruns, R.E.; Tavares, M.F.M. (**2001**). Factorial design of electrolyte systems for the separation of fatty acids by capillary electrophoresis. *Journal of Chromatography A, 924,* 533-539.

De Oliveira, M.A.L.; Solis, V.E.S.; Gioielli, L.A.; Polakiewicz, B.; Tavares, M.F.M. (**2003**). Method development for the analysis of trans-fatty acids in hydrogenated oils by capillary electrophoresis. *Electrophoresis,* 24, 1641-1647.

Drange, E.; Lundanes, E. (**1997**). Determination of long-chained fatty acids using non-aqueous capillary electrophoresis and indirect UV detection *Journal of Chromatography, A, 771,* 301-309.

Durst, H.D.; Milano, M.; Kikta, E.J.; Connelly, S.A.; Grushka, E. (**1975**). Phenacyl esters of fatty acids via crown ether catalysts for enhanced ultraviolet detection in liquid chromatography. *Analytical Chemistry 47,* 1797-1801.

Erim, F.B.; Xu, X.; Kraak, J.C. (**1995**). Application of micellar electrokinetic chromatography and indirect UV detection for the analysis of fatty acids. *Journal of Chromatography A, 694,* 471-479.

Gallaher, D.L.,Jr.; Johnson, M.E. (**2000**). Nonaqueous capillary electrophoresis of fatty acids derivatized with a near-infrared fluorophore. *Analytical Chemistry, 72,* 2080-2086.

Gunstone, F.D. (**2002**). Vegetables Oils in Food Technology; Blackwell Publishing, CRC Press: Boca Raton, Florida.

Gutnikov, G. (**1995**). Fatty acid profiles of lipid samples. *Journal of Chromatography B, 671*, 71-89.

Haddadian, F.; Shamsi, S.A.; Warner, I.M. (**1999**). Separation of saturated and unsaturated free fatty acids using capillary electrophoresis with indirect photometric detection. *Journal of Chromatographic Science, 37*, 103-107.

Heinig, K.; Hissner, F.; Martin, S.; Vogt, C. (**1998**). Separation of saturated and unsaturated fatty acids by capillary electrophoresis and HPLC. *American laboratory, 30*, 24-29.

Jee, M. (**2002**). Oils and fat authentication; Blackwell Publishing, CRC Press: Boca Raton, Florida.

Jordi, H.C. (**1978**). Separation of long and short chain fatty acids as naphthacyl and substituted phenacyl esters by high performance liquid chromatography. *Journal of Liquid Chromatography, 1*, 215-230.

Li, M.; Zhou, Z.; Nie, H.; Bai, Y. (**2011**). Recent advances of chromatography and mass spectrometry in lipidomics. *Analytical and Bioanalytical Chemistry, 399*, 243-249.

Liu, X.; Cao, Y.; Chen, Y. (**2005**). Separation of conjugated linoleic acid isomers by cyclodextrin-modified micellar electrokinetic chromatography. *Journal of Chromatography A, 1095*, 197-200.

Miwa, H.; Yamamoto, M.; Nishida, T.; Nunoi, K.; Kikuchi, M. (**1987**). High-performance liquid chromatographic analysis of serum long-chain fatty accids by direct derivatization method. *Journal of Chromatography B* 1987, 416, 237-245.

Mofaddel, N.; Desbene-Monvernay, A. (**1999**). Fatty acid analysis using capillary electrophoresis. *Analusis, 27*, 120-124.

Mossoba, A.M.; Lee, T. (**2000**). Rapid determination of total trans fat content by attenuated total reflection infrared spectroscopy. *Journal of the American Oil Chemists' Society, 77*, 457-462.

Mossoba, M.M. (**1999**). In Spectral Methods in Food Analysis: Instrumentation and Applications; Dekker: New York.

Nikolova-Damyanova, B.; Momchilova, S. (**2001**). Silver ion thin-layer chromatography of fatty acids. A survey. *Journal of Liquid Chromatography & Related Technologies, 24*, 1447-1466.

Ohman, M.; Wan, H.; Hamberg, M.; Blomberg, L.G. (**2002**). Separation of conjugated linoleic acid isomers and parinaric fatty acid isomers by capillary electrophoresis. *Journal of Separation Sciencia, 25*, 499-506.

Otieno, A.C.; Mwongela, S.M. (**2008**). Capillary electrophoresis-based methods for the determination of lipids a review. *Analytica Chimica Acta*, *624*, 163-174.

Roldan-Assad, R.; Gareil, R. (**1995**). Capillary zone electrophoretic determination of C_2C_{18} linear saturated free fatty acids with indirect absorbance detection. *Journal of Chromatography A, 708*, 339-350.

Surowiec, I.; Kaml, I.; Kenndler, E. (**2004**). Analysis of drying oils used as binding media for objects of art by capillary electrophoresis with indirect UV and conductivity detection. *Journal of* Chromatography A, 1024, 245-254.

Vallejo-Cordoba, B.; Mazorra-Manzano, M.A.; Gonzalez-Cordova, A. F. (**1998**). Determination of short-chain free fatty acids in lipolyzed milk fat by capillary electrophoresis. *Journal of Capillary Electrophoresis, 5*, 111-114.

Vandeginste, B.G.M.; Massart, D.L.; Buydens, L.M.C.; De Jong, S.; Lewi, P.J.; Smeyers-Verbeke, J. (**1998**). In data handling in science and technology, Part B; Elsevier Science: Amsterdam, The Netherlands, p 237.

Williams, C.M.; Mander, L.N. (**2001**). Chromatography with silver nitrate. *Tetrahedron, 57,* 425-447.

Yeung, E.S. (**1995**). Optical detectors for capillary electrophoresis. *Advances in Chromatography, 35,* 1-51.

Chapter 17. Acrylate ester-based monolithic columns for capillary electrochromatography separation of triacylglycerols in vegetable oils

Journal of Chromatography A, 1218 (2011) 7528–7533

Contents lists available at ScienceDirect

Journal of Chromatography A

journal homepage: www.elsevier.com/locate/chroma

Acrylate ester-based monolithic columns for capillary electrochromatography separation of triacylglycerols in vegetable oils

M.J. Lerma-García, M. Vergara-Barberán, J.M. Herrero-Martínez, E.F. Simó-Alfonso*

Departamento de Química Analítica, Universidad de Valencia, C. Doctor Moliner 50, E-46100 Burjassot, Valencia, Spain

A simple and reliable method for the evaluation of TAGs in vegetable oils by CEC with UV-Vis detection, using octadecyl acrylate (ODA) ester-based monolithic columns, has been developed. The percentages of the porogenic solvents in the polymerization mixture, and the mobile phase composition, were optimized. The optimum monolith was obtained at the following ratios: 40:60% (wt/wt) monomers/porogens, 60:40% (wt/wt) ODA/1,3-butanediol diacrylate and 23:77% (wt/wt) 1,4-butanediol/1-propanol (14 wt% 1,4-butanediol in the polymerization mixture). A satisfactory resolution between TAGs was achieved in less than 12 min with a 65:35 (v/v) acetonitrile/2-propanol mixture containing 5 mM ammonium acetate. The method was applied to the analysis of TAGs of vegetable oil samples. Using linear discriminant analysis of the CEC, TAG profiles, the vegetable oils belonging to six different botanical origins (corn, extra virgin olive, hazelnut, peanut, soybean and sunflower) were correctly classified with an excellent resolution among all the categories.

Keywords: Capillary electrochromatography; botanical origin; linear discriminant analysis; triacylglycerols; octadecyl acrylate-based monolithic columns; vegetable oils

17.1. Introduction

Vegetable oils are primarily a mixture of TAGs, with some free fatty acids, mono- and diacylglycerols, and non-glyceridic constituents (0.5 – 1.5%). The composition and structure of TAGs determine, to a large extent, the functionality of oils as food ingredients, and their physiological effects as components of the human diet. TAG profile is characteristic of the original oil source (Belitz, 1999; Jakab, 2002; Holčapek, 2005), which can be useful for the identification of the botanical origin of the oil. For this reason, the determination of these components could be of great value in establishing oil genuineness.

TAGs in vegetable oils have been usually determined by LC, including both non-aqueous RP-HPLC (Carelli, 1993; Parcerisa, 1995; Jakab, 2002; Fauconnot, 2004; Holčapek, 2005; Cunha, 2006) and silver-ion HPLC (Schuyl, 1998; Macher, 2001; Adlof, 2002). The first provides separation according to hydrophobicity, while the latter gives separations according to degree of insaturation. On the other hand, selectivity and high peak capacities have been achieved by using comprehensive two-dimensional chromatography, by combining both a C18 column with a second column load with silver ions (Robison, 1985; Dugo, 2006; van der Klift, 2008). Other analytical technique also used for TAG determination has been high temperature capillary gas chromatography (Carelli, 1993; Aparicio, 2000). On the other hand, the official method of analysis involves the use of a HPLC coupled with a RI detector (Parcerisa, 1995), but, since it is not compatible with the use of gradient elution (desirable to reduce analysis times and to improve chromatographic resolution), other detectors have been also used, such as UV at low wavelengths (Holčapek, 2005; Carelli, 1993; van der Klift, 2008), ELSD (Macher, 2001; Holčapek, 2005; van der Klift, 2008) or MS (Holčapek, 2005; van der Klift, 2008). However, most of these techniques provide long analysis times being thus desiderable the development of other

analytical methods to solve this problem.

CEC is a hybrid separation technique, which combines the selectivity of HPLC with the high efficiency of CE. Among CEC supports, the use of monolithic columns has extensively grown in the last few years. Their advantages compared with CEC packed columns are: (i) simple preparation, (ii) absence of retaining frits, (iii) adjustable porosity and pore size, allowing the use of long columns to achieve highly efficient separations, and (iv) the wide variety of monomers available for the synthesis of stationary phases with different functionalities (Legido-Quigley, 2003; Svec, 2003). Briefly, monolithic materials can be classified into two categories, organic polymer- and silica-based monoliths (Svec, 2003). Among these polymeric stationary phases, acrylate- (Ngola, 2001; Bedair, 2003; Barrioulet, 2005; Augustin, 2006; Cantó-Mirapeix, 2009) and methacrylate-based (Peters, 1998; Yu, 2002; Eeltink, 2005; Cantó-Mirapeix, 2009) monoliths are the most popular materials used for CEC applications. These monoliths are usually prepared by *in situ* polymerization of a mixture composed of functional monomer/s, cross-linker, porogens, and a free radical initiator. Polymerization reaction is commonly initiated thermally (Peters, 1998; Yu, 2002; Bedair, 2003; Eeltink, 2005), by UV irradiation (Augustin, 2006; Ngola, 2001; Barrioulet, 2005; Yu, 2002), or by a chemical system (Peters, 1998; Cantó-Mirapeix, 2009). Advantages of photo-initiation are speed and easy selection of polymerization regions by using masks, which is particularly important in relation to the manufacturing of microfluidic chips.

The potential of this monolithic technology has been demonstrated in the determination of tocopherols (Lerma-García, 2007) and sterols (Lerma-García, 2008) in vegetable oils, and phenolic compounds (Lerma-García, 2009) in extra virgin olive oils. On the other hand, CEC using packed columns has been used to determine TAGs in fish oils (Dermaux, 1998, Dermaux, 1999) and in several vegetable oils (corn, peanut, primrose and walnut)

(Sandra, 1997). However, and to our knowledge, any work has been published using TAG profiles established by CEC to classify edible oils according to their botanical origin. Then, it could be interesting to develop a classification method using TAG profiles established by CEC, since usually analysis times are lower than those obtained by LC techniques.

The aim of this work was to evaluate the TAG profiles of vegetable oils from different botanical origins by using a simple and reliable CEC method. The characterization of TAG profile using octadecyl acrylate (ODA) ester-based monolithic columns was optimized in terms of composition of polymerization mixture (i.e. porogenic solvents) and mobile phase composition. The classification of vegetable oil samples according to their botanical origin was performed by LDA.

17.2. Materials and methods

17.2.1. Reagents and samples

ODA, 1,3-butanediol diacrylate (BDDA), lauroyl peroxide (LPO), [2-(methacryloyloxy)ethyl] trimethyl ammonium chloride (75% in water, META), 1,4-butanediol and 3-(trimethoxysilyl)propyl methacrylate from Aldrich (Milwaukee, WI, USA), methanol, 2-propanol, 1-propanol and ACN from Scharlau (Barcelona), *n*-hexane and ammonium acetate (Riedel-de Haën, Seelze, Germany) were employed. Deionized water was obtained with a Barnstead deionizer (Sybron, Boston, MA, USA). Fused-silica capillaries of 33.5 cm length and 375 μm O.D. × 100 μm I.D. with UV-transparent external coating (Polymicro Technologies, Phoenix, AZ, USA) were used.

The vegetable oil samples employed in this study are summarized in **Table 17.1.** These oils were either purchased or kindly donated by the manufacturers. The botanical origin and quality grade of all the samples were guaranteed by the suppliers.

Table 17.1

Botanical origin, number of samples and brand of the vegetable oil samples used in this work.

Origin	No. of samples	Brand
Corn	2	Guinama
	1	Asua
	1	Cristal
	1	Gloria
	1	Mazola
Extra virgin olive	1	Borges
	1	Carbonell
	1	Coosur
	1	Grupo Hojiblanca
	1	Vea
	1	Torrereal
Hazelnut	3	Guinama
	3	Percheron
Peanut	2	Coppini
	2	Guinama
	2	Maurel
Soybean	2	Coosur
	2	Guinama
	1	Biolasi
	1	Coppini
Sunflower	2	Hacendado
	2	Coosur
	2	Koipesol

17.2.2. Instrumentation

CEC experiments were performed on an HP^{3D}CE instrument (Agilent Technologies, Waldbronn, Germany), equipped with a diode array UV-Vis detector and provided with an external nitrogen supply. Data acquisition was performed with ChemStation Software (Rev.A.10.01, Agilent). Before use, all the eluents for CEC were degassed with a D-78224 ultrasonic bath (Elma, Germany). To photoinitiate polymerization, capillaries were placed into an UV crosslinker (model CL1000) from UVP Inc. (Upland, CA, USA) equipped with five UV lamps (5 × 8 W, 254 nm). Scanning electron microscope (SEM) photographs of monolithic materials were taken with a SEM model S-4100 (Hitachi, Ibaraki, Japan) provided with a field emission gun, a BSE AUTRATA detector and an EMIP 3.0 image data acquisition system.

17.2.3. Preparation and characterization of the polymeric monolithic columns

Before preparation of the columns, and in order to enable covalent attachment of the monolith to the wall, surface modification of the inner wall of the fused-silica capillaries with 3-(trimethoxysilyl)propyl methacrylate was performed (Peters, 1998). Monoliths were prepared using polymerization mixtures containing a bulk monomer (ODA), a cross-linker (BDDA), pore-forming solvents (1,4-butanediol/1-propanol) and a positively charged monomer (META), which was added to assure EOF. LPO (1 wt% with respect to the monomers) was employed as initiator. After mixing, and to obtain a clear solution, sonication for 10 min followed by deareation with nitrogen for 10 more min was applied. The preconditioned capillary (33.5 cm) was filled with the polymerization mixture up to a total length of 25 cm. Photo-polymerization was accomplished by irradiation of the capillaries inside the UV crosslinker at 0.9 J/cm^2 for 10 min (Bernabé-Zafón, 2009). After polymerization and using an HPLC pump, the resulting columns were flushed

first with methanol to remove the pore-forming solvents and possible unreacted monomers or oligomers, and then with mobile phase for 30 min.

17.2.4. CEC procedures

The monolithic column was placed in the instrument and equilibrated with the mobile phase as follows. Using nitrogen, a pressure of 10 bar (1 MPa) was applied to both ends of the column (Peters, 1998; Eeltink, 2005), and the voltage was stepwise raised from -5 to -25 kV, with increments of 5 kV. Each voltage was kept until a constant current and a stable baseline were achieved. Separations were performed at -25 kV with the column kept at 20ºC, and the inlet and outlet vials pressurized to 1 MPa with nitrogen. Sample extracts were injected electrokinetically under -10 kV for 3 s. Detection was performed at 192 nm.

17.2.5. Sample preparation, data treatment and statistical analysis

Vegetable oil samples were injected into the CEC system after a simple dilution to 3% in a 2:2:1 ACN/2-propanol/*n*-hexane (v/v/v) ternary mixture. All samples were injected three times. Using peanut oil as reference sample, the common peaks for all vegetable oils studied were selected. The peak area of each compound was measured, and a data matrix was constructed using the areas of all the peaks as original variables. After normalization of the variables, statistical data treatment was performed using SPSS (v. 15.0, Statistical Package for the Social Sciences, Chicago, IL, USA). LDA, a supervised classificatory technique, is widely recognized as an excellent tool to obtain vectors showing the maximal resolution between a set of previously defined categories. In LDA, vectors minimizing the Wilks' lambda, $\lambda_{w,}$ are obtained (Vandeginste, 1998). This parameter is calculated as the sum of squares of the distances between points belonging to the same category divided by the total sum of squares. Values of λ_w approaching zero are

obtained with well resolved categories, whereas overlapped categories made λ_w to approach one. Up to N−1 discriminant vectors are constructed by LDA, being N the lowest value for either the number of predictors or the number of categories. The selection of the predictors to be included in the LDA models was performed using the SPSS stepwise algorithm. According to this algorithm, a predictor is selected when the reduction of λ_w produced after its inclusion in the model exceeds F_{in}, the entrance threshold of a test of comparison of variances or F-test. However, the entrance of a new predictor modifies the significance of those predictors which are already present in the model. For this reason, after the inclusion of a new predictor, a rejection threshold, F_{out}, is used to decide if one of the other predictors should be removed from the model. The process terminates when there are no predictors entering or being eliminated from the model. The probability values of F_{in} and F_{out}, 0.05 and 0.10, respectively, were adopted.

17.3. Results and discussion

17.3.1. Optimization TAGs separation

The conditions to prepare photo-polymerized ODA-based monoliths were adapted from a previous work, where CEC columns were chemically polymerized using LPO as initiator (Cantó-Mirapeix, 2009). Initially, the selected composition of the polymerization mixture was 40 wt% monomers (59.7 wt% ODA, 40 wt% BDDA and 0.3 wt% META) and 60 wt% porogens (13 wt% 1,4-butanediol and 87 wt% 1-propanol) in the presence of 0.3 wt% LPO. According to Sandra and co-workers (Sandra, 1997; Dermaux, 1998; Dermaux, 1999), mobile phases containing ACN, 2-propanol, and mixtures of them with small amounts of *n*-hexane, all of them containing ammonium acetate as background electrolyte, have been used to separate TAGs by CEC. Accordingly, an ACN/2-propanol (65:35 v/v) mixture containing 5 mM

ammonium acetate was firstly tried. However, at this 1,4-butanediol content in the polymerization mixture (8 wt%), the column exhibited poor permeability, leading to blockage problems. For this reason, polymerization mixtures containing higher 1,4-butanediol contents (10-16 wt%) were studied. This increase in the 1,4-butanediol content led to a reduction in the analysis time. This retention behaviour was attributed to the increase of the globule size, which was corroborated by the SEM pictures shown in **Figure 17.1**.

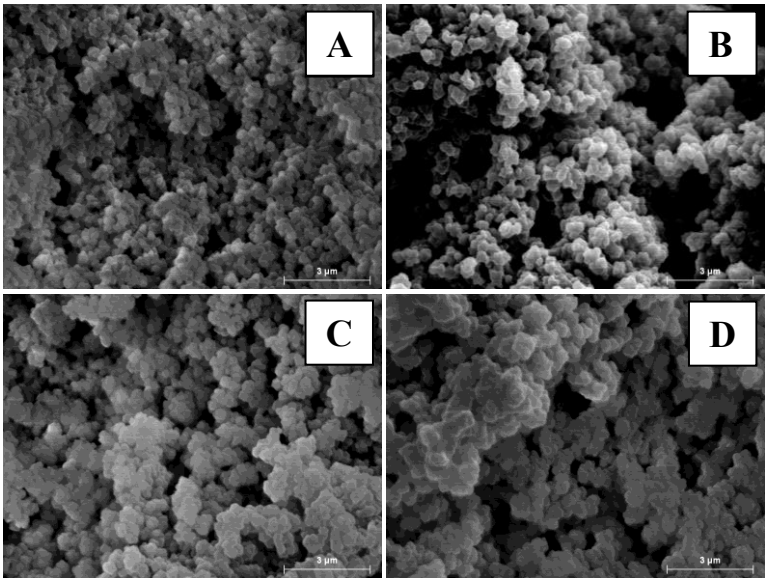

Figure 17.1. SEM micrographs of ODA-based monolithic columns prepared with (A) 9%, (B), 10%, (C) 12% and (D) 14% 1,4-butanediol in the polymerization mixture. The bar lengths stand for 3 μm.

Monolith prepared with 10 wt% 1,4-butanediol showed poor efficiencies which could be explained by the double-layer overlap, as suggested by other authors (Jiang, 2001; Eeltink, 2005). When the 1,4-butanediol content was increased up to 14 wt%, an increase in peak resolution was observed. However, when a 16 wt% 1,4-butanediol was used, resolution decreased, which was consistent with the large globules sizes obtained for this monolith (**Figure 17.1D).** At the sight of these results, a monolith containing 14 wt% 1,4-butanediol in the polymerization mixture was selected for further studies.

In order to improve the quality of separation, the influence of mobile phase composition was studied. The ACN/2-propanol ratio, containing 5 mM ammonium hydroxide, was varied between 70:30 and 50:50 v/v. **Figure 17.2** shows the electrochromatograms obtained under these ACN/2-propanol ratios.

At 70:30 v/v (**Figure 17.2A**), a decrease in peak resolution regarding to 65:35 v/v (**Figure 17.2B**) was evidenced. A progressive increase in 2-propanol content (**Figure 17.3C and D**) led to an increase in the analysis time jointly with a loss of peak resolution, being especially dramatic at 50:50 v/v (**Figure 17.3D**). This retention behaviour can be explained in terms of a conjunction of two factors, the eluotropic strength of solvent composition and EOF (2-propanol showed lower polarity and higher eluotropic strength than ACN). In addition, a reduction of EOF could be due to the reduction of the electric permittivity/viscosity ratio (ε/η 99 and 9 for pure ACN and 2-propanol at 25ºC, respectively). As a result of this study, a mobile phase containing 65:35 v/v ACN/2-propanol with 5 mM ammonium acetate was chosen for oil sample analysis.

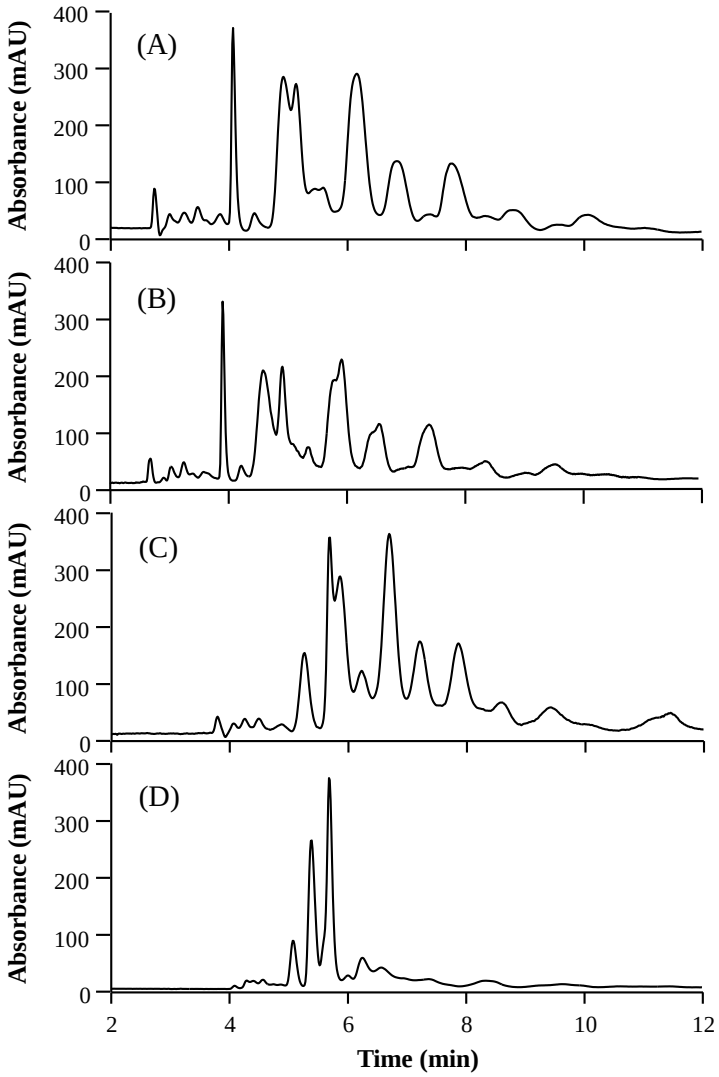

Figure 17.2. Influence of the mobile phase composition on the separation of TAG compounds in a peanut oil sample: (A) 70:30, (B) 65:35 (C) 60:40 and (D) 50:50 (v/v) ACN/2-propanol mixtures containing 5 mM ammonium acetate. CEC conditions: ODA-based monolithic column prepared with 14 wt% 1,4-butanediol in the polymerization mixture; electrokinetic injection, -10 kV for 3 s; separation voltage, -25 kV; wavelength detection: 192 nm.

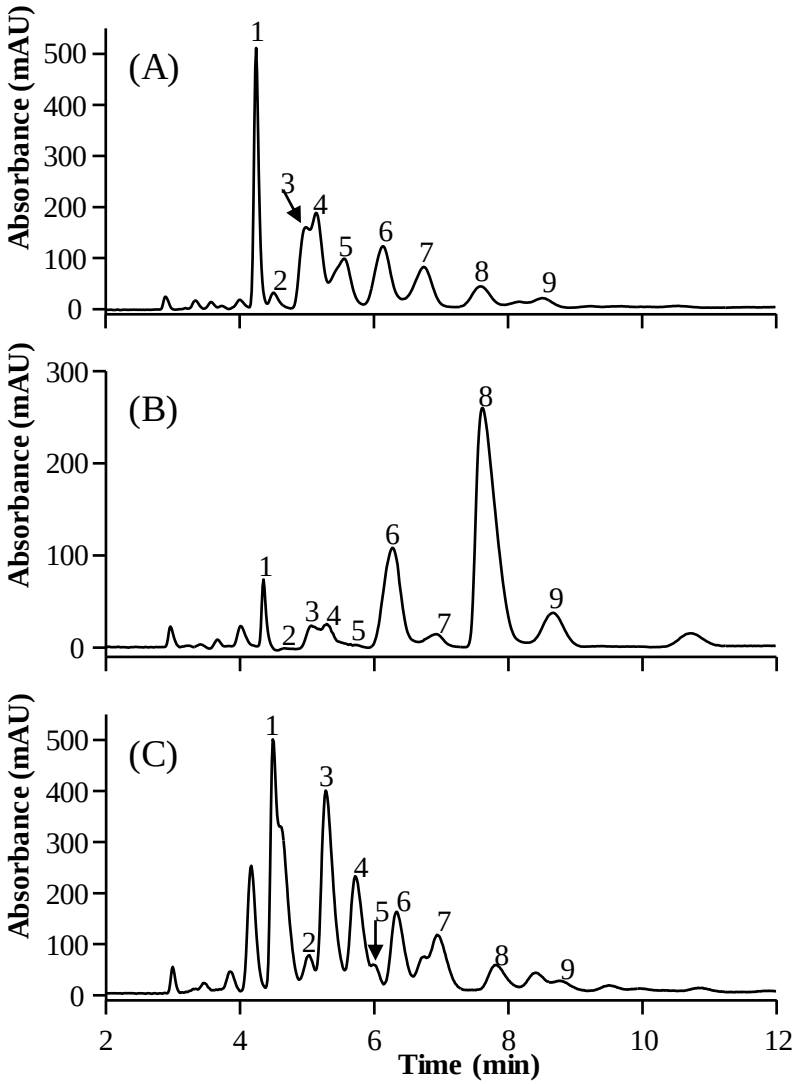

Figure 17.3. Electrochromatograms of a (A) corn, (B) hazelnut and (C) soybean oils obtained on an ODA-based monolithic capillary under the optimal conditions. Other experimental conditions as in **Figure 17.2.**

17.3.2. Characterization of the TAGs of vegetable oils

The optimized method was applied to the analysis of vegetable oil samples. Representative electrochromatograms of corn (A), hazelnut (B) and soybean (C) oils are shown in **Figure 17.3**. As observed in **Figure 17.2B** and **Figure 17.3**, a total of 9 common peaks were present in the four representative botanical origins in less than 12 min. In order to assure a correct peak assignment, peanut oil (which was used as reference sample) was mixed with the other studied vegetable oils. Since any sample treatment was done to the vegetable oils employed in the study (oils were only diluted to a 3% in a hexane 2:2:1 ACN/2-propanol/*n*-hexane (v/v/v) ternary mixture), these peaks were attributed to TAGs, which are the most abundant compounds present in vegetable oils. Thus, the different profiles observed should be related with the different botanical origins of the oil samples. The differences observed in oil fingerprints were enhanced when chemometric analysis of the data was performed.

17.3.3. Normalization of the variables and construction of LDA models

In order to reduce the variability associated to sources of variance that can affect the sum of the areas of all the peaks, normalized rather than absolute peak areas were used. In order to normalize the variables, the area of each peak was divided by each one of the areas of the other 8 peaks; in this way, and taking into account that each pair of peaks should be considered only once, (9 x 8)/2 = 36 non-redundant peak ratios were obtained to be used as predictors.

Using the normalized variables, an LDA model capable of classifying the vegetable oil samples according to their respective botanical origin was constructed. From the 36 samples of **Table 17.1**, a matrix containing 108 injections (all samples were injected three times), was constructed and used for evaluation purposes. To construct the LDA training matrix, only the means

of the replicates of the samples were included (36 objects); in this way, the internal dispersion of the categories was reduced, which was important to reduce the number of variables selected by the SPSS stepwise algorithm during model construction. A response column, containing the six categories corresponding to the six botanical origins of the oil, was added to both matrices. When the LDA model was constructed, an excellent resolution between all the category pairs was achieved (**Figure 17.4**, $\lambda_w = 0.051$).

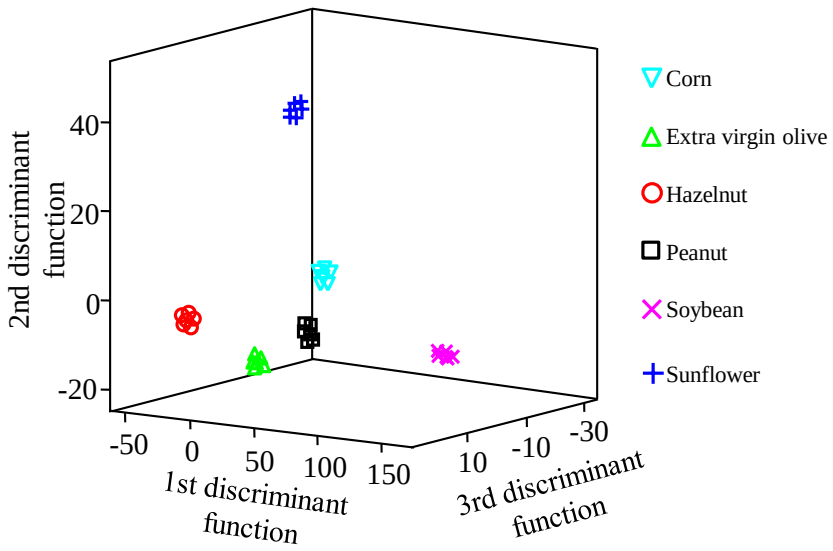

Figure 17.4. Score plot on an oblique plane of the 3-D space defined by the three first discriminant functions of the LDA model constructed to classify vegetable oils according to their botanical origin.

The variables selected by the SPSS stepwise algorithm, and the corresponding standardized coefficients of this model, showing the predictors with large discriminant capabilities, are given in **Table 17.2**.

Table 17.2

Predictors selected and corresponding standardized coefficients of the LDA model constructed to classify vegetable oils according to their botanical origin.

Predictors[a]	f_1	f_2	f_3	f_4	f_5
1/4	-0.11	-0.03	3.45	-2.13	1.51
2/8	2.03	-0.53	-0.29	-0.72	-0.18
3/6	-0.67	1.16	-3.10	3.43	-1.61
3/9	2.64	-0.34	0.70	-0.71	0.31
4/6	2.08	4.60	0.88	0.95	-0.71
5/6	-0.55	1.09	-0.79	1.15	0.97
6/7	-0.24	0.68	1.00	1.14	-0.12
7/8	-4.47	-4.31	-0.61	-0.36	-0.04

[a] Pairs of peak areas identified according to figure labels.

For this model, and using leave-one-out validation, all the points of the training set were correctly classified. The corresponding evaluation set, containing the 36 original data points, was then used to check the prediction capability of the model. Using a 95% probability, all the objects were correctly assigned.

The results obtained could be compared with those previously obtained by our research group in which vegetable oils were classified according to their botanical origin using alcohol profiles obtained by HPLC after a previous derivatization step with diphenic anhydride (Lerma-García, 2009B). In both cases, an excellent resolution among all oil categories was obtained. However, the λ_w obtained when alcohol profiles were used as predictors was 0.163, while the one obtained using TAG profiles was 0.051. This lower λ_w value could be attributed to the selection of a lower number of predictors by the model constructed using TAG profiles (8 predictors against the 12 selected using alcohol profiles). On the other hand, TAG profiles were obtained after a simple sample dilution, whereas a tedious sample treatment was needed in order to obtain alcohol profiles, being also necessary the application of a

previous derivatization step in order to enhance alcohol detection (Lerma-García, 2009B).

The proposed method was also compared with other methodologies previously published in literature to determine TAG profiles (Parcerisa, 1995; Sandra, 1997; Dermaux, 1998; Macher, 2001; Adlof, 2002; Jakab, 2002; Fauconnot, 2004; Holčapek, 2005; Cunha, 2006; Dugo, 2006). Sandra *et al.* have determine TAG profiles by CEC in several vegetable oils (corn, peanut, primrose and walnut) (Sandra, 1997) and in fish oils (Dermaux, 1998) using a commercially packed 3 µm Hypersil C18 column; however, our method is largely faster (12 min against *ca*. 80 min) and present the advantage that our column is a monolithic one, which is prepared by us in the laboratory; then its cost is very low, and their morphological properties (pore size, macro and microporous and globule size) could be adapted to our convenience.

On the other hand, analysis time was also largely reduced when comparing the proposed CEC methodology (12 min) with the chromatographic ones, which are close to 30 min or higher (Parcerisa, 1995; Macher, 2001; Adlof, 2002; Jakab, 2002; Fauconnot, 2004; Holčapek, 2005; Cunha, 2006; Dugo, 2006; van der Klift, 2008), being necessary in some cases the use of two columns connected in series (Holčapek, 2005; Adlof, 2002) or the use of comprehensive two-dimensional chromatography (Dugo, 2006; van der Klift, 2008). In addition, our CEC method allows the classification of the studied vegetable oils with a high assignment probability due to the lower λ_w value obtained, which improves the discrimination between the different oils previously obtained by other authors by LDA (Jakab, 2002) or by principal component analysis (Cunha, 2006).

17.4. Conclusions

Using ODA ester-based monolithic columns, a simple and reliable CEC method for the analysis of TAG profiles of vegetable oils has been developed. The best TAG separations were obtained in less than 12 min with an ODA-based column prepared with 14 wt% 1,4-butanediol in the polymerization mixture, and using a mobile phase containing 65:35 (v/v) ACN/2-propanol (5 mM ammonium acetate). Using CEC data and LDA, the vegetable oil samples belonging to the six different botanical origins (corn, extra virgin olive, hazelnut, peanut, soybean and sunflower) were correctly classified with an excellent resolution among all the categories. A next step of this work will be the identification of the different TAGs by interfacing CEC with MS or by injection of single TAGs previously collected by HPLC.

Acknowledgements

Work supported by project CTQ2010-15335/BQU (MEC and FEDER funds). M.J. Lerma García thanks the Generalitat Valenciana for an FPI grant for PhD studies.

17.5. References

Adlof, R.O.; Menzel, A.; Dorovska-Taran, V. (**2002**). Analysis of conjugated linoleic acid-enriched triacylglycerol mixtures by isocratic silver-ion high-performance liquid chromatography. *Journal of Chromatography A,* 953 293-297.

Aparicio, R.; Aparicio-Ruíz, R. (**2000**). Authentication of vegetable oils by chromatographic techniques. *Journal of Chromatography A, 881*, 93-104.

Augustin, V.; Jardy, A.; Gareil, P.; Hennion, M.C. (**2006**). *In situ* synthesis of monolithic stationary phases for electrochromatographic separations: Study of polymerization conditions. *Journal of Chromatography* A, 1119, 80-87.

Barrioulet, M.P.; Delaunay-Bertoncini, N.; Demesmay, C.; Rocca, J.L. (**2005**). Development of acrylate-based monolithic stationary phases for electrochromatographic separations. *Electrophoresis 26,* 4104-4115.

Bedair, M.; El Rassi, Z. (**2003**). Capillary electrochromatography with monolithic stationary phases: II. Preparation of cationic stearyl-acrylate monoliths and their electrochromatographic characterization. *Journal of Chromatography A, 1013,* 35-45.

Belitz, H.D.; Grosch, W. (**1999**). Food Chemistry, Springer, Berlin.

Bernabé-Zafón, V.; Cantó-Mirapeix, A.; Simó-Alfonso, E.F.; Ramis-Ramos, G.; Herrero-Martínez, J.M. (**2009**). Comparison of thermal- and photo-polymerization of lauryl methacrylate monolithic columns for CEC. *Electrophoresis, 30*, 1929-1936.

Cantó-Mirapeix, A.; Herrero-Martínez, J.M.; Mongay-Fernández, C.; Simó-Alfonso, E.F. (**2009**). Chemical initiation for butyl and lauryl acrylate monolithic columns for CEC. *Electrophoresis, 30,* 599-606.

Carelli, A.A.; Cert, A. (**1993**). Comparative study of the determination of triacylglycerol in vegetable oils using chromatographic techniques. *Journal of Chromatograpy A, 630,* 213-222.

Cunha, S.C.; Oliveira, M.B.P.P. (**2006**). Discrimination of vegetable oils by triacylglycerols evaluation of profile using HPLC/ELSD. *Food Chemistry, 95,* 518-524.

Dermaux, A.; Sandra, P.; Ksir, M.; Zarrouck F.F. (**1998**). Analysis of triglycerides and free and derivatized fatty acids in fish oil by capillary electrochromatograpy. *Journal of Separation Science, 21,* 545-548.

Dermaux, A.; Medvedovici, A.; Ksir, M.; Van Hove, E.; Talbi, M.; Sandra. P. (**1999**). Elucidation of the triglycerides in fish oil by packed-column supercritical fluid chromatography fractionation followed by capillary electrochromatography and electrospray mass spectrometry. *Journal of Microcolumn Separations, 11,* 451-459.

Dugo, P.; Kumm, T., Crupi, M.L.; Cotroneo, A.; Mondello, L. (**2006**). Comprehensive two-dimensional liquid chromatography combined with mass spectrometric detection in the analyses of triacylglycerols in natural lipidic matrixes. *Journal of Chromatography A, 1112*, 269-275.

Eeltink, S.; Herrero-Martínez, J.M.; Rozing, G.P.; Schoenmakers, P.J.; Kok, W.Th. (**2005**). Tailoring the morphology of methacrylate ester-based monoliths for optimum efficiency in liquid chromatography. *Analytical Chemistry, 77,* 7342-7347.

Fauconnot, L.; Hau, J.; Aeschlimann, J.M.; Fay, L.B.; Dionisi, F. (**2004**). Quantitative analysis of triacylglycerol regioisomers in fats and oils using

reversed-phase high-performance liquid chromatography and atmospheric pressure chemical ionization mass spectrometry. *Rapid Communications in Mass Spectrometry, 18*, 218-222.

Holčapek, M.; Lísa, M.; Jandera, P.; Kabátová, N. (**2005**). Quantitation of triacylglycerols in plant oils using HPLC with APCI-MS, evaporative light-scattering, and UV detection. *Journal of Separation Science, 28*, 1315-1333.

Jakab, A.; Héberger, K.; Forgács, E. (**2002**). Comparative analysis of different plant oils by high-performance liquid chromatography-atmospheric pressure chemical ionization mass spectrometry. *Journal of Chromatography A, 976*, 255-63.

Jiang, T.; Jiskra, J.; Claessens, H.A.; Cramers, C.A. (**2001**). Preparation and characterization of monolithic polymer columns for capillary electrochromatography. *Journal of Chromatography* A, 923, 215-227.

Legido-Quigley, C.; Marlin, N.D.; Melin, V.; Manz, A.; Smith, N.W. (**2003**). Advances in capillary electrochromatography and micro-high performance liquid chromatography monolithic columns for separation science. *Electrophoresis, 24*, 917-944.

Lerma-García, M.J.; Simó-Alfonso, E.F.; Ramis-Ramos, G.; Herrero-Martínez, J.M. (**2007**). Determination of tocopherols in vegetable oils by CEC using methacrylate ester-based monolithic columns. *Electrophoresis 28*, 4128-4135.

Lerma-García, M.J.; Simó-Alfonso, E.F.; Ramis-Ramos, G.; Herrero-Martínez, J.M. (**2008**). Rapid determination of sterols in vegetable oils by CEC using methacrylate ester-based monolithic columns. *Electrophoresis, 29*, 4603-4611.

Lerma-García, M.J.; Lantano, C.; Chiavaro, E.; Cerretani, L.; Herrero-Martínez, J.M.; Simó-Alfonso, E.F. (**2009A**). Classification of extra virgin olive oils according to their geographical origin using phenolic compound profiles obtained by capillary electrochromatography. *Food Research International, 42*, 1446-1452.

Lerma-García, M.J.; Ramis-Ramos, G.; Herrero-Martínez, J.M.; Gimeno-Adelantado, J.V.; Simó-Alfonso, E.F. (**2009B**). Characterization of the alcoholic fraction of vegetable oils by derivatization with diphenic anhydride followed by high-performance liquid chromatography with spectrophotometric and mass spectrometric detection. *Journal of* Chromatography A, 1216, 230-263.

Macher, M.B.; Holmqvist, A. (**2001**). Triacylglycerol analysis of partially hydrogenated vegetable oils by silver ion HPLC. *Journal of Separation Science*, *24*, 179-185.

Ngola, S.M.; Fintschenko, Y.; Choi, W.Y.; Shepodd, T.J. (**2001**). Conduct-as-cast polymer monoliths as separation media for capillary electrochromatography. *Analytical Chemistry*, *73*, 849-856.

Parcerisa, J.; Boatella, J.; Codony, R.; Rafecas, M.; Castellote, A. I.; García, J.; López, A.; Romero, A. (**1995).** Comparison of fatty acid and triacylglycerol compositions of different hazelnut varieties (*Corylus avellana L.)* cultivated in Catalonia (Spain). *Journal of Agriculture and Food Chemistry*, *43*, 13-16.

Peters, E.C.; Petro, M.; Svec, F.; Fréchet. J.M.J. (**1998**). Molded rigid polymer monoliths as separation media for capillary electrochromatography. Effect of chromatographic conditions on the separation. *Analytical Chemistry, 70*, 2288-2302.

Robison, J.L.; Tsimidou, M.; Macrae, R.. (**1985**). Evaluation of the mass detector for quantitative detection of triglycerides and fatty acid methyl esters. *Journal of Chromatography A, 324*, 35-51.

Sandra, P.; Dermaux, A.; Ferraz, V.; Dittmann, M.M.; Rozing. G. (**1997**). Analysis of triglycerides by capillary electrochromatography. *Journal of Microcolumn Separations, 9*, 409-419.

Schuyl, P.J.W.; de Joode, T.; Vasconcellos, M.A.; Duchateau, G.S.M.J.E. (**1998**). Silver-phase high-performance liquid chromatography–electrospray mass spectrometry of triacylglycerols. *Journal of Chromatography A*, 810, 53-61.

Svec, F.; Tennikova, T.B.; Deyl, Z. (**2003**). Monolithic materials: preparation, properties and applications. *Journal of Chromatography Library*, Vol. 67.

Vandeginste, B.G.M.; Massart, D.L.; Buydens, L.M.C.; De Jong, S.; Lewi, P.J.; Smeyers-Verbeke, J. (**1998**). Data Handling in Science and Technology, Part B, Elsevier, Amsterdam

Van der Klift, E.J.C.; Vivó-Truyols, G.; Claassen, F.W.; van Holthoon, F.L.; van Beek, T. A. (**2008**). Comprehensive two-dimensional liquid chromatography with ultraviolet, evaporative light scattering and mass spectrometric detection of triacylglycerols in corn oil. *Journal of Chromatography A, 1178*, 43-55.

Yu, C.; Xu, M.; Svec, F.; Fréchet, J.M.J. (**2002**). Preparation of monolithic polymers with controlled porous properties for microfluidic chip applications using photoinitiated free-radical polymerization. *Journal of Polymeric Chemistry, 40*, 755-769.

III.B. Application of spectroscopic techniques

Chapter 18. Cultivar discrimination of Spanish olives by using direct FTIR data combined with linear discriminant analysis

Eur. J. Lipid Sci. Technol. 2015, *117*, 1473–1479

Research Article

Cultivar discrimination of Spanish olives by using direct FTIR data combined with linear discriminant analysis

María Vergara-Barberán, María Jesús Lerma-García, José Manuel Herrero-Martínez and Ernesto Francisco Simó-Alfonso

ATR-FTIR, followed by LDA of spectral data, was used to discriminate olive fruits according to their cultivar. For this purpose, the spectral data of 136 olives coming from 17 cultivars, collected at different Spanish locations, were recorded. Up to 24 frequency regions were selected on the spectra, which corresponded to a peak or shoulder. The normalized absorbance peak areas within these regions were used as predictors. Although a good resolution was achieved among all categories, a second LDA model was also constructed to improve cultivar discrimination. With both models, evaluation set samples were correctly classified with assignment probabilities higher than 95%. Thus, it is demonstrated that FTIR followed by LDA of the spectral data presents a high potential to discriminate olives from a high number of different cultivars.

Keywords: ATR-FTIR; cultivar discrimination; linear discriminant analysis, olive fruits

18.1. Introduction

Olive tree (*Olea europeaea L.*) is a typical species grown throughout the Mediterranean regions. It is one of the oldest known cultivated trees in the world, being also an economically important crop due to the high quality of its oil. Virgin olive oil (VOO) quality can be affected by different parameters, such as the agronomic technique used, varietal and geographic origin, olive fruit quality, ripening stage, and oil extraction process, among others (Dupuy, 2010; Salguero-Chaparro, 2013). Thus, the production of good-quality VOOs should start with raw materials that gather well-defined quality standards (Gómez-Caravaca, 2008). In order to assure the real quality of this oil, it is necessary to develop analytical methods able to control raw materialquality, and also to control its origin since olive oil producershave to include in their manufactured products both the genetic variety (monovarietal oils) and the geographical origin of the olives (protected designation of origin) according to the European Community (EC) regulation 182/2009 (EC, 2009).

Among the different methodologies used for this scope, spectroscopic techniques have been significantly usedto establish the origin and to discriminate food products in the last years (Terouzi, 2011). IR is a rapid, low cost, and non-destructive technique used for the study of a wide variety of food and food processes, which requires minimum sample preparation. It allows qualitative determination since the characteristic vibrational mode of each molecular group produces the appearance ofbands in the IR spectrum, which are influenced by the surrounding functional groups (Vlachos, 2006).Moreover, IR is also an excellent tool for quantitative analysis, because the intensities of the spectral bands are proportional to the concentration. In addition, IR data have been often treated with multivariate chemometric techniques to develop methods of classification and characterization (Terouzi, 2011). Thus, IR (near and medium, and mostly Fourier-transform infrared spectroscopy, FTIR) has been effectively employed to predict quality

parameters of both olives and VOOs (Mailer, 2004; Ayora-Canada, 2005; Jiménez-Marquez, 2005; Vlachos, 2006; Cayuela, 2010; Casale, 2010;Dupuy, 2010; Morales-Sillero, 2011; Toreozi, 2011, Salguero-Chaparro, 2013; Inarejos,-García, 2013; Cayuela, 2013), and also to classify them according to their genetic variety (Gurdeniz, 2007; Concha-Herrera, 2009; De Luca, 2012), geographical origin (Tapp, 2003; Bendini, 2007; Galtier, 2007), to detect VOO adulteration (Ozen, 2002; Tay, 2002; Vlachos, 2006; Lerma-García, 2010), to evaluate VOO freshness (Sinelli, 2007), and early stages of VOO autoxidation (Nenadis, 2013). Regarding classification models of olive fruits according to their cultivar, Dupuy *et al.* (Dupuy, 2010) used NIR and MIR spectral data followed by partial least squares-discriminant analysis (PLS-DA) to classify the olives into five French cultivar origins. After using the K-means clustering method on the PLS-DA scores, all samples were correctly classified into the five cultivars. A similar study was developed by Terouzi *et al*. (Terouzi, 2011) using FTIR and PLS-DA to discriminate olives from four Moroccan varieties. Also in this case, the model was able to separate the four classes and to classify new objects with a percentage prediction of 97%. Moreover, De Luca *et al*. (De Luca, 2012) constructed a principal component analysis-linear discriminant analysis (PCA-LDA) model to classify Moroccan olives according to their cultivar by using ATR-FTIR spectra of endocarps. With PCA, samples were clustered into the five cultivars by using the two first principal components with an explained variance of 98.16%, while with LDA the 92% of an external set of new samples was correctly classified. However, the use of PLS or PCA before the application of LDA, requires the use of all the original variables in order to reduce dimensions, while in LDA, only the employ of the variables selected by the model should be performed. In this work, a direct and fast classification of Spanish olive fruits according to their cultivar was performed by using the ATR-FTIR spectral data, followed by LDA. For this purpose, FTIR spectrawere divided into 24 frequency regions, using the normalized absorbance peak areas as predictor variables.

18.2. Materials and methods

18.2.1. Olive fruits

A total of 136 olive fruit samples, coming from 17 different cultivars have been used in this study (see **Table 18.S1** of supplementary material). To assure a correct sampling, healthy and non-damage olives have been recollected during the harvesting period (October–February) of four crop seasons (2011/2012–2014/2015) at different Spanish regions (see **Table 18.S1**). All the olives employed were manually harvested to assume the absence of mold or other microorganisms, washed with water to remove dust or airborne particles settled on the olive. To assure a uniform distribution of the samples, the olive fruit pulp was removed from almost 30 olives for each sample. From the whole, about 20 g of fresh pulp was frozen in liquid nitrogen and ground to a fine powder with a pre-cooled mortar and pestle, lyophilized, and the resulting powder was homogenized and directly measured.

18.2.2. ATR-FTIR spectra

FTIR spectra were obtained using a Jasco 4100 type A spectrophotometer (Jasco, Easton, MD) fitted with a single reflection attenuated total reflectance (ATR) accessory. Analysis was carried out at room temperature and to reduce the background noise measurements for each sample were the mean of 50 scans acquired with a resolution of 4 cm^{-1}. Spectra were recorded in the absorbance mode from 3000 to 700 cm^{-1}. Data handling was performed with spectra manager version 2.07.00 software (Jasco). For each sample, the absorbance spectrum was collected against a background obtained with a dry and empty ATR cell. Three spectra were recorded for each sample per day, during three consecutive days, to consider the possible variability associated

with the FTIR measurements. Before each spectrum was acquired, the ATR crystal was cleaned with a cellulose tissue soaked in acetone and dried.

18.2.3. Data treatment and statistical analysis

The ATR-FTIR spectra were divided into the 24 frequency regions described in **Table 18.1**. Each selected region corresponds to a peak or a shoulder, which conveyed absorbance associated to structural or functional group information. Peaks or shoulders were not necessarily specific, since they could be due to contributions of more than a single transition, arising from a given compound or from several compounds, including lipids or minor components of the samples (see **Table 18.1**). For each region, the peak/shoulder area was measured. In order to minimize variability associated to sources of variance affecting the intensity of all the peaks, such as radiation source intensity, normalized rather than absolute areas were used (Concha-Herrera, 2009; Lerma-García, 2010). To normalize the variables, the area of each region was divided by each one of the areas of the other 23 regions; in this way and because any pair of areas should be considered only once, (24 x 23)/2 = 276 normalized variables were obtained. These predictors were used to construct LDA models. For this purpose, the SPSS software package (v. 12.0.1, SPSS, Inc., Chicago, IL) was used. LDA, a supervised classificatory technique, is widely recognized as an excellent tool to obtain vectors showing the maximal resolution between a set of previously defined categories. The LDA discriminating vectors are frequently obtained by minimizing a parameter called the Wilks' lambda (λ_w) (Vandeginste, 1998). This parameter is calculated as the sum of squares of the distances between points belonging to the same category, divided by the total sum of squares. Values of λ_w approaching zero are obtained with well-resolved categories, whereas overlapped categories made λ_w to approach one. Up to N-1 discriminant vectors are constructed by an LDA, with N being the lowest value for either the number of predictors or the number of categories.

Table 18.1

FTIR spectral regions selected as predictor variables for statistical data treatment.

Identification No.	Range, cm^{-1}	Functional group	Mode of vibration
1	3050-2990	=C-H (trans) =C-H (cis)	stretching stretching
2	2990-2881	-C-H (CH_2)	stretching (asym)
3	2881-2770	-C-H (CH_2)	stretching (sym)
4	2408-2338	alkane	stretching
5	2338-2276	alkane	stretching
6	2276-2237	C=C aromatic	bending (scissoring)
7	2237-2180	N-H	stretching
8	1814-1715	-C=O	stretching
9	1715-1698	-C=O	stretching
10	1698-1680	-C=O	stretching
11	1680-1666	-C=O (acid)	stretching
12	1666-1652	-C=C- (cis)	stretching
13	1652-1631	-C=C-	stretching
14	1596-1559	$-COO^-$	stretching (asym)
15	1559-1539	N-H	bending
16	1539-1524	N-H	bending
17	1524-1490	-C-H_3	bending
18	1490-1403	-C-H (CH_2) -C-H (CH_3) C-O-H	bending (scissoring) bending (asym) bending (in plane)
19	1403-1334	=C-H -C-H (CH_3)	bending bending (sym)
20	1305-1212	=C-H (cis) -C-O -CH_2	bending stretching bending
21	1212-1119	-C-O -CH_2- -C-O	stretching bending stretching
22	1119-1049	-C-O -C-O	stretching stretching
23	1049-982	-C-O	stretching
24	982-932	-HC=CH- (cis)	bending (out of plane)

Selection of predictors to be included in the LDA models was performed by using the SPSS stepwise algorithm. According to this algorithm, a predictor is selected when the reduction of λ_w produced after its inclusion in the model exceeds the entrance threshold of a test of comparison of variances or $F_{\text{-test}}$ (F_{in}). However, the entrance of a new predictor modifies the significance of those predictors which are already present in the model. For this reason, after the inclusion of a new predictor, a rejection threshold, F_{out}, is used to decide if one of the other predictors should be removed from the model. The process terminates when there are no predictors entering or being eliminated from the model. The significances of F_{in} and F_{out} were set to 0.01 and 0.10, respectively.

18.3. Results and discussion

18.3.1. ATR-FTIR analysis

ATR-FTIR spectra of the 136 olive samples shown in **Table 18.S1** were collected. **Figure 18.1** shows the spectra of five olives, corresponding to five different cultivars. As it can be observed, FTIR spectra were closely similar, being also comparable for the other cultivars not depicted in **Figure 18.1**. Thus, to enhance the small differences that were not appreciated straight away in the spectra of samples obtained from different cultivars, the peak areas of the 24 selected regions were conveniently handled by multivariate statistical techniques.

18.3.2. Classification of olive fruits according to their cultivar using LDA

An LDA model was constructed to classify olive samples according to their cultivar. For this purpose, a matrix containing 136 objects, which corresponded to the average of all the spectra recorded for each sample, and

the 276 predictors obtained after variable normalization, was constructed. A response column, containing the categories corresponding to the 17 olive cultivars, was added to this matrix.

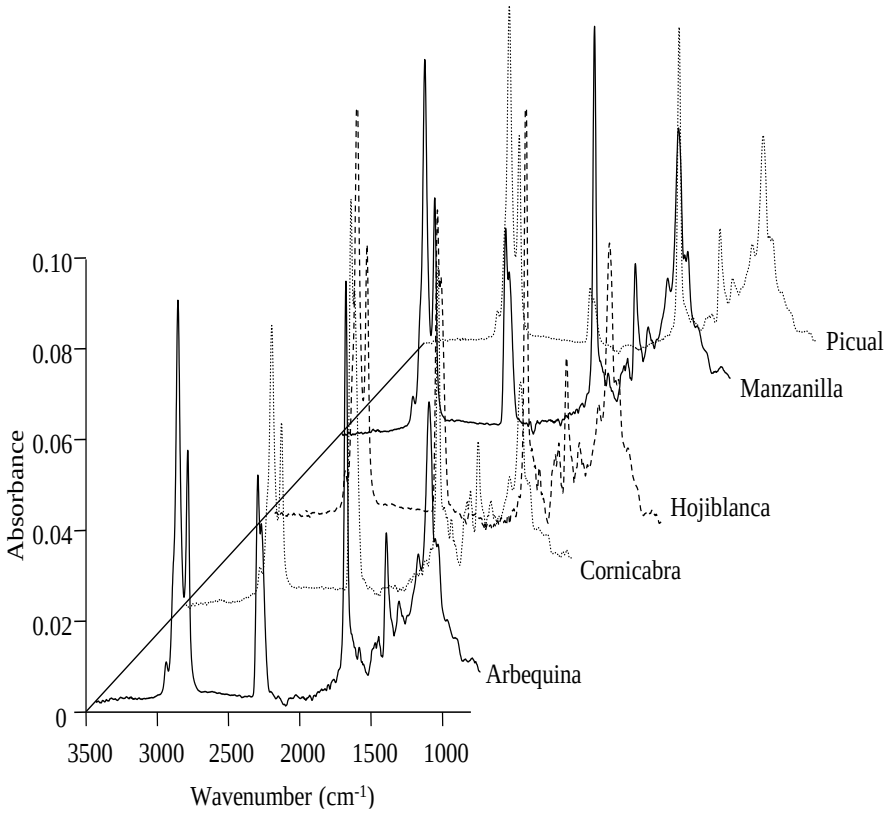

Figure 18.1. ATR-FTIR spectra directly recorded from the endocarp of olive fruits from different Spanish cultivars.

This matrix was divided into two groups, training and evaluation sets. The training set was composed of six samples for each cultivar (6 x 17 = 102 objects), which were randomly selected, while the evaluation set was performed with the remaining samples (34 objects). A good resolution between the 17 categories was achieved when the LDA model was constructed (λ_w <0.01). The variables selected by the SPSS stepwise algorithm and the corresponding standardized coefficients of the six first

discriminant functions of the model are given in **Table 18.2** (see **Table 18.S2** of supplementary material for all the discriminant functions). According to this table, the main frequency regions selected by the algorithm to construct the LDA model were 9/23, 21/24, and 3/22 area ratios, corresponding to the 1715–1698 cm^{-1} region, which arises from the stretching vibration of the ester carbonyl functional group of the triglycerides, the 1212–932 cm^{-1} interval of frequencies, which was assigned to stretching of –C–O bond, to vibrations out of plane of disubstituted olefins, and to bending vibrations of methylene groups, and the 2881–2770 cm^{-1} region, which corresponded to a symmetric stretching vibration of methylene groups.

Table 18.2

Predictors selected and corresponding standardized coefficients of the six first discriminant functions of the LDA model constructed to classify olive fruits according to the 17 different cultivars.

Predictors[a]	f_1	f_2	f_3	f_4	f_5	f_6
1/20	0.30	-4.44	-2.96	-5.23	-2.18	2.41
1/21	-3.61	6.23	5.13	3.25	4.98	-9.10
1/23	5.09	-1.81	-1.97	3.92	-1.89	7.66
2/19	4.77	4.32	1.32	0.47	-0.33	0.28
2/21	-1.60	1.23	-7.44	0.26	-0.33	3.72
3/18	-0.97	1.81	0.66	-2.58	1.35	-2.03
3/22	-6.96	-9.05	10.11	1.86	0.99	-3.18
8/22	-5.35	0.06	-5.55	0.12	-6.96	4.55
9/23	-11.76	0.79	-3.93	-0.72	1.93	-1.61
11/24	2.48	0.53	2.24	1.78	2.04	6.36
17/23	4.19	1.98	1.62	-0.88	2.34	-11.05
19/22	4.64	2.94	-0.75	-1.65	5.27	8.62
19/24	0.47	2.18	1.56	-2.98	-5.39	-7.65
21/24	7.33	4.04	-2.79	-1.95	6.48	-3.10
22/24	3.71	-4.85	2.06	5.56	0.77	5.23

[a] Area ratios of the frequency regions identified according to **Table 18.1.**

The score plot of the projections of the objects on the 3D space defined by the three first discriminant functions is shown in **Figure 18.2**. As it can be observed, Frantoio, Blanqueta, Gordal, Llorona, Morruda, Serrana, and Villalonga cultivars appeared greatly separated from the other cultivars, being Canetera, Lechín de Granada, and Piñon also well resolved. However, the other seven cultivars (Arbequina, Cornicabra, Grosal de Albocacer, Hojiblanca, Manzanilla, Picual, and Solá) seemed overlapped in the 3D space, although the projections of the objects on the space provided by the 15 discriminant functions allowed for the distinction of at least a different category.

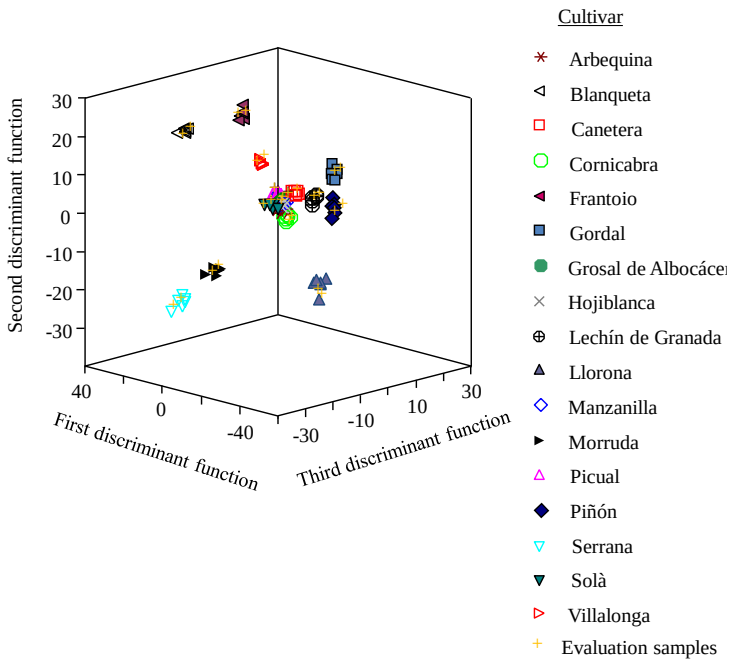

Figure 18.2. Score plot on an oblique plane of the three-dimensional space defined by the three first discriminant functions of the LDA model constructed to classify olive fruits according to the 17 cultivars. Evaluation set samples are labeled with a cross symbol.

When the leave-one-out validation was applied to the training set, all the objects were correctly assigned to their corresponding category. Moreover, the samples of the evaluation set were also used to test the capability assignation to a determine category of the model. Also, in this case, all the objects were correctly classified with an assignment probability higher than 95%. The evaluation set samples are marked with a cross in **Figure 18.2.**

Finally, another chemometric technique (PCA-LDA) was applied to the FTIR data, in order to compare both, the previously developed stepwise-LDA model with the model obtained by this technique. As reported by De Luca *et al.* (De Luca, 2012), PCA-LDA was performed in two steps: in the first step, a PCA model was constructed using the training set samples and the 276 predictors obtained after data normalization. The explained variances (%) obtained by the PCA model constructed are shown in **Table 18.S3** of supplementary material. As it can be observed, at least 10 PCs should be considered in order to explain a 95% of variance. The 3D score plot obtained using the three first PCs is shown in **Figure 18.S1** of Supplementary material. As it can be observed, only the cultivars Blanqueta, Serrana, Morruda, and Llorona are well-separated from the other cultivars. Next, using the score values calculated for the 10 first PCs as predictors (95% explained variance), an LDA model was constructed. The 3D score plot obtained by the three first discriminant functions is shown in **Figure 18.S2,** being the standardized coefficients of the discriminant functions included in **Table 18.S4**. As shown in **Figure 18.S2**, most categories are resolved; however, some samples of the training set (20 objects) are not correctly classified. Thus, the rate of correct classification was *ca.* 80% within the training set. In any case, the samples of the evaluation set were also used to test the capability assignation to a determine category of the model. Using a 95%probability, a total of 15 objects were not correctly assigned; thus, the prediction capability of the PCA-LDA was 56%. Thus, and due to the fact that the statistical method proposed in this article provides a 100% prediction capability, being also simpler and quicker than the PCA-LDA model, since only themeasurement of the variables

selected by themodel should be performed, the usefulness of the proposed stepwise-LDA model has been demonstrated.

18.4. Conclusions

In this work, the possibility of using ATR-FTIR data to discriminate Spanish olives according to their cultivar has been demonstrated. Using LDA, all the olive samples were correctly classified into their corresponding 17 cultivars. Moreover, evaluation set samples were correctly classify with assignment probabilities higher than 95%. Thus, it is demonstrated that FTIR followed by LDA of the spectral data presents a high potential to discriminate olives from a high number of different cultivars.

Acknowledgements

M. Vergara-Barberán thanks the MEC for an FPU grant for PhD. studies. M.J. Lerma-García thanks the Generalitat Valenciana for a VALi+d postdoctoral contract.

The authors have declared no conflict of interest.

18.5. References

Ayora-Canada, M.J.; Muik, B.; Garcia-Mesa, J.A.; Ortega-Calderon, D.; Molina-Diaz, A. (**2005**). Fourier-transform near-infrared spectroscopy as a tool for olive fruit classification and quantitative analysis. *Spectroscopy Letters, 38,* 769-785.

Baeten, V.; Fernández Pierna, J.A.; Dardenne, P.; Meurens, M.; García-González, D.L.; Aparicio-Ruiz, R. (**2005**). Detection of the presence of hazelnut oil in olive oil by FT-Raman and FT-MIR spectroscopy. *Journal of Agricultural and Food Chemistry, 53,* 6201-6206.

Bendini, A.; Cerretani, L.; Carrasco-Pancorbo, A.; Gómez-Caravaca, A. M.; Segura-Carretero, A.; Fernández-Gutiérrez, A.; Lercker, G. (**2007**). Phenolic molecules in virgin olive oils: a survey of their sensory properties, health effects, antioxidant activity and analytical methods. An overview of the last decade. *Molecules, 12*, 1679-1719.

Casale, M.; Zunin, P.; Cosulich, M.E.; Pistarino, E.; Perego, P.; Lanteri, S. (**2010**). Characterization of table olive cultivar by NIR spectroscopy. *Food Chemistry, 122,* 1261-1265.

Cayuela Sánchez, J.A.; Moreda, W.; García, J.M. (**2013**). Prediction of quality of intact olives by near infrared spectroscopy. *Journal of Agricultural and Food Chemistry*, 61, 8056–8062.

Cayuela, J.A.; Perez Camino, M.C. (**2010**). Prediction of quality of intact olives by near infrared spectroscopy. *European Journal of Lipid Science and Technology, 112,* 1209-1217.

Commission regulation (EC) number 182/2009 of 6 March 2009 amending regulation (EC) number 1019/2002 on marketing standards for olive oil. 0ff. J. Eur. Union **2009**, L63, 6-8.

Concha-Herrera, V.; Lerma-García, M. J.; Herrero-Martínez, J. M.; Simó-Alfonso, E. F. (**2009**). Prediction of the genetic variety of extra virgin olive

oils produced at La Comunitat Valenciana, Spain, by Fourier transform infrared spectroscopy. *Journal of Agricultural and Food Chemistry*, 57, 9985-9989.

Concha-Herrera, V.; Lerma-García, M.J.; Herrero-Martínez, J.M.; Simó-Alfonso, E.F. (**2009**). Prediction of the genetic variety of extra virgin olive oils produced at La Comunitat Valenciana, Spain, by Fourier Transform Infrared Spectroscopy. *Journal of Agricultural and Food Chemistry, 57*, 9985-9989.

De Luca, M.; Terouzi, W.; Kzaiber, F.; Ioele, G.; Oussama, A.; Ragno, G. (**2012**). Classification of Moroccan olive cultivars by linear discriminant analysis applied to ATR–FTIR spectra of endocarps *International Journal of Food Science & Technology, 47*, 1286-1292.

Dupuy, N.; Galtier, O.; Le Dréau, Y.; Pinatel, C.; Kister, J.; Artaud, J. (**2010**). Chemometric analysis of combined NIR and MIR spectra to characterize French olives. *European Journal of Lipid Science and Technology, 112*, 463-475.

Galtier, O.; Dupuy, N.; Le Dréau, Y.; Ollivier, D.; Pinatel, C.; Kister, J.; Artaud, J. (**2007**). Geographic origins and compositions of virgin olive oils determinated by chemometric analysis of NIR spectra. *Analytica Chimica Acta, 595*, 136–144.

Gómez-Caravaca, A.M.; Cerretani, L.; Bendini, A.; Segura-Carretero, A.; Fernández-Gutiérrez, A.; Del Carlo, M.; Compagnone, D.; Cichelli, A. (**2008**). Effects of fly attack (Bactroceraoleae) on the phenolic profile and selected chemical parameters of olive oil. *Journal of Agricultural and Food Chemistry, 56*, 4577-4583.

Guillén, M.D.; Cabo, N. (**1998**). Characterization of edible oils and lard by Fourier transform infrared spectroscopy. Relationships between composition and frequency of concrete bands of the fingerprint region. *Journal of Agricultural and Food Chemistry, 46*, 1788-1793.

Gurdeniz, G.; Tokatli, F.; Ozen, B. (**2007**). Differentiation of mixtures of monovarietal olive oils by mid-infrared spectroscopy and chemometrics. *European Journal of Lipid Science and Technology, 109*, 1194-1202.

Inarejos-García, A.M.; Gómez-Alonso, S.; Fregapane, G.; Salvador, M.D. (**2013**). Evaluation of minor components, sensory characteristics and quality of virgin olive oil by near infrared (NIR) spectroscopy. *Food Research International, 50*, 250-258.

Jiménez-Marquez, A.; Molina-Díaz, A.; Pascual-Reguera, M.I. (**2005**). Using optical NIR sensor for on-line virgin olive oils characterization. *Sensors Actuators B Chemistry, 107*, 64-68.

Lerma-García, M.J.; Ramis-Ramos, G.; Herrero-Martínez, J.M.; Simó-Alfonso, E.F. (**2010**). Authentication of extra virgin olive oils by Fourier-transform infrared spectroscopy. *Food Chemistry*, *118*, 78-83.

Lerma-García, M.J.; Ramis-Ramos, G.; Herrero-Martínez, J.M.; Simó-Alfonso, E.F. (**2010**). Authentication of extra virgin olive oils by Fourier-transform infrared spectroscopy. *Food Chemistry, 118*, 78-83.

Mailer, R.J. (**2004**). Rapid evaluation of olive oil quality by NIR reflectance spectroscopy. *Journal of the American Oil Chemists' Society, 8*1, 823-827.

Morales-Sillero, A.; Fernández-Cabanás, V.M.; Casanova, L.; Jiménez, M.R.; Suárez, M.P.; Rallo, P. (**2011**). Feasibility of NIR spectroscopy for non-destructive characterization of table olive traits. *Journal of Food Engineering, 107*, 99-106.

Nenadis, N.; Tsikouras, I.; Xenikakis; P.; Tsimidou, M.Z. (**2013**). Fourier transform mid-infrared spectroscopy evaluation of early stages of virgin olive oil autoxidation. *European Journal of Lipid Science and Technology*, *115*, 526-534.

Ozen, B.; Mauer, L.J. (**2002**). Detection of hazelnut oil adulteration using FTIR spectroscopy. *Journal of Agricultural and Food Chemistry, 50*, 3898-3901.

Salguero-Chaparro, L.; Baeten, V.; Fernández-Pierna, J. A.; Peña-Rodríguez, F. (**2013**). Near Infrared spectroscopy (NIRS) for on-line determination of quality parameters in intact olives. *Food Chemistry*, *139*, 1121-1126.

Silverstein, R.M.; Bassler, G.C.; Morrill, T.C. (**1981**). Spectrometric identification of organic compounds. John Wiley & Sons: Chichester.

Sinelli, N.; Cosio, M.S.; Gigliotti, C.; Casiraghi, E. (**2007**). Preliminary study on application of mid infrared spectroscopy for the evaluation of the virgin olive oil "freshness". *Analytica Chimica Acta*, *598*, 128-134.

Tapp, H. S.; Defernez, M.; Kemsley, E. K. (**2003**). FTIR spectroscopy and multivariate analysis can distinguish the geographic origin of extra virgin olive oils, *Journal of Agricultural and Food Chemistry, 51*, 6110-6115.

Tay, A.; Singh, R.K.; Krishnan, S.S.; Gore, J.P. (**2002**). Authentication of olive oil adulterated with vegetable oils using Fourier transform infrared spectroscopy. LWT - Food Science and Technology, 35, 99-103.

Terouzi, W.; De Luca, M.; Bolli, A.; Oussama, A.; Patumi, M.; Ioele, G.; Ragno, G. (**2011**). A discriminant method for classification of Moroccan olive varieties by using direct FT-IR analysis of the mesocarp section. *Vibrational Spectroscopy, 56*, 123-128.

Vandeginste, B.G.M.; Massart, D.L.; Buydens, L.M.C.; De Jong, S.; Lewis, J.; Smeyers-Verbeke, J. (**1998**). Data handling in science and technology, part B., Elsevier, Ed.; 18th ed.; Amsterdam.

Vlachos, N.; Skopelitis, Y.; Psaroudaki, M.; Konstantinidou, V.; Chatzilazarou, A; Tegou, E. (**2006**). Applications of Fourier transform-infrared spectroscopy to edible oils. *Analytica Chimica Acta, 573*, 459-465.

Suplementary material

Table 18.S1

Cultivar, geographical origin and number of samples of the olive fruits used in this study.

Cultivar	Geographical origin	Crop season	Nº of samples
Arbequina	Altura (Castellón)	2011/2012 2014/2015	2
	Puente Genil (Córdoba)	2011/2012 2013/2014	2
	Jumilla (Murcia)	2012/2013 2013/2014	2
	Alicante	2012/2013 2014/2015	2
Blanqueta	Alicante	2011/2012 2014/2015	2
	Alcalatén *comarca* (Castellón)	2011/2012 2012/2013	2
	Pobla del Duc (Valencia)	2012/2013 2013/2014	2
	Benigànim (Valencia)	2013/2014 2014/2015	2
Canetera	Altura (Castellón)	2011/2012 2012/2013 2014/2015	3
	Adzaneta (Castellón)	2012/2013 2013/2014	2
	La Plana *comarca* (Castellón)	2012/2013 2013/2014 2014/2015	3
Cornicabra	Requena (Valencia)	2011/2012 2013/2014	2
	Daimiel (Ciudad Real)	2011/2012 2013/2014	2
	Jumilla (Murcia)	2012/2013 2013/2014	2
	Villapalacios (Albacete)	2012/2013 2014/2015	2

Frantoio	Puente Genil (Córdoba)	2011/2012 2012/2013 2013/2014	3
	Jumilla (Murcia)	2011/2012 2012/2013 2013/2014	3
	Altura (Castellón)	2012/2013 2013/2014	2
Gordal	Altura (Castellón)	2011/2012 2012/2013 2013/2014	3
	Pobla del Duc (Valencia)	2012/2013 2013/2014 2014/2015	3
	Jérica (Castellón)	2012/2013 2013/2014	2
Grosal de Albocácer	Requena (Valencia)	2011/2012 2012/2013 2013/2014	3
	Pobla del Duc (Valencia)	2011/2012 2013/2014 2014/2015	3
	La Noguera (Lleida)	2012/2013 2013/2014	2
Hojiblanca	Estepa (Sevilla)	2011/2012 2012/2013 2013/2014	2
	Jumilla (Murcia)	2011/2012 2012/2013 2013/2014	2
	Puente Genil (Córdoba)	2012/2013 2013/2014	2
	Fuente de Piedra (Málaga)	2012/2013 2013/2014	2

Lechín de Granada	Jumilla (Murcia)	2011/2012 2012/2013 2013/2014	3
	Tabernas (Almería)	2012/2013 2013/2014 2014/2015	3
	Puente Genil (Córdoba)	2012/2013 2013/2014	2
Llorona	Altura (Castellón)	2011/2012 2012/2013 2013/2014	3
	Artana (Castellón)	2012/2013 2013/2014 2014/2015	3
	Jérica (Castellón)	2012/2013 2014/2015	2
Manzanilla	Altura (Castellón)	2011/2012 2012/2013	2
	Puente Genil (Córdoba)	2011/2012 2012/2013	2
	Requena (Valencia)	2012/2013 2013/2014	2
	Ahigal (Cáceres)	2012/2013 2013/2014	2
Morruda	Altura (Castellón)	2011/2012 2013/2014	2
	Artana (Castellón)	2011/2012 2012/2013 2013/2014	3
	Jérica (Castellón)	2011/2012 2012/2013 2013/2014	3
Picual	Puente Genil (Córdoba)	2011/2012 2012/2013	2
	Jumilla (Murcia)	2011/2012 2012/2013	2
	Requena (Valencia)	2012/2013 2013/2014	2
	Villapalacios (Albacete)	2012/2013 2013/2014	2

Piñón	Pobla del Duc (Valencia)	2011/2012 2012/2013 2013/2014	3
	Alicante	2012/2013 2013/2014	2
	Benigànim	2011/2012 2012/2013 2013/2014	3
Serrana	Altura (Castellón)	2011/2012 2012/2013	2
	Viver (Castellón)	2011/2012 2012/2013	2
	Artana (Castellón)	2012/2013 2013/2014	2
	Jérica (Castellón)	2012/2013 2013/2014	2
Solà	Altura (Castellón)	2011/2012 2012/2013 2013/2014	3
	Viver (Castellón)	2012/2013 2013/2014 2014/2015	3
	Jérica (Castellón)	2011/2012 2012/2013	2
Villalonga	Altura (Castellón)	2011/2012 2012/2013 2014/2015	3
	Requena (Valencia)	2011/2012 2012/2013 2013/2014	3
	Pobla del Duc (Valencia)	2012/2013 2013/2014	2

Table 18.S1

Cultivar, geographical origin and number of samples of the olive fruits used in this study.

Predictors[a]	f_1	f_2	f_3	f_4	f_5	f_6	f_7	f_8	f_9	f_{10}	f_{11}	f_{12}	f_{13}	f_{14}	f_{15}
1/20	0.30	-4.44	-2.96	-5.23	-2.18	2.41	-1.36	0.20	-1.26	-2.05	-0.52	0.50	-1.20	-1.13	0.77
1/21	-3.61	6.23	5.13	3.25	4.98	-9.10	2.45	0.95	-0.05	1.10	-0.04	-1.18	0.91	1.57	-0.98
1/23	5.09	-1.81	-1.97	3.92	-1.89	7.66	0.74	-0.53	1.01	0.66	-0.48	0.45	0.01	-0.08	-0.25
2/19	4.77	4.32	1.32	0.47	-0.33	0.28	1.29	-1.01	-0.03	1.41	0.16	0.24	0.58	0.05	-0.69
2/21	-1.60	1.23	-7.44	0.26	-0.33	3.72	-1.74	0.76	0.19	-1.65	0.18	0.07	0.19	-1.84	0.31
3/18	-0.97	1.81	0.66	-2.58	1.35	-2.03	0.50	-0.16	1.08	-0.74	-0.06	0.29	0.55	1.29	0.33
3/22	-6.96	-9.05	10.11	1.86	0.99	-3.18	-2.30	-0.27	-2.01	3.40	-1.82	-3.73	-0.64	-1.25	1.80
8/22	-5.35	0.06	-5.55	0.12	-6.96	4.55	-0.34	-0.74	0.60	-2.10	3.90	1.24	-1.63	2.03	-1.67
9/23	-11.76	0.79	-3.93	-0.72	1.93	-1.61	0.24	0.36	-0.25	-0.21	-0.25	-0.10	-0.16	-0.12	0.24
11/24	2.48	0.53	2.24	1.78	2.04	6.36	-0.72	-0.26	-0.12	-0.40	-0.44	0.20	0.52	-0.17	-0.18
17/23	4.19	1.98	1.62	-0.88	2.34	-11.05	1.02	-0.08	1.83	2.30	0.46	0.45	0.74	1.63	0.50
19/22	4.64	2.94	-0.75	-1.65	5.27	8.62	4.45	-0.19	-1.12	-1.33	-0.85	4.50	3.33	-0.43	1.09
19/24	0.47	2.18	1.56	-2.98	-5.39	-7.65	-1.36	-1.65	2.61	1.96	2.04	-2.38	-3.28	0.32	-0.38
21/24	7.33	4.04	-2.79	-1.95	6.48	-3.10	-0.14	3.15	-1.05	-1.71	-2.11	0.04	2.38	-0.76	-0.01
22/24	3.71	-4.85	2.06	5.56	0.77	5.23	0.95	-0.50	-0.61	0.18	0.69	0.95	-0.03	0.07	0.36

Table 18.S3

Explained variances (%) obtained from the full cross-validation of the PCA model constructed to discriminate olive fruits according to their cultivar.

PCs	Exp. % variance
1	42.076
2	60.731
3	73.026
4	78.908
5	83.314
6	87.508
7	90.049
8	92.212
9	93.877
10	95.461
11	96.285
12	96.853
13	97.334
14	97.749
15	98.092

Table 18.S4

Standardized coefficients of the 10 PCs of the LDA model constructed to classify olive fruits according to the 17 different cultivars.

PCs	f_1	f_2	f_3	f_4	f_5	f_6	f_7	f_8	f_9
1	1.26	0.04	0.14	0.65	-0.53	-0.04	-0.01	-0.01	-0.03
2	-0.19	0.33	0.03	0.36	0.12	0.25	-0.03	0.92	0.20
3	1.76	-0.40	0.10	-0.19	0.20	-0.09	-0.01	0.03	0.03
4	1.28	0.90	0.34	0.13	0.39	0.60	-0.04	-0.10	-0.13
5	0.20	0.48	0.26	-0.01	0.07	-0.14	0.93	0.02	0.01
6	-0.83	-0.22	0.66	0.62	0.46	-0.16	-0.06	-0.06	0.07
8	-0.51	-1.25	0.14	0.05	-0.15	0.41	0.16	-0.02	0.01
9	0.61	0.48	-0.33	0.08	-0.11	0.26	0.02	-0.29	0.89
10	0.25	-0.18	-0.82	0.53	0.34	0.01	0.07	-0.02	-0.04

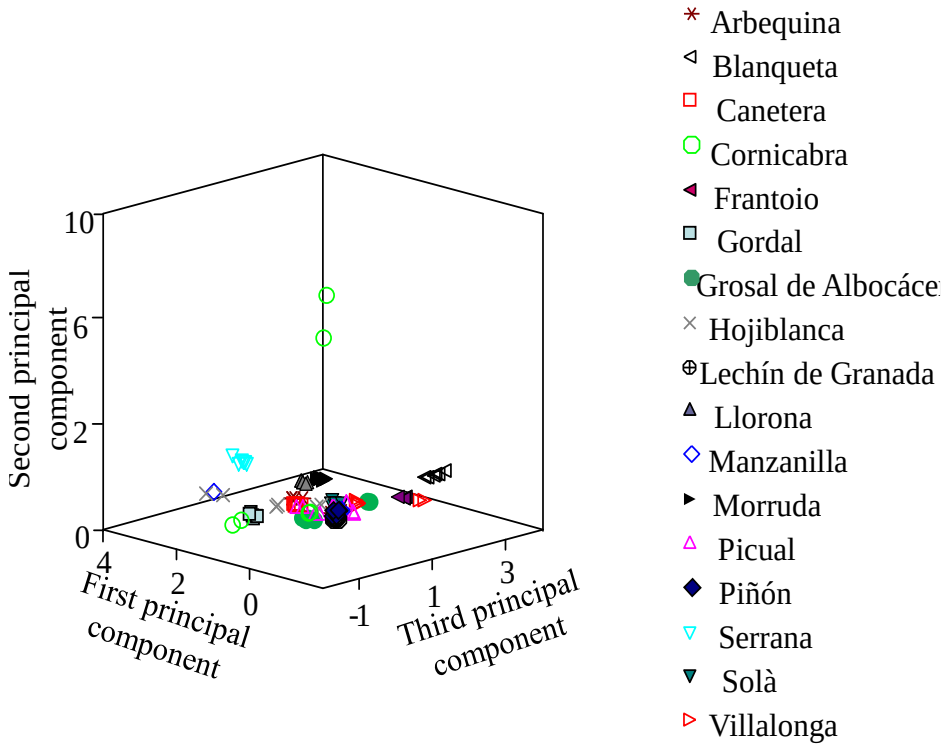

Figure 18.S1. 3D score plot (PCs 1-3) obtained by the PCA model constructed to discriminate olive fruits according to their cultivar.

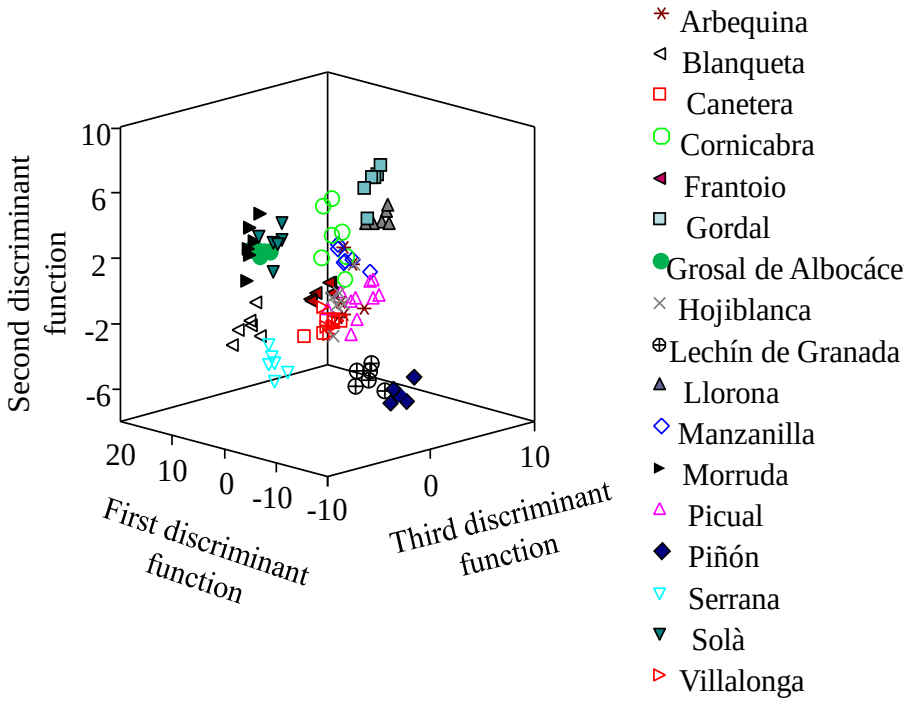

Figure 18.S2. Score plot on an oblique plane of the three-dimensional space defined by the three first discriminant functions of the LDA model constructed using the 10 PCs as predictors.

Chapter 19. Cultivar discrimination and prediction of mixtures of Tunisian extra virgin olive oils by FTIR

Eur. J. Lipid Sci. Technol. 2015, *117*, 0000–0000

Short Communication

Cultivar discrimination and prediction of mixtures of Tunisian extra virgin olive oils by FTIR

Marwa Abdallah[1], María Vergara-Barberán[2], María Jesús Lerma-García[2], José Manuel Herrero-Martínez[2], Ernesto F. Simó-Alfonso[2] and Mokhtar Guerfel[1]

[1] Laboratoire Biotechnologie de l'Olivier, Centre de Biotechnologie de Borj Cedria, Hammam-Lif, Tunisia
[2] Department of Analytical Chemistry, Faculty of Chemistry, University of Valencia, Burjassot, Valencia, Spain

Fourier-transform infrared spectroscopy, followed by multivariate treatment of the spectral data, was used to classify Tunisian EVOOs according to their cultivar. Moreover, these data were also employed to establish the composition of binary mixtures of EVOOs from different cultivars. For this purpose, the spectra were divided in 20 regions, being the normalized peak areas within these regions used as predictors. Using linear discriminant analysis, an excellent resolution between EVOOs from different cultivar was obtained. Moreover, multiple linear regression models were used to predict the composition of binary mixtures of EVOOs, being in all cases capable of predicting the percentage of one of the oils with average validation errors below 6%. Thus, the FTIR method proposed in this work, followed by chemometric analysis, could be used in an industrial setting since no complicated laboratory facilities are required, which could save great deal of time and money.

Keywords: ATR-FTIR; cultivar; linear discriminant analysis; multiple linear regression

19.1. Introduction

The olive tree crop is widespread in the Mediterranean area. From the fruits of this tree, EVOO is obtained by physical methods without any refining operations (Youssef, 2011). EVOO is a fundamental constituent of the Mediterranean diet owing to its highly appreciated organoleptic attributes and its health (Gimeno, 2002; Matos, 2007; Ben Youssef, 2010) and nutritional properties (Bendini, 2007).

Olive oil plays an important role in the Tunisian agronomy and economy, being the second most producer of EVOO in the world after the European Community (Faostat, 2012). The Tunisian olive grove lands are dominated by two major varieties, Chemlali in the south and centre and Chétoui in the north, although a great genetic diversity among its olive trees could be found throughout the country.

Olive oil quality is related to a large number of factors, such as geographical origin (Tapp, 2003; Bendini, 2007; Guerfel, 2009; Youssef, 2011), climatic conditions (Mannina, 1999; Baccouri, 2007), agronomic techniques (Kricheme, 2010), harvesting systems and processing technologies (Gimeno, 2002), among which the genetic variety (Gutiérrez, 1991; Mannina, 1999; Zamora, 2001; Matos, 2007; Haddada, 2007; Baccouri, 2007; Baccouri, 2008; Concha-Herrera, 2009; Guerfel, 2009; Oueslati, 2009; Sinelli, 2010; Youssef, 2011; Vichi, 2012; Yorulmaz, 2013; Gouvinhas, 2015) and the olive ripening stage are two of the most important ones (Gutiérrez, 1991; Salvador, 2001; Gimeno, 2002; Rotondi, 2004; Baccouri, 2007; Matos, 2007; Baccouri, 2008; Ben Youssef, 2010; Vichi, 2012; Bengana, 2013; Yorulmaz, 2013; Gouvinhas, 2015).

Regarding genetic variety, olive oils produced from a given cultivar (monovarietal oils) have specific physical and biochemical characteristics, which provide them with typical compositions and attributes. The

development of methods to distinguish olive cultivar is important because, according to the European Community (EC) regulation 182/2009, olive oil producers have to include in their manufactured products the genetic variety of the olives.

There are several studies that have investigated the influence of these factors (cultivar and maturity index) on Tunisian cultivars (Youssef, 2011; Ben Youssef, 2010; Guerfel, 2009; Baccouri, 2007; Haddada, 2007; Baccouri, 2007; Baccouri, 2008; Oueslati, 2009; Vichi, 2012; Bengana, 2013). However, most of these studies have been focused on the improvement and characterization of the two main cultivars (Chétoui and Chemlali) (Baccouri, 2007; Bacouri, 2008; Ben Youssef, 2010; Vichi, 2012), which causes a lack of information of several minor cultivars that could provide a better oil quality (higher phenolic content, better organoleptic properties, etc). Thus, to diversify Tunisian olive oil resources and improve the quality of olive oil produced in Tunisia, research on additional cultivars needs to be conducted.

Among the different methodologies used to study olive oil quality, spectroscopic techniques, such as Fourier transform infrared spectroscopy (FTIR), has been successfully used. FTIR is a rapid, low cost and non-destructive powerful analytical tool used for the study of a wide variety of food and food processes, which requires minimum sample preparation. FTIR is also an excellent tool for quantitative analysis, because the intensities of the spectral bands are proportional to the concentration. In addition, FTIR data have been often treated with multivariate chemometric techniques to develop methods of classification and characterization (Teouzi, 2011). This fruitful combination constitutes a very powerful tool to be adopted for quality control purposes by food industries and even by regulatory agencies. For this reason, FTIR has mainly been used to distinguish EVOOs from different geographical origins (Tapp, 2003; Bendini, 2007; Faostat, 2012) and genetic varieties (Concha-Herrera, 2009; Sinelli, 2010; Gouvinhas, 2015), to detect olive oil

adulteration (Baeten, 2005; Vlachos, 2006; Lerma-García, 2010), and to distinguish mixtures of monovarietal EVOOs (Gurdeniz, 2007).

In this work, ATR FTIR followed by LDA of the spectral data was used to classify Tunisian EVOOs according to their cultivar. Also, data treatment by multiple linear regression (MLR) was used to evaluate the possibility of detecting mixtures of EVOOs from different cultivars.

19.2. Materials and methods

19.2.1. EVOO samples and binary mixtures

The present work was carried out using a total of 55 EVOOs, arising from seven Tunisian cultivars (see **Table 19.1**). All these samples were used to develop a classificatory method according to their variety. To minimize the influence of the geographical origin, harvesting season and maturity index, the sampling was accomplished as next indicated. The EVOOs were obtained from ca. 1 kg of healthy and non-damaged olives, which have been hand picked at different periods during the 2012/2013 and 2013/2014 harvesting seasons from olive orchards located in the Tunisian geographical areas indicated in **Table 19.1.** After harvesting, olives were deleafed, crushed with a hammer crusher, mixed at ambient temperature for 30 min and centrifuged without addition of water or chemicals; then, EVOOs were transferred into dark glass bottles and stored at 4 °C until analysis.

Table 19.1

Genetic variety, number of samples, maturity index and geographical origin of the EVOO samples employed in this study.

Genetic variety	No. of samples	Crop season	Maturity index	Geographical origin
Chemchali	1	2012/2013	1	Gafsa
	2	2013/2014		
	2	2012/2013	2	
	1	2013/2014		
	2	2012/2013	3	
	1	2013/2014		
	1	2012/2013	4	
	2	2013/2014		
	2	2012/2013	5	
	1	2013/2014		
Chemlali	1	2012/2013	3.1	Sousse
	1	2013/2014	3.7	Sfax
	2	2012/2013	3.5	Sidi Bouzid
		2013/2014	4.0	
Dhokar	2	2012/2013	3.9	Ben Gardène
		2013/2014	3.2	
	2	2012/2013	3.7	Tataouine
		2013/2014	3.5	
Fouji	2	2012/2013	1	Gafsa
	1	2013/2014		
	2	2012/2013	2	
	1	2013/2014		
	1	2012/2013	3	
	2	2013/2014		
	1	2012/2013	4	
	2	2013/2014		
	1	2012/2013	5	
	2	2013/2014		

Table 19.1

Cont.

Genetic variety	No. of samples	Crop season	Maturity index	Geographical origin
Jemri	2	2012/2013 2013/2014	4.2 3.8	Ben Gardène
	2	2012/2013 2013/2014	3.1 3.7	Medenine
Zalmati	2	2012/2013 2013/2014	3.3 3.6	Medenine
	2	2012/2013 2013/2014	3.1 3.9	Zarzis
Zarrazi	2 1	2012/2013 2013/2014	1	Gafsa
	2 1	2012/2013 2013/2014	3	
	2 1	2012/2013 2013/2014	4	

In order to obtain the EVOOs of different maturity indexes, *ca*. 10 kg olives were collected from the same olive tree at different periods, and then classified according to the maturity levels established by the National Institute of Agronomical Research of Spain, described by the IOOC (IOOC, 2011), which is based on a subjective evaluation of olive skin and pulp colours. For Chemchali and Fouji cultivars, five maturity levels were identified (1, yellowish green; 2, green with reddish spots; 3, reddish brown; 4, black with white flesh and 5, black with < 50% purple flesh), while for Zarrazi variety only three maturity levels were observed (1, 3 and 4).

On the other hand, for Chemlali, Dhokar, Jemri and Zalmati varieties, the maturity index of each sample was calculated according to the IOOC methodology (IOOC, 2011), which is based on the assessment of the colour of the skins of 100 olives which were randomly drawn from 1 kg of the sample.

To evaluate the possibility of detecting mixtures of EVOOs from different cultivars, binary mixtures containing Chemchali and increasing percentages of Fouji or Zarrazi were prepared. To improve the robustness of MLR models, mixtures were prepared using EVOOs from different maturity index, which were randomly selected and mixed. For instance, for the Fouji-Chemchali, EVOOs from different maturity index were selected to prepare a total of 20 mixtures containing 0, 10, 20, 40 and 50% Fouji EVOO. Another set of 20 mixtures containing the same percentages of Zarrazi EVOO was also prepared for the Zarrazi-Chemchali pairs. Thus, a total of 40 mixtures were obtained.

19.2.2. FTIR spectra

FTIR spectra were obtained using a Jasco 4100 type A spectrophotometer (Jasco, Easton, MD) fitted with a single reflection ATR accessory. All analyses were carried out at room temperature and to reduce the background noise all samples were measured as the mean of 50 scans acquired with a resolution of 4 cm^{-1}. The FTIR spectra were obtained from 4000 to 600 cm^{-1} in the absorbance mode. Data handling was performed with spectra manager version 2.07.00 software (Jasco). For each sample, *ca*. 50 μL was deposited on the ATR surface. The absorbance spectrum was recorded against a background obtained using a dry and empty ATR cell. At the beginning of the working session and between runs, the ATR crystal was repeatedly cleaned with a cellulose tissue soaked in n-hexane, rinsed with acetone, and dried. Three spectra were recorded for each sample, during 2 consecutive days, to avoid possible irreproducibility in the FTIR measurements.

19.2.3. Data treatment and statistical analysis

All ATR-FTIR spectra were divided into the 20 regions described in **Table 19.2**. These regions correspond to a peak or a shoulder related with structural or functional group information. Peaks or shoulders were not necessarily specific, since they could be due to contributions of more than a single transition, arising from a given compound or from several compounds, including lipids or minor components of the samples. For each region, the peak/shoulder area was measured. In order to reduce the variability associated with the total amount of oil sample used and to minimize other sources of variance also affecting the intensity of all of the peaks, the areas were normalized, and these values were considered as predictors. To normalize the variables, the area of each region was divided by each one of the areas of the other 19 regions; in this way and because any pair of areas should be considered only once, a number of (20 x 19)/2 = 190 normalized variables were obtained. These predictors were used to construct LDA and MLR models. For this purpose, the SPSS software (v. 12.0.1, SPSS Inc., Chicago, IL, USA) was used.

LDA, a supervised classificatory technique, uses a linear combination of predictor variables to obtain new axes (called discriminant functions) that show the maximal resolution between a set of previously defined categories (Vandeginste, 1998). Up to N-1 discriminant vectors are constructed by LDA, being N the lowest value for either the number of predictors or the number of categories. In LDA, vectors minimizing Wilks' lambda (λw) are calculated as the sum of squares of the distances between points belonging to the same category, divided by the total sum of squares. Values of λw approaching zero are obtained with well-resolved categories, whereas overlapped categories made λw to approach one.

Table 19.2

FTIR spectral regions selected as predictor variables for statistical data treatment

Identification No.	Range, cm^{-1}	Functional group[a]	Mode of vibration
1	3039-2989	=C-H (trans) =C-H (cis)	stretching stretching
2	2989-2949	-C-H (CH_3)	stretching (asym)
3	2949-2880	-C-H (CH_2)	stretching (asym)
4	2880-2886	-C-H (CH_2)	stretching (sym)
5	2866-2755	-C-H (CH_2)	stretching (sym)
6	2383-2283	C=C (aromatic)	bending (scissoring)
7	1802-1672	-C=O (ester) -C=O (acid)	stretching stretching
8	1483-1443	-C-H (CH_2)	bending(scissoring)
9	1443-1425	-C-H (CH_3)	bending(asym)
10	1425-1407	=C-H (cis)	bending (rocking)
11	1407-1392	=C-H	bending
12	1392-1368	=C-H -C-H (CH_3)	bending bending (sym)
13	1368-1356	O-H	bending (in plane)
14	1356-1343	O-H	bending (in plane)
15	1251-1216	-C-O -CH_2	stretching bending
16	1216-1145	-C-O -CH_2	stretching bending
17	1145-1127	-C-O	stretching
18	1127-1107	-C-O	stretching
19	1107-1068	-C-O	stretching
20	785-643	-C-H -$(CH_2)_n$- -HC=CH- (cis) C⋯⋯C O-H	bending (out of plane) rocking bending (out of plane) bending (out of plane) bending (out of plane)

19.3. Results and discussion

19.3.1. ATR-FTIR analysis

ATR-FTIR spectra of the 55 EVOOs included in **Table 19.1** and of the Fouji- and Zarrazi-Chemchali binary mixtures were collected. Representative spectra of 7 EVOOs, one for each cultivar, are depicted in **Figure 19.1**. As it can be observed, comparable profiles were obtained for the seven cultivars studied. The same pattern was also observed when the binary mixtures were compared (data not shown). Thus, to enhance the small differences that were not visibly detected in the spectra of samples, the peak areas of the 20 selected regions were normalized according to section 2.3.

19.3.2. Discrimination of EVOOs according to their cultivar using LDA

An LDA model was constructed to classify EVOO samples according to their cultivar. To obtain this model, a matrix containing 55 objects which corresponded to the mean of 6 spectra (3 replicates x 2 days) of samples included in **Table 19.1,** was constructed. This matrix also contained the 190 predictors obtained after application of the normalization procedure indicated above, and a response column, which included the categories corresponding to the 7 cultivars. This matrix was divided in two groups of objects to constitute the training and the evaluation sets. The training set was composed by 10 objects for Chemchali and Fouji varieties (2 samples x 5 maturity indexes) and 6 objects for Zarrazi (2 samples x 3 maturity indexes) and 3 objects for the other varieties, while the evaluation set was constituted by the remaining samples (17 objects).

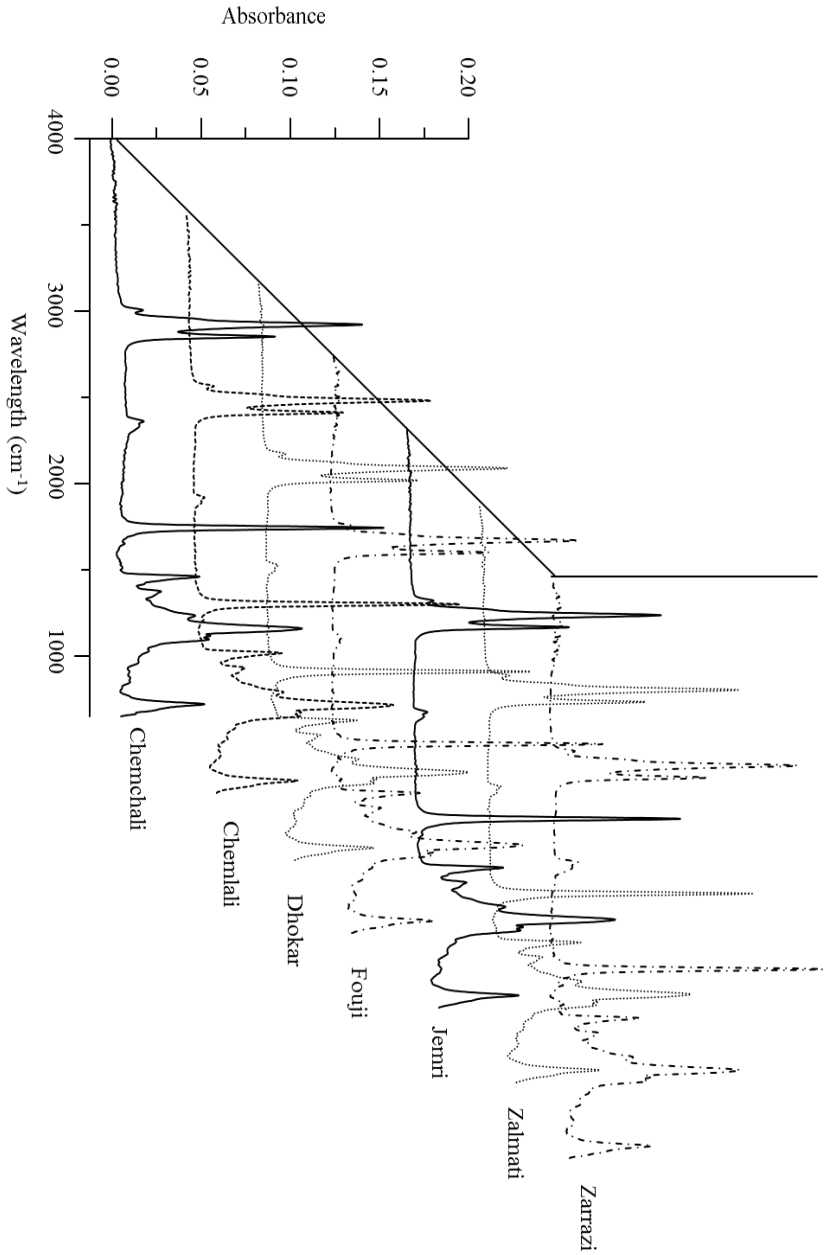

Figure 19.1. ATR-FTIR spectra of representative EVOOs from 7 Tunisian cultivars.

As shown in **Figure 19.2**, a good resolution between the seven categories was achieved when the LDA model was constructed ($\lambda_w < 0.01$).

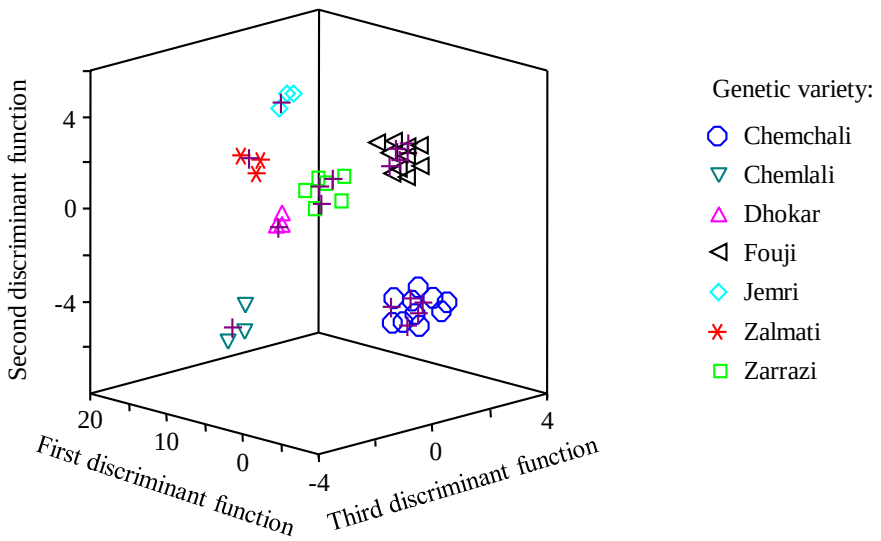

Figure 19.2. Score plot on an oblique plane of the three-dimensional space defined by the three first discriminant functions of the LDA model constructed to classify EVOOs according to their cultivar. Evaluation set samples are labelled with a cross symbol.

The region area ratios selected by the model, which had the highest contribution, and the corresponding standardized coefficients are given in Table S1. According to this table, the main region area ratios selected by the SPSS stepwise algorithm were 6/18, 6/9, 12/15 and 16/17. The selected regions mainly corresponded to vibrations associated to C-H, C-O, C=C (aromatic) and =C-H groups (see **Table 19.2**). To validate the LDA model, two different methods were employed. In first place, leave-one-out validation was applied. With this method, one object was removed from the model and used as evaluation set, while the remaining objects were used as training set. This process is repeated for each sample of the original training set. With this methodology, all the objects were correctly classified. In the second place, the

prediction capability of the model was evaluated using the evaluation set. In this case, all the objects (represented with a cross symbol in **Figure 19.2**) were correctly assigned within a 95% probability level.

Finally, another chemometric technique (PCA-LDA) was applied to the FTIR data, in order to compare both, the previously developed stepwise-LDA model with the model obtained by this technique. PCA-LDA was performed in two steps (De Luca, 2012): in the first step, a PCA model was constructed using the training set samples and the 190 predictors obtained after data normalization. The explained variances (%) obtained by the PCA model constructed are shown in **Table 19.S2** of supplementary material. As it can be observed, at least 8 PCs should be considered in order to explain a 95% of variance. The 3D score plot obtained using the three first PCs is shown in **Figure 19.S1** of supplementary material. As it can be observed, any category was well-resolved from the other categories. Next, using the score values calculated for the 8 first PCs as predictors (95% explained variance), an LDA model was constructed. The 3D score plot obtained by the three first discriminant functions is shown in **Figure 19.S2**, being the standardized coefficients of the discriminant functions included in **Table 19.S3.** As shown in **Figure 19.S2**, most categories are resolved; however, some samples of the training set (8 objects) are not correctly classified. Thus, the rate of correct classification was *ca.* 80% within the training set.

In any case, the samples of the evaluation set were also used to test the capability assignation to a determined category of the model. Using a 95% probability, a total of 6 objects were not correctly assigned; thus, the prediction capability of the PCA-LDA was 65%. Thus, and due to the fact that the statistical method proposed in this article provides a 100% prediction capability, being also simpler and quicker than the PCA-LDA model, since only the measurement of the variables selected by the model should be

performed, the usefulness of the proposed stepwise-LDA model has been demonstrated.

19.3.3. MLR model construction to predict the added amount of Fouji and Zarrazi EVOOs in Chemchali EVOO

Finally, to evaluate the possibility of detecting Fouji- and Zarrazi-Chemchali mixtures, two MLR models were constructed. To select the predictors used in the construction of MLR models, the SPSS stepwise algorithm, with the default probability values of F_{in} and F_{out}, 0.05 and 0.10, respectively, was adopted. For MLR studies, calibration and external validation sets were constructed, one for each pair of EVOOs. The calibration matrices contained 15 objects (mean of the replicated spectra of 3 mixtures x 5 concentration levels). The external validation matrices were constructed with the 5 remaining mixtures (1 mixture x 5 concentration levels). These matrices contained also the 190 predictors, and a response column with the Fouji or Zarrazi percentage. A plot showing the predicted versus the nominal oil percentages for the two types of binary mixtures is shown in **Figure 19.3**.

The predictors selected and their corresponding non-standardized model coefficients are given in **Table 19.3**. According to **Table 19.2**, the main transitions selected to construct the MLR model for the Fouji-Chemchali pair were -C-H (CH_2) and -C-O, while for the Zarrazi-Chemchali pair were -C-H (CH_2), -C-H (CH_3), -C-O and O-H. The regression coefficients and the average prediction errors (calculated as the sum of the absolute differences between expected and predicted oil percentages divided by the number of predictions) are also given in **Table 19.3.** For both models, and using leave-one-out validation, the average prediction errors were lower than 4%.

Finally, when the models were applied to the validation sets, an excellent prediction capability was observed (**Figure 19.3** red cross symbols), being the average validation errors below 6%.

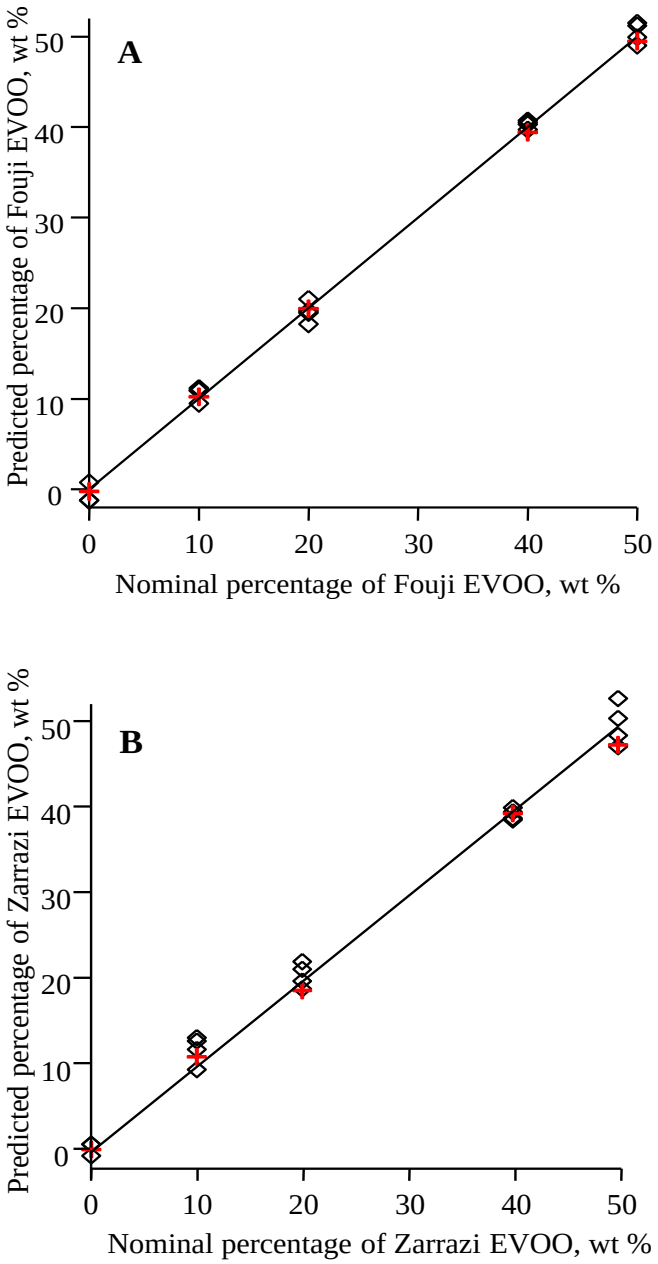

Figure 19.3. Predicted (MLR) versus nominal oil percentages for binary mixtures of Chemchali with (A) Fouji and (B) Zarrazi EVOOs. External validation set samples are labelled with a cross symbol. The straight line is y = x.

Table 19.3

Predictors selected and their corresponding non-standarized model coefficients (Coef.), linear regression coefficients (R^2) and average prediction errors (Av. pred. error) obtained for the MLR models constructed to predict Fouji- and Zarrazi-Chemchali binary mixtures.

Binary mixture	Predictor	Coef.	R^2	Av. pred. error %	RMSEC[a] value
Fouji-Chemchali	Constant	1178.37	0.998	1.09	2.40
	1/9	90.48			
	3/4	-47.77			
	8/15	-297.84			
	13/20	-190.41			
	15/17	-735.78			
	15/18	378.74			
Zarrazi-Chemchali	Constant	1321.32	0.956	3.88	5.90
	2/4	359.48			
	13/15	248.42			

[a] RMSEC = Root Mean Square Error of Calibration

19.4. Conclusions

FTIR in combination with chemometric techniques has been employed with the aim of distinguishing EVOOs from different cultivar. Using 20 spectral regions, all the samples were correctly classified with an excellent resolution among the categories. In addition, the possibility of detecting mixtures of EVOO from different variety was also evaluated using MLR. In both cases, the models constructed were able to predict the percentage of one of the oils with average validation errors below 6%. Thus, the results obtained in this study showed that FTIR spectroscopy jointly with chemometric techniques, such as LDA or MLR models, provides a simple and fast approach to be used by the olive industry for the classification of EVOO as well as to

quantify EVOO blends. In fact, only FTIR equipment (common analytical lab instrumentation) and a chemometric software, are just required to implement the proposed method.

Acknowledgments

M. Vergara-Barberán thanks the MEC for an FPU grant for PhD studies. M.J. Lerma-García thanks the Generalitat Valenciana for a VALi+d postdoctoral contract.

19.5. References

Baccouri, B.; Zarrouk, W.; Krichene, D.; Nouairi, I.; Youssef, N.B.; Daoud, D.; Zarrouk, M. (**2007A**). Influence of fruit ripening and crop yield on chemical properties of virgin olive oils from seven selected oleasters. *Agronomy Journal, 6*, 388-396.

Baccouri, O.; Cerretani, L.; Bendini, A.; Caboni, M.F.; Zarrouk, M.; Pirrone, L.; Daoud Ben Miled, D. (**2007B**). Preliminary chemical characterization of Tunisian monovarietal virgin olive oils and comparison with Sicilian ones. *European Journal of Lipid Science and Technology, 109,* 1208-1217.

Baccouri, O.; Guerfel, M.; Baccouri, B.; Cerretani, L.; Bendini, A.; Lercker, G.; Zarrouk, M.; Daoud, D. (**2008**). Chemical composition and oxidative stability of Tunisian monovarietal virgin olive oils with regard to fruit ripening. *Food Chemistry, 109*, 743-754.

Baeten, V.; Fernández Pierna, J.A.; Dardenne, P.; Meurens, M.; García-González, D.L.; Aparicio-Ruiz, R. (**2005**). Detection of the presence of hazelnut oil in olive oil by FT-Raman and FT-MIR Spectroscopy. *Journal of Agricultural and Food Chemistry, 53,* 6201–6206.

Ben Youssef, N.; Zarrouk, W.; Carrasco-Pancorbo, A.; Ouni, Y.; Segura-Carretero, A.; Fernández-Gutiérrez, A.; Daoud, D.; Zarrouk, M. (**2010**). Effect of olive ripeness on chemical properties and phenolic composition of Chétoui virgin olive oil. *Journal of the Science of Food and Agriculture, 90,* 199-204.

Bendini, A.; Cerretani, L.; Carrasco-Pancorbo, A.; Gómez-Caravaca, A.M.; Segura-Carretero, A.; Fernández-Gutiérrez, A.; Lercker, G. (**2007**). Phenolic molecules in virgin olive oils: A survey of their sensory properties, health effects, antioxidant activity and analytical methods. An overview of the last decade. *Molecules, 12,* 1679-1719.

Bengana, M.; Bakhouchev, A.; Lozano-Sánchez, J.; Amir, Y.; Youyou, A.; Segura-Carretero, A.; Fernandez-Gutiérrez, A. (**2013**). Influence of olive ripeness on chemical properties and phenolic composition of Chemlal extra-virgin olive oil. *Food Research International, 54*, 1868-1875.

Concha-Herrera, V.; Lerma-García, M.J.; Herrero-Martínez, J.M.; Simó-Alfonso, E. F. (2009). Prediction of the genetic variety of extra virgin olive oils produced at La Comunitat Valenciana, Spain, by Fourier Transform Infrared Spectroscopy. *Journal of Agricultural and Food Chemistry,* 57, 9985-9989.

De Luca, M.; Terouzi, W.; Kzaiber, F.; Ioele, G.; Oussama, A.; Ragno, G. (**2012**). Classification of moroccan olive cultivars by linear discriminant analysis applied to ATR–FTIR spectra of endocarps. *International Journal of Food Science & Technology, 47*, 1286–1292.

FAOSTAT. (**2012**). Crops processed data for olive oil.

Gimeno, E.; Castellote, A.I.; Lamuela-Raventos, R.M.; De la Torre, M.C.; Lopez-Sabater, M.C. (**2002**). The effects of harvest and extraction methods on the antioxidant content (phenolics, α-tocopherol, and β-carotene) in virgin olive oil. *Food Chemistry, 78*, 207-211.

Gouvinhas, I.; de Almeida, J.M.M.M.; Carvalho, T.; Machado, N.; Barros, A.I.R.N.A. (**2015**). Discrimination and characterisation of extra virgin olive oils from three cultivars in different maturation stages using Fourier transform infrared spectroscopy in tandem with chemometrics. *Food Chemistry*, 174, 226-232.

Guerfel, M.; Ouni, Y.; Taamalli, A.; Boujnah, D.; Stefanoudaki, E.; Zarrouk, M. (**2009**). Effect of location on virgin olive oils of the two main Tunisian olive cultivars. *European Journal of Lipid Science and Technology, 111*, 926-932.

Guillén, M.D.; Cabo, N. (**1998**). Relationships between the composition of edible oils and lard and the ratio of the absorbance of specific bands of their Fourier Transform Infrared spectra. Role of some bands of the fingerprint región. *Journal of Agricultural and Food Chemistry, 46,* 1788-1793.

Gurdeniz, G.; Tokatli, F.; Ozen, B. (**2007**). Differentiation of mixtures of monovarietal olive oils by mid-infrared spectroscopy and chemometrics. *European Journal of Lipid Science and Technology, 109,* 1194-1202.

Gutiérrez, F.; Jiménez, B.; Ruíz, A.; Albi, M.A. (**1991**). Effect of olive ripeness on the oxidative stability of virgin olive oil extracted from the varieties picual and hojiblanca and on the different components involved. *Journal of Agricultural and Food Chemistry, 47,* 121–127.

Haddada, F.M.; Manai, H.; Oueslati, I.; Daoud, D.; Sánchez, J.; Osorio, E.; Zarrouk, M. (**2007**). Fatty acid, triacylglycerol, and phytosterol composition in six Tunisian olive varieties. *Journal of Agricultural and Food Chemistry,* 55, 10941-10946.

International Olive Oil Council. (IOOC) (**2011**). Olive oil exportations. http://www.internationaloliveoil.org.

Krichene, D.; Allalout, A.; Mancebo-Campos, V.; Salvador, M.D.; Zarrouk, M.; Fregapane, G. (**2010**). Stability of virgin olive oil and behaviour of its natural antioxydants under medium temperature accelerated storage conditions. *Food Chemistry, 121,* 171-177.

Lerma-García, M. J.; Ramis-Ramos, G.; Herrero-Martínez, J.M.; Simó-Alfonso, E.F. (**2010**). Authentication of extra virgin olive oils by Fourier-transform infrared spectroscopy. *Food Chemistry, 118,* 78–83.

Mannina, L.; Barone, P.; Patumi, M.; Fiordiponti, P.; Emanuele, M.C.; Segre, A.L. (**1999**). Cultivar and pedoclimatic effects in the discrimination of

olive oils: a high-field NMR study. *Recent research developments in oil chemistry, 3*, 85-92.

Matos, L.C.; Cunha, S.C.; Amaral, J.S.; Pereira, J.A.; Andrade, P.B.; Seabra, R.M.; Oliveira, B.P.P. (**2007**). Chemometric characterization of three varietal olive oils (Cvs. Cobrançosa, Madural and Verdeal Transmontana) extracted from olives with different maturation indices. *Food Chemistry, 102*, 406-414.

Oueslati, I.; Manai, H.; Haddada, F.M.; Daoud, D.; Sánchez, J.; Osorio, E.; Zarrouk, M. (**2009**). Sterol, triterpenic dialcohol, and triacylglycerol compounds of extra virgin olive oils from some Tunisian varieties grown in the region of Tataouine. *Food Science and Technology International, 15*, 5-13.

Rotondi, A.; Bendini, A.; Cerretani, L.; Mari, M.; Lercker, G.; Toschi, T.G. (**2004**). Effect of olive ripening degree on the oxidative stability and organoleptic properties of cv. Nostrana di Brisighella extra virgin olive oil. *Journal of Agricultural and Food Chemistry*, *52*, 3649–3654.

Salvador, MD.; Aranda, F.; Fregapane, G. (**2001**). Influence of fruit ripening on "Cornicabra" virgin olive oil quality. A study of four successive crop seasons. *Food Chemistry, 73*, 45-53.

Silverstein, R.M.; Bassler, G.C.; Morril, T.C. (**1981**). Spectrometric identification of organic compounds; John Wiley & Sons, Chichester.

Sinelli, N.; Casale, M.; Di Egidio, V.; Oliveri, P.; Bassi, D.; Tura, D.; Casiraghi, E. (**2010**). Varietal discrimination of extra virgin olive oils by near and midinfrared spectroscopy. *Food Research International, 43*, 2126-2131.

Tapp, H. S.; Defernez, M.; Kemsley, E.K. (**2003**). FTIR spectroscopy and multivariate analysis can distinguish the geographic origin of extra virgin olive oils. *Journal of Agricultural and Food Chemistry, 51,* 6110-6115.

Terouzi, W.; De Luca, M.; Bolli, A.; Oussama, A.; Patumi, M.; Ioele, G.; Ragno, G. (**2011**). A discriminant method for classification of Moroccan olive varieties by using direct FT-IR analysis of the mesocarp section. *Vibrational Spectroscopy, 56,* 123-128.

Vandeginste, B.G.M.; Massart, D.L.; Buydens, L.M.C.; De Jong, S.; Lewis, J.; Smeyers-Verbeke, J. (**1998**). Data handling in science and technology, part B, 18th edn. Elsevier, Amsterdam.

Vichi, S.; Lazzez, A.; Grati-Kamoun, N.; Caixach, J. (**2012**). Modifications in virgin olive oil glycerolipid fingerprint during olive ripening by MALDI-TOF MS analysis. *LWT - Food Science and Technology, 48,* 24-29.

Vlachos, N.; Skopelitis, Y.; Psaroudaki, M.; Konstantinidou, V.; Chatzilazarou, A.; Tegou, E. (**2006**). Applications of Fourier transform-infrared spectroscopy to edible oils. *Analytica Chimica Acta, 573,* 459-465.

Yorulmaz, A.; Erinc, H.; Tekin, A. (**2013**). Changes in olive and olive oil characteristics during maturation. *Journal of the American Oil Chemists' Society, 90,* 647-658.

Youssef, O.; Guido, F.; Daoud, D.; Mokhtar, Z. (**2011**). Effect of cultivar on minor components in Tunisia olive fruits cultivated in microclimate. *Journal of Horticulture and Forestry, 31,* 13-20.

Youssef, O.; Guido, F.; Manel, I.; Ben Youssef, N.; Pier Luigi, C.; Mohamed, H.; Dauja, D.; Mokhtar, Z. (**2011**). Volatile compounds and compositional quality of virgin olive oil from Oueslati variety: Influence of geographical origin. *Food Chemistry, 124,* 1770-1776.

Zamora, R.; Alaiz, M.; Hidalgo, F.J. (**2001**). Influence of cultivar and fruit ripening on olive (Olea europaea) fruit protein content, composition, and antioxidant activity *Journal of Agricultural and Food Chemistry*, *49*, 4267-4270.

Suplementary material

Table 19.S1

Predictors selected and corresponding standardized coefficients of the LDA model constructed to predict the genetic variety of Tunisian EVOOs.

Predictors[a]	f_1	f_2	f_3	f_4	f_5	f_6
1/3	-4.12	6.39	0.13	5.09	-2.37	-3.73
1/7	1.10	5.92	5.03	2.98	0.52	3.29
1/8	1.90	-1.07	-0.19	1.74	1.66	0.93
2/8	-3.06	-2.09	1.10	-4.48	2.23	3.14
6/9	11.03	5.55	8.20	11.30	23.51	2.29
6/18	12.70	7.39	5.85	11.21	19.22	0.69
7/8	1.43	0.33	-1.93	-0.25	-0.97	-1.07
12/15	-10.54	-5.96	-6.72	-6.83	-21.56	-4.36
12/16	0.41	-4.79	-1.09	-1.82	-2.63	0.28
16/17	-5.78	0.42	2.44	-0.90	2.16	1.40
17/18	-2.63	-5.03	1.06	-0.24	3.41	1.62

[a] Pairs of wavelength regions identified according to **Table 16.2.**

Tble 19.S2

Explained variances (%) obtained from the full cross-validation of the PCA model constructed to predict the genetic variety of Tunisian EVOOs.

PCs	Exp. Variance (%)
1	56.92
2	72.48
3	78.68
4	83.40
5	87.54
6	91.03
7	93.76
8	95.54

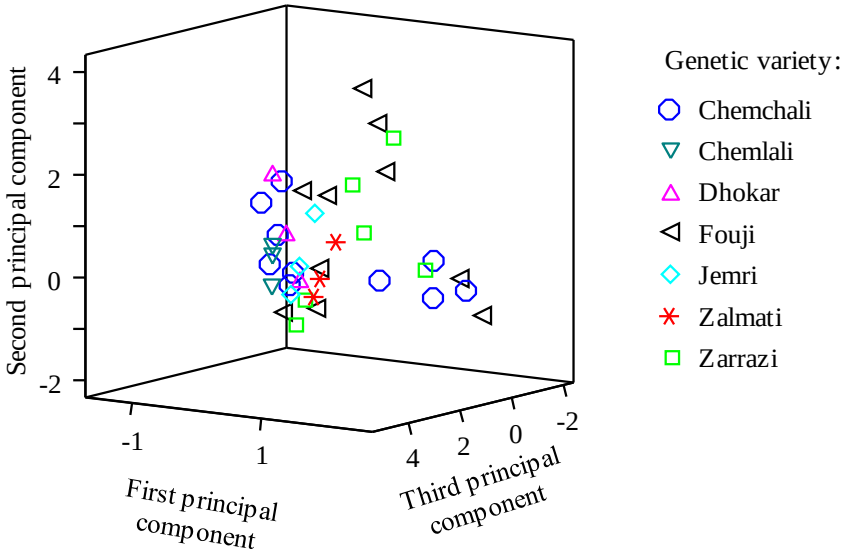

Figure 19.S1. 3D score plot (PCs 1-3) obtained by the PCA model constructed to discriminate EVOOs according to their genetic variety.

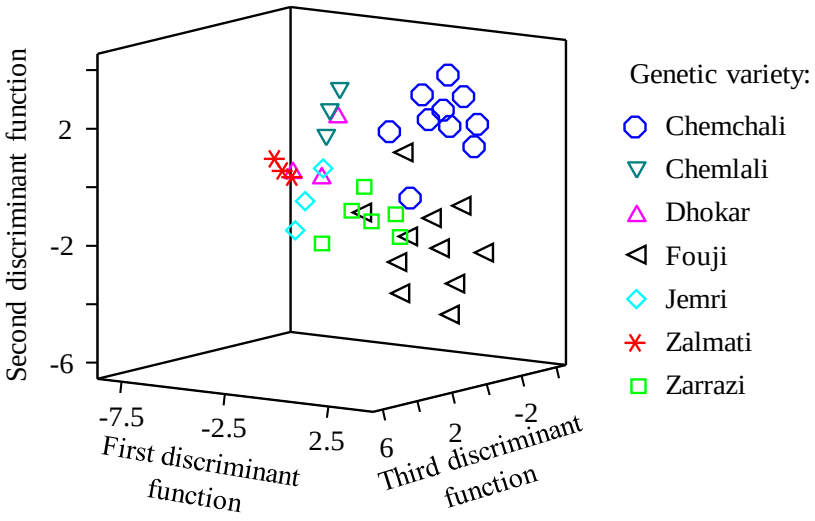

Figure 19.S2. Score plot on an oblique plane of the three-dimensional space defined by the three first discriminant functions of the LDA model constructed using the 8 PCs as predictors.

Table 19.S3

Principal components selected and corresponding standardized coefficients of the LDA model constructed to classify EVOOs according to the 7 different genetic varieties.

PCs	f_1	f_2	f_3	f_4	f_5	f_6
1	-1.17	0.51	0.39	0.63	-0.42	-0.04
3	0.17	0.01	0.74	0.26	0.71	-0.27
5	1.49	-0.25	-0.10	0.40	0.10	0.64
6	-0.76	-0.31	0.92	-0.29	-0.08	0.37
7	-0.66	1.32	-0.18	-0.06	0.18	0.17
8	1.07	0.86	0.36	-0.07	-0.17	-0.08

Chapter 20. Classification of Tunisian extra virgin olive oils according to their genetic variety and maturity index using fatty acid profiles established by direct infusion mass spectrometry

Eur. J. Lipid Sci. Technol. 2016, *118*, 735–743

Research Article

Classification of Tunisian extra virgin olive oils according to their genetic variety and maturity index using fatty acid profiles established by direct infusion mass spectrometry

Marwa Abdallah[1], María Vergara-Barberán[2], María Jesús Lerma-García[2], José Manuel Herrero-Martínez[2], Ernesto F. Simó-Alfonso[2] and Mokhtar Guerfel[1]

The usefulness of fatty acid profiles established by direct infusion mass spectrometry (DIMS) as a tool to discriminate between seven genetic varieties of Tunisian EVOOs was evaluated in this work. Moreover, the discrimination of EVOOs from the genetic varieties Chemchali, Fouji, and Zarrazi, characterized with different maturity indices, was also studied. For DIMS, EVOO samples were diluted with an 85:15 propanol/methanol (v/v) mixture containing 40 mM ammonia and directly infused into the mass spectrometer using a syringe pump. The establishment of ratios of the peak abundances of the free fatty acids followed by linear discriminant analysis was employed to predict both genetic variety and maturity index. In all cases, an excellent resolution between all category pairs was achieved, which demonstrated that fatty acid profiles are a good marker of both genetic variety and maturity index of EVOOs.

Keywords: direct infusion mass spectrometry; fatty acid profiles; genetic variety; maturity index; Tunisian extra virgin olive oils

20.1. Introduction

EVOO is the only edible oil obtained by physical methods from the fruits *Olea europaea L.* without any refining operations (IOOC, 2004; Taamalli, 2012). This oil plays an important role in the Tunisian agronomy and economy, as it occupies the second position in the world after the European Union in terms of olive oil exportation, with an average export over 10 000 metric tons (Alonso-Salces, 2011). More than 50 different cultivars are found throughout Tunisia, which are cultivated under different climatic conditions all over the country (Giacometti, 2001; Lagarda, 2006).

Olive oil is a product with high-nutritional value and its regular use is believed to result in significant health benefits, such as a low incidence of cardiovascular diseases, neurological disorders, breast and colon cancers, and with hipolipidemic and antioxidant properties (Richelle, 2004; Sotiroudis, 2008; Gylling, 2014; Cárdeno, 2014). These benefits have been related either to its well-balanced fatty acid composition, where oleic acid is the main component, or to the presence of minor biomolecules such as phytosterols, carotenoids, tocopherols, and phenols (Sotiroudis, 2008; Boskou, 2011). Thus, olive oil has become an important component of the human diet (Sánchez-Casas, 2004).

Olive oil quality is related to a large number of factors, such as genetic variety, geographical origin, maturity index, climatic conditions, agronomic techniques, harvesting systems, and processing technologies, among which the genetic variety and the olive maturity stage are two of the most important ones (Cañabate, 2007; Martínez-Vidal, 2007; Ben Temime, 2008; Lerma-García, 2008; Azadmard.Damirchi, 2010; Al-Ismail, 2010; Gylling, 2014). Regarding genetic variety, olive oils produced from a given cultivar (monovarietal oils) have specific physical and biochemical characteristics, which provide them with typical compositions and performances. In this way, the group of Simal-

Gandara (Berenguer, 2006; Ilyasoglu, 2010) have evaluated the improvement of EVOO quality by co-crushing two Spanish major cultivars (Arbequina and Picual) with a minor olive variety (Local cultivar). In all cases, the cocrushing process improved sensory and health properties of the EVOOs, producing high quality oils with predictable phenolic and aromatic profiles.

On the other hand, during ripening, many metabolic processes and transformations occur inside the olives, which produce several variations on the profiles of some compounds. Thus, it is of great importance to find parameters that allow olive oil classification according to these variables (Reboredo-Rodríguez, 2014).

Different olive oil components, such as triacylglycerols, phenols, sterols, volatile compounds, fatty acids, etc., have been employed to discriminate between olive oils according to their genetic variety (Gylling, 2014; Bouaiz, 208; Krichène, 2010; Fuentes de Mendoza, 2013), quality grade (Manai, 2012), geographical origin (Cunha, 2006; Lerma-García, 2008A; Lerma-García, 2008B), maturity index (Gylling, 2014; Cárdeno, 2014; Cañabate, 2007; Fuentes de Mendoza, 2013; Martínez-Vidal, 2007; Segura-Carretero, 2008; EC, 2002), etc. In particular, fatty acid profiles have been used to characterize olive oils from different genetic varieties (Vandeginste, 1998; Ouni, 2011), or from different maturity indexes (EC, 2002; Cañabate, 2007; Martínez-Vidal, 2007; Fuentes de Mendoza, 2013; Cárdeno, 2014; Gylling, 2014;).

According to the International Olive Oil Council, fatty acids are usually determined by gas chromatography (GC) coupled with a flame ionization detector after conversion to fatty acid methyl esters (Alonso-Salces, 2011; Noorali, 2014), although GC coupled with mass spectrometry (MS) (Gutíerrez, 1999; Rivera del Álamo, 2004) and capillary zone electrophoresis have been also used for this purpose (Koutsaftakis, 1999; Miler, 2010). However, there is a continuous need of new methodologies, taking into

account that an ideal method will be the one that requires minimal sample preparation, permits an automatic analysis of many samples with negligible reagent costs, provides an accurate determination, and straightforward automation. In this way, direct infusion mass spectrometry (DIMS) has been proposed as a very fast, versatile, reproducible, and sensitive technique, which is capable of ionizing a wide range of molecules, especially polar ones (Alves, 2010). DIMS requires any or little sample preparation providing almost instantaneous information about the composition of a given sample, as any prior chromatographic separation is needed. Different studies have been published regarding the use of this methodology for oil authentication, followed in most cases by multivariate statistical analysis of data (Goodacre, 2002; Catharino, 2005; García, 2008; Alves, 2010; Lerma- Reboredo, 2015). In particular, fatty acid profiles established by DIMS have been used to classify Spanish EVOO according to their genetic variety (Lerma-García, 2008A) and to distinguish between olive oils from different quality grade (Lerma-García, 2008).

The aim of this work was to investigate the possibility of using fatty acid profiles established by DIMS, followed by LDA of the spectral data, to classify Tunisian EVOOs according to their genetic variety (Chemchali, Fouji, Zarrazi, Dhokar, Chemlali, Jemri, and Zalmati), and to discriminate Chemchali, Fouji, and Zarrazi EVOOs according to their maturity index. For this purpose, DIMS profiles were used to construct the classification methods.

20.2. Materials and methods

20.2.1. Chemicals and samples

MeOH, n-propanol (PrOH), and ammonia from Scharlau (Barcelona, Spain), were used. A total of 55 EVOOs, coming from seven Tunisian genetic varieties, were employed in this study (**Table 20.1**). All these samples were

used to develop a classificatory method according to their genetic variety. On the other hand, a study to classify the samples according to their maturity index was also carried out using only the samples of known maturity level. The EVOOs were obtained from *ca.* 1 kg of healthy and non-damage olives, which have been hand picked during the 2012/2013 and 2013/2014 harvesting seasons from olive orchards located in the Tunisian geographical areas indicated in **Table 20.1.** After harvesting, olives were deleafed, crushed with a hummer crusher, mixed at ambient temperature for 30 min, and centrifuged without addition of water or chemicals; then, EVOOs were transferred into dark glass bottles and stored at 4°C until analysis.

In order to obtain the EVOOs of different maturity indexes, *ca.* 10 kg olives were collected from the same olive tree at different periods, and then classified according to the maturity levels established by the National Institute of Agronomical Research of Spain, described by the IOOC (IOOC, 2011), which is based on a subjective evaluation of olive skin and pulp colors. For Chemchali and Fouji varieties, five maturity levels were identified (1, yellowish green; 2, green with reddish spots; 3, reddish brown; 4, black with white flesh and 5, black with <50% purple flesh), whereas for Zarrazi variety only three maturity levels were observed (1, 3, and 4).

On the other hand, for Chemchali, Dhokar, Jemri, and Zalmati varieties, the maturity index of each sample was calculated according to the IOOC methodology (IOOC, 2011), which is based on the assessment of the color of the skins of 100 olives which were randomly drawn from 1 kg of the sample.

Table 20.1
Genetic variety, number of samples, maturity index and geographical origin of the EVOO samples employed in this study.

Genetic variety	No. of samples	Crop season	Maturity index	Geographical origin
Chemchali	1	2012/2013	1	Gafsa
	2	2013/2014		
	2	2012/2013	2	
	1	2013/2014		
	2	2012/2013	3	
	1	2013/2014		
	1	2012/2013	4	
	2	2013/2014		
	2	2012/2013	5	
	1	2013/2014		
Chemlali	1	2012/2013	3.1	Sousse
	1	2013/2014	3.7	Sfax
	2	2012/2013	3.5	Sidi Bouzid
		2013/2014	4.0	
Dhokar	2	2012/2013	3.9	Ben Gardène
		2013/2014	3.2	
	2	2012/2013	3.7	Tataouine
		2013/2014	3.5	
Fouji	2	2012/2013	1	Gafsa
	1	2013/2014		
	2	2012/2013	2	
	1	2013/2014		
	1	2012/2013	3	
	2	2013/2014		
	1	2012/2013	4	
	2	2013/2014		
	1	2012/2013	5	
	2	2013/2014		
Jemri	2	2012/2013	4.2	Ben Gardène
		2013/2014	3.8	
	2	2012/2013	3.1	Medenine
		2013/2014	3.7	
Zalmati	2	2012/2013	3.3	Medenine
		2013/2014	3.6	
	2	2012/2013	3.1	Zarzis
		2013/2014	3.9	

Table 20.1

Cont.

Zarrazi	2	2012/2013	1	Gafsa
	1	2013/2014		
	2	2012/2013	3	
	1	2013/2014		
	2	2012/2013	4	
	1	2013/2014		

20.2.2. Instrumentation and working conditions

An HP 1100 series ion trap mass spectrometer provided with an electrospray ionization source (Agilent Technologies, Waldbronn, Germany) was used. A syringe pump (KD Scientific, Holliston, MA, USA) was used to infuse the samples at 0.5 mL/h through a 50 mm i.d. PEEK tube. The MS working conditions were: nebulizer gas pressure, 25 psi; dry temperature, 200°C; dry gas, 5 L/min; capillary voltage, 3.5 kV; voltages of skimmers 1 and 2, -26.8 and -6.0 V, respectively. Nitrogen was used as nebulizer and dry gas (Gaslab NG LCMS 20 generator, Equcien, Madrid, Spain). The mass spectrometer was scanned within the *m/z* 100–800 range in the negative-ion mode. The target mass was set at *m/z* 281 ($[M-H]^-$ oleic acid peak).Maximum loading of the ion trap was 3×10^4 counts, and maximum collection time was 300 ms. Instrument control and data acquisition were performed using the LC/MSD Trap software 5.2 (Bruker Daltonics, Bremen, Germany).

20.2.3. Procedures

For DIMS, the oil samples were 1:4 (v/v) diluted with an 85:15 (v/v) PrOH/MeOH mixture containing 40mM ammonia (lower dilutions led to a significant increase in background noise). This mixture was also used to rinse and clean the PEEK tube between successive infusions. Rinsing for 5 min was enough to achieve a satisfactory reduction of the background noise and reproducible oil profiles. Before data acquisition, the diluted sample was infused until the signal remained constant. All samples were injected three times, and each time the data were averaged for 1 min.

20.2.4. Statistical analysis

LDA models were constructed using the SPSS software (v. 12.0.1, SPSS, Inc., Chicago, IL, USA). LDA, a supervised classificatory technique, is widely recognized as an excellent tool to obtain vectors showing the maximal resolution between a set of previously defined categories. The LDA discriminating vectors are frequently obtained by minimizing a parameter called the Wilks' lambda (λ_w) (Vandeginste, 1998). This parameter is calculated as the sum of squares of the distances between points belonging to the same category, divided by the total sum of squares. Values of λ_w approaching zero are obtained with well-resolved categories, whereas overlapped categories made λ_w to approach one. Up to N-1 discriminant vectors are constructed by an LDA, with N being the lowest value for either the number of predictors or the number of categories.

Selection of predictors to be included in the LDA models was performed by using the SPSS stepwise algorithm. According to this algorithm, a predictor is selected when the reduction of λ_w produced after its inclusion in the model exceeds the entrance threshold of a test of comparison of variances or $F_{\text{-test}}$ (F_{in}). However, the entrance of a new predictor modifies the significance of those predictors which are already present in the model. For

this reason, after the inclusion of a new predictor, a rejection threshold, F_{out}, is used to decide if one of the other predictors should be removed from the model. The process terminates when there are no predictors entering or being eliminated from the model. The significances of F_{in} and F_{out} were set to 0.05 and 0.10, respectively.

20.3. Results and discussion

20.3.1. Determination of fatty acids by DIMS

In DIMS, all EVOO samples showed the $[M-H]^-$ peaks of the following fatty acids in the MS spectra: myristic (*m/z* 227), palmitoleic (*m/z* 253), palmitic (*m/z* 255), linolenic (*m/z* 277), linoleic (*m/z* 279), oleic (*m/z* 281) and stearic (*m/z* 283). A representative DIMS spectrum of a Chemchali EVOO from the maturity index 3 is shown in **Figure 20.1**.

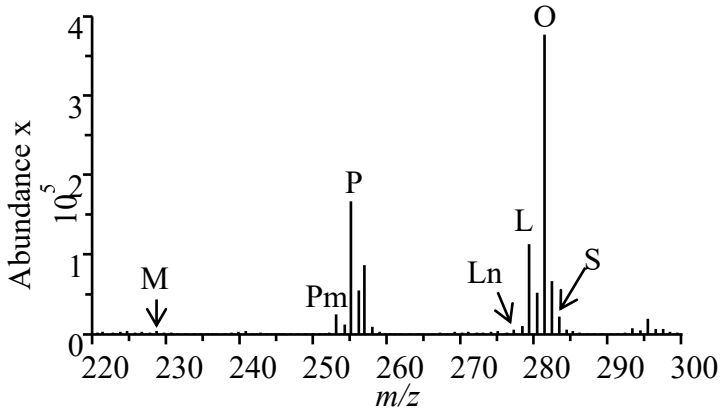

Figure 20.1. Representative DIMS spectra of a Chemchali EVOO from the maturity index 3. Peak identification: M = myristic acid; Pm = palmitoleic acid; P = palmitic acid; Ln = linolenic acid; L = linoleic acid; O = oleic acid; S = stearic acid.

However, to make comparison easier, relative peak intensities of fatty acids are depicted in **Figure 20.2.**

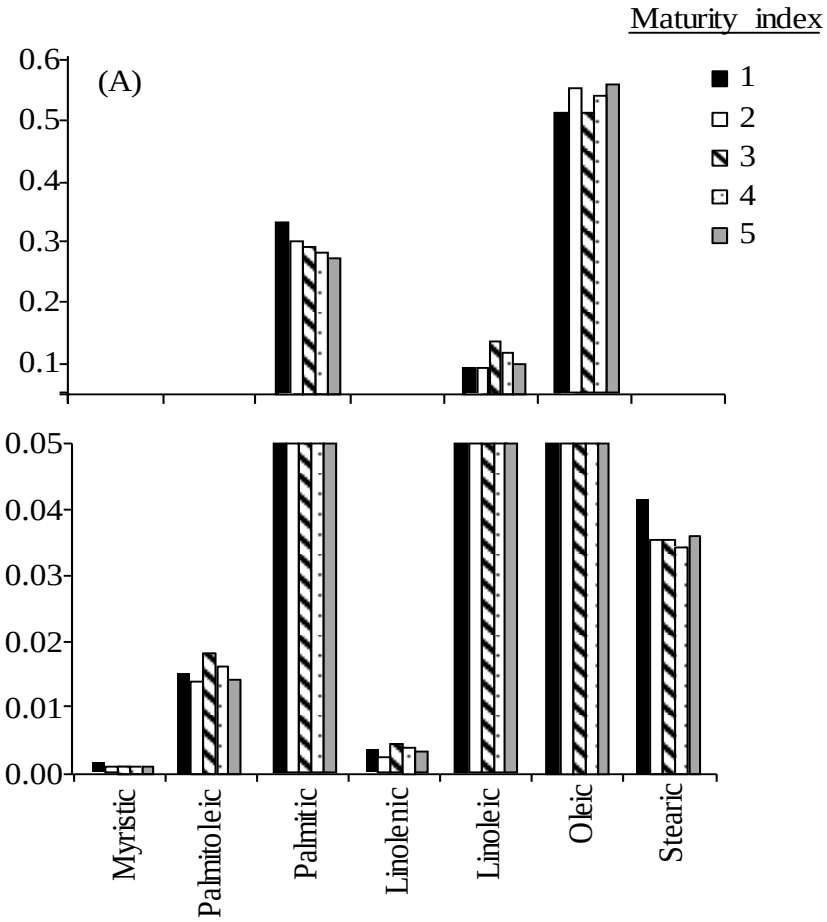

Figure 20.2A. Relative peak intensities of fatty acids observed in the mass spectra of Chemchali EVOOs at different maturity indexes.

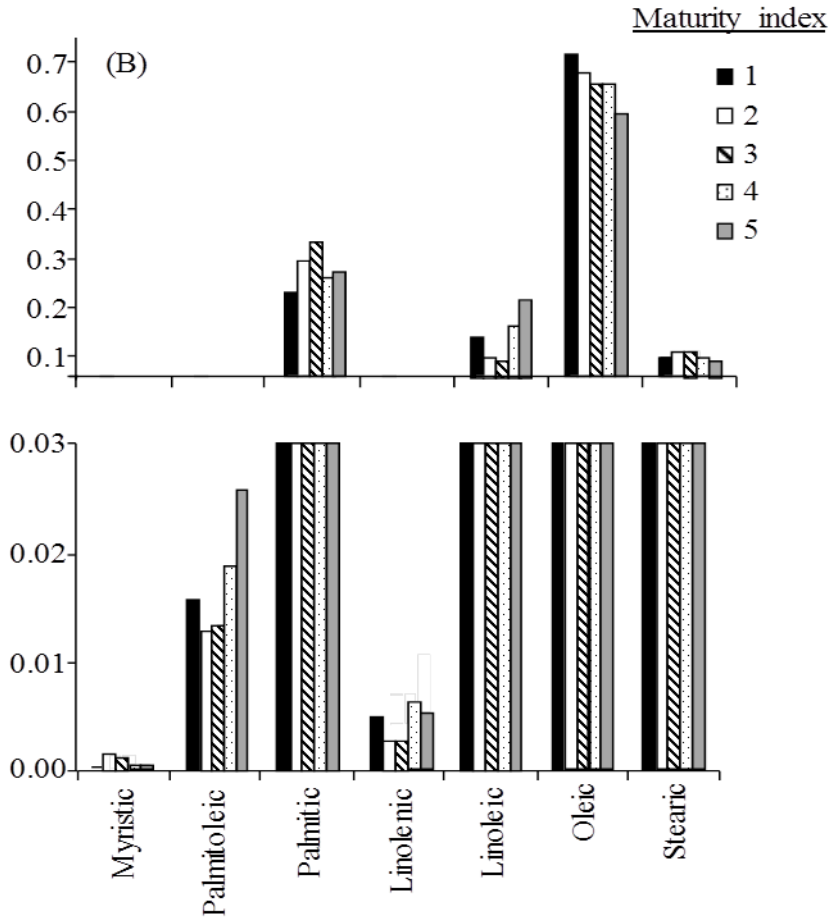

Figure 20.2B. Relative peak intensities of fatty acids observed in the mass spectra of Fouji EVOOs at different maturity indexes.

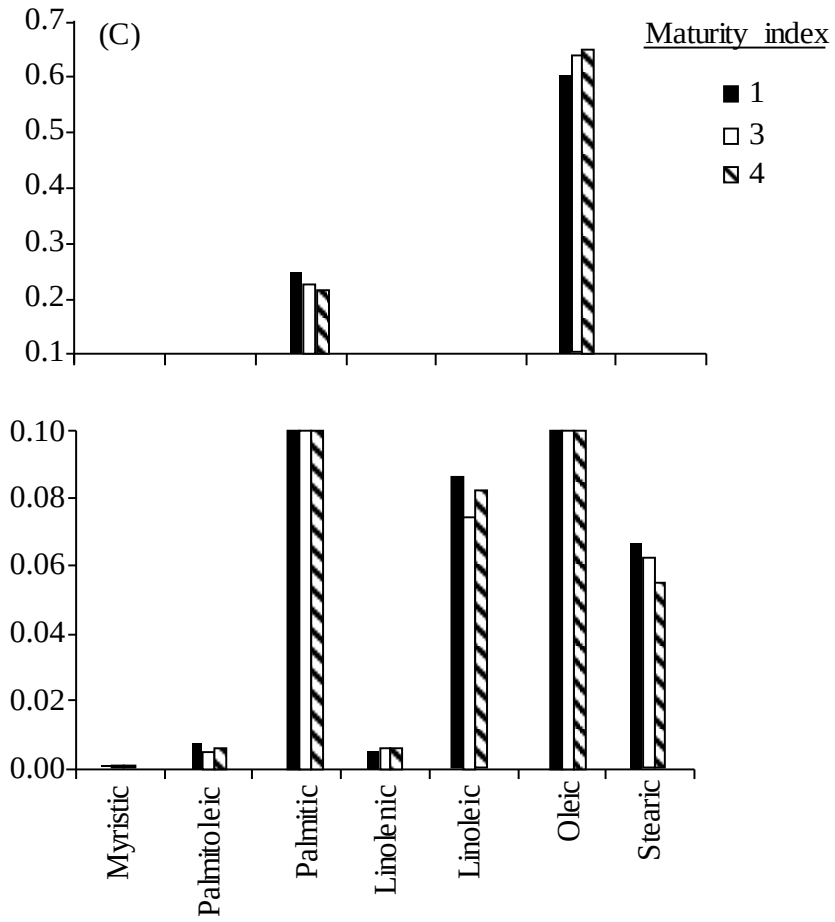

Figure 20.2C. Relative peak intensities of fatty acids observed in the mass spectra of Zarrazi EVOOs at different maturity indexes.

These relative peak intensities were obtained by dividing each fatty acid peak abundance by the sum of the abundances of all fatty acids. The percentages of fatty acids present in the total fatty acid fraction of all EVOO considered in this study are shown in **Table 20.2.**

Table 20.2

Percentages of fatty acids present in the total fatty acid fraction of the EVOO considered in this study.

Genetic variety	Maturity index	*m/z* 227	*m/z* 253	*m/z* 255	*m/z* 277	*m/z* 279	*m/z* 281	*m/z* 283
Chemchali	1	0.14	1.50	32.86	0.34	9.27	51.75	4.14
	2	0.11	1.19	30.30	0.25	8.80	55.24	4.12
	3	0.11	1.82	29.26	0.43	13.22	51.64	3.53
	4	0.12	1.63	28.39	0.40	11.56	54.48	3.43
	5	0.10	1.42	27.93	0.33	10.30	56.31	3.60
Fouji	1	0.01	1.55	17.71	0.47	8.47	67.79	3.99
	2	0.14	1.28	24.61	0.28	4.43	64.01	5.26
	3	0.11	1.32	28.20	0.27	3.16	61.75	5.20
	4	0.04	1.87	20.89	0.63	10.66	61.77	4.15
	5	0.04	2.58	21.94	0.51	16.51	55.18	3.24
Zarrazi	1	0.17	1.57	23.69	0.52	8.51	58.98	6.55
	3	0.12	1.12	21.75	0.63	7.36	62.89	6.14
	4	0.15	1.27	20.84	0.61	8.15	63.58	5.41
Dhokar	-	0.15	3.37	25.43	0.45	12.25	55.11	3.24
Chemlali	-	0.28	3.37	28.64	0.65	15.21	48.54	3.31
Jemri	-	0.25	3.05	23.90	0.67	15.87	53.17	3.09
Zalmati	-	0.04	2.54	22.17	0.66	16.80	55.14	2.64

As deduced from this table and **Figure 20.2** for Chemchali variety (trace A), palmitic and stearic acid percentages decreased when the maturity index increased, while oleic acid percentage increased. The same tendency was also observed for the Zarrazi variety (trace C). This tendency was in agreement with the results previously published in literature for Memecik and Edremit cultivars (Yorulmaz, 2013). However, for the Fouji variety (trace B), the tendency observed was a decrease of the oleic acid percentage, which is contrary to that observed for the other varieties. This behaviour found for oleic acid was consistent to that reported in literature, where some studies have shown increases in oleic acid content due to triacylglycerol biosynthesis (Gutíerrez, 1999; Issaoui, 2010), while other works have determined an oleic acid content decrease (Baccouri, 2008; Ben Yousef, 2010). Regarding the other fatty acids, their content did not seem to vary during maturation, which is in agreement with literature (Ouni, 2011; Matos, 2007; Skevin, 2003; Baccouri, 2007). However, to enhance small differences that were not appreciated straight away in the data, the peak abundances of the 7 fatty acids were conveniently handled by multivariate statistical techniques in order to check their suitability as both genetic variety and maturity index predictors.

20.3.2. Normalization of the variables for statistical analysis

In order to minimize variability associated to sources of variance affecting the intensity of all the peaks, normalized rather than absolute peak intensities were used. For this purpose, the abundance of each fatty acid was divided by each one of the abundances of the other 6 fatty acids; in this way, and since each pair of peaks should be considered only once, (7 x 6) / 2 = 21 normalized predictors were obtained. These predictors were used to construct LDA models.

20.3.3. Classification of EVOOs according to their genetic variety

A first LDA model was constructed to classify the EVOO samples according to their variety (see **Table 20.1**). For this purpose, a matrix containing 55 objects and the 21 predictors obtained after application of the normalization procedure indicated above, was constructed. A response column, containing the categories corresponding to the 7 genetic varieties, was added. This matrix was divided in two groups of objects to constitute the training and evaluation sets. The training set was composed by 38 objects (10 objects from Chemchali and Fouji, and 6 from Zarrazi (2 samples for each maturity index) and 3 objects from the other varieties), while the evaluation set was constituted by the remaining samples (17 objects). When the LDA model was constructed, an excellent resolution between all the category pairs was achieved (**Figure 20.3**, $\lambda_w < 0.01$). The variables selected by the SPSS stepwise algorithm, and the corresponding standardized coefficients of the model, showing the predictors with large discriminant capabilities, are given in **Table 20.3**.

Table 20.3
Predictors selected and corresponding standardized coefficients of the LDA model constructed to classify EVOO samples according to their genetic variety.

Predictors[a]	f_1	f_2	f_3	f_4	f_5	f_6
227/253	4.04	5.24	2.05	2.05	0.07	-0.67
227/255	0.41	-4.79	-1.09	-1.82	-2.63	0.28
227/281	-6.74	-6.51	-5.89	-3.35	2.24	-2.50
227/283	1.10	5.92	5.03	2.98	0.52	3.29
253/255	-4.09	-6.61	0.77	7.43	-3.77	4.92
253/281	12.59	19.36	8.08	0.68	4.70	-5.05
253/283	-2.06	-9.58	-10.25	-7.27	-3.19	-0.07
255/279	1.90	-1.07	-0.19	1.74	1.66	0.93
255/283	-4.44	-2.24	-0.45	1.82	-2.34	1.10
279/283	-2.63	-5.03	1.06	-0.24	3.41	1.62
281/283	3.81	6.85	1.09	-0.06	2.84	-2.77

[a] *m/z* values of the ratios of abundances of fatty acid peak pairs

According to this table, the main fatty acids selected by the algorithm to construct the LDA model corresponded to oleic, palmitoleic and myristic acids (ratios at *m/z* 253/281 and 227/281). Using this model and leave-one-out validation, all the objects of the training set were correctly classified. Concerning to the prediction capability of the model, all the objects of the evaluation set (represented with crosses in **Figure 20.3**) were correctly assigned within a 95% probability level.

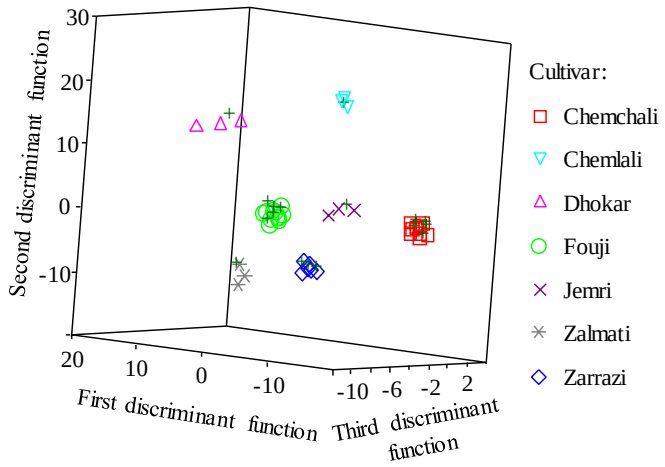

Figure 20.3. Score plot on an oblique plane of the 3D space defined by the three first discriminant functions of the LDA model constructed to classify EVOOs according to their genetic variety. Evaluation set samples are labelled with a cross symbol.

20.3.4. Classification of EVOO from the Chemchali, Fouji and Zarrazi varieties according to their maturity index

Next, the EVOOs from the Chemchali, Fouji and Zarrazi varieties were also classified according to their maturity index. For this purpose, three matrices were constructed: two matrices (for Chemchali and Fouji) containing 15 objects each, and one more matrix (for Zarrazi) with 9 objects. These matrices also contained the 21 predictors obtained after normalization and a response column in which the different maturity levels were included. All matrices were also divided in the training and evaluation sets. Thus the training sets were composed by 10 objects for Chemchali and Fouji and by 6 objects for Zarrazi, while the evaluation sets were composed by 5 objects (Chemchali and Fouji) and 3 objects (Zarrazi). Three LDA models, one for each genetic variety, were next constructed. The corresponding score plots are shown in **Figure 20.4.**

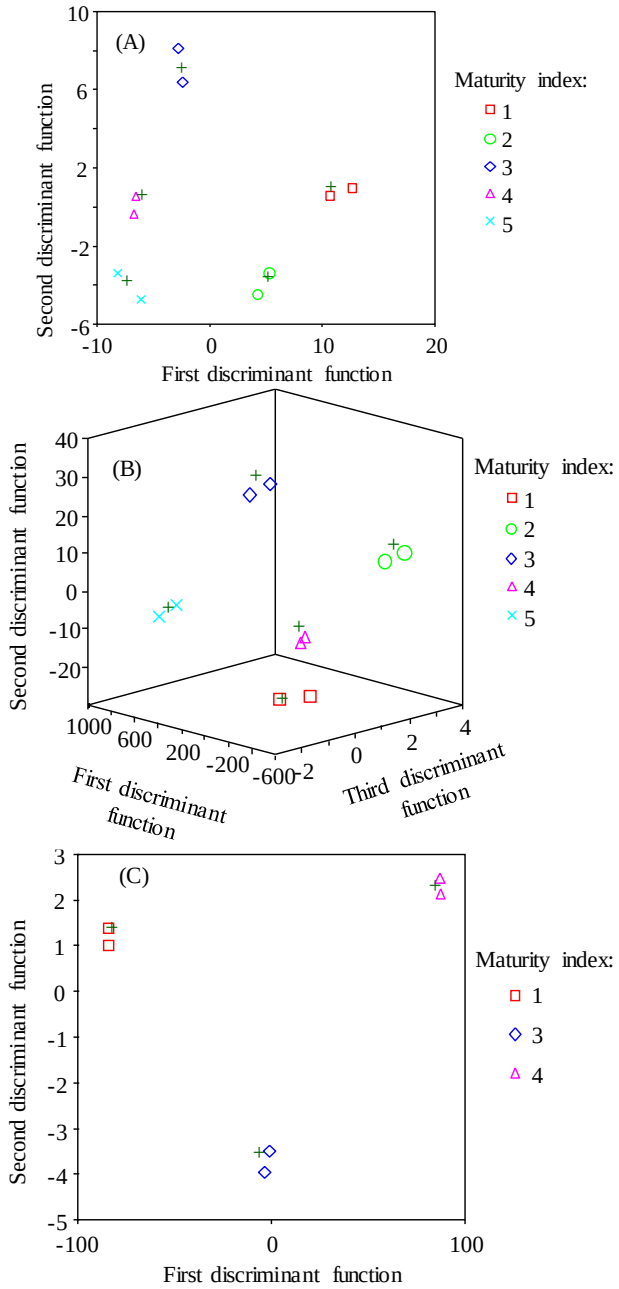

Figure 20.4. Score plots of the discriminant functions of the LDA models constructed to classify Chemchali (A), Fouji (B) and Zarrazi (C) EVOOs according to their maturity index. Evaluation set samples are labelled with a cross symbol.

In all cases, and excellent resolution between all category pairs was obtained, being $\lambda_w < 0.01$. The variables selected by the SPSS stepwise algorithm, and the corresponding standardized coefficients of the models, showing the predictors with large discriminant capabilities, are given in **Table 20.4.**

Table 20.4

Predictors selected and corresponding standardized coefficients of the LDA model constructed to predict the maturity index of EVOOs.

Genetic variety	Predictors[a]	f_1	f_2	f_3	f_4
Chemchali	255/279	2.19	0.63	-	-
	279/281	1.69	1.53	-	-
Fouji	227/255	9.65	0.09	0.79	0.66
	253/279	-3.43	1.00	-0.34	0.17
	253/281	27.96	0.06	-0.22	0.18
	255/281	27.75	0.82	0.40	-0.36
Zarrazi	279/281	-0.85	0.98	-	-
	281/283	1.29	0.03	-	-

[a] *m/z* values of the ratios of abundances of fatty acid peak pairs

According to this table, the fatty acids selected to discriminate among the maturity index of Chemchali EVOOs corresponded to palmitic, linoleic and oleic acids (ratios at *m/z* 255/279 and 279/281). The selection of these predictors to construct the model was expected, since these fatty acids were those that provided higher variability in fatty acid content (see **Table 20.2** and **Figure 20.2**). Moreover, and as observed in **Figure 20.4A,** *f1* was mainly constructed with the 255/279 ratio, which values decreased when the maturity index was increased. As observed, the projections of the objects over this function appeared in order (maturity index 5 to 1 when *f1* values increased).

On the other hand, for the Fouji EVOOs the main fatty acids selected were palmitoleic, palmitic and oleic acids (ratios at *m/z* 253/281 and 255/281). Finally, the linoleic, oleic and stearic acids (ratios at *m/z* 279/281 and 281/283) were those selected for the classification of Zarrazi varieties according to the maturity index.

When leave-one-out validation was applied to the three models, all the objects of the training set were correctly classified. Next, the prediction capability of the models was also evaluated using the evaluation sets. Using a 95% probability, all the objects were correctly classified; thus, the prediction capability of the three models was 100%.

20.4. Conclusions

The possibility of distinguishing Tunisian EVOOs according to their genetic variety and maturity index by using fatty acid profiles established by DIMS has been demonstrated in this work. Since different fatty acid patterns were observed for the EVOOs obtained from different genetic variety and maturity index, fatty acids were used as predictors for the construction of LDA models. EVOOs belonging to 7 Tunisian genetic varieties, and EVOOs from the Chemchali, Fouji and Zarrazi obtained at different maturity indexes, were correctly classified with an excellent resolution among all the categories, being in all cases the assignment probability of the models higher than 95%. Thus, it was demonstrated that fatty acid profiles present a high potential to discriminate EVOOs obtained from different genetic variety and maturity index.

Acknowledgements

M. Vergara-Barberán thanks the MEC for an FPU grant for PhD studies. M.J. Lerma-García thanks the Generalitat Valenciana for a VALi+d postdoctoral contract.

20.5. References

Perez-Jimenez, F.; Alvarez de Cienfuegos, G.; Badimon, L.; Barja, G.; Battino, M.; Blanco, A. (**2005**). International conference on the healthy effect of virgin olive oil. *European Journal of Clinical Investigation*, *35*, 421–424.

Alves, J.O.; Neto, W.B., Mitsutake, H., Alves, P.S.P. (**2010**). Extra virgin (EV) and ordinary (ON) olive oil: distinction and detection of adulteration (EV with ON) as determined by direct infusion electrospray ionization mass spectrometry and chemometric approaches. *Rapid Communications in Mass Spectrometry*, *24*, 1875–1880.

Alves, M. R.; Cunha, S. C.; Amaral, J. S.; Pereira; J. A., Oliveira, M. B. (**2005**). Classification of PDO olive oils on the basis of their sterol composition by multivariate analysis. *Analytica Chimica Acta, 549*, 166–178.

Aparicio, R.; Aparicio-Ruíz, R. (**2002**). Authentication of vegetable oils by chromatographic techniques. *Journal of. Chromatography A*, *881*, 93–104.

Baccouri B, Zarrouk W; Krichene D, Nouairi I; Youssef, N. B.; Daoud D, Zarrouk, M. (**2007**). Influence of fruit ripening and crop yield on chemical properties of virgin olive oils from seven selected oleasters (Olea europaea L.). *Journal of Agronomy*, *6*, 388–396.

Baccouri, O.; Guerfel, M.; Baccouri, B.; Cerretani, L.; Bendini, A.; Lercker, G.; Zarrouk, M.; Daoud, D. (**2008**). Chemical composition and oxidative stability of Tunisian monovarietal virgin olive oils with regard to fruit ripening. *Food Chemistry*, *109*, 743-754.

Ben Youssef, N.; Zarrouk, W.; Carrasco-Pancorbo, A.; Ouni, Y.; Segura-Carretero, A.; Fernández-Gutiérrez, A.; Daoud, D.; Zarrouk, M. (**2010**).

Effect of olive ripeness on chemical properties and phenolic composition of Chétoui virgin olive oil. *Journal of the Science of Food and Agriculture, 90*, 199-204.

Boggia, R.; Borgogni, C.; Hysenaj, V.; Leardi, R.; Zunin, P. (**2014**). Direct GC-(EI)MS determination of fatty acid alkyl esters in olive oils. *Talanta, 119*, 60–67.

Bucci, R.; Magrí, A. D.; Magrí, A.L.; Marini; D., Marini; F. (**2002**). Chemical authentication of extra virgin olive oil varieties by supervised chemometric procedures *Journal of Agricultural and Food Chemistry*, *50*, 413–418.

Catharino, R.R.; Haddad, R.; Cabrini, L.G.; Cunha, I.B.S., Sawaya; A. C.H.F., Eberlin, M.N. (**2005**). Characterization of vegetable oils by electrospray ionization mass spectrometry fingerprinting: classification, quality, adulteration, and aging. *Analytical Chemistry, 77*, 7429–33.

Garcia, J.M.; Seller, S.; Pérez-Camino, M.C. (**1996**). Influence of fruit ripening on olive oil quality. *Journal of Agricultural and Food Chemistry, 44*, 3516–3520.

Garrido-Delgado, R.; Arce, L.; Valcárcel, M. (**2012**). Multi-capillary column-ion mobility spectrometry: a potential screening system to differentiate virgin olive oils. *Analytical and Bioanalytical Chemistry, 402*, 489–498.

Gimeno, E.; Fitó, M.; Lamuela-Raventós, R. M.; Castellote, A. I.; Covas, M.; Farré, M., (**2002**). Effect of ingestion of virgin olive oil on human low-density lipoprotein composition. *European Journal of Clinical Nutrition, 56*, 114–120.

Goodacre, R.; Vaidyanathan, S.; Bianchi, G.; Kell, D. B. **(2002**). Metabolic profiling using direct infusion electrospray ionisation mass spectrometry for the characterisation of olive oils. *The Analyst*, *127*, 1457–1462.

Gutiérrez, F.; Jímenez, B.; Ruíz, A.; Albi, M. A. (**1999**). Effect of olive ripeness on the oxidative stability of virgin olive oil extracted from the varieties picual and hojiblanca and on the different components involved. *Journal of Agricultural and Food Chemistry*, *47*, 121–127.

IOOC. (**2004**). Olive Oil Exportations, International Olive Oil Council, http:// www.internationalolive oil.org 2011.oil.org. (2011).

Issaoui, M.; Flamini, G.; Brahmi, F.; Dabbou, S.; Ben Hassine, K.; Taamali, A., Chehab, H.; Ellouz, M.; Zarrouk, M;. Hammami, M.; (**2010**). Effect of the growing area conditions on differentiation between Chemlali and Chétoui olive oils. *Food Chemistry, 119*, 220–225.

Kalua, C.M.; Allen, M.S.; Bedgood, D.R.; Bishop, A.G.; Prenzler, P.D. (**2005**). Discrimination of olive oils and fruits into cultivars and maturity stages based on phenolic and volatile compounds. *Journal of Agricultural and Food Chemistry*, *53*, 8054–8062.

Kammoun; N.G., Zarrouk, W. (**2012**). Exploratory chemometric analysis for the characterisation of Tunisian olive cultivars according to their lipid and sterolic profiles. *International Journal of Food Science*, *47*, 1496–1504.

Kesen, S.; Kelebek, H.; Selli, S. (**2013**). LC–ESI–MS characterization of phenolic profiles turkish olive oils as influenced by geographic origin and harvest year. *Journal of the American Oil Chemists' Society*, *91*, 385–394.

Kiritsakis, A.; Nanos, G.D.; Polymenopoulos, Z.; Thomai, T.; Sfakiotakis, E.M. (**1998**). Effect of fruit storage conditions on olive oil quality. *Journal of the American Oil Chemists' Society, 75*, 721–724.

Lanteri, S.; Armanino, C.; Perri, E.; Palopoli, A. (**2002**). Study of oils from Calabrian olive cultivars by chemometric methods. *Food Chemistry, 76*, 501–507.

Lerma-García, M.J.; Herrero-Martínez, J.M.; Ramis-Ramos, G.; Simó-Alfonso, E.F., (**2008A**). Prediction of the genetic variety of Spanish extra virgin olive oils using fatty acid and phenolic compound profiles established by direct infusion mass spectrometry. *Food Chemistry, 108*, 1142–1148.

Lerma-García, M.J.; Herrero-Martínez, J.M.; Ramis-ramos, G.; Simó-Alfonso, E.F. (**2008B**). Evaluation of the quality of olive oil using fatty acid profiles by direct infusion electrospray ionization mass spectrometry. *Food Chemistry, 107*, 1307–1313.

Lerma-García, M.J.; Lantano, C.; Chiavaro, E.; Cerretani, L.; Herrero-Martínez, J.M.; Simó-Alfonso, E.F. (**2009**). Classification of extra virgin olive oils according to their geographical origin using phenolic compound profiles obtained by capillary electrochromatography. *Food Research International, 42*, 1446–1452.

López-Feria, S.; Cárdenas, S.; García-Mesa, J. A.; Fernández-Hernández, A.; Valcárcel, M. (**2007**). Quantification of the intensity of virgin olive oil sensory attributes by direct coupling headspace-mass spectrometry and multivariate calibration techniques. *Journal of Chromatography A, 1147*, 144–152.

Manai, H.; Mahjoub-Haddada, F.; Oueslati, I.; Daoud, D.; Zarrouk, M. (**2008**). Characterization of monovarietal virgin olive oils from six crossing varieties. *Scientia Horticulturae, 115*, 252–260.

Mannina, L.; Barone, P.; Patumi, M.; Fiordiponti, P.; Emanuele, M. C.; Segre, A.L. (**1999**). Cultivar and pedoclimatic effects in the discrimination of olive oils: a high-field NMR study. *Recent Research &. Developments in. Oil Chemistry, 3*, 85–92.

Matos, L.C.; Cunha, S.C.; Amaral, J.S.; Pereira, J.A.; Andrade, P.B.; Seabra, R.M.; Oliveira, B.P.P. (**2007**). Chemometric characterization of three varietal olive oils (Cvs. Cobrançosa, Madural and Verdeal Transmontana) extracted from olives with different maturation indices. *Food Chemistry, 102*, 406-414.

Medeiros, M.D. (**2001**). *The Handbook of Nutraceuticals and Functionals Foods*. (W. REC.CRC, Ed.) 261–267.

Ouni, Y.; Guido, F.; Daoud, D.; Zarrouk, M. (**2011**). Effect of cultivar on minor components in Tunisia olive fruits cultivated in microclimate. *Journal of Horticultural Science, 3*, 13–20.

Reboredo-Rodríguez, P.; González-Barreiro, C.; Cancho-Grande, B.; Simal-Gándara, J. (**2014**). Quality of extra virgin olive oils produced in an emerging olive growing area in north-western Spain. *Food Chemistry, 164*, 418–426.

Reboredo-Rodríguez, P.; González-Barreiro, C.; Cancho-Grande, B.; Fregapane, G.; Salvador, M.D.; Simal-Gándara, J. (**2015**). Blending Local olive oils with Arbequina or Picual oils produces high quality, distinctive EVOOs. *European Journal of Lipid Science and Technology, 116*, in press.

Reboredo-Rodríguez, P.; González-Barreiro, C.; Cancho-Grande, B.; Fregapane, G.; Salvador, M.D.; Simal-Gándara, J. (**2015**) Characterisation of extra virgin olive oils from Galician autochthonous varieties and their co-crushings with Arbequina and Picual cv. *Food Chemistry,176*, 493-503.

Rotondi, A.; Bendini, A.; Cerretani, L.; Mari, M.; Lercker, G.; Toschi, T.G. (**2004**). Effect of olive ripening degree on the oxidative stability and organoleptic properties of cv. Nostrana di Brisighella extra virgin olive oil. *Journal of Agricultural and Food Chemistry, 52*, 3649–3654.

Salvador, M.D.; Aranda, F.; Fregapane, G. (**2001**). Influence of fruit ripening on "Cornicabra" virgin olive oil quality. A study of four successive crop seasons. *Food Chemistry, 73*, 45-53.

Sato, R.T.; Coelho Castro, R.J.; De Castro Barra, P.M.; De Oliveira, M. A.L. (**2014**). Rapid separation of free Fatty acids in vegetable oils by capillary zone electrophoresis. *Phytochemical Analysis*, *25*, 241–246.

Skevin D, Rade D, Strucelj D, Mokrovcak Z, Nederal S, Bencic D (**2003**). The influence of variety and harvest time on the bitterness and phenolic compounds of olive oil. *European Journal of Lipid Science and Technology*, *105*, 536-541.

Taamalli, A.; Arráez-Román, D.; Zarrouk, M.; Valverde, J.; Segura-Carretero, A.; Fernández-Gutiérrez, A. (**2012**). The occurrence and bioactivity of polyphenols in Tunisian olive products and by-products: a review. *Journal of Food Science*, *77*, 83–92.

Vandeginste, B. G. M.; Massart, D. L.; Buydens, L. M. C.; De Jong, S.; Lewis, J.; Smeyers-Verbeke, J. (**1998**). Data handling in science and technology, part B. (Elsevier, Ed.) (18th ed., p. 237), Amsterdam.

Vergara-Barberán, M.; Escrig-Doménech, A.; Lerma-García, M.J.; Simó-Alfonso, E.F.; Herrero-Martínez, J.M. (**2011**). Capillary electrophoresis of free fatty acids by indirect ultraviolet detection: application to the classification of vegetable oils according to their botanical origin. *Journal of Agricultural and Food Chemistry*, 10775–10780.

Yang, Y.; Ferro, M.D.; Cavaco, I.; Liang, Y. (**2013**). Detection and identification of extra virgin olive oil adulteration by GC-MS combined with chemometrics. *Journal of Agricultural and Food Chemistry*, *61*, 3693–3702.

Yorulmaz, A.; Erinc, H.; Tekin, A. (**2013**). Changes in olive and olive oil characteristics during maturation. *Journal of the American Oil Chemists' Society*, *90*, 647-658.

Zamora, R.; Alaiz, M.; Hidalgo, F.J. (**2001**). Influence of cultivar and fruit ripening on olive (Olea europaea) fruit protein content, composition, and antioxidant activity *Journal of Agricultural and Food Chemistry*, *49*, 4267-4270.

SECTION IV. SUMMARY OF RESULTS, DISCUSSION AND CONCLUSIONS

This PhD thesis reports the development of novel separation systems to determine biomolecules from complex matrices, especially in vegetal samples. In the first part of this thesis, extraction methodologies were designed to isolate proteins, constituting a significant contribution in the sample preparation field. Thus, the development of novel in-house sorbents based on organic polymers modified with Au and AgNPs for SPE with improved properties, the proper selection of enzyme preparations (either alone or in mixtures) for efficient release of these biomacromolecules from plant cells, and the use of CPLLs to preconcentrate LAPs in complex matrices have been accomplished. Significant enhancements such as large protein extraction yield, tunable selectivity, cost-effective, environmentally friendly and other advantages should place the developed methodologies in a competitive position compared to commercial SPE materials or other traditional extraction methodologies (that imply the use of organic solvents).

Another part covered by this thesis was the development of methods for the characterization and determination of several compounds in olive products using different chromatographic and spectrometric techniques.

For this purpose, different profiles belong to components present in these matrices, such as proteins, TAGs, sterols and fatty acids were considered. These profiles allowed a discrimination of vegetable oils according to their botanical origin, and also the characterization and authentication of Spanish and Tunisian olive oils in relation to their genetic variety. The proposed methodologies are of utmost interest to assure product quality and to investigate fraudulent practices in food science.

In this section of the PhD Thesis, and as required by the aforementioned regulation of the University of Valencia, a summary of the results shown in the successive articles jointly with Sections II and III and the most relevant conclusions of each work is briefly presented here.

Part I: Development of novel extraction techniques for protein extraction in vegetable samples

I.A. SPE based on ground methacrylate monolith modified with gold nanoparticles for isolation of protein

A SPE sorbent based on a powdered GMA monolith for protein extraction from vegetal samples has been developed in this work. A GMA polymer was selected as the parent monolith, since it is chemically and mechanically stable and contains reactive moieties (epoxy groups) susceptible of undergoing functionalization thus allowing the attachment of organic material or even metallic NPs such as gold. Thus, once GMA-based monolith was synthesized, it was ground in powder and subsequently amino groups were introduced onto the surface of the material by reacting epoxy groups with ammonia. Then, AuNPs, which have a strong interaction with the amino groups, were immobilized onto the GMA powder monolith surface. This AuNP-modified GMA material was chosen as "reactive support" to extract thiol-containing compounds such as proteins. SEM/BSE micrographs of this material were taken, showing an excellent surface coverage of polymer with AuNPs. The Au content was also measured by both UV-vis spectroscopy and EDAX analysis giving values comprised between 0.4-0.5 wt%. After packing the material in an SPE cartridge, the extraction conditions and other parameters of the SPE support (loading capacity and regenerative ability of sorbent) were optimized using proteins as test solutes. The results indicated that pH plays an important role on the protein extraction, since by simply adjusting the pH of the loading and washing solution close to pI values of proteins of interest, the biomacromolecules were readily adsorbed onto the AuNPs surface. With regard to protein recovery and loading capacity of the SPE sorbent, satisfactory results were obtained (95-98 % and 16 mg/g sorbent, respectively). In addition, a study based on the reusability of this material

revealed that the sorbent can be reused for 20 times without significant efficiency losses (satisfactory recoveries comprised between 81.3-97.6%).

The applicability of this methodology was firstly demonstrated by the isolation of cyt c from BSA followed by SDS-PAGE analysis. Also, this sorbent was applied to the isolation of lectins from mistletoe. Thus, these glycoproteins were efficiently isolated, placing the developed method as a promising alternative to affinity chromatography, which is the most commonly employed method for their purification. In any case, the results obtained here showed that the developed sorbent could be useful for the selective separation and/or preconcentration of protein species of interest (according to pI) in complex real samples.

I.B. Polymeric sorbents modified with Au and AgNPs for SPE of proteins followed by MALDI-TOF analysis

In this work, novel SPE sorbents with enhanced properties were designed for selectively extraction of proteins from complex matrices. For this purpose, a ground GMA based polymer was treated with two different ligands, ammonia and cysteamine. The resulting polymers containing amine or thiol groups (GMA-NH_2 and GMA-SH, respectively), were allowed to react with metallic NPs, concretely AuNPs and AgNPs. The presence of AuNPs and AgNPs was demonstrated by SEM micrographs of materials and their Au and Ag content was measured by ICP-MS. The results showed that the material containing thiol functionalities (GMA-SH) afford a large coverage of AuNPs or AgNPs onto the polymer surface due to the large affinity of thiol moieties and these NPs. Then, these GMA-modified materials were used as SPE sorbents. Several SPE parameters such as loading and elution pHs were optimized using BSA as test solute. Satisfactory protein recovery values were found for all the four sorbents synthesized (>90 %). Loading capacity of GMA-SH-Au and GMA-SH-Ag sorbents was also established (29.3 and 17.6 $\mu g \cdot mg^{-1}$ of sorbent, for Au and AgNPs, respectively). With regard to the

reusability of the developed SPE cartridges, the results showed that BSA adsorption capacity decreased only 5.3% after 20 cycles. The LOD of BSA using standard BSA spiked in water using the GMA-SH-Au sorbent, gave a value of 0.1 nM.

To demonstrate the applicability of these sorbents, they were employed to selectively isolate and preconcentrate viscotoxins (thionins) from mistletoe samples. The optimized SPE procedure allowed the isolation of the thionins by simply adjusting the loading pH at its pI, and eluting at pH above 11. The enriched mistletoe fractions were subjected to MALDI-TOF analysis to underpin their selectivity.

The methodology proposed here can be considered as a potential tool in proteomic field, since protein isolation and preconcentration always imply time-consuming processes. This methodology compared to other existing NP-based methods for sample preparation in MALDI-TOF analysis is simpler, more cost-effective, and shorter in terms of processing time. Moreover, this SPE protocol simplifies the handling of more samples simultaneously and speeds (10 samples h^{-1} vs 1-2 samples h^{-1} reported in other NP-based protocols) the preconcentration process of proteins.

I.C. Use of an enzyme-assisted method to improve protein extraction from olive leaves

The isolation of proteins from vegetal samples, such olive leaves, constitutes a difficult task due to the low crude protein content present (and the high level of interfering compounds). To overcome this problem, in this work, a cellulase enzyme was selected (Celluclast® 1.5L) to efficiently extract proteins from olive leaves. This enzyme was selected since it can hydrolyze cellulose, hemi-cellulose and pectins from the cell walls of olive leaves. Several parameters that affect the extraction process, (such as the influence and amount of organic solvent, enzyme amount, pH and extraction

temperature and time) were optimized The influence of these factors was examined by measuring the total protein amount by the standard Bradford assay, being next the extracted proteins charactetized by SDS-PAGE. The optimum extraction parameters were: 30% ACN, 5 % (v/v) Celluclast® 1.5L at pH 5.0 and 55 ºC for 15 min. Using the optimal extraction conditions, several protein extracts from olive leaves of different genetic variety were analysed and compared by SDS–PAGE, being the total protein content of the extracts also established. The values found were *ca.* 2-3 folds higher than those reported (for the same genetic varieties). The repeatability of the extraction protocol was also evaluated, giving in all cases satisfactory RSD values (below 5.2 %). In addition, the electrophoretic protein profiles obtained by SDS-PAGE showed differences in some protein bands, which could be helpful to distinguish the olive leaf tissues according to their genetic variety. Thus, the procedure developed stands out amongst the traditional protein extraction methodologies due to the mild extraction conditions employed, its lower environmental impact and shorter processing time.

I.D. Efficient extraction of olive and stone proteins by using an enzyme-assisted method

In this work, an efficient protein extraction protocol for proteins from olive pulp and stone by using enzymes was developed. For this purpose, the strategy described in the previous section was adopted. However, in this case, olive pulp and stone were selected as matrices, and different enzymes were tested to assist the extraction. In particular, individual enzymes (lipase, cellulase and phospholipase) and a commercial multienzyme preparation (arabanase, cellulase, beta-glucanase, hemicellulose and xylanase) were investigated. The main parameters that affect the protein yield, type of enzyme, enzyme content, pH and extraction temperature and time, were studied. The best extraction conditions for pulp and stone proteins were achieved at pH 7 and 5% (v/v) Palatase® 20000 L or Lecitase® Ultra content, respectively. The optimal

extraction temperature and time were 30 and 40 ºC for 15 min for pulp and stone tissues, respectively. Under these conditions, several protein extracts coming from olive pulp and stone of different genetic variety were analyzed, and their profiles compared by SDS-PAGE. In the case of stone proteins, different electrophoretic patterns and band intensities were found, which could be helpful to distinguish samples according to their genetic variety. The developed enzyme-assisted extraction method also showed advantages (such as high recovery and reduced solvent usage) and it can be considered as a feasible technology to extract proteins from these matrices.

I.E. Enzyme-assisted extraction of proteins from Citrus fruits and prediction of their cultivar using protein profiles obtained by CGE

This work was also framed within the application of enzyme-assisted methodology to vegetal samples. In this study, the objectives were: i) to verify the effectiveness of several enzyme-aid extraction (cellulase and lipase) in the protein release from pulp and peel from *Citrus* fruits (orange and tangerine), and ii) to compare this enzymatic approach with non-enzymatic methods and iii) use of established protein profiles by CGE as a tool to discriminate between *Citrus* cultivars.

After testing different extraction methodologies, the enzyme-assisted treatment (applied to both peel and pulp of *Citrus* fruits) gave protein contents higher than the traditional native buffer (containing Tris-HCl). The best results were achieved using 5% (v/v) Celluclast® 1.5L (cellulase) and 5% (v/v) Palatase® 20000 L (lipase) buffers for *Citrus* peel and pulp protein extracts, respectively. Then, the protein extracts were subjected to CGE analysis, and 14 and 8 protein peaks for peel and pulp, respectively, were identified. The reproducibility of the method was also evaluated obtaining good RSD values (3.6 and 3.7% for peel and pulp samples). All the protein peak areas were normalized for their use as predictors in the construction of LDA models, which were able to distinguish *Citrus* peel and pulp samples according to their

cultivar. All the samples included in this work, coming from different Spanish regions, were properly assigned with very good resolution among categories.

This work evidenced again the feasibility of the enzyme-assisted methodology to extract proteins from complex matrices (e.g. *Citrus* peel and pulp tissues). In addition, it was demonstrated the potential of protein profiles obtained by CGE (after efficient extraction) as a tool to discriminate *Citrus* samples according to their cultivar.

I.F. Proteomic fingerprinting of mistletoe (Viscum Album L) via CPLLs and MS analysis

An entire investigation of mistletoe proteome, by using CPLLs technology coupled to MS analysis, was accomplished in this work. As mentioned in **Section II.11**, CPLLs are able to preconcentrate low abundance proteins reducing at the same time the high abundance ones. For this purpose, proteins were captured with CPLLs conducting the experiments at two different pHs (2.2 and 7.2). The eluted proteins, which were desorbed with SDS, were characterized by SDS-PAGE. The sample bands were subjected to tryptic digestion and subsequently analyzed by MS. Using a specific database, a total of 295 and 257 proteins were identified in untreated control sample and with CPLL treatment, respectively, while only 96 were commonly recognize in both samples. The proposed methodology was able to extract not only lectins and viscotoxins, which are the most deeply described in literature, but also other proteins involved in metabolic processes related to pharmacological activities. In addition, in the present research, an evaluation of the biological function of identified proteins was carried out in order to ascertain their role on human health and the potential benefits of mistletoe extracts in medicine.

Part II. Development of methods for the discrimination of olive products according to their genetic and botanical origin

II.A. Use of protein profiles established by CZE to predict the cultivar of olive leaves and pulps

A CZE method to separate olive leaf and pulp intact proteins was developed and applied to predict the cultivar of olive leaves and pulps using protein peaks as predictors. Firstly, the enzyme-assisted method previously optimized to extract proteins from olive leaves and pulps (using cellulase and lipase enzymes, respectively) was applied (see **Section I.C** and **I.D**). The intact proteins were then separated by CZE, after optimization of different experimental conditions such as separation buffer, voltage of separation and conditions of injection (type, time and pressure). The best separation performance was obtained with a BGE composed of 50 mM phosphate, 50 mM tetraborate and 0.1% PVA at pH 9, a separation voltage of +10 kV and and hydrodynamic injection of 50 mbar for 3 s. When compared to other previously reported protocols for the same matrix in literature, the methodology developed here showed lower analysis times and better reproducibilities. A total of 9 and 14 common electrophoretic peaks, for leaf and pulp samples, respectively, were identified in the 9 cultivars considered in this work. The protein peak areas were normalized and used as predictors to construct LDA models able to classify the olive leaf and pulp samples according to their cultivar. All types of samples (leaf and pulp) were correctly classified with a good resolution between all category pairs, which demonstrated that intact protein profiles are characteristic of each cultivar.

II.B. Classification of olive leaves and pulps according to their cultivar by using protein profiles established by CGE

In this work, a classification of different olive leaves and pulps according to their genetic origin using protein profiles established by CGE was

accomplished. Also in this case, the previously optimized enzyme-assisted extraction protocol was employed (**Section I.C** and **I.D).** The protein extracts of samples coming from 12 different cultivars were next subjected to CGE analysis, and 10 and 9 common peaks were observed for leaf and pulp samples, respectively. Next, the molecular masses of these proteins were established by using two calibration curves (one for leaf and another for pulp), being consistent with those reported in literature. The precision of the method was also evaluated by studying the reproducibility of migration times of some protein peaks. The results showed in all cases RSD values lower than 2.6%.

Finally, two LDA models, for leaf and for pulp samples, respectively, were constructed using the normalized protein peak areas as predictors. In both cases, olive leaf and pulp samples belonging to twelve cultivars from different Spanish regions were correctly classified with an excellent resolution among all the categories, which demonstrated that protein profiles were characteristic of each cultivar.

II.C. Use of TAG profiles established by HPLC-UV and ELSD to predict cultivar and maturity of Tunisian olive oils

In this work, TAG profiles have been established by HPLC-UV and ELSD detection to classify Tunisian EVOOs according to their cultivar and maturity index. A total of 19 peaks, which were common to all the EVOOs studied, were observed with both detectors. However, and in order to select which data is the most adequate for statistical analysis, the response of both UV and ELSD detectors was compared in order to see if the obtained response is the same with both of them, and to check if there is an exaltation of the signal with one of the detectors with the aim of maximizing the possible differences between the different studied EVOOs. ELSD peak areas were selected since this detector, in general, provided higher signal-to-noise ratios than those found in UV.

Then TAG content present in Tunisian olive oils was established. Several changes in the TAG percentages according to the different cultivars and maturity indexes were evidenced. Thus, these differences were enhanced by using TAG peaks as predictors for the construction of LDA models. EVOOs belonging to 7 Tunisian cultivars, and EVOOs from the Chemchali, Fouji and Zarrazi cultivars obtained at different maturity indexes, were correctly classified with an excellent resolution among all the categories. Thus, it shows that TAG profiles are a good marker of both cultivar and maturity index of EVOOs.

II.D. Sterol profiles of Tunisian EVOOs: Classification among different cultivars and maturity indexes.

In this study, Tunisian EVOOs arising from different cultivars and different maturity index has been classified on basis of their sterol profiles. For this purpose, sterols were extracted according to the procedure established by the European Union and then analyzed by HPLC-MS. A total of 12 sterols were identified and their content in the different samples was established. The results showed that sterol composition varied significantly among the cultivars and also among the different maturity index. As previously stated in II.C for TAGs, these differences will be enhanced using chemometric techniques, such as LDA. Also, in this case, EVOOs coming from 7 different cultivars, and EVOOs from the Chemchali, Fouji, and Zarrazi cultivars from different maturity indexes, were properly classified with an outstanding separation among all the categories using sterol peak ratios as predictors, which proved that the proposed method is of interest to control the genetic origin and the maturity index of the olives used to obtain the EVOOs.

II. E. Capillary electrophoresis of free fatty acids by indirect UV detection: application to the classification of vegetable oils according to their botanical origin

A CE method using indirect UV detection was developed to determine free fatty acids from vegetable oils. By using indirect UV detection, the use of derivatization reactions is avoided, which could produce incomplete conversion of the analytes and undesirable interfering side products. The separation of fatty acids was optimized by selecting BGE composition (Brij surfactant nature and content, and percentage of organic modifier). The best results were obtained with a BGE containing 10 mM p-hydroxybenzoate, 5 mM Tris at pH 8.8, 80 mM Brij 98, 40% acetonitrile, and 10% 2-propanol. Under the selected conditions, the method precision and its LOD were evaluated, giving values ca. 3% and 0.020 mM, respectively. Next, fatty acid contents from five vegetable oils coming from different botanical origins (avocado, corn, extra virgin olive, hazelnut, and soybean) were established. Finally, an LDA model was constructed using fatty acid peak areas as predictors obtaining an excellent resolution among all category pairs. Thus, the developed methodology is a promising alternative to the traditional GC method with the advantages of simplicity and lower consumption of reagents. Therefore, the present procedure is of great interest for routine quality control or adulteration purposes in vegetable oil samples.

II.F. Acrylate ester-based monolithic columns for capillary electrochromatography separation of triacylglycerols in vegetable oils

A CEC method using laboratory-made acrylate monolithic columns for the determination of TAGs in vegetable oils has been developed. For this purpose, the preparation of octadecyl acrylate (ODA) ester-based monoliths was first optimized in terms of composition of polymerization mixture. The best resolution was achieved at the following ratios: 40:60% (wt/wt)

monomers/porogens, 60:40% (wt/wt) ODA/1,3-butanediol diacrylate and 23:77% (wt/wt) 1,4-butanediol/1-propanol (14 wt% 1,4-butanediol in the polymerization mixture). After a simple dilution to the vegetable oil samples, the best separation was accomplished giving a total of 9 common peaks (in less than 12 min) using a mobile phase containing 65:35 (v/v) acetonitrile/2-propanol mixture and 5 mM ammonium acetate. Then, the CEC data (TAG peak areas) followed by LDA was employed to classify these samples according to their botanical origin, and in all cases the vegetable oil samples belonging to the different botanical origins (corn, extra virgin olive, hazelnut, peanut, soybean and sunflower) were correctly classified with an excellent separation among all the categories.

The proposed procedure can be an interesting approach to develop a classification method using TAG profiles established by CEC in combination with LDA, being analysis times lower than those obtained by LC techniques.

II.G. Cultivar discrimination of Spanish olives by using direct FTIR data combined with linear discriminant analysis

A direct and fast method capable of classifying Spanish olive fruits according to their cultivar was performed using ATR-FTIR spectroscopy and LDA as a chemometric tool. Thus, the spectral data of 136 olives coming from 17 cultivars, collected at different Spanish locations, were recorded. The spectra were divided into 24 frequencies. The normalized absorbance peak areas within these regions were used as predictors to construct LDA models. Although this model showed an excellent prediction capability (100%) to classify Spanish olives, a second chemometric approach was accomplished (PCA-LDA). This latter chemometric tool was not able to separate all the evaluation set samples (56 % prediction capability). Thus, the stepwise LDA model was selected due to its simpler, faster, and larger discrimination power than the PCA-LDA approach.

II.H. Cultivar discrimination and prediction of mixtures of Tunisian extra virgin olive oils by FTIR

This study can be considered an extension of the applicability of the ATR-FTIR technique in combination with multivariate data analysis (LDA and MLR). In this case, Tunisian EVOOs arising from different cultivars and maturity indexes were assayed. Thus, the constructed LDA model had the capability to discriminate between EVOOs belong to different genetic origin and maturity index. Also, MLR was used to evaluate the possibility of detecting mixtures of EVOOs from different cultivars. In this case, the model was able to predict the percentage of one of the oils with average validation errors below 6%. Thus, the results obtained in this study showed that FTIR spectroscopy jointly with chemometric techniques, such as LDA or MLR models, provides a simple and fast approach to be used by the olive industry for the classification of EVOO as well as to quantify EVOO blends. In fact, only FTIR equipment (common analytical lab instrumentation) and a chemometric software, are just required to implement the proposed method.

II.I. Classification of Tunisian EVOOs according to their genetic variety and maturity index using fatty acid profiles established by direct infusion MS

The aim of this work is to demonstrate the usefulness of fatty acid profiles established by DIMS as a tool to discriminate seven Tunisian EVOOs according to their genetic variety (Chemchali, Fouji, Zarrazi, Dhokar, Chemlali, Jemri, and Zalmati), and to differenciate Chemchali, Fouji, and Zarrazi EVOOs regarding to their maturity index. In addition, the discrimination of EVOOs from the genetic varieties Chemchali, Fouji, and Zarrazi, characterized with different maturity indices, was also evaluated. For this purpose, EVOO samples were properly diluted in a mixture of 85:15 propanol/methanol (v/v) mixture containing 40 mM ammonia without any

previous extraction and injected into MS, followed by the measurement of fatty acid profiles. Differences in patterns were evidenced depending on genetic variety and maturity index.

Then, fatty acid peak areas were employed to build LDA models in order to predict both parameters. In all cases, an excellent resolution between all category pairs was achieved, which demonstrated that fatty acid profiles are target solutes to classify EVOOs according to both genetic variety and maturity index of EVOOs.

Other developments

This PhD thesis should also include four other chapters whose experimental parts are today finished, but the writing is still being done. Due to time requirements to present the thesis, these four parts have not been included in this report but have been recorded here to be considered as genuine part of the thesis. These four parts are next shortly indicated:

a) Poly(ethylene glycol) diacrylate-based monolithic capillary columns for analysis of apolar and polar solutes by capillary electrochromatography

b) Preparation and characterization of polymeric monoliths modified with gold nanoparticles for their use in pippete-tip extraction of proteins

c) Combination of CE-MS and advanced chemometric tools for proteomic profiling of vegetable samples (olive leaves, pulp, and mistletoe).

d) Enhanced analysis of porcine seminal plasma proteome by using polymeric sorbents modified with gold nanoparticles.